Use of HiTran inserts to enhance heat transfer and control fouling from hydrocarbons

Shalhi, Ahmed Mohadab

Award date:
1993

Awarding institution:
University of Bath

Use of HiTran inserts to enhance heat transfer and control fouling from hydrocarbons

Submitted by Ahmed Mohadab Shalhi

for the Degree of Ph.D.

of the University of Bath

1993

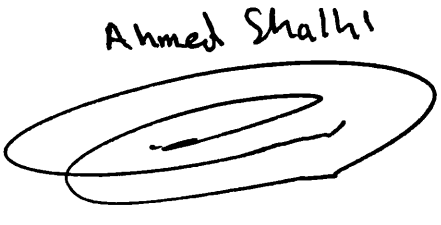

ProQuest LLC
789 East Eisenhower Parkway
P.O. Box 1346
Ann Arbor, MI 48106-1346

This work is dedicated to
My wife

Acknowledgements

I am most grateful to my supervisor Professor B.D. Crittenden for his able supervision throughout the course of my research and for his constructive criticisms and unfailing guidance during the preparation of the thesis.

I would like to express my sincere gratitude to Dr S.T. Kolaczkowski for his help and encouragement over the course of the study.

I would also like to express my gratitude to Professor J.A. Howell , Head of the School of Chemical Engineering, for his encouragement and provision of the research facilities and equipment. Thanks are especially due to Mr P. McDonald for his excellent help in obtaining the experimental results.

I am grateful to the Petroleum Research Centre, Tripoli, Libya , for financing my stay and study. I would also like to thank Umm AL- Jawaby Oil Service Co. Ltd. , London, for their service .

I would like to thank Cal Gavin Ltd, Birmingham , for suppling the **HiTran** inserts and for the provision of funds to carry out this research .

Finally it is impossible to mention by name all of those who have helped in accomplishing this work and to all of them I would like to express my thanks.

Summary

A pilot - scale apparatus has been used to study the effect of **HiTran** inserts on the heat transfer, friction factor and fouling characteristics of hydrocarbons.

Correlations for a bare tube and for a tube fitted with various **HiTran** inserts have been generated for the ranges of $500 < Re < 34000$ and $30 < Pr < 187$ for Santotherm 55 (a non-fouling fluid) and tested with data obtained using Arabian light crude oil under similar experimental conditions. These empirical correlations could be used to aid the design of refinery heat exchangers with **HiTran** inserts fitted inside tubes since the test section tubes used in the present study are identical to those used in refinery equipment.

HiTran inserts enhanced the heat transfer j_H-factor over that of the bare tube case by between 1.3 and 5.8 times, depending on the value of Re and the insert used . The concomitant increase in the pressure drop was between 8.5 and 50 times that of the bare tube . **HiTran** inserts reduced the inner surface temperature by as much as 100 °C from that of the bare tube. The consequences of this on chemical reaction fouling are believed to be significant .

Fouling of crude oil was found to be inhibited by nucleate boiling and by degassing of dissolved nitrogen on hot surfaces due to the solubility difference at the bulk fluid and surface temperatures. Both nucleate boiling and bubble nucleation due to gas solubility difference can provide an enhancement in the heat transfer coefficient and a reduction in the inner surface temperature , the latter being beneficial in reducing chemical reaction fouling .

Contents

Nomenclature

SI units are used throughout and are defined in the text where the symbol first occur

A : frequency factor (equation 1.9)

A_1 , .., A_{13} : constants defined in the text

A_i : inside surface area of tube

A_o : outside surface area of tube

A_{oin} : outside surface area of the insulation around the heated test section

A_t : heat transfer surface area at the location of the wall thermocouples

a : constant (equation 3.4)

a_1 : constant (equation 4.4)

B : constant (equation 1.53)

b : constant (equation 3.4)

b_1 : constant (equation 4.4)

C_i : parameter (equation 1.9)

C_p : heat capacity

C_{pa} : specific heat of the air

C_a : function (equation 3.93)

C_b : function (equation 3.55)

c : constant (equation 3.4)

D_{J_i} : jacket tube inside diameter

D_{J_o} : jacket tube outside diameter

D_i : inner tube diameter

D_{in} : outside diameter of the insulation

D_o : outside tube diameter

E : activation energy

EF : enhancement factor (equation 1.99)

F : correction factor (equation 1.23)

FI : flow rate

f : Fanning friction factor

f_a : friction factor (equation 1.104)

f_b : Fanning friction factor for bare tube

f_c : friction factor (equations 1.50 & 1.51)

f_D : Darcy friction factor

f_e : Fanning friction factor for enhanced tube

f_{is} : isothermal Fanning friction factor

f_{nis} : non-isothermal Fanning friction factor

f_R : Fanning friction factor for rough tubes

f_S : Fanning friction factor for smooth tubes

g : standard acceleration of gravity

g_c : the gravitational acceleration conversion factor

G_z : Graetz number (equation 1.56)

Gr_D : Grashof number of air (equation 3.50)

h_i : film heat transfer coefficient of fluid inside tube

h_o : film heat transfer coefficient of fluid outside tube

h_c : natural convection heat transfer coefficient

h_r : radiation heat transfer coefficient

j_H : Sieder and Tate heat transfer factor (equation 1.95)

j_h : Colburn heat transfer factor (equation 1.96)

j_{HM} : modified heat transfer factor (equation 3.114)

k : thermal conductivity

k_a : thermal conductivity of the air

k_j : thermal conductivity of the jacket tube

k_f : deposit thermal conductivity

k_s : thermal conductivity of the test section

L : tube length

L_{hy} : hydrodynamic entrance length

L_{hy}^+ : dimensionless hydrodynamic entrance length

L_{in} : insulation length

L_p : the length between two tapping (equation 3.78)

L_{th} : thermal entrance length

$L_{(ost)}$: Ostwald coefficient

L_{th}^+ : dimensionless thermal entrance length

M : mass deposition per unit surface area

m : mass flow rate

Nu : Nusselt number (equation 1.54)

Nu_b : Nusselt number for bare tube

Nu_D : Nusselt number of natural convection for a horizontal cylinder

Nu_e : Nusselt number for enhanced tube

Nu_l : Nusselt number for uniform wall temperature

$Nu_{(m)}$: mean Nusselt number

Nu_o : Nusselt number for uniform heat flux

Nu_R : Nusselt number for rough tubes

Nu_s : Nusselt number for smooth tubes

Nu_t : Nusselt number (equations 1.92 & 1.94)

$Nu_{(\infty)}$: fully developed Nusselt number

P : pressure

$P_{(g)}$: gas partial pressure

Pe : Peclet number (Pr Re)

Pr : Prandtl number ($C_p \mu / k$)

Pr : Prandtl number ($C_p \mu / k$)

Pr_a : Prandtl number of air

Q : heat duty

$Q_{(loss)}$: heat loss (equation 3.38)

$Q_{(sup)}$: direct wattmeter reading

q : heat flux

q_r : heat transfer per unit area due to radiation to the surroundings

R : universal gas constant

Ra_D : Rayleigh number of air (Pr_a Gr_D)

Re : Reynolds number (v D_i ρ / μ)

R_f : fouling resistance

$R_{f(App)}$: apparent fouling resistance

$R_{f(hard)}$: fouling resistance due to hard coke deposit layer

R_{fi} : fouling resistance on inside of tube

R_{fo} : fouling resistance on outside of tube

$R_{f(tarry)}$: fouling resistance due to tarry deposit layer

$\dot{R}_{f(\theta)}$: net rate of fouling deposition

R_{Nu} : ratio of enhanced to bare Nusselt numbers

R_o : overall resistance (equation 1.4)

R_w : tube wall resistance

$R_{\Delta p}$: ratio of enhanced to bare pressure drop

r_i : inside tube radius

S : cross section area of the test section

St : Stanton number (Nu / Re Pr)

T : temperature

T_{av} : average bulk fluid temperature

T_b : bulk fluid temperature

$T_{c(in)}$: inlet temperature of cold fluid

$T_{c(out)}$: outlet temperature of cold fluid

T_f : film temperature

$T_{h(in)}$: inlet temperature of hot fluid

$T_{h(out)}$: outlet temperature of hot fluid

T_i : inner surface temperature

$T_{i(mf)}$: the temperature at which the fouling rate is maximum

T_s : surface temperature

T_w : wall temperature

T_∞ : room temperature

t : time

U_c : clean overall heat transfer coefficient

U_f : fouling overall heat transfer coefficient

U_o : overall heat transfer coefficient based on outside surface area

U_t : overall heat transfer coefficient based on area A_t

v : fluid velocity

$V^o(l)$: molar volume of liquid

X : wall thickness of the test section

X_d : deposit thickness

X_m : mole fraction solubility

x : axial distance

x^* : dimensionless axial distance

β_a : coefficient of thermal expansion of the air

Δp : pressure drop

ΔT : temperature difference

δ : boundary layer thickness

ϵ : height of surface roughness element

ϵ_i : the emissivity of the insulation

Γ	:	function (equation 1.54)
ϕ	:	net fouling flux
ϕ_{CT}	:	removal rate by conversion of tarry layer to coke
ϕ_d	:	gross deposition flux
ϕ_{Fr}	:	removal rate by fluid shear
ϕ_r	:	removal flux
ϕ_{Td}	:	deposition rate of tarry layer
ϕ_{Tr}	:	removal rate of tars by mass transfer to fluid bulk
η	:	test section efficiency
μ	:	fluid dynamic viscosity
μ_a	:	dynamic viscosity of the air
μ_b	:	dynamic viscosity at the bulk fluid temperature
μ_f	:	dynamic viscosity at the film temperature
μ_w	:	dynamic viscosity at the wall temperature
ν	:	kinematic viscosity
ρ	:	density
ρ_a	:	air density
ρ_f	:	deposit density
σ	:	Stefan - Boltzmann
τ	:	shear stress
Ψ	:	constant (equation 3.66)

Introduction

"Fouling has been with us since fire was discovered" (59)

Fouling can be defined as the formation of undesired solid material on heat transfer surfaces that impede heat transfer and increase the resistance to the flow of fluids over the surface(54-63). Fouling has been a problem since the first heat exchanger was invented(40). Shell - and - tube heat exchangers and condensers are among the most common and widely used pieces of equipment within the petroleum and chemical process industries. Today, with the aid of computer technology , the design of heat exchanger and heat exchanger networks has reached a level that was never possible before . Many heat transfer enhancement techniques have been applied , and the modern plants now have fewer and smaller heat exchangers, achieve higher levels of heat recovery , and require lower levels of heat input(196-200,227) . Yet , despite the best designs , heat exchanger fouling remains a problem in many plants . This " silent thief robs the plant of its efficiency , creates bottlenecks , increases energy consumption , cuts down production , creates maintenance problems , causes equipment failure , reduces profit , and creates nightmares for design engineers and plant operators "(227) .

Although difficult to estimate , the total fouling costs for the U.K and U.S.A have been estimated to be as follows :

U.K (1979): £ 3×10^8 to £ 5×10^8 [125]
U.S.A (1985): \$ 8×10^9 to \$ 10×10^9 [39]

For oil refining , early estimates suggest that the cost ranges from \$ 37 [125] to \$330 [77] per 1000 barrels of oil processed. The latter figure is based on Exxon Chemical Company's estimates of the total fouling - related expenses in a 100,000 barrel per day refinery being \$ 9.875 million per annum[77]. It is obvious that the goal of substantial savings in such financial penalties could be obtained through a better understanding not only of the fouling problem itself, but also of practical ways in which it can be overcome[78].

Twenty years ago a now classical article in two parts was published with the title " **Fouling - The Major Unresolved Problem in Heat Transfer** "[102] . This article was important , not only because of its substantive contents but also by virtue of its title , which challenged engineers and scientists to attack this major problem , resulting in the significant increase in literature on the subject and a resolution of the various aspects of the problem[62]. Despite the amount of research attention it has created , and the new knowledge that has been generated in the past 20 years , fouling still remains one of the most poorly understood aspects of heat exchanger design and operation[40,134]. Even now there is

still little other than qualitative relationships together with improved treatment and cleaning methods that can be used to attack the problem. One main difficulty is getting information to the designer. The amount and quality of information that the designer receives varies amongst organizations (in-house designers, engineering contractors , or vendors). The ultimate user who initially specifies the equipment needs to provide the designer with much more information than a fouling resistance on a specification sheet[134]. Bott[40], however, attempts to fill this gap by providing a background to heat exchanger fouling and the opportunities available for overcoming or reducing the problem in industrial operations. This is useful for heat exchanger designers and users alike .

Hydrocarbon fouling is possibly one of the most complex phenomena in chemical engineering. It involves momentum , heat and mass transfer as well as chemical reaction kinetics[64-68,82]. One would have to agree that the extent of knowledge lies somewhere between poor and scant[82]. Crude oil fouling , which is an important example of hydrocarbon fouling , has been little investigated in the laboratory , most likely due to safety reasons. Available information on crude oil fouling comes either from industrial plant data or from laboratory experiments designed to scale - down substantially the actual heat exchanger and so to accelerate the fouling process. Unfortunately , both of

these methods can suffer from serious limitations[83,89]. A careful crude oil fouling investigation in a tube of typical industrial dimensions operating under typical industrial conditions but in a laboratory , with full control of process variables (temperature , flow rate , pressure , .etc) , has never been attempted before .

The **HiTran** insert , which is a wire wound turbulence promoter used for in-tube heat transfer enhancement[19-25] has been found[19,24] to provide a substantial reduction in hydrocarbon fouling . The reason why this improvement should have happened is not fully understood. Thus it is the aim of this study to investigate the performance of the **HiTran** insert under clean and fouling conditions , in order to provide a clear picture of the role of this device in the fouling process. This could also lead to a better understanding of fouling phenomena in general. The important case of crude oil fouling has been chosen for this laboratory study .

Chapter 1

Literature Survey

1.1 Fouling of heat transfer equipment

1.1.1 General background

In his survey on the history of fouling of heat transfer surfaces, Somerscales[59] identified four epochs of fouling up to 1979 ;

a- The period until 1920 , which was mostly concerned with observing and devising methods to eliminate fouling or to minimize its consequences

b- 1920 - 1935 , when methods for the measurement and the representation of fouling were first formulated;

c- 1935 - 1945 , the era of the fouling factor, and ;

d- 1945 - 1979 , when a more scientific approach to understanding fouling gained acceptance .

During the past twenty years, fouling has been the subject of books[39,40] , treatises[41-53] and hundreds, if not thousands, of scientific papers. Fouling references of general interest , based on recent conferences , workshops and surveys , which

reflect the current state of the art , are provided by Somerscales and Knudsen[54], Chenoweth and Impagliazza[55] , Bryers[57] , Suitor and Pritchard[56] , and Melo *et al*[58] .

Fouling may be classified in different ways. Epstein[60,61] however , has developed the following classification scheme, which has received wide acceptance :

- **Precipitation fouling** .The precipitation of dissolved substances onto a heat transfer surface . When the dissolved substances have inverse solubility - vs.- temperature behaviour (such as $CaCO_3$, $CaSO_4$, $MgSiO_3$, and $NaSO_4$ in water) , the precipitation occurs on superheated surfaces and the process is often referred to as scaling .
- **Particulate fouling** .The accumulation of finely divided solids suspended in the fluid onto the heat transfer surface . In a minority of instances settling by gravity prevails , and the process is then referred to as sedimentation fouling .
- **Chemical reaction fouling** . Deposits formed at the heat transfer surface by chemical reactions in which the surface material itself is not a reactant .
- **Corrosion fouling** . The heat transfer surface itself reacts to produce corrosion products (in situ corrosion fouling) which thermally insulate (foul) the surface and may promote the attachment of other foulants .

- **Biological fouling** . The attachment of macroorganisms (macrofouling) and/or microorganisms (microfouling or microbial fouling) to a heat transfer surface , along with the adherent slimes often generated by the latter .
- **Solidification fouling** . Freezing of a liquid , or some of its higher - melting constituents , or liquid components in a gas stream onto a subcooled heat transfer surface .

Two or more of the above fouling types can occur simultaneously and in some cases may be synergistic , i.e, hydrocarbon fouling is often a combination of chemical reaction, crystallization (solidification or precipitation), particulate and corrosion processes.

Epstein[62] also proposed five major categories of fouling events which may play a role in all types of fouling , as follows :

1- **Initiation**, which may include surface conditioning;
2- **Transport** of foulant ;
3- **Attachment** to the surface ;
4- **Removal** of the deposit ; and
5- **Aging** of the deposit on the surface .

Epstein[62] provides a 5 by 5 fouling matrix shown in Fig 1.1 which is a combination of five fouling types , i.e, crystallization, particulate , chemical reaction , corrosion and biological fouling , and the five fouling events (initiation, transport,

	1. Crystallization Fouling	2. Particulate Fouling	3. Chemical-Reaction Fouling	4. Corrosion Fouling	5. Biological Fouling
1. Initiation	1,1	1,2	1,3	1,4	1,5
2. Transport	2,1	2,2	2,3	2,4	2,5
3. Attachment	3,1	3,2	3,3	3,4	3,5
4. Removal	4,1	4,2	4,3	4,4	4,5
5. Aging	5,1	5,2	5,3	5,4	5,5

Fig 1.1 Fouling matrix of Epstein[62]

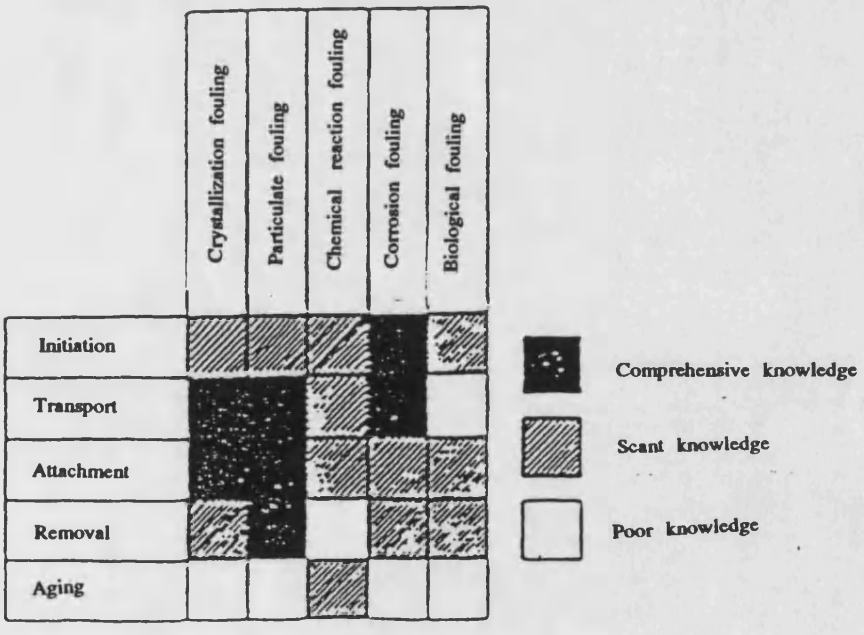

Fig 1.2 Bohnet's assessment[63] of state of knowledge of fouling matrix

attachment, removal and aging). It contributes both a conceptual framework for the study of fouling, and a focus for research.

Using Epstein's fouling matrix, Bohnet[63] presented an assessment of the extent of knowledge in each element in the matrix , as shown in Fig 1.2. It is clear from Bohnet's assessment that some elements of the fouling matrix have received more attention than others, e.g, the extent of knowledge in removal of particulate fouling is comprehensive while it is poor in chemical reaction fouling .

The current investigation concerns hydrocarbon fouling, more precisely fouling of crude oil. Consequently, chemical reaction, particulate, precipitation and corrosion fouling would be expected to occur while biological fouling would not.

1.1.2 Fouling of hydrocarbons

Fouling of hydrocarbons, sometimes referred to as organic fluid fouling, can lead to enormous financial penalties in terms of additional energy consumption and debits in through-put[20]. It can occur in any process environment in which hydrocarbons are heated , including , oil , chemical

and petrochemical industries[64,65]. It has been the subject of several reviews[49,65,78-80,82], the most recent, critical and comprehensive being provided by Watkinson[82]. He examined existing data that can be used for the development of mechanism - related models , reviewed chemical and physical analyses that have been conducted for organic fluid fouling, reviewed analyses that could be used to determine key variables and their effects on organic fluid fouling and finally listed several recommendations for organic fluid fouling research. Watkinson[82] concluded that for a broad range of organic fluids, fouling occurs by production of soluble low molecular weight precursors which subsequently react to form substances of higher molecular weight, which are insoluble . The predominant mechanism of precursor formation at temperatures below about 350 °C and in the presence of traces of oxygen is autoxidation , whereas at higher temperatures and in the absence of oxygen it is thermal decomposition. These routes, however, have been established largely through fluid aging and mass deposition studies ; confirmatory experiments in thermal fouling are required[82] . Watkinson[82] believed that similar kinds of reactions are involved in the fouling of many organic fluids. Consequently, a general understanding of the organic fluid fouling process could possibly be obtained without studying an inordinately large number of different fluids.

However, this is a speculative conclusion . Fouling of crude oil which is a very complex fluid , for instance , will not be completely understood by studying the polymerisation of styrene in kerosene[49,81].

The literature on hydrocarbon fouling can be put into different categories of study, which may overlap to some extent, as follows :

1- Reviews containing a significant hydrocarbon or organic reaction fouling content ;
2- Thermal fouling studies in laboratory test rigs ;
3- Industrial thermal fouling reports or studies in actual full scale heat exchangers ;
4- Mass deposition studies in laboratory apparatus ;
5- Aging and thermal stability studies for soluble and insoluble gum formation ;
6- Coke formation studies ;
7- Studies of kinetics of reactions implicated in fouling such as autoxidation and pyrolysis ;
8- Additive studies for fouling prevention;
9- Deposit characterization ; and
10- Fouling tendency studies .

Table 1.1 summarises many of the articles covered in this review keyed by numbers to these categories .

Table 1.1 Hydrocarbon Fouling References by Category

Category	Primary Subject	Reference By Number
1	Reviews with significant content of hydrocarbon fouling	49,65,78,79,80,82
2	Thermal fouling studies in laboratory test equipment s .	66,67,86,80,81,87,88,107, 108,114,117,120,122,139
3	Industrial thermal fouling studies in actual full scale heat exchangers .	19,21,39,72,73,77,89,90, 92,94,95,96,97,89,127
4	Mass deposition studies in laboratory apparatus .	86,109,113,118,119,140
5	Aging and thermal stability studies for soluble and insoluble gum formation.	91,109,115,116,126,128, 129,130
6	Coke formation studies .	79,109,114,122,130,131,230
7	Studies of kinetics of reactions implicated in fouling .	46,66,67,69,73,80,81,86, 90,97,99,100,101,117,126, 129,131
8	Additive studies for fouling prevention .	67,68,73,92,98,127,139
9	Deposit characterisation .	19,21,66,68,69,73,107,117, 120,139
10	Fouling tendency studies .	66,67,68,86,98,145,

Thermal fouling studies refer to cases where heat transfer of some kind is occurring and where thermal resistance is normally the primary response measured. In mass deposition studies the fouling deposit is weighed but its thermal resistance not measured . The link between thermal fouling and mass deposition studies arises through the following equation which is valid for thin deposits (x_d) ;

$$R_f = \frac{x_d}{k_f} = \frac{M}{\rho_f k_f} \qquad (1.1)$$

Mass deposition per unit surface area (M) data can be converted to thermal resistance (R_f) only if the deposit density (ρ_f) and thermal conductivity (k_f) are known .

The aging and thermal stability category refers to studies of deposit formation either at or near room temperature (aging) or under thermal stressing . Coke formation studies have been listed as a separate category , as they include mainly high temperature mass deposition studies often from pure component feedstocks .

Table 1.2 lists the key studies of thermal fouling and mass deposition which form the bulk of published hydrocarbon fouling literature. This includes research on crude oils , and refinery cuts of various types , including kerosenes , gas oils and jet fuels. Thermal fouling in polymerising systems has been examined only for the case of styrene polymerisation as a model reaction[49,81].

Most of the studies listed in Table 1.2 used experimental conditions which would induce measurable effects over relatively short timescales. Thus , processes which may occur in industrial exchangers over periods of months are measured under more severe operating conditions over periods of hours or days[87,65].The uncertainties introduced by using such an approach are undoubtedly worse in chemical reaction fouling than in other types of fouling, since the nature of the reactions occurring

and the selectivity to certain reaction products may be a strong function of conditions[82,83] .

Table 1.2 Experimental Hydrocarbon Fouling Studies

Fouling fluids	Test rig and measurement	Temperature, Pressure and Time	Authors
Gas oil	Heated tube Thermal fouling	$T_i < 175$ °C $T_b < 100$ °C P=101.3 kPa t < 430 h	Watkinson and Epstein[107]
Kerosenes	Heated tube Thermal fouling	$130 < T_b < 100$ °C t < 650 h	Smith[108]
Jet fuels	Heated tube Mass deposition	$150 < T_b < 260$ °C $20 < P < 6990$ kPa t < 4 h	Taylor[113,118] Taylor and Frankenfeld[140]
Oil refinery feedstocks	Hot wire probe Thermal fouling	$175 < T_s < 400$ °C $T_b < 100$ °C P=1480 kPa t < 50 h	Braun[66] Hausler and Thalmayer[117]
Crude oil	Heated tube Thermal fouling	$365 < T_i < 447$ °C $345 < T_b < 365$ °C P=4100 kPa t < 400 h	Scarborough *et al*[122]
Jet fuel	Isothermal Mass deposition	$120 < T_b < 355$ °C P < 4235 kPa t < 16 h	Vranos *et al*[109]
Styrene in heptane	Hot wire annular probes Thermal fouling	$T_s < 180$ °C $T_b < 107$ °C P = 650 kPa t < 72 h	Fetissoff *et al*[120]
Kerosene (air saturated)	Tube side Vaporizer Thermal fouling	$T_s < 287$ °C $106 < P < 253$ kPa t < 110 h	Crittenden and Khater[87]
Crude oil refinery cuts	Autoclaves (rotating cylinder) probe Thermal fouling	$160 < T_i < 380$ °C $71 < T_b < 287$ °C P = 2000 kPa t < 20 h	Eaton and Lux[86]
1% Styrene in kerosene	Heated Tube Thermal fouling	$22 < T_i < 249$ °C $22 < T_b < 229$ °C t < 12 h	Crittenden *et al*[80,81]
Crude oil with asphaltenes	TFT (Thermal Fouling Tester)[138] Fouling tendency	$332 < T_b < 266$ °C t < 4 h	Dickakian and Seay[67]

Modelling is an important part of the research process and many reviews of fouling models can be found in the open literature . Epstein[84] , and Crittenden[65] have provided recent reviews on thermal fouling and chemical reaction fouling models respectively. Most fouling models are based on the Kern and Seaton[85] assumption that the net fouling flux (ϕ) is the difference between a gross deposition flux (ϕ_d) and a removal flux (ϕ_r) as follows :

$$\phi = \phi_d - \phi_r \qquad (1.2)$$

Kern and Seaton[85] believed that the deposition flux (ϕ_d) should be constant at constant conditions of flow rate , temperature and fluid quality , and postulated that the removal flux (ϕ_r) is proportional to the deposit thickness (x_d) and to the shear stress (τ) at the fluid - deposit interface.

Chemical reaction fouling models are listed in Table 1.3 in chronological order. It is only in Crittenden *et al*'s[80] model in which the kinetics of a reaction (polymerisation of styrene) were separately established and then used to interpret data and provide the basis for a mathematical model of the fouling process . The other models listed in Table 1.3 are either empirical or semi - empirical based , in many cases, on industrial data in which the kinetics of the fouling reaction were not known. Moreover , most of these models refer to chemical

reaction only, even for situations where particulates are involved or corrosion processes occur. Crittenden[64] has explained the interference between chemical reaction and corrosion fouling .

Table 1.3 Hydrocarbon Fouling Models

Authors (year)	Application	Deposition term	Removal term	Remarks
Nelson[69] (1934)	Oil refining	Rate is directly dependent upon thickness of thermal boundary layer	None considered	Fouling rate can be reduced by increasing fluid velocity
Atkins[90] (1962)	Fired heaters in oil industry	Constant monthly increase in coke resistance for various refinery steams	None considered	Two layer concept porous coke adjacent to fluid and hard coke adjacent to wall
Nijsing[229] (1964)	Organic coolant in nuclear reactors	Hydrodynamic boundary layer and diffusion partial differential equations	Product diffusion back to the fluid bulk	Solution with diffusion control fits plant data , fouling rate predicted to increase with velocity
Watkinson and Epstein[107] (1969)	Liquid phase fouling from gas oil	Mass transfer and adhesion of suspended particles	First order Kern and Seaton shear removal term	(1) Correct prediction of initial rate dependence on velocity (2) Incorrect prediction of asymptotic resistance on velocity
Fernandez-Baujin and Solomon[124 (1976)	Vapour phase pyrolysis	Kinetics and/or mass transfer control with first order reaction	None considered	Solution with mass transfer control fits plant run-time date
Crittenden and Kolaczko-wski[100,101] (1979)	Hydrocarbons in general	Kinetics and/or mass transfer control with first order reaction	(1) Diffusion of foulant back into fluid bulk (2) First order Kern and Seaton shear removal term	(1) Limited testing (2) Complex - many parameters (3)Extended to two layer concept proposed by Atkins[90] .
Crittenden *et al* (80) (1987)	Dilute solution polymerisation of styrene	Non-zero order kinetics	(1) Diffusion of foulant back into fluid bulk (2) First order Kern and Seaton shear removal term	
Kolaczkowski *et al* (99) (1988)	Crude oils	kinetics control	First order Kern and Seaton shear removal term	Demonstrated interactive nature of fouling in process networks

Table 1.3 continued

Authors (year)	Application	Deposition term	Removal term	Remarks
Yen *et al*[131] (1988)	Fluid catalytic cracking	Coke formation is kinetics control with fourth order reaction	None considered	(1) Complex - many parameters (2) Tested against actual coke data from both pilot and commercial FCCU's (Fluid Catalytic Cracking Units)
Takatsuka *et al*[114] (1989)	Residual oil	Coke formation is kinetics control	None considered	Predicts the effects of major operation conditions i.e. velocity , surface temperature ..etc of cracking furnaces on tubular fouling
Crittenden *et al* (97) (1992)	Crude oils	kinetics control	None considered	Plant data used to obtain coefficients in predictive model ; good fits obtained

Models which are specifically related to crude oil fouling will be discussed in chronological order in the next section.

1.1.2.1 Fouling of crude oil

Crude oil is a combination of hundreds of hydrocarbon compounds , some of which contain sulphur , oxygen , and nitrogen atoms. Salts such as magnesium chloride and metallo - organic compounds containing iron , nickel , vanadium , arsenic, etc., are also found in crude oil[70] .

The specific components of crude oils that contribute to fouling are dissolved gases, salts, inorganic silicates , metal oxides or sulphides

which may combine with organic polymers and gums, oxidation products, resins and asphaltenes[66-68]. The extent however to which each of these and other components (e.g corrosion products) contributes to fouling can not easily be quantified. Moreover, the mechanism by which each of these components affects fouling is not fully known[68] .

Fouling of crude oil has a long history. It has probably existed since the first petroleum refinery was built in 1860[70]. In the early days , when the fouling process was not generally realised, the reduction of heat transfer coefficients often led plant engineers to believe that something must have been wrong with the film coefficients that were published[70] .

The earliest reference to the fouling of crude oils was published by Nelson[69,70]. He provides numerical values for fouling resistance due to various petroleum feedstocks , wax deposits , coke deposits in pipe stills and precipitation fouling on the water side of shell - and - tube heat exchangers. More general fouling resistance values have been tabulated in **TEMA** "Standards of the Tubular Exchanger Manufacturers Association " since the first edition on 1941[71] . The allowance for fouling in design is through the use of individual fouling resistance values, R_{f_i} and R_{f_o} for the two

sides of the heat transfer surface . Thus for the tube of a heat exchanger subject to fouling :

$$\frac{1}{U_o} = \frac{1}{h_o} + R_{f_o} + R_w + R_{f_i}\,\frac{A_o}{A_i} + \frac{1}{h_i}\,\frac{A_o}{A_i} \qquad (1.3)$$

Where :

U_o = overall heat transfer coefficient based on outside surface area ($W\ m^{-2}\ K^{-1}$)

h_o = film coefficient of fluid outside tube ($W\ m^{-2}\ K^{-1}$)

h_i = film coefficient of fluid inside tube ($W\ m^{-2}\ K^{-1}$)

R_{f_o} = fouling resistance on outside of tube ($m^2\ K\ W^{-1}$)

R_{f_i} = fouling resistance on inside of tube ($m^2\ K\ W^{-1}$)

R_w = tube wall resistance based on outside surface ($m^2\ K\ W^{-1}$)

$\frac{A_o}{A_i}$ = ratio of outside to inside surface of tube

The influence of the **TEMA** fouling resistance tables on the design of heat exchangers has been substantial. In the absence of any other systematic source , it is still widely (and often blindly) accepted as the true standard[76]

It is interesting to note that the values of fouling resistance given by **TEMA** are specific minimum values to be used to design a **TEMA** standard heat exchanger which is subject to fouling. The often single values of fouling resistance from the **TEMA** pay only scant regard to the effects that process variables such as temperature, flow rate, or composition can have on the fouling process. It has

been reported on several occasions[72,73] that in oil refineries the **TEMA** design fouling resistances are often exceeded in very short time - scales , as shown in Fig 1.3 . The most recent edition of **TEMA**[74] , which is a revision[75] of the 1978 edition, contains general comments abstracted from the literature regarding fouling types and factors influencing deposition and removal. In the new edition some previous values of fouling resistance have been updated and about 20 values for organic compounds added. Despite such revisions, Taborek[76] has reviewed the new **TEMA** edition and criticised it for not providing a systematic overhaul of the fouling tables .

Fouling in preheat equipment of crude oil distillation units (CDUs) is a serious operating problem which leads to increased energy consumption, increased pressure drops , reduction or complete loss of throughput , and increased maintenance costs[77,78]. The mechanism is complex and involves crystallisation of inorganics , corrosion , chemical reactions of organics and particulate deposition . Asphaltene precipitation, believed to be responsible for the organic content of the deposits , is in itself a complex mechanism[67,78]. Laboratory experimental studies on crude oil fouling are very limited in extent[66,86,67]. Since the available experimental studies have used modified process

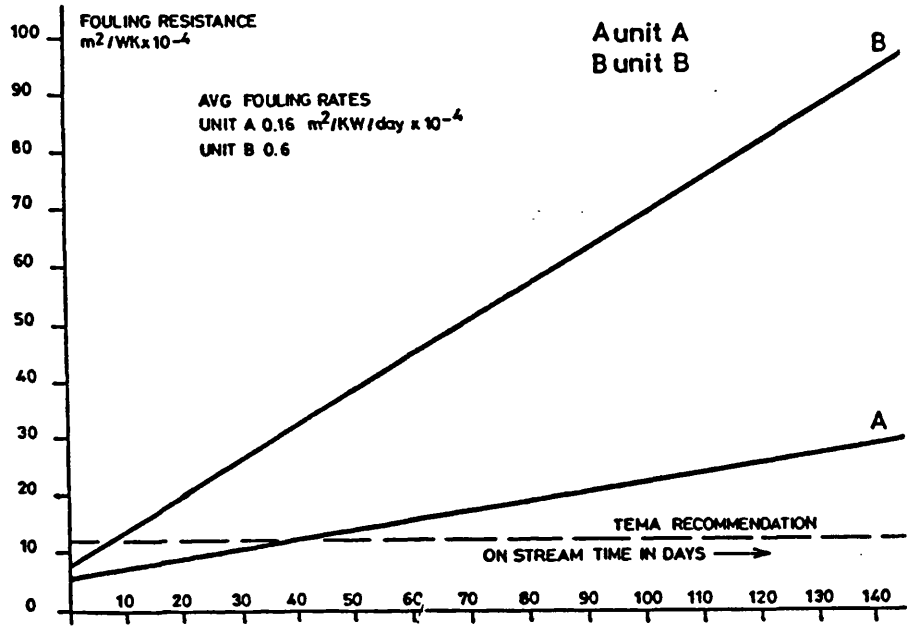

Fig 1.3 Evolution of fouling resistances for crude / residue exchangers
Work of Lambourn and Durrieu[73] on crude oil

parameters to scale - down the actual heat exchanger and to give an accelerated fouling rate, they at best can only give a comparative effectiveness of a particular anti - foulant treatment or sometimes can test the comparative fouling tendency of different refinery feedstocks. None of these studies has used tubular test sections and thus the heat transfer process must be expected to differ from that of industrial heat exchangers. Moreover , the effect of process parameters ,such as velocity , on fouling will not be easy to interpret. Despite these shortcomings , Braun[66] was able to provide useful information about the threshold (break-point) temperature above which fouling occurred and below which none occurred . Eaton and Lux[86] examined the effect of dissolved oxygen on the fouling of crude oil and some other refinery cuts. Dickakian and Seay[67] and also Eaton and Lux[86] demonstrated the effect of asphaltenes . This will be described in section 1.1.3 of this chapter

As laboratory studies are limited , it is not surprising to find that most information on crude oil fouling has come from actual plant data or from industrial plant studies[19,21,39,69,73,77,89,90,92-98]. Plant data often suffers from poor accuracy[83]. Moreover , it is not possible to mount scientific experiments without interfering with the normal business of production . Crittenden *et al*[89] listed the disadvantages of using industrial plant data in

fouling research. The pros and cons of plant and laboratory experiments will be discussed in more detail in section 1.1.4 .

Models related to crude oil fouling , which are listed in Table 1.3 , are those of Nelson(1934)[69], Atkins(1962)[90] , Kolaczkowski *et al*(1988)[99], , and Crittenden *et al*(1992)[97] . Models of Crittenden and Kolaczkowski(1979)[100,101] are considered to be valid for fouling of hydrocarbons in general .

Nelson[69] , provided the first model for crude oil fouling . He assumed that the rate of coke deposition is directly dependent upon the thickness of the thermal boundary layer (the heat transfer film thickness) . The thicker the thermal boundary layer the greater the volume of oil that is exposed to high temperature. For fully developed turbulent flow the thermal boundary layer becomes very thin and thus the deposition rate may be reduced by increasing the fluid velocity. Nelson's model does not include a removal rate term.

Atkins[90] observed that fouling in fired process heater tubes manifests itself in two layers, a porous coke or tarry layer and a hard crust layer. He believed that on exposure to high temperature the hydrocarbon deposits in the tarry layer can undergo further reactions (decomposition) leading to the

formation of the hard coke layer . Gas from this decomposition can add to the bulk of the fouling deposit by inflating small pockets or cells and by opening up pores and crevices during its escape back to the main fluid body . Atkins presumed that the overall resistance to the temperature gradient is a combination of four resistances, as shown in Fig 1.4 :

$$R_o = \frac{1}{h_i} + R_w + R_{f(hard)} + R_{f(tarry)} \qquad (1.4)$$

Where :

R_o	= overall resistance	(m^2 K W^{-1})
h_i	= film coefficient	(W m^{-2} K)
R_w	= tube wall resistance	(m^2 K W^{-1})
$R_{f(hard)}$	= thermal resistance due to hard coke deposit layer	(m^2 K W^{-1})
$R_{f(tarry)}$	= thermal resistance due to tarry deposit layer	(m^2 K W^{-1})

Although Atkins[90] did not consider any removal mechanism , the passage of gas bubbles from the hard deposit layer to the bulk of the fluid *via* the tarry layer could possibly enhance the film coefficient through a nucleate boiling mechanism. It could be postulated that if bubble nucleation became very rapid, then the subsequential enhancement in film coefficient could be sufficient to counteract the insulating effect of the deposits themselves .

Crittenden and Kolaczkowski[100,101] developed two semi-empirical models to account for chemical reaction fouling in hydrocarbons. The first model

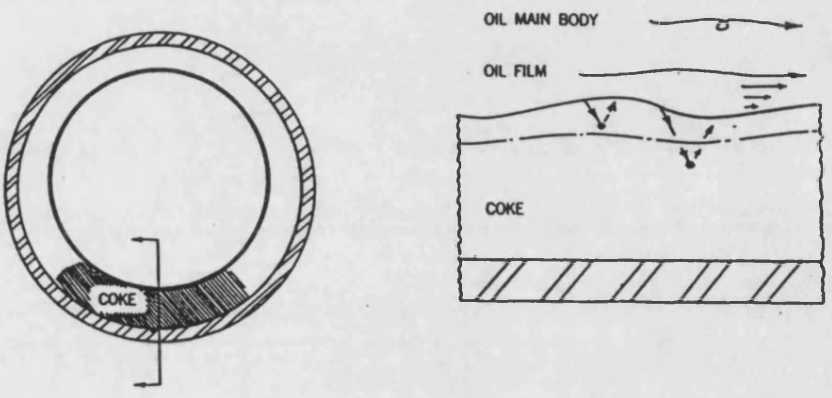

Fig 1.4 Atkins's two layers fouling resistance model[90]

was based on the Kern and Seaton[85] model and developed for a single layer of foulant deposited on a heat exchanger tube. The following was proposed[100]:

$$\dot{R}_{f(\theta)} = \phi_d - \phi_r \qquad (1.5)$$

Where :

$\dot{R}_{f(\theta)}$ = the net rate of deposition .
ϕ_d = deposition rate .
ϕ_r = removal rate .

The deposition of foulant material , D , was assumed to be caused by transport of the foulant precursors , P , present in the fluid , normal to the tube surface where they then decomposed or polymerised close to or at the heating surface . The deposition rate was assumed to occur under constant heat flux, constant mass flow rate and constant precursor bulk concentration. The foulant material is formed by the irreversible reaction as follows :

$$P \longrightarrow D + \text{light products} \qquad (1.6)$$

The removal rate was assumed to depend on fluid shear (τ) and foulant thickness (x_d).

The second Crittenden-Kolaczkowski model[101] is a modification of the first model by taking into account the two layer deposition mechanism proposed by Atkins[90] :

$$\dot{R}_{f(\theta)} = \phi_{Td} - \phi_{Tr} - \phi_{CT} - \phi_{Fr} \qquad (1.7)$$

Where :

ϕ_{Td} = deposition rate of tarry layer ;

ϕ_{Tr} = removal rate of tars by mass transfer to fluid bulk ;

ϕ_{CT} = removal rate by conversion of tarry layer to coke ;

ϕ_{Fr} = removal rate by fluid shear .

The foulant (coke) was assumed to form *via* two consecutive reactions as follows :

$$\text{Precursors (in fluid bulk)} \longrightarrow \text{Tarry foulant} + \text{Products} \longrightarrow \text{Coke} + \text{Products} \qquad (1.8)$$

Crittenden - Kolaczkowski models[100,101] contain all the parameters which are likely to contribute to chemical reaction fouling , including mass flow rate, temperature, concentration of precursor, physical properties, etc. Consequently, complex mathematical expressions were obtained even making several assumptions and approximations, e.g. physical properties independent of temperature . To date , the Crittenden-Kolaczkowski models have been little tested. They have been incorporated in a simulation package[99] known as **MINERVA** designed to provide amongst other things the following :

1- the simulation of an existing net work of preheat exchangers in a crude distillation unit (CDU) ;

2- the selection of alternative exchangers ;

3- the effect of operating conditions ;

4- the evaluation of the cost effectiveness of anti - foulants

The **MINERVA** program is considered to complement, not replace , the existing range of heat transfer software through it's ability to predict the dynamic behaviour not only of individual exchangers but also of existing and re-vamped series networks[64]. Kolaczkowski *et al*[99] claimed that by using the **MINERVA** program , the **TEMA** standards do not necessarily have to be used at the design stage. Instead , any selected design resistance(s) can be incorporated into a fouling model and the simulation run to establish the optimum operating strategy. This package however has not been practically tested yet[64] .

Very recently Crittenden *et al*[97] have developed a simple model based on plant data from a major European refinery. A simple correlation has been established between the fouling rate and the tube wall temperature of individual heat exchangers in the crude distillation unit (CDU) preheat train as follows :

$$R_f = C_i + \int [A \exp(-E / R T_w)]\, dt \qquad (1.9)$$

Where ;

R_f = fouling resistance (m^2 K kW^{-1})

C_i = parameter to allow for the idiosyncrasies of individual heat transfer units (m^2 K kW^{-1})

A = frequency factor (m^2 K kW^{-1})

R = universal gas constant (kJ mol^{-1} K^{-1})

E = activation energy (kJ mol^{-1})

T_w = the mean tube wall temperature over the extended period of measurement (K)

Values of activation energy , E , can indicate whether the fouling mechanism is dominated by chemical reaction or by physical mechanisms. For example, a value in excess of 40 kJ mol^{-1} generally indicates that the mechanism of fouling is predominantly chemical reaction in nature , whilst a value below 40 kJ mol^{-1} indicates that physical mechanisms , perhaps crystallisation or particulate deposition , are important as well .

Values of activation energy , E , obtained from various laboratory and industrial studies are shown in Table 1.4 .

Table 1.4 Activation energies for chemical reaction fouling

Fluid	Activation energy kJ mol^{-1}	Surface temperature range , ° C	Reference
Gas oil	120	146 - 204	Watkinson and Epstein(107)
Crude oil	53	365 - 447	Scarborough *et al*(122)
Jet fuels	42	150 - 260	Taylor(118)
Kerosene	70	160 - 380	Crittenden and Khater(87)
Crude oil	36	287	Eaton and Lux(86)
Styrene polymerisation	39	22 - 98	Crittenden *et al*(80)
Liquid jet fuels	42	149 - 260	Vranos *et al*(109)
Light crude oil	33	160 - 280	Crittenden *et al*(97)
Heavy crude oil	21	160 - 280	Crittenden *et al*(97)

Crittenden *et al*[97] found that for light crude oils , i.e those with a specific gravity of less than 0.87 (>31 ^{o}API) , the activation energy for the fouling process was about **33 kJ mol^{-1}** , which lies in the region for a mixture of chemical and physical mechanisms . For heavier crude oils (<31 ^{o}API) , the activation energy was found to be much lower , around **21 kJ mol^{-1}**, which indicates not only a higher fouling rate for a given temperature, but also the predominance of a physical mechanism such as asphaltene precipitation.

The simple Crittenden *et al*[97] model was used to predict the fouling behaviour after the refinery CDU had been shut down for a thorough clean. Fig 1.5 shows how well the model was able to predict the performance of an example exchanger.

Lambourn and Durrieu[73] used another computer program (**HTRI's ST-4**) in their research on fouling of CDU preheat exchangers on the **TOTAL-C.F.R** refinery . This program was used to check the efficiency of a cleaning technique . Data input was simplified by using **HTRI's ST-4** program to generate simple power type relationships based on flow rates and physical properties such as viscosity. These are then placed in the on - line computer for daily use by operating personnel. Lambourn and Durrieu[73], however, did not mention the source or the fundamental basis of **HTRI's ST- 4** program.

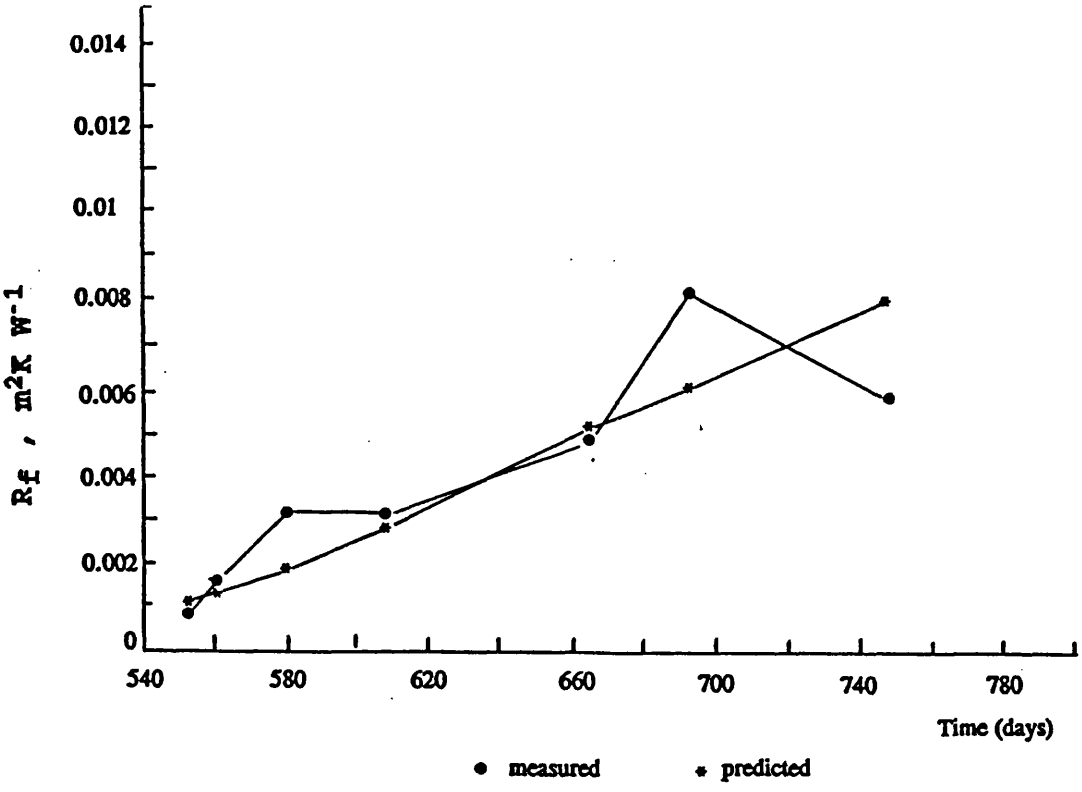

Fig 1.5 Comparison between experimental and predicted fouling resistance Work of Crittenden *et al*[97] on crude oil

1.1.3 Conditions influencing fouling of hydrocarbons

Conditions that influence fouling can be classified as , time , operating parameters , fluid properties , and heat exchanger design parameters[39], Those parameters which are affecting and affected by hydrocarbon deposition are summarised[64] in Fig 1.6.

1.1.3.1 Time

Fig 1.7 shows several possible effects of time on fouling resistance. For hydrocarbon fouling the dependency has been found to be linear[73,87,88,90,93,106-109] , falling rate[93,110], asymptotic[86,107] , falling rate + linear[106,111,112] or even of a saw-tooth shape[97] . In general , it is not possible to determine whether or not an initial linear behaviour would eventually yield either a falling rate or an asymptotic behaviour , given a sufficiently long period of operation[60,61,65]. Possible induction periods and even negative values of fouling resistance during the initial stages of the fouling process are reported in many studies[87,88,103,104,106]. Negative fouling resistances have been suggested to be caused by small amounts of deposit creating a rough surface in the early stages of fouling and thereby increasing the film heat transfer coefficient to an extent sufficient to counteract the additional thermal resistance due to the deposit itself[61,88,105]. Moreover, if the

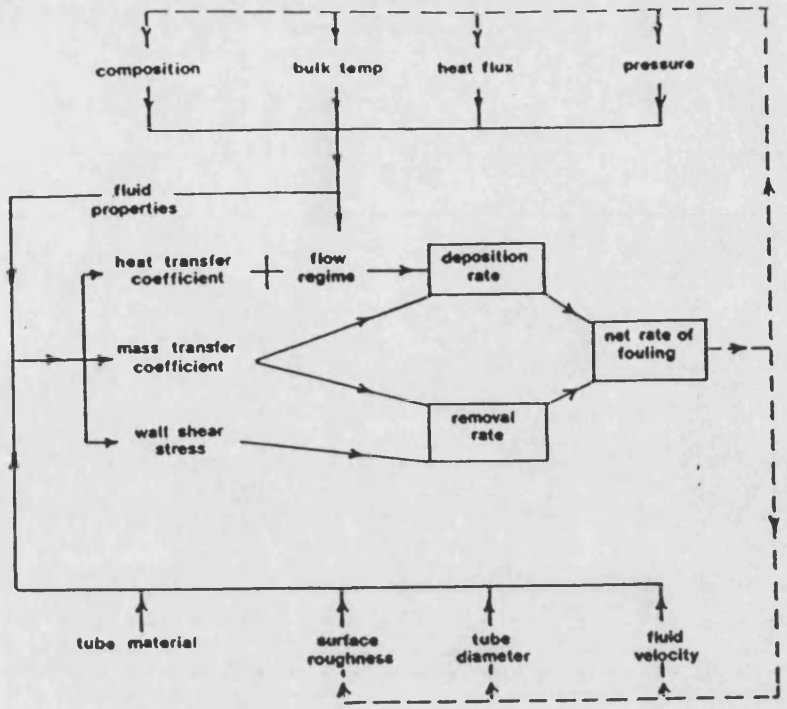

Fig 1.6 Parameters affecting and affected by deposition(64)

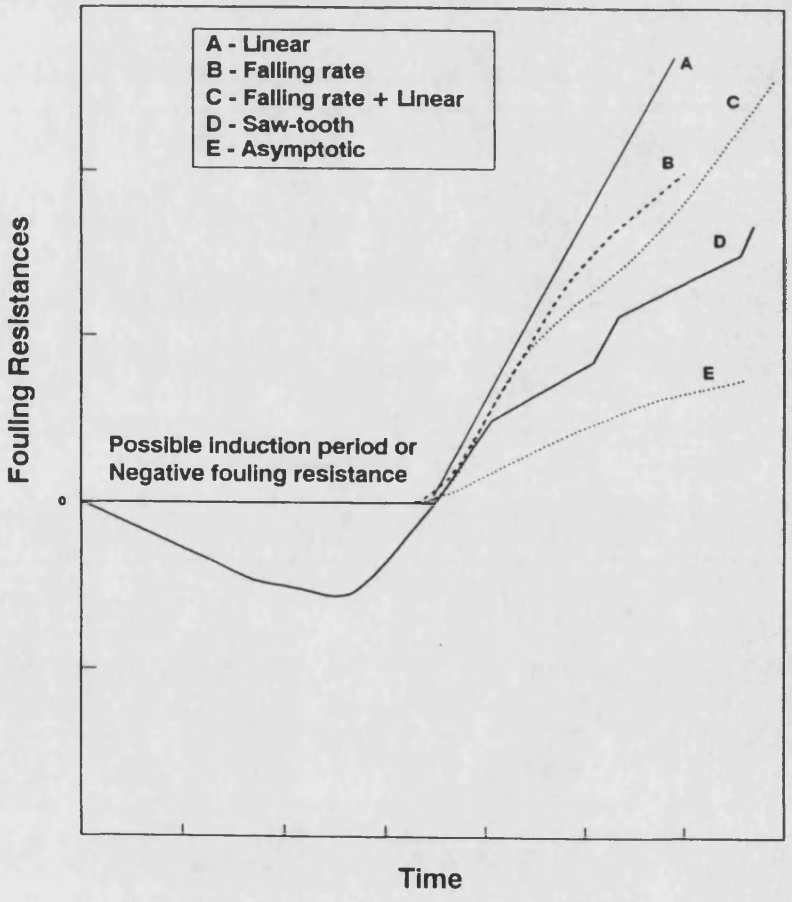

Fig 1.7 The effect of time (t) on the fouling resistances (R_f)

increase in the film heat transfer coefficient is just balanced by the deposit thermal resistance, then one can expect that the net result of equation 1.10 will be to yield a zero fouling resistance ;

$$R_f = \frac{1}{U_f} - \frac{1}{U_c} \qquad (1.10)$$

where :

R_f = fouling resistance (m^2 $K.W^{-1}$)

U_f = fouling overall heat transfer coefficient ($W\ m^{-2}\ K^{-1}$)

U_c = clean overall heat transfer coefficient ($W\ m^{-2}\ K^{-1}$)

This could be one explanation for the presence of an induction period .

1.1.3.2 Operating parameters

Many operating parameters can affect hydrocarbon fouling namely, temperature, velocity, heat flux and pressure , see Fig 1.6. The importance of each of these parameters depends on the nature of the heat transfer process .

1 - Temperature

The dependence of fouling rate on the temperature is complex[65,114]. Many studies have shown that the rate of chemical reaction fouling increases exponentially with absolute surface temperature[66,81,90,97,107]. Arrhenius-type equations have often been used to fit the experimental data as follows :

$$\frac{dR_f}{d_t} \alpha \exp(-E/RT_w) \qquad (1.11)$$

Therefore , a plot of the logarithm of the fouling rate $(\frac{dR_f}{d_t})$ as a function of reciprocal absolute surface temperature $(\frac{1}{T_W})$ will provide the value of activation energy, E , from the slope as shown in Fig 1.8. Use of this expression implies that there is a constant concentration and order of reaction. Some workers however have found complex plots of the shape shown in Fig 1.9 . At a certain temperature , $\overset{*}{T}$, the fouling rate appears to decrease with temperature[87,88,118] and at higher temperature to increase again[47]. Such results are almost certainly indicative of a change in the predominant fouling mechanism[87,88,118], and/or perhaps due to a change from liquid to vapour phase[65] .

Braun[66] obtained another type of relationship between fouling rate and surface temperature. He found that maximum fouling rates for hydrodesulphurizer samples occurred at intermediate temperatures, and that the maximum rate was dependent on the sample , as shown in Fig 1.10. Braun[66] claimed that his results were in concurrence with Watt's results[116] for fouling of jet fuels . However no explanation was given by Braun for why a maximum in the fouling rate temperature graph should have occurred.

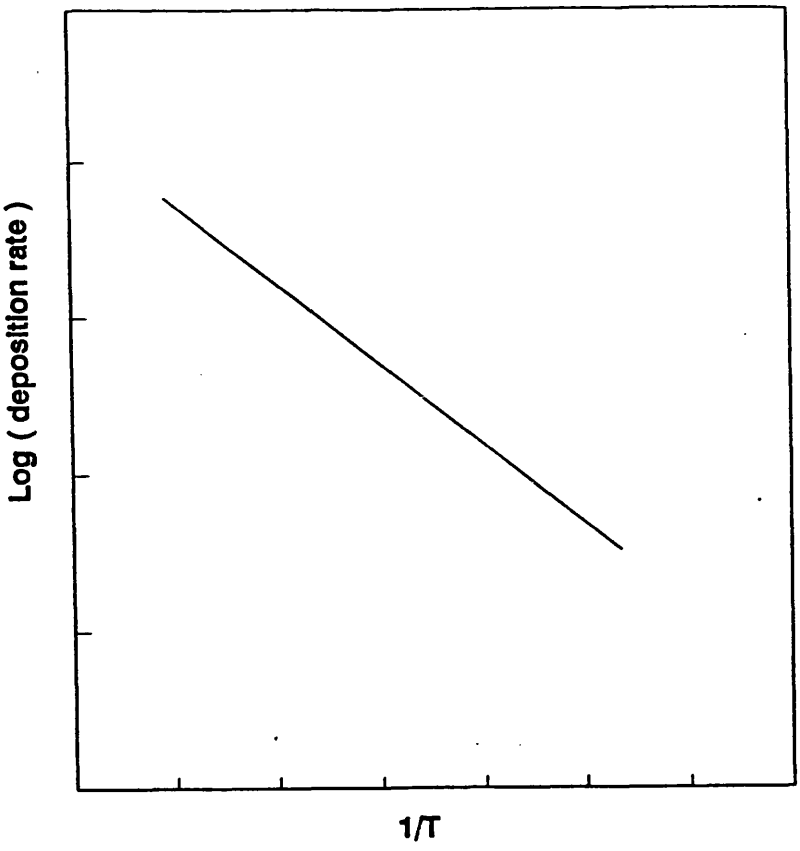

Fig 1.8 Arrhenius plot for determination of the activation energy (E)

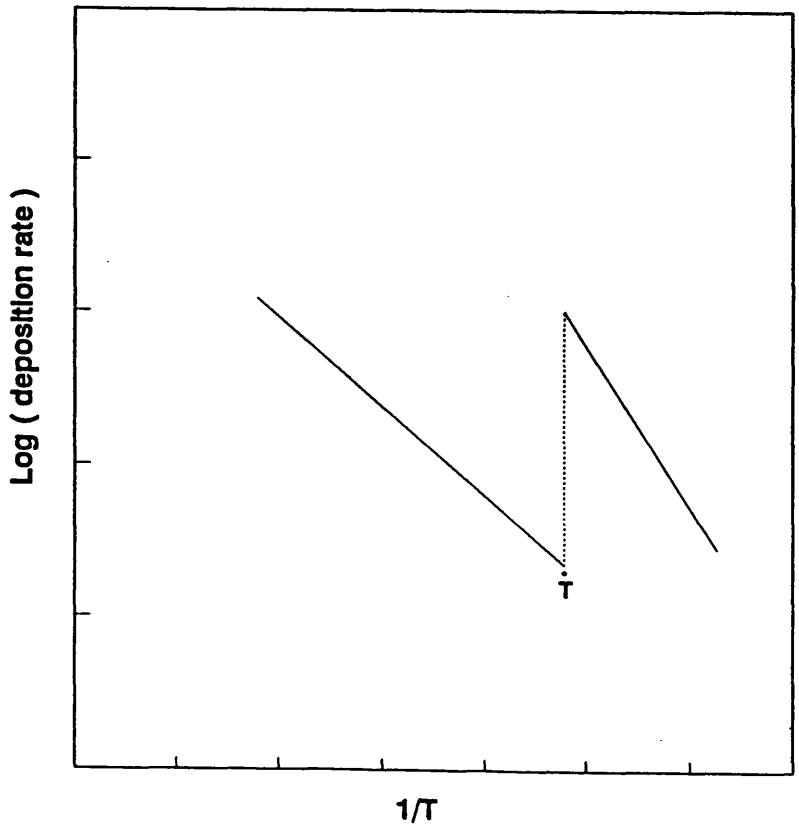

Fig 1.9 Arrhenius plot showing change of mechanism[87,88,118]

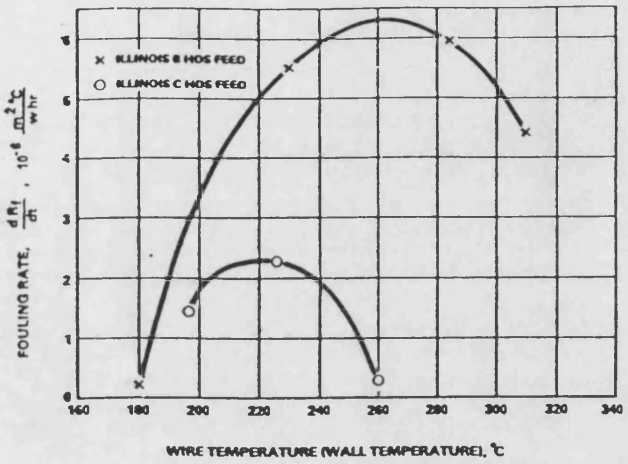

Fig 1.10 Effect of surface temperatures on fouling rate (Braun[66])

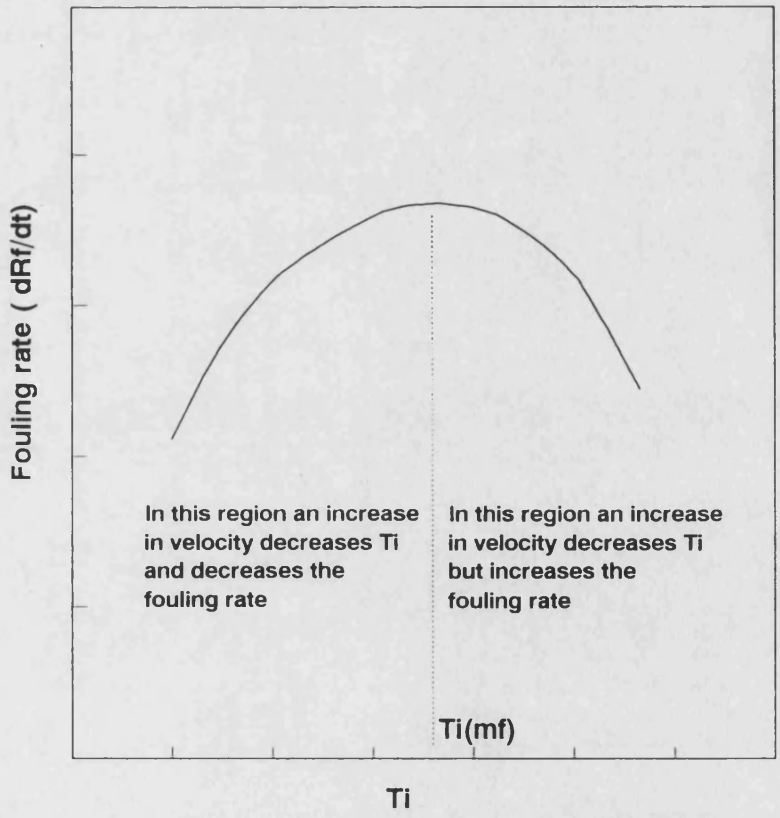

Fig 1.11 Effect of surface temperature and velocity on the fouling rate

Several studies[66,115,117] have reported a threshold (break point) surface temperature above which fouling occurred and below which none occurred. The threshold temperature seems to depend on the hydrocarbon under study. Hausler and Thalmayer[117] provide the following expression which is not of an Arrhenius type but does imply the presence of a threshold temperature ;

$$\left(\frac{dR_f}{dt}\right)_{t=0} = 3.7 \times 10^{-7} \exp\left[\left(T_s\,(^{\circ}F) - 100\right) / 100\right] \qquad (1.12)$$

Where ,

$\left(\frac{dR_f}{dt}\right)_{t=0}$ = the initial fouling rate ($^{\circ}F\ ft^2\ Btu^{-1}$)

T_s = surface temperature ($^{\circ}F$)

The bulk fluid temperature has received only a little attention in hydrocarbon fouling studies. Eaton and Lux[86] found that an increase in bulk temperature caused a decrease in fouling rate for the same initial surface temperature . However, this result could be the effect of temperature difference, ΔT_i , between the bulk fluid and the surface , which has been found to be important[119] in the deposition of wax from hydrocarbon solutions. It is well established[104,40] that the temperature difference can play a major role in the precipitation of inverse solubility salts such as $CaCO_3$, $CaSO_4$ .etc. Hydrocarbons such as asphaltenes in crude oil may show inverse solubility with temperature , as will be discussed in

section 1.1.3.3. The effect of ΔT_i on the fouling of hydrocarbons in a heating process has never been investigated before .

2 -Velocity

It is a generally accepted rule in the oil and chemical industries that the problem of hydrocarbon fouling can be alleviated to some extent by the use of higher velocities[65]. There is conflicting evidence , however , in a number of hydrocarbon studies . An increase in velocity can decrease fouling[70,74,94,107,122], increase it[108,109,123,124] have a complex effect[81,111], or have no effect[120,112], as summarised in Table 1.5 . If the fouling deposition process is controlled solely by a chemical reaction which is not influenced by mass transfer , then the fouling rate should be independent of velocity[82]. There is some belief[70] that crude oil fouling can be alleviated by increasing the velocity .

Changes in velocity of a fluid stream can affect deposition rates in four important ways ;

I- As velocity increases , the viscous sub - layer close to the wall becomes thinner thereby reducing the resistance to diffusion and transfer generally from the bulk towards the wall[40]

II- As velocity increases, the shear force at the wall is increased, thus the removal rate can increase to a greater extent so

that the overall rate of fouling and the eventual steady state deposition thickness are decreased ;

III- Velocity affects the surface temperature which is extremely important for chemical reaction fouling ; and

IV- As velocity increases the residence time of fouling precursors near the surface can be reduced[40] .

Table 1.5 Effect of velocity on deposition rate in hydrocarbon fouling

Authors (year)	System studied	Dependence of deposition rate on increasing velocity	Tube diameter (m)	Temperature range (°C)	Velocity or flow rate	Remarks
Nelson[70] (1958)	Oil refining	decreases	not specified	$T_b > 260$	$0.3 < m\ s^{-1} < 2.1$	Industrial plant data
Chantry and Church[94] (1958)	Forced circulation reboilers	decreases	not specified	not specified	$3 < m\ s^{-1} < 10$	
Watkinson and Epstein[107] (1969)	Liquid sour gas oils	decreases	0.0087	146 - 204	$9800 < Re < 10^4$	
Smith[108] (1969)	Liquid aviation kerosene	increases	0.0021 to 0.0028	160-260	$4500 < Re < 10^4$	ASTM fuel coker
Chen and Maddock[123] (1973)	Cracking furnace for ethylene	increases	0.05 to 0.2	900 - 1000	not specified	Kinetics may control at lower temperature
Fernandez-Baujin and Solomon[124] (1976)	Vapour phase pyrolysis of naphtha and light gas oil	increases	not specified	high	not specified	Comparison of model with plant data
Shah *et al*[111] (1976)	Vapour phase thermal cracking of n-Octane	Complex increases or decreases	0.0046 to 0.0064	750 - 800	0.1 < space time (sec) < 15	Maximum in rate-flow rate relationship
Vranos *et al*[109] (1981)	Liquid jet fuels	increases	0.0018 to 0.0048	149 - 260	$600 < Re < 10^4$	Rate α $Re^{0.6}$
Crittenden *et al*[81] (1987)	polymeri-sation of styrene	Complex increases or decreases	0.002	22 - 249	$1000 < Re < 5200$	Maximum in rate-flow rate relationship

For a constant heat flux process , the inner tube surface temperature, T_i , may be determined as follows:

$$T_i = T_b + \frac{q}{h_i} \qquad (1.13)$$

Where :

T_b = bulk fluid temperature (K)

q = heat flux ($W\ m^{-2}$)

h_i = film heat transfer coefficient ($W\ m^{-2}\ K^{-1}$)

From the Dittus - Boelter[12] correlation the relationship between, h_i , and the fluid velocity, v, is expressed to a first order approximation as follows ;

$$h_i \ \alpha \ v^{0.8} \qquad (1.14)$$

Thus an increase in velocity , v , will increase the film coefficient and the inner surface temperature , T_i , will decrease . However according to Braun's results[66] shown in Fig 1.10 , a decrease in T_i may decrease or increase the fouling rate according to whether the inner surface temperature is less or more than $T_{i(mf)}$, the temperature at which the fouling rate is maximum . These conflicting effects are illustrated in Fig 1.11. It is clear that the complex effect of velocity needs further investigation.

3 -Heat flux

Increases in heat flux , according to equation 1.13 , can increase the inner tube surface temperature if both bulk fluid temperature and fluid

velocity are maintained constant . Heat flux can also control the fluid phase behaviour , e g. at a certain heat flux , nucleate boiling can start and the film heat transfer coefficient can rapidly increase with an increase in heat flux[147]. Consequently , if equation 1.10 is used in fouling resistance calculations , it is very important that h_i is calculated properly, otherwise very small or even negative values of R_f may be determined. The effect of heat flux on phase change will be discussed in Chapter 4 , section 4.6.2.3

Hydrocarbon fouling studies involving phase change are very rare[43,47] . The work of Crittenden and Khater[88] on fouling from vaporising kerosene appears to be unique in this field . If heat fluxes rather than surface temperatures , however , were used for interpreting the experimental data , then a plot with less intricacy than that shown in Fig 1.12, might be expected .

4 -Pressure

Clearly an increase of pressure can also affect the phase behaviour of the fluid , e g . it can increase the initial boiling point or the onset of nucleate boiling of the fluid. Crittenden and Khater[87,88] found that the fouling rate of vaporising kerosene was generally increased with pressure in the range of 1 to 2.5 bar . This was possibly due to the suppression of nucleate boiling with increasing pressure, however the effect of

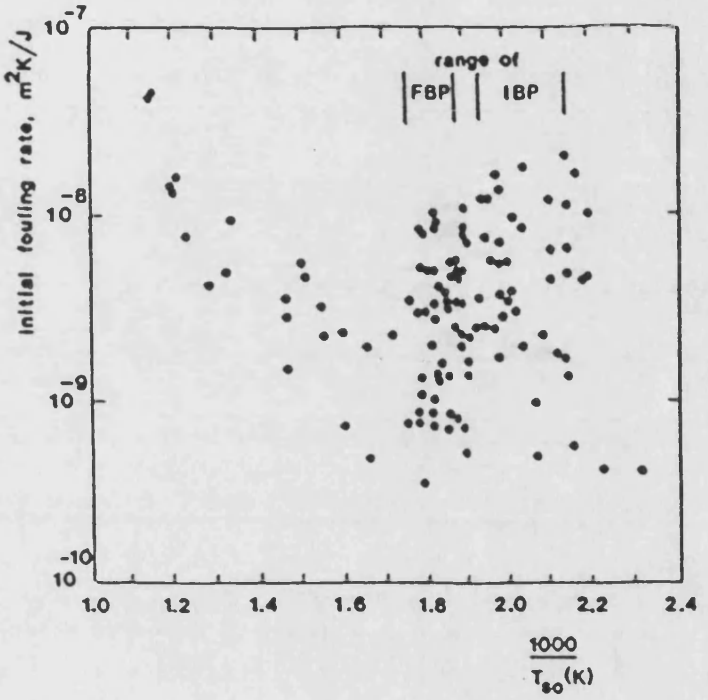

Fig 1.12 Complex relationship between T_S and initial fouling rate
Work of Crittenden and Khater[88] on vaporising kerosene

dissolved oxygen was also believed to be a key factor. Nucleate boiling can on the other hand provide a substantial reduction in fouling rate as found by Palen and Westwater[135] in their study on fouling rates during pool boiling of calcium sulphate solutions . This effect has been confirmed by Muller-Steinhagen *et al*[136] working on fouling of alumina particles suspended in heptane during boiling and non - boiling conditions . The effect of nucleate boiling on chemical reaction fouling of hydrocarbon fluids has never been investigated before .

1.1.3.3 Fluid properties

Both the basic composition of the fluid and the nature of the species dissolved or entrained in it can have a significant impact on fouling[39].

1- Feedstock composition

The open literature shows that an increase in composition of some species such as sulphur compounds, nitrogen compounds , dissolved oxygen and oxygenated species , dissolved metallic ions, etc., can increase the fouling rate from hydrocarbons. The presence of asphaltenes and resins has been reported[67,73,86] to be the major factor in precipitation fouling in crude oils .

a - The role of asphaltenes and resins in fouling of crude oil

Asphaltenes comprise a fraction of crude oil which is insoluble in non-polar solvents such as

pentane or hexane , but can be soluble in solvents of high surface tension such as pyridine , carbon disulphide , carbon tetrachloride , benzene , toluene or xylene[86,137]. Asphaltenes have a wide range of molecular weights[67,86], typically 530-5270 kg $kmol^{-1}$ and contain 79-85% C , 7.4-8% H , 1.5-4% O and 7.5-8% S[137,86]. The percentage of asphaltenes in crude oils varies from less than 1% for light crude oils (^{o}API > 40) to about 9% for heavier crude oils (^{o}API < 22) . Resins are soluble in the liquids which precipitate asphaltenes. They are very adhesive materials of molecular weight around 800 (kg $kmol^{-1}$) containing 82-88% C and 9.5-11.5% H. They are less aromatic than asphaltenes and much smaller molecules[137] .

It has been suggested[82] that asphaltenes are polymeric homologs of condensed aromatics found in the resins and indeed that reactions such as 1.15 can produce the asphaltenes ;

$$\text{Oils} \xrightarrow[\text{Condensation}]{\text{Oxidative}} \text{Resins} \xrightarrow[\text{Condensation}]{\text{Oxidative}} \text{Asphaltenes} \qquad (1.15)$$

Eaton and Lux[86] proposed the following reaction for fouling by deposition of asphaltenes ,

$$\text{S.H} \xrightarrow[\text{Acids}]{\text{Inorganic}} \text{Un.S.H} \xrightarrow[\text{Heat}]{O_2} \text{O.A} \xrightarrow[\text{Heat}]{\text{Wall}} \text{R+A} \xrightarrow[\text{Heat}]{\text{Wall}} \text{D} \qquad (1.16)$$

Where :

S.H = Saturated hydrocarbons .
Un.S.H = Unsaturated hydrocarbons .
O.A = Organic acids .
R + A = Resins and asphaltenes .
D = Coke - like deposit .

Eaton and Lux[86] found that the presence of 5% asphaltic pitch (containing 16% asphaltenes) in a paraffin oil caused a large increase in thermal fouling compared to the base case of the same oil containing 10% resins. They believed that resins will cause significant fouling only after degradation to asphaltenes.

Dickakian and Seay[67] used a pilot scale test unit called the Thermal Fouling Tester (TFT), originally invented by Dickakian[138] , for studying the effect of asphaltenes on the fouling of hundreds of crude oil feedstocks. They reported that asphaltene precipitation and subsequent carbonisation is the major mechanism of crude oil heat exchanger fouling although other mechanisms may contribute . The mere presence of asphaltenes does not necessarily mean a crude oil will foul, however, as the asphaltenes may remain in solution. Analysis of deposits indicated that when asphaltenes were precipitated and adhered to the metal surface then they could be carbonized into infusible coke. Dickakian and Seay[67] proposed the following mechanism :

- incompatibility between asphaltenes and the oil initiates precipitation of some asphaltenes ;
- precipitated asphaltenes adhere to the hot metal surface ;
- asphaltenes carbonize to infusible coke .

The Dickakian and Seay[67] mechanism seems to be in good agreement with Atkins's model[90] in which asphaltenes could provide the tarry layer which then undergoes degradation to the hard coke layer. This two stage mechanism is also suitable for inclusion in Crittenden and Kolaczkowski's second model[101] for hydrocarbon fouling .

The solubility of asphaltenes has been related to fouling rates in several studies[67,73,86]. Lambourn and Durrieu[73] found complex solubility relationships with temperature for asphaltenes as shown in Fig 1.13. For some crude oils such as **"Safaniya"**, they[73] found that the solubility of asphaltenes can behave normally, i.e the solubility increases with increasing temperature, up to a certain temperature (around 130 °C) then start to show inverse solubility behaviour, i.e the solubility decreases with increasing the temperature. Thus a precipitation fouling mechanism, similar to that suggested by Ritter[104] for precipitation of inverse solubility salts , could be

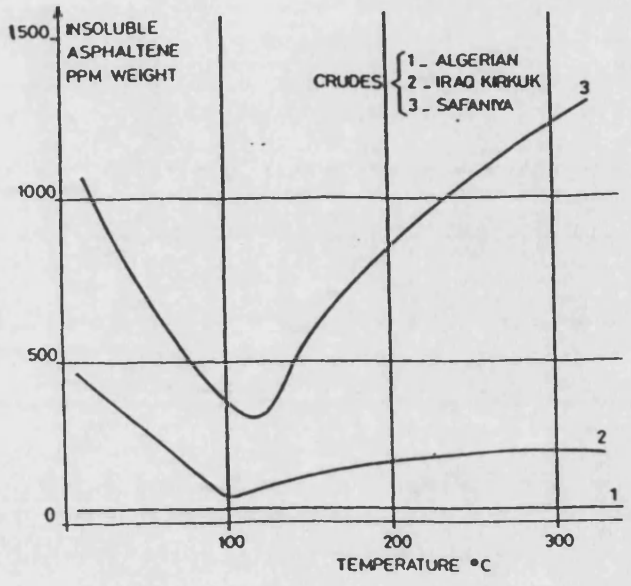

Fig 1.13 Thermal evolution of insoluble asphaltenes in crude oil
Work of Lambourn and Durrieu[73] on crude oil

expected if such crude oils were exposed to temperatures typically higher than 130 °c .

b - The role of dissolved oxygen and oxygenated species

The importance of dissolved oxygen is well established for low temperature storage instability and for higher temperature fouling. Many workers[66,86,88,93,113,118,139,140] have commented on the key role of oxygen in hydrocarbon fouling and have suggested that removal of oxygen will reduce or at least control fouling . Removal of oxygen by employing nitrogen blanketed storage or by introducing an oxygen stripper has led to successful control of crude oil fouling[66,139] .

It is generally accepted that deposition at low temperature , particularly for hydrocarbons in the liquid phase , is due to free-radical autoxidation reactions to form polymer precursors followed by their polymerisation to insoluble gums or sludges[64,82]. These reactions are initiated by hydrogen abstraction from the substrate molecule R - H by a free-radical $\dot{X}$ as follows ;

Initiation

$$R - H + \dot{X} \longrightarrow \dot{R} + XH \qquad (1.17)$$

Propagation

$$\dot{R} + O_2 \longrightarrow R\dot{O}O \qquad (1.18)$$

$$R\dot{O}O + R - H \longrightarrow ROOH + \dot{R} \qquad (1.19)$$

Possible termination steps are :

$$\dot{R} + \dot{R} \longrightarrow R - H \qquad (1.20)$$

$$\dot{R} + R\dot{O}O \longrightarrow ROOR \qquad (1.21)$$

$$R\dot{O}O + R\dot{O}O \longrightarrow ROOR + O_2 \qquad (1.22)$$

Here $\dot{R}$ represents an organic radical , ROOH is a hydroperoxide and ROOR is a dialkyl or diaryl peroxide. It is obvious from reaction 1.18 that the presence of O_2 is very important for the propagation reaction .

Oxygenated species such as peroxides, carboxylic acids , phenols, furans , alcohols, ketones and esters , have been found to increase deposit formation[82]. Taylor and Frankenfeld[140] showed that under de-oxygenated, high temperature (371 - 538 ^{o}C) and high pressure (69 atm) conditions, the addition of some oxygenated species at 100 ppm to jet - fuels caused significant increases in the mass of deposits formed on a tube wall .

2 - Particulates

Particulates such as salts , corrosion products or even precipitated asphaltenes can play a major role in hydrocarbon fouling. Lambourn and Durrieu[73] noted that colloidal particles containing asphaltenes, iron oxide/sulphide species and water were formed in crude oil heating and then deposited

on the tube wall. The exact role of particulates in chemical reaction fouling has not been elucidated[82], They can, however, initiate polymerisation reactions[40].

1.1.3.4 Heat transfer surface parameters

Heat transfer surfaces on which the fouling occurs have a significant effect on all types of fouling[39,40]. Bott[40] identifies two effects of heat transfer surface on the fouling problem : (a) "*that the surfaces in contact with process streams become corroded to a greater or lesser extent depending upon conditions , thus a less corrosive material must be used , and ;* (b) *whether the surface itself is smooth or rough. It is generally appreciated that very smooth surfaces are less likely to receive and retain a dirt layer than are rougher surfaces*"[40]

The type of heat exchanger can also determine the extent of fouling. Shell - and - tube exchangers are more prone to fouling than plate - and - frame or spiral heat exchangers .

1.1.4 Equipment and methods used for fouling studies

Methods used for fouling studies fall into two categories[141] , namely those which interpret industrial plant data and those which use specially designed laboratory-scale equipment to simulate actual plant equipment . Fig 1.14 summarizes these

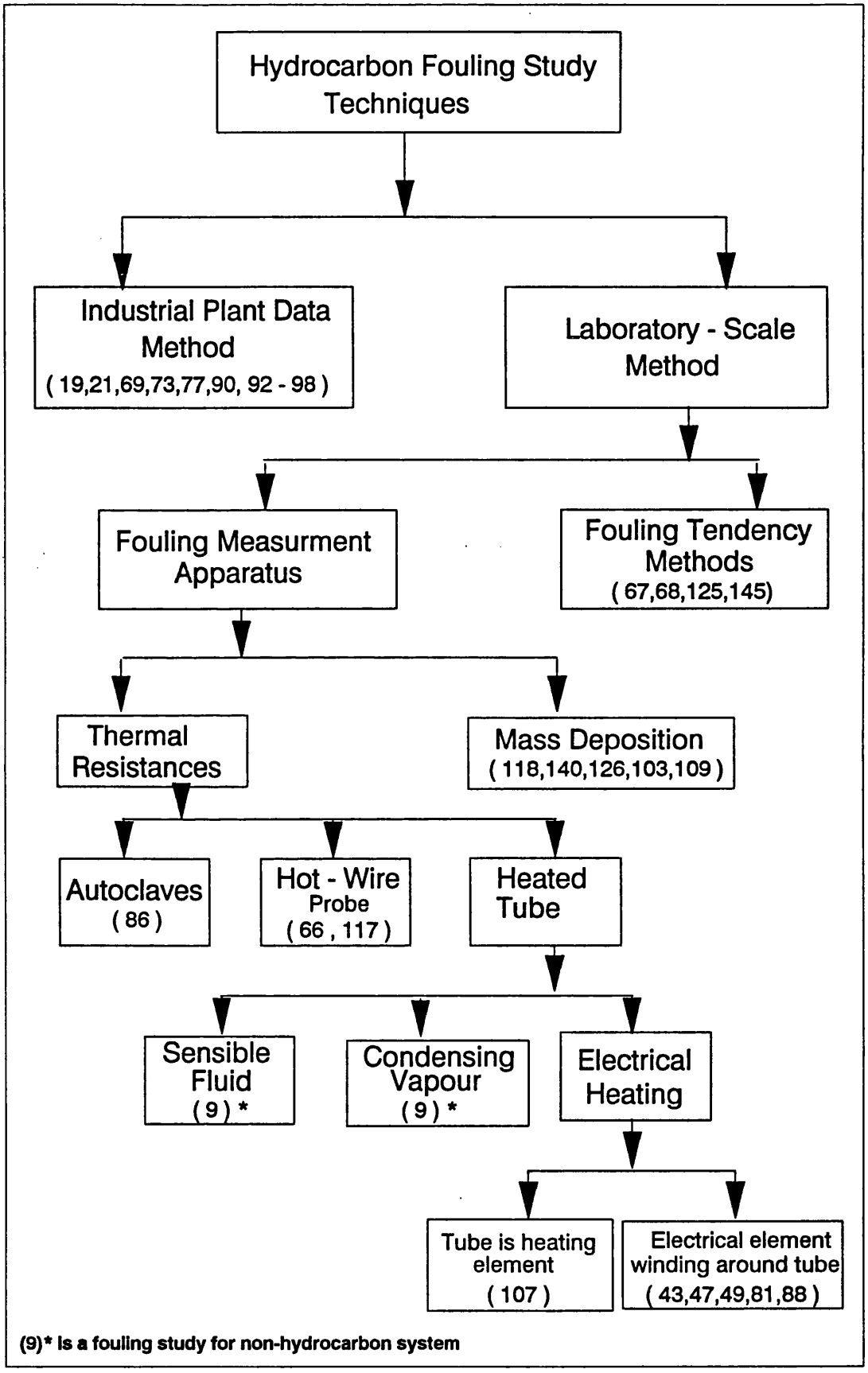

Fig 1.14 Schematic diagram of methods used for hydrocarbon fouling studies

methods and how they been used for hydrocarbon fouling studies .

1.1.4.1 Industrial plant data method

Actual plant data may be used as a source of information to derive the thermal fouling resistance R_f. This method can however suffer from poor accuracy[83]. Crittenden *et al*[89] found that a small error in temperature readings and an inaccuracy in flow rate measurement could yield, in some cases, as high as 100% error in the overall heat transfer coefficient calculated by equation 1.23 below, which, consequently , would affect the accuracy of R_f calculated from equation 1.10 .

$$U_f = \frac{Q}{F\, A_o\, LMTD} \qquad (1.23)$$

Where :

U_f = actual overall heat transfer coefficient (fouled) at any time ($W\ m^{-2}\ K^{-1}$)

A_o = heat transfer surface area based on the outside diameter of the tubes (m^2)

Q = heat duty (W)

$$Q = m\, c_p\, (T_{c\,(out)} - T_{c\,(in)}) \qquad (1.24)$$

Where :

m = mass flow rate of the cold fluid ($kg\ s^{-1}$)

c_p = cold fluid heat capacity ($kJ\ kg\ K^{-1}$)

F = Correction factor for multipass shell and tube heat exchanger

$LMTD$ = log mean temperature difference (K)

$$LMTD = \frac{\Delta T_2 - \Delta T_1}{\ln(\frac{\Delta T_2}{\Delta T_1})} \qquad (1.25)$$

ΔT_1 and ΔT_2 are explained schematically by the following diagram for a two tube pass single shell pass counter - current shell - and - tube heat exchanger.

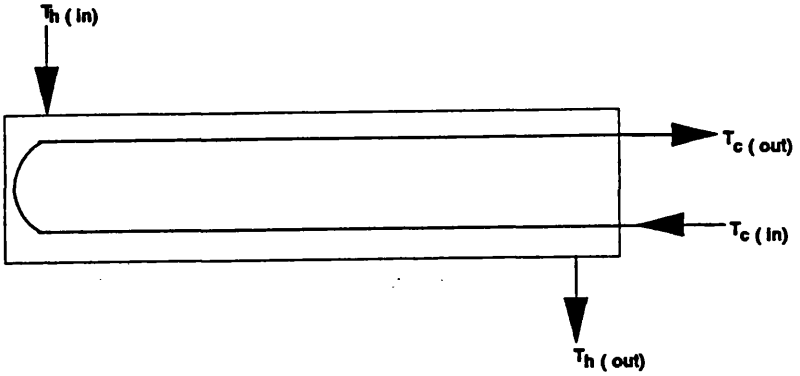

Thus ,

$$\Delta T_1 = (T_{h\,(in)} - T_{c\,(out)}) \qquad (1.26)$$

$$\Delta T_2 = (T_{h\,(out)} - T_{c\,(in)}) \qquad (1.27)$$

Where :

$T_{(in)}$ = inlet temperature of(h/c) fluid (K)

$T_{(out)}$ = outlet temperature of(h/c) fluid (K)

subscripts h and c refer to the hot and cold fluids respectively .

Another potential error may arise in equation 1.10 if U_C is calculated as follows ;

$$\frac{1}{U_C} = \frac{1}{h_o} + R_w + \frac{1}{h_i}\frac{A_o}{A_i} \qquad (1.28)$$

Where, U_C, h_o, h_i, R_w, and $\frac{A_o}{A_i}$ were already defined in equations 1.3 and 1.10 .

Poor selection of mathematical correlations to predict the coefficients h_o and h_i can,

unfortunately, lead to a significant error in U_C. For example , Merry and Polley[141] found that the widely used Dittus and Boelter[12] correlation overpredicts the tube side heat transfer coefficient , h_i, by around 15%, while the ESDU[190] correlation was found to be in very good agreement with their experimental data .

Crittenden *et al*[89] have listed many limitations and difficulties in the use of industrial plant data in fouling research. Thus it is not surprising that industrial plant studies need to be well supported by laboratory - scale experimentation .

1.1.4.2 Laboratory - scale method

Laboratory - scale equipments have been designed in order to simulate fouling in actual plant heat exchangers. However , the scale - down of a single heat exchanger tube, especially for hydrocarbon fouling studies , requires that compromises must inevitably be made between the principles of geometric , dynamic , thermal and chemical similarity . Consequently , deposits with different chemical composition , structure and morphology from those found in the field may occur when using laboratory - scale equipment[81,83]. Clearly the balance of mechanisms may have been altered on scale down .

Several comprehensive reviews are available on laboratory-scale methods, including those provided by Epstein[60,61], Knudsen[10], Somerscales[143], Melo and Pinheiro[144] and later by Chenoweth[142].

Melo and Pinheiro[144] presented a detailed list of topics for research on fouling and related areas. They also presented a matrix of interactions between experimental factors and deposit formation processes, which may assist in designing a programme for fouling research .

Generally laboratory - scale techniques and apparatus used for fouling studies can be classified into two main categories , as shown in Fig 1.14 ;

- Firstly , those for determining a fouling tendency which are mainly used for studying the effectiveness of anti - fouling chemicals in hydrocarbon processes. For example Fields *et al*[68] used a pilot scale test unit called INSITE for studying the fouling tendency of many crude oils. This apparatus is a two - step process that incorporates selective solvent extraction and spectrophotometry . A proprietary reagent is used to selectively extract specific components from crude oil which, when quantified, can be translated into a crude oil's resistance to foul. The INSITE equipment was used to measure the potential to foul relative to a known standard. Using a standard, a scale of zero (low fouling severity) to 100

(high fouling severity) was established. Through repeated testing, a profile of fouling severity versus time can be readily produced and can be used to optimise antifoulant feedrate .

- Secondly , those designed to study the thermal resistance , mass or thickness of the fouling deposit .

Knudsen[10] has listed the experimental parameters which should be measured in any fouling test section in order to provide a sound basis for the thermal fouling resistance calculation:

1 - Heat flux (q)	(W m^{-2})
2 - Flow velocity (v)	(m s^{-1})
3 - Bulk fluid temperature (T_b)	(K)
4 - Surface temperature of deposit at interface separating flowing fluid and deposit (Ti)	(K)
5 - Wall temperature at the heat transfer surface (Tw)	(K)

It should be possible to overcome most of the disadvantages of laboratory - scale equipment by designing a test apparatus which simulates closely the actual heat transfer equipment without the need to scale down the test section or accelerate the experimental conditions . This may not always be an easy task , especially for fouling of crude oil when many constraints , most of them relating to safety , can confront the researcher. Nevertheless, this is the challenge provided in the present study. Chapter 2 describes a solution, although not perfect, to this challenge.

1.2 Heat transfer and friction in circular tubes

The field of heat transfer research has grown substantially in the last 20 years . One subfield of great industrial importance is convective heat transfer . This has been the subject of many books, including those by Shah and London[13], Kays and Crawford[29] , Arpaci and Larsen[154], and Burmeister[155] , and numerous scientific papers. A handbook on single-phase convective heat transfer is edited by Kakaç *et al*[14] .

Convective heat transfer in circular tubes may be divided into two main categories , namely :

1- Convective heat transfer in bare tubes .

2- Enhanced Convective heat transfer in tubes.

1.2.1 Convective heat transfer in bare tubes

Plane or bare tubes are the most common type of heat transfer ducts used in heat exchangers . Bare tubes can be smooth or rough. Few commercial heat exchanger tubes can be regarded as hydrodynamically smooth since they usually have a natural roughness caused by the methods of manufacture[38,40]. Many investigations[38,153-159] have indicated an increase in convective heat transfer coefficient by roughness in the turbulent flow region, i.e $Re > 10^4$. However roughness has no effect on the heat transfer coefficient for laminar flow ($Re < 2100$). Roughness can also affect the pressure

drop (Δ_P) across the tube length (L) by increasing the friction factor in the turbulent flow region .

1.2.1.1 Friction factor models

Friction factor is a dimensionless parameter defined by Fanning as a ratio of wall shear stress (τ) to the flow kinetic energy per unit volume , $(\frac{\rho\ v^2}{2g_c})$. According to Shah[13] the Fanning friction factor (f) is expressed as follows :

$$f = \frac{r_i}{L}\frac{\Delta P}{\rho\ v^2/2g_c} \qquad (1.29)$$

Where :

r_i	= inside tube radius	(m)
L	= the tube length	(m)
Δ_P	= pressure drop across the tube length	(N m^{-2})
ρ	= fluid density	(kg m^{-3})
v	= fluid velocity	(m s^{-1})
g_C	= the gravitational acceleration conversion factor = 1	$(\frac{kg\ m}{N\ s^2})$

Another friction factor , however , may be found in the literature defined as :

$$f_D = 4f \qquad (1.30)$$

Here , f_D is the Darcy friction factor , sometimes referred to as the Darcy - Weisbach friction factor. It is this friction factor which was used by Moody[15] in his chart . A third friction factor, f_C , has been used particularly by Churchill[35,173] in which :

$$f = 2f_C \qquad (1.31)$$

The friction factor for laminar flow is unaffected by roughness . For fully developed laminar flow of incompressible Newtonian fluids , such as water , oils , etc ., under isothermal condition with no heat added to or removed from the tube, Poiseuille[160] provides the following expression for the Fanning friction factor :

$$f_{is} = \frac{16}{Re} \qquad (1.32)$$

Where :

f_{is} = the isothermal Fanning friction factor

Re = Reynolds number = $\frac{v \rho D_i}{\mu}$

D_i = inner tube diameter = $2 r_i$ (m)

μ = fluid dynamic viscosity (N s m^{-2})

For - non isothermal conditions , Sieder and Tate[36] provide the following modification to Poiseuille's equation 1.32 ;

$$f_{nis} = 1.1 \, f_{is} \, (\frac{\mu_b}{\mu_w})^{0.25} \qquad (1.33)$$

Or ,

$$f_{nis} = 1.1 \, (\frac{16}{Re}) \, (\frac{\mu_b}{\mu_w})^{0.25} = \frac{17.6}{Re} \, (\frac{\mu_b}{\mu_w})^{0.25} \qquad (1.34)$$

Where ;

f_{nis} = non - isothermal Fanning friction factor

μ_b and μ_w are the fluid dynamic viscosities at bulk fluid and wall temperatures respectively .

Sieder and Tate[36] used equation 1.34 for laminar friction factor calculations in heating and cooling processes alike .

There are several mathematical models which can be used for calculate the friction factor in smooth and rough tubes for fully developed turbulent flow. Most of these models are listed in Table 1.6 in chronological order as equations 1.35 to 1.49 .

Table 1.6 Fully Developed Turbulent Flow Friction Factor Correlations for Smooth and Rough Circular Tubes

f_S is the Fanning friction factor for smooth tubes = $f_D / 4$
f_R is the Fanning friction factor for rough tubes = $f_D / 4$

Authors (year)	Correlation		Recommended Range	Remarks
Blasius[161] (1913)	$f_S = 0.0791\ Re^{-0.25}$	(1.35)	$4x10^3 < Re < 10^5$	Smooth tubes
van Kàrmàn[162] (1931)	$\frac{1}{\sqrt{f_R}} = 3.36 - 1.763Ln(\frac{\epsilon}{r_i})$	(1.36)	$Re > 10^4$	Rough tubes
Drew *et al*[163] (1932)	$f_S = 0.0014 + 0.125Re^{-0.32}$	(1.37)	$4x10^3 < Re < 10^5$	Smooth tubes
Nikuradse[157] (1933)	$\frac{1}{\sqrt{f_R}} = 3.48 - 1.737Ln(\frac{\epsilon}{r_i})$	(1.38)	$Re > 10^4$	Rough tubes
Colebreek[164] (1939)	$\frac{1}{\sqrt{f_R}} = 3.48 - 1.737Ln(\frac{\epsilon}{r_i} + \frac{9.35}{Re\sqrt{f_R}})$	(1.39)	$Re > 10^4$	This Correlation was chosen by Kakaç *et al*[14] as the most accurate model for rough tube
	$\frac{1}{\sqrt{f_S}} = 1.737Ln(\frac{Re}{7})$	(1.40)	$2100 < Re < 10^4$	Smooth tubes
Moody[15] (1944)	$f_R = 1.375x10^{-3}\ [1 + 21.54(\frac{\epsilon}{ri} + \frac{100}{Re})^{1/3}]$	(1.41)	$2100 < Re < 10^8$ $2x\ 10^{-8} < \frac{\epsilon}{r_i} < 0.1$	Rough tubes The friction factor used by Moody was f_D which is $4\ f_R$

Table 1.6 continued

Authors (year)	Correlation	Recommended Range	Remarks
McAdams [3] (1954)	$f_s = 0.046\ Re^{-0.2}$ (1.42)	$4x10^3 < Re < 10^5$	Smooth tubes
Techo *et al* [165] (1965)	$\frac{1}{\sqrt{f_s}} = 1.737\ Ln\left(\frac{Re}{(1.964\ Re - 3.82)}\right)$ (1.43)	$10^4 < Re < 10^7$	Smooth tubes
Nikuradse[166] (1966)	$f_s = 0.0008 + 0.0553\ Re^{-0.237}$ (1.44)	$10^5 < Re < 10^7$	Smooth tubes
Prandtl[168] Kàrmàn[167] Nikuradse[166] (1966)	$\frac{1}{\sqrt{f_s}} = 1.737\ Ln(Re\sqrt{f_s}) - 0.3946$ (1.45)	$4x10^3 < Re < 10^7$	1- This model is referred to as PKN 2-chosen by Kakaç *et al*[14] as the most accurate model for Smooth tubes 3-The appearance of f_s in both sides of equation 1.45 , is the main disadvantage of PKN model.
Swamee and Jain[169] (1976)	$f_s = 3.4769 - 1.737\ Ln\left[\frac{\epsilon}{r_i} + \frac{42.48}{Re^{0.9}}\right]$ (1.46)	$4000 < Re < 10^8$ $2x\ 10^{-8} < \frac{\epsilon}{r_i} < 0.1$	Rough tubes
Jain[170] (1980)	$f_R = 4.215 - 1.564\ Ln\left[\frac{\epsilon}{r_i} + \frac{96.3}{Re}\right]$ (1.47)	$4000 < Re < 10^8$ $2x\ 10^{-8} < \frac{\epsilon}{r_i} < 0.1$	Rough tubes in good agreement with equation 1.41
Haaland[171] (1983)	$f_R = 3.474 - 1.564\ Ln\left[(\frac{\epsilon}{r_i})^{1.11} + \frac{63635}{Re}\right]$ (1.48)	$4000 < Re < 10^8$ $2x\ 10^{-8} < \frac{\epsilon}{r_i} < 0.1$	Rough tubes
Bhatti and Shah[172] (1987)	$f_s = 0.00128 + 0.1143\ Re^{-0.311}$ (1.49)	$4000 < Re < 10^7$	Smooth tubes

Churchill developed general correlations for both smooth[35] and rough[173] tubes which may be applied to all three flow regimes : laminar , transition , and turbulent as follows :

1 -<u>for smooth tube</u>

$$f_c = \left[\frac{1}{\left[\left(\frac{8}{Re} \right)^{10} + \left(\frac{Re}{36500} \right)^{20} \right]^{0.5}} + 2.21 \ln \left(\frac{Re}{7} \right) \right]^{-0.2} \qquad (1.50)$$

2 -<u>for rough tube</u>

$$f_c = \left[\left(\frac{8}{Re} \right)^{12} + (A1 + B1)^{-1.5} \right]^{1/12} \qquad (1.51)$$

Where :

$$A1 = \left[2.2088 + 2.457 \ln \left(\frac{\epsilon}{r_i} + 42.683 \, Re^{-0.9} \right) \right]^{16} \qquad (1.52)$$

$$B1 = \left[\frac{37530}{Re} \right]^{16} \qquad (1.53)$$

ϵ = height of surface roughness element (m)

Although equations 1.50 and 1.51 are applicable to the whole Re range , Churchill[35] suggested that for Re < 2100 , equation 1.32 should be used. Churchill's correlations[35,173] are complex and unsuitable for manual calculations . Moreover , the prediction for friction factor in the transition flow region , 2100 < Re < 4000 , is subject to some uncertainty[14]. Despite this , Churchill's correlations are the only ones available for the whole range of Re . They can of course be used in computer programs for friction factor and pressure drop calculations of tubular heat exchangers .

1.2.1.2 Heat transfer models

According to Nusselt[174] the convective heat transfer in a tube can be represented in the form of dimensionless groups as follows :

$$Nu = \left(\frac{h_i D_i}{k}\right) = \Gamma \left(Re, Pr, \frac{L}{D_i} \right) \quad (1.54)$$

Where ;

Nu = Nusselt number

Pr = Prandtl number = $\left(\frac{c_p \mu}{k} \right)$

k = fluid thermal conductivity (W m K^{-1})

It has been the object of numerous theoretical and experimental studies to find the nature of the function Γ and these studies have in general been limited to ascertaining the effects of Re , Pr and $\frac{L}{D_i}$. It is a matter of fact that most early studies paid no attention to the effect of roughness on the convective heat transfer coefficient. The main important models used for forced convection heat transfer coefficient calculations are discussed below .

a- Laminar flow (Re < 2100)

For fully developed laminar flow , Nusselt[175] theoretically found that Nu is a constant value, equal to 3.65 for uniform wall temperature conditions. This figure has been confirmed by Shah[30] who also obtained a value of $\frac{48}{11}$ for Nu in fully developed laminar flow at uniform heat flux

conditions. Hydrodynamic and thermal entrance lengths, which are required for velocity and temperature profiles to be fully developed, are discussed in detail in chapter 3 , section 3.5.2.1

For thermally developing laminar flow, Lévêque[176] provides the following expression ,

$$Nu = 1.75\ Gz^{1/3} \qquad (1.55)$$

Where :

Gz = Graetz number

$$Gz = \left(\frac{m\, c_p}{k\, L}\right) = \left(\frac{Re\, Pr\, (\pi\, D_i)}{4\, L}\right) = \frac{\pi}{4} RePr \frac{D_i}{L} \qquad (1.56)$$

Or ,

$$Gz = \frac{11}{14}\ Re\, Pr\, \frac{D_i}{L} \qquad (1.57)$$

Therefore , equation 1.55 may be re-expressed as follows ;

$$Nu = 1.75\ \left(\frac{11}{14}\ Re\ Pr\ \frac{D_i}{L}\right)^{1/3}$$

Or ,

$$Nu = 1.614\ \left(Re\, Pr \frac{D_i}{L}\right)^{1/3} \qquad (1.58)$$

Sieder and Tate[36] considered the effect of a radial temperature gradient on the distribution of the axial and the radial components of velocity, and provided the following empirical correlation, which is in the form of equation 1.58 :

$$Nu = 1.86\ \left(Re\ Pr \frac{D_i}{L}\right)^{1/3} \left(\frac{\mu_b}{\mu_w}\right)^{0.14} \qquad (1.59)$$

The Sieder and Tate[36] correlation is only valid for a fully established velocity profile. It is not suitable for the hydrodynamic entrance region.

b- Turbulent flow (Re > 10000)

There are numerous empirical and theoretical correlations for predicting the heat transfer coefficient in fully developed turbulent flow. Most of these correlations are listed in Table 1.7 as equations 1.60 to 1.89 . Kakaç *et al*[14] compared many of these correlations and have chosen Gnielinski's correlations[37] , equations 1.80 - 1.82 in Table 1.7 , as the most accurate. Hydrodynamic and thermal entrance lengths which are needed for turbulent flow to be fully developed, are discussed in detail in chapter 3 (section 3.5.2.1).

Table 1.7 Fully Developed Turbulent Flow Nusselt Number Correlations for Smooth (Nu_S) and Rough (Nu_R) Circular Tubes

f_S is the Fanning friction factor in a smooth tube which may be calculated from the PKN correlation (equation 1.45) or any of smooth tube friction factor correlations shown in Table 1.6

f_R is the friction factor in a rough tube which may be calculated from Nikuradse correlation (equation 1.38) or any of rough tube friction factor correlations shown in Table 1.6

Authors (year)	Correlation	Recommended Range	Remarks
Reynolds[178] (1874)	$Nu_S = \frac{f_S}{2} Re\ Pr$ (1.60)	$Pr = 1$ $Re > 10^4$	1- Smooth tubes 2- Theoretical model sometimes referred to as Reynolds analogy
Nusselt[175] (1910)	$Nu_S = 0.024\ Re^{0.786}\ Pr^{0.45}$ (1.61)	$5x10^3 < Re < 5x10^6$ $Pr < 1$	1- Smooth tubes 2- Originated by Nusselt and modified by many other investigators
Prandtl[179] (1910) Taylor[180] (1916)	$Nu_S = \frac{\frac{f_S}{2} Re\ Pr}{(1 + 5\sqrt{f_S/2}\,(Pr - 1))}$ (1.62)	$5000 < Re < 5x10^5$ $Pr < 10$	1- Smooth tubes 2- Theoretical model has been derived independently by Prandtl[179] in 1910 and by Taylor[180] in 1916
Dittus and Boelter[12] (1930)	For heating : $Nu_S = 0.024\ Re^{0.8}\ Pr^{0.4}$ (1.63) For cooling : $Nu_S = 0.024\ Re^{0.8}\ Pr^{0.3}$ (1.64)	$2500 < Re < 1.24x10^5$ $0.7 < Pr < 120$	1- Smooth tubes 2- This empirical correlation was widely used for heat exchanger design.However, it is within -10% to +21% comparing with Gnielinski[37] correlation
Colburn[181] (1933)	$Nu_S = 0.024\ Re^{0.8}\ Pr^{1/3}$ (1.65)	$10^4 < Re < 10^5$ $0.5 < Pr < 3$	1- Smooth tubes 2- within -20% to +21% comparing with Gnielinski[37] correlation

Table 1.7 (Continuation 1)

Authors (year)	Correlation	Recommended Range	Remarks
Sieder and Tate (36) (1936)	$Nu_S = 0.027\ Re^{0.8}\ Pr^{1/3} (\frac{\mu_b}{\mu_w})^{0.14}$ (1.66)	$2100 < Re < 10^6$ $158 < Pr < 16700$	1- Commercial tubes were used ,but no attention was paid to the effect of roughness on the heat transfer . 2- Within -10% to +30 % comparing with Gnielinski(37) correlation
van Kàrmàn(182) (1939)	$Nu_S = \frac{\frac{f_S}{2} Re\ Pr}{(1 + 5 (\sqrt{f_S/2}) [Pr - 1 + Ln(\frac{5\ Pr+1}{6})])}$ (1.67)	$10^4 < Re < 10^6$ $0.5 < Pr < 10$	1- Smooth tubes 2- Within -11% to +16 % comparing with Gnielinski(37) correlation
Drexel and McAdams(183) (1945)	$Nu_S = 0.021\ Re^{0.8}\ Pr^{0.4}$ (1.68)	$10^4 < Re < 10^6$ $Pr < 0.7$	1- Smooth tubes 2-Within -10% to +21% comparing with Gnielinski(37) correlation
Martinelli(184) (1947)	$Nu_R = \frac{Re\ Pr \sqrt{f_R/2}}{(5 [Pr + Ln(1+5\ Pr)] + 0.5\ Ln(A2))}$ (1.69) Where: $A2 = \frac{Re \sqrt{f_R/2}}{60}$ (1.70)	None stated	Used for metal liquids in rough tubes
Nunner(156) (1956)	$Nu_R = \frac{\frac{f_R}{2} Re\ Pr}{(1+1.5\ Re^{-1/8}\ Pr^{-1/6} [Pr(\frac{f_R}{f_S} - 1)])}$ (1.71)	$500 < Re < 8x10^6$ $Pr = 0.7$	Used for air in rough pipes
Friend and Metzner(185) (1958)	$Nu_S = \frac{\frac{f_S}{2} Re\ Pr}{(1.2+11.8 \sqrt{f_S/2} (Pr-1) Pr^{-1/3})}$ (1.72)	$4000 < Re < 5x10^6$ $50 < Pr < 600$	1- Smooth tubes 2- Within -2% to +8% comparing with Gnielinski(37) correlation

Table 1.7 (Continuation 2)

Authors (year)	Correlation	Recommended Range	Remarks
Petukhov *et al*[186] (1958)	$Nu_S = \frac{\frac{f_S}{2} Re\, Pr}{(A3 + 12.7\sqrt{f_S/2}\,(Pr^{2/3} - 1))}$ (1.73) Where : $A3 = 1.07 + (\frac{900}{Re}) - [\frac{0.63}{(1+10Pr)}]$ (1.74) $Nu_S = \frac{\frac{f_S}{2} Re\, Pr}{(1.07 + 12.7\sqrt{f_S/2}\,(Pr^{2/3} - 1))}$ (1.75)	$4000 < Re < 5x10^6$ $0.5 < Pr < 10^6$	1- Smooth tubes 2- The first Petukhov's model agrees with most heat transfer experimental data to an accuracy of ±5% 3- The second model is a simplified version of the first one .
Dipprey and Sabersky[187] (1963)	$Nu_R = \frac{\frac{f_R}{2} Re\, Pr}{(1 + 12.7\sqrt{f_R/2}[5.19\,(Re_\epsilon)^{0.2} Pr^{0.44} - 8.48])}$ (1.76) Where : $Re_\epsilon = \frac{\epsilon\, v\, \rho}{\mu}$ (1.77)	$1.4x10^4 < Re < 10^5$ $1.2 < Pr < 5.94$ $0.0024 < \frac{\epsilon}{Di} < 0.049$	1- Rough tubes 2-Sand grain roughness
Gowen and Smith[188] (1968)	$Nu_R = \frac{\sqrt{f_R/2}\, Re\, Pr}{(4.5 + [0.155\,(Re\sqrt{f_R/2})^{0.54} + \sqrt{f_R/2}\,]\, Pr^{0.5})}$ (1.78)	$10^4 < Re < 5x10^4$ $0.7 < Pr < 14.3$ $0.021 < \frac{\epsilon}{D_i} < 0.095$	Rough tubes
Walker and Bott[38] (1973)	$Nu_R = 0.0114\,(\frac{f_R}{2})^{0.5} Re^{1.174} Pr^{0.5}$ (1.79)	$10^4 < Re < 5x10^4$ $2 < Pr < 5.5$	1- Natural roughness of commercial tubes 2- Artificial "sand grain" roughness
Gnielinski[37] (1976)	$Nu_S = \frac{\frac{f_S}{2}(Re - 1000)\, Pr}{(1 + 12.7(\frac{f_S}{2})^{1/2}(Pr^{2/3} - 1))}$ (1.80) $Nu_S = 0.0214\,(Re^{0.8} - 100)\, Pr^{0.4}$ (1.81) $Nu_S = 0.012\,(Re^{0.87} - 280)\, Pr^{0.4}$ (1.82)	$2300 < Re < 5x10^6$ $0.5 < Pr < 2000$ $10^4 < Re < 5x10^6$ $0.5 < Pr < 1.5$ $3000 < Re < 10^6$ $1.5 < Pr < 500$	1- Smooth or commercial tubes 2- Based on the second Petukhov's model 3-Chosen by Kakaç *et al*[14] as the most accurate correlation for smooth tube heat transfer coefficient calculation 4- The second and third correlations are simplified versions of the first one .

Table 1.7 (Continuation 3)

Authors (year)	Correlation	Recommended Range	Remarks
Butterworth[189] (1977)	$Nu_R = E_t' Re^{0.795} Pr^{0.795}$ (1.83) Where : $E_t' = 0.0225 \exp[-0.0225 (Ln(Pr))^2]$ (1.84)	$Re > 10^4$ $0.5 < Pr < 400$	1- Commercial tubes 2-Based on the work of ESDU[190]
Kays and Crawford[29] (1980)	$Nu_S = 0.022 Re^{0.8} Pr^{0.5}$ (1.85)	$10^4 < Re < 10^6$ $0.5 < Pr < 1$	1- Smooth tubes 2-within -2.5% to +6.6% comparing with Gnielinski[37] correlation
Sandall *et al*[191] (1980)	$Nu_R = \frac{Re\, Pr \sqrt{f_R/2}}{(12.485\, Pr^{2/3} - 7.85\, Pr^{1/3} + 3.61\, Ln(Pr) + 5.8 + A4)}$ (1.86) Where : $A4 = 2.78 \ln(\sqrt{f_R/8}\,(\frac{Re}{45}))$ (1.87)	$10^4 < Re < 5x10^6$ $0.5 < Pr < 2000$	1- Smooth tubes 2-within -4% to +6.6% comparing with Gnielinski[37] correlation
Kawase and De[192] (1984)	$Nu_R = 0.047\, Re \sqrt{Pr} \sqrt{f_R}\,[1.11 + 0.44\, Pr^{-1/3} - 0.7\, Pr^{-1/6}]$ (1.88)	$5000 < Re < 5x10^5$ $5.1 < Pr < 390$	1-Fully rough tubes 2-In agreement with the experimental data[14]
Bhatti and Shah[172] (1987)	$Nu_R = \frac{Re\, Pr\, (f_R/2)}{(1 + \sqrt{f_R/2}[4.5\, (Re_\epsilon)^{0.2} Pr^{0.5} - 8.48])}$ (1.89) Where : $Re_\epsilon = \frac{\epsilon\, v\, \rho}{\mu}$	$Re > 10^4$ $0.5 < Pr < 400$	1-Fully rough tubes 2-Within 5% with the available experimental data[14]

c - Transition region (2100 < Re < 10000)

The transition region between fully laminar and fully turbulent flow is unstable and the heat transfer coefficient cannot be predicted with certainty[189,177]. Some of the correlations listed

in Table 1.7 , such as Gnielinski's correlation[37] (equation 1.80) are valid for transition as well as for turbulent flow. Churchill[35] provides a general correlation for predicting the fully developed heat transfer coefficient in smooth tubes for $0 < Pr < 10^6$ and $10 < Re < 10^6$, conditions which span the laminar , transition and turbulent flow regimes :

$$Nu = \left[(Nu_l)^{10} + \left[A_5 \, Nu_l^{-2} + Nu_t^{-2} \right]^{-5} \right] \qquad (1.90)$$

Where :

$$A_5 = \exp\left((2200 - Re) / 365 \right) \qquad (1.91)$$

$$Nu_t = Nu_0 + \left[\frac{0.079 \sqrt{f_c} \, Re \, Pr}{\left(1 + Pr^{4/5} \right)^{5/6}} \right] \qquad (1.92)$$

Nu_o = 4.8 for uniform wall temperature

Nu_o = 6.3 for uniform heat flux

Nu_l = 3.657 for uniform wall temperature

Nu_l = 4.364 for uniform heat flux

f_c = friction factor for smooth tube which may be calculated from equation 1.50 .

Thus , for fully developed flow at uniform heat flux , equations 1.90 & 1.92 may be re-written as follows ;

$$Nu = \left[2.505 \times 10^6 + \left[\frac{A_5}{19.05} + Nu_t^{-2} \right]^{-5} \right]^{1/10} \qquad (1.93)$$

And ,

$$Nu_t = 6.3 + \left[\frac{0.079 \sqrt{f_c} \, Re \, Pr}{\left(1 + Pr^{4/5} \right)^{5/6}} \right] \qquad (1.94)$$

Therefore , for $Re < 2100$, equation 1.93 yields $Nu = 4.364$, which is the same value reported by Shah[30] for fully developed laminar

flow at uniform heat flux conditions . For $0 < Pr < 10^6$ and $2100 < Re < 10^4$ equation 1.93 can predict Nu values in agreement with experimental results for transition flow[14] . It is, however, within +13.7% and -10.5% compared to Gnielinski's correlations (equations 1.80 to 1.82) for the range of $0.5 < Pr < 2000$ and $10^4 < Re < 10^6$. Consequently , equation 1.93 can be safely used for the prediction of h_i in the fully developed transition region . The hydrodynamic and thermal entrance lengths, needed for transition flow to be fully developed, are discussed in detail in chapter 3 (section 3.5.2.1).

Sieder and Tate[36] provide a dimensionless parameter for heat transfer , called j_H - factor [193] , plotted against Re for all flow regimes (laminar, transition and turbulent) , Fig 1.15 . The j_H - factor is defined as follows:

$$j_H = Nu \; Pr^{-1/3} \left(\frac{\mu_b}{\mu_w}\right)^{-0.14} \qquad (1.95)$$

Another j_h - factor has been defined by Colburn[181] and is shown in Fig 1.16 :

$$j_h = St \, Pr^{2/3} \left(\frac{\mu_b}{\mu_f}\right)^{-0.14} \qquad (1.96)$$

Where ,

$$St = \text{Stanton number} = \frac{Nu}{Re \, Pr} = \frac{h_i}{\rho \, v \, c_p} \qquad (1.97)$$

μ_b and μ_f are the dynamic viscosities at bulk fluid (T_b) and film (T_f) temperatures respectively .

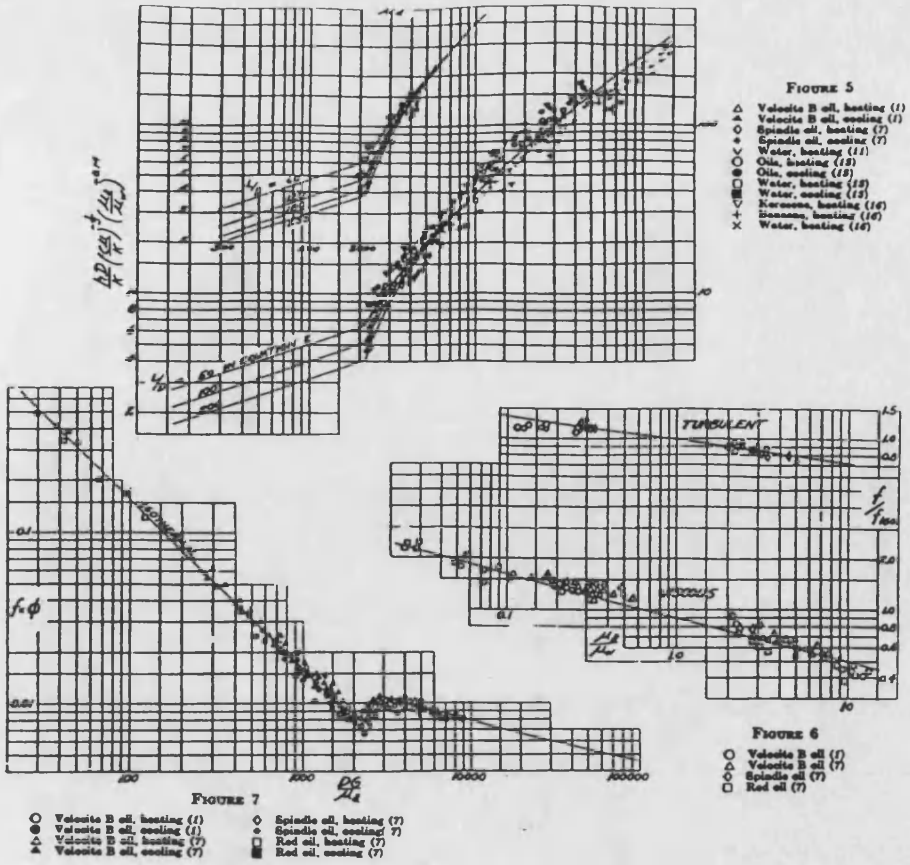

Fig 1.15 Sieder and Tate[36] j_H - factor

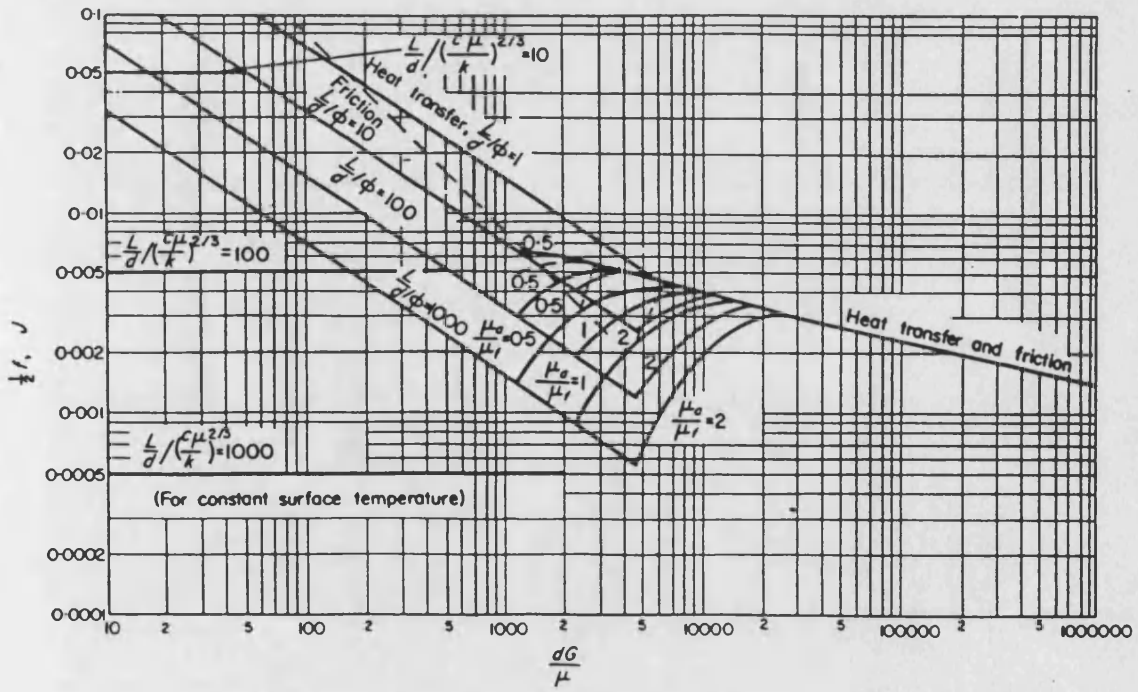

Fig 1.16 Colburn[181] j_h - factor

$$T_f = \frac{T_w + T_b}{2} \qquad (1.98)$$

It is very important to notice here that the viscosity correction factor $\frac{\mu_b}{\mu_f}$ used in equation 1.96 is different from the one used by Sieder and Tate[36] , $\frac{\mu_b}{\mu_w}$, in equation 1.95 . Sieder and Tate[36] used the viscosity (μ_w) at the inner wall temperature , T_w , while Colburn[181] used the viscosity (μ_f) at the film temperature , T_f . Thus j_H from equation 1.95 is not necessarily equal to j_h Re from equation 1.96 .

1.2.2 Enhanced convective heat transfer in tubes

Various techniques for achieving improved heat transfer are usually referred to as heat transfer augmentation or heat transfer enhancement. This subject has developed to the stage that it is of serious interest for heat - exchanger applications, and can be regarded as a major field of endeavour. The need to conserve energy has resulted in a substantial growth in research and development to improve heat transfer equipment . Industry has used enhanced heat transfer surfaces for two purposes ; firstly to obtain compact and less expensive heat exchangers , and , secondly , to increase the overall heat transfer coefficient - surface area

product (UA) of a heat exchanger . The higher UA value is exploited in one of two ways[194,196,200]:

a- to obtain an increased heat transfer rate for fixed fluid inlet temperatures , or

b- to reduce the mean temperature difference (LMTD) for the heat exchanger

A number of surveys on the subject of heat transfer enhancement has been published including those by Bergles[194-196] and Webb[197-200]. Bergles[195] presents a chart , Fig 1.17 , which shows that references dealing with heat transfer enhancement have grown substantially in number since 1861 when Joule[201] reported a significant improvement in the overall heat transfer coefficient for the in - tube condensation of steam when a wire was inserted in the cooling water jacket. It is now estimated[196] that each year over 500 papers , reports and patents are published on the subject .

The various techniques to enhance heat transfer inside tubes are generally classified[202] into two categories :

1- **Passive techniques** , in which no external energy, other than pump work, is required to produce the enhancement.

2- **Active techniques** , where external energy is needed .

These techniques are further classified as shown in Table 1.8 .

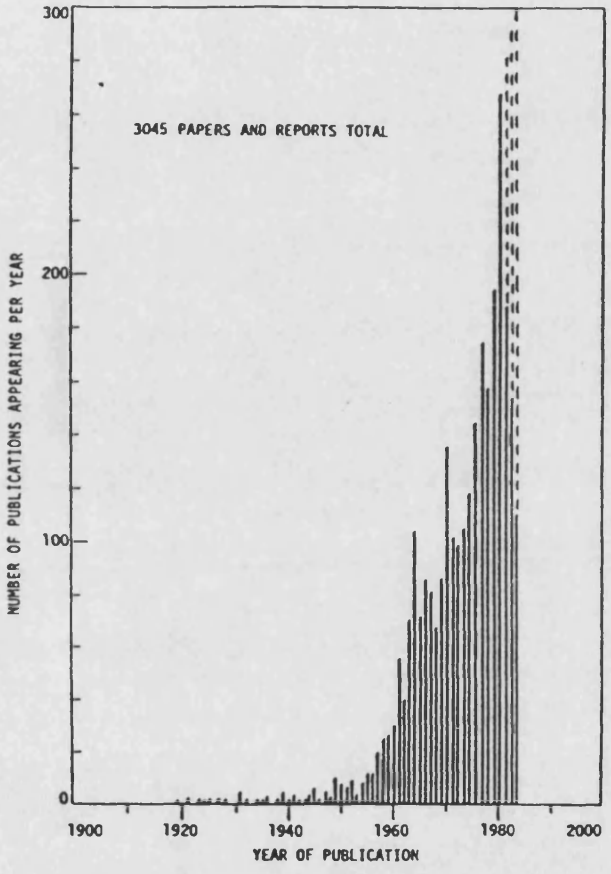

Fig 1.17 Annual publications worldwide in heat transfer enhancement[195]

Table 1.8 Classification of Enhancement Techniques

Passive	Reference by Number	Active	Reference by Number
Surface roughness	156 , 205 - 208	Mechanical aids	233 - 237
Internal extended surface	18 , 209 - 212	Heated surface vibration	238
Displaced promoters	213 - 218	Fluid vibration or pulsation	239
Swirl flow	219 - 224	Electrostatic fields	240 , 241
Additives	196 , 231	Suction or injection	242
Compound techniques	232		

Passive techniques are less expensive and easier to apply than active techniques. Consequently , it is not surprising that most of the passive techniques have received intensive investigation during the past twenty years . The important studies of passive and active techniques are described below :

1- Passive techniques

(I) Surface roughness, including internally knurling or threading a tube[204,205], inserting rings of various height and shape[156,205], inserting thin wire spirals which are in good contact with the tube wall[206], spirally grooving the tube[207], or convoluting the tube[208] .

(II) Internally extended surface, including the use of internally finned tubes[209-211] or finned annular gaps of double pipe exchangers[212,18].

(III) Displaced promoters , such as static mixers[214,215] , rings[213] , disks[213]

or coiled wire turbulence promoters[216,217] one of which is known as the **HiTran** insert[218] and is described in more detail in section 1.2.2.1 .

(IV) Swirl flow , which may be produced by inlet vortex generators[219,220] or by using twisted tape inserts[221-224], The enhancement occurs for several reasons: increased path length of flow, secondary flow effects , and , in the case of the tapes, fin effects .

(V) Additives, include solid particles and gas bubbles in single phase flows[231] and liquid trace additives for boiling systems[196] .

(VI) Compound enhancement, in which more than one of above techniques may be used simultaneously[232] .

2- Active techniques

(I) Mechanical aids, including scraped-surface heat transfer[233] , a straight tube rotating about its own axis[234] , a straight tube rotating around a parallel axis[235], a rotating circular tube[236,237] .

(II) Heated surface vibration, including the inner tube vibrated transversely, or a

rectangular channel with a flexible vibrating side[238] .

(III) Fluid vibration or pulsation, which is the most practical type of vibration enhancement[196]. The vibration range can be from pulsations of about 1 Hz to ultrasound[239] .

(IV) Electrostatic fields, which can be directed to cause greater bulk mixing of fluid in the vicinity of the heat transfer surface[196] . An electrical field and a magnetic field may be combined to provide a forced convection *via* electromagnetic pumping[196,202]. Some impressive enhancements (at least 100% improvements in heat transfer rate) have been recorded with electric fields, particularly in the laminar flow region[240,241] .

(V) Injection or suction. Injection involves supplying gas to a flowing liquid through a porous heat transfer surface or injecting similar fluid upstream of the heat transfer section . Surface degassing of liquids can produce augmentation similar to gas injection[196,239] . Suction involves either vapour removal through a porous heated surface in nucleate or film boiling, or fluid withdrawal through a porous heated surface in single - phase flow[196].

Kinney[242] reported a large increase in heat transfer coefficient for laminar flow with surface suction .

For most of the passive techniques, the enhancement in heat transfer rate is usually obtained simultaneously with an increase in friction factor or pressure drop over and above the bare tube values. Bergles and Joshi[202] have compared many published heat transfer and friction factor data in laminar flow, and have concluded that techniques such as twisted - tape inserts , inner finned tubes, and a combination of the two seem to be especially effective for applications where pumping power is a limiting factor . Static mixers provide large heat transfer enhancements but the increases in pressure drop are also very large.

In order to provide a clear picture on the benefit of using a heat transfer enhancement technique to improve a heat transfer rate against the disbenefit of an increase in friction factor or pressure drop, the following three methods can be applied :

A- Nusselt number ratio, $(\frac{Nu_e}{Nu_b})$, may be plotted as a function of the friction factor ratio $(\frac{f_e}{f_b})$ where, the subscripts e and b refer to the enhanced and bare tubes respectively . This method was

used by Trupp and Soliman[211] for providing the optimum fin height and fin number that can be used in internally finned tubes , as shown in Fig 1.18 .

B- Enhancement factor (EF), which is defined as follows:

$$EF = \frac{(R_{Nu} - 1)}{(R_{\Delta p} - 1)} \qquad (1.99)$$

Where ,

$$R_{Nu} = \frac{\text{Nu for enhanced tube}}{\text{Nu for bare tube}} \qquad (1.100)$$

$$R_{\Delta p} = \frac{\Delta p \text{ for enhanced tube}}{\Delta p \text{ for bare tube}} \qquad (1.101)$$

This method was used by Agrawal and Sangupta[18] in their study on the use of a finned annular gap in a double pipe exchanger. Agrawal and Sangupta's data is shown in Fig 1.19 .

Use of the EF method can provide a clear comparison between different heat transfer enhancement techniques . The higher the EF value the better the enhancement . It is clear that no enhancement in Nu or increase in Δp would be expected if the bare tube alone is used in equation 1.99. Therefore the EF value is believed to be equal to zero for bare tube .

c- Ratio of the overall performance , $(\frac{j_H}{f})$, where j_H is the Sieder and Tate[36] heat

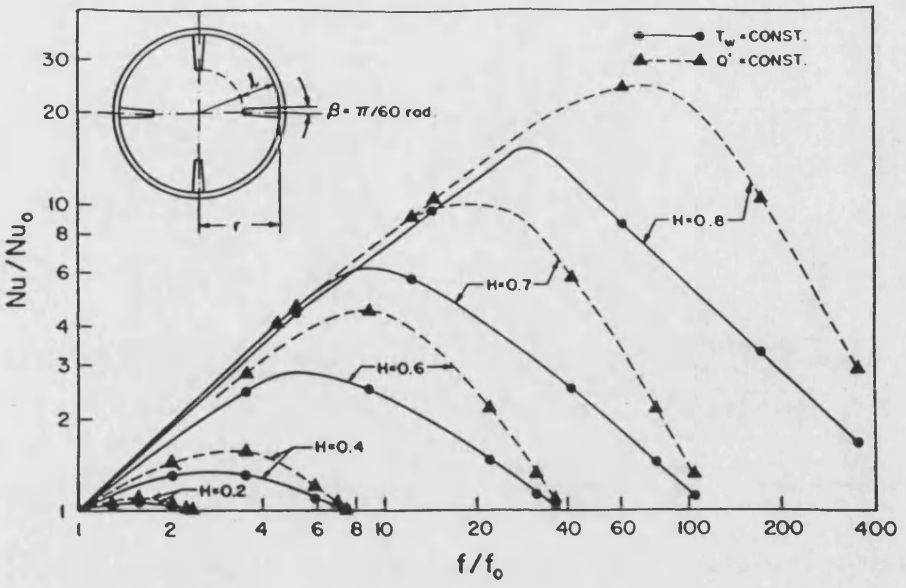

Fig 1.18 Use of Nusselt number - friction factor ratios
Work of Trupp and Soliman(211)

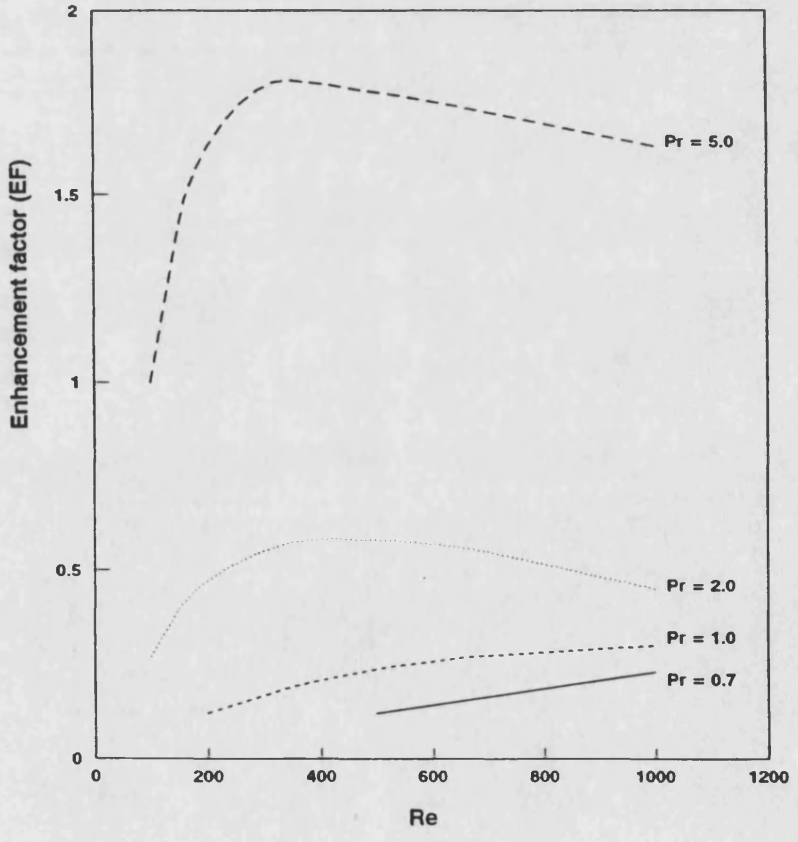

Fig 1.19 Use of enhancement factor (EF)
Results of Agrawal and Sengupata(18)

transfer factor and f is the Fanning friction factor . This method was used by Gough *et al*[19] in their study on the performance of the **HiTran** insert and is discussed in more detail in section 1.2.2.1 .

Fouling of enhanced tube surfaces will be discussed separately in section 1.3.

1.2.2.1 Use of HiTran inserts

The **HiTran** insert has been designed to position a matrix of wire filaments close to the inside wall of a tube , as shown in Fig 1.20 . The filaments are supported by a central spine to form a skeletal structure through which the tube - side fluid flows. In addition to supporting the filaments , the central spine provides the means of pulling the insert into the tube , which may have diameters from 4 mm to at least 150 mm , and lengths up to 15 m . The insert design enables the filaments to be sprung on to the tube wall to achieve good wire - wall contact[218,23] .

The **HiTran** insert , formerly called the Heatex tube insert, has been used in several studies[19-25] some of them using actual plant heat exchangers[25], to achieve an improvement in heat transfer rate of between 6 and 10 times that for the bare tube cases. The enhancement in heat transfer depends on the relative loop density , that is the number of

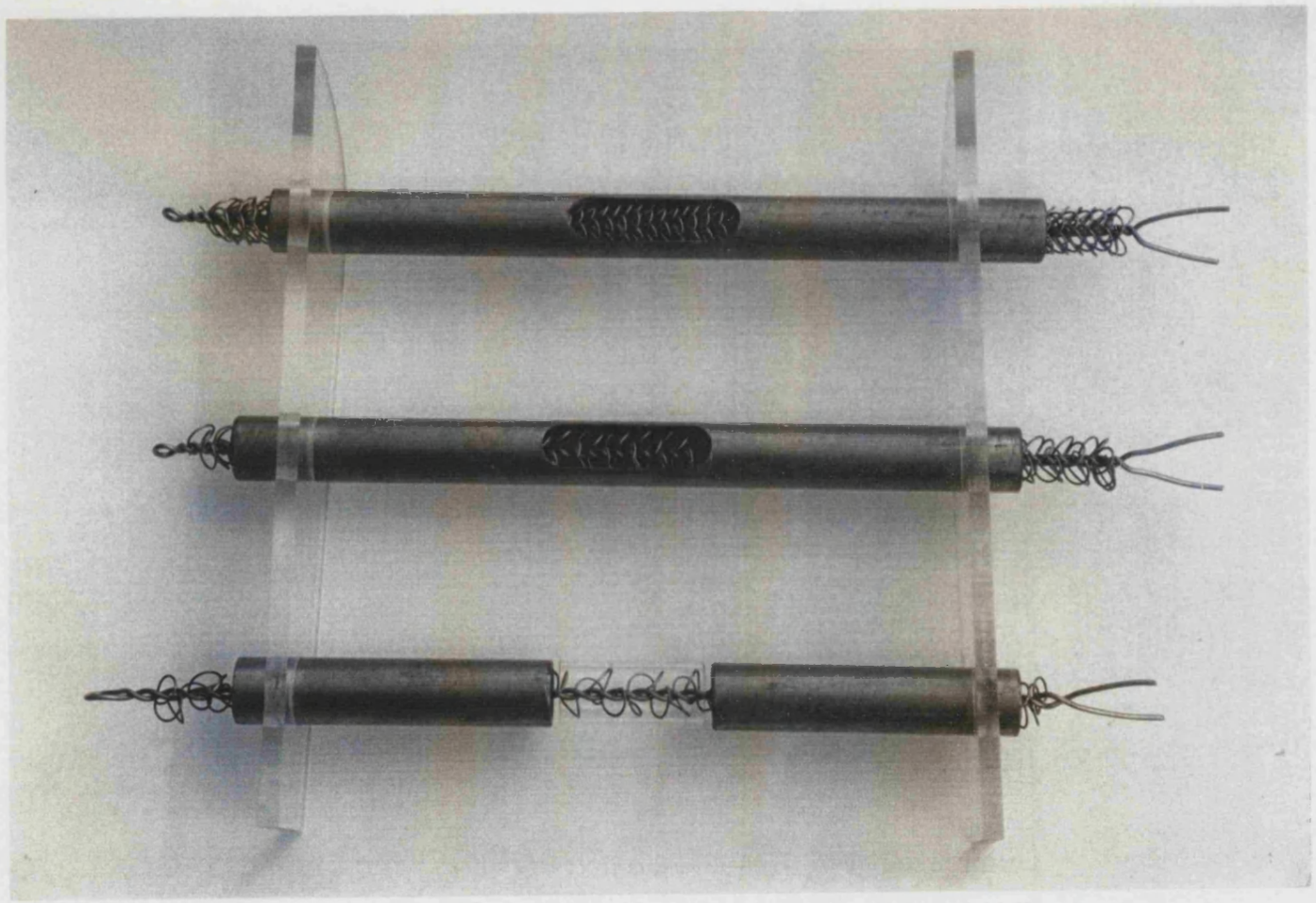

Fig (1.20) The way of fitting the HiTran inserts inside the tublular test sections

insert loops per unit length of insert. The penalty of heat transfer improvement is of course an increase in pressure drop which could be as high as 28 times[19] that of the bare tube .

Gough *et al*[19] studied the effect of using **HiTran** inserts on the tube side heat transfer and friction factor to a hot viscous fluid flowing, in laminar flow , inside a tube which was cooled by cold water passing counter - currently through an annular jacket of a double - pipe heat exchanger. Gough *et al*[19] compared the heat transfer factor (j_H) and the friction factor (f) with and without the use of the **HiTran** insert and found that the increase in j_H was increased by an increase in Re . At constant Re , j_H could also be increased by increasing the relative loop density . The friction factor f , however , increased as well and thus the ratio of the overall performance ($\frac{j_H}{f}$) was found to decrease with an increase in the loop density. Gough *et al*[19] claimed that if an air cooler was designed to operate with **HiTran** inserts fitted in tubes , then the surface area required could be reduced to at least a fifth in comparison with the bare tube design .

In another study , Oliver and Aldington[23] investigated the effect of using **HiTran** inserts on the heat transfer and friction factor of Newtonian and non-Newtonian fluids in the range of

40 < Pr < 550 and 5 < Re < 1600 for both heating and cooling . They found that the **HiTran** insert provided an enhancement in j_H by up to 5 times compared with the bare tube case. The pressure drop, however , was increased by a factor of up to 20 times compared with the bare tube case . Oliver and Aldington[23] obtained the following heat transfer and friction factor correlations for heating or cooling a glycerol/water mixture, a Newtonian fluid , in a tube fitted with a **HiTran** insert of medium density in the range of 40 < Pr < 550 and 5 < Re < 1600 :

$$Nu = 0.232\, Re^{0.54}\, Pr^{0.46} \qquad (1.102)$$

$$Ln\,(f_a) = 5.57 - 1.32\,(Ln(Re)) + 0.0627\,(Ln(Re))^2 \qquad (1.103)$$

Where f_a is the Fanning friction factor defined by the following equation ;

$$f_a = \left(\frac{\Delta p\, D_i}{2\, L\, \rho\, v^2}\right) \qquad (1.104)$$

They also reported useful information about non - Newtonian fluids but this subject is beyond the scope of this project .

The Fanning friction factor as defined by equation 1.104 is slightly different ,however, than the usual definition given in equation 1.29 .

Equations 1.102 and 1.103 are experimental correlations based on Aldington's work[22] and have not been tested on different systems .

1.3 Fouling of tubes with enhanced surfaces

There is a general feeling among heat exchanger users that enhanced tubes in dirty service would foul faster , that the heat transfer performance would drop to low values in short times and that the equipment would be almost impossible to clean. This might be the case in some situations but evidence from the few available industrial and laboratory investigations which have used enhanced surface tubes in fouling conditions , indicates otherwise . Indeed fouling can be reduced or even eliminated by employing a successful heat transfer enhancement technique .

Enhanced tubes, as far as fouling is concerned, may be divided into two main categories:

1- Those with extended surface or surface roughness, i.e finned tubes , knurling or threading tubes .etc, sometimes referred to as **structured surfaces** .

2- Those enhanced by means of displacement promoters or swirl flow , i.e static mixers , **HiTran** inserts, twisted tape inserts . etc, sometimes referred to as **unstructured surfaces** .

1.3.1 Fouling of structured surfaces

The literature contains very little data on fouling in tubes with structured surfaces. The few investigations that have been carried out address particulate and precipitation fouling. Watkinson[225] reviewed this subject and came to the following conclusions :

1- For internally finned tubes with area increase factors of 2.4, simulated cooling tower water studies show that a fouling resistance of about 1.2 times that of a plain tube should be used for design .

2- For extended longitudinally finned tubes with a total external area ratio of 3.4 in scaling service , a fouling resistance equal to that of a plain tube should be used for design .

3- For extended radially finned tubes with a total external area ratio of 2.4 in oil cooling service , a fouling resistance of 60% of the plain - tube value is tentatively recommended , although there is some evidence that a larger percentage should be used .

4- For enhanced surfaces with no extension of heat transfer area , in tube - side cooling water applications , fouling resistances equivalent to those of

plane tubes at the same velocity are recommended .

In a recent study , Kim and Webb[226] investigated the particulate fouling of water in tubes having a two - dimensional roughness geometry and found that enhanced tubes fouled almost the same as the smooth bare tube at Re = 30000 . At lower Reynolds numbers , however , the enhanced tubes showed higher fouling resistances .

1.3.2 Fouling of unstructured surfaces

Although many investigations have used static mixers , coiled wire promoters or twisted tape inserts for achieving higher in-tube heat transfer rates , none of them have suggested the use of these devices in fouling environments. This is possibly because of the corrosion risk . However the risk of corrosion may be overcome by proper choice of insert material .

Gough and Rogers[21] have reported an important case study involving severe fouling. A multitubular tar oil heater required cleaning after two months operation due to excessive pressure drop and reduced throughput resulting from the accumulation of deposits on the inside of the tube , through which the tar oil was passed . Tests carried out showed that the performance of the heater was decreased by 50% over the 4 month period . By using

HiTran inserts inside the tubes , the fouling resistance remained essentially zero over four months and cleaning was not required for at least twelve months. New heaters were built with **HiTran** inserts fitted , and operated for over four years without the need to shut-down for cleaning . The mechanism by which the **HiTran** insert can reduce fouling is not fully understood however. It could be due to turbulence created on the inside of the tube wall, which provides a similar effect to increasing velocity . However the inner surface temperature of a tube fitted with a **HiTran** insert is expected to be lower than that for the bare tube case in fluid heating applications, due to the higher heat transfer coefficient. Thus , if fouling is controlled by a chemical reaction mechanism then less fouling might be expected at a lower surface temperature . Elucidation of the mechanism by which **HiTran** inserts can reduce hydrocarbon fouling is one of the main objectives of the current study .

Chapter 2

Equipment Design and Operational Procedure

2.1 Introduction

The test equipment was designed in order to simulate the events inside a tube of a refinery heat exchanger. The apparatus which is shown schematically in Figs 2.1 and 2.2 is described in detail in section 2.2.

Local heat transfer coefficients were obtained for two hydrocarbon fluids using two horizontal heated tubular test sections. Santotherm 55, which is a non-fouling fluid, was used for studying the performance of the test equipment under clean conditions with or without the use of a **HiTran** Insert. Arabian light crude oil which is a potentially fouling fluid, was used for the fouling study (see Chapters 3 and 4). The liquid to be studied (Santotherm 55 or crude oil) was circulated around a closed heat transfer loop at a measured flow rate. The tubular test sections were heated indirectly by electrical elements externally wound around a thick tube jacket. After passing through the test sections the fluid was returned to the feed reservoir.

There are several advantages in this experimental arrangement over small-scale test apparatus. These include,

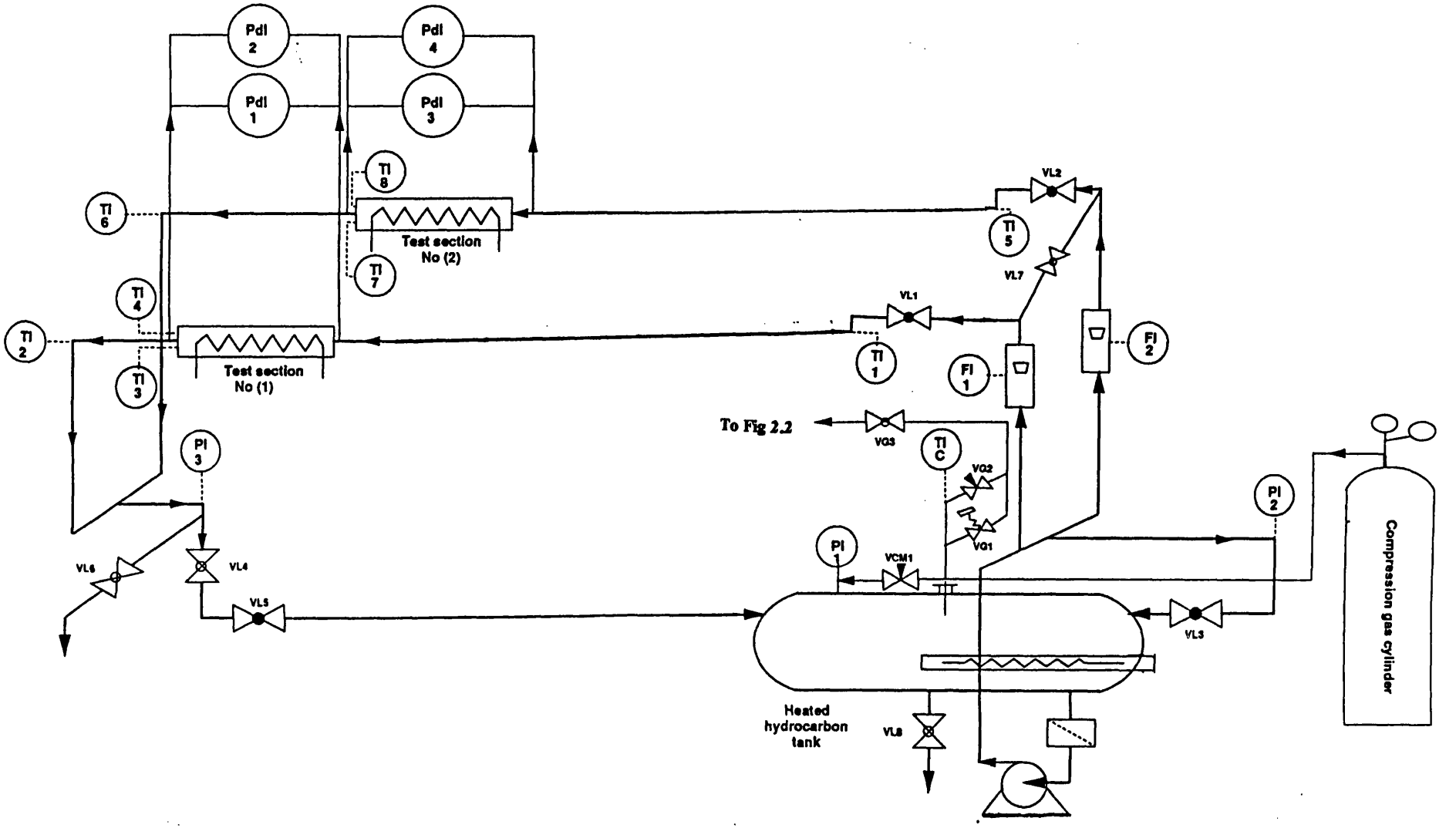

Fig 2.1 Schematic of Hydrocarbon Flow Loop

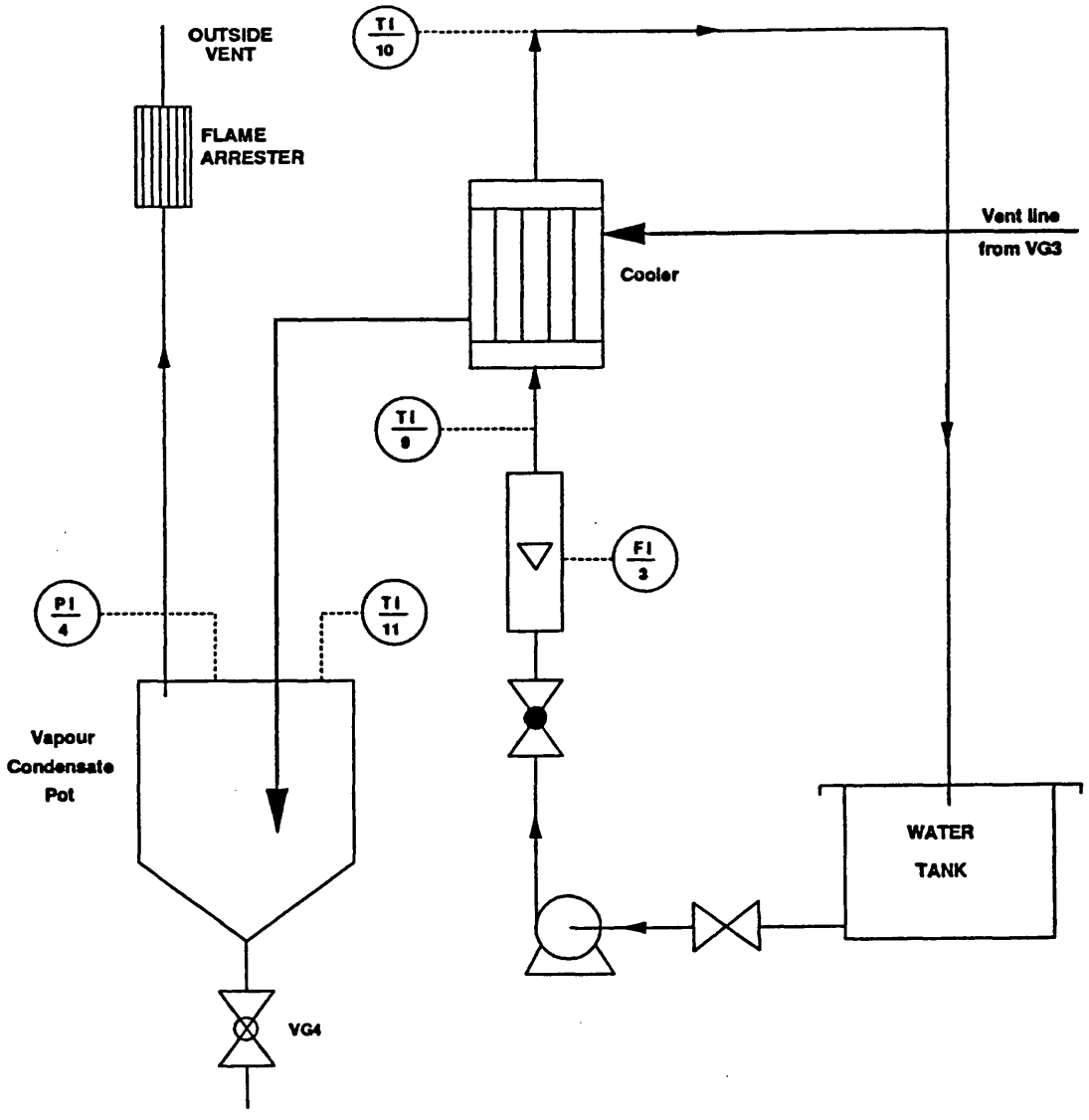

Fig 2.2 Schematic of Vapour Condensate system

1- The use of the same type of heat exchanger tubes in the experimental test sections as those used in refinery heat exchangers (3/4 inch BWG14 carbon steel).

2- Process variables such as, flow rate, heat flux, pressure and temperature could be controlled to values similar to those typically found in crude distillation unit preheat exchangers.

3- The test equipment was designed to consist of two horizontal tubular test sections connected in parallel, in which one could be fitted with a **HiTran** insert and the other left bare; both test sections were identical in design and could be controlled under the same operating conditions of flow rate, heat flux, etc.

Continual re-circulation of the test fluid (either Santotherm 55 or crude oil) around a closed circuit, rather than on a once-through basis, is the main difference between operation of this experiment and that of industrial practice. It might be considered that constant re-circulation of test fluid, especially crude oil, for a long period of time could affect its composition. It could possibly lead to loss of foulant precursors which would thereby make the absolute values of fouling

resistance or fouling rate somewhat different to the values found in actual refinery heat exchangers. However, the use of test sections of short length (27.2 cm each) provides a volume hold-up of 1:2200 between the test section and the volume of test fluid in the whole apparatus. Depending on the flow rate used, the number of complete reservoir changes may vary from 2.5 to 15 per hour for each test section. The residence time of the fluid in each test section is typically in the range of 0.06 to 0.6 second per cycle, Consequently, for 100 hrs of continuous operation the total residence time in each heated test section is between 2.5 and 25 minutes, which is equivalent to 0.042% - 0.42% of the total operating time. Thus the exposure of the re-circulated bulk fluid to elevated surface temperatures is small. On the positive side the heat transfer coefficients, with or without using **HiTran** inserts, should be very similar to those in the industrial heat exchangers. Furthermore, if the operating conditions of the experiments are maintained to simulate those of actual heat exchangers in the pre-heating train of a crude distillation unit, then it is believed that the effect of process variables on the fouling behaviour will be more or less the same.

2.2 Apparatus

There are two parts to the experimental apparatus, namely, the hydrocarbon recycle flow loop (see Fig 2.1), which contains the test sections, and the vapour vent condensation system (see Fig. 2.2). The latter is used for venting and depressurising the system since the test apparatus is designed to operate at pressures up to 15 bar.

2.2.1 Hydrocarbon recycle flow loop

A schematic diagram of the hydrocarbon recycle flow loop is shown in Fig 2.1 and a photograph is shown in Fig 2.3. The test fluid is pumped around a closed circuit by a centrifugal pump. The recycle flow loop contains two sections connected in parallel. Each section comprises a flow meter, a control valve and a heated test section. The detailed design of the heated sections is described in section 2.3. Both sections are joined together at the exit end and the test fluid is re-cycled back to the feed reservoir.

The major parts in the hydrocarbon flow loop are as follows:

a- A pressure vessel. This is used as a feed reservoir with a capacity of 23 gallons (105 litres) and was tested to 500 PSI (34.5 Bar). It is fitted with an electrical heater (2 kW) for pre-heating

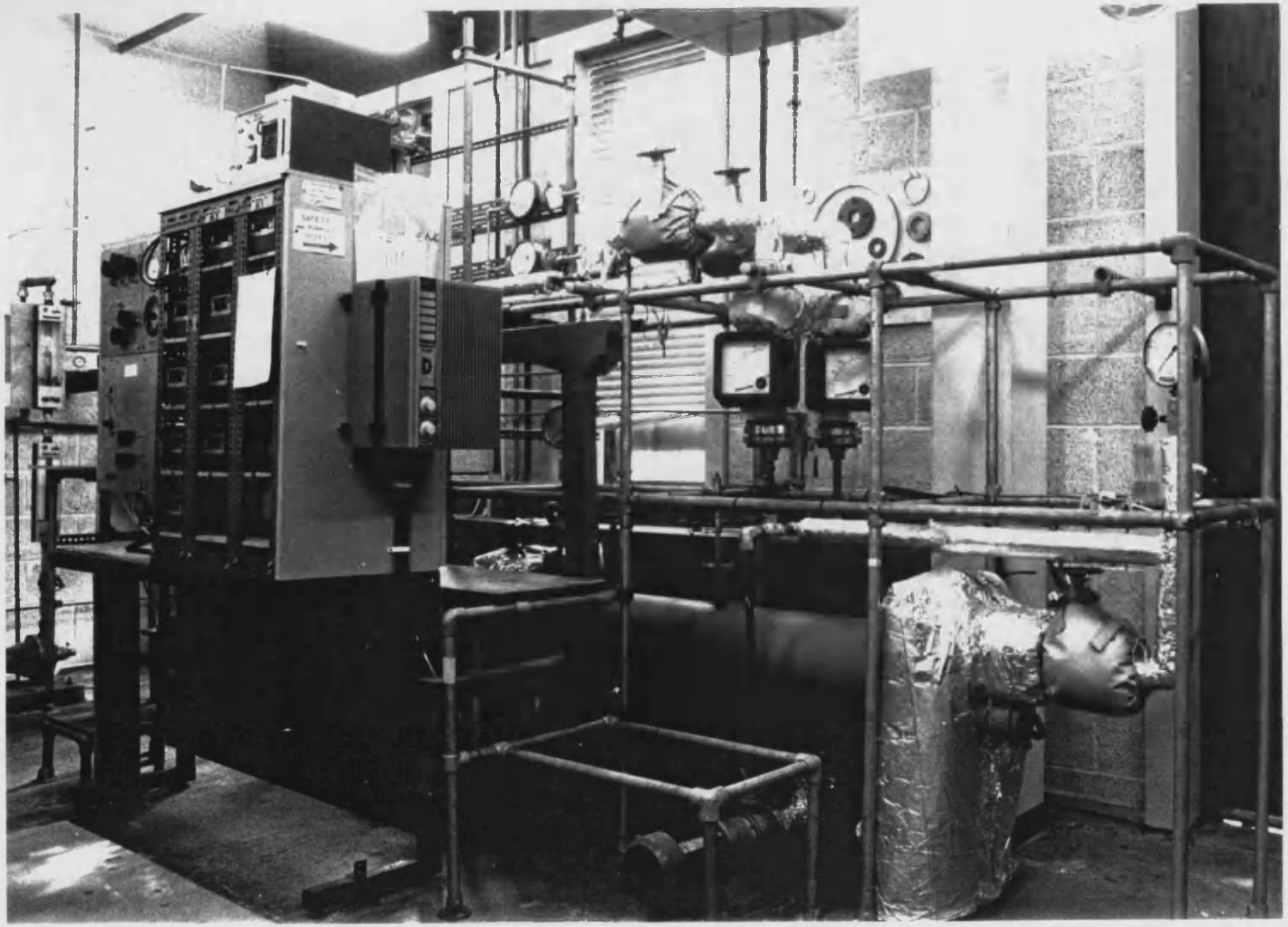

Fig (2.3) Photograph of the experimental apparatus

the fluid. A ball valve (VL8) is fitted in the drainage line in the bottom of the tank. The pressure vessel was specially manufactured by Heatrae Industrial Ltd (works order UO 2746 item 01).

b- A Magnetic Drive Centrifugal Pump (supplied by Worthington Simpson Ltd), designed to deliver 5 m^3/hr of test fluid at a bulk temperature up to 250 ^oC. The pump can generate a head up to 20.4 m , and it is suitable for working pressures up to 20 bar. A motor speed controller supplied by Danfoss Ltd (F on Fig 2.9) is used for controlling the hydrocarbon flow rate in the apparatus.

c- Two sections connected in parallel, in which each had it's own flow meter, power supply and temperature and pressure drop instrumentation; the two sections are very similar and can be controlled under the same operating conditions. Variable Area Flowmeters (Model 9300 supplied by KDG Flowmeters) are used to measure the flow rate of test fluid in each section [FI1 for test section No (1) and FI2 for test section no (2)].

d- Budenberg 316 S.S tube pressure gauges (PI1, PI2 and PI3), each with 0 - 20 bar scale are used to measure the total pressure at three different locations on the hydrocarbon flow loop (see Fig. 2.1). Microvar differential pressure gauges, with 0 - 0.25 and 0 - 0.7 bar ranges and 60 bar maximum working pressure are connected using tappings at X and Y (see Figs 2.4 and 2.8) in order to measure the pressure drop across each test section.

e- Three manual control valves, VL1, VL2 and VL3 (see Fig 2.1) are connected to the test section no (1), test section No (2) and by-pass loop respectively. These valves are used for controlling the flow rate and/or to isolate the relevant test section or by-pass loop. Another large manual control valve VL5 is used for fluid re-cycle control. Three Whitey "60" series ball valves VL4, VL6 and VL7 are fitted to the test loop. VL4 and VL6 are used for calibration of the flowmeters. VL7 is used to link the flowmeters together to one heated test section.

2.2.2 Venting system

The main purpose of the venting system is to protect the equipment and the operator from potential hazards, which could occur if the system pressure were to increase beyond the desired limit. The venting system is shown schematically in Fig 2.2 and it consisted of :

a- An in-line adjustable pressure relief valve (VG1) supplied by Swagelok. This has an operating range of 0 to 15 bar.

b- A bellows valve (VG2) supplied by Swagelok. This valve is used for regulating the depressurisation of the system in a controlled manner and is designed to operate at high pressure and high temperature.

c- A quick 1/4 turn actuation ball valve (VG3) supplied by Swagelok. This valve would only be used in the case of mechanical failure of valves VG1 and VG2.

d- A multi-tubular cooler (supplied by Bowman) in which a large quantity of water is re-circulated counter-currently to the hydrocarbon vapours.

All vapours condensed in the cooler are collected in a large glass reservoir, while the non-condensable gases are vented outside the laboratory

via a flame arrester. 1/2 inch O.D pipe is used throughout the vent system.

2.3 Heated test section design

Both heated test sections are made from 3/4 inch BWG14 carbon steel tube. The overall dimensions of each heated test section within the flow loop are shown in Fig 2.4 . The design specification of each test section is follows:

Outside diameter	(D_o)	= 1.905 cm (3/4 in)
Inside diameter	(D_i)	= 1.483 cm (0.584 in)
Wall thickness	(x)	= 0.211 cm (0.083 in)
Heated length	(L)	= 27.2 cm (10.71 in)
Jacket tube outside diameter	(D_{Jo})	= 3.81 cm (1.5 in)
Jacket tube inside diameter	(D_{Ji})	= 1.905 cm (3/4 in)

A calming section of 73 inner pipe diameters (107.8 cm from the inlet end) is used to ensure that the flow boundary layer is fully developed on entry to the heated section. In the position shown in Fig 2.4, the heating jacket tube was tightly clamped over the outer surface of each test section as follows:

- the jacket tube was heated to a high temperature,
- the test section tube was filled with liquid nitrogen and inserted into the jacket tube.
- by expansion of the test section tube and contraction of the jacket tube, latter

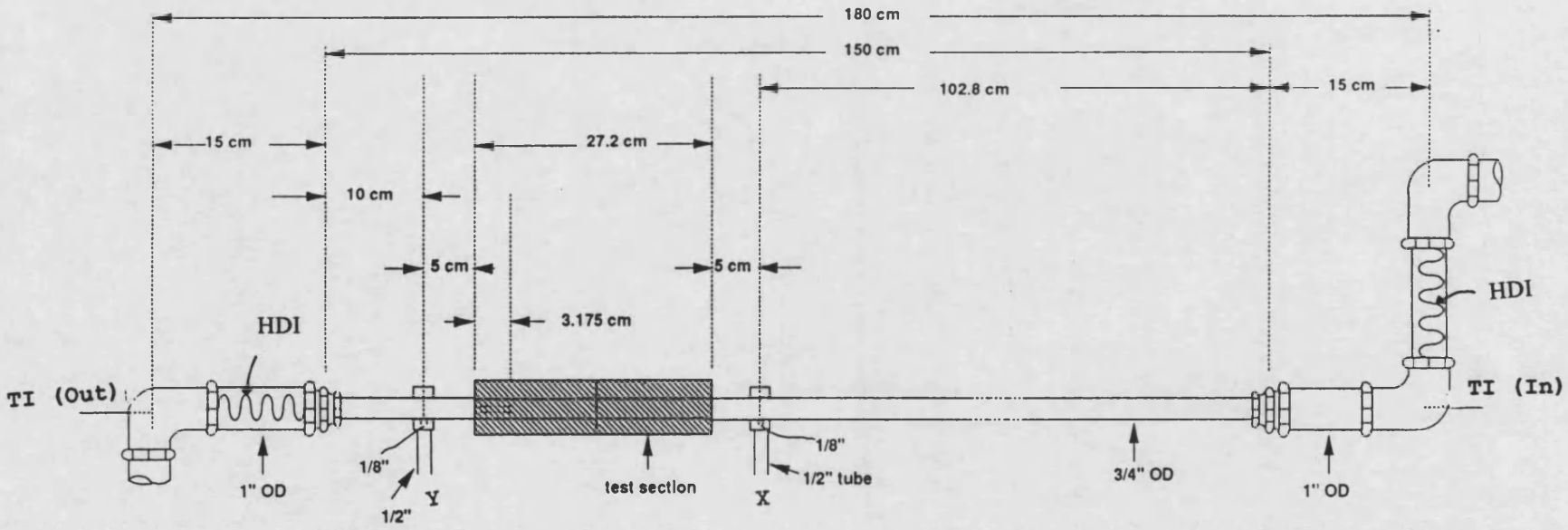

Fig 2.4 The Heated Test Section Location within the Test Loop

was fixed permanently over the outer surface of the test section as shown in Fig. 2.5.

In order to provide uniform indirect heating for each test section, four electrical heating elements, each one 165.1 cm (65 in) long and 0.1588 cm(1/16 in) O.D, were used as shown in Figs. 2.6 and 2.7. The following procedure was applied to fit the electrical elements;

- A 5 mm pitch channel was machined on to the outer surface of the jacket tube.
- Four electrical cables were tightly wound (one after the other) into the channel.
- The four heating elements were connected in series to one power supply.

2.4 Process variable measurements

The effect of process variables such as temperature, power supply, flow rate, and pressure on heat transfer parameters and fouling were extensively studied during this research. Process variables were measured with precision using the calibrated instruments in order to minimise experimental errors.

2.4.1 Temperature measurements

Temperature measurement is the main source of heat transfer and fouling data in this experimental study. Temperatures of the test fluid, and of the

Fig (2.5) Photograph of the jacket tube over the test section

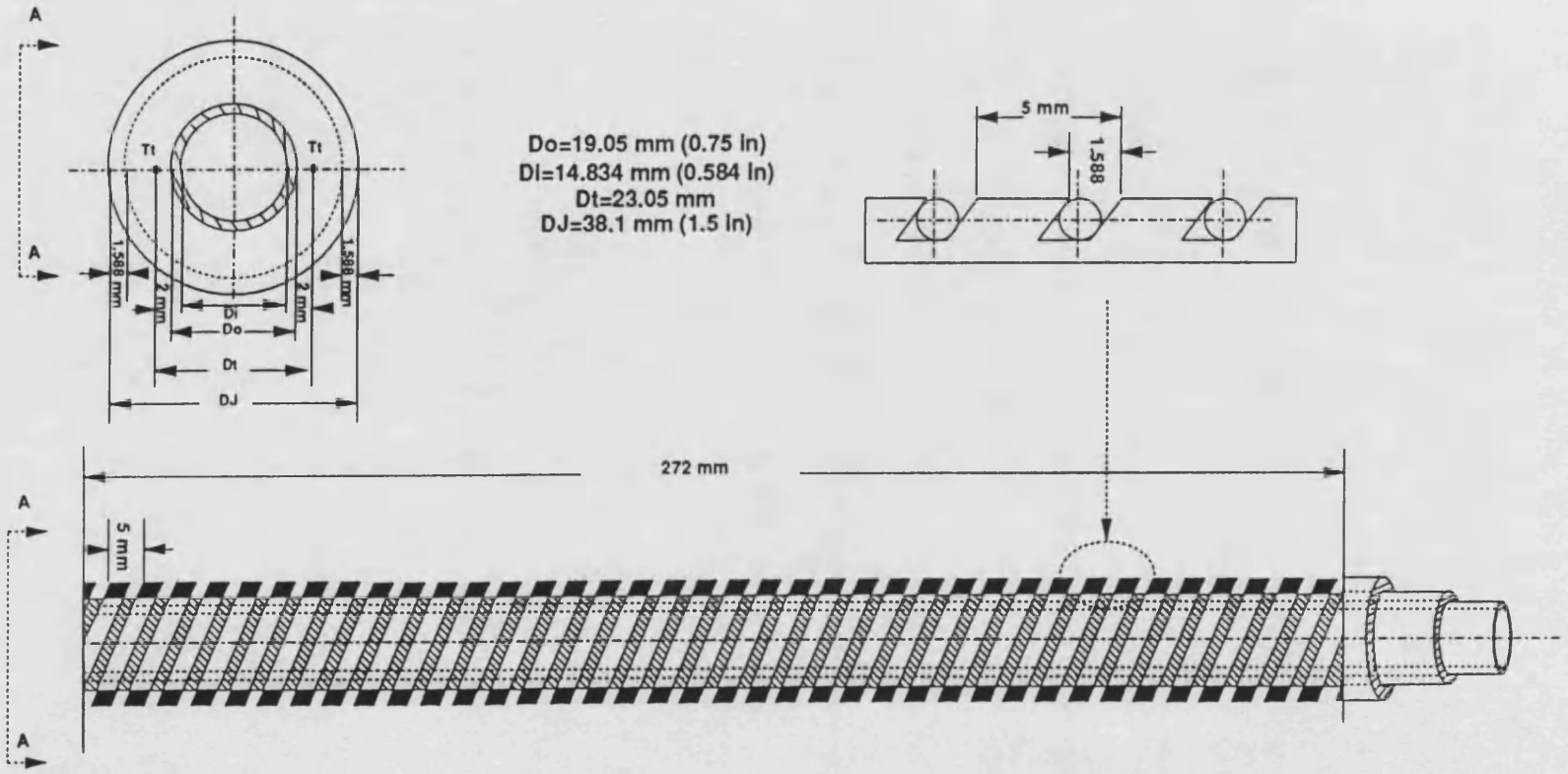

Fig 2.6 The heating Element Configuration on the Outer Surface of the Jacket Tube

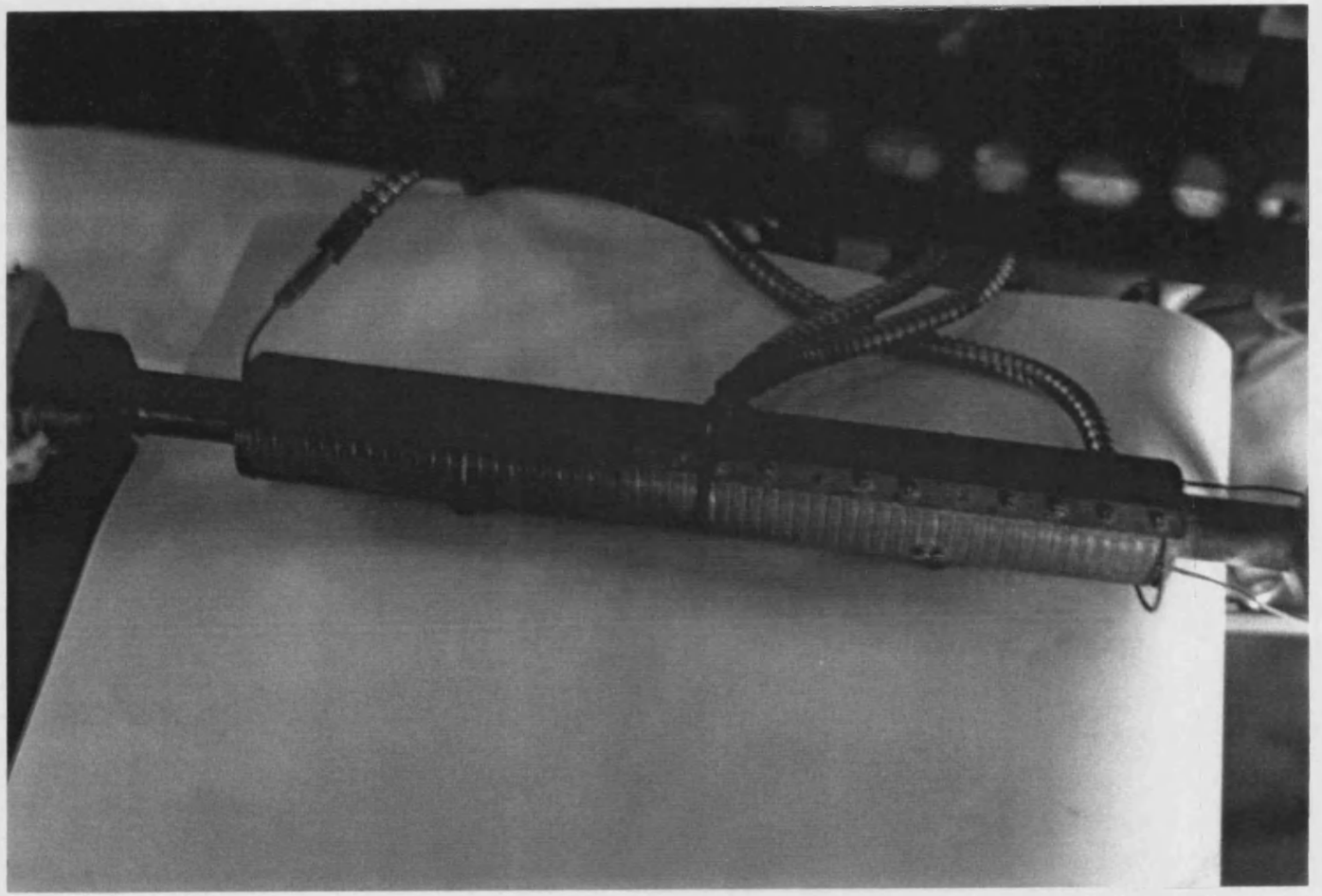

Fig (2.7) Photograph of the heated test section

test section tube wall were measured using chromel-alumel thermocouples. The locations of the thermocouples for both test sections are shown in Fig 2.8 .

Two thermocouples were used for measuring the tube wall temperature in each test section [T_3 and T_4 for test section No (1) and T_7 and T_8 for test section No (2)]. The thermocouples were embedded, then silver soldered into axial holes inside the wall of the jacket tube (one into each side). Each hole was drilled 31.8 mm (1.25 in) from the exit and 2 mm from the inner surface of the jacket tube.

A single thermocouple was used to measure the test fluid inlet temperature for each test section, T_1 and T_5 for test sections No (1) and No (2) respectively. The outlet temperature of the test fluid was also measured by a single thermocouple, T_2 for test section No (1) and T_6 for test section No (2). In order to avoid radial temperature variations and also to improve accuracy, the test fluid passed through a 10 cm length of high density **HiTran** insert (HDI) immediately prior to an inlet or outlet bulk fluid thermocouple as shown in Fig 2.4 .

There were two reasons for using only two thermocouples for tube wall temperature measurements:

1- The length of the test section is too short to accommodate more than two axial thermocouples.

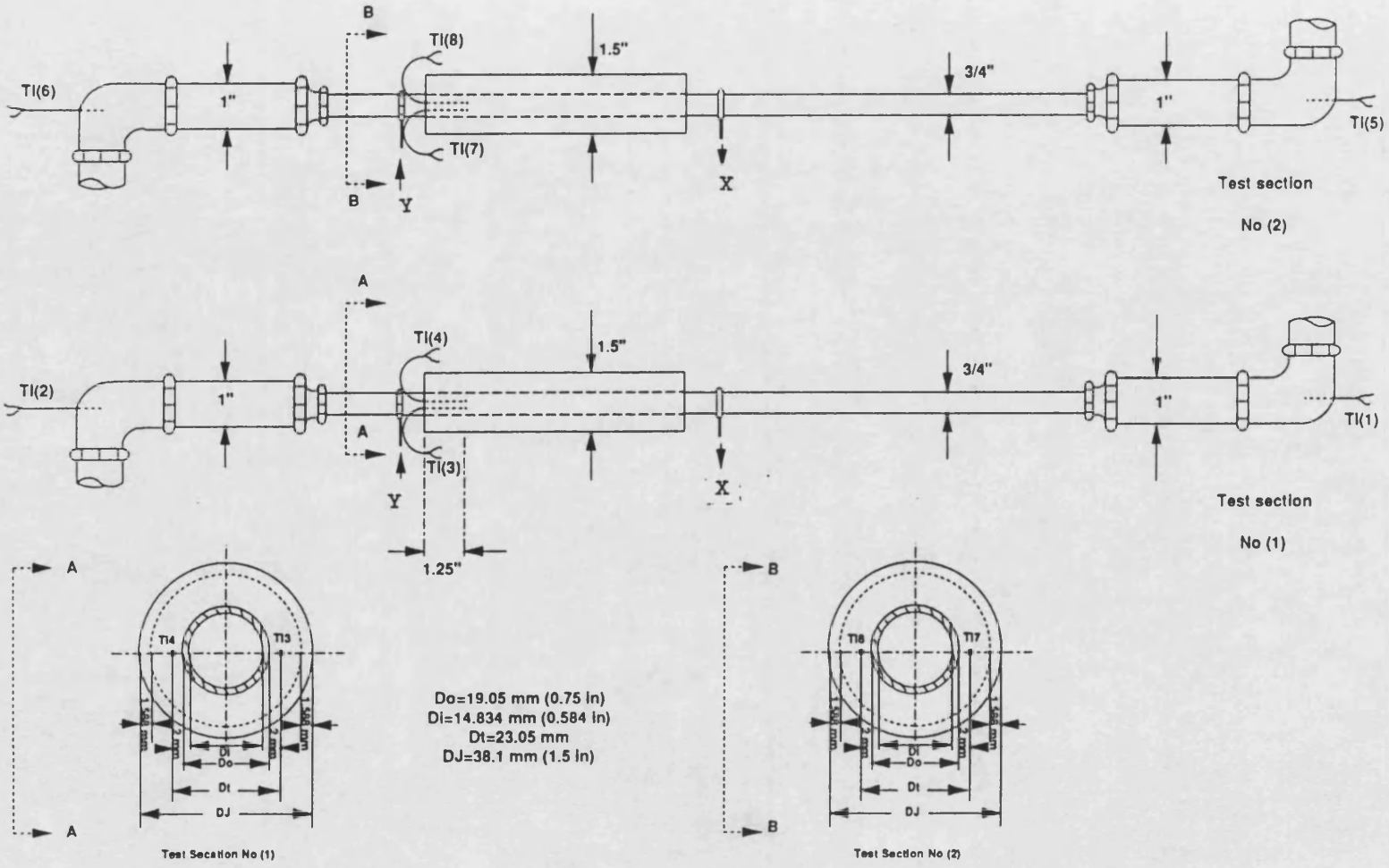

Fig 2.8 Schematic of The Thermocouples Location for Both Test Sections

2- The location for thermocouples near to the exit end of the test section is the best position for local heat transfer coefficient and local fouling resistance studies since the thermal and velocity profiles would be developed.

Such a thermocouple location has been used by other workers. For example, Ritter[104] used the HTRI test section for his crystallisation fouling studies. Only the data from two thermocouples near the exit end of the test section were considered in evaluating the results. The data from five other thermocouples were not of any significant value.

In this study, all thermocouples were calibrated against a thermocouple which had been calibrated previously by National Physical Laboratory Instruments. The calibration results were within ±0.3 ^{o}C for all the original thermocouples and ±1.5 ^{o}C for two replacement thermocouples T_2 and T_6 for which correction factors were applied.

2.4.2 Power measurement

The four heating elements of each test section were connected in series to one Fi-monitor Triac Regulator (Variac), supplied by Fisons, [shown as M1 for Test Section No (1) and M2 for test section No (2) in Fig 2.9]. Both M1 and M2 were linked via a selector switch (S) to a digital wattmeter,

supplied by Tabor Electronics Ltd. The power supplied to each test section was controlled by adjusting the Variac and the readings were taken directly from the digital wattmeter, which is within ±2W accuracy (manufacturer's specification).

2.4.3 Flow rate measurement

The flow rate of the test fluid in each test section was measured as a percentage of the full scale flowmeter reading (% F.S.R). The flowmeters were originally designed for a capacity of 2.5 m^3/hr of water at 20 ^oC. However, they were re-calibrated twice during the experimental study using Santotherm 55 and Arabian light crude oil (see Chapters 3 and 4).

The flowmeters comprised two main sub-assemblies. These were the main body of the flowmeter and the basic indicator.

The principle of flowmeter operation is summarised as follows:

When the test fluid passes through the body of the meter, the float within the body is carried upwards, within the divergent metering tube, to the level where the force exerted against the float equals that of the float weight. Thus the greater the flow rate, the higher the float level. The float rises to a height which is proportional to the rate of flow calibrated from 10 - 100% of full scale position.

The position of the bar magnet in the float is sensed by the follower magnet assembly on the end of the indicator spindle. As the float rises or falls according to the flow rate, the indicator pointer will swing across the scale over an arc of 100%.

2.4.4 Pressure measurement

In the crude oil study, the test equipment was operated under elevated pressure using either nitrogen or helium above the liquid surface in the reservoir. The total pressure was monitored to ensure that the crude oil would not vaporise at the operating bulk fluid temperature which ranged from 70 to 150 ^{o}C.

In enhancement of heat transfer studies, pressure drop (Δp) measurements were also important for enhancement factor (EF) calculations, equation 1.99 , when **HiTran** inserts were used.

2.5 Equipment operation and experimental procedure

Detailed specifications of the two different hydrocarbon liquids studied (Santotherm 55 and Arabian light crude oil) are given in Chapters 3 and 4.

The experimental procedure for both hydrocarbon fluids may be summarised as follows (refer to Figs 2.1, 2.2 and 2.9):

2.5.1 Preparation of equipment.
2.5.2 Pre-heating procedure.
2.5.3 Normal operation and data acquisition for Santotherm 55.
2.5.4 Normal operation and data acquisition for crude oil.
2.5.5 Shut-down procedure.
2.5.6 Dismantling of the test sections.

2.5.1 Preparation of equipment

The drainage valves VL6 and VL8 were closed and the reservoir was filled with test fluid (Santotherm 55 or crude oil) . The heating element inside the tank was always covered by liquid. The test equipment was checked for leaks under 15 bar gauge of N_2 gas pressure. For the crude oil study the pressure relief valve (VG1) was manually adjusted to 13 - 15 bar (according to the operating conditions).

2.5.2 Pre-heating procedure

The heating element inside the reservoir was switched on to bring the fluid to a desired bulk temperature. It could take 7 - 8 hrs to bring the fluid temperature up to 150 ^{o}C. The pump was started and the test fluid was circulated around the by-pass loop at a low pump speed (controlled by " F "). For the crude oil study, the fluid was blanketed with nitrogen (sufficient to raise the pressure by 1 bar) to avoid any oxidation problems. For the Santotherm 55 study, the pre-heating period could be reduced to 2 - 3 hrs by recycling the fluid around the test

loops and supplying 1 kW power to each test section. This procedure was not adopted for the fouling fluid, crude oil.

2.5.3 Normal operation and data acquisition for the Santotherm 55 study

Santotherm 55 is a non-fouling fluid (see Chapter 3). Thus it was used for studying the heat transfer coefficients of the test sections with and without HiTran inserts under clean conditions at different bulk fluid temperatures, heat fluxes and flow rates.

When the desired bulk temperature was obtained, the power supplied to the relevant test sections was controlled at the required operating value using M1 and M2. The flow rate (% F.S.R) in each test section was controlled by using controller "F" and/or by opening/closing the valves VL1, VL2, VL3 and VL5.

During the run, which usually took 8 hrs, the following variables were monitored and recorded on data sheets at agreed intervals of not less than 10 mins:

Time	: local
% F.S.R	: FI_1, FI_2
Temperature (^oC)	: $T_1, T_2, T_3, T_4, T_5, T_6, T_7, T_8$.
Pressure (bar)	: P_1, ΔP_1, ΔP_2, ΔP_3, ΔP_2.
Power supplied (in Watts)	: No (1) and No (2)

An example data sheet used to record this information is shown in Appendix (A).

2.5.4 Normal operation and data acquisition for the crude oil study

Arabian light crude oil was used for the fouling study. Changes in heat transfer coefficients of the test sections were followed with time. One of the test sections was fitted with a low density **HiTran** insert (LDI) and the other left bare.

When the desired bulk temperature was achieved, the crude oil was circulated around the test loops and the equipment was pressurised to the desired operating pressure. 15 to 20 mins later the flow rate (% F.S.R) was controlled to the required level, and the power supply to the relevant test section was turned on and controlled to the desired wattmeter reading.

The same variables which were monitored in section 2.5.3 were recorded for the crude oil on similar data sheets at an agreed interval of not less than 30 mins. Runs lasted from about 19 to 185 hours (see Chapter 4).

2.5.5 Shut-down procedure

At the end of each run, the power supply to the equipment was turned off. The test fluid was allowed to circulate for 15 - 20 minutes before the pump could be isolated. For the crude oil study, the system was carefully depressurised using the valve VG2, when the crude oil had sufficiently cooled, i.e., $T_1 < 30\ ^{o}C$.

Under emergency conditions, the shut-down was possible by turning isolators "A" and "G".

2.5.6 Dismantling of test sections

The test sections had to be dismantled either to change in-tube HiTran inserts (for the Santotherm 55 study) or to inspect the inner surface of test sections for fouling deposits in the crude oil study. After the test sections were reassembled, a pressure check was made and the equipment was prepared for the next run.

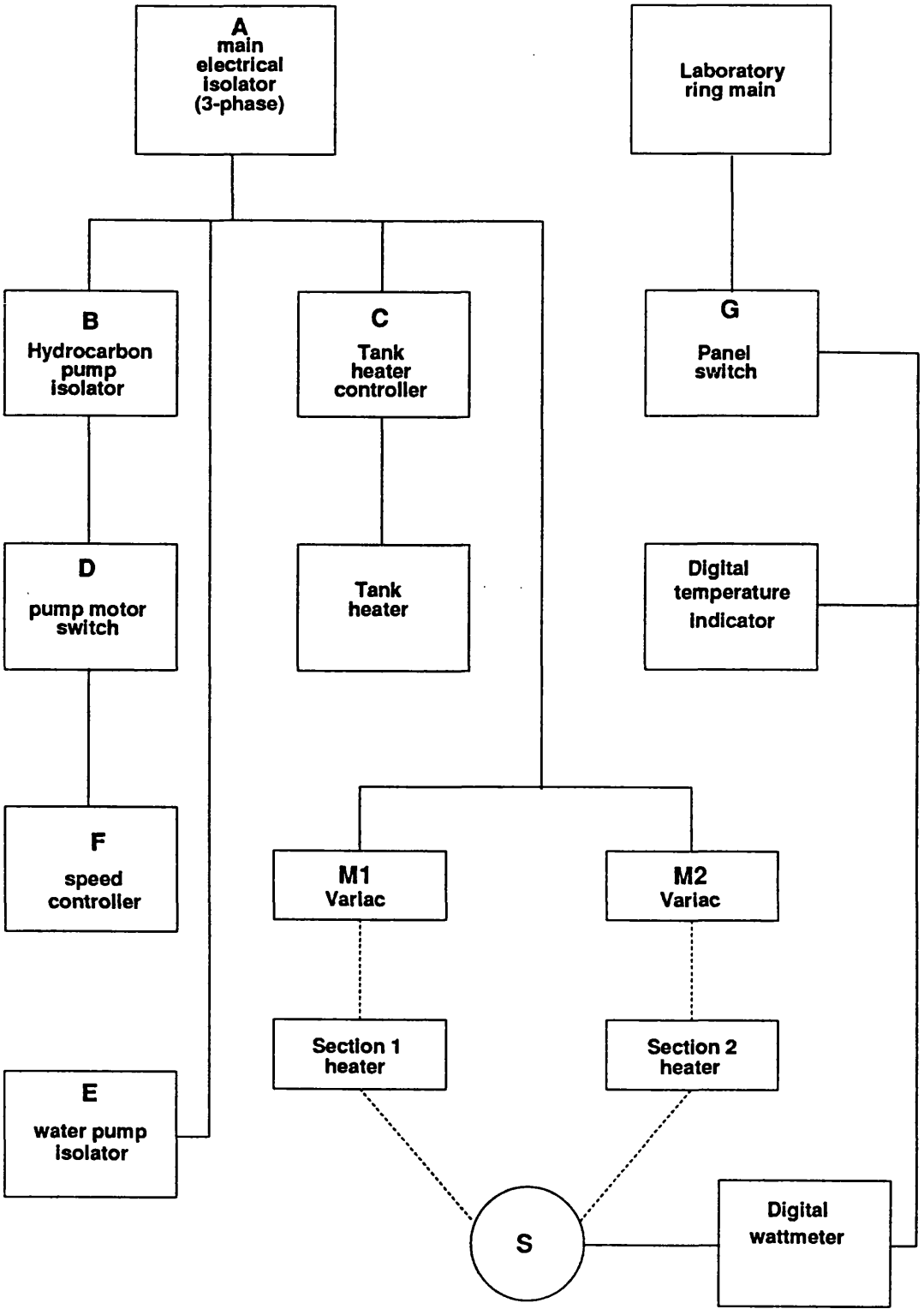

Fig 2.9 Schematic of The Electrical Network

Chapter 3
Santotherm 55 Study

3.1 Introduction

In order to provide a sound basis for heat transfer and friction factor calculations, Santotherm 55 fluid was used in the apparatus as a non-fouling fluid . Santotherm 55 is a synthetic hydrocarbon fluid used for heat transfer applications where operating temperatures are moderate.

The study to monitor the heat transfer performance of the test sections was carried out for both the bare tube and for the tube fitted with different types of **HiTran** insert. Comparisons have been made for various experimental conditions.

3.2 Specification of Santotherm 55 fluid

Santotherm 55 has an operating range of -18 ^{o}C to 316 ^{o}C (0 ^{o}F to 600 ^{o}F) and a pour point of -40 ^{o}C. As a heat transfer fluid , it has a wide viscosity range (from 16 $N.s.m^{-2}$ at -20 ^{o}C to $3.6x10^{-3}$ $N.s.m^{-2}$ at 340 ^{o}C), high specific heat and high thermal conductivity . It is one of a series of six Monsanto synthetic heat transfer fluids, covering an operating range from -50 ^{o}C to 400 ^{o}C, as seen in Table 3.1.

Table 3.1 Comparison between six different Santotherm fluids

Fluid type	Operating range °C	Flash Point°C	Max.Bulk temp.°C	Max.Film temp.°C	Av. M.wt kg kmol^{-1}	Boiling Range°C for 10%	for 90%
Santotherm 44	-50 to 220	207	204	246	367	337	390
Santotherm 55	-18 to 316	177	288	340	340	335	355
Santotherm 60	-50 to 316	154	327	346	250	288	394
Santotherm 66	0 to 350	177	343	374	240	339	353
Santotherm 75	75 to 350	199	399	429	255	NA	NA
Santotherm 88	140 to 400	NA	NA	NA	NA	NA	NA

3.2.1 Thermal stability

Santotherm 55 has a superior stability compared with many mineral, oil based, heat transfer fluids. Monsanto claims this superiority has been demonstrated over many millions of hours of successful system operations in laboratories.

The risk of fouling or coking on heat transfer surfaces , due to the formation of polymeric degradation products which are known as "high boilers" is considered to be the most critical indicator of a fluid's stability and ultimate life. The time taken to reach 10 percent "high boiler" level is used as a measure of performance in comparative tests .

Table 3.2 High boiler formation - Comparison between Santotherm 55 and some mineral oils.

Temp. (°C)	Time to reach 10% "high boiler" (hours)		
	Santotherm 55	Mineral oil M600	Mineral oil T65
288	37000	6000	12000
316	5000	1000	1500
343	500	200	200

Table 3.2 shows that if Santotherm 55 fluid is left for 37000 hours at 288 °C, then 10% of the total weight will be degraded. In the present study, the maximum bulk temperature was 150 °C and the maximum surface temperature was 220 °C and the total operating time was less than 2500 hours. Therefore it is a reasonable assumption that there would be no risk of thermal degradation and hence no risk of fouling from the use of Santotherm 55 .

3.2.2 Physical properties

The most important physical properties of Santotherm 55 fluid as provided by the supplier are listed in Table 3.3

The variation of some physical properties, such as density (ρ), specific heat (C_p), thermal conductivity (k), and kinematic viscosity (υ), with temperature as supplied by the manufacturer are shown in Figs. 3.1 to 3.4 . The data have been correlated as follows :

$$\rho \ (kg\ m^{-3}) = 1086.14 - 0.671\ T \quad (3.1)$$

$$C_p \ (kJ\ kg^{-1}\ K^{-1}) = 0.797 + 3.767 \times 10^{-3}\ T \quad (3.2)$$

$$k \ (W\ m\ K^{-1}) = 0.1647 - 9.463 \times 10^{-5}\ T \quad (3.3)$$

$$\upsilon \ (mm^2\ s^{-1}) = 10^{(e^a/T^b)} - c \quad (3.4)$$

where:

T is absolute temperature (K)

a is constant = 22.336

b is constant = 3.825

c is constant = 0.7526

An average error of ±1.5% can be expected from equation 3.4 for the temperature range 40-340 °C.

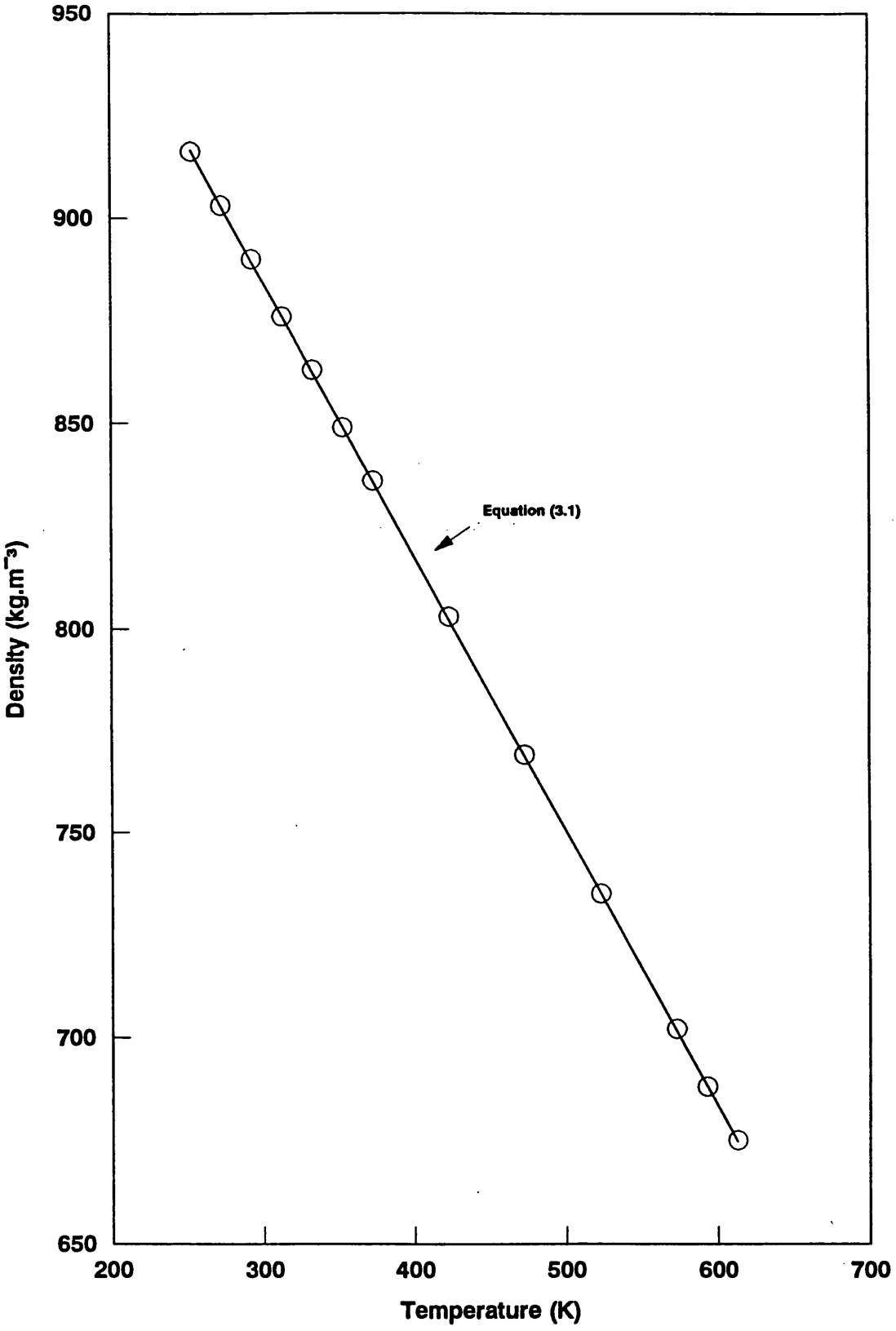

Fig(3.1) Density (ρ) Vs. Absolute Temperature for Santotherm 55

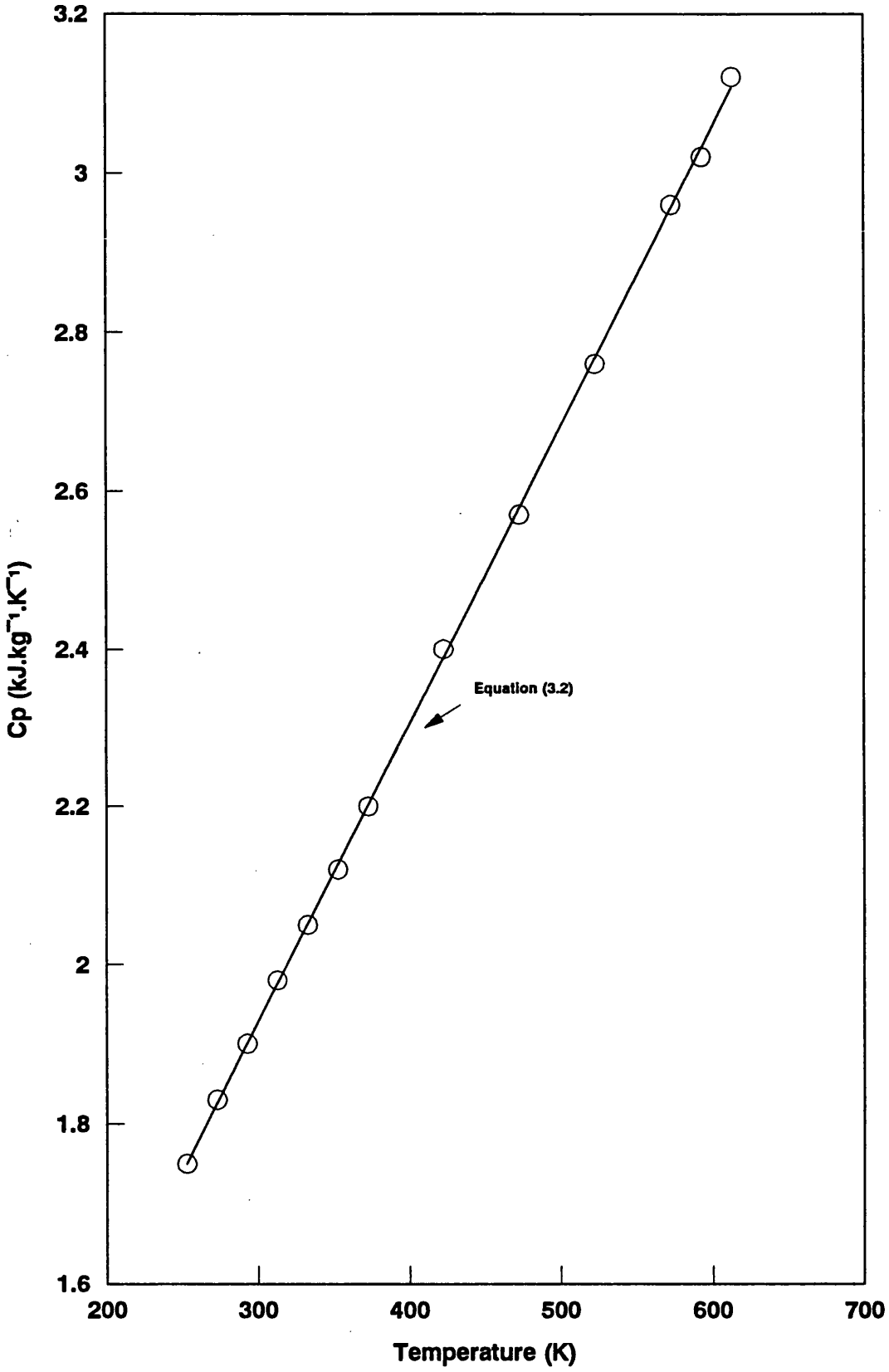

Fig(3.2) Specific heat (Cp) Vs. Absolute Temperature for Santotherm 55

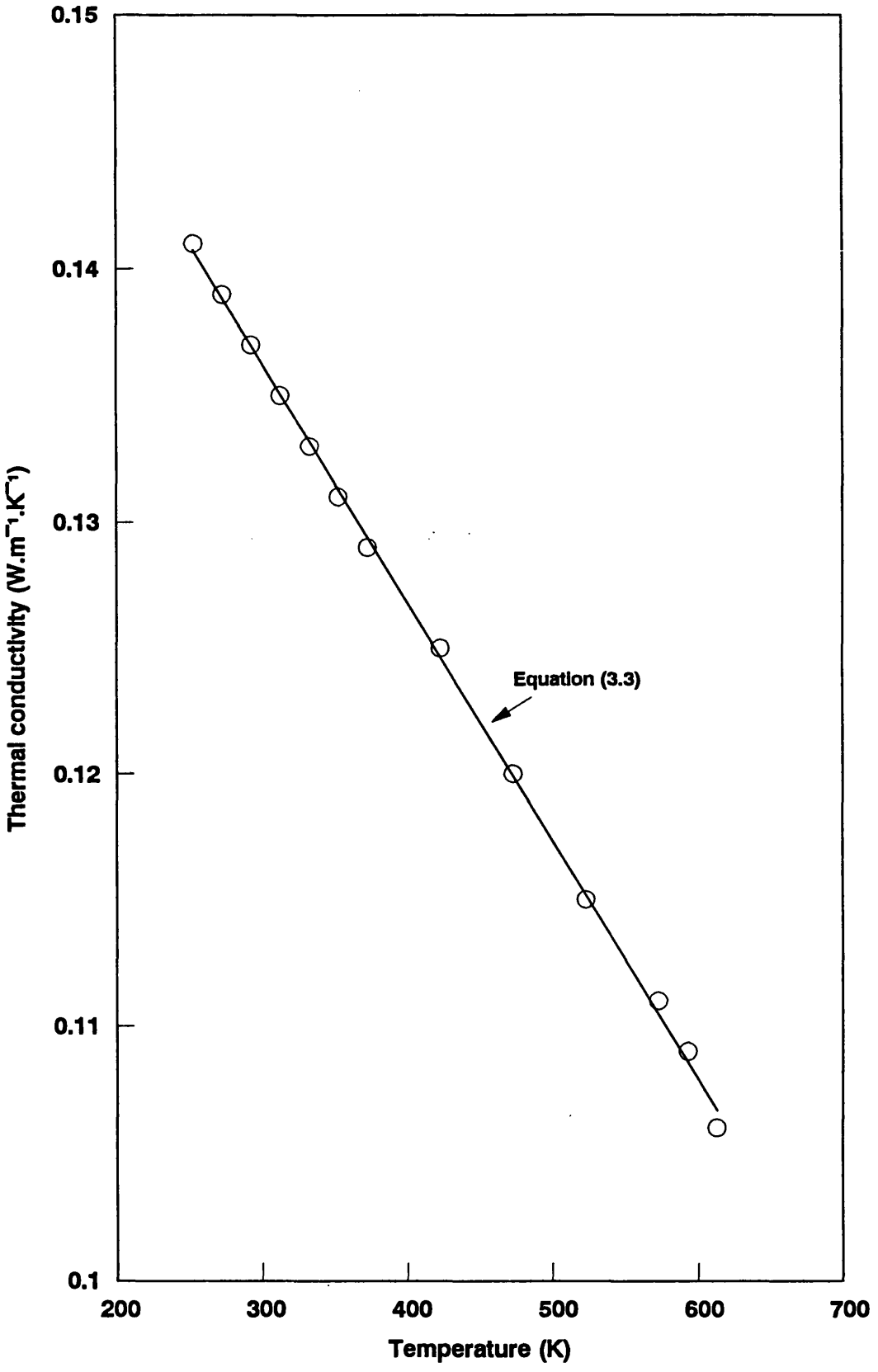

Fig(3.3) Thermal conductivity Vs. Absolute Temperature for Santotherm 55

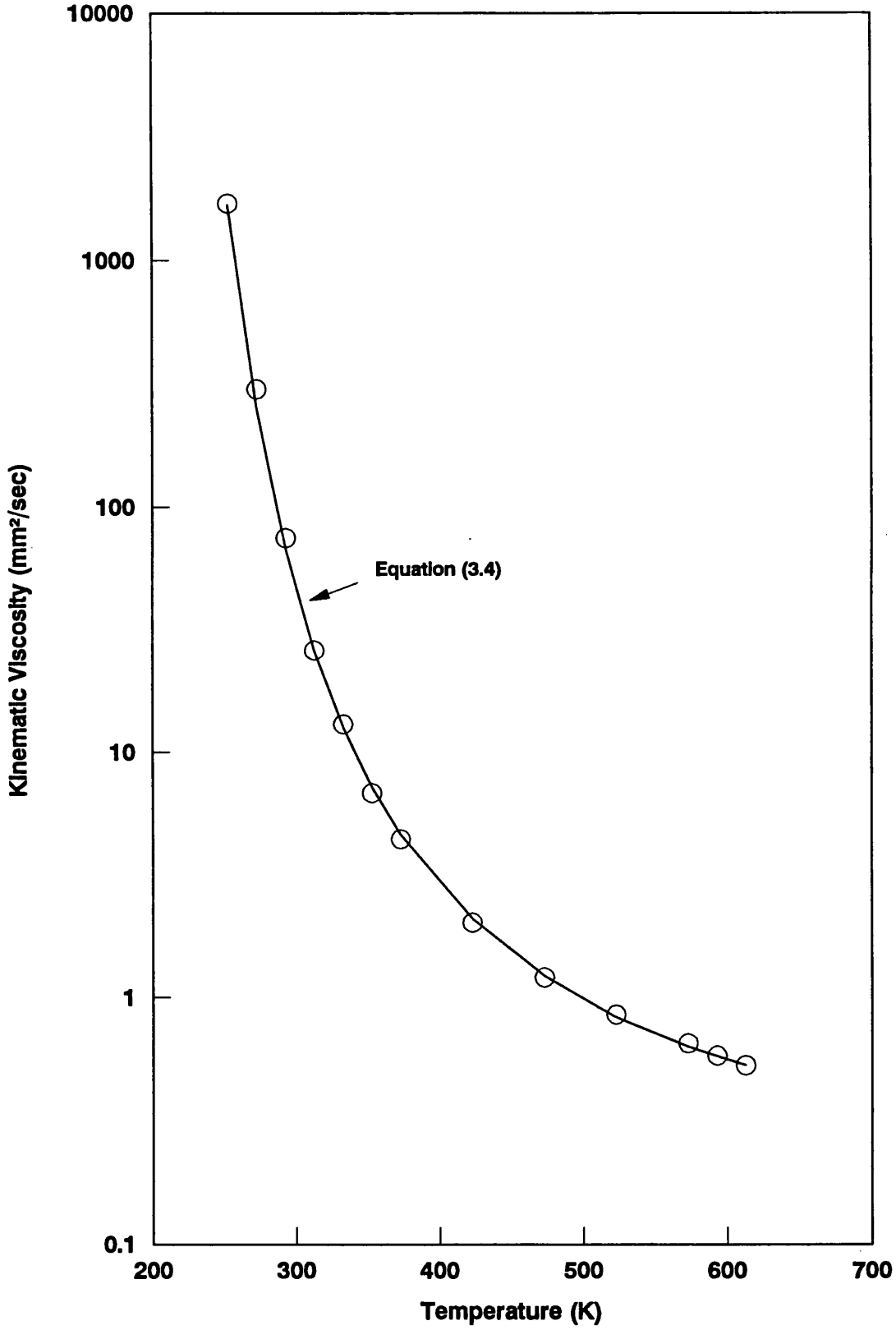

Fig (3.4) kinematic viscosity Vs. Absolute Temperature for Santotherm 55

Table (3.3) Physical Properties of Santotherm 55

Composition	Synthetic hydrocarbon mixture
Appearance	clear yellow liquid
Density at 15 °C	893 (Kg m^{-3})
°API	27
Temp. for Kinematic Viscosity of 300 cst (mm^2 s^{-1})	0 °C
Kinematic viscosity at 50 °C	12-26 (mm^2 s^{-1})
Flash point	177 °C
Fire point	240 °C
Autoignition point	357 °C
Pour point	-40 °C
Boiling range 10% 90% Coefft. of thermal expansion for the range 40 - 315 °C	 335 °C 355 °C 0.00075/ °C
Average molecular weight	340 (kg $kmol^{-1}$)

3.3 Calibration of Flowmeters

Having obtained a well-conditioned flow, it was necessary to measure the flow rate with precision. This required either the measure of a certain volume passed in a measured time, or the mass passed in a measured time[1].

Both flowmeters were calibrated at 10 values of % full scale reading (% F.S.R) . The calibration was by the measurement of mass collected in a known amount of time at seven different bulk temperatures (in the range of 50-150 °C) as shown in Table 3.4. For each bulk temperature and % F.S.R , three measurements for mass flow rate were made and the average value is reported in Table 3.5 .

Table 3.4 Flowmeter calibrations

% F.S.R	Bulk temperatures in Flow meter No(1)							Bulk temperatures in Flow meterNo(2)						
10	49.4	69.0	74.8	96.0	118.0	131.6	151.4	50.0	68.5	89.5	97.8	112.0	129.4	151.1
20	49.8	71.8	82.5	98.0	118.0	130.3	151.0	50.3	70.2	89.8	98.6	112.0	126.6	151.8
30	50.2	71.6	86.8	99.3	118.8	127.4	148.0	49.7	72.4	86.5	99.6	114.5	126.6	148.0
40	50.2	71.9	86.5	99.3	114.5	126.4	145.1	50.2	70.7	86.7	100.0	116.7	127.7	145.7
50	50.5	69.0	87.5	99.3	114.2	126.9	144.6	50.0	69.1	87.3	100.0	116.0	125.5	145.0
60	51.2	70.0	88.4	99.0	114.0	125.7	145.2	49.9	71.7	87.4	100.0	116.0	126.4	144.8
70	51.3	70.0	88.8	99.0	113.9	125.7	145.1	50.0	72.5	87.6	100.7	116.2	125.5	144.7
80	50.5	70.7	89.4	99.8	113.9	126.5	144.6	50.3	70.9	88.3	100.7	116.3	125.2	144.7
90	50.0	70.7	89.8	100.5	115.7	125.0	144.8	50.5	71.5	89.7	99.6	117.0	126.0	145.0
100	50.8	70.9	90.6	100.5	117.2	125.1	144.9	50.6	69.7	90.3	99.9	118.0	125.1	144.9

The mass flow rate for a given % F.S.R was found to be dependent on temperature due to the variation of density and viscosity with this parameter . Thus for constant % F.S.R, the mass flow rate was plotted against temperature and linear least squares regression analysis was applied to the data shown in Figs 3.5 to 3.10 to obtain the following calibration equations :

For Flowmeter No (1)

M_1 (10%) = 260.484 - 0.0455 T (^oC) (3.5)
r = -0.998

M_1 (20%) = 490.950 - 0.2292 T (^oC) (3.6)
r = -0.980

M_1 (30%) = 718.580 - 0.4053 T (^oC) (3.7)
r = -0.996

M_1 (40%) = 935.222 - 0.4607 T (^oC) (3.8)
r = -0.988

M_1 (50%) = 1134.455 - 0.3424 T (^oC) (3.9)
r = -0.992

M_1 (60%) = 1360.910 - 0.2625 T (^oC) (3.10)
r = -0.954

M_1 (70%) = 1552.00 - 0.1206 T (^oC) (3.11)
r = -0.938

M_1 (80%) = 1801.624 - 0.4142 T (^oC) (3.12)
r = -0.952

Table 3.5 Calibration of Flow meters using santotherm 55 fluid

Flow meter No (1) in Test section No (1)						
% F.S.R	Bulk Temperature (°C)	Mass Flow Rate (Kg/hr)	Flowmeter Flow Rate (m^3/hr)	Velocity (m/sec)	Kinematic Viscosity (mm^2/sec)	Re
10	49.4	258.16	0.2968	0.4773	18.120	390.64
	69.0	257.31	0.3004	0.4830	9.671	740.73
	74.8	257.14	0.3015	0.4849	8.255	871.21
	96.0	256.20	0.3055	0.4913	5.018	1451.99
	118.0	255.12	0.3097	0.4980	3.321	2223.91
	131.6	254.58	0.3125	0.5026	2.677	2784.27
	151.4	253.48	0.3163	0.5087	2.039	3700.06
20	49.8	477.34	0.5490	0.8828	17.859	733.07
	71.8	476.15	0.5570	0.8958	8.947	1484.87
	82.5	471.72	0.5565	0.8950	6.796	1952.92
	98.0	471.09	0.5627	0.9049	4.815	2787.07
	118.0	463.72	0.5629	0.9053	3.321	4042.30
	130.3	460.20	0.5643	0.9075	2.730	4930.54
	151.0	455.67	0.5684	0.9141	2.049	6615.62
30	50.2	696.73	0.8015	1.2890	17.604	1085.87
	71.6	689.76	0.8068	1.2975	8.996	2138.94
	86.8	685.04	0.8110	1.3042	6.141	3149.57
	99.3	679.04	0.8119	1.3057	4.689	4129.26
	118.8	669.58	0.8133	1.3080	3.277	5919.60
	127.4	668.04	0.8172	1.3142	2.853	6830.57
	148.0	657.33	0.8179	1.3154	2.130	9159.15
40	50.2	911.55	1.0486	1.6864	17.604	1420.66
	71.9	904.41	1.0581	1.7017	8.922	2828.33
	86.5	895.75	1.0602	1.7049	6.183	4088.99
	99.3	889.61	1.0637	1.7106	4.689	5409.72
	114.5	878.16	1.0630	1.7094	3.526	7189.03
	126.4	876.21	1.0710	1.7223	2.898	8813.63
	145.1	871.17	1.0814	1.7391	2.213	11655.62
50	50.5	1115.85	1.2800	2.0648	17.415	1758.26
	69.0	1112.69	1.3000	2.0888	9.670	3203.12
	87.5	1103.83	1.3100	2.1026	6.042	5160.13
	99.3	1101.60	1.3200	2.1183	4.689	6698.86
	114.2	1093.61	1.3200	2.1283	3.544	8903.90
	126.9	1092.26	1.3400	2.1479	2.875	11077.33
	144.6	1084.40	1.3500	2.1638	2.227	14405.92
60	51.2	1346.50	1.5500	2.4930	16.986	2176.43
	70.0	1343.49	1.5700	2.5240	9.403	3980.83
	88.4	1338.35	1.5900	2.5512	5.920	6390.46
	99.0	1335.96	1.6000	2.5683	4.718	8072.92
	114.0	1328.30	1.6100	2.5847	3.557	10775.24
	125.7	1324.26	1.6200	2.6015	2.930	13167.60
	145.2	1319.60	1.6400	2.6345	2.210	17680.27
70	51.3	1544.20	1.7800	2.8592	16.927	2505.02
	70.0	1543.62	1.8000	2.9000	9.403	4573.83
	88.8	1542.36	1.8300	2.9410	5.867	7433.77
	99.0	1541.84	1.8400	2.9641	4.718	9317.02
	113.9	1537.65	1.8600	2.9918	3.564	12450.67
	125.7	1538.05	1.8800	3.0215	2.930	15293.43
	145.1	1532.60	1.9000	3.0594	2.213	20505.05
80	50.5	1775.14	2.0426	3.2848	17.415	2797.13
	70.7	1778.24	2.0786	3.3426	9.222	5375.51
	89.4	1765.35	2.0942	3.3678	5.789	8628.17
	99.8	1762.67	2.1085	3.3908	4.642	10831.68
	113.9	1750.34	2.1177	3.4056	3.564	14172.87
	126.5	1752.83	2.1426	3.4457	2.893	17660.39
	144.6	1738.75	2.1574	3.4695	2.228	23098.75
90	50.0	1989.80	2.2910	3.6806	17.731	3078.43
	70.7	1987.86	2.3221	3.7367	9.222	6009.18
	89.8	1976.30	2.3533	3.7715	5.737	9749.04
	100.5	1969.71	2.3612	3.7912	4.578	12281.74
	115.7	1958.40	2.3714	3.8160	3.454	16384.95
	125.0	1949.22	2.3825	3.8270	2.963	19158.08
	144.8	1944.65	2.4118	3.8810	2.222	25907.56
100	50.8	2203.87	2.5416	4.0791	17.223	3510.89
	70.9	2201.31	2.5714	4.1386	9.171	6692.39
	90.6	2200.10	2.6121	4.2012	5.636	11054.63
	100.5	2196.65	2.6374	4.2280	4.578	13696.80
	117.2	2193.40	2.6611	4.2791	3.366	18850.80
	125.1	2191.06	2.6819	4.3022	2.958	21570.86
	144.9	2188.30	2.7242	4.3676	2.219	29194.97

Table 3.5 (Continued)

Flow meter No (2) in Test section No (2)						
% F.S.R	Bulk Temperature (°C)	Mass Flow Rate (Kg/hr)	Flowmeter Flow Rate (m^3/hr)	Velocity (m/sec)	Kinematic Viscosity (mm^2/sec)	Re
10	50.0	265.60	0.3055	0.491	17.731	410.91
	68.5	262.83	0.3067	0.493	9.809	745.68
	89.8	258.77	0.3071	0.494	5.737	1276.51
	97.8	258.49	0.3087	0.496	4.835	1522.80
	112.0	256.26	0.3096	0.498	3.685	2003.40
	129.4	253.74	0.3109	0.500	2.767	2679.73
	151.1	249.11	0.3108	0.500	2.047	3621.48
20	50.3	486.70	0.5599	0.900	17.541	761.31
	70.2	482.65	0.5639	0.907	9.351	1438.33
	89.8	474.64	0.5632	0.906	5.737	2341.39
	98.6	472.80	0.5650	0.909	4.756	2833.01
	112.0	466.83	0.5639	0.907	3.685	3649.60
	126.6	464.15	0.5674	0.912	2.889	4684.11
	151.8	452.72	0.5651	0.909	2.029	6644.13
30	49.7	698.98	0.8038	1.293	17.924	1069.50
	72.4	693.38	0.8116	1.305	8.802	2198.96
	86.5	687.78	0.8140	1.309	6.183	3139.63
	99.6	681.18	0.8147	1.310	4.661	4168.40
	114.5	670.95	0.8122	1.306	3.526	5492.73
	126.6	667.38	0.8159	1.312	2.889	6735.09
	148.0	657.86	0.8186	1.316	2.130	9166.50
40	50.2	908.15	1.0447	1.680	17.604	1415.35
	70.7	902.80	1.0553	1.697	9.222	2729.10
	86.7	898.70	1.0638	1.711	6.155	4122.10
	100.0	892.90	1.0682	1.718	4.624	5509.89
	116.7	890.44	1.0798	1.736	3.395	7584.81
	127.7	882.80	1.0802	1.737	2.840	9070.71
	145.7	873.94	1.0854	1.745	2.195	11792.20
50	50.0	1117.07	1.2800	2.066	17.730	1728.22
	69.1	1110.98	1.3000	2.086	9.643	3207.51
	87.3	1108.31	1.3100	2.111	6.070	5156.56
	100.0	1106.22	1.3200	2.128	4.623	6826.23
	116.0	1101.51	1.3300	2.147	3.436	9265.67
	125.5	1098.78	1.3400	2.158	2.939	10889.48
	145.0	1094.49	1.3600	2.185	2.215	14622.74
60	49.9	1345.46	1.5500	2.489	17.794	2073.92
	71.7	1342.54	1.5700	2.526	8.971	4174.94
	87.4	1328.52	1.5700	2.530	6.056	6195.80
	100.0	1330.32	1.5900	2.559	4.623	8209.11
	116.0	1327.86	1.6100	2.588	3.436	11169.72
	126.4	1324.86	1.6200	2.604	2.897	13326.53
	144.8	1317.68	1.6400	2.630	2.222	17554.76
70	50.0	1557.50	1.7900	2.881	17.731	2409.61
	72.5	1556.81	1.8200	2.931	8.778	4950.98
	87.6	1547.02	1.8300	2.947	6.029	7249.03
	100.7	1547.74	1.8500	2.979	4.559	9690.77
	116.2	1538.24	1.8600	2.999	3.424	12985.97
	125.5	1541.61	1.8800	3.028	2.939	15278.10
	144.7	1531.10	1.9000	3.055	2.224	20369.11
80	50.3	1779.27	2.0470	3.292	17.541	2783.19
	70.9	1781.26	2.0824	3.349	9.171	5415.35
	88.3	1766.61	2.0939	3.367	5.934	8415.57
	100.7	1763.96	2.1115	3.396	4.560	11044.56
	116.3	1746.68	2.1174	3.405	3.418	14772.13
	125.2	1744.27	2.1299	3.425	2.953	17200.79
	144.7	1732.30	2.1496	3.457	2.225	23045.79
90	50.5	1997.70	2.3012	3.697	17.416	3147.82
	71.5	1995.81	2.3324	3.754	9.021	6171.56
	89.7	1986.37	2.3601	3.790	5.750	9776.09
	99.6	1982.41	2.3715	3.813	4.661	12131.19
	117.0	1969.30	2.3901	3.841	3.378	16864.64
	126.0	1967.80	2.4009	3.867	2.916	19663.77
	145.0	1956.13	2.4315	3.905	2.216	26134.52
100	50.6	2224.17	2.5611	4.116	17.353	3517.50
	69.7	2218.15	2.5905	4.166	9.482	6516.06
	90.3	2211.70	2.6310	4.222	5.673	11036.70
	99.9	2208.85	2.6410	4.249	4.634	13601.90
	118.0	2199.35	2.6720	4.294	3.321	19171.97
	125.1	2196.77	2.6810	4.313	2.958	21627.08
	144.9	2188.97	2.7211	4.369	2.218	29203.91

M_1 (90%) = 2021.698 - 0.5398 T (^oC) (3.13)

r = -0.978

M_1 (100%) = 2213.761 - 0.1738 T (^oC) (3.14)

r = -0.983

and for Flowmeter No (2)

M_2 (10%) = 273.613 - 0.1582 T (^oC) (3.15)

r = -0.99615

M_2 (20%) = 504.982 - 0.3352 T (^oC) (3.16)

r = -0.99426

M_2 (30%) = 723.689 - 0.4422 T (^oC) (3.17)

r = -0.99136

M_2 (40%) = 927.502 - 0.3480 T (^oC) (3.18)

r = -0.984

M_2 (50%) = 1128.27 - 0.2317 T (^oC) (3.19)

r = -0.995

M_2 (60%) = 1359.33 - 0.2845 T (^oC) (3.20)

r = -0.952

M_2 (70%) = 1573.897 - 0.2829 T (^oC) (3.21)

r = -0.955

M_2 (80%) = 1814.10 - 0.5519 T (^oC) (3.22)

r = -0.96675

M_2 (90%) = 2025.97 - 0.4666 T (^oC) (3.23)

r = -0.980

M_2 (100%) = 2244.7 - 0.3794 T (^oC) (3.24)

r = -0.934

where:

M_1 and M_2 are mass flow rates in (kg hr^{-1}) for flowmeters No (1) and No (2) respectively, at given % F.S.R ,

T is the bulk temperature (^oC) ,

and r is a correlation coefficient measuring how well the regression line fits the data[2] .

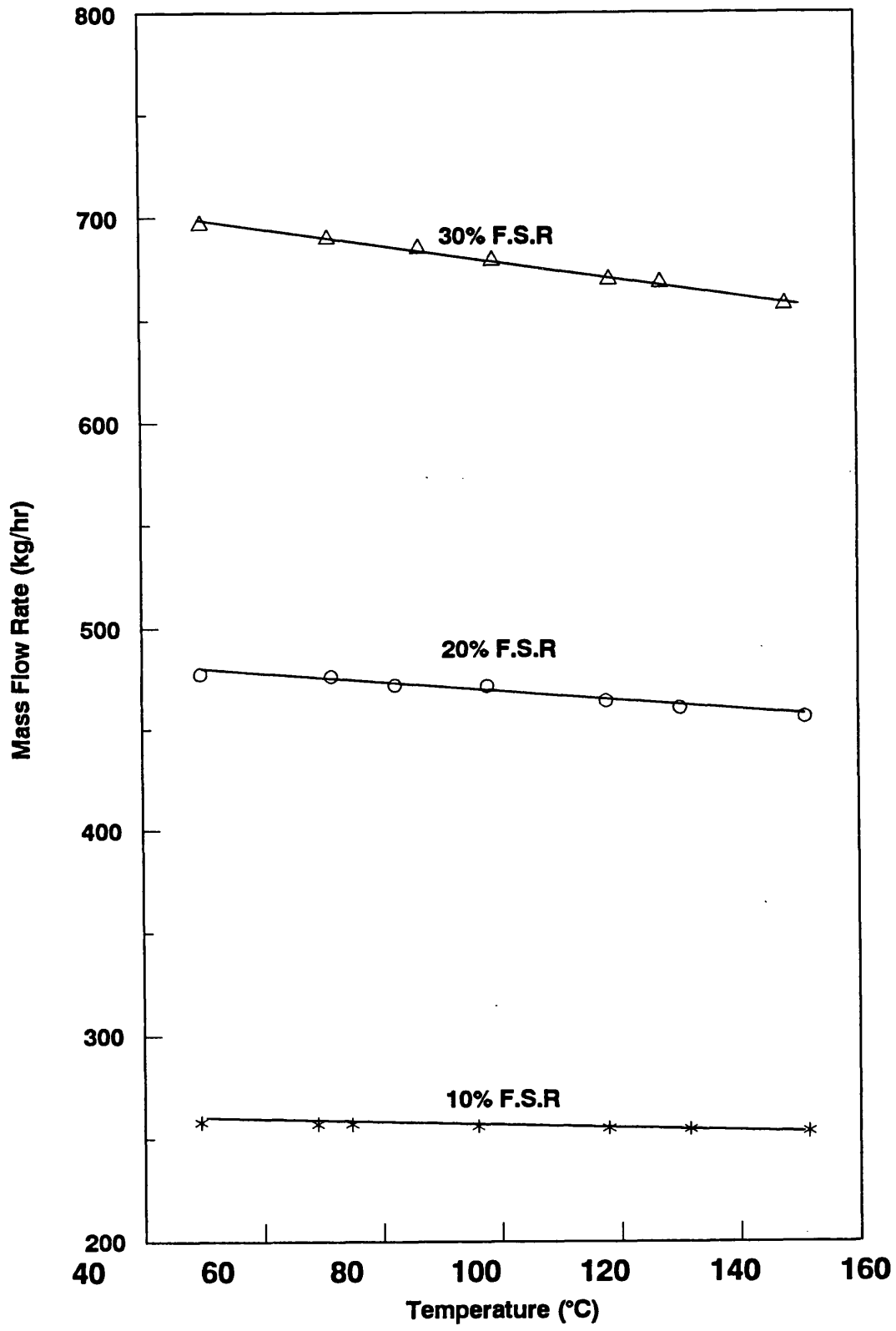

Fig (3.5) Calibration of Flowmeter No(1)

Using Santotherm 55 fluid at 10% - 30% F.S.R

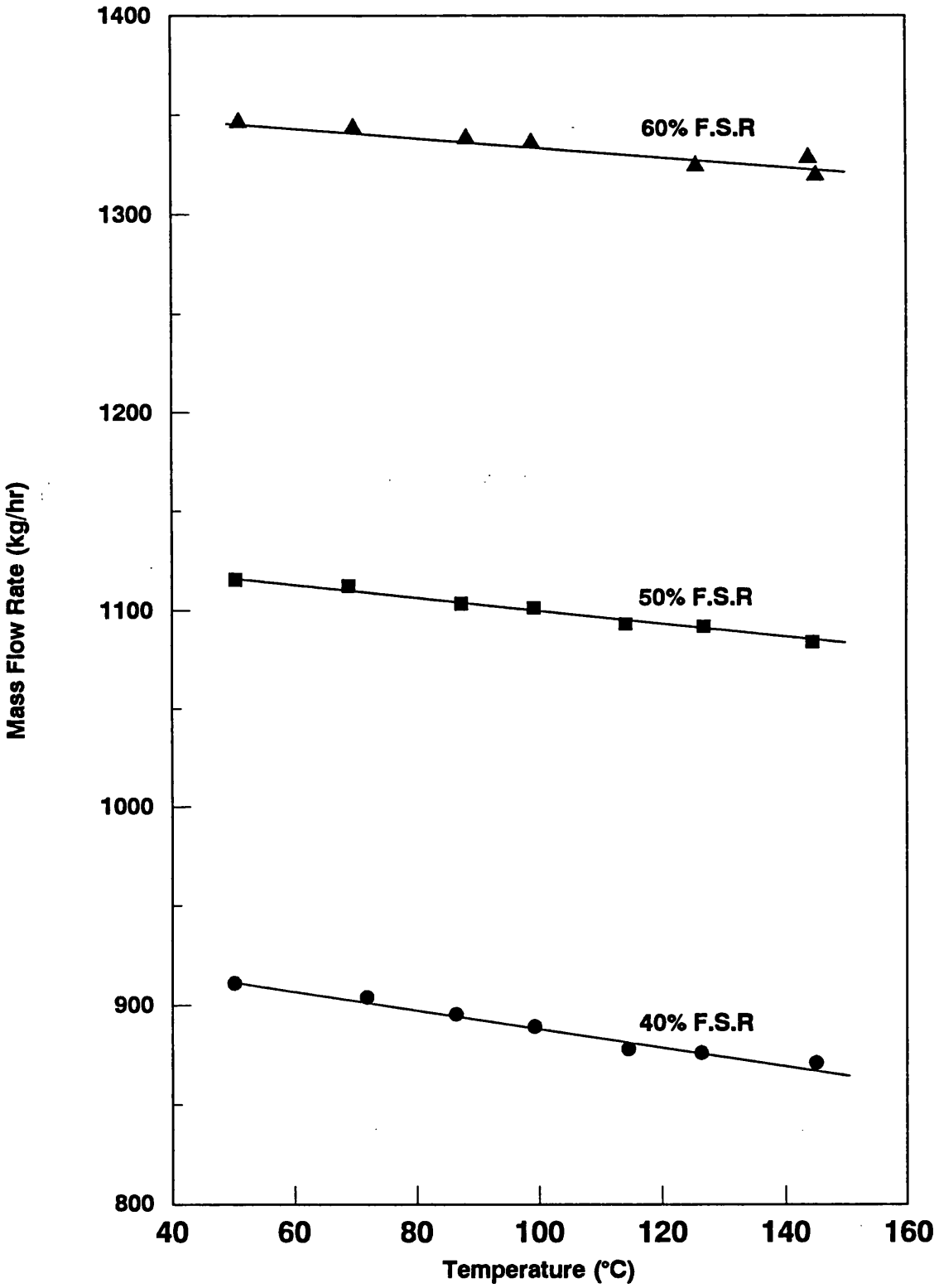

Fig (3.6) Calibration of Flowmeter No(1)

Using Santotherm 55 fluid at 40% - 60% F.S.R

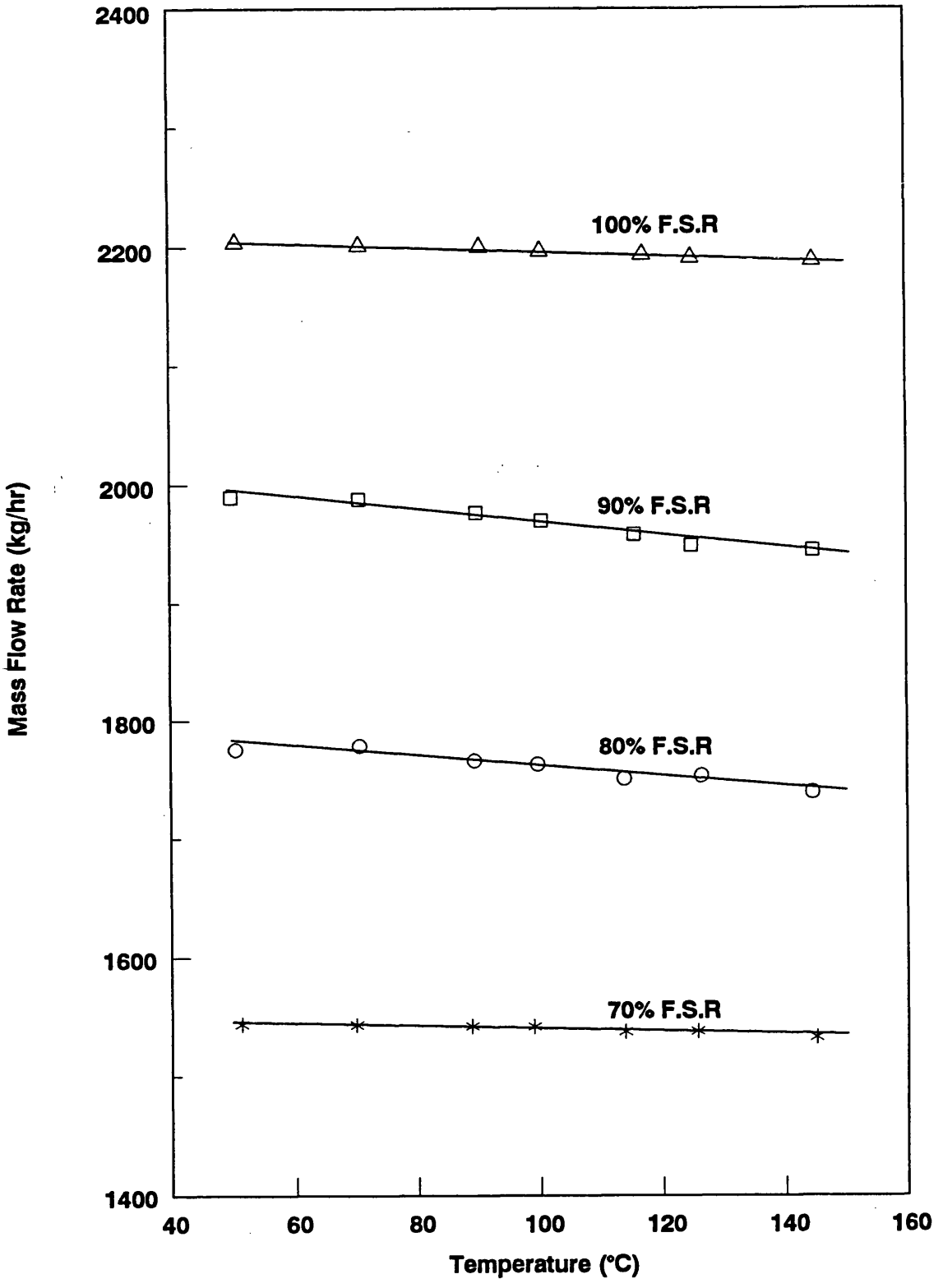

Fig (3.7) Calibration of Flowmeter No(1)

Using Santotherm 55 fluid at 70% - 100% F.S.R

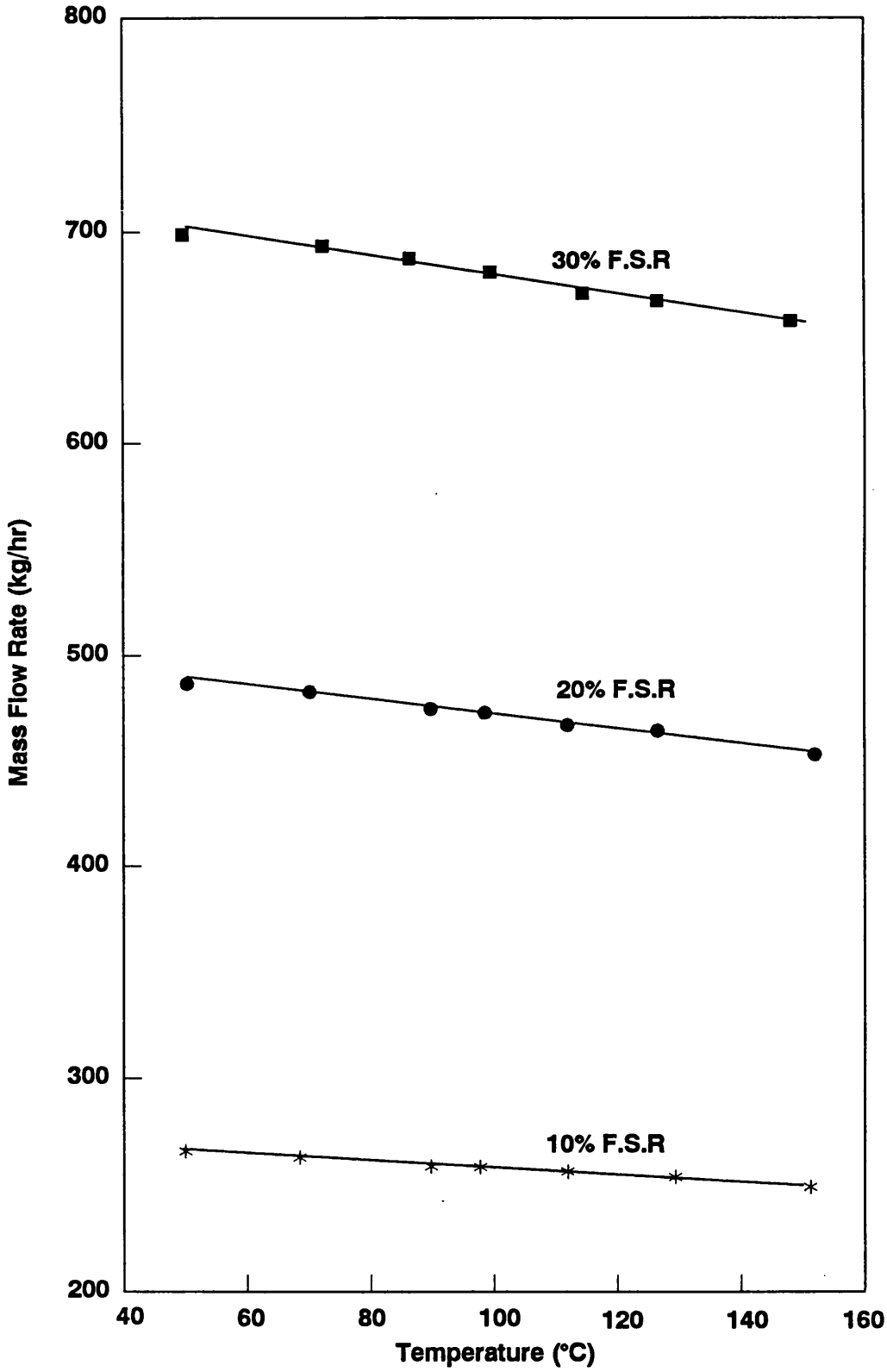

Fig (3.8) Calibration of Flowmeter No(2)

Using Santotherm 55 fluid at 10% - 30% F.S.R

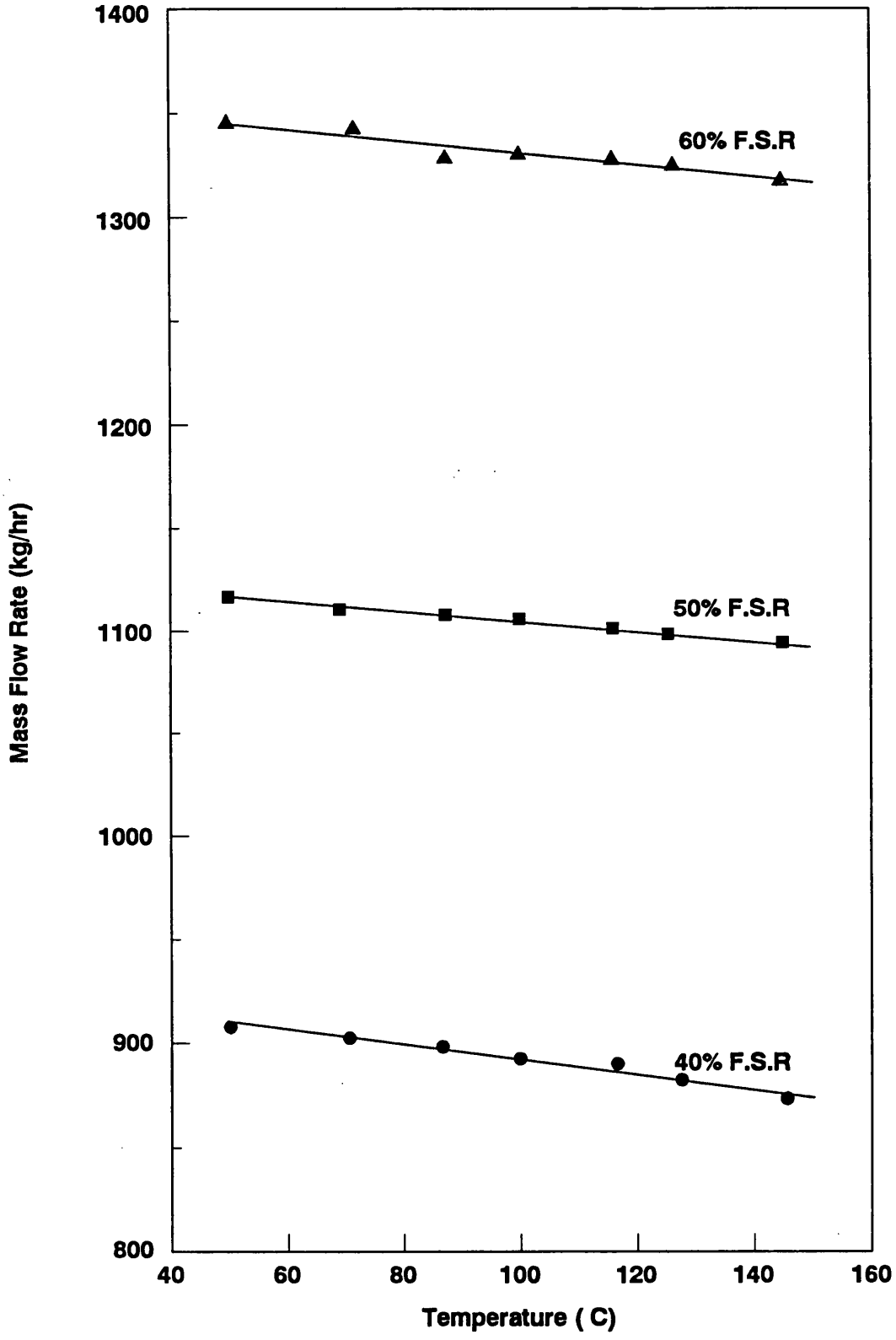

Fig (3.9) Calibration of Flowmeter No(2)

Using Santotherm 55 fluid at 40% - 60% F.S.R

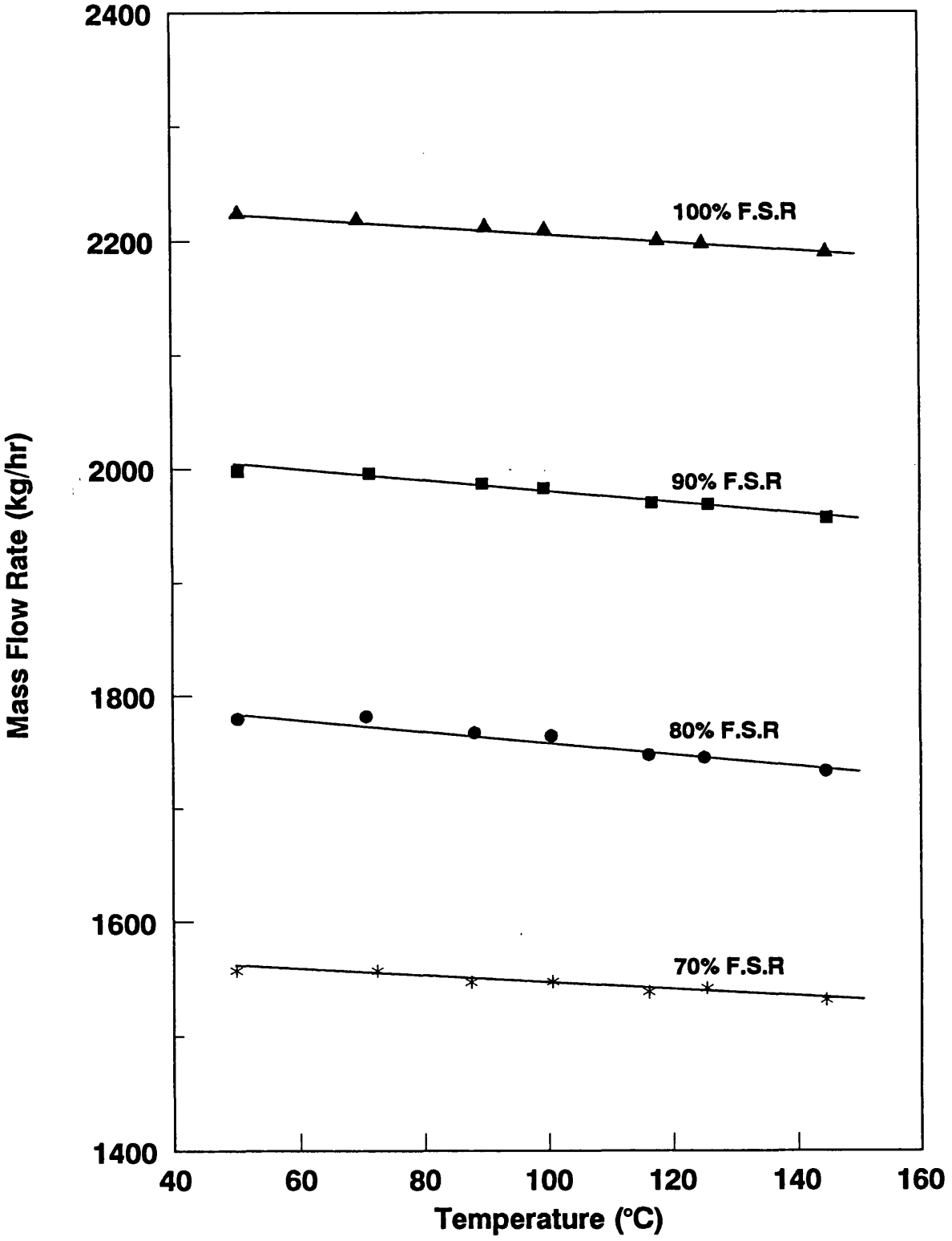

Fig (3.10) Calibration of Flowmeter No(2)

Using Santotherm 55 fluid at 70% - 100% F.S.R

3.4 Heat transfer and friction factor calculations

The methods of calculating the heat transfer and friction factor parameters are presented in the following sections :

3.4.1- Heat transfer coefficient (h_i) .

3.4.1.1- Determination of test section efficiency (η).

3.4.1.2- Determination of thermal wall resistance (R_w).

3.4.1.3- Heat transfer dimensionless groups .

3.4.2- Inner surface temperature (T_i).

3.4.3- Friction factor .

3.4.4- Enhancement factor (EF).

3.4.1 Heat transfer coefficient (h_i)

Local heat transfer coefficients (h_i) were calculated for the bare tube and for the tube fitted with different types of **HiTran** inserts . The effects of various experimental conditions such as bulk temperature, heat flux and flow rate (fluid velocity) on the heat transfer coefficient were studied . Reference should be made to Fig 2.8 for the labelling of temperature measurements.

The overall heat transfer coefficient is dependant on temperature , heat duty and heat transfer area as follows:

$$U_t = \frac{Q}{A_t\ (T_w - T_b)} \qquad (3.25)$$

However,

$$\frac{1}{U_t} = \frac{1}{h_i}\frac{A_t}{A_i} + R_w \qquad (3.26)$$

or,

$$\frac{1}{h_i} = \left(\frac{1}{U_t} - R_w \right) \frac{A_i}{A_t} \qquad (3.27)$$

Therefore,

$$\frac{1}{h_i} = \frac{(Tw-Tb)}{Q/A_i} - Rw \ \frac{A_i}{A_t} \qquad (3.28)$$

where,

U_t is the overall heat transfer coefficient based on area A_t ($W\ m^{-2}\ K^{-1}$)

A_t is the heat transfer area at the location of the wall thermocouples (m^2)

$A_t = \pi\ D_t\ L = 1.97 \times 10^{-2}$ (m^2)

A_i is the heat transfer area based on the inner tube diameter. (m^2)

$A_i = \pi\ D_i\ L = 1.268 \times 10^{-2}$ (m^2)

T_w is the average measured wall temperature (°C)

T_b is the bulk temperature at the axial location of the wall thermocouples. (°C)

Rw is the wall thermal resistance between the inner tube surface and the thermocouple location ($m^2\ K\ W^{-1}$)

Q is the thermal duty (W)

The actual thermal duty is related to the power output measured by the Wattmeters :

$$Q = \eta\ Q_{(sup)} \qquad (3.29)$$

where,

η is the test section efficiency

$Q_{(sup)}$ is the direct Wattmeter reading (W)

By substituting A_t and A_i values into equation 3.28 :

$$\frac{1}{h_i} = \frac{(T_w - T_b)}{78.864\ \eta Q_{(sup)}} - 0.6437\ R_w \qquad (3.30)$$

The average wall temperature (T_w) for test sections No(1) and No(2) were calculated respectively as follows:

$$T_{w_1} = \frac{(T_3 + T_4)}{2} \qquad (3.31)$$

$$T_{w_2} = \frac{(T_7 + T_8)}{2} \qquad (3.32)$$

The bulk temperature (T_b) was assumed to increase linearly with the length of the heated tube. The following expression was used to calculate T_b for use in equation 3.30 ,

$$T_b = \frac{(T_{out} - T_{in})}{L} x + T_{in} \qquad (3.33)$$

where:

L is the total length of heated test section = 0.272 m

x is the axial heated length at the thermocouple location

x = (0.272 - 0.03175) = 0.240 m

Therefore,

$$T_b = [\frac{(T_{out}-T_{in})}{0.272}]0.240 + T_{in}$$

Or,

$$T_b = 0.1176\ T_{in} + 0.8824\ T_{out} \qquad (3.34)$$

Where,

T_{in} is the inlet bulk temperature (°C)

T_{out} is the outlet bulk temperature (°C)

The bulk temperature (T_b) for each test section, (see Fig 2.8 for the labelling of the thermocouples) , was calculated as follows:

$$T_{b1} = 0.1176\ T_1 + 0.8824\ T_2 \qquad (3.35)$$

$$T_{b2} = 0.1176\ T_5 + 0.8824\ T_6 \qquad (3.36)$$

In order to calculate the heat transfer coefficient (h_i) from equation (3.30) , the efficiency (η) and the wall thermal resistance (R_w) of each test section had to be determined.

3.4.1.1 Determination of test section efficiency (η)

The efficiency of each heated test section (η) is defined by the following expression,

$$\eta = 1 - \frac{Q(loss)}{Q(sup)} \qquad (3.37)$$

in which the heat loss ($Q_{(loss)}$) from the heated test section *via* the insulation is calculated based on natural convection and radiation heat transfer coefficients[3,7] as follows:

$$Q_{(loss)} = A_{oin}\ (h_C + h_r)\ (T_S - T_\infty) \qquad (3.38)$$

Where:

A_{oin} is the outer surface area of the insulation around the heated test section (m^2)

T_S is the average surface temperature of the insulation (K)

T_∞ is the room temperature (K)

h_C is the natural convection heat transfer coefficient ($W\ m^{-2}\ K^{-1}$)

h_r is the radiation heat transfer coefficient ($W\ m^{-2}\ K^{-1}$)

(i) **McAdams** Correlation[3];

$$Nu_D = 0.53\ (Ra_D)^{1/4} \qquad (3.44)$$

for $10^4 < Ra_D < 10^9$

Thus ,

$$h_C = 0.53\ \frac{k_a}{L_{in}}(Ra_D)^{1/4} \qquad (3.45)$$

(ii) **Churchill and Chu** correlation[5]

$$Nu_D = \left[0.60 + \frac{0.387\ Ra_D^{1/6}}{[1+ (0.559/Pr_a)^{9/16}]^{8/27}}\right]^2 \qquad (3.46)$$

for $10^{-5} < Ra_D < 10^9$

Thus ,

$$h_C = \frac{k_a}{L_{in}}\left[0.60 + \frac{0.387\ Ra_D^{1/6}}{[1+ (0.559/Pr_a)^{9/16}]^{8/27}}\right]^2 \qquad (3.47)$$

Where;

Ra_D (Rayleigh number of air) $= Gr_D\ Pr_a$ (3.48)

Pr_a (Prandtl number of air) $= Cp_a\ \mu_a/k_a$ (3.49)

Gr_D (Grashof number of air) $= \dfrac{(D_{in})^3\ (\rho_a)^2\ g\ \beta_a \Delta T}{(\mu_a)^2}$ (3.50)

D_{in} is the outside diameter of the insulation

$D_{in} = 0.129$ (m)

ρ_a is density of the air (kg m^{-3})

g is standard acceleration of gravity

$g = 9.807$ (m s^{-2})

β_a is coefficient of thermal expansion for the air (K^{-1})

μ_a is dynamic viscosity of the air (N s m^{-2})

Cp_a is specific heat of the air (kJ kg^{-1} K^{-1})

$$\Delta T = T_s - T_\infty \qquad (3.51)$$

The physical properties involved in equations 3.43 to 3.50 are evaluated at the film temperature (T_f) of the air;

where:

$$T_f = \frac{T_s + T_\infty}{2} \qquad (3.52)$$

The temperature of the outside surface of the insulation around each heated test section was measured at 12 different positions as shown in Fig 3.11. A portable digital thermocouple was used for the surface (T_s) and room temperature (T_∞) measurements. At each % F.S.R the mean average temperature reading for all twelve temperatures was calculated and used as T_s in equations 3.39 to 3.52.

The radiation heat transfer coefficient (h_r) was calculated from equation 3.42 . In order to provide greater accuracy in h_c calculations , both equations 3.45 and 3.47 were used and a comparison between them is reported in Tables 3.6 and 3.7 for test sections No(1) and No(2) respectively .

The Prandtl number (Pr_a) of air[6] was plotted against the absolute temperature (T_f) in Fig 3.12. The following equation correlated the data to ± 0.1%

$$Pr_a = 0.8489 - 7.313\times10^{-4}\,(T_f) + 9.93\times10^{-7}\,(T_f)^2 - 4.08\times10^{-10}(T_f)^3 \qquad (3.53)$$

The group of air properties[6] $[(\rho_a)^2\ g\ \beta_a/(\mu_a)^2]$ which are used in Gr_D calculations (equation 3.50)

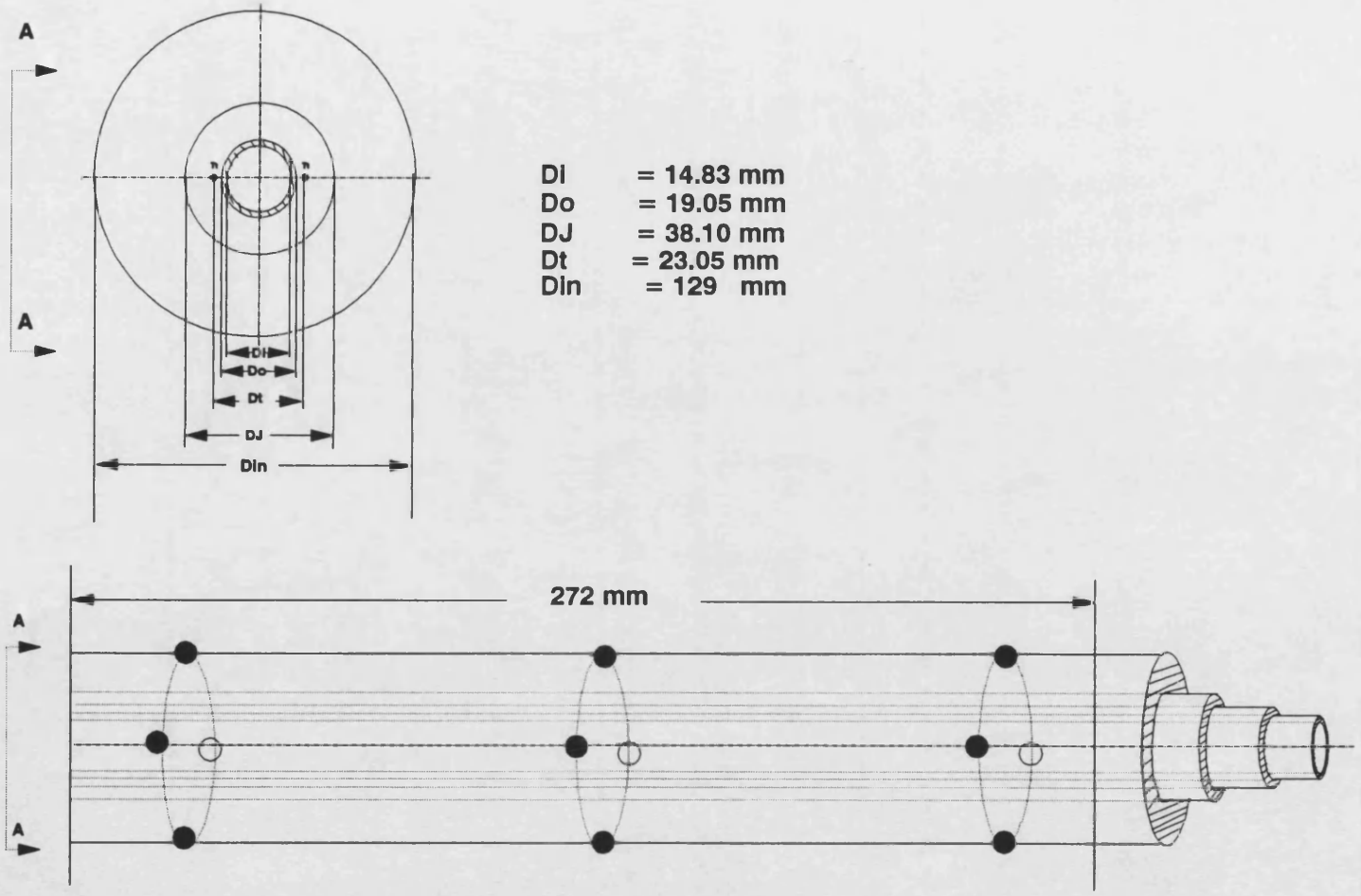

Fig (3.11) Diagram of the heated test section showing the position of temperature measurements on the outer surface of the insulation

Table 3.6 Heat loss and efficiency (η) calculation for test section No(1)

Q(sup.) W	%F.S.R	T(∞) K	Ts K	Tf K	Dt (Equ.) (3.51)	hr (Equ.) (3.42)	Pra (Equ.) (3.53)	C (Equ.) (3.54)	Grd (Equ.) (3.56)	Rad (Equ.) (3.49)	Ka (Equ.) (3.57)	Based on McAdams Correlation			Based on Churchill & Chu Correlation		
												hc (Equ.) (3.45)	Q(loss) (Equ.) (3.38)	% Efficiency (Equ.) (3.37) * 100	hc (Equ.) (3.47)	Q(loss) (Equ.) (3.38)	% Efficiency (Equ.) (3.37) * 100
216.6	10	290	301.8	295.9	11.8	0.415	0.7011	1.41E+08	5.55E+06	2.49E+06	0.0260	1.207	3.459	98.384	1.141	3.357	98.450
216.6	30	291	304.0	297.5	13.0	0.421	0.7006	1.37E+08	3.84E+06	2.69E+06	0.0261	1.236	3.956	98.173	1.172	3.803	98.244
216.6	50	291	300.9	296.0	9.9	0.415	0.7011	1.41E+08	3.00E+06	2.10E+06	0.0260	1.157	2.862	98.678	1.087	2.734	98.737
216.6	80	290	299.8	294.9	9.8	0.411	0.7014	1.43E+08	3.02E+06	2.12E+06	0.0259	1.156	2.828	98.694	1.086	2.702	98.752
216.6	100	290	299.3	294.7	9.3	0.409	0.7015	1.44E+08	2.88E+06	2.02E+06	0.0259	1.141	2.657	98.773	1.071	2.536	98.829
424.2	10	290	307.3	298.6	17.3	0.426	0.7002	1.35E+08	5.00E+06	3.50E+06	0.0262	1.325	5.546	98.692	1.269	5.371	98.734
424.2	30	291	303.3	297.2	12.3	0.420	0.7007	1.38E+08	3.66E+06	2.56E+06	0.0261	1.220	3.714	99.124	1.155	3.566	99.159
424.2	50	291	301.5	296.3	10.5	0.416	0.7010	1.40E+08	3.16E+06	2.21E+06	0.0260	1.173	3.064	99.278	1.104	2.931	99.309
424.2	80	290	301.3	295.7	11.3	0.414	0.7012	1.41E+08	3.44E+06	2.41E+06	0.0260	1.197	3.351	99.210	1.130	3.212	99.243
424.2	100	290	301.8	295.9	11.8	0.415	0.7011	1.41E+08	3.58E+06	2.51E+06	0.0260	1.209	3.528	99.168	1.144	3.386	99.202
625.8	10	290	307.1	298.5	17.1	0.426	0.7002	1.35E+08	4.96E+06	3.47E+06	0.0262	1.322	5.482	99.124	1.266	5.307	99.152
625.8	30	289	306.3	297.6	17.3	0.422	0.7005	1.37E+08	5.08E+06	3.56E+06	0.0261	1.326	5.537	99.115	1.272	5.365	99.143
625.8	50	289	305.5	297.3	16.5	0.421	0.7007	1.38E+08	4.89E+06	3.42E+06	0.0261	1.312	5.249	99.161	1.256	5.080	99.188
625.8	80	289	304.5	296.8	15.5	0.418	0.7008	1.39E+08	4.63E+06	3.24E+06	0.0260	1.292	4.869	99.222	1.235	4.705	99.248
625.8	100	289	303.8	296.4	14.8	0.417	0.7009	1.40E+08	4.45E+06	3.12E+06	0.0260	1.279	4.618	99.262	1.220	4.458	99.288
821.5	10	289	316.3	302.6	27.3	0.444	0.6989	1.27E+08	7.44E+06	5.20E+06	0.0265	1.479	9.622	98.829	1.440	9.430	98.852
821.5	30	289	309.4	299.2	20.4	0.429	0.7000	1.34E+08	5.87E+06	4.11E+06	0.0262	1.381	6.785	99.174	1.332	6.601	99.196
821.5	50	289	308.8	298.9	19.8	0.428	0.7001	1.34E+08	5.73E+06	4.01E+06	0.0262	1.371	6.551	99.203	1.321	6.370	99.225
821.5	80	289	308.6	298.8	19.6	0.427	0.7002	1.35E+08	5.66E+06	3.97E+06	0.0262	1.367	6.452	99.215	1.317	6.271	99.237
821.5	100	289	307.8	298.4	18.8	0.426	0.7003	1.36E+08	5.48E+06	3.84E+06	0.0262	1.354	6.155	99.251	1.303	5.977	99.272
1020.2	10	290	323.2	306.6	33.2	0.462	0.6976	1.20E+08	8.53E+06	5.95E+06	0.0268	1.547	12.235	98.801	1.515	12.043	98.820
1020.2	30	291	319.4	305.2	28.4	0.456	0.6981	1.22E+08	7.46E+06	5.21E+06	0.0267	1.490	10.154	99.005	1.452	9.952	99.025
1020.2	50	290	315.0	302.5	25.0	0.444	0.6989	1.27E+08	6.84E+06	4.78E+06	0.0265	1.447	8.680	99.149	1.405	8.484	99.168
1020.2	80	290	313.3	301.7	23.3	0.440	0.6992	1.29E+08	6.46E+06	4.52E+06	0.0264	1.424	7.985	99.217	1.379	7.791	99.236
1020.2	100	290	313.0	301.5	23.0	0.439	0.6993	1.29E+08	6.38E+06	4.46E+06	0.0264	1.419	7.847	99.231	1.373	7.654	99.250

Table 3.7 Heat loss and efficiency (η) calculation for test section No(1)

Q(sup.) W	%F.S.R	T(oo) K	Ts K	Tf K	Dt (Equ.) (3.51)	hr (Equ.) (3.42)	Pra (Equ.) (3.53)	C (Equ.) (3.54)	Grd (Equ.) (3.56)	Rad (Equ.) (3.49)	Ka (Equ.) (3.57)	Based on McAdams Correlation: hc (Equ.) (3.45)	Q(loss) (Equ.) (3.38)	% Efficiency (Equ.) (3.37)*100	Based on Churchill & Chu Correlation: hc (Equ.) (3.47)	Q(loss) (Equ.) (3.38)	% Efficiency (Equ.) (3.37)*100
225.2	10	290	298.83	294.42	8.83	0.408	0.7016	1.44E+08	1.18E+07	8.27E+06	0.0259	2.702	4.930	97.811	2.688	4.907	97.821
225.2	30	290	299.08	294.54	9.08	0.409	0.7016	1.44E+08	1.21E+07	8.49E+06	0.0259	2.721	5.100	97.735	2.710	5.082	97.743
225.2	50	290	300.08	295.04	10.08	0.411	0.7014	1.43E+08	1.33E+07	9.35E+06	0.0259	2.791	5.793	97.428	2.792	5.795	97.427
225.2	80	291	299.75	295.38	8.75	0.412	0.7013	1.42E+08	1.15E+07	8.07E+06	0.0259	2.693	4.875	97.835	2.676	4.848	97.847
225.2	100	290	300.33	295.17	10.33	0.412	0.7014	1.42E+08	1.36E+07	9.56E+06	0.0259	2.808	5.968	97.350	2.812	5.976	97.346
424.6	10	289	304.58	296.79	15.58	0.419	0.7008	1.39E+08	2.01E+07	1.41E+07	0.0260	3.106	9.854	97.679	3.168	10.026	97.639
424.6	30	289	302.33	295.67	13.33	0.414	0.7012	1.41E+08	1.75E+07	1.22E+07	0.0260	2.991	8.144	98.082	3.030	8.238	98.060
424.6	50	289	302.42	295.71	13.42	0.414	0.7012	1.41E+08	1.76E+07	1.23E+07	0.0260	2.996	8.207	98.067	3.036	8.303	98.044
424.6	80	289	301.67	295.33	12.67	0.412	0.7013	1.42E+08	1.67E+07	1.17E+07	0.0259	2.954	7.650	98.198	2.986	7.723	98.181
424.6	100	290	302.33	296.17	12.33	0.416	0.7010	1.40E+08	1.60E+07	1.12E+07	0.0260	2.932	7.407	98.256	2.958	7.465	98.242
634.9	10	288	310.25	299.13	22.25	0.429	0.7001	1.34E+08	2.76E+07	1.93E+07	0.0262	3.387	15.230	97.601	3.508	15.716	97.525
634.9	30	288	305.17	296.58	17.17	0.418	0.7009	1.39E+08	2.22E+07	1.55E+07	0.0260	3.183	11.089	98.253	3.262	11.333	98.215
634.9	50	288	302.92	295.46	14.92	0.413	0.7013	1.42E+08	1.96E+07	1.37E+07	0.0259	3.077	9.339	98.529	3.135	9.494	98.505
634.9	80	288	302.08	295.04	14.08	0.411	0.7014	1.43E+08	1.86E+07	1.31E+07	0.0259	3.034	8.705	98.629	3.084	8.831	98.609
634.9	100	290	301.67	295.83	11.67	0.414	0.7011	1.41E+08	1.52E+07	1.07E+07	0.0260	2.892	6.921	98.910	2.911	6.961	98.904
833.3	10	290	316.58	303.29	26.58	0.447	0.6987	1.26E+08	3.10E+07	2.16E+07	0.0265	3.525	18.944	97.727	3.672	19.643	97.643
833.3	30	290	314.58	302.29	24.58	0.443	0.6990	1.28E+08	2.91E+07	2.03E+07	0.0264	3.460	17.214	97.934	3.593	17.799	97.864
833.3	50	290	310.83	300.42	20.83	0.434	0.6996	1.31E+08	2.54E+07	1.77E+07	0.0263	3.327	14.057	98.313	3.431	14.448	98.266
833.3	80	290	306.83	298.42	16.83	0.426	0.7003	1.36E+08	2.11E+07	1.48E+07	0.0262	3.161	10.831	98.700	3.232	11.044	98.675
833.3	100	290	306.75	298.38	16.75	0.425	0.7003	1.36E+08	2.10E+07	1.47E+07	0.0262	3.157	10.766	98.708	3.227	10.975	98.683
1036.7	10	289	319.67	304.33	30.67	0.452	0.6984	1.24E+08	3.52E+07	2.46E+07	0.0266	3.649	22.564	97.823	3.825	23.533	97.730
1036.7	30	289	313.33	301.17	24.33	0.438	0.6994	1.30E+08	2.93E+07	2.05E+07	0.0264	3.456	16.997	98.360	3.590	17.582	98.304
1036.7	50	289	311.83	300.42	22.83	0.434	0.6996	1.31E+08	2.78E+07	1.94E+07	0.0263	3.404	15.723	98.483	3.527	16.227	98.435
1036.7	80	289	311.75	300.38	22.75	0.434	0.6996	1.32E+08	2.77E+07	1.94E+07	0.0263	3.401	15.653	98.490	3.523	16.152	98.442
1036.7	100	290	310.58	300.29	20.58	0.434	0.6997	1.32E+08	2.51E+07	1.76E+07	0.0263	3.317	13.851	98.664	3.420	14.229	98.627

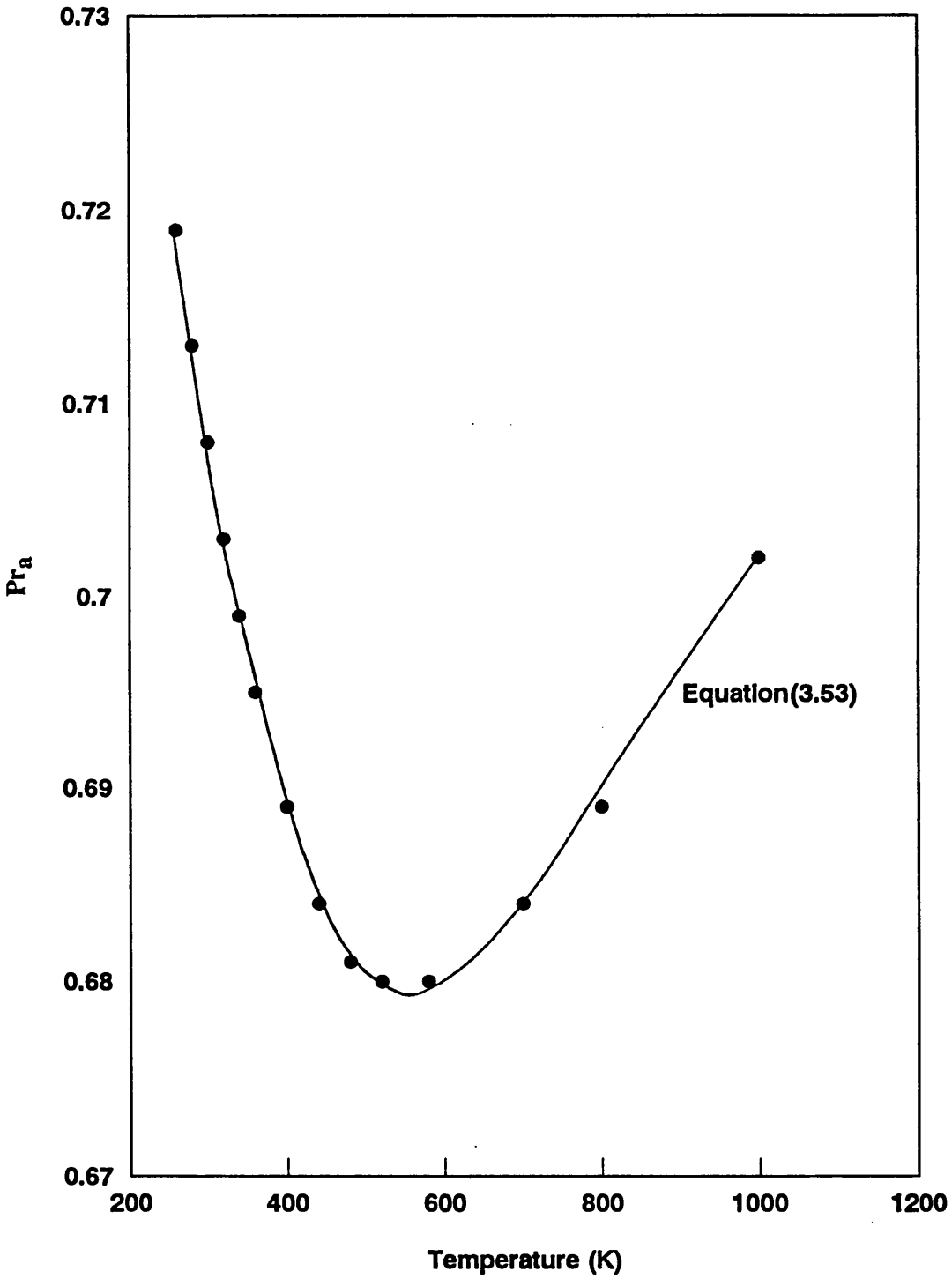

Fig (3.12) Prandtl number (Pr_a) of Air vs absolute temperature (K)

are plotted against T_f (K) in Fig 3.13 and correlated within ± 1.4% by the following equation:

$$\log C_b = A_6 + A_7 \log T_f + A_8 (\log T_f)^2 + A_9 (\log T_f)^3 + A_{10} (\log T_f)^4 \quad (3.54)$$

where,

$$C_b = \frac{(\rho_a)^2 g \beta_a}{(\mu_a)^2} \quad (3.55)$$

A6 = 352.746
A7 = -506.497
A8 = 283.291
A9 = -71.042
A10 = 6.681

The Grashof number (Gr_D) is calculated from equations 3.50 and 3.51 as follows:

$$Gr_D = C (D_{in})^3 (T_s - T_\infty) \quad (3.56)$$

The Rayleigh number (Ra_D) is calculated from equation 3.48 . The thermal conductivity (k_a) of air[6] is plotted against T_f (K) in Fig 3.14 and correlated to ± 0.7% using the following equation :

$$k_a = 1.757 \times 10^{-3} + 8.863 \times 10^{-5} T_f - 2.3 \times 10^{-8} (T_f)^2 \quad (3.57)$$

Sample calculations for both test sections are presented in Tables 3.6 and 3.7 for $Q_{(sup)}$ in the range of 200 to 1000 W. The h_c calculations based on equations 3.45 and 3.47 are in close agreement.

The % efficiency (η) values listed in Tables 3.6 and 3.7 vary slightly with % F.S.R as shown in Figs 3.15 and 3.16 for test sections No(1) and No(2)

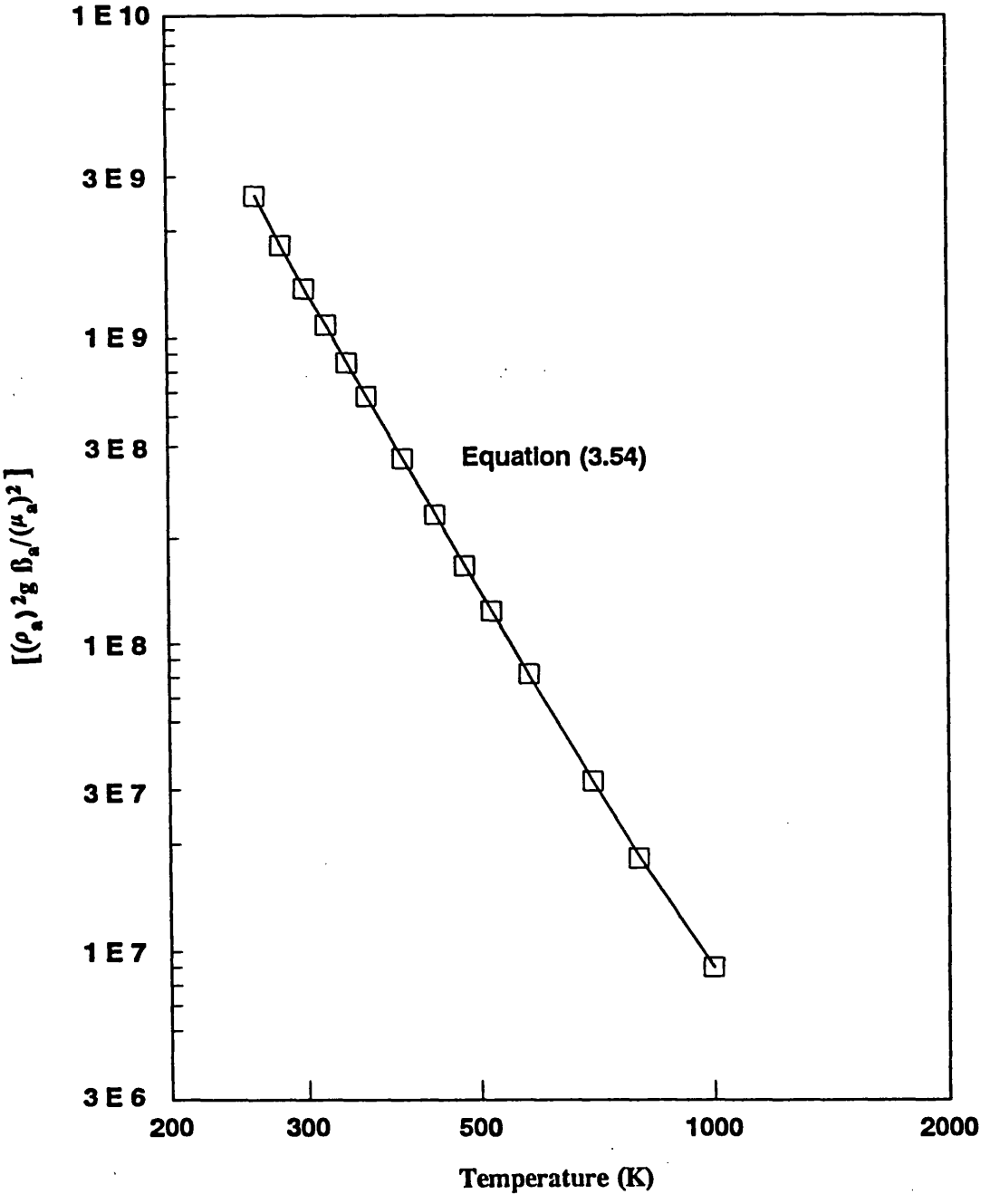

Fig 3.13 Variation of Air properties $[\rho_a)^2 g\ \beta_a/(\mu_a)^2]$ with absolute temperature (K)

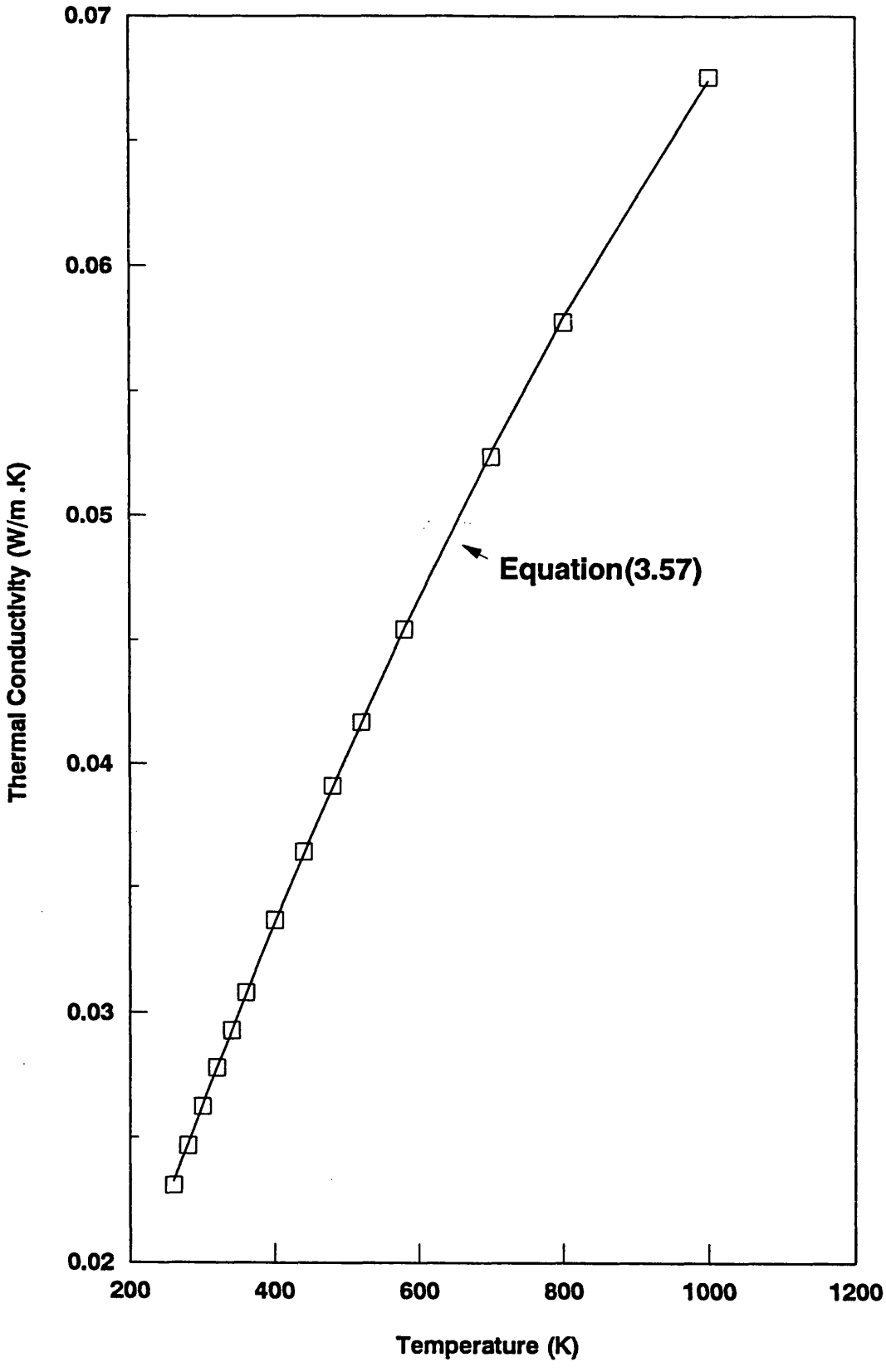

Fig (3.14) Thermal conductivity of the Air vs. absolute temperature (K)

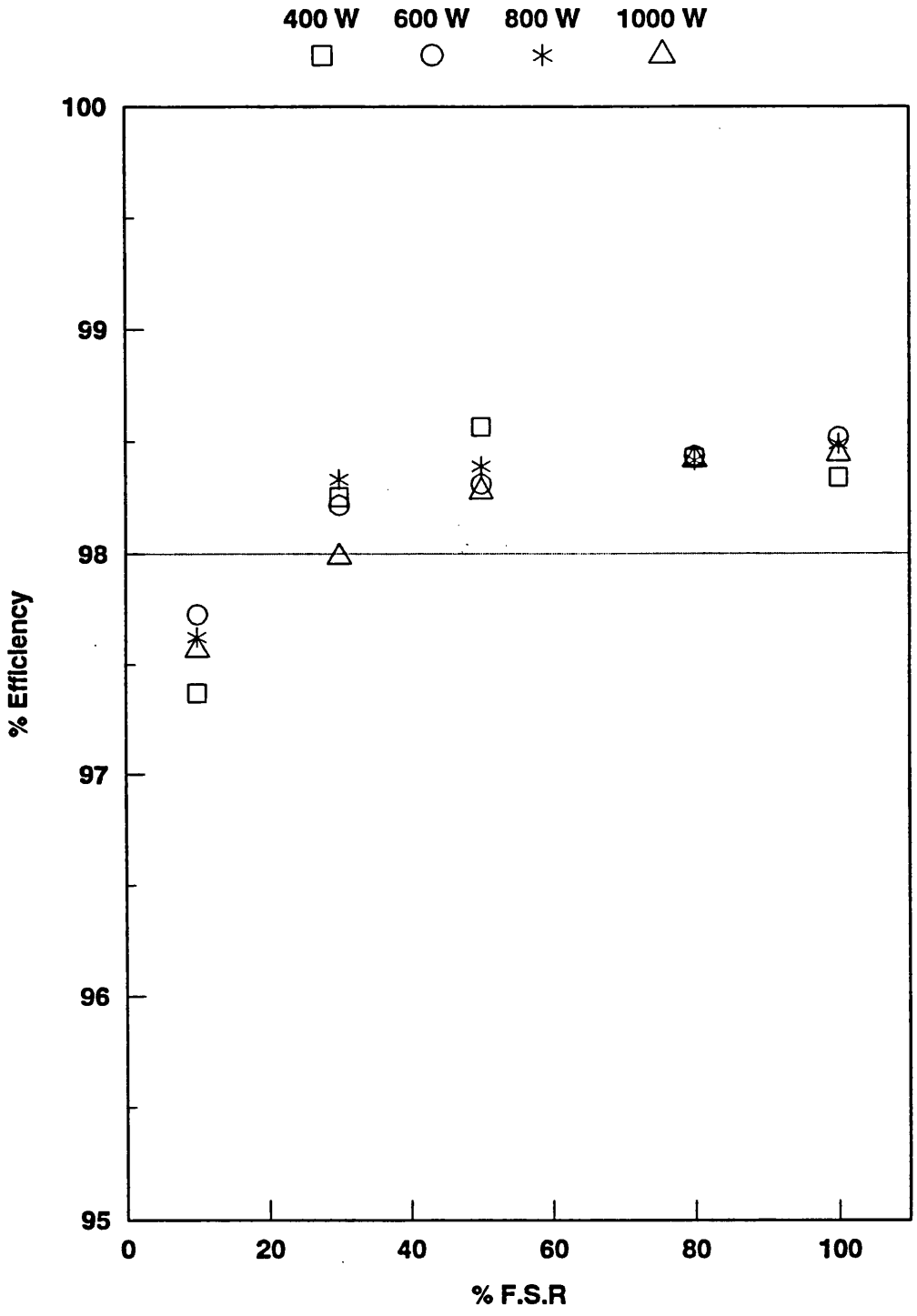

Fig (3.15) Percentage of Efficiency (% η) Vs % F.S.R

Test Section No(1) with using Santotherm 55 Fluid

400 W < Q(sup) < 1000 W ; (24 kW/m² < q < 60.2 kW/m²)

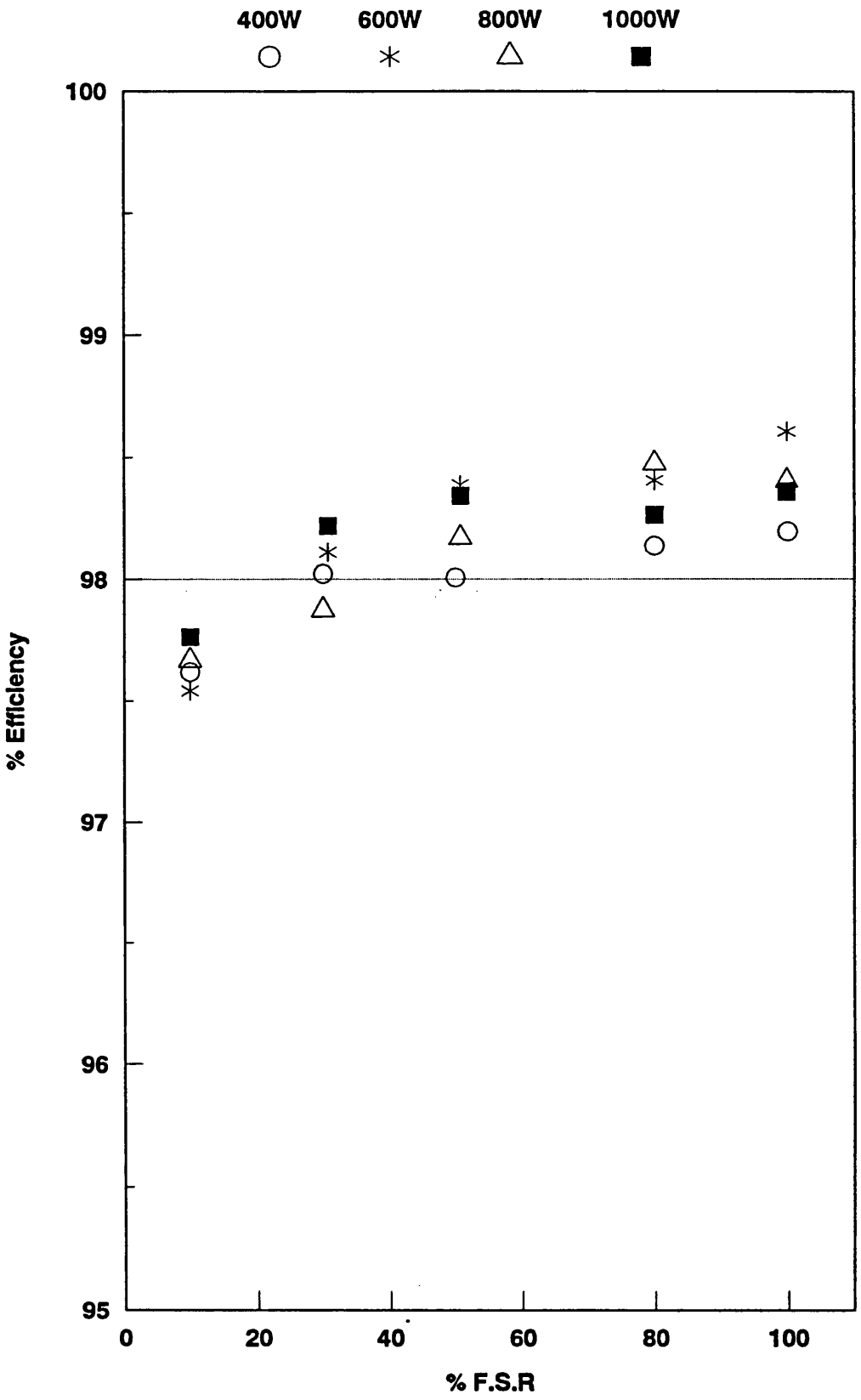

Fig (3.16) Percentage of Efficiency (% η) Vs % F.S.R

Test Section No(2) with using Santotherm 55 Fluid

400 W < Q(sup) < 1000 W ; (24 kW/m² < q < 60.2 kW/m²)

respectively. The average value of % η is 98%. Thus the efficiency (η) of each test section was taken to be 0.98 for all heat transfer calculations for both Santotherm 55 and crude oil studies. An efficiency cross check was made whenever the test section was dismantled and re-connected and no significant change in η values was observed.

3.4.1.2 Determination of test section wall resistance (Rw)

The thermal resistance between the wall thermocouple and the inner surface of the test section (R_w) may be calculated in one of two ways :

(a) Concentric cylinder

If a perfect contact between adjacent layers (the outer surface of heated test section and the inner surface of jacket tube), is assumed to exist, the following expression for concentric tubes may be applied[7,8],

$$R_W = \frac{Dr_s\ At}{k_s\ Alm\ ,\ s} + \frac{Dr_j\ At}{k_j\ Alm\ ,\ j} \qquad (3.58)$$

Where,

$$Dr_s = (D_o - D_i)/2 \qquad (3.59)$$

$$Dr_j = (D_t - D_o)/2 \qquad (3.60)$$

$$Alm,s = \frac{A_o - A_i}{\ln (A_o/A_i)} = \frac{\pi L\ (D_o - D_i)}{\ln (D_o/D_i)} \qquad (3.61)$$

$$Alm,_j = \frac{A_t - A_o}{\ln (A_t/A_o)} = \frac{\pi L\ (D_t - D_o)}{\ln (D_t/D_o)} \qquad (3.62)$$

$$A_t = \pi \, L \, D_t \qquad (3.63)$$

Therefore,

$$R_w = \frac{D_t \ln (D_o/D_i)}{2k_s} + \frac{D_t \ln (D_t/D_o)}{2k_j} \qquad (3.64)$$

Where:

D_i is the inside diameter of the test section

$D_i = 1.483 \times 10^{-2}$ (m)

D_o is the outside diameter of the test section

$D_o = 1.905 \times 10^{-2}$ (m)

D_t is the distance between the wall thermocouples

$D_t = 2.305 \times 10^{-2}$ (m)

L is the heated length of the test section

$L = 0.272$ (m)

k_s is thermal conductivity of the test section material (carbon steel)

k_s[4] = 51.87 (W m^{-1} K^{-1})

k_j is the thermal conductivity of the jacket tube material (mild steel)

k_j[4] = 45.3 (W m^{-1} K^{-1})

Therefore,

$$R_w = 5.564 \times 10^{-5} + 4.84912 \times 10^{-5}$$

$$R_w = 1.0413 \times 10^{-4} \quad (m^2 \, K \, W^{-1})$$

However, such perfect contact between two metals has probably never been achieved in the majority of industrial systems. The contact resistance caused by blowholes, bubbles, rough surfaces etc., is very likely to be present where two solids are brought together[3,8]. The contact resistance could be large enough to be a significant percentage of the total . For a practical solution,

Wilson's method has been used for the wall thermal resistance determination[9,10].

(b) Wilson's method for thermal wall resistance calculation

Wilson[11] developed a graphical technique which can be used for the R_w determination. Starting with a clean surface and using a non-fouling fluid (Santotherm 55 in the present study) , a series of data is obtained at various rates of flow. At each flow rate, the overall heat transfer coefficient (U_t) between the wall sensor and the bulk fluid is calculated from equation 3.25 .

In equation 3.26 , if a single-phase fluid is flowing in fully developed turbulent flow inside the heated test section, the convective coefficient (h_i) may be estimated by the Dittus and Boelter correlation[12] as follows :

$$\frac{h_i D_i}{k} = 0.023 \left(\frac{D_i v \rho}{\mu}\right)^{0.8} \left(\frac{C_p \mu}{k}\right)^{0.3} \qquad (3.65)$$

Where:

v	is the fluid velocity	(m s^{-1})
ρ	is the density of fluid	(kg m^{-3})
μ	is the viscosity of fluid	(N s m^{-2})
C_p	is the specific heat of fluid	(kJ kg^{-1} K^{-1})
k	is the fluid thermal conductivity	(W m^{-1} K^{-1})

In equation 3.65 the heat transfer coefficient (h_i) is proportional to $v^{0.8}$ if all other properties are constant.

Thus, equation 3.26 may be rearranged as follows,

$$\frac{1}{U_t} = R_w + \frac{\psi}{v^{0.8}} \left(\frac{A_t}{A_i}\right) \qquad (3.66)$$

Where :

ψ is a constent

Consequently, a plot of $\frac{1}{U_t}$ versus $\frac{1}{v^{0.8}}$ should be a straight line with a slope of $(\psi)\left(\frac{At}{Ai}\right)$ and an intercept of R_w when $\frac{1}{v^{0.8}}$ equals zero i.e., when v is infinity.

Wilson's method was applied to both test sections. The basic experimental data for test sections No(1) and No(2) are shown respectively in Tables 3.8 and 3.9 and the Wilson plots are shown in Fig.3.18 based on the calculated results in Table 3.10.

From Fig. 3.18, the thermal wall resistance for test section No(1) , Rw_1 is equal to 1.19×10^{-3} (K m^2 W^{-1}) and that for test section No(2) , Rw_2 is equal to 6.75×10^{-4} (K m^2 W^{-1}). The value of Rw_1 is 1.76 times that of Rw_2. The values of Rw_1 and Rw_2 are respectively, 11.43 and 6.48 times those calculated on the basis of equation 3.64. Consequently, the contact resistance is significant .

Table 3.8 Wilson plot calculation for test section No (1) using Santotherm 55

Q(sup) = 403.4 W
At(surfas) = 0.01969 m2
Ai(surfas) = 0.01267 m2
Eff. = 0.98

%F.S.R No(1)	%F.S.R No(2)	T(1) C	T(2) C	T(3) C	T(4) C	Dt C	T(Bulk) C	T(wall) C	T(Avrag) C	M1 kg/h	M2 kg/h	M (M1+M2) kg/h	Density Kg/m3	Velocity m/sec	1/(V^.8)	1/Ut	(1/V^.8) *(At/Ai)	Kinematic Viscosity mm2/sec	Re
30	30	101.3	103.9	144.8	144.2	0.4	101.7	144.5	101.5	677.4	680.0	1357.4	834.85	2.613	0.4637	2.13E-03	0.7205	4.505	8604.60
30	40	100.0	102.5	141.7	141.4	0.3	100.3	141.6	100.2	678.0	892.6	1570.6	835.76	3.021	0.4130	2.06E-03	0.6417	4.628	9681.56
40	40	99.5	101.9	139.8	139.4	0.2	99.7	139.6	99.6	889.3	892.8	1782.2	836.13	3.426	0.3734	1.99E-03	0.5802	4.680	10859.86
40	50	99.2	101.7	138.6	138.3	0.3	99.5	138.5	99.4	889.4	1105.3	1994.7	836.29	3.834	0.3413	1.94E-03	0.5303	4.703	12091.27
50	50	99.5	101.9	137.3	137.0	0.2	99.7	137.2	99.6	1100.3	1105.2	2205.5	836.13	4.240	0.3149	1.87E-03	0.4893	4.680	13439.69
50	60	103.2	105.5	139.9	139.7	0.1	103.3	139.8	103.3	1099.1	1330.0	2429.1	833.68	4.683	0.2908	1.82E-03	0.4518	4.353	15957.68
60	60	103.3	105.7	139.2	139.0	0.2	103.5	139.1	103.4	1332.8	1329.9	2662.7	833.58	5.134	0.2701	1.77E-03	0.4198	4.341	17546.03
60	70	103.5	105.8	138.6	138.4	0.1	103.6	138.5	103.6	1332.8	1544.6	2877.4	833.48	5.549	0.2539	1.74E-03	0.3945	4.328	19017.94
70	70	103.7	106.0	138.1	137.9	0.1	103.8	138.0	103.8	1539.5	1544.5	3084.0	833.34	5.949	0.2401	1.70E-03	0.3732	4.311	20466.17
70	80	104.1	106.4	138.1	137.9	0.1	104.2	138.0	104.2	1539.4	1756.6	3296.0	833.07	6.360	0.2276	1.68E-03	0.3537	4.278	22049.81

Test section No(1) at power supply 801.8 W

Q(sup) = 801.8 W
At(surfas) = 0.01969 m2
Ai(surfas) = 0.01267 m2
Eff. = 0.98

%F.S.R No(1)	%F.S.R No(2)	T(1) C	T(2) C	T(3) C	T(4) C	Dt C	T(Bulk) C	T(wall) C	T(Avrag) C	M1 kg/h	M2 kg/h	M (M1+M2) kg/h	Density kg/m3	Velocity m/sec	1/(V^.8)	1/Ut	(1/V^.8) *(At/Ai)	Kinematic Viscosity mm2/sec	Re
60	0	103.4	104.2	187.0	191.3	0.7	104.0	189.2	103.8	1332.7	0.0	1332.7	833.34	2.571	0.4699	2.13E-03	0.7301	4.311	8844.13
70	0	104.6	105.3	184.7	189.2	0.6	105.1	187.0	104.9	1539.3	0.0	1539.3	832.57	2.972	0.4184	2.05E-03	0.6501	4.217	10453.52
80	0	105.6	106.2	181.8	186.4	0.5	106.0	184.1	105.9	1757.8	0.0	1757.8	831.93	3.396	0.3760	1.96E-03	0.5843	4.142	12164.00
90	0	105.5	106.1	179.8	184.6	0.5	105.9	182.2	105.8	1964.6	0.0	1964.6	832.00	3.795	0.3440	1.91E-03	0.5346	4.149	13568.46
100	0	105.0	105.5	176.6	181.4	0.4	105.4	179.0	105.2	2195.4	0.0	2195.4	832.37	4.239	0.3149	1.85E-03	0.4893	4.193	14997.77
50	60	101.7	102.2	173.0	177.9	0.4	102.1	175.5	101.9	1099.6	1330.3	2429.9	834.58	4.680	0.2909	1.84E-03	0.4521	4.470	15530.14
60	60	103.7	104.0	172.0	176.9	0.2	103.9	174.5	103.8	1332.7	1329.8	2662.5	833.31	5.136	0.2701	1.77E-03	0.4197	4.307	17686.60
60	70	109.3	109.7	175.8	180.7	0.3	109.6	178.3	109.5	1330.9	1542.9	2873.8	829.52	5.569	0.2532	1.72E-03	0.3934	3.873	21327.55
70	70	110.1	110.4	175.6	180.8	0.2	110.3	178.2	110.2	1538.7	1542.7	3081.4	829.01	5.975	0.2393	1.70E-03	0.3719	3.820	23197.08
80	70	110.8	111.1	175.6	180.8	0.2	111.0	178.2	110.9	1755.7	1542.5	3298.2	828.54	6.398	0.2265	1.69E-03	0.3520	3.772	25159.89

Table 3.9 Wilson plot calculation for test section No (2) using Santotherm 55

Q(sup) = 401.8 W
At(surfas) = 0.01969 m2
Ai(surfas) = 0.01267 m2
Eff. = 0.98

%F.S.R No(1)	%F.S.R No(2)	T(5) C	T(6) C	T(7) C	T(8) C	Dt C	T(Bulk) C	T(wall) C	T(Avrag) C	M1 kg/h	M2 kg/h	M (M1+M2) kg/h	Density Kg/m3	Velocity m/sec	1/(V^.8)	1/Ut	(1/V^.8) *(At/Ai)	Kinematic Viscosity mm2/sec	Re
20	40	99.9	102.0	132.5	135.0	0.4	100.3	133.8	100.1	438.0	892.7	1330.7	835.79	2.559	0.4716	1.68E-03	0.7327	4.633	8193.84
30	40	99.3	101.3	129.1	131.6	0.3	99.6	130.4	99.5	678.3	892.9	1571.2	836.23	3.020	0.4130	1.54E-03	0.6418	4.694	9543.97
30	50	99.4	101.4	127.1	129.5	0.3	99.7	128.3	99.6	678.2	1105.2	1783.4	836.16	3.428	0.3732	1.43E-03	0.5799	4.684	10856.15
40	50	99.3	101.2	126.3	128.9	0.2	99.5	127.6	99.4	889.4	1105.2	1994.7	836.26	3.834	0.3413	1.41E-03	0.5303	4.699	12103.77
40	60	99.5	101.5	125.3	127.9	0.3	99.8	126.6	99.7	889.3	1331.0	2220.3	836.09	4.268	0.3132	1.34E-03	0.4866	4.675	13543.74
40	70	100.1	101.9	124.5	127.1	0.1	100.2	125.8	100.2	889.1	1545.6	2434.6	835.76	4.682	0.2908	1.28E-03	0.4519	4.628	15007.36
40	80	100.5	102.3	124.0	126.6	0.1	100.6	125.3	100.6	888.9	1758.6	2647.5	835.49	5.093	0.2719	1.24E-03	0.4225	4.591	16455.84
50	80	100.9	102.7	123.7	126.3	0.1	101.0	125.0	101.0	1099.9	1758.4	2858.3	835.22	5.501	0.2557	1.20E-03	0.3973	4.555	17913.87
60	80	101.6	103.4	123.8	126.4	0.1	101.7	125.1	101.7	1333.4	1758.0	3091.4	834.75	5.953	0.2400	1.17E-03	0.3730	4.492	19656.65
60	90	102.6	104.4	124.3	127.0	0.1	102.7	125.7	102.7	1333.1	1978.1	3311.1	834.08	6.381	0.2270	1.15E-03	0.3528	4.405	21489.21

Test section No(2) at power supply 801.2 W

Q(sup) = 801.2 W
At(surfas) = 0.01969 m2
Ai(surfas) = 0.01267 m2
Eff. = 0.98

%F.S.R No(1)	%F.S.R No(2)	T(5) C	T(6) C	T(7) C	T(8) C	Dt C	T(Bulk) C	T(wall) C	T(Avrag) C	M1 kg/h	M2 kg/h	M (M1+M2) kg/h	Density Kg/m3	Velocity m/sec	1/(V^.8)	1/Ut	(1/V^.8) *(At/Ai)	Kinematic Viscosity mm2/sec	Re
0	60	99.9	102.6	162.9	169.4	0.8	100.6	166.2	100.3	0.0	1330.8	1330.8	835.66	2.560	0.4715	1.64E-03	0.7326	4.614	8228.82
0	70	100.2	102.9	159.4	166.1	0.8	100.9	162.8	100.6	0.0	1545.4	1545.4	835.46	2.973	0.4182	1.55E-03	0.6499	4.587	9615.84
0	80	100.6	103.1	155.6	162.4	0.6	101.1	159.0	100.9	0.0	1758.4	1758.4	835.25	3.384	0.3771	1.45E-03	0.5860	4.559	11009.22
0	90	100.8	103.2	153.6	160.4	0.5	101.2	157.0	101.1	0.0	1978.8	1978.8	835.15	3.809	0.3431	1.40E-03	0.5331	4.546	12427.76
0	100	101.2	103.6	151.5	158.5	0.5	101.6	155.0	101.5	0.0	2206.2	2206.2	834.89	4.247	0.3144	1.34E-03	0.4886	4.510	13970.54
40	70	101.3	103.7	150.1	157.2	0.5	101.7	153.7	101.6	888.4	1545.2	2433.6	834.82	4.686	0.2907	1.30E-03	0.4517	4.501	15442.37
50	70	101.5	103.8	148.3	155.5	0.4	101.9	151.9	101.7	1099.6	1545.1	2644.8	834.72	5.093	0.2719	1.26E-03	0.4225	4.488	16834.07
50	80	101.5	103.8	147.0	154.3	0.4	101.9	150.7	101.7	1099.6	1758.0	2857.6	834.72	5.503	0.2556	1.22E-03	0.3972	4.488	18188.81
60	80	101.2	103.5	145.5	152.8	0.4	101.6	149.2	101.4	1333.5	1758.1	3091.6	834.92	5.952	0.2400	1.19E-03	0.3730	4.514	19557.15
60	90	100.7	102.9	144.1	151.4	0.3	101.0	147.8	100.9	1333.6	1978.9	3312.6	835.29	6.374	0.2272	1.17E-03	0.3531	4.564	20718.18

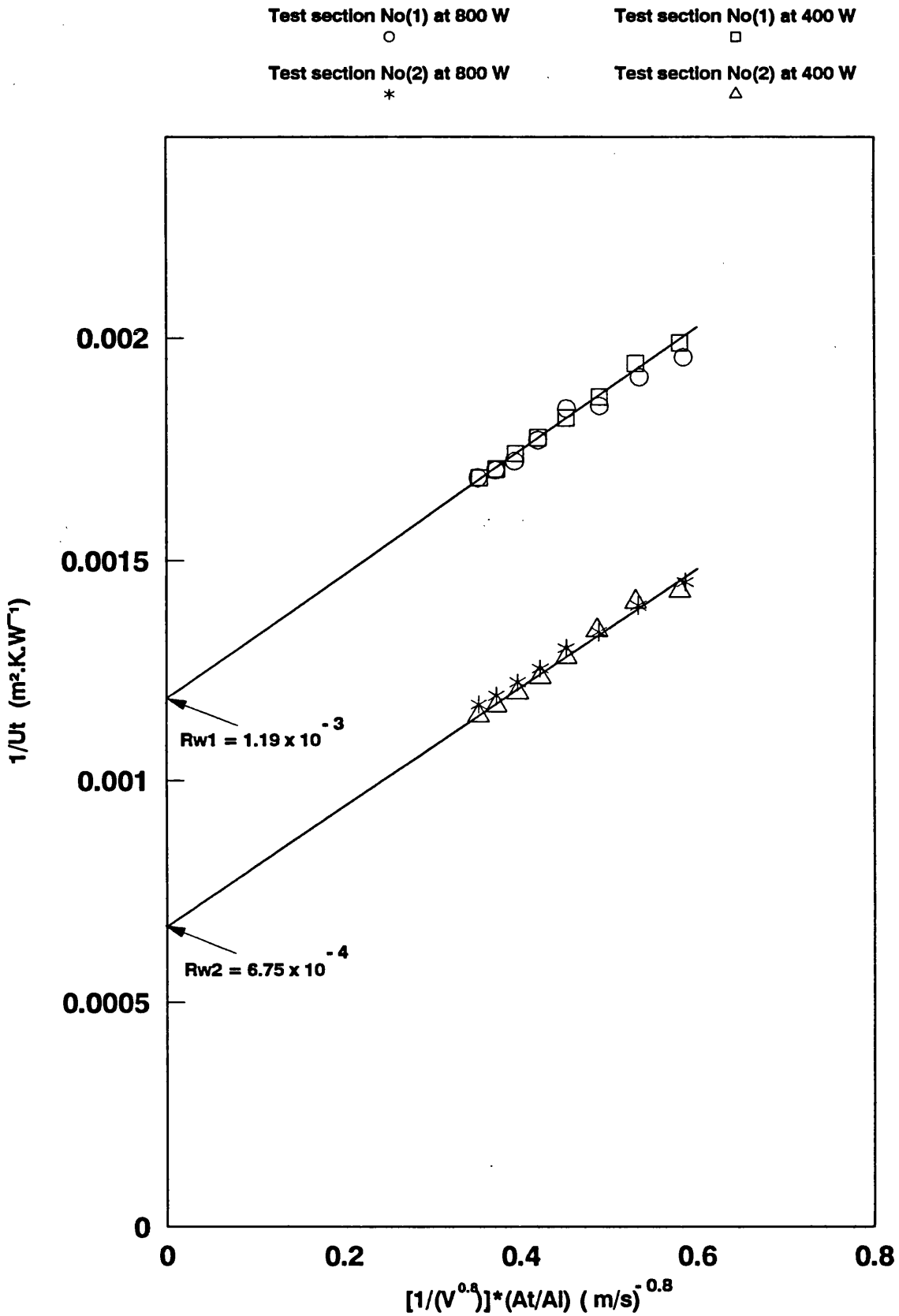

Fig (3.18) Wilson plot for thermal resistance calculation

Both bare tube test sections using Santotherm 55

Table 3.10 Wilson plot data used in Fig (3.18)

Test section No(1) Santotherm 55						Test section No(2) Santotherm 55					
Q(sup) = 400 W			Q(sup) = 800 W			Q(sup) = 400 W			Q(sup) = 800 W		
Re	(1/V^0.8) *(At/Ai)	1/Ut	Re	(1/V^0.8) *(At/Ai)	1/Ut	Re	(1/V^0.8) *(At/Ai)	1/Ut	Re	(1/V^0.8) *(At/Ai)	1/Ut
8604.595	0.720527	0.002134	8844.130	0.730133	0.002133	8193.841	0.732747	0.001675	8228.817	0.732600	0.001644
9681.556	0.641706	0.002056	10453.51	0.650130	0.002050	9543.965	0.641822	0.001539	9615.835	0.649877	0.001551
10859.85	0.580217	0.001989	12164.00	0.584295	0.001956	10856.15	0.579907	0.001432	11009.21	0.585994	0.001451
12091.27	0.530296	0.001942	13568.45	0.534577	0.001911	12103.77	0.530286	0.001406	12427.75	0.533114	0.001398
13439.68	0.489258	0.001867	14997.77	0.489305	0.001846	13543.73	0.486641	0.001342	13970.54	0.488562	0.001338
15957.67	0.451837	0.001819	15530.13	0.452103	0.001839	15007.35	0.451907	0.001281	15442.36	0.451655	0.001302
17546.02	0.419785	0.001774	17686.60	0.419707	0.001769	16455.83	0.422491	0.001236	16834.07	0.422529	0.001255
19017.93	0.394502	0.001739	21327.54	0.393392	0.001721	17913.87	0.397276	0.001201	18188.80	0.397159	0.001224
20466.17	0.373161	0.001704	23197.07	0.371861	0.001702	19656.64	0.372955	0.001171	19557.14	0.372994	0.001193
22049.81	0.353740	0.001684	25159.88	0.352016	0.001685	21489.20	0.352790	0.001148	20718.18	0.353078	0.001173

3.4.1.3 Heat transfer dimensionless groups

The heat transfer dimensionless groups such as Nusselt Number (Nu), Stanton Number (St) and j_H Factor can be calculated based on the in-tube heat transfer coefficient (h_i) as follows:

$$Nu = \frac{h_i D_i}{k} \qquad (3.67)$$

$$St = Nu/Pr.\ Re \qquad (3.68)$$

$$j_H = Nu.\ (Pr)^{-1/3}\ (\mu_b/\mu_w)^{-0.14} \qquad (3.69)$$

Where:

$$Re\ (Reynolds\ Number) = \frac{v\ D_i\ \rho}{\mu} = \frac{vD_i}{\nu} \qquad (3.70)$$

$$Pr\ (Prandtl\ Number) = \frac{\mu\ C_p}{k} \qquad (3.71)$$

where:

μ, ν , ρ, k and C_p are the physical properties of Santotherm 55 given in section 3.2. The subscripts b and w refer to the viscosity of the Santotherm 55 at the bulk fluid and inner tube wall temperatures respectively.

3.4.2 Inner Surface temperature (T_i)

The heat transfer coefficient (h_i) based on the internal area of the test section is expressed as follows:

$$h_i = \frac{Q/A_i}{(T_i - T_b)} \qquad (3.72)$$

Or,

$$\frac{1}{h_i} = \frac{(T_i - T_b)}{Q/A_i} \qquad (3.73)$$

However, from equation 3.28,

$$\frac{1}{h_i} = \frac{A_i}{Q}(T_w - T_b) - R_w \frac{A_i}{A_t}$$

Therefore,

$$\frac{A_i}{Q}(T_w - T_b) - R_w \frac{A_i}{A_t} = \frac{(T_i - T_b)}{Q/A_i}$$

Thus,

$$T_i = T_w - (Q/A_t) R_w \qquad (3.74)$$

Where,

T_i is the inner surface temperature of the test section (°C)

The inner surface temperature (T_i) for each test section may be calculated as follows :

$$T_{i(1)} = T_{w(1)} - \frac{\eta_1 Q_{(sup)1}}{At} R_{w(1)}$$

Or,

$$T_{i(1)} = \frac{T_3 + T_4}{2} - \frac{0.98\, Q_{(sup)1}}{1.97 \times 10^{-2}} (1.19 \times 10^{-3})$$

$$T_{i(1)} = \frac{T_3 + T_4}{2} - 0.0592 Q_{(sup)1} \qquad (3.75)$$

And,

$$T_{i(2)} = T_{w(2)} - \frac{\eta_2 Q_{(sup)2}}{At} R_{w(2)}$$

$$T_{i(2)} = \frac{T_7 + T_8}{2} - \frac{0.98\, Q_{(sup)2}}{1.97 \times 10^{-2}} (6.75 \times 10^{-4})$$

$$T_{i(2)} = \frac{T_7 + T_8}{2} - 0.03358\, Q_{(sup)2} \qquad (3.76)$$

3.4.3 Friction factor

The pressure drop across the heated test section was measured as previously described in Chapter 2. The Fanning friction factor for the bare tube and with a **HiTran** insert may be calculated as follows[13,14]:

$$f\frac{L_p}{r_i} = \frac{\Delta p}{\rho v^2/2g_c} \qquad (3.77)$$

Or,

$$f = \frac{2r_i \Delta p\, g_c}{L_p \rho v^2} \qquad (3.78)$$

Where:

f is the Fanning friction factor

r_i is the inner tube radius

$r_i = D_i/2 = 7.415 \times 10^{-3}$ (m)

L_p is the length between the two tappings (X and Y in Fig 2.4 of Chapter 2)

$L_p = 0.372$ (m)

g_c is the gravitational acceleration conversion factor = 1 $(\frac{kg\ m}{N\ s^2})$

v is the average velocity of the fluid ($m\ s^{-1}$)

$$v = \frac{m}{\rho S \times 3600} \qquad (3.79)$$

where:

m is the mass flow rate at a given % F.S.R and T_{av} ($kg\ hr^{-1}$)

ρ is the density of fluid at given T_{av} ($kg\ m^{-3}$)

T_{av} is the average bulk fluid temperature (^oC)

$$T_{av} = (T_{out} + T_{in})/2 \qquad (3.80)$$

S is the cross section area of test section (m^2)

$$S = \frac{\pi D_i^2}{4} = 1.7273\times10^{-4} \qquad (m^2)$$

Therefore,

$$v = \frac{m}{0.62183\,\rho} \qquad (3.81)$$

And,

$$f = 3986.56\frac{\Delta p}{\rho\, v^2} \qquad (3.82)$$

Where ,

Δp is pressure drop across L_p (bar)

For fully hydrodynamically developed flow, f is called the Fanning (or Skin) friction factor and is defined as the ratio of wall shear stress (τ) to the flow kinetic energy per unit volume ($\rho v^2/2g_c$). However, if the fluid is not in fully developed flow, f is called the apparent Fanning friction factor (f_{app}) which is a combination of both the skin friction and the friction due to the change in the shape of the velocity profile in the hydrodynamic entrance region[13,14].

3.4.4 Enhancement factor (EF)

The use of a **HiTran** insert, as well as any other heat transfer enhancement techniques, causes an increase in the heat transfer coefficient and a substantial increase in pressure drop over the bare tube case .

In order to provide a simple and practical means which can demonstrate the effect of using **HiTran** inserts, on both the heat transfer coefficient and the pressure drop simultaneously, the enhancement factor (EF) (method b in chapter 1 section 1.2.2 , equation 1.99) which is introduced by Agrawal and Senguptel[18], is used in the present study :

$$EF = \frac{(R_{Nu} - 1)}{(R_{\Delta p} - 1)} \qquad (3.83)$$

Where ;

$$R_{Nu} = \frac{\text{Nu for insert case}}{\text{Nu for bare tube case}} \qquad (3.84)$$

$$R_{\Delta p} = \frac{\Delta p \text{ for insert case}}{\Delta p \text{ for bare tube case}} \qquad (3.85)$$

The Nusselt numbers and pressure drops for both cases (with and without **HiTran** inserts) must be measured under similar conditions of bulk temperature, heat flux and mass flow rate.

Using an EF technique makes it possible to compare different types of **HiTran** inserts.

3.5 Results and Discussion for Santotherm 55 study

3.5.1 Results

The experimental conditions for the Santotherm 55 study are summarized in Tables 3.12 to 3.17. Examples of the friction factor and the heat transfer results are tabulated in Appendix (B)

This study was carried out for the bare tube and for the tube fitted with different types of HiTran inserts (low, medium and high loop densities as shown in Fig 3.20). These HiTran inserts were similar to those used in other investigations[19-25] .

Two sets of HiTran inserts (labelled A and B) , of similar physical dimension but from different sources , were tested. The first set (LDI-A. MDI-A and HDI-A) was supplied by Cal Gavin Ltd, U.K, while the other set (LDI-B. MDI-B and HDI-B) was supplied by Norton Co. USA.

A comprehensive comparison between the performance of the bare tube and the tube fitted with different types of HiTran insert from the two sources was carried out for three different bulk temperatures (80 °C, 100 °C and 150 °C). At each bulk temperature , the power supplied , $Q_{(sup)}$, to each test section , was varied as follows:

$Q_{(sup)}$ = 200, 400, 600, 800, 1000 W ;

LDI [Low loop density insert (2.7 loops per cm)]

MDI [Medium loop density insert (6.4 loops per cm)]

HDI [High loop density insert (10.5 loops per cm)]

Fig (3.20) Three different types of HiTran inserts used in the present study

The relationship between $Q_{(sup)}$ and heat flux (q) , based on outer surface area of heated test section (A_o), is as follows,

$$q = \frac{\eta Q_{(sup)}}{A_o} \qquad (3.86)$$

Where :

η is the test section efficiency = 0.98

A_o is the outside surface area of the heated test section (m^2)

$A_o = \pi L D_o = \pi (0.272)(1.905 \times 10^{-2}) = 1.628 \times 10^{-2}$ (m^2)

Therefore ,

$$q = 6.02 \times 10^{-2} \; Q_{(sup)} \qquad (3.87)$$

Values of q ($kW\ m^{-2}$) based on equation 3.87 are plotted against $Q_{(sup)}$ in Fig. (3.21). For each, $Q_{(sup)}$, the following flow rates were used :

% F.S.R = 10, 20. 30, 40, 50, 60, 70, 80, 90 and 100%

At each % F.S.R , temperature and pressure drop measurements in Table 3.11 were collected for five power supplies as shown in Tables 3.12 to 3.17 :

Table 3.11 Temperature and pressure drop measurements

	test section No(1)	test section No(2)
inlet temperature	T_1	T_5
outlet temperature	T_2	T_6
wall temperatures	T_3 and T_4	T_7 and T_8
pressure drop	Δp_1	Δp_2

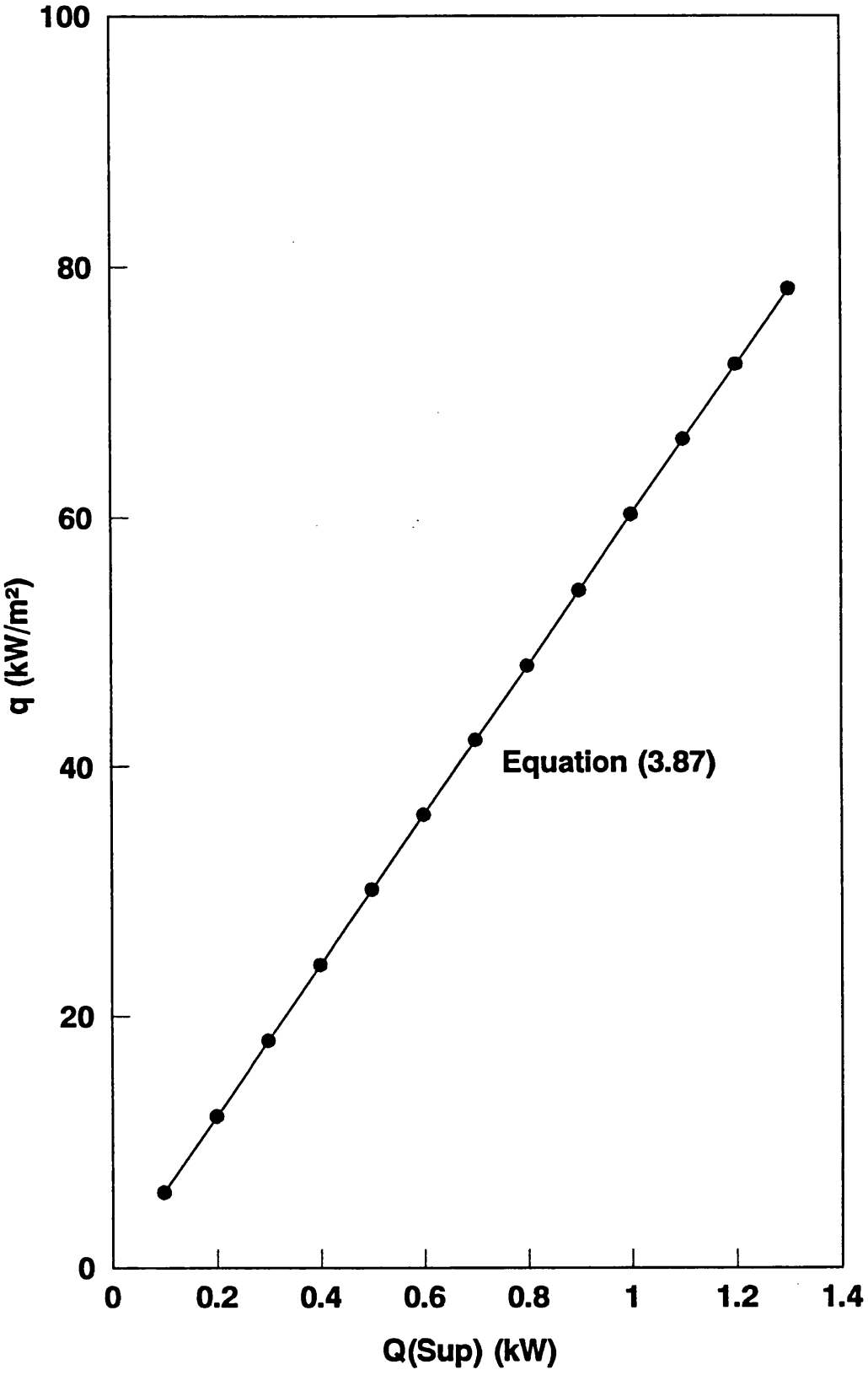

Fig (3.21) Heat flux q(kW/m²) vs power supply (Q(sup)

Heat flux q based on the outer surface area (Ao) of heated test section

Table No(3.12) Summary of Experimental Conditions of Santotherm 55 Study

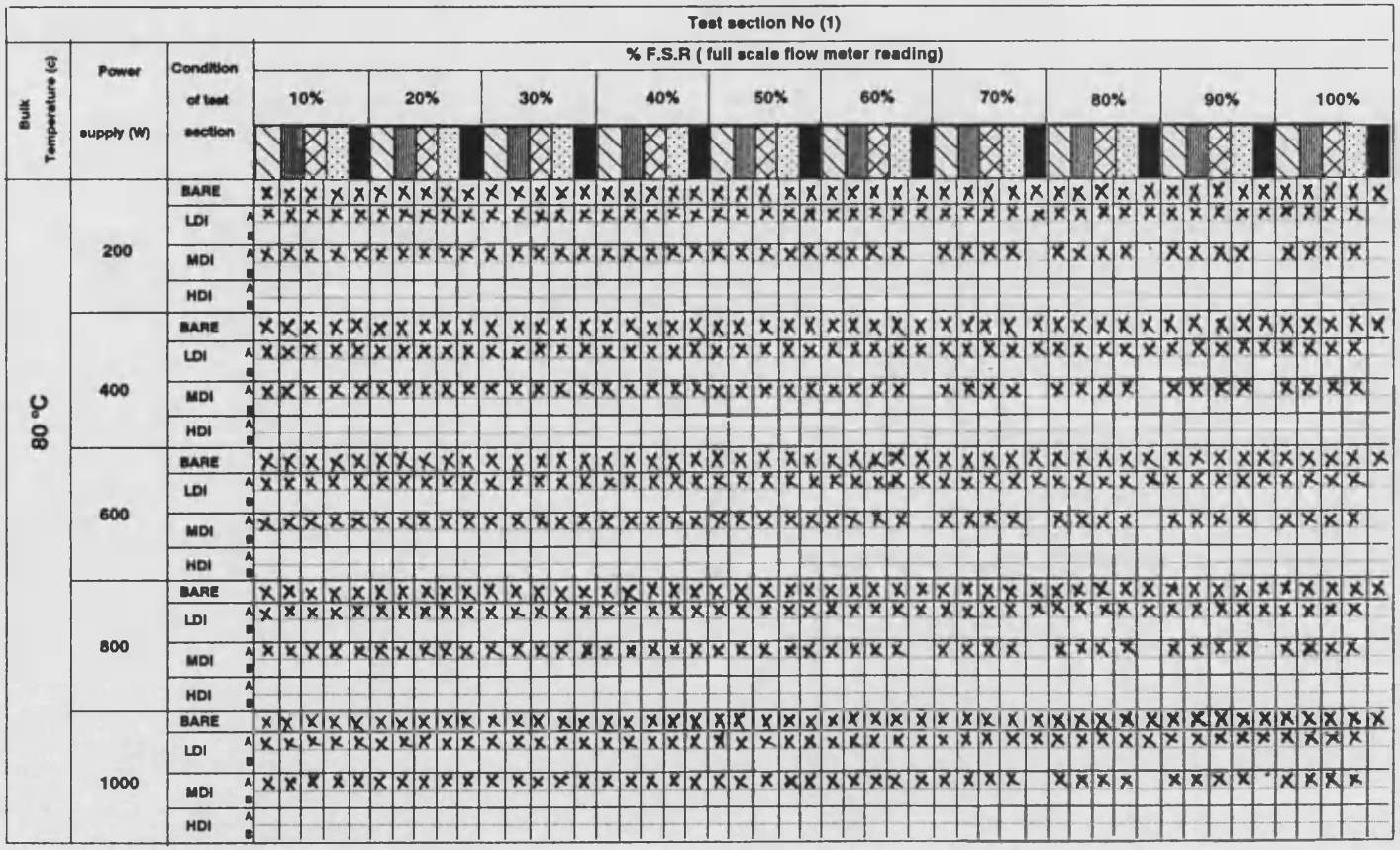

T1
T2
T3
T4
ΔP1

Number of measurements :

- x once
- * twice
- ▲ three times
- ■ four times

Type of HiTran Inserts :

- LDI (low loop density)
- MDI (medium loop density)
- HDI (high loop density)

The supplier of HiTran Inserts :

- A - set supplied by Cal Gavin Ltd.
- B - set supplied by Norton Co.

Table No(3.13) Summary of Experimental Conditions of Santotherm 55 Study

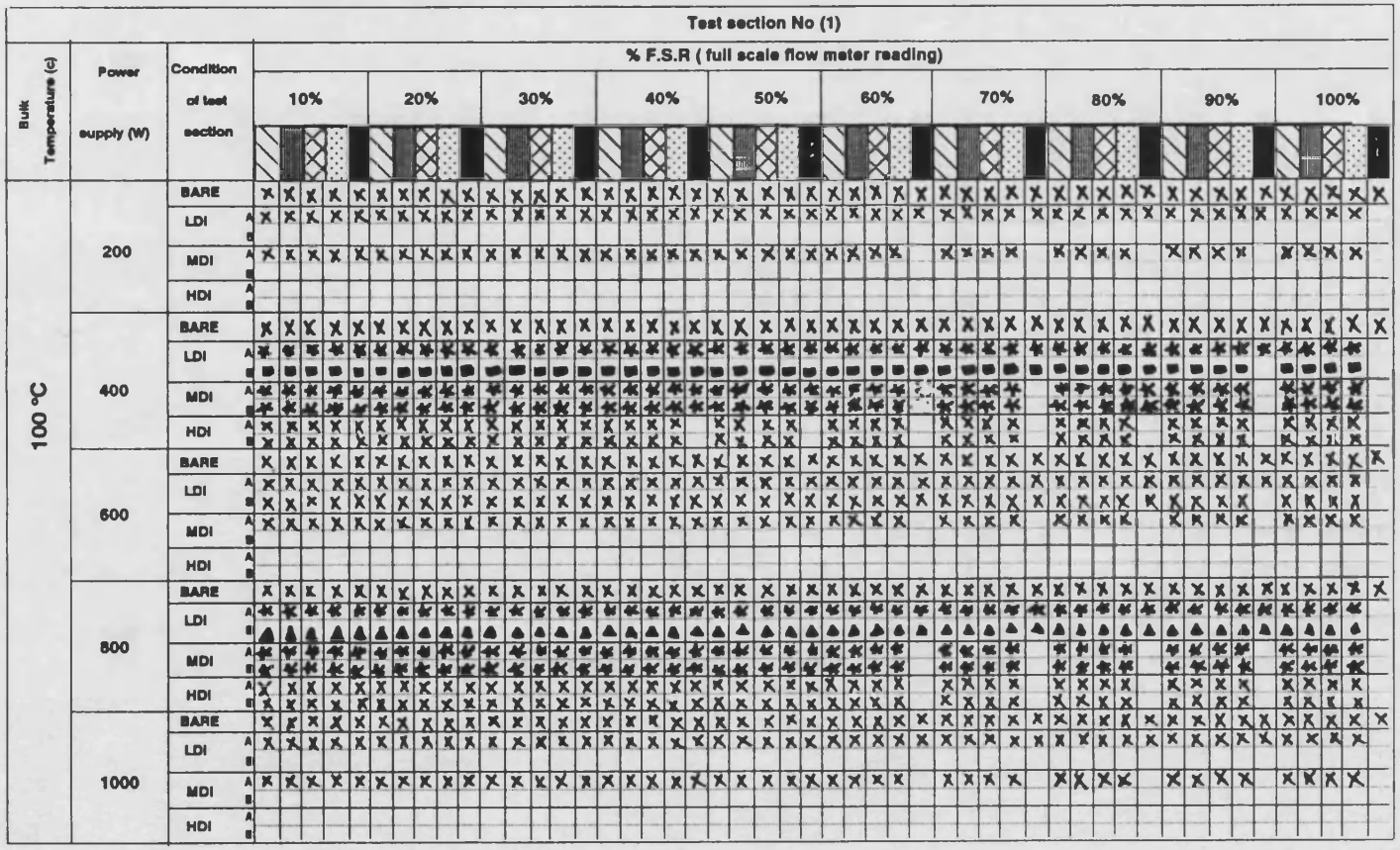

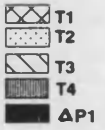

Number of measurements :

- x once
- * twice
- ▲ three times
- ■ four times

Type of HiTran inserts :

- LDI (low loop density)
- MDI (medium loop density)
- HDI (high loop density)

The supplier of HITran inserts :

- A - set supplied by Cal Gavin Ltd.
- B - set supplied by Norton Co.

Table No(3.14) Summary of Experimental Conditions of Santotherm 55 Study

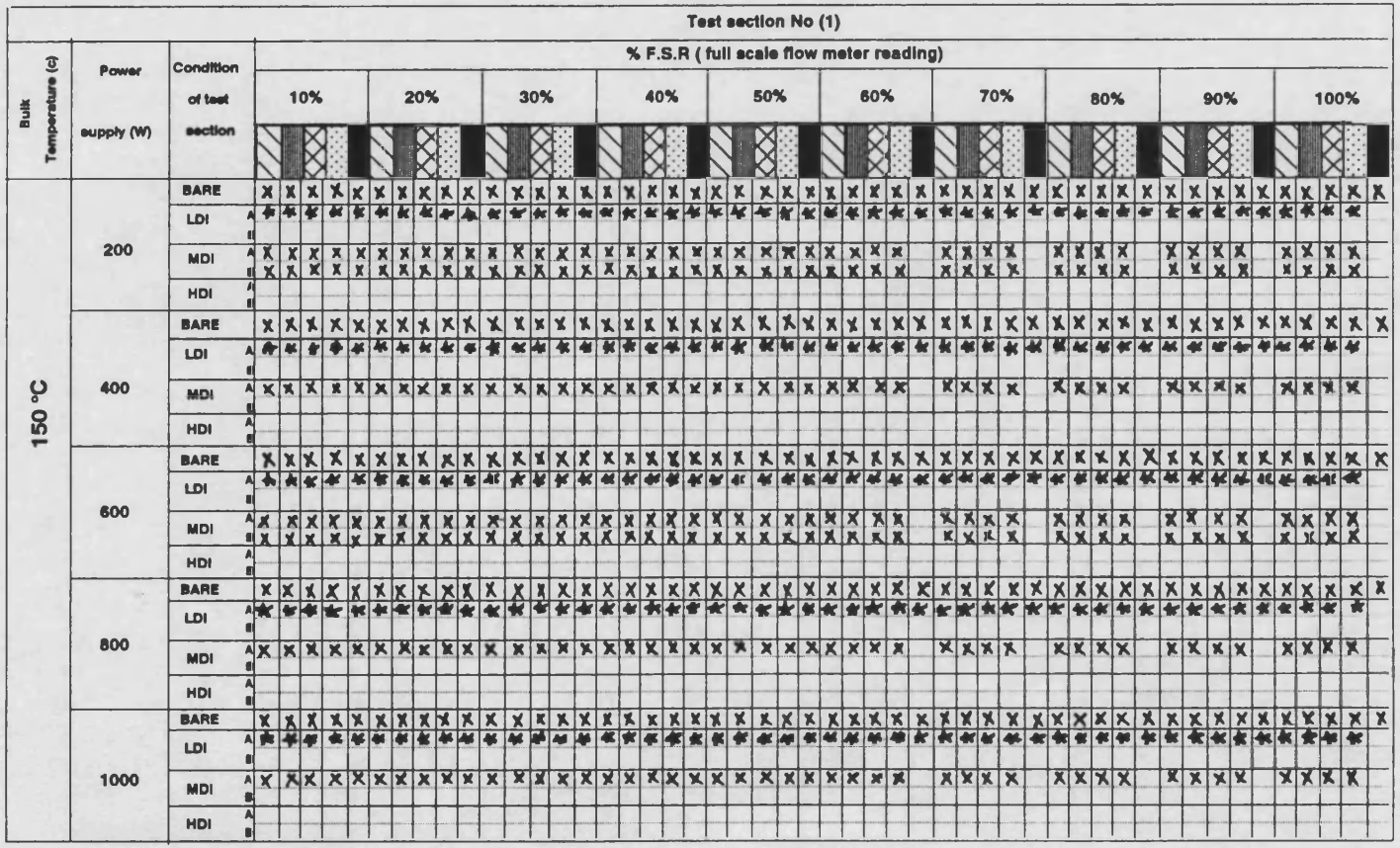

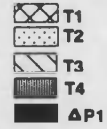

Number of measurements :

- x once
- * twice
- ▲ three times
- ■ four times

Type of HITran Inserts :

- LDI (low loop density)
- MDI (medium loop density)
- HDI (high loop density)

The supplier of HITran Inserts :

- A - set supplied by Cal Gavin Ltd.
- B - set supplied by Norton Co.

Table No(3.15) Summary of Experimental Conditions of Santotherm 55 Study

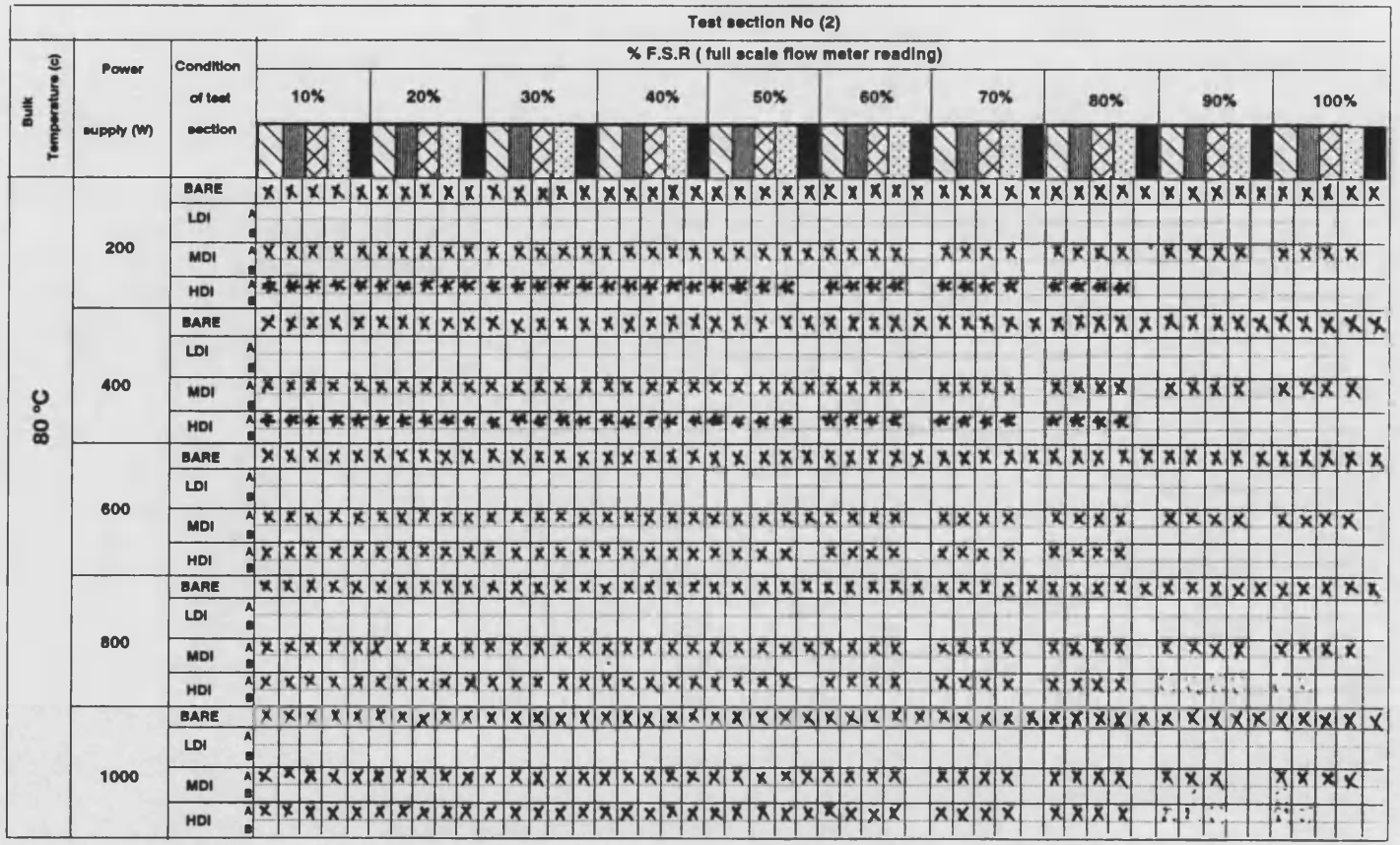

T5
T6
T7
T8
ΔP2

Number of measurements :

x once
∗twice
▲ three times
■ four times

Type of HiTran inserts :

LDI (low loop density)
MDI (medium loop density)
HDI (high loop density)

The supplier of HiTran inserts :

A - set supplied by Cal Gavin Ltd.
B - set supplied by Norton Co.

Table No(3.16) Summary of Experimental Conditions of Santotherm 55 Study

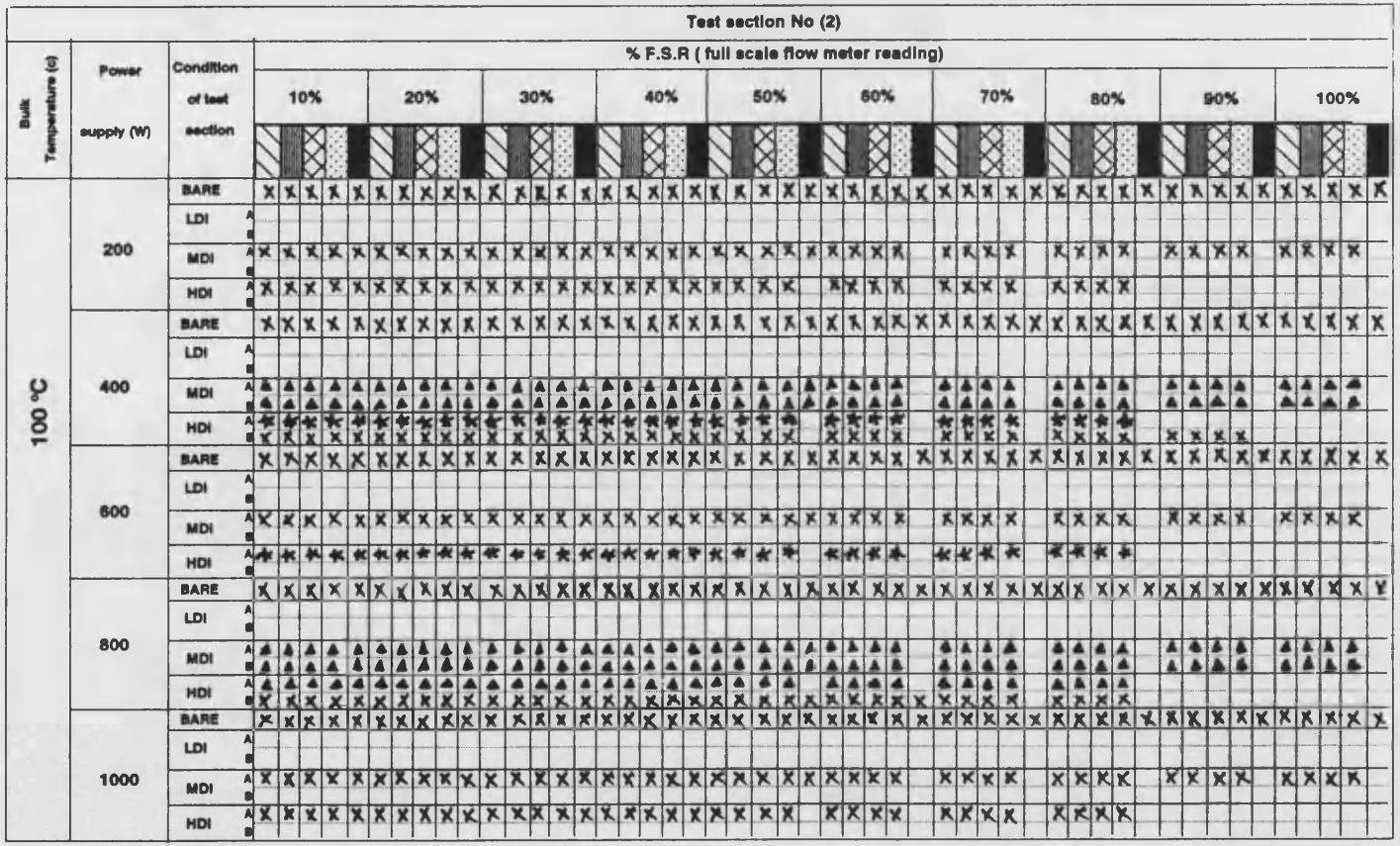

T5
T6
T7
T8
ΔP2

Number of measurements :

- x once
- * twice
- ▲ three times
- ■ four times

Type of HITran inserts :

- LDI (low loop density)
- MDI (medium loop density)
- HDI (high loop density)

The supplier of HITran inserts :

- A - set supplied by Cal Gavin Ltd.
- B - set supplied by Norton Co.

Table No(3.17) Summary of Experimental Conditions of Santotherm 55 Study

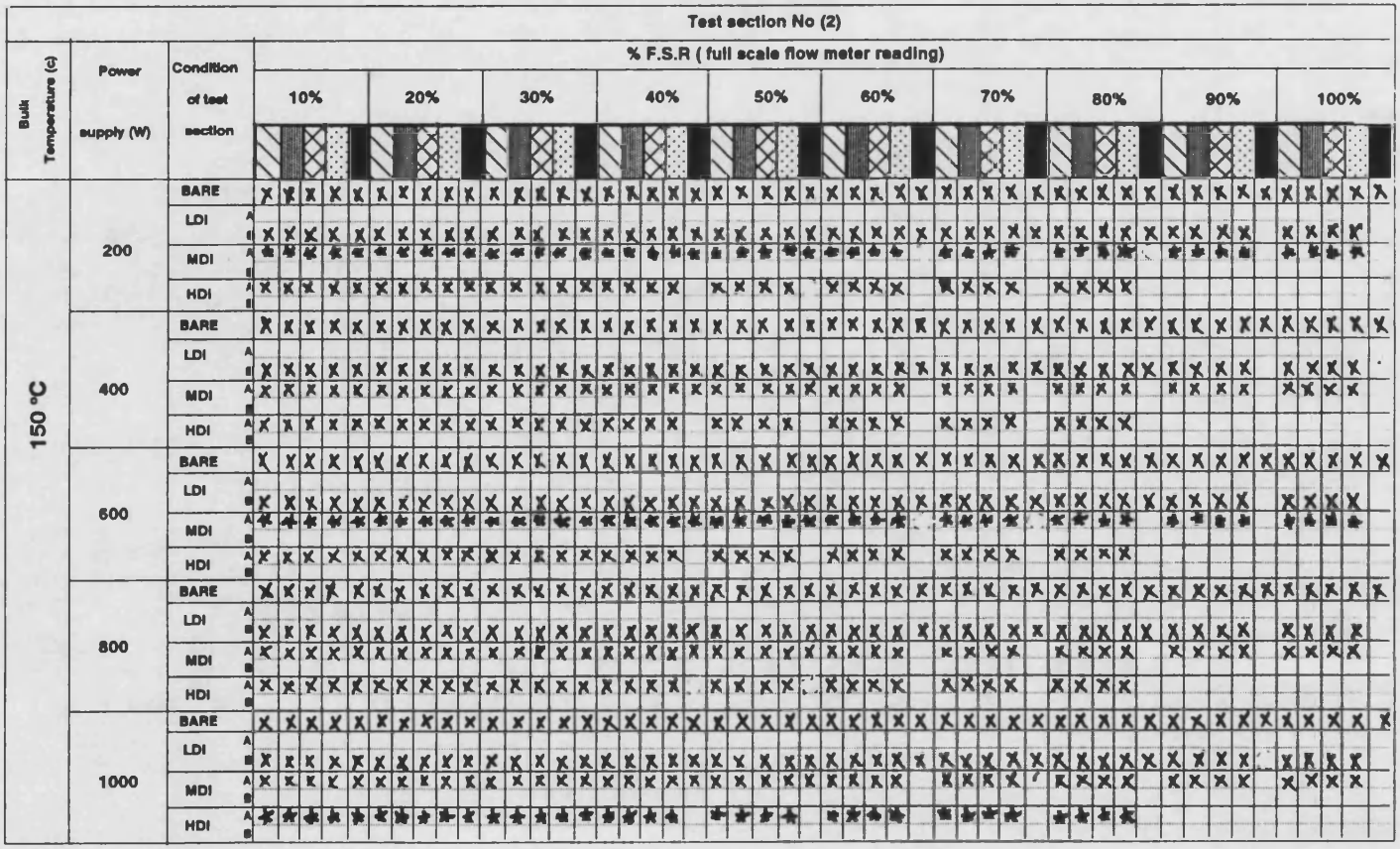

T5
T6
T7
T8
ΔP2

Number of measurements :

x once
* twice
▲ three times
■ four times

Type of HITran inserts :

LDI (low loop density)
MDI (medium loop density)
HDI (high loop density)

The supplier of HITran inserts :

A - set supplied by Cal Gavin Ltd.
B - set supplied by Norton Co.

The total number of readings (data points) taken was approximately 6500 of which 1500 were for the bare tube and around 5000 for the tube fitted with **HiTran** inserts. The ranges of Reynolds number (Re) and Prandtl number (Pr) tested were as follows; $500 < Re < 34000$ and $30 < Pr < 187$.

3.5.2 Discussion

The results of the Santotherm 55 fluid study will be discussed under the following headings;

3.5.2.1- Entrance lengths (L_{hy}) and (L_{th})

a- Theoretical background .

b- Determination of (L_{hy}) and (L_{th}) .

3.5.2.2- Friction factors .

3.5.2.2.1- Bare tube test sections .

3.5.2.2.2- Test sections fitted with HiTran inserts .

I- Low loop density insert (LDI) .

II- Medium loop density insert (MDI) .

III- High loop density insert (HDI) .

IV- Effect of re-using the same HiTran insert.

V- Effect of rotating a HiTran insert inside the test section .

3.5.2.2.3- Comparison between the bare tube and the tube fitted with an insert.

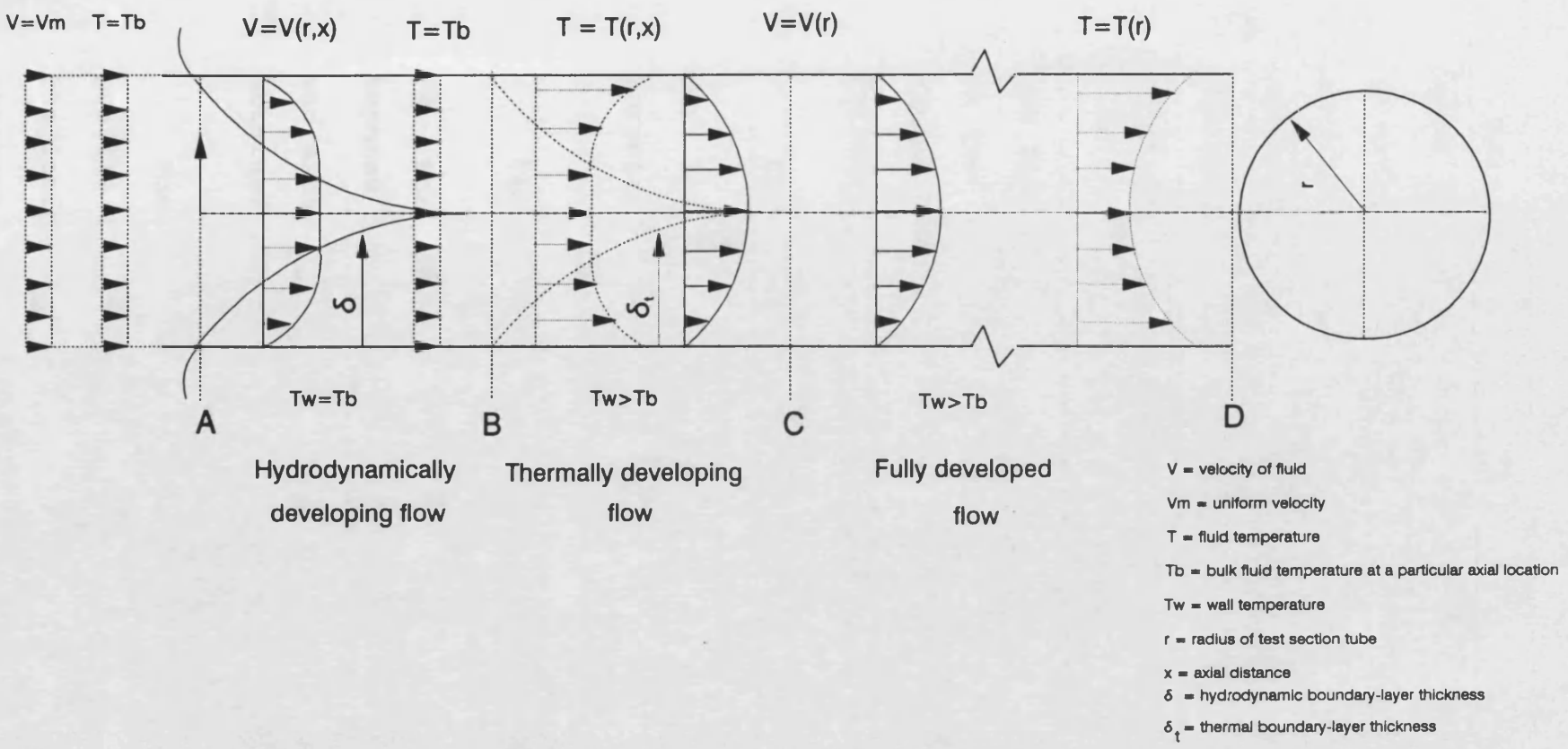

Fig (3.22) Illustration of fluid flow inside the tubular test section at uniform heat flux under laminar flow conditions

increases and in laminar flow fills the tube. Consequently, the velocity profile varies with all space coordinates i.e., v = v (r,x). At the length at which the velocity profile ceases to change, the flow is hydrodynamically developed. The hydrodynamic entrance length (L_{hy}) is defined as the axial distance required to attain 99% of the ultimate fully developed maximum velocity when the entering flow is uniform[3,13]. The value of $(\frac{L_{hy}}{D_i})$ at which the flow becomes hydrodynamically developed, depends on the type of entry and Reynolds number (Re). The dimensionless hydrodynamic length is expressed as follows:

$$L_{hy}^{+} = \frac{L_{hy}}{D_i \, Re} \qquad (3.88)$$

For laminar flow (Re < 2100) the following correlation was obtained by Chen[26] :

$$L_{hy}^{+} = 0.056 + \frac{0.60}{Re\,(0.035\,Re + 1)} \qquad (3.89)$$

For Re > 400 , the second part of equation 3.89 becomes insignificant and $L_{hy}^{+} = 0.056$. This value was experimentally confirmed by Hornbeck[27]. Liu[28] obtained another value of L_{hy}^{+} for liquid metals .

For turbulent flow (Re > 4000) the velocity profile becomes established much more rapidly than the laminar profile because of the much larger shear stresses that a given velocity gradient will

sustain[29]. Thus, the final profile is typically almost fully established[29] in less than 10 tube diameters ($\frac{L_{hy}}{D_i}$ < 10) . In smooth pipes the fully turbulent velocity profile exists[156] after an inlet length of 25-40 tube diameters ($\frac{L_{hy}}{D_i}$ = 25 to 40).

For transition flow (2100 < Re < 4000) the boundary layer thickness also increases very rapidly. The value of $\frac{L_{hy}}{D_i}$ at Re = 2500 is quoted[17] to be in the range of 50 - 100.

II- Thermally developing region

In this region (section B-C in Fig 3.22) the test section is heated by uniform heat flux and the local heat transfer coefficient (h_i) decreases with an increase in axial distance. At the point at which h_i is independent of the tube length, the fluid becomes fully thermally developed. The thermal entrance length (L_{th}) is defined as the duct length required to achieve a local Nusselt number ($Nu_{(x)} = \frac{h_i D_i}{k}$) equal to 1.05 times that for fully thermally developed flow[14] .

The dimensionless thermal entrance length (L_{th}^+) is expressed[13] as:

$$L_{th}^+ = \frac{L_{th}}{D_i Pe} \qquad (3.90)$$

Where:

Pe (Peclet number) = Re Pr
Re (Reynolds number) = $v\rho D_i / \mu$
Pr (Prandtl number) = $\mu Cp / k$

For laminar flow (Re < 2100), a graphical solution for the L_{th}^{+} calculation is provided by Shah[30] . Fig. 3.23 shows the local $Nu_{(x)}$ and mean $Nu_{(m)}$ Nusselt numbers as a function of x^*, where $x^* = (\frac{x}{D_i Pe})$ and x is the axial heated distance. Both $Nu_{(x)}$ and $Nu_{(m)}$ decreased with the increase in x^*. For thermally developed flow, $Nu_{(x)}$ approaches a constant value of 4.364 for a round tube , and Fig 3.23 gives $L_{th}^{+} = 0.0430$. Fig.3.23 also shows that the values of $Nu_{(m)}$ are about 30% higher than $Nu_{(x)}$ values at a given x^* .

For turbulent flow ($Re > 10^4$) and for fluids with high Pr, the thermal resistance is primarily very close to the wall, yielding a temperature profile that is essentially flat over most of the cross section, regardless of thermal boundary layer. Thus there is generally no need to analyse[14] the boundary layer for turbulent flows for fluids with $Pr > 0.5$.

Latzko[32] provides the following expression for L_{th} for turbulent flow in a smooth pipe,

$$\frac{L_{th}}{D_i} = 0.693\, Re^{1/4} \qquad (3.91)$$

Notter and Sleicher[33] provided solutions for several Pr values in the range of $0 < Pr < 10^4$ and stated that for $Pr > 3$ the value of $\frac{L_{th}}{D_i}$ is in the range of 2 to 5 . Kays and London[34] plotted

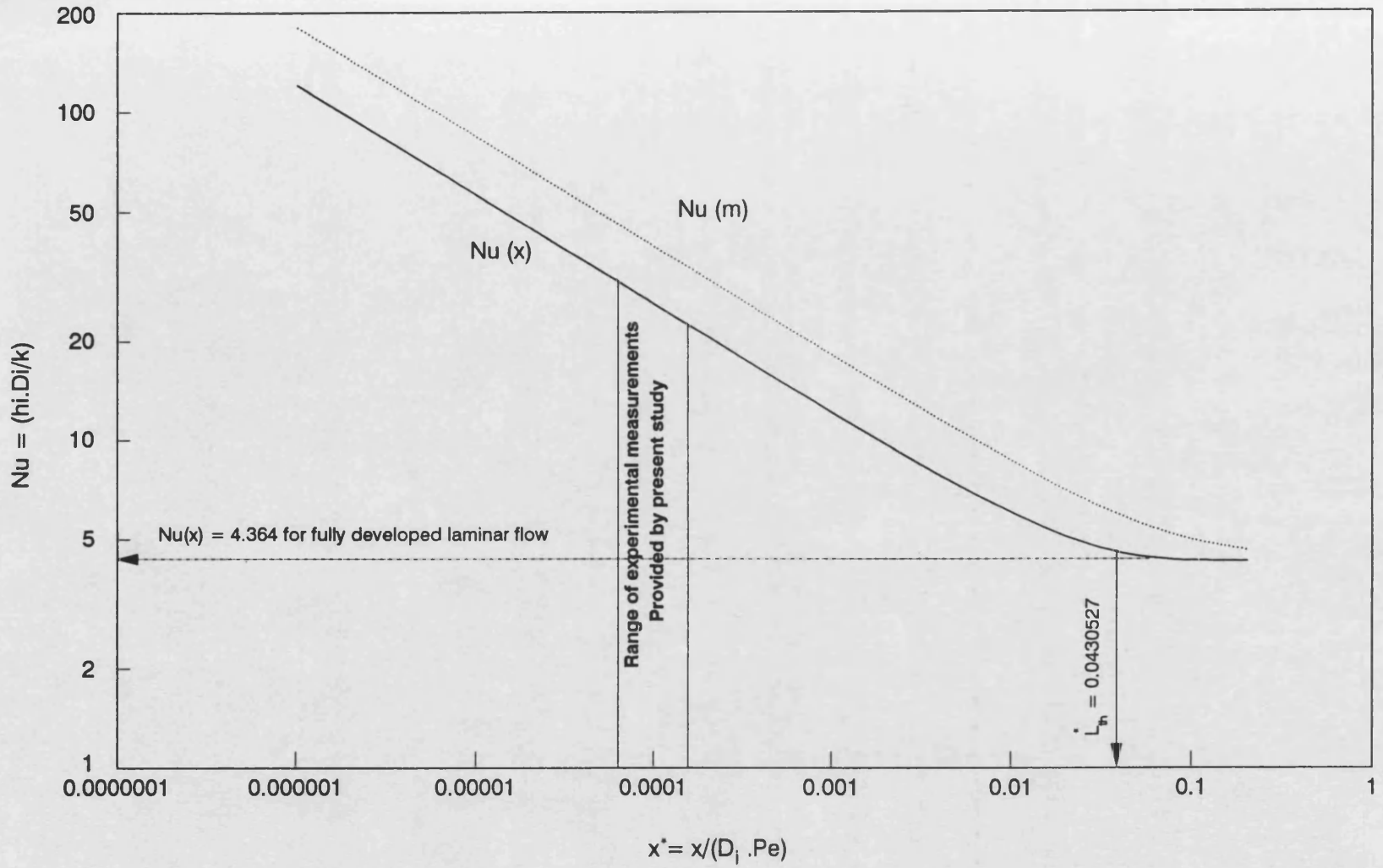

Fig (3.23) Determination of L^*_{th} [after Shah calculation (30)]

$\frac{Nu_{(m)}}{Nu_{(\infty)}}$ versus (x/D_i) for different Pr values at $Re = 10^5$ as shown in Fig. 3.24 , where $(Nu_{(m)}$ and $Nu_{(\infty)}$ are mean and fully developed Nusselt numbers respectively. For fully developed flow at $(\frac{Nu_{(m)}}{Nu_{(\infty)}}) = 1.05$, the value of (x/D_i) decreases with an increase in Pr.

For transition flow ($2100 < Re < 10^4$) the thermal entrance length L_{th} is difficult to determine due to instability in this region[14]. However, Al-Arabi[31] developed the following correlation which may be used for L_{th} estimation within ± 30% error for the ranges of $5000 < Re < 10^4$, $0.7 < Pr < 75$ and $x/D_i > 3$, as,

$$\frac{Nu_{(m)}}{Nu_{(\infty)}} = 1 + \frac{C_a}{x/D_i} \qquad (3.92)$$

$$C_a = \frac{(x/D_i)^{0.1}}{Pr^{1/6}} (0.68 + \frac{3000}{Re^{0.81}}) \qquad (3.93)$$

However, for a fully developed thermal boundary layer (at $x = L_{th}$) the value of $Nu_{(m)} = 1.05\ Nu_{(\infty)}$; therefore,

$$\frac{Nu_{(m)}}{Nu_{(\infty)}} = 1.05 = 1 + \frac{C_a}{(L_{th}/D_i)}$$

or,

$$\frac{L_{th}}{D_i} = \left[\frac{(0.68 + \frac{3000}{Re^{0.81}})}{0.05\ Pr^{1/6}}\right]^{10/9} \qquad (3.94)$$

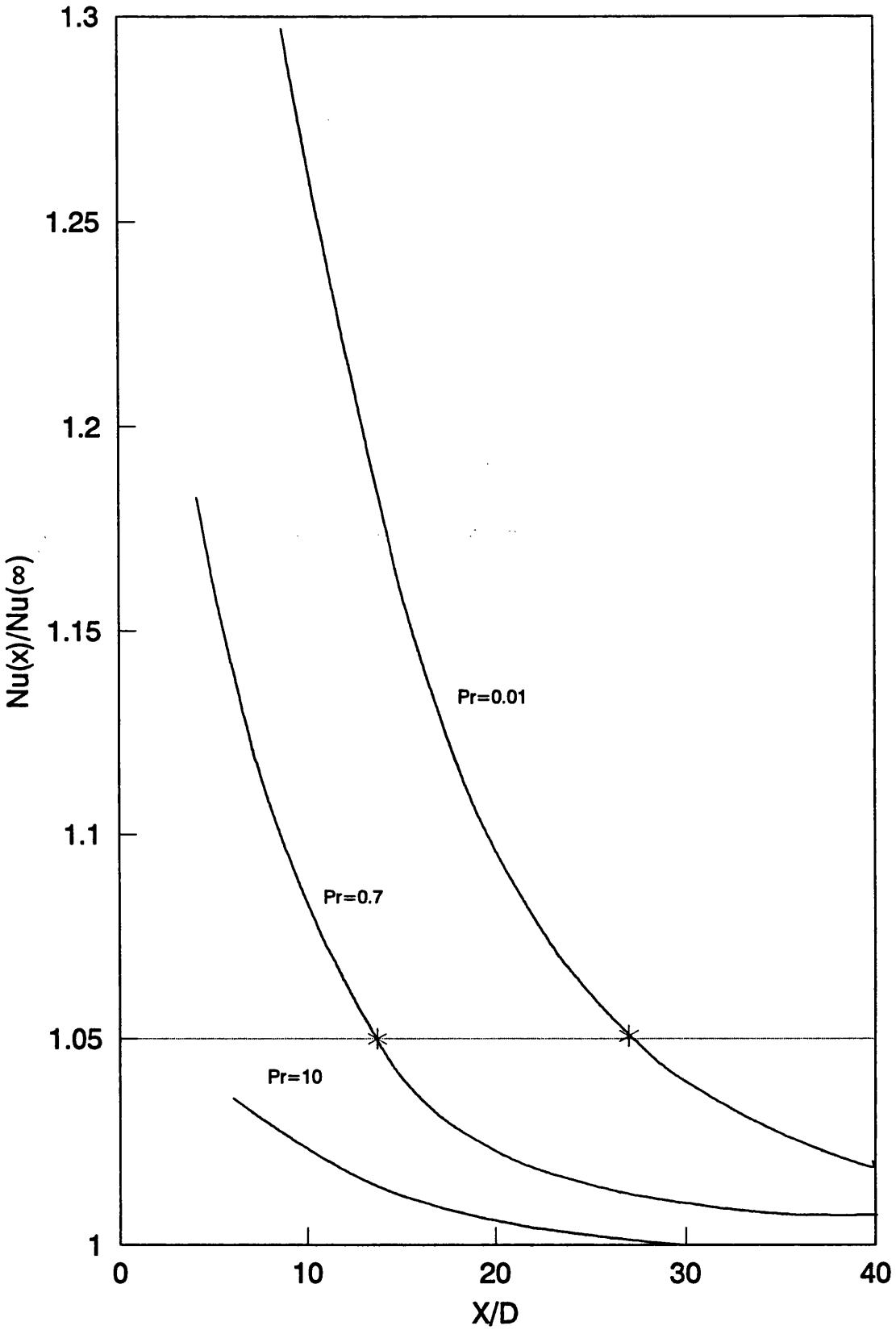

Fig(3.24) Effect of Prandtl number (Pr) on thermal-entry-length for
Hydrodynamically developed turbulent flow at Re = 100,000
Kays and London (34)

III- Fully developed flow

In this region (section C-D in Fig 3.22) both the velocity and temperature profiles are fully developed and the local heat transfer coefficient (h_i) does not change with the axial distance[3].

b - Determination of (L_{hy}) and (L_{th})

The experimentally available hydrodynamic entrance length (L_{hy}) was 108 cm i.e., 73 D_i, and the experimentally available thermal entrance length (L_{th}) was 24.06 cm i.e 16.22 D_i.

The following procedure was applied in order to verify whether the fluid was fully developed , hydrodynamically and thermally , for the ranges of Re and Pr studied .

I- Hydrodynamic entrance length (L_{hy})

For the range of 100 < Re < 2100, L_{hy} was calculated using equation 3.89 (in which D_i = 1.483 cm) and plotted in Fig 3.25 . At Re = 2500 the L_{hy} was taken to be in the band of 50 to 100 Di (as quoted by[17]). For turbulent flow (Re > 4000) the values of $\frac{L_{hy}}{D_i}$ were taken[156,10] as 45 and 10 for Re = 4000 and 10000 respectively. A horizontal line at the experimental value of L_{hy} = 108 cm was drawn to provide a distinction between developed and undeveloped flow . From Fig 3.25 the fluid was hydrodynamically developed

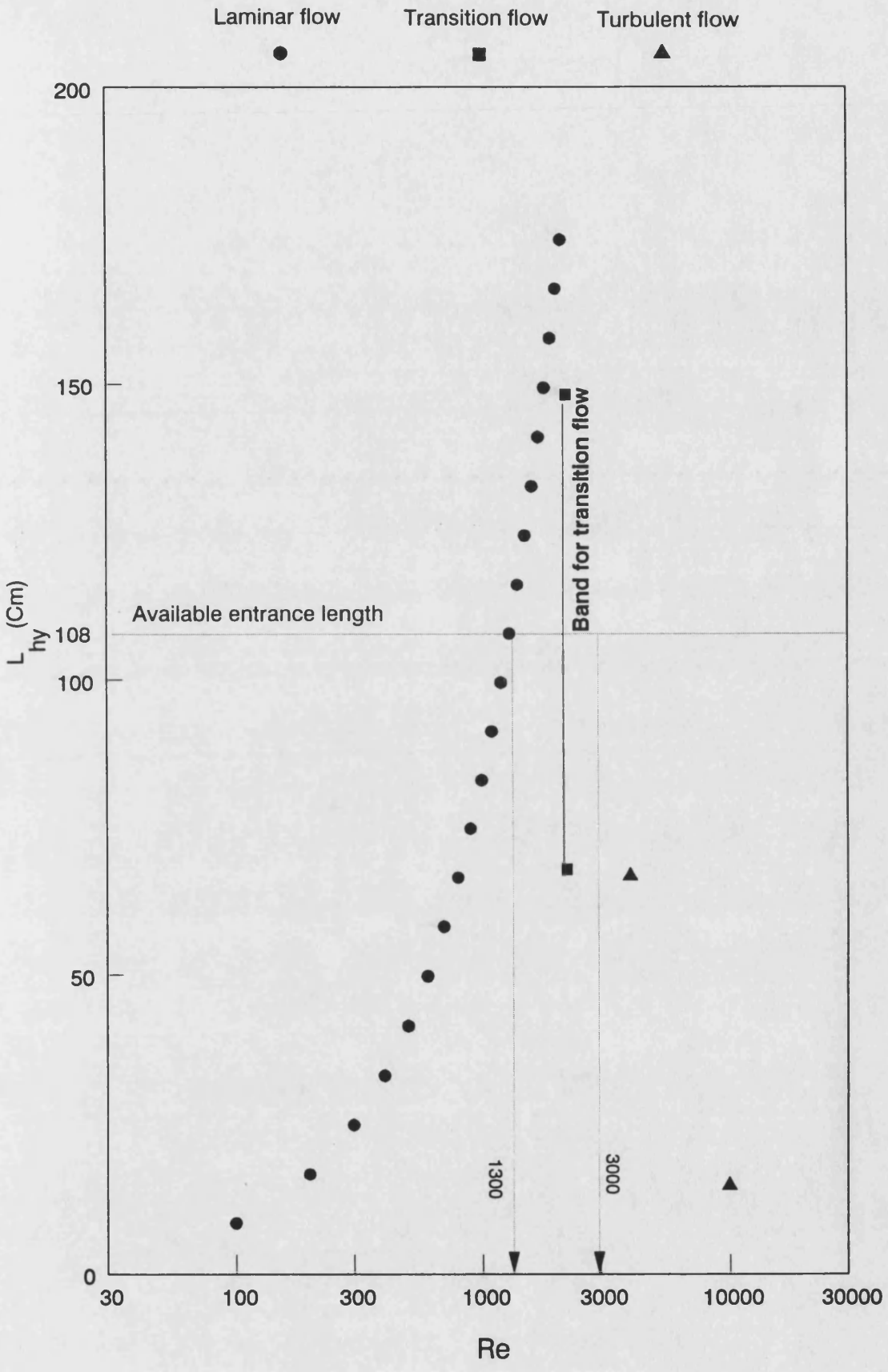

Fig (3.25) Determination of hydrodynamic entrance length

for the whole range of Re except possibly in the range of 1300 < Re < 3000 .

II- Thermal entrance length (L_{th})

The ranges of Re and Pr studied were 570 < Re < 34000 and 30 < Pr < 187 . The values of Re , Pr , Pe and x^* provided by the present study for laminar flow are reported in Table 3.18 . Consequently , from Table 3.18 the values of x^* were in the range of 6.21×10^{-5} to 1.68×10^{-4} , as shown in Fig 3.23. Throughout the range, the x^* values were less than L^+_{th} provided by Shah[30] ($L^+_{th} = 0.043$) . Therefore, the laminar flow in the present study was thermally developing.

For turbulent flow ($Re > 10^4$) , Pr was in the range of 30 to 82 which is much higher than values shown in Fig 3.24 . Thus, the value of L_{th} provided (24.05 cm) should have enabled the fluid to be in fully thermally developed flow.

For transition flow ($2100 < Re < 10^4$), the thermal entrance length L_{th} estimated by equation 3.94 was in the range of 57.56 to 125.5 cm i.e. 2.4 to 5.2 times L_{th} provided by the present experimental study. Thus, for this Re range the fluid was also thermally developing .

Table 3.18 Experimental data ranges for Santotherm 55 in bare tube

(for the laminar flow region)

Re	Pr	Pe	x^*
515.4	187.0	9.64 E+04	1.68 E-04
723.3	133.5	9.66 E+04	1.68 E-04
728.9	135.6	9.89 E+04	1.64 E-04
817.0	121.5	9.93 E+04	1.63 E-04
908.3	108.4	9.84 E+04	1.65 E-04
938.6	106.8	1.00 E+05	1.62 E-04
977.1	101.4	9.91 E+04	1.64 E-04
1060.6	94.1	9.98 E+04	1.63 E-04
1080.1	165.1	1.78 E+05	9.10 E-05
1201.8	85.0	1.02 E+05	1.59 E-04
1291.3	78.8	1.02 E+05	1.59 E-04
1335.2	135.3	1.81 E+05	8.98 E-05
1398.1	120.4	1.68 E+05	9.64 E-05
1466.0	70.9	1.04 E+05	1.56 E-04
1500.2	121.3	1.82 E+05	8.91 E-05
1533.1	68.0	1.04 E+05	1.56 E-04
1551.7	66.8	1.04 E+05	1.56 E-04
1575.0	107.8	1.70 E+05	9.55 E-05
1584.1	66.0	1.05 E+05	1.55 E-04
1613.8	64.5	1.04 E+05	1.56 E-04
1634.3	64.2	1.05 E+05	1.55 E-04
1652.1	103.2	1.70 E+05	9.52 E-05
1657.2	63.4	1.05 E+05	1.54 E-04
1681.9	153.8	2.59 E+05	6.27 E-05
1693.8	108.4	1.84 E+05	8.84 E-05
1788.1	95.9	1.72 E+05	9.42 E-05
1966.4	132.8	2.61 E+05	6.21 E-05
1976.1	54.0	1.07 E+05	1.52 E-04
2074.4	51.7	1.07 E+05	1.51 E-04
2123.6	81.9	1.74 E+05	9.32 E-05

The expected states of hydrodynamic and thermal developement for Santotherm 55 in the bare tube are summarised in Table 3.19 .

Table 3.19 The expected conditions of Santotherm 55 in bare tube test sections

	Laminar flow	Transition flow	Turbulent flow
Hydrodynamically	fully developed for Re < 1300 possibly developing for the range of 1300 < Re < 2100	fully developed for Re > 2500 possibly developing for the range of 2100 < Re < 2500	fully developed
Thermally	developing	developing	fully developed

For the cases in which a **HiTran** insert was fitted inside a test section, the flow would be expected to develop very rapidly . Consequently, the fluid was believed to be fully developed both hydrodynamically and thermally at the axial position where wall temperature measurements were taken, i.e 132.05 cm from the inlet of the test section (108 + 24.05 cm).

3.5.2.2 Friction factors

The friction factor (f) results for the bare tube and for the tube fitted with HiTran inserts are shown in Figs 3.26 to 3.39 .

The friction factor (f) for both bare tube and insert cases was calculated from equation 3.82. In order to compare the experimental results with the theoretical correlations, both Churchill's correlations for smooth[35] tubes (equation 1.50) and for rough[173] tubes (equation 1.51) were plotted as

reference curves throughout all friction factor figures , as follows ;

(1) Churchill correlation for smooth tubes:

$$f = 2\left[\frac{1}{f_1} + f_2\right]^{-1/5} \qquad (3.95)$$

where:

$$f_1 = \left[\left(\frac{8}{Re}\right)^{10} + \left(\frac{Re}{36500}\right)^{20}\right]^{1/2} \qquad (3.96)$$

$$f_2 = [2.21 \ln\left(\frac{Re}{7}\right)]^{10} \qquad (3.97)$$

(1) Churchill correlation for rough tubes:

$$f = 2\left[\left(\frac{8}{Re}\right)^{12} + (A1 + B1)^{-1.5}\right]^{1/12} \qquad (3.98)$$

Where ;

$$A1 = \left[2.2088 + 2.457 \ln\left(\frac{\epsilon}{r_i} + 42.683\, Re^{-0.9}\right)\right]^{16} \qquad (3.99)$$

$$B1 = \left[\frac{37530}{Re}\right]^{16} \qquad (3.100)$$

ϵ is the height of surface roughness element (m)

$\epsilon = 1.5 \times 10^{-5}$ (m) for drawn tubing[17]

r_i is the inside radius of the tubular test section .

$r_i = 7.415 \times 10^{-3}$ (m)

3.5.2.2.1 - Bare tube test sections

The effect of using different heat fluxes in the range of 12 kW/m^2 < q < 60 kW/m^2 at three bulk temperatures (80 °C , 100 °C and 150 °C) on the friction factor of the bare tube is shown in Fig 3.26a. The

effect of the three bulk temperatures (80 °C , 100 °C and 150 °C) at five heat fluxes in the range of 12 kW/m^2 < q < 60 kW/m^2 is shown in Fig 3.26b .

Figs 3.26a and 3.26b show that the experimental results are closer to Churchill's correlation for a smooth tube , equation 3.95 , rather than to the rough tube correlation , equation 3.98 . This suggests that the test sections used in the present study are much smoother than drawn tubing . Consequently , a lower value of ϵ than 1.5×10^{-5} should be used in equation 3.98 . The experimental values of friction factor in the range of fully developed turbulent flow (Re > 10^4) were about 10% higher than those predicted by equation 3.95. The following correlation fits the experimental data for the bare tube in the region of fully developed flow (Re > 10^4) to within ± 5% :

$$f = 0.117\, Re^{0.283} \qquad (3.101)$$

Figs 3.26a and 3.26b also show that the friction factor results in the region of laminar and transition flow i.e, Re < 4000 vary with heat flux (q) and bulk temperature (T_b) . In order to investigate the cause of this variation, a viscosity correction factor , $(\mu_b/\mu_w)^{0.25}$, the same as that used by Sieder and Tate[36] for non - isothermal flow, was applied as shown in Figs 3.27a and 3.27b . Unfortunately , the use of this viscosity correction

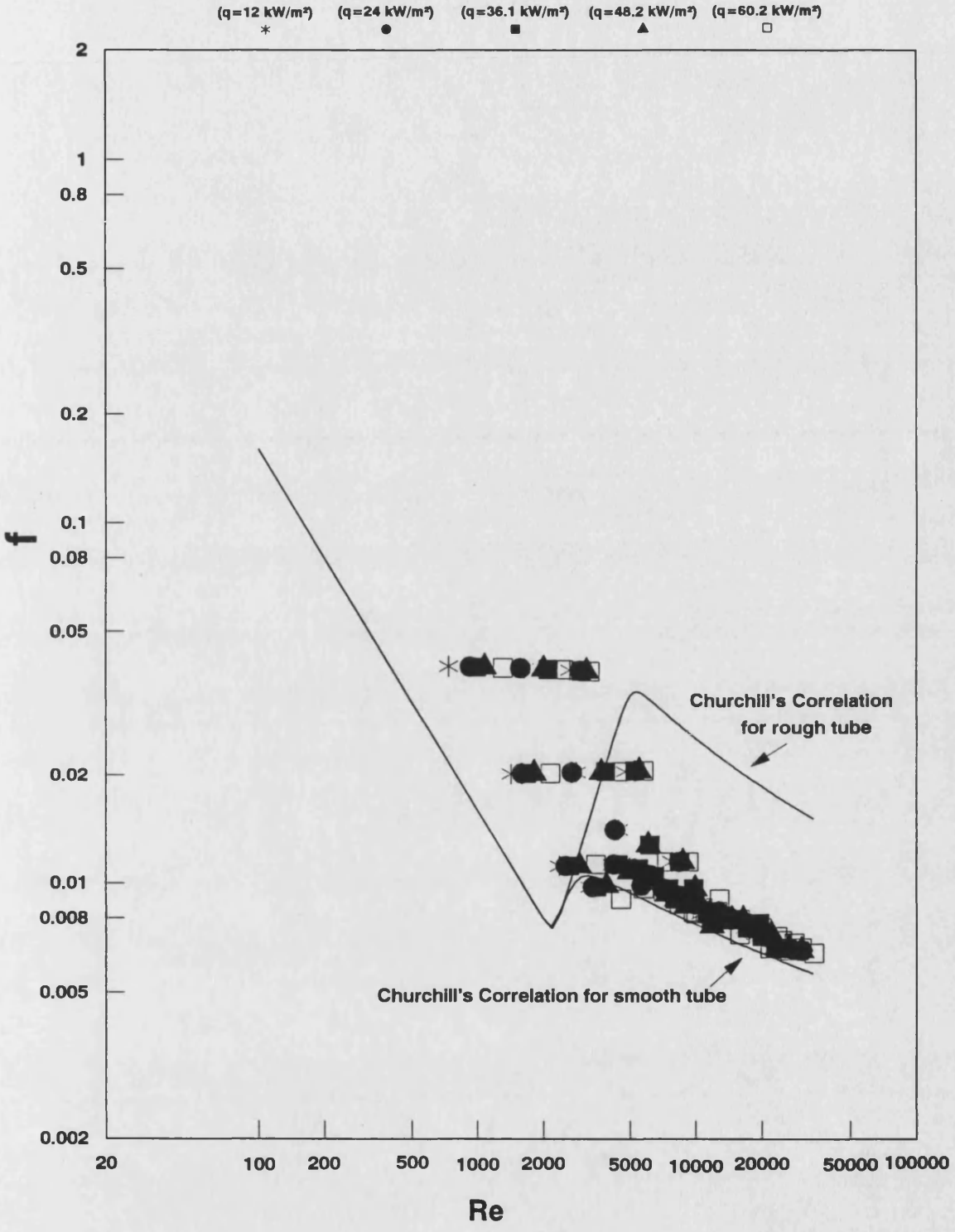

Fig (3.26a) Friction factor (f) vs Reynolds number (Re)

Santotherm 55 in bare tube test sections (30 < Pr < 158)

Effect of heat flux in the range of 12 < q < 60.2 kW/m²

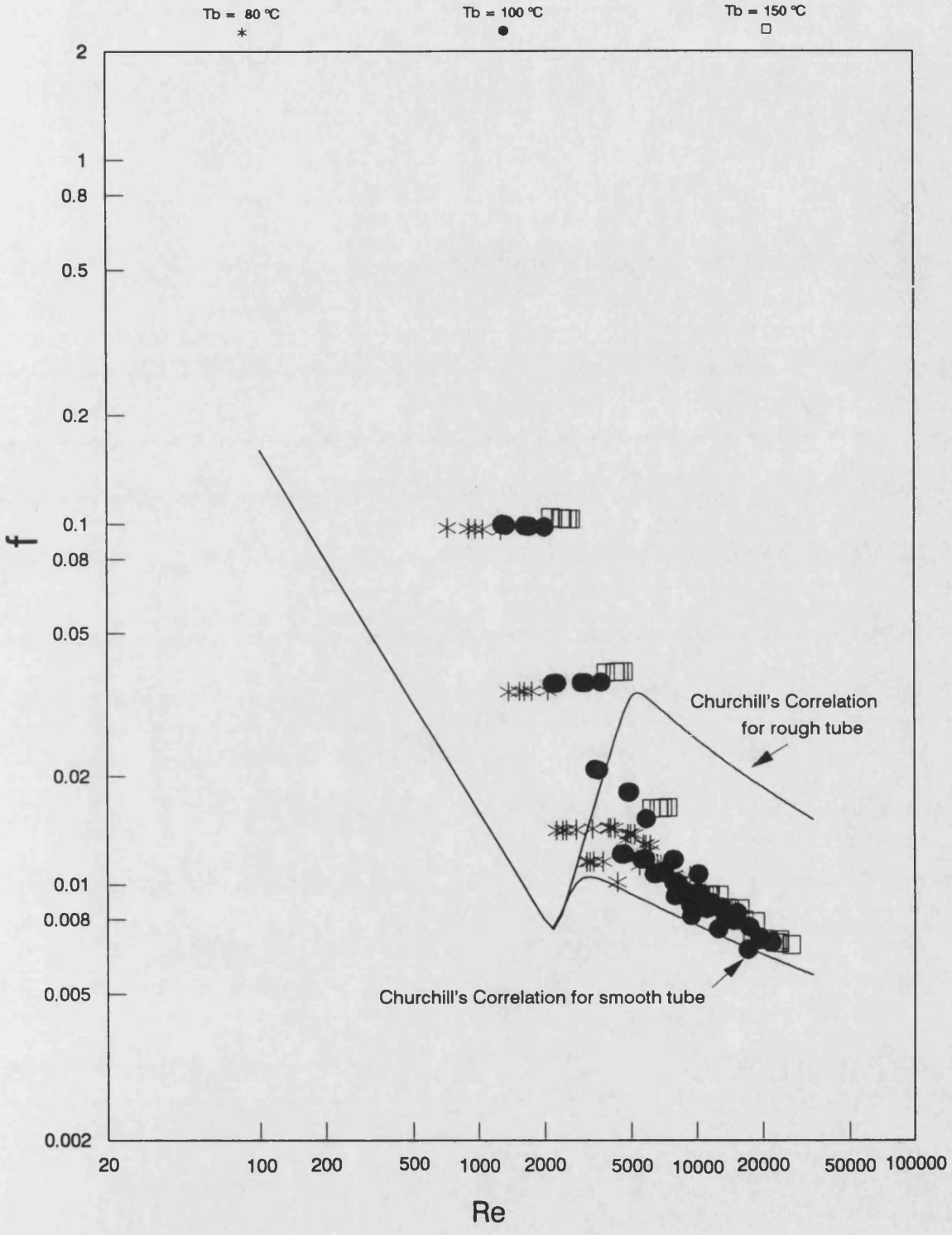

Fig (3.26b) Friction factor (f) vs Reynolds number (Re)

Santotherm 55 in bare tube test sections (30 < Pr < 158)

Effect of bulk temperature in the range of 80 °C < Tb < 150 °C

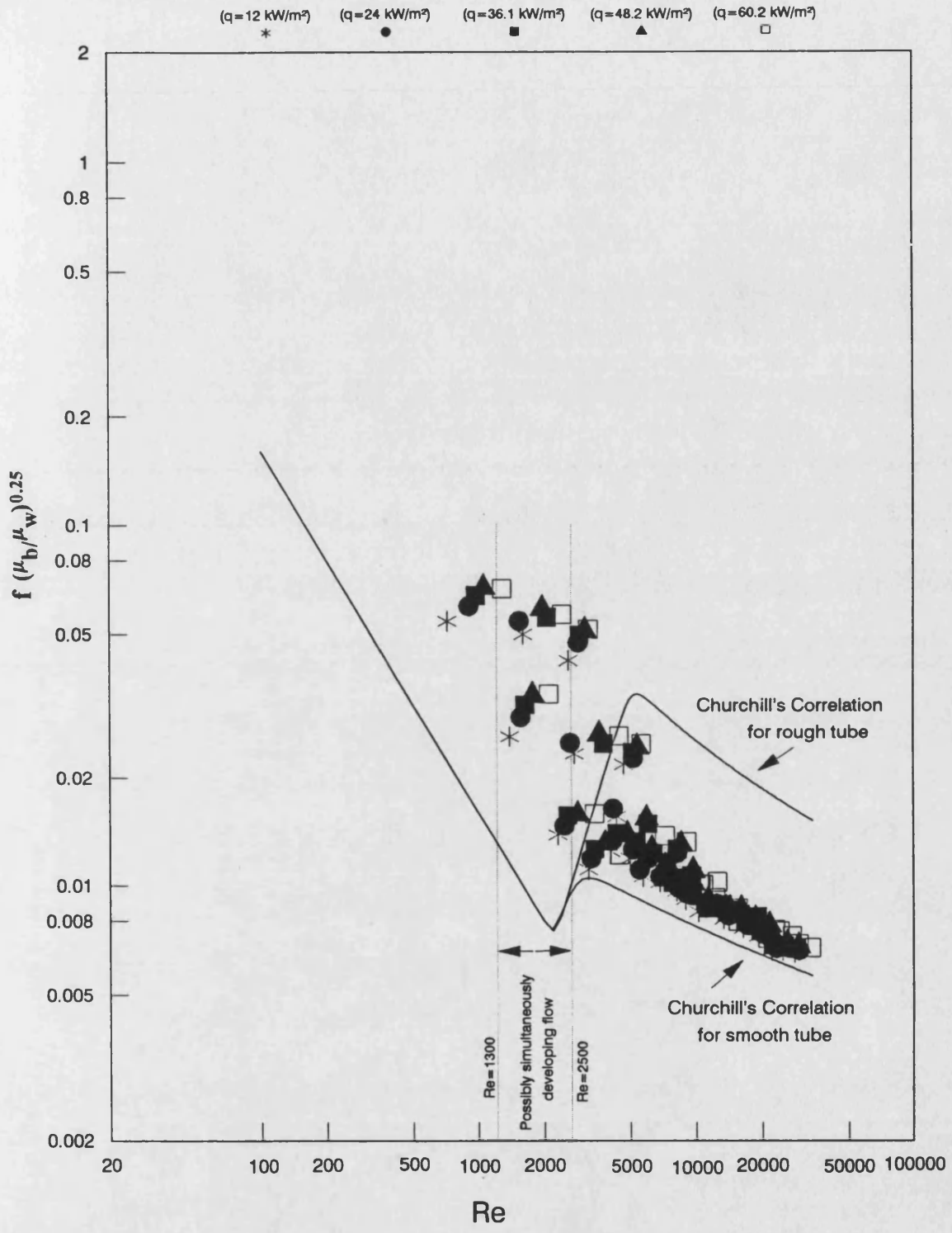

Fig (3.27a) Friction factor [$f\ (\mu_b/\mu_w)^{0.25}$] vs Reynolds number (Re)

Santotherm 55 in bare tube test sections (30 < Pr < 158)
Effect of bulk temperature in the range of 80 °C < Tb < 150 °C
(Use of viscosity correction factor for non-isothermal process)

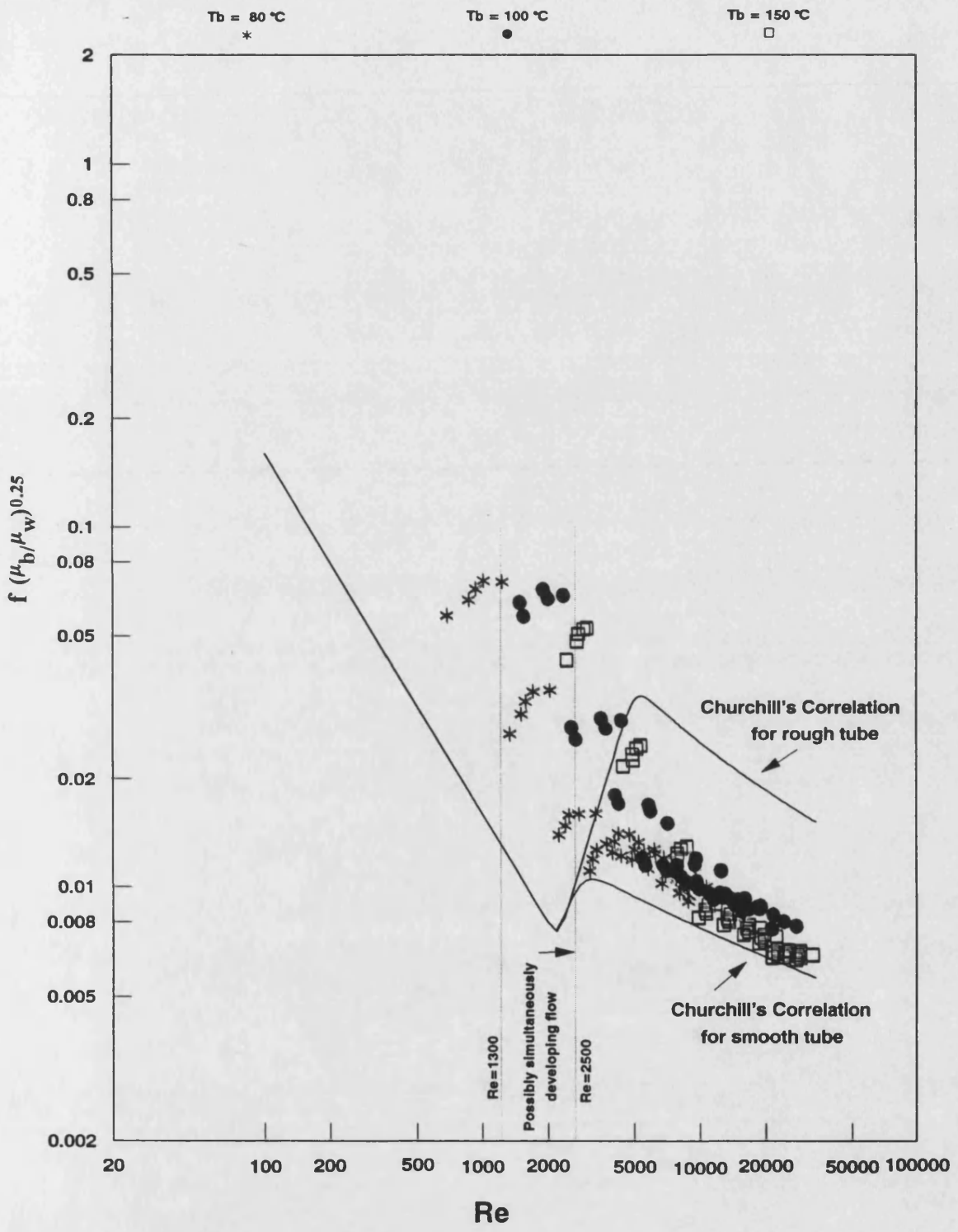

Fig (3.27b) Friction factor [$f\ (\mu_b/\mu_w)^{0.25}$] vs Reynolds number (Re)

Santotherm 55 in bare tube test sections (30 < Pr < 158)
Effect of bulk temperature in the range of 80 °C < Tb < 150 °C
(Use of viscosity correction factor for non-isothermal process)

factor did not significantly improve the correlation of experimental points in the laminar and transition flow regions , especially in the range 1300 < Re < 2500 where the flow is expected to be developing both hydrodynamically and thermally. For developing flow the friction factor is called the apparent Fanning friction factor[13,14], which is a combination of both the Fanning friction factor and the friction due to the change in the shape of the velocity profile in the hydrodynamic entrance region.

3.5.2.2.2 -Test sections fitted with different types of HiTran inserts

The effect of using six types of HiTran insert, namely: LDI-A, LDI-B, MDI-A, MDI-B, HDI-A and HDI-B, on the friction factor is demonstrated in Figs 3.28 , 3.29 and 3.31 - 3.35 .

I - Low loop density inserts (LDI-A and LDI-B)

Fig 3.28 shows the values of friction factor of test section No(1) fitted with LDI-A . No effect of bulk temperature or heat flux on the friction factor was noted . The following equation correlates the data to within ± 8% :

$$f\,(\text{LDI-A}) = A_{11} + 60000/Re^2 \qquad (3.102)$$

where:

$$\text{Log}_{10}(A_{11}) = 1.24 - 0.33\,\text{Log}_{10}(Re^3) + 0.01216\,(\text{Log}_{10}\,Re^3))^2 \qquad (3.103)$$

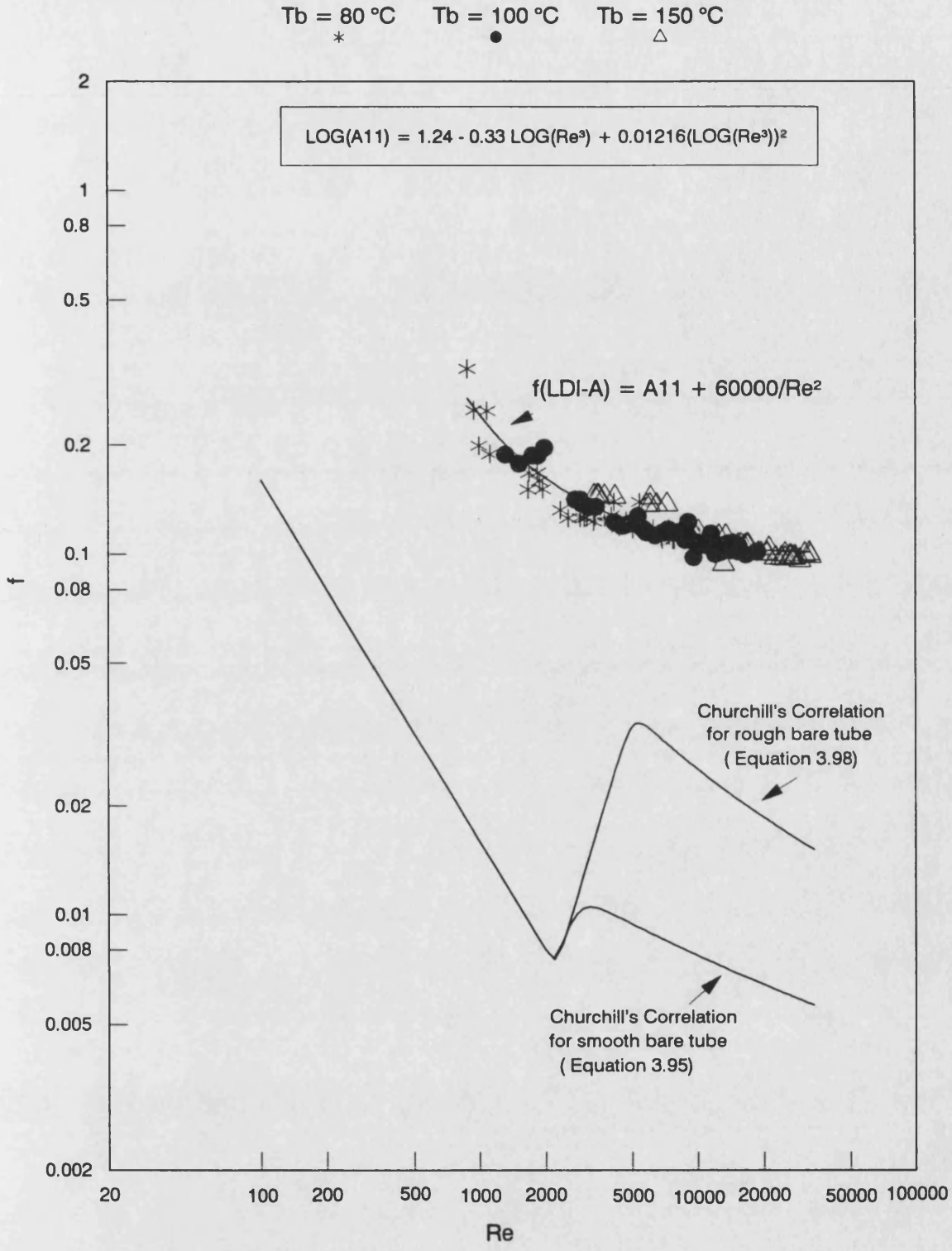

Fig (3.28) Friction factor (f) vs Reynolds number (Re)

Test section No1 fitted with LDI-A ; Santotherm 55 fluid

At 12 kW/m² < q < 60 kW/m² : 30 < Pr < 187

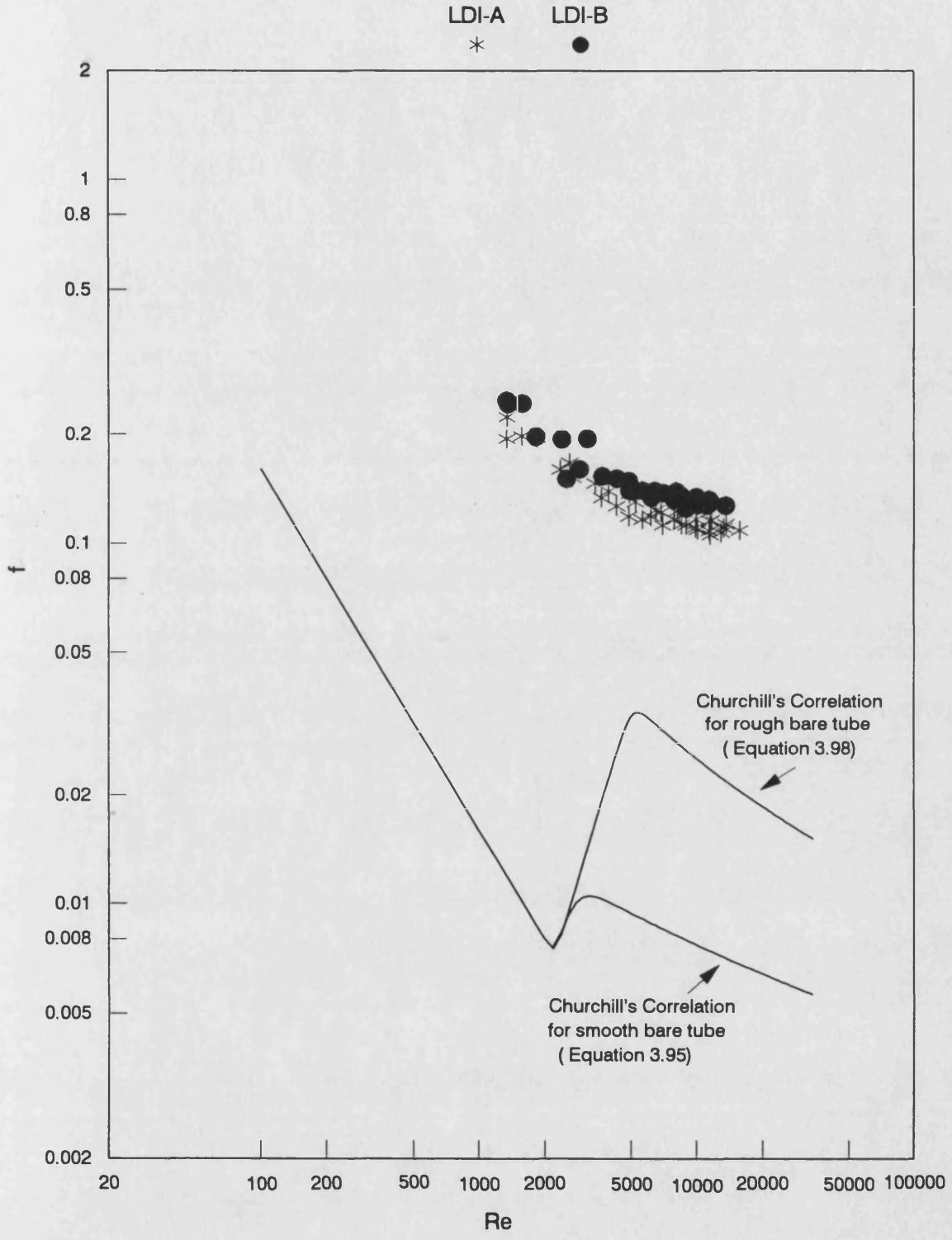

Fig (3.29) Friction factor (f) vs Reynolds number (Re)

Comparison between LDI-A and LDI-B ; Santotherm 55 fluid

At 24 kW/m² < q < 48.2 kW/m² : 60 < Pr < 178

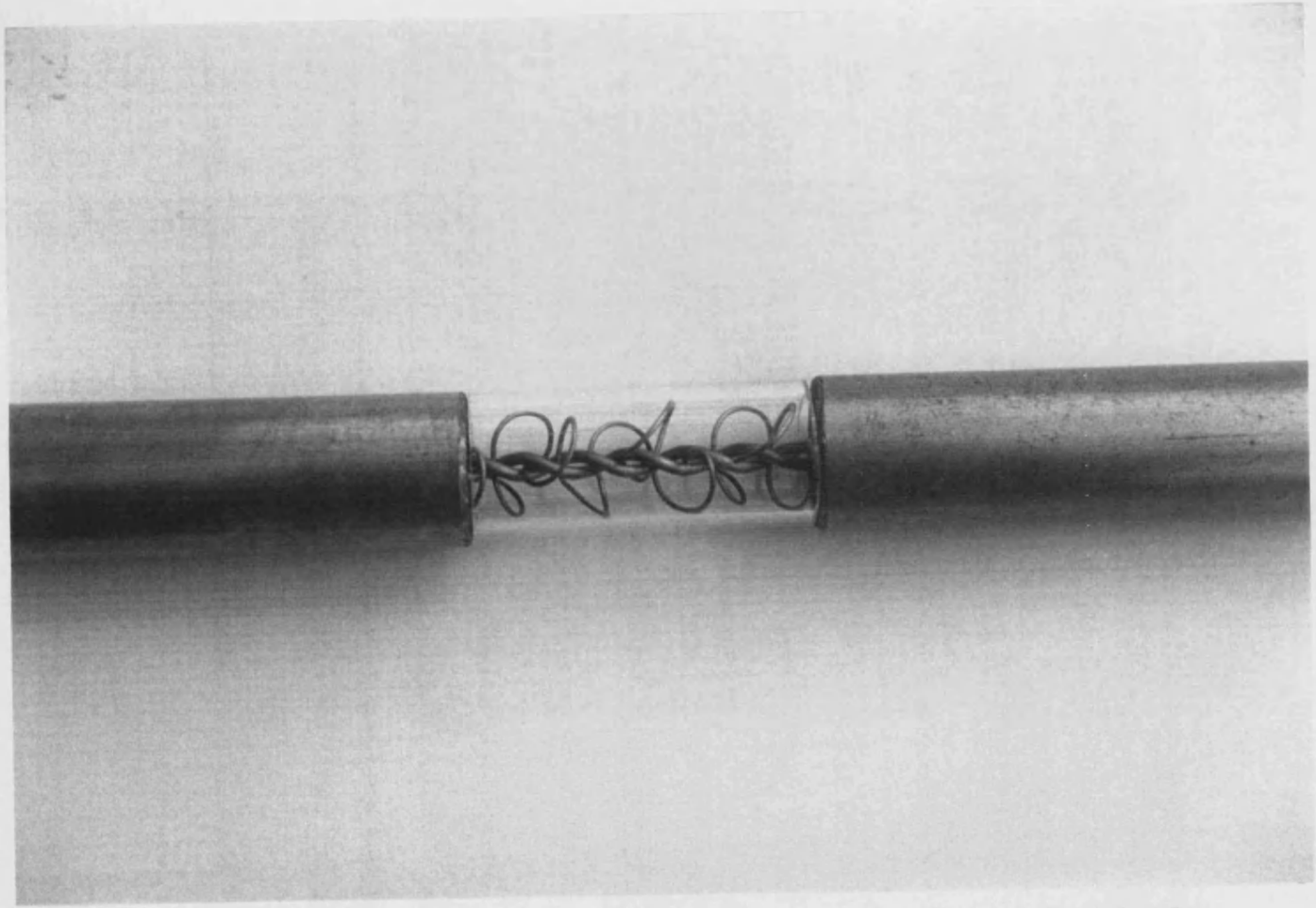

Fig (3.30) The contact of HiTran insert loops with the inner surface of the tublular test section

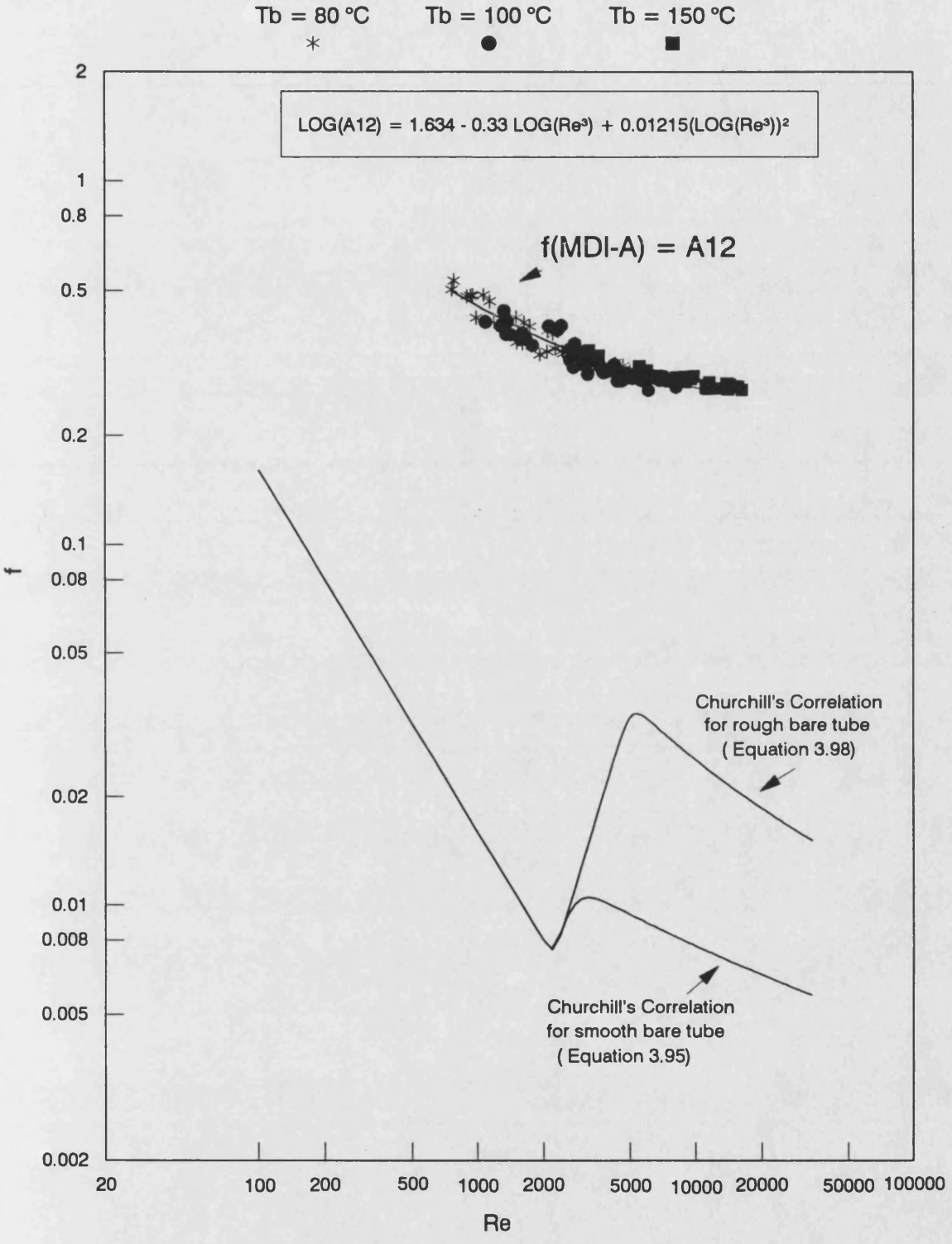

Fig (3.31) Friction factor (f) vs Reynolds number (Re)

Test sections No1 and No2 fitted with MDI-A ; Santotherm 55 fluid

At 12 kW/m² < q < 60.2 kW/m² : 34 < Pr < 129

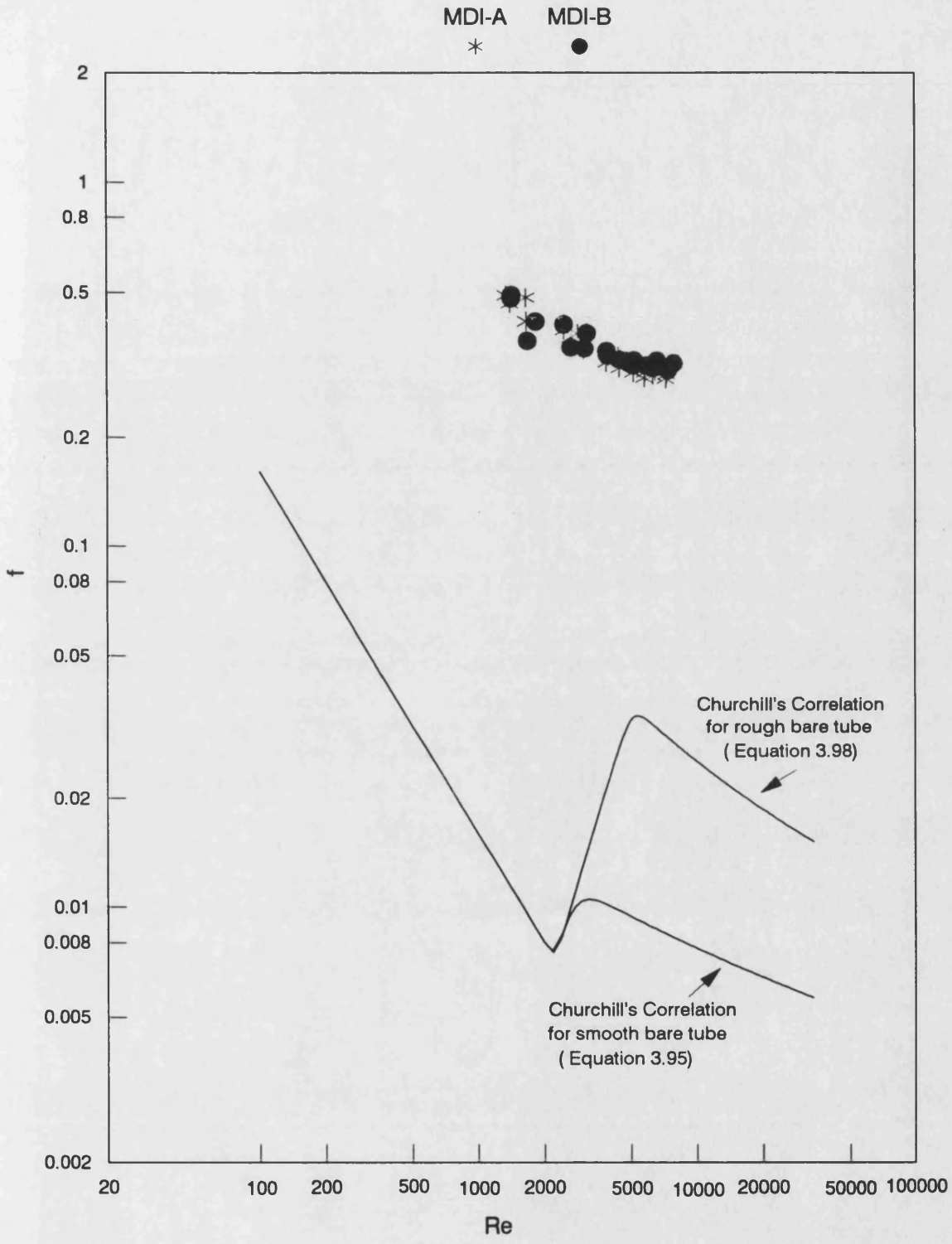

Fig (3.32) Friction factor (f) vs Reynolds number (Re)

Comparison between MDI-A and MDI-B in test section No 1 ; Santotherm 55 fluid

At 24 kW/m² < q < 48.2 kW/m² : 60 < Pr < 178

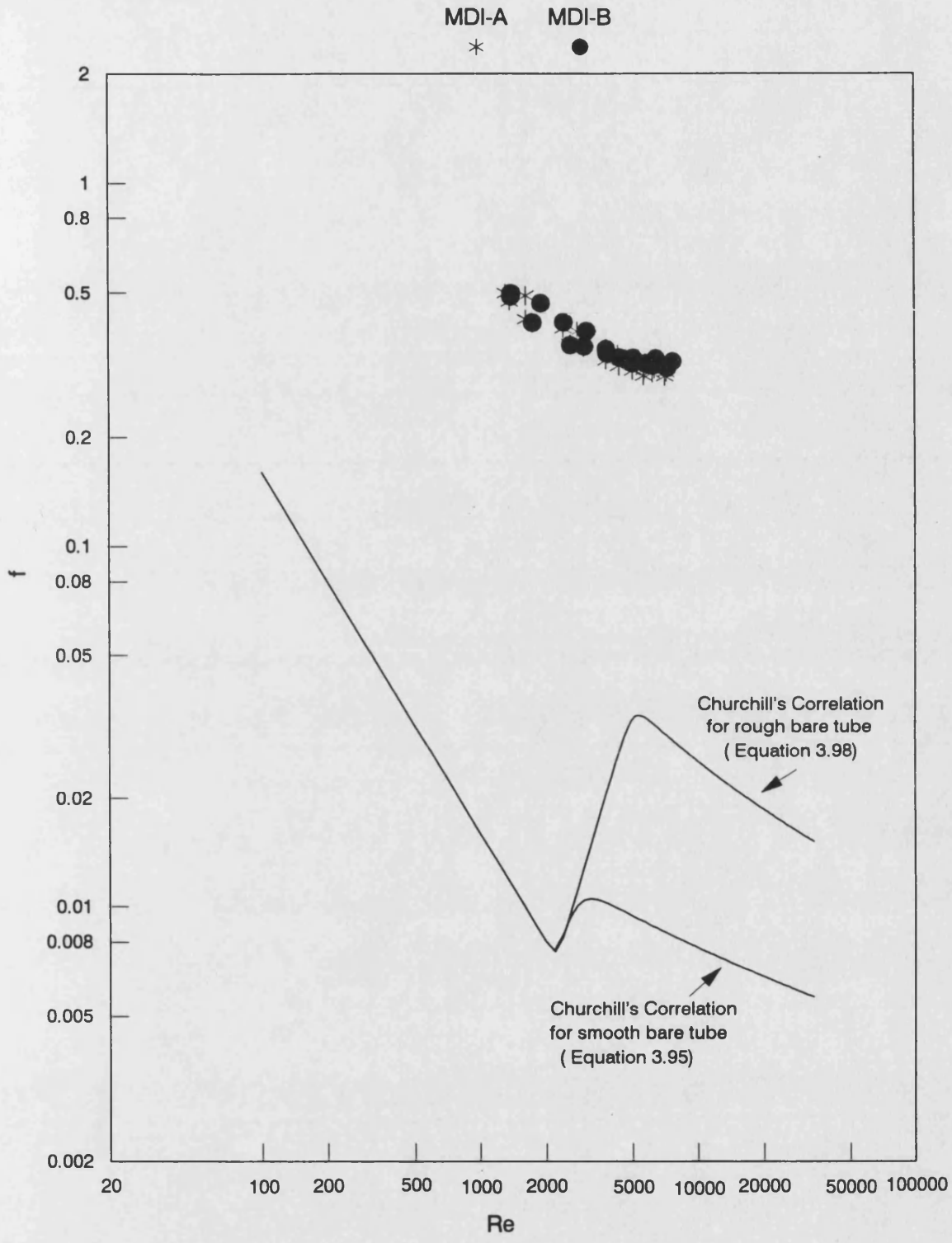

Fig (3.33) Friction factor (f) vs Reynolds number (Re)

Comparison between MDI-A and MDI-B in test section No 2 ; Santotherm 55 fluid

At 24 kW/m² < q < 48.2 kW/m² : 60 < Pr < 178

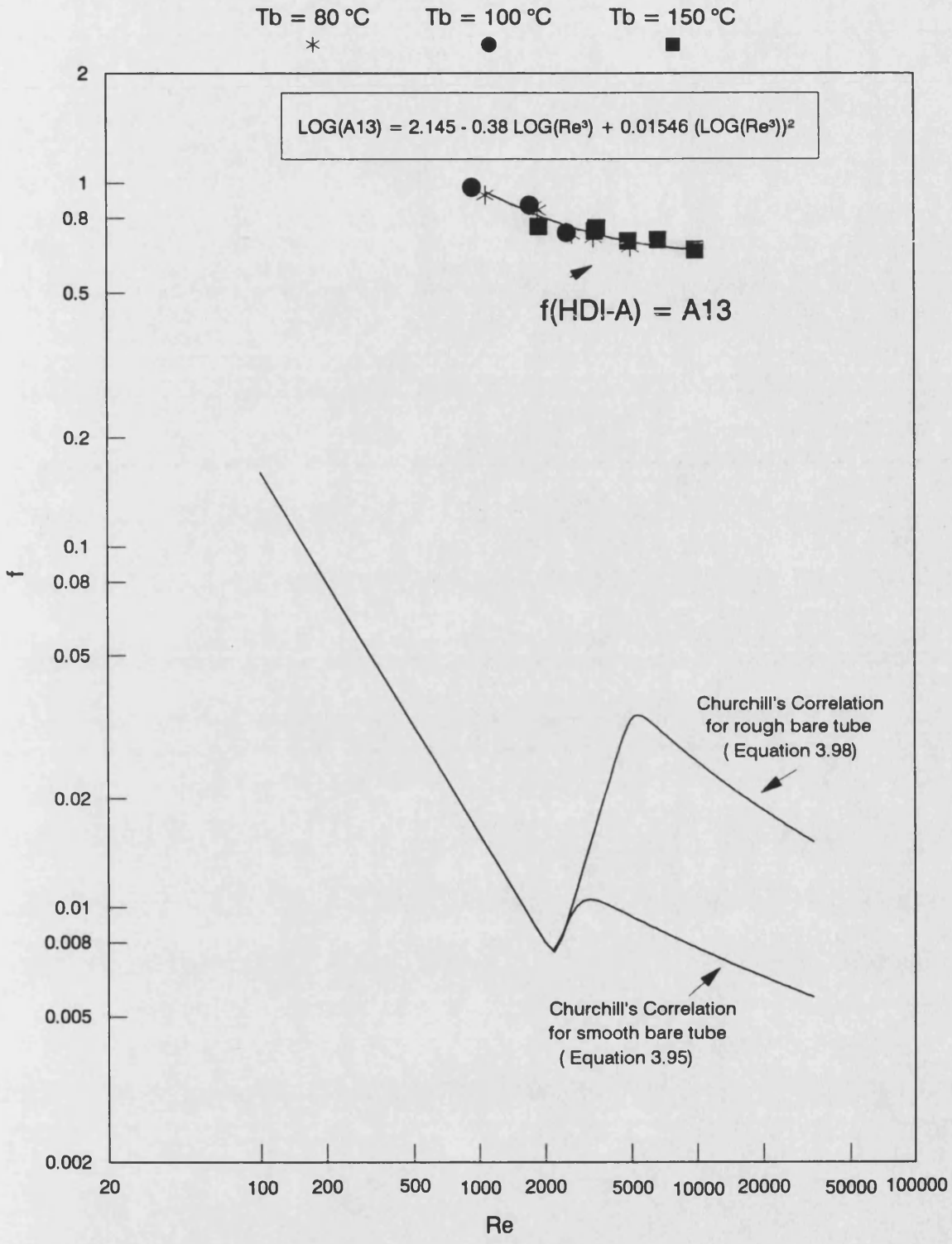

Fig (3.34) Friction factor (f) vs Reynolds number (Re)

Test sections No2 fitted with HDI-A ; Santotherm 55 fluid

At 12 kW/m² < q < 60.2 kW/m² : 30 < Pr < 111

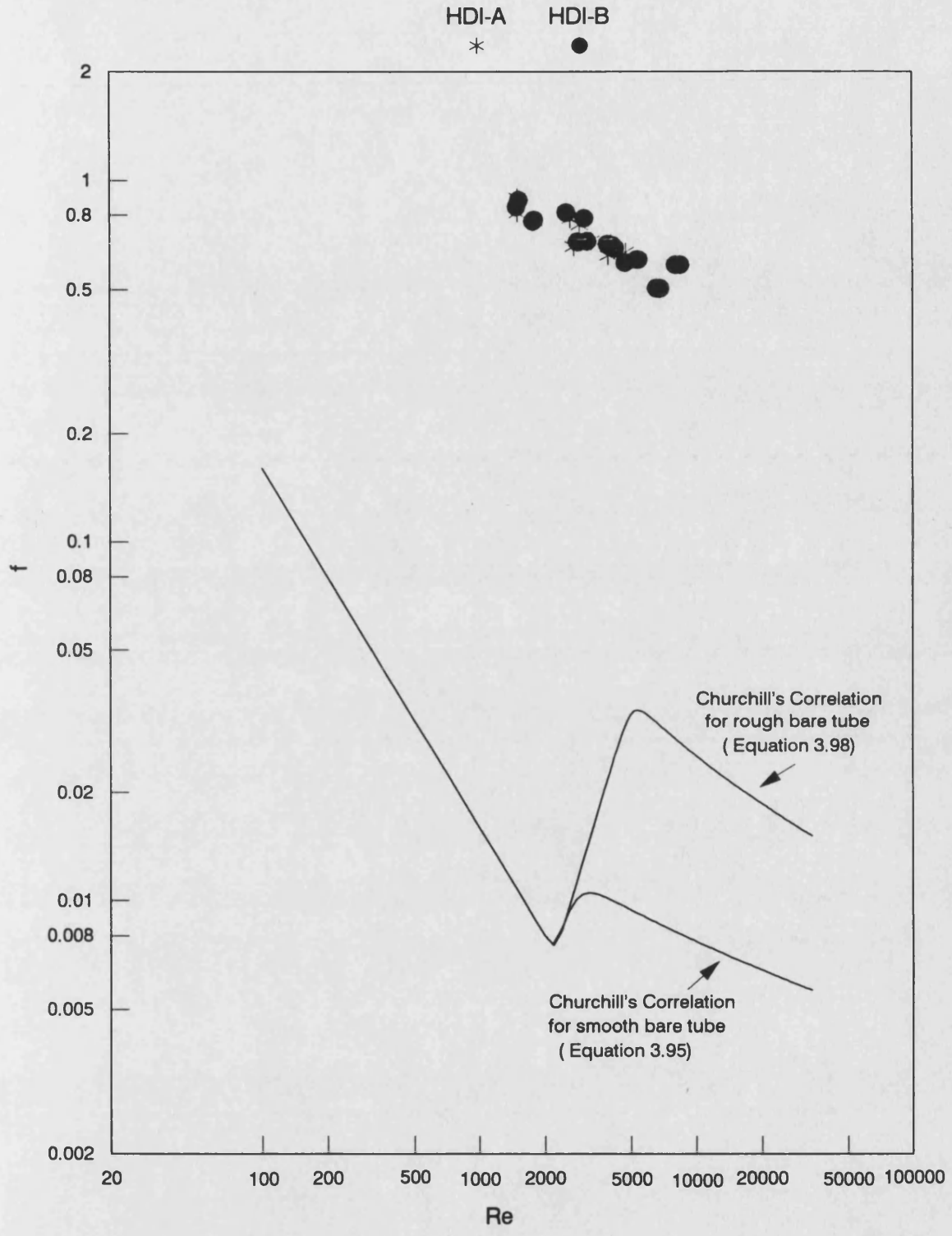

Fig (3.35) Friction factor (f) vs Reynolds number (Re)

Comparison between HDI-A and HDI-B ; Santotherm 55 fluid

At 24 kW/m² < q < 48.2 kW/m² : 60 < Pr < 178

This correlation is valid for Santotherm 55, in the ranges of $1000 < Re < 34000$ and $30 < Pr < 178$.

A comparison between the friction factor for test section No(1) fitted with LDI-A and the same test section fitted with LDI-B is shown in Fig 3.29. Although LDI-A and LDI-B were physically similar (but from different manufacturers) the friction factor obtained with LDI-B was about 10% higher than that with LDI-A . However, it is worthwhile to note that LDI-A was used many times before this experimental comparison took place. Consequently, if some loops of insert LDI-A were to lose their contact with the inner surface of the test section, then there could be some effect on the friction factor comparison . The way which the HiTran insert loops contact the inner surface of the test section is illustrated in Fig 3.30 . The glass tube has a similar diameter to that of the test section. The total number of loops in insert LDI-A was 73 loops . Therefore, poor contact of only one loop with the surface of the test section would create 1.3% loss in the total number of contact points which would have an effect on the friction factor.

II - Medium loop density inserts (MDI-A and MDI-B)

Fig 3.31 shows the friction factor of MDI-A fitted into both test sections , No(1) and No(2) . The friction factor of the tube fitted with MDI-A is not affected by either heat flux or bulk temperature.

The following mathematical correlation was found to fit the friction factor results to within ± 7% :

$$f(\text{MDI-A}) = A_{12} \qquad (3.104)$$

where:

$$\text{Log}_{10}(A_{12}) = 1.634 - 0.33\,\text{Log}_{10}(Re^3) + 0.01215\,(\text{Log}_{10}Re^3))^2 \qquad (3.105)$$

This correlation is valid for Santotherm 55, in the ranges of 750 < Re < 15500 and 34 < Pr < 129. A comparison between the friction factor of MDI-A and MDI-B fitted in test sections No(1) and No(2) is shown in Figs 3.32 and 3.33 respectively. No significant difference between the friction factors for both inserts was noted .

III - High loop density inserts (HDI-A and HDI-B)

The friction factor of test section No(2) fitted with HDI-A is shown in Fig 3.34 . A mathematical correlation for friction factor of the tube fitted with HDI-A is as follows :

$$f(\text{HDI-A}) = A_{13} \qquad (3.106)$$

where:

$$\text{Log}_{10}(A_{13}) = 2.143 - 0.38\,\text{Log}_{10}(Re^3) + 0.01546\,(\text{Log}_{10}Re^3))^2 \qquad (3.107)$$

This correlation is accurate to within ± 2% for Santotherm 55 , in the ranges of 900 < Re < 13300 and 30 < Pe < 111 .

A comparison between the friction factors for test section No(2) fitted with HDI-A then with HDI-B is shown in Fig 3.35 . No difference between them is noted .

IV -Effect of re-using the same HiTran insert

In order to demonstrate the effect of re-using a HiTran insert in the same test section , MDI inserts (both MDI-A and MDI-B) were tested twice under similar experimental conditions. Insert MDI-A was fitted inside test section No(1) and tested at T_b = 100 °C and q = 24 and 48.2 kW/m^2 . The insert was removed from the test section and then re-fitted and tested under similar conditions. The results of the two runs are shown in Fig 3.36 . In the same way two runs were carried out for MDI-B fitted into test section No(1) and the results are shown in Fig 3.37 . In both cases, using MDI-A and MDI-B, the friction factor was unaffected by re-insertion. This is possibly because the number of insert loops of MDI , ether MDI-A or MDI-B , was about 185 . Thus , the poor contact of a few loops would not have a great effect on the friction factor .

V-Effect of rotating a HiTran insert inside the test section

The effect of rotating a HiTran insert inside a test section is demonstrated as follows; MDI-A was fitted into test section No2 and tested at T_b = 100 °C and q = 24 and 48.2 kW/m^2 . The insert was rotated 90° anti-clockwise and then tested under similar conditions. The results of the two runs are shown in Fig 3.38 . There was no effect of rotating the HiTran insert on the friction factor .

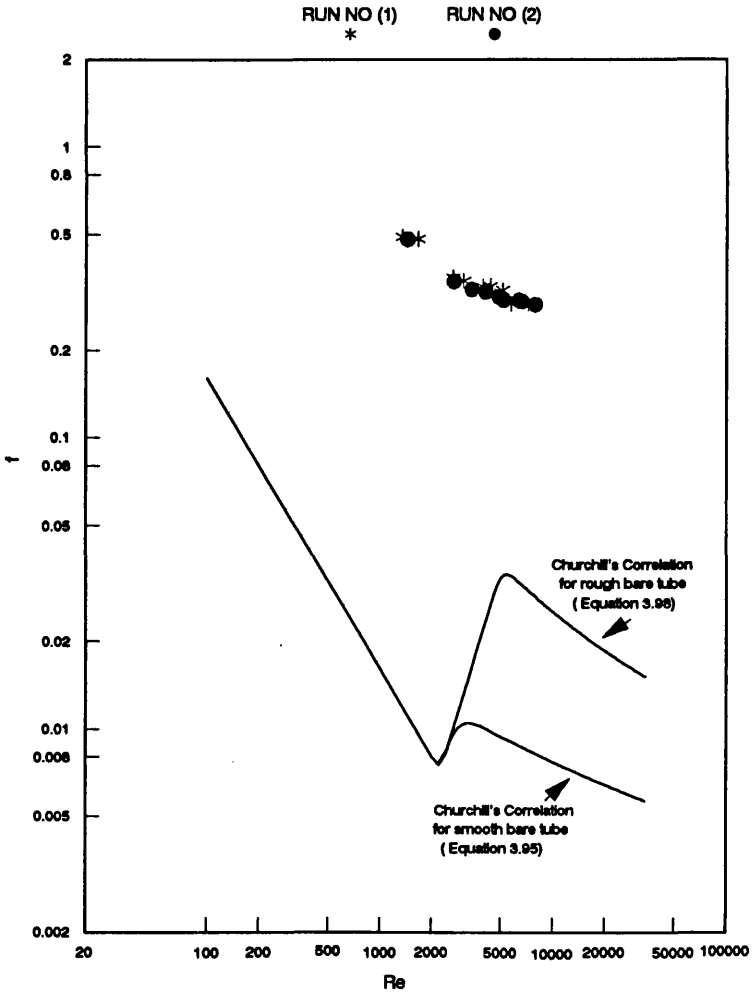

Fig (3.36) Friction factor (f) vs Reynolds number (Re)

Re-using of MDI-A fitted inside test section No1 ; Santotherm 55 fluid

At Tb = 100 °C ; 12 kW/m² < q < 48.2 kW/m² : 34 < Pr < 90

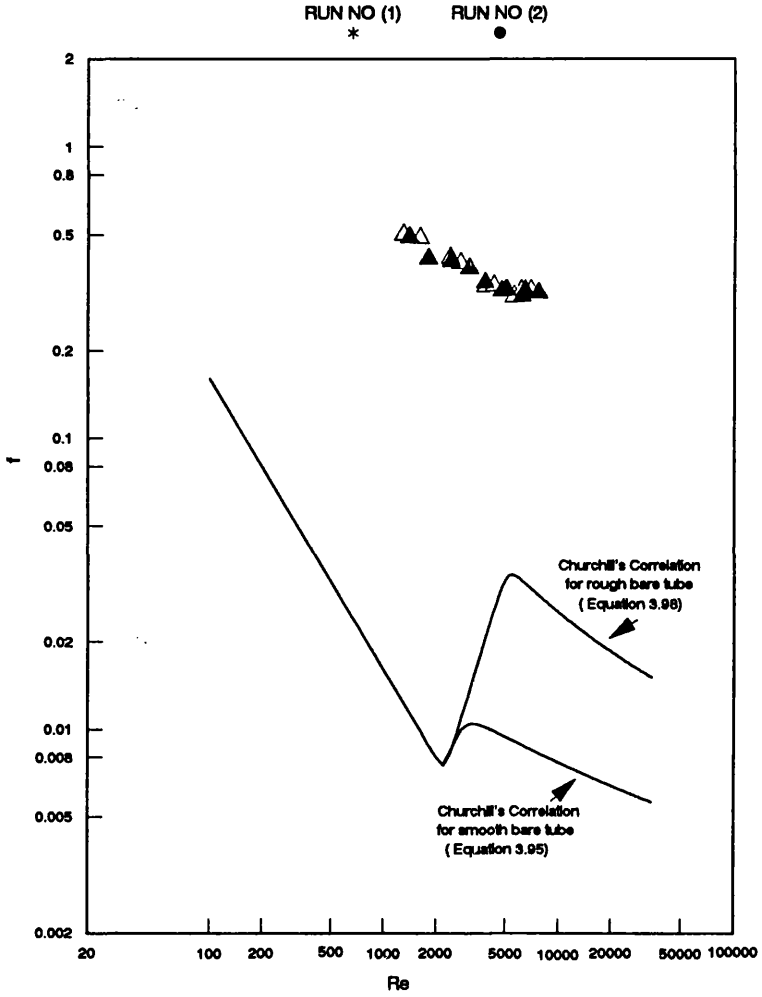

Fig (3.37) Friction factor (f) vs Reynolds number (Re)

Re-using of MDI-B fitted inside test section No 2 ; Santotherm 55 fluid

At Tb = 100 °C ; 12 kW/m² < q < 48.2 kW/m² : 34 < Pr < 90

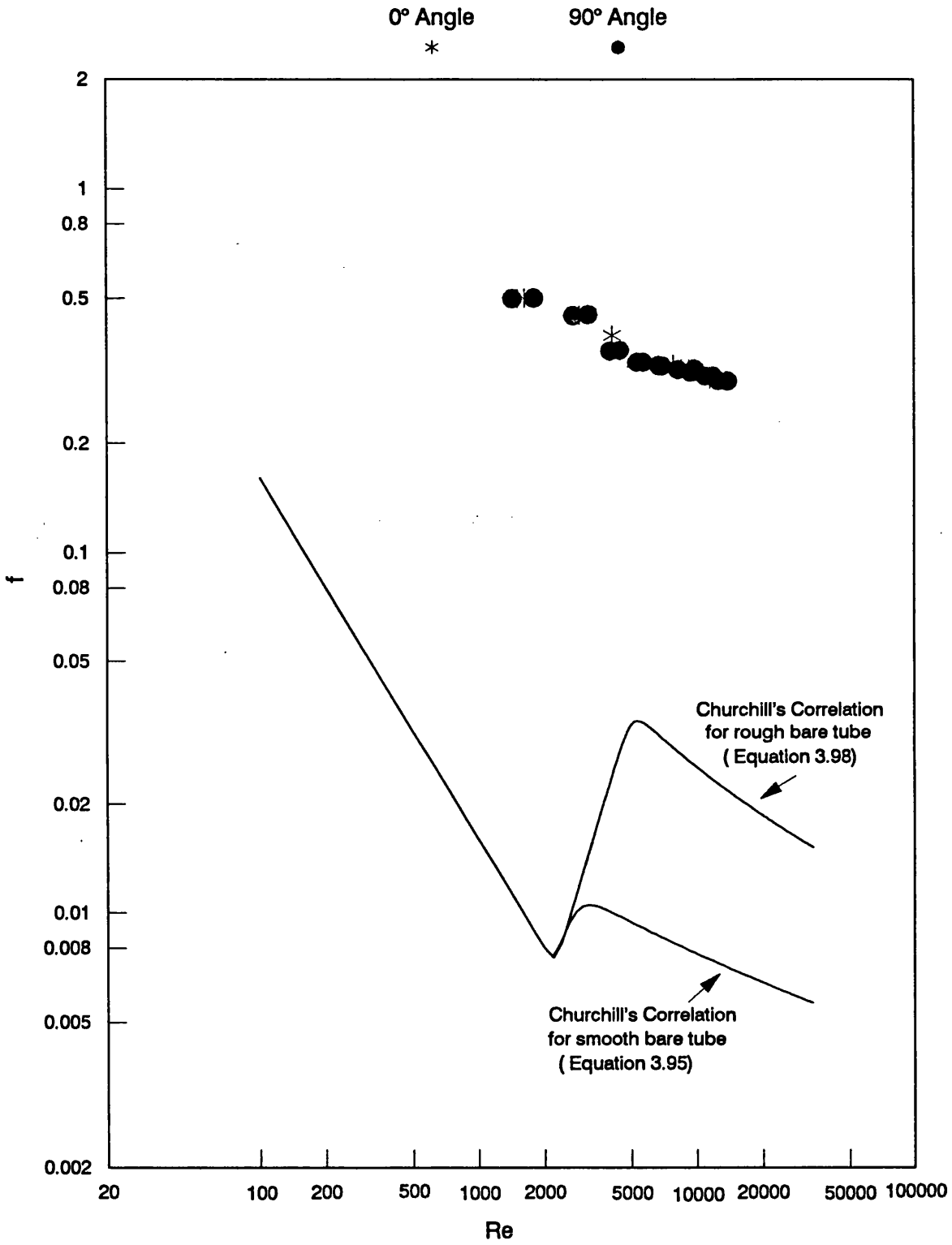

Fig (3.38) Friction factor (f) vs Reynolds number (Re)

Rotation of MDI-A inside test section No 1 ; Santotherm 55 fluid

At Tb = 100 °C ; q = 24 and 48.2 kW/m² and 34 < Pr < 90

3.5.2.2.3 -Comparison between the bare tube and tube fitted with HiTran insert

An overall comparison between the friction factor of the bare tube and the tube fitted with different types of HiTran insert (LDI-A, MDI-A and HDI-A) is shown in Fig 3.39. The Oliver and Aldington[23] correlation for the friction factor (for a tube fitted with a HiTran insert with glycerol/water mixtures, (equation 3.108)) is also shown in Fig 3.36. The friction factor of fully developed flow is represented by equation 3.101.

$$\text{Ln}(f_a) = 5.57 - 1.32\,(\text{Ln}(\text{Re})) + 0.0627\,(\text{Ln}(\text{Re}))^2 \qquad (3.108)$$

It important to note that although f_a was defined by Oliver and Aldington[23] somewhat differently to the usual definition of Fanning friction factor , equation 3.108 appears to be in reasonably good agreement with equation 3.104 for the MDI in the present study . Oliver and Aldington[23] did not state the number of loops per unit length which might have been different from that used in the present study .

The friction factor of the tube fitted with a **HiTran** insert increases as expected with an increasing loop density and decreases with an increase in Reynolds number (Re). Table 3.20 shows a comparison between friction factors for the tube fitted with **HiTran** insets and values predicted from Churchill's correlations for smooth (equation 3.95) and rough (equation 3.98) bare tubes .

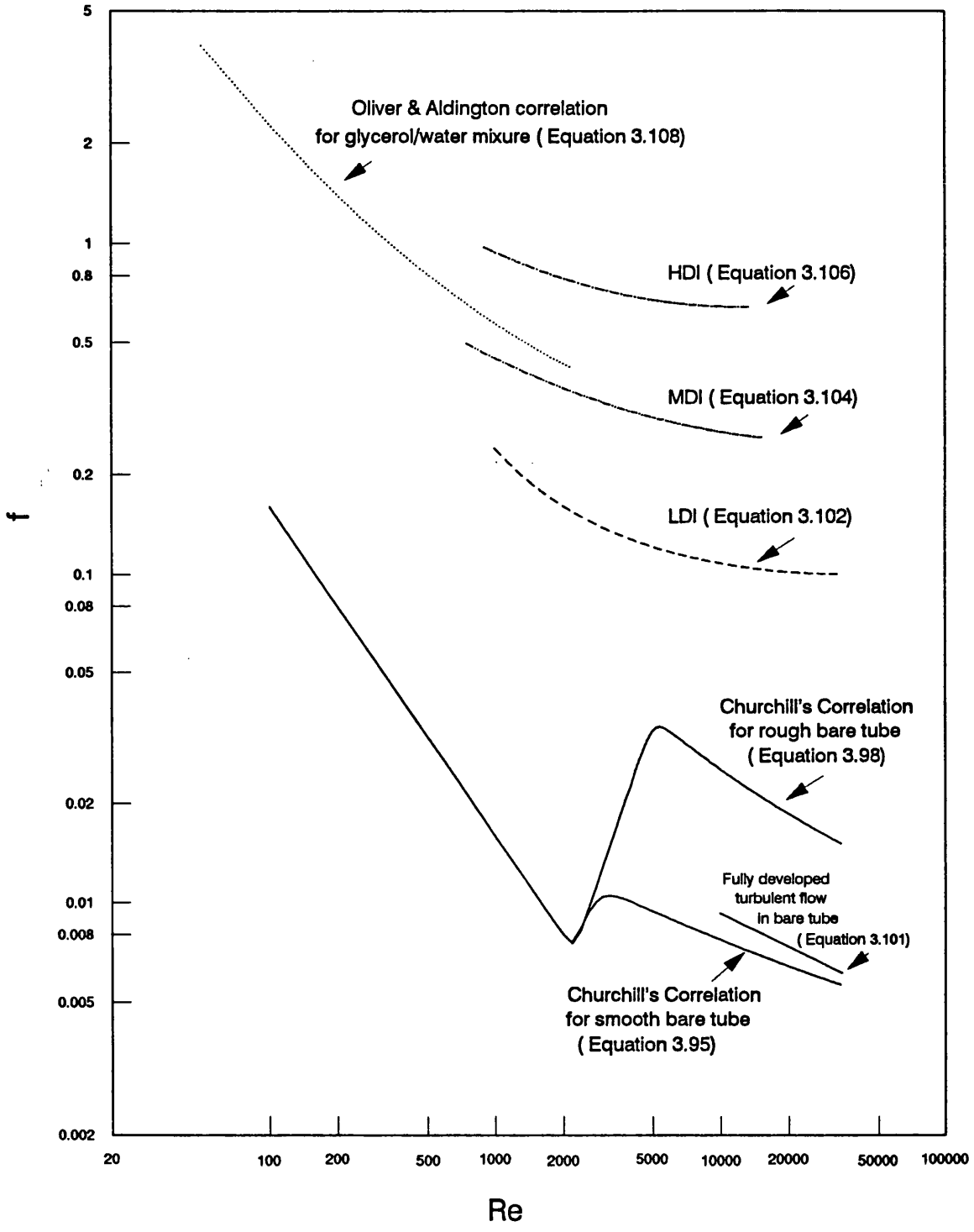

Fig (3.39) Friction factor (f) vs Reynolds number (Re) for Santother 55 fluid

Comparison between bare tube and tube fitted with HiTran insert

For the ranges of 750 < Re < 34000 and 30 < Pr < 187

Table 3.20 Comparison between friction factors of tube fitted with HiTran inserts and friction factors predicted from Churchill's correlations

Type of HiTran insert	Laminar flow 500<Re<2100		Transition flow 2100<Re<4000		Turbulent flow Re>4000	
	f (insert) / f (equ.3.95)	f (insert) / f (equ.3.98)	f (insert) / f (equ.3.95)	f (insert) / f (equ.3.98)	f (insert) / f (equ.3.95)	f (insert) / f (equ.3.98)
Low loop density insert LDI (2.7 loops per cm)	15 - 20.3	15 - 20.3	20.3 - 12.5	20.6 - 5.6	12.6 - 17.8	5.1 - 6.8
Medium loop density insert MDI (6.4 loops per cm)	18.1 - 45.5	18.1 - 45.5	46.6 - 30.4	47.2 - 13.7	30.5 - 37.5	12.3 - 12.7
High loop density insert HDI (10.5 loops per cm)	54.8 - 98.2	54.8 - 98.2	101 - 67.9	102.2 - 30.5	68.5 - 89.3	27.6 - 29.2

3.5.2.3 Heat transfer j_H - factors

The heat transfer factor was calculated from equation 3.69 and the complete set of results is shown in Figs 3.40 to 3.90 for the bare tube and for the tube fitted with a **HiTran** insert.

In order to provide a sound basis for comparison with the literature, the well-known Sieder and Tate correlation[36] was plotted as a reference curve on all Figures.

The Sieder-Tate correlation is a combination of two parts as follows :

For laminar flow (Re < 2100),

$$Nu = 1.86 \left(Re\, Pr \frac{Di}{L} \right)^{1/3} \left(\frac{\mu_b}{\mu_w} \right)^{0.14} \qquad (3.109)$$

In this experiment , D_i = 1.483 cm and L = 24.025 cm

Therefore,

$$Nu = 0.7419 \left(Re\, Pr \right)^{1/3} \left(\frac{\mu_b}{\mu_w} \right)^{0.14} \qquad (3.110)$$

For transition and turbulent flow (Re > 2100) ,

$$Nu = 0.027\, Re^{0.8}\, Pr^{0.33} \left(\frac{\mu_b}{\mu_w} \right)^{0.14} \qquad (3.111)$$

3.5.2.3.1 Heat transfer j_H - factor of bare tube

The results for the bare tube are shown in Figs 3.40 to 3.46. In Fig 3.40 j_H vs Re is plotted for both bare tube test sections for T_b = 80 °C and under heat fluxes in the range of 12 kW/m^2 < q < 60.2 kW/m^2 . At this bulk temperature, the experimental points for Re < 2100 were below the line predicted by equation 3.110. However, as already discussed in section 3.5.2.1, the fluid flow was probably still thermally developing for Re < 10000 and probably still developing both hydrodynamically and thermally in the range of 1300 < Re < 2500 . For transition and turbulent flow (Re > 2100) the experimental results fit very well with equation 3.111 and have a regular distribution on either side of the Sieder-Tate curve. At 80 °C the Prandtl number is in the range of 110 to 187 which is partially in the range of Prandtl numbers studied by Sieder and Tate (151 < Pr < 16700).

At T_b = 100 °C and 12 kW/m^2 < q < 60.2 kW/m^2 , j_H is shown in Fig 3.41 . At this bulk temperature for which 60 < Pr < 80 , the experimental values of j_H-factor are slightly higher than the previous case and closer to the Sieder-Tate curve for Re < 2100. However , for Re > 2100 the majority of data points are above the Sieder-Tate curve by about 5 to 8%.

At T_b = 150 °C and 12 kW/m^2 < q < 60.2 kW/m^2 , j_H for the bare tube is shown in Fig 3.42 . At this

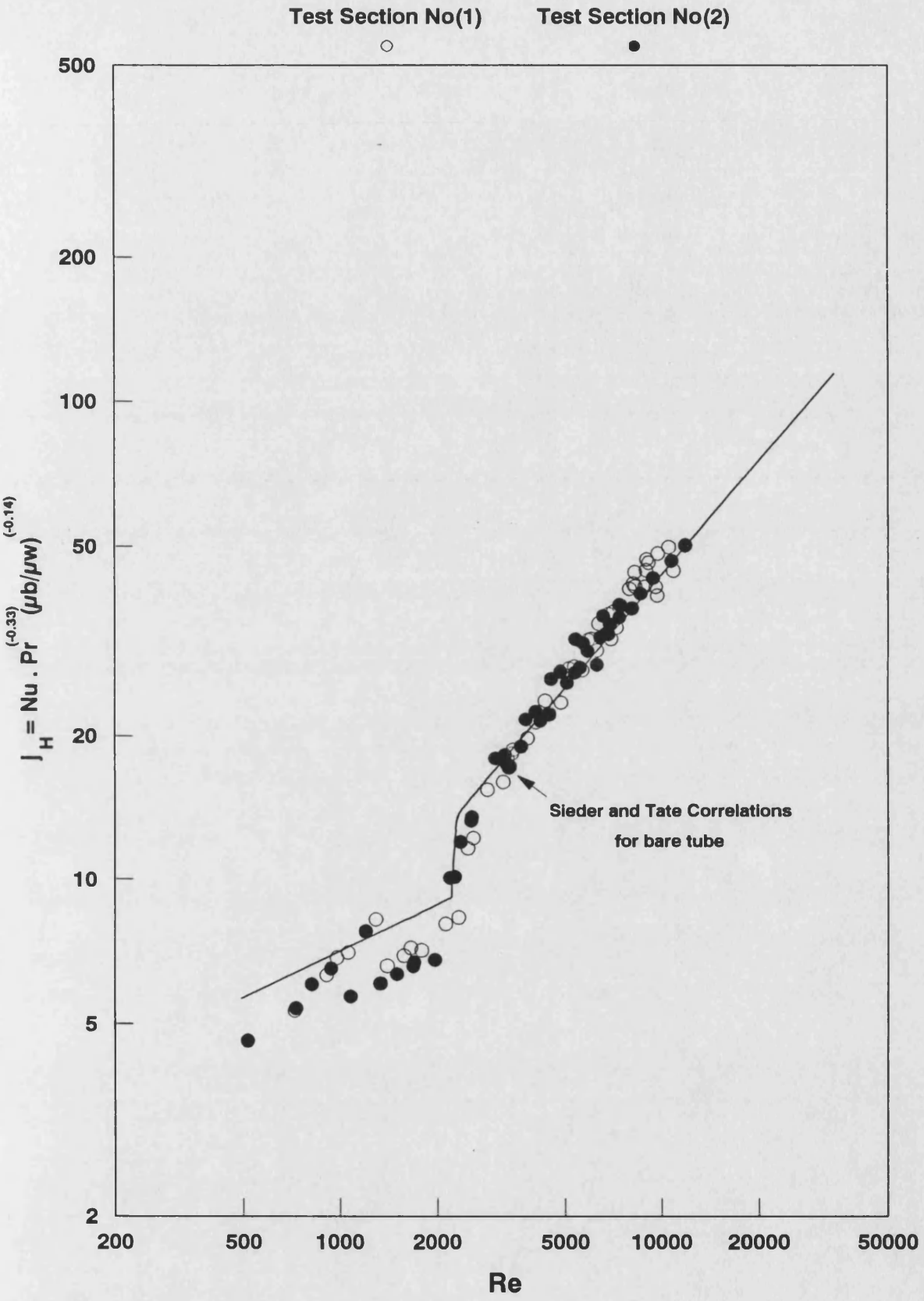

Fig (3.40) Heat transfer factor (j_H) vs Reynolds number (Re)

Santotherm 55 for bare tube ; both test sections at Tb = 80 °C
(110 < Pr < 187)

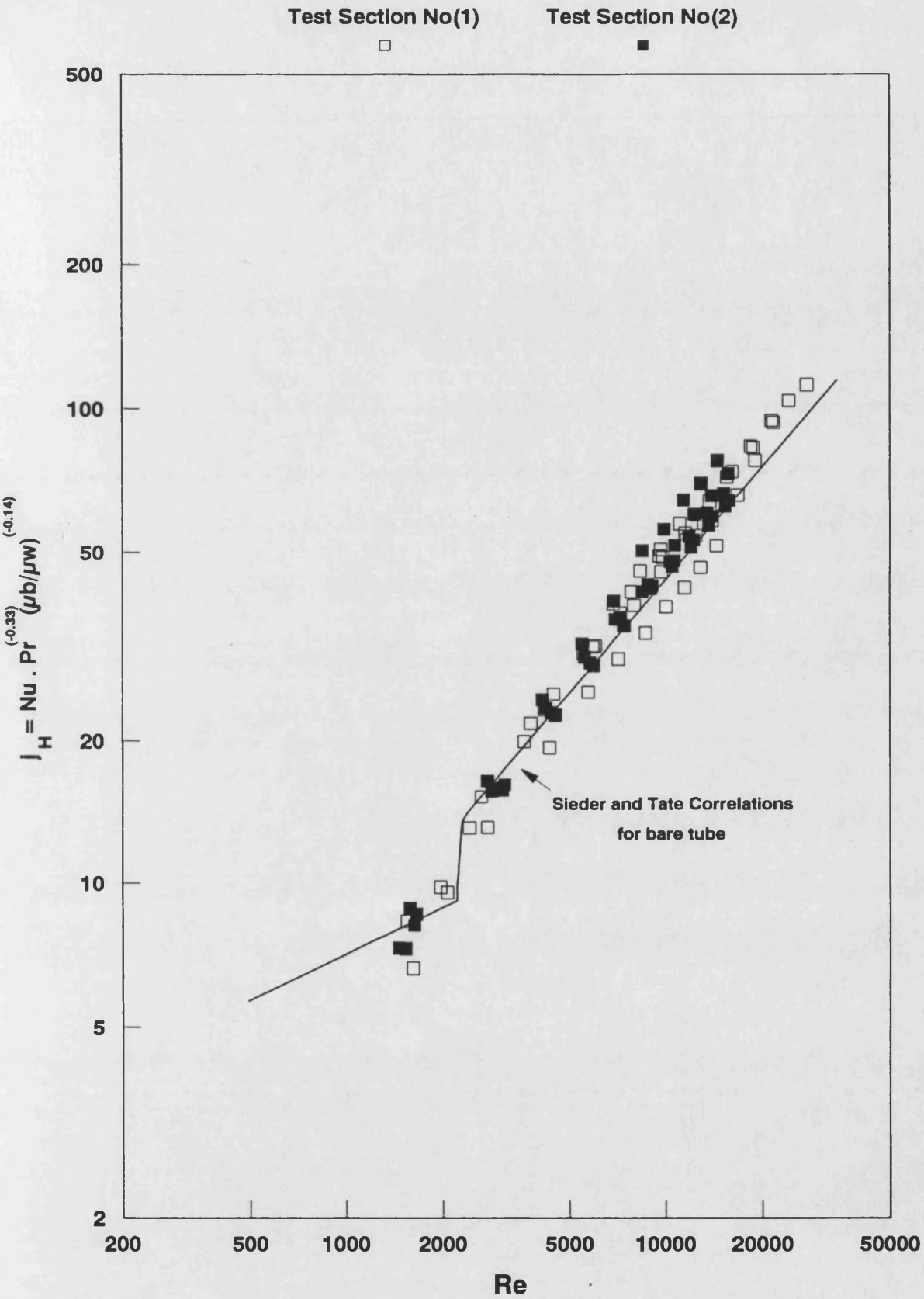

Fig (3.41) Heat transfer factor (j_H) vs Reynolds number (Re)

Santotherm 55 for bare tube ; both test sections at Tb = 100 °C

(60 < Pr < 90)

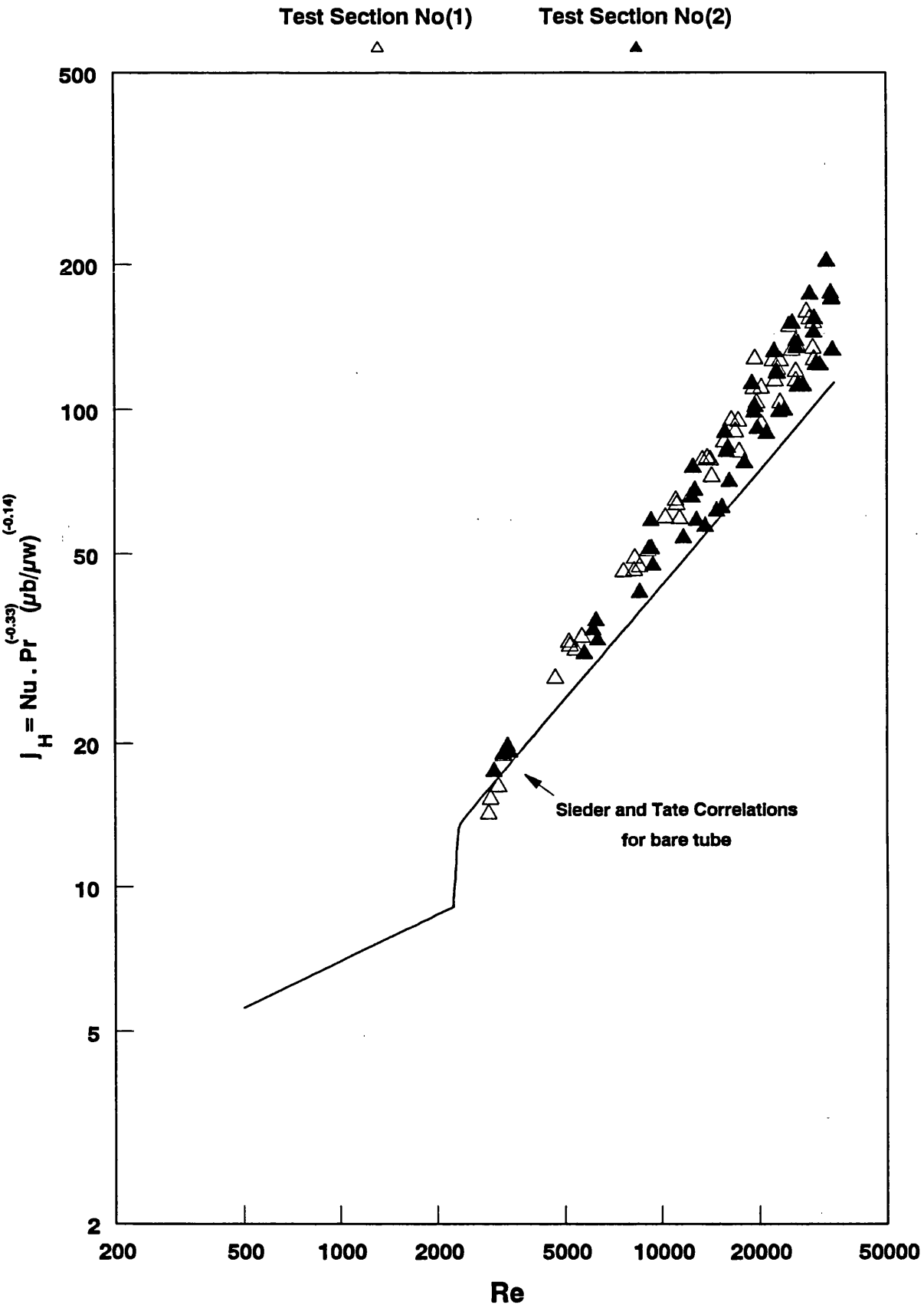

Fig (3.42) Heat transfer factor (j_H) vs Reynolds number (Re)

Santotherm 55 for bare tube ; both test sections at Tb = 150 °C

(30 < Pr < 60)

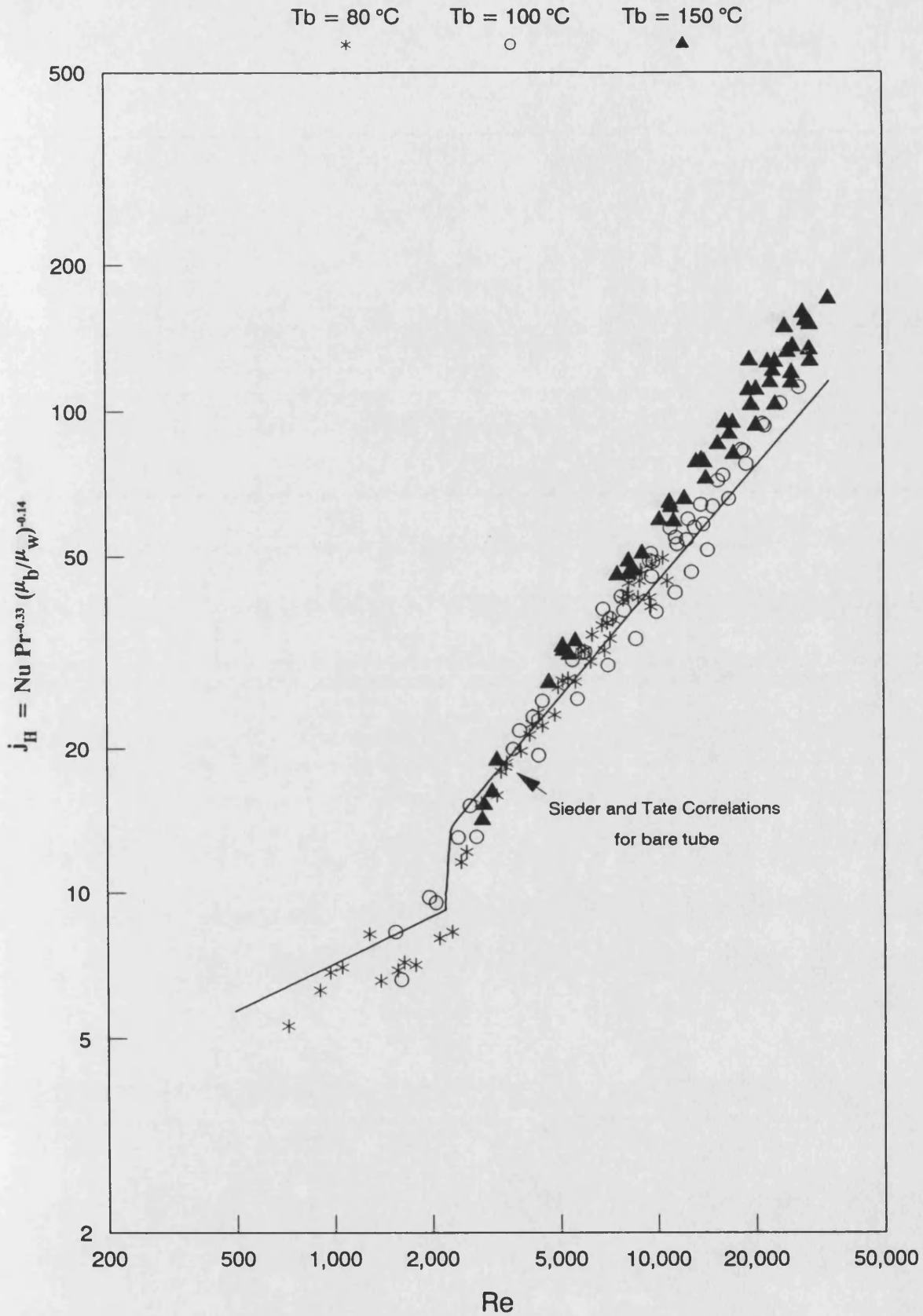

Fig (3.43) Heat transfer factor (j_H) vs Reynolds number (Re)

Santotherm 55 for bare tube ; test sections No 1 at 12 kW/m² < q < 60.2 kW/m²

(30 < Pr < 187)

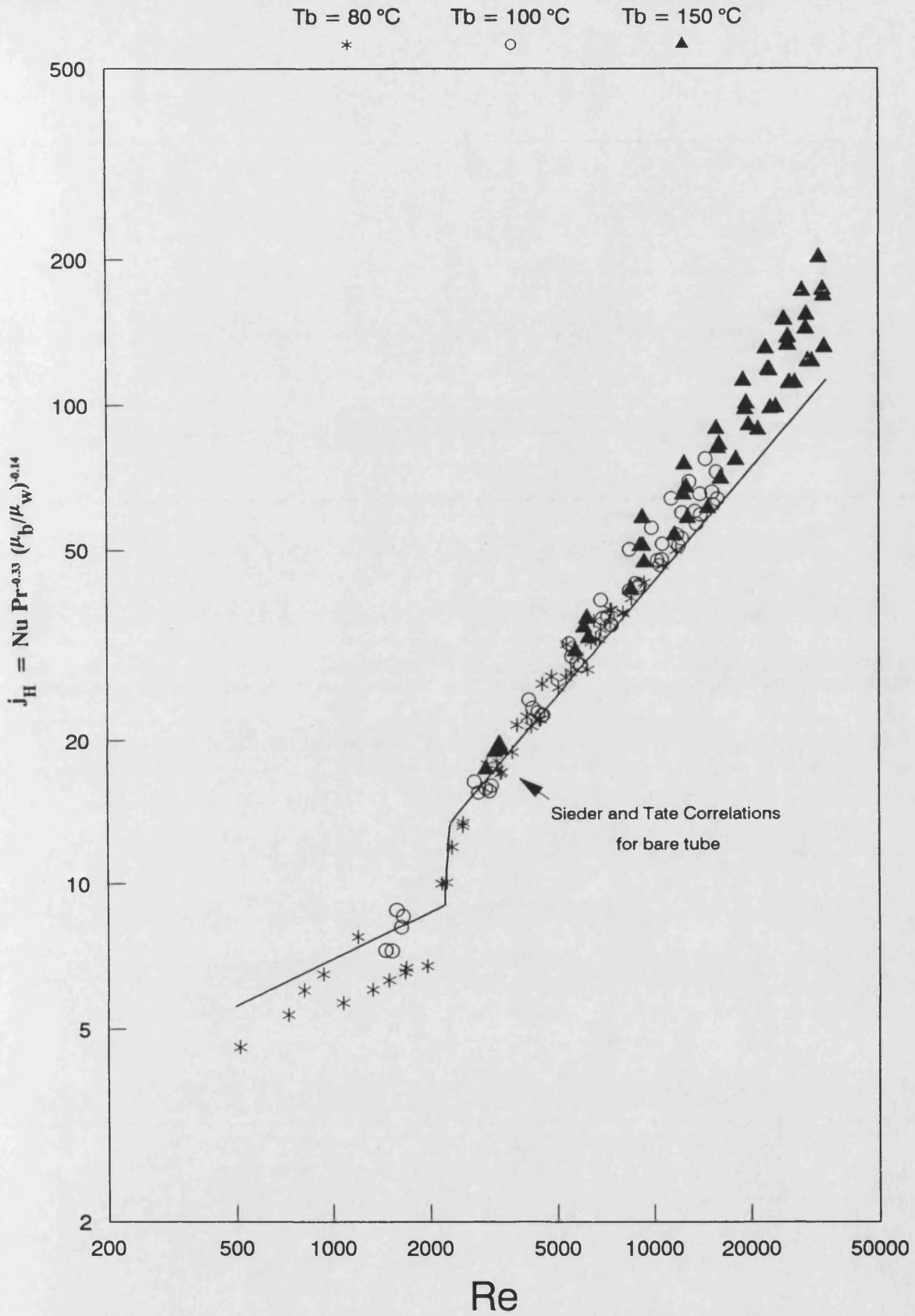

Fig (3.44) Heat transfer factor (j_H) vs Reynolds number (Re)

Santotherm 55 for bare tube ; test sections No 2 at 12 kW/m² < q < 60.2 kW/m²

(30 < Pr < 187)

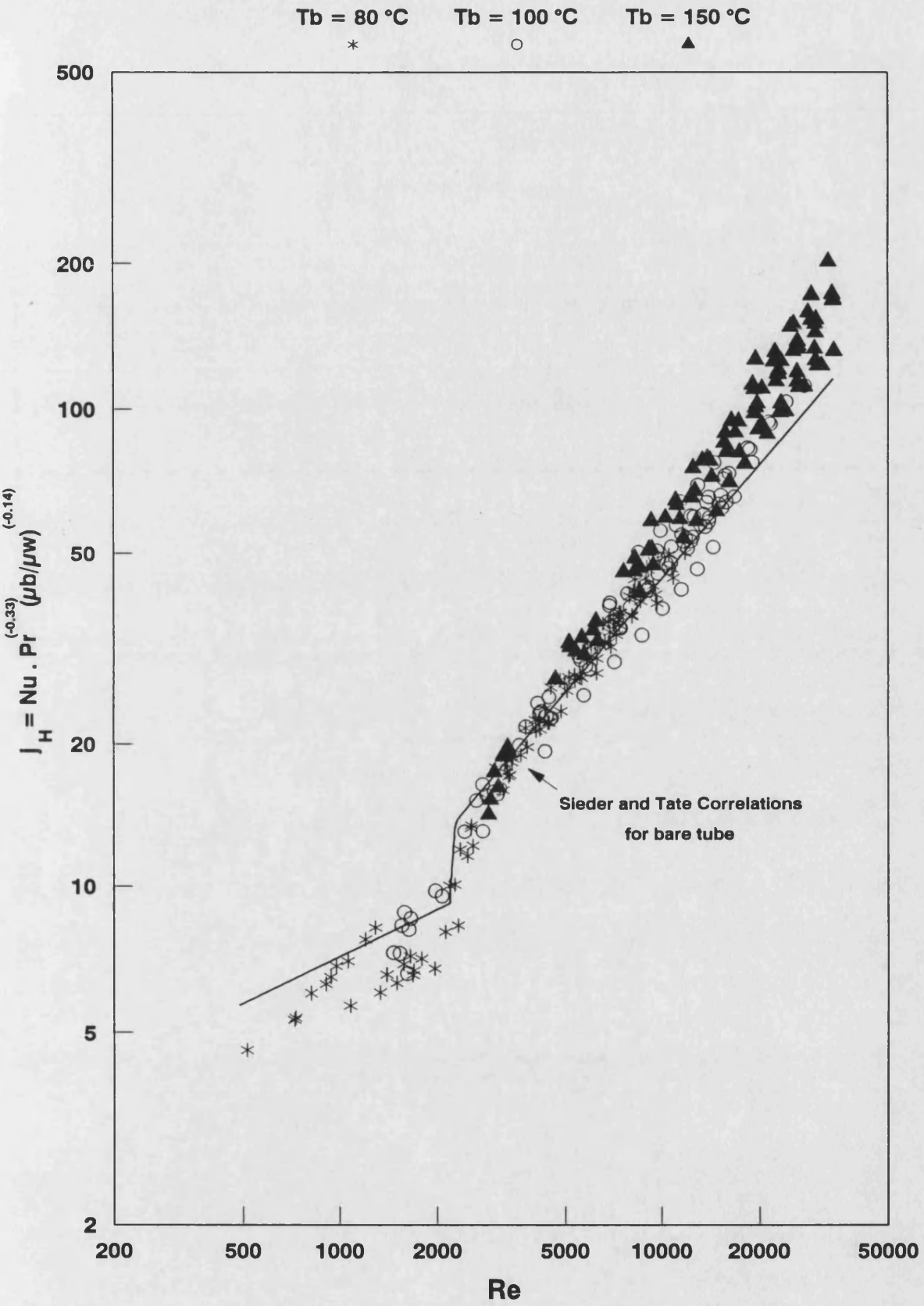

Fig (3.45) Heat transfer factor (j_H) vs Reynolds number (Re)

Santotherm 55 for bare tube ; both test sections at 12 kW/m² < q < 60.2 kW/m²
(30 < Pr < 187)

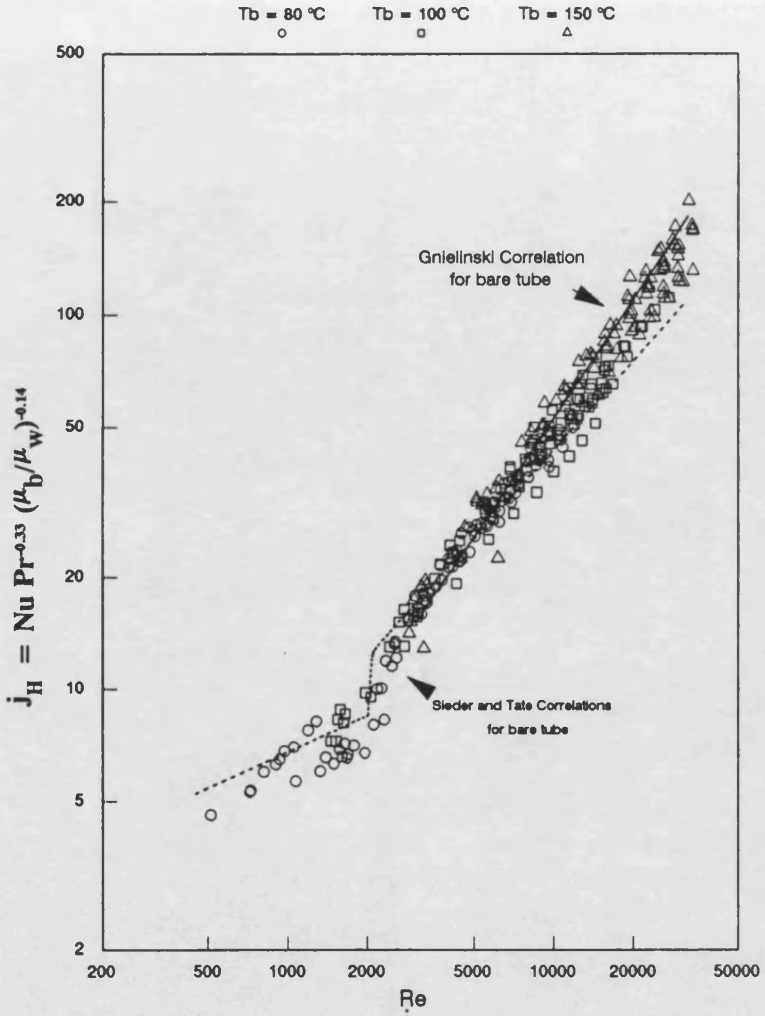

Fig (3.46) Heat transfer factor (j_H) vs Reynolds number (Re)

Santotherm 55 for bare tube ; both test sections at 12 kW/m² < q < 60.2 kW/m²

Comparing the experimental results with Sieder-Tate and Gnielinski correlations

(30 < Pr < 187)

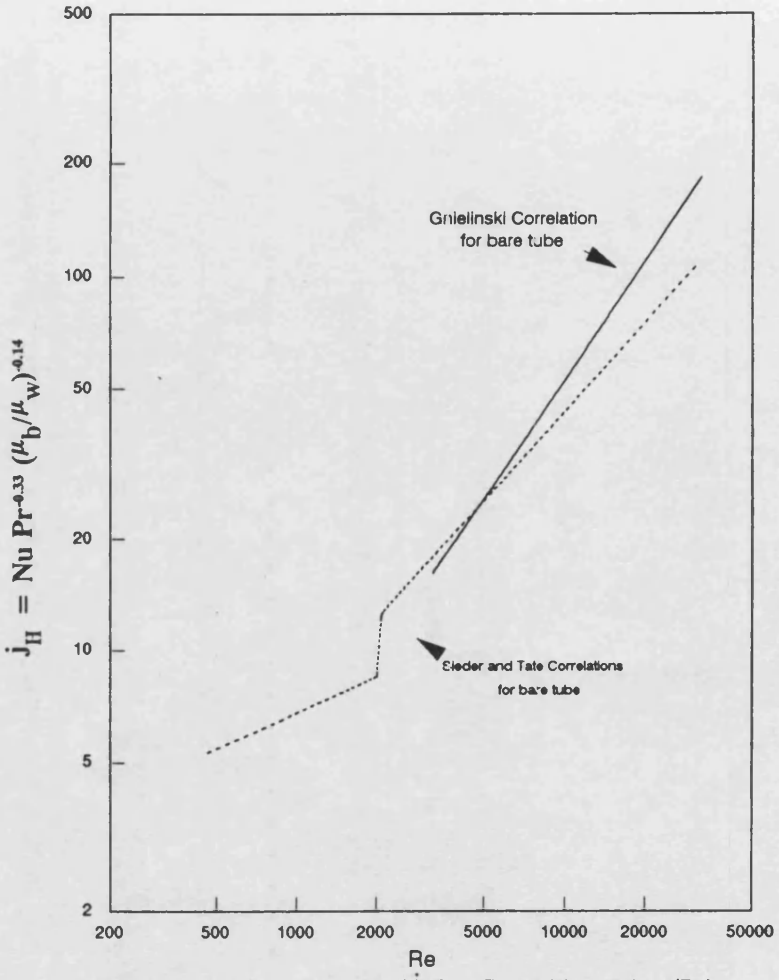

Fig (3.47) Heat transfer factor (j_H) vs Reynolds number (Re)

Comparsion between Sieder-Tate and Gnielinski correlations

(30 < Pr < 187)

temperature, for which 30 < Pr < 60 there were no data points for Re < 2100 . For Re > 2100, the experimental values of j_H-factor are well above the Sieder-Tate correlation by about 20 to 30% and as much as 50% for some extreme points.

For each test section in turn , the j_H-factor for all three temperatures is shown in Figs 3.43 (test section No 1) and 3.44 (Test section No 2) . All the data for both test sections are shown in Fig 3.45 . It may be concluded that there is no significant difference between the test sections.

The Sieder-Tate model appears to be unsuitable over the entire range of experimental conditions studied . The reasons behind this are twofold.

Firstly , the thermal entrance length (L_{th}) used in present study was 16.22 D_i which is much shorter than that used by Sieder and Tate ($50 < \frac{L}{D_i} < 235$) . Moreover , in the Sieder and Tate study the fluid was fully developed hydrodynamically, whilst in the present study in the range of 1300 < Re < 2500 it is believed to be in simultaneously developing flow .

Secondly , In the original work of Sieder and Tate, the fluids tested had Prandtl numbers in the range of 151 to 16700 only and no low Pr fluids were tested. The agreement between the experimental points in

this study with the Sieder and Tate correlation (Fig 3.40) with 110 < Pr <187 is further evidence that the correlation is applicable for fluids with high Prandtl numbers.

For fully developed turbulent flow , equation 3.111 was found by Kakaç *et al*[14] to give results in the range of 10% below to 21% above those from the Gnielinski correlation[37] (equation 1.80). Gnielinski correlations were chosen by Kakaç *et al*[14] as the most accurate heat transfer correlations for turbulent flow.

In Fig 3.46 the experimental results are compared with both the Sieder-Tate[36] and Gnielinski[37] correlations. In order to provide a clearer comparison between Sieder-Tate and Gnielinski correlations the latter was modified in this study by incorporating the viscosity correction factor as in equation 3.112 :

$$Nu = 0.012\,(Re^{0.87} - 280)\,Pr^{0.4}\,(\mu_b/\mu_w)^{0.14} \qquad (3.112)$$

Better agreement of the experimental data in this study with the Gnielinski correlation was found than with the Sieder-Tate correlation . For ease of interpretation Fig 3.47 shows the comparison between the Sieder-Tate and the modified Gnielinski correlations without the data points.

3.5.2.3.2 Heat transfer j_H - factor for tube fitted with different types of HiTran insert

j_H-factors for tubes fitted with different types of HiTran insert are shown in Figs 3.48 to 3.88 . The Sieder-Tate and the modified Gnielinski correlations for the bare tube are used as reference curves on all Figures.

I - Low loop density inserts (LDI-A and LDI-B)

The effect of supplying different heat fluxes in the range of $12 < q < 60.2$ kW/m^2 to test section No(1) fitted with LDI-A is shown in Figs 3.48 , 3.49 and 3.50 for T_b = 80, 100 and 150 °C respectively.

For T_b = 80 and 100 °C the effect of q on j_H is very small as shown in Figs 3.48 and 3.49 . At each bulk temperature the experimental data could be fitted to a straight line. For T_b = 150 °C j_H varies with q . This variation was within ± 5 to 15% for $12 < q < 60.2$ kW/m^2 .

The effect of bulk temperature on j_H for the tube fitted with LDI-A at constant heat flux (q) is shown in Figs 3.51 and 3.52 for q = 24 kW/m^2 and 48.2 kW/m^2 respectively . Fig 3.53 shows the results for $12 < q < 60.2$ kW/m^2 and for the three bulk temperatures (80, 100 and 150 °C) . For T_b < 100 °C , j_H was not affected by T_b . However , for T_b > 100 °C the values of j_H are higher. This is perhaps due to a decrease of Pr and $(\mu_b/\mu_w)^{0.14}$ at higher bulk temperatures, because these changes can increase the values of the product $Pr^{-1/3}$ $(\mu_b/\mu_w)^{0.14}$ in equation

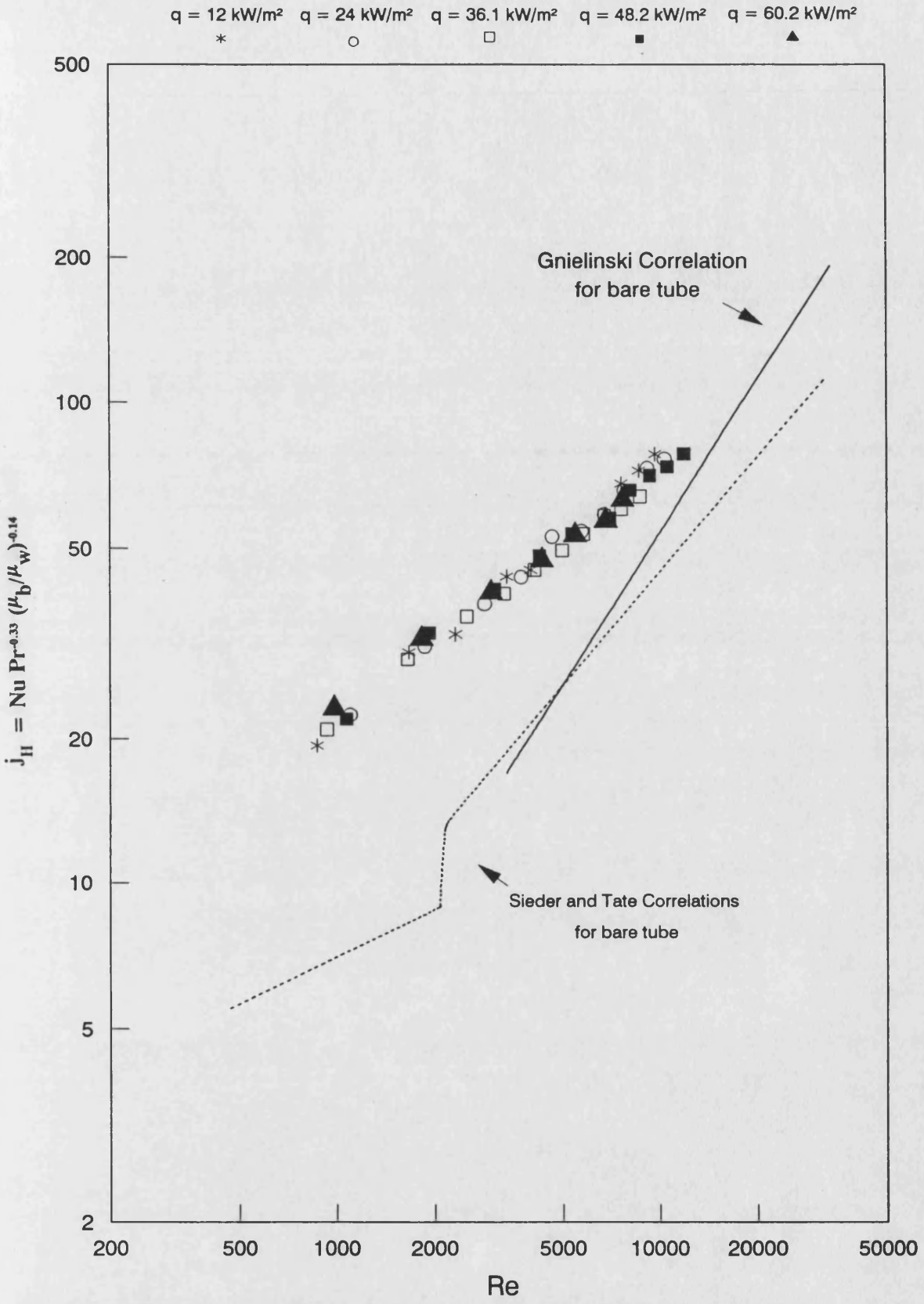

Fig (3.48) Heat transfer factor (j_H) vs Reynolds number (Re)

Santotherm 55 for tube fitted with LDI-A at Tb = 80 °C

(100 < Pr < 170)

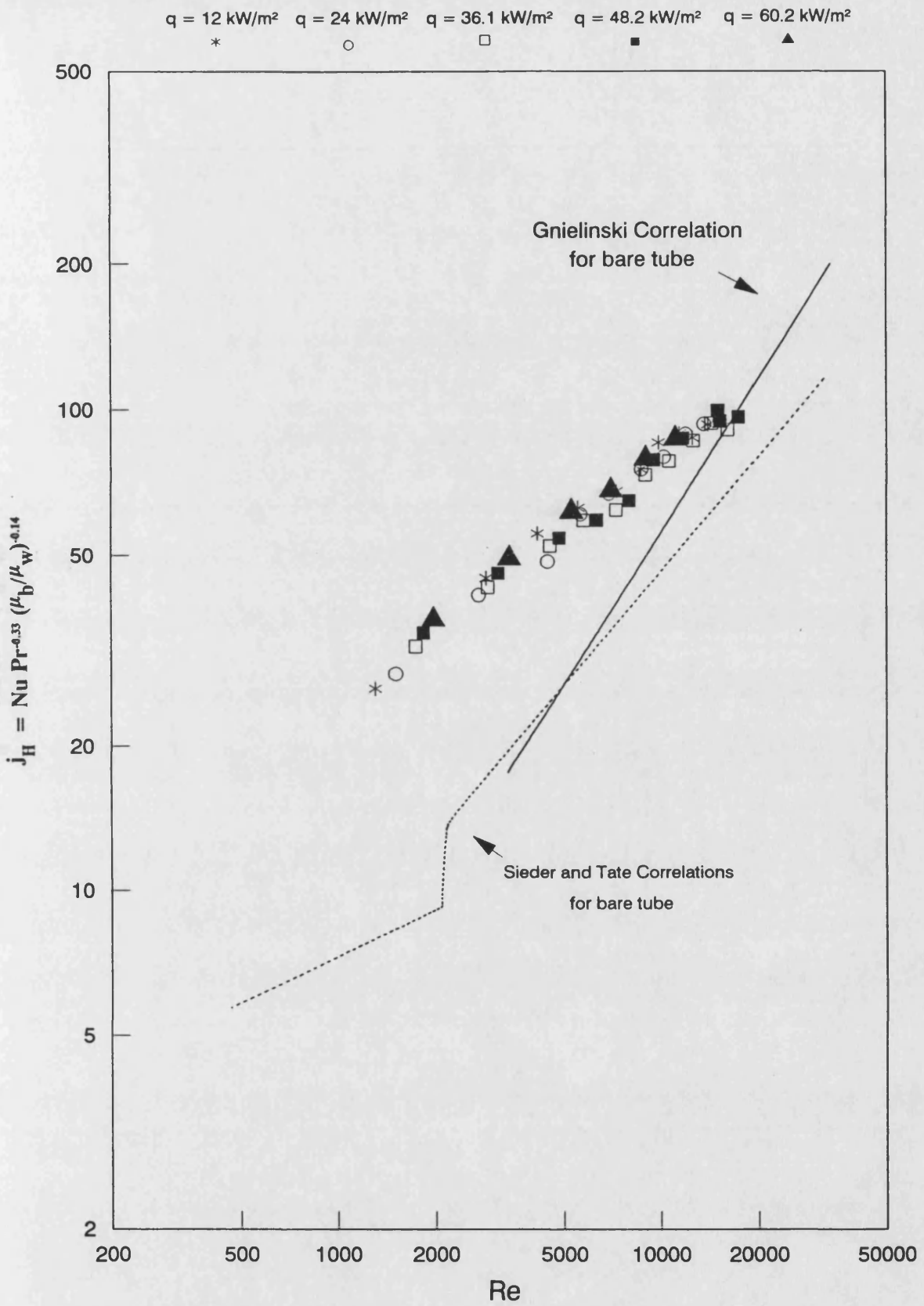

Fig (3.49) Heat transfer factor (j_H) vs Reynolds number (Re)

Santotherm 55 for tube fitted with LDI-A at Tb = 100 °C

(60 < Pr < 80)

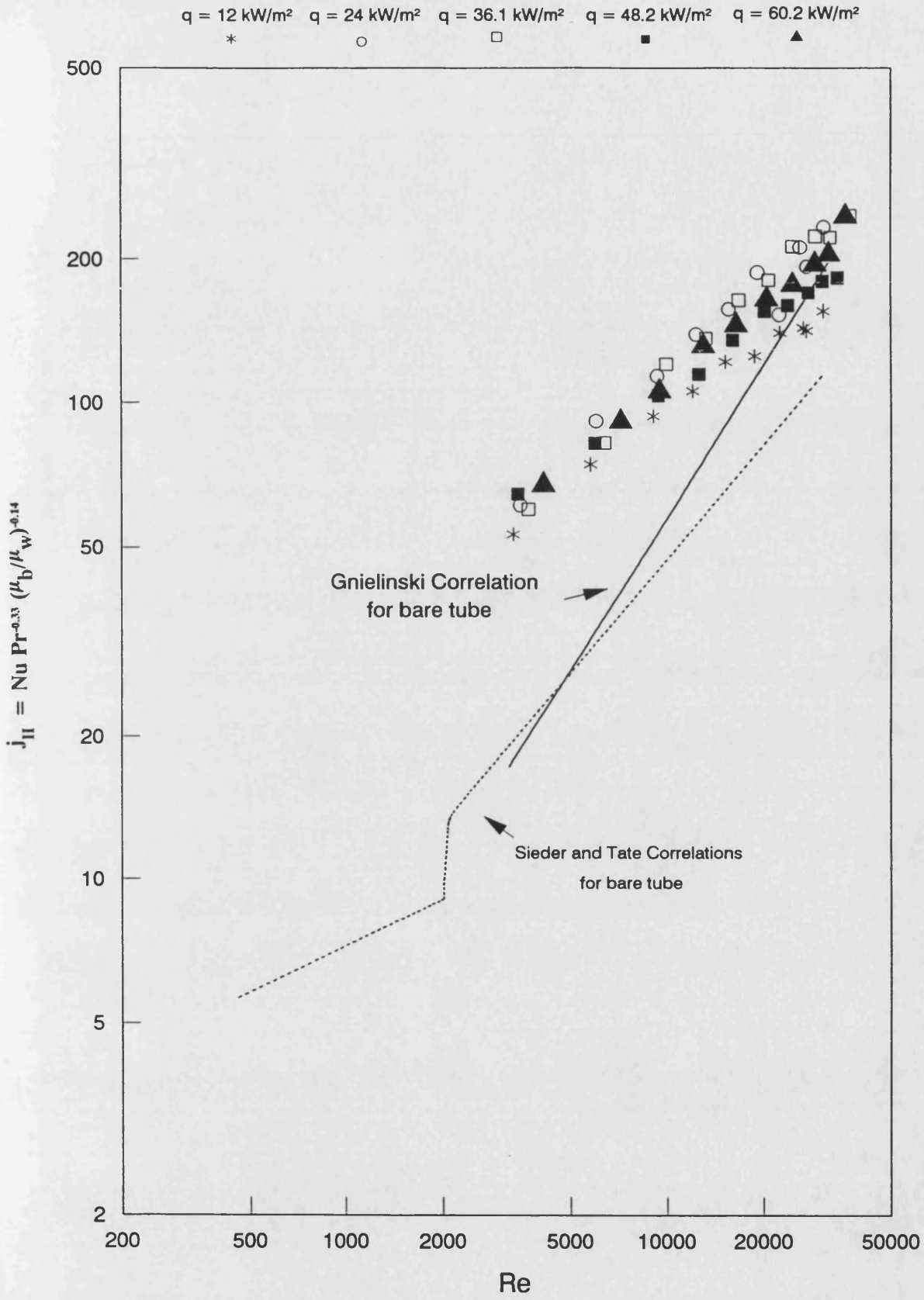

Fig (3.50) Heat transfer factor (j_H) vs Reynolds number (Re)

Santotherm 55 for tube fitted with LDI-A at Tb = 150 °C

(30 < Pr < 60)

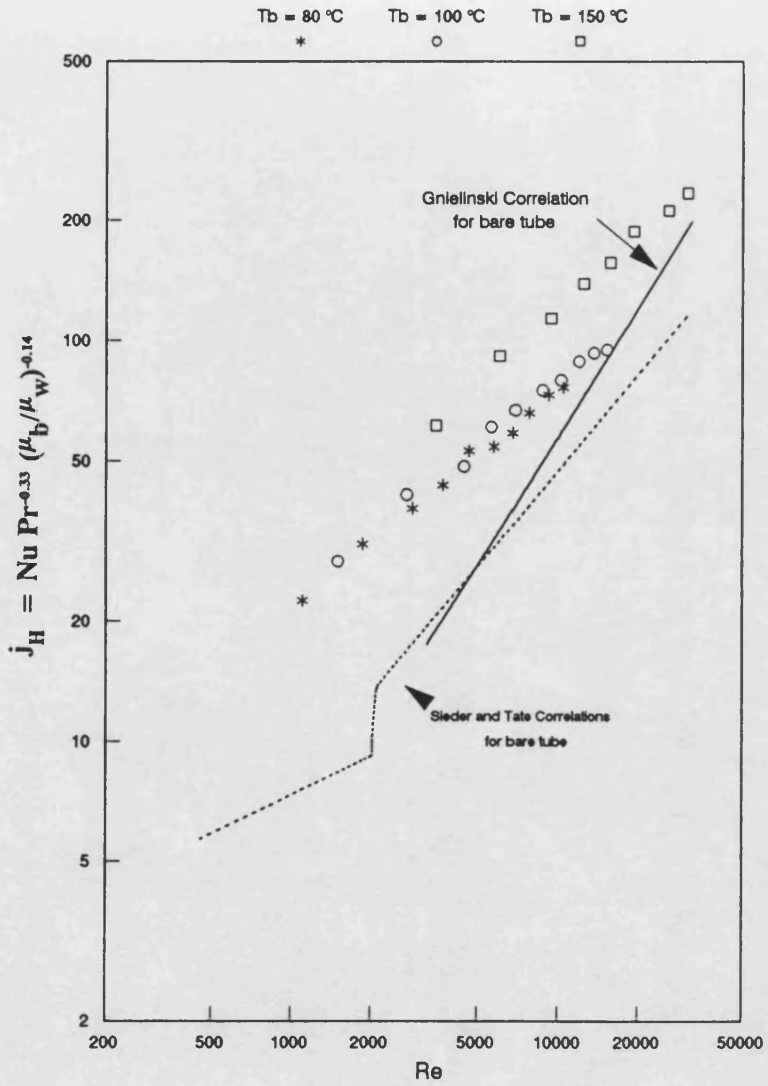

Fig (3.51) Heat transfer factor (j_H) vs Reynolds number (Re)
Santotherm 55 for tube fitted with LDI-A at q = 24 kW/m²
(30 < Pr < 178)

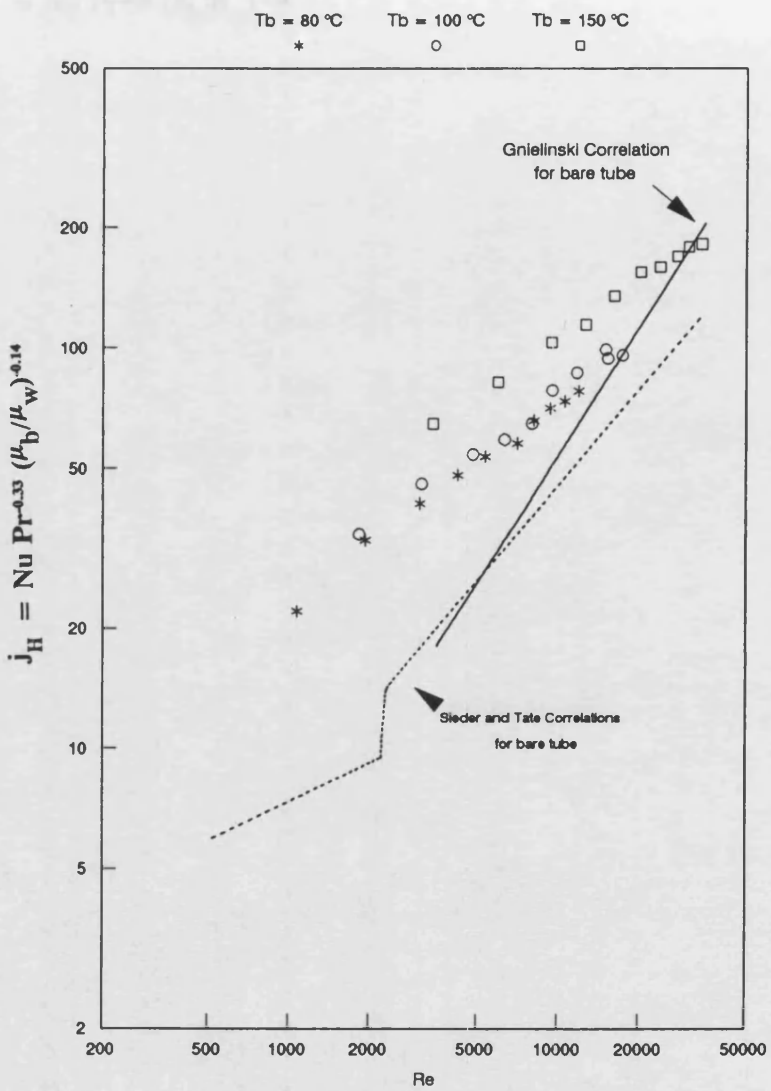

Fig (3.52) Heat transfer factor (j_H) vs Reynolds number (Re)
Santotherm 55 for tube fitted with LDI-A at q = 48.2 kW/m²
(30 < Pr < 178)

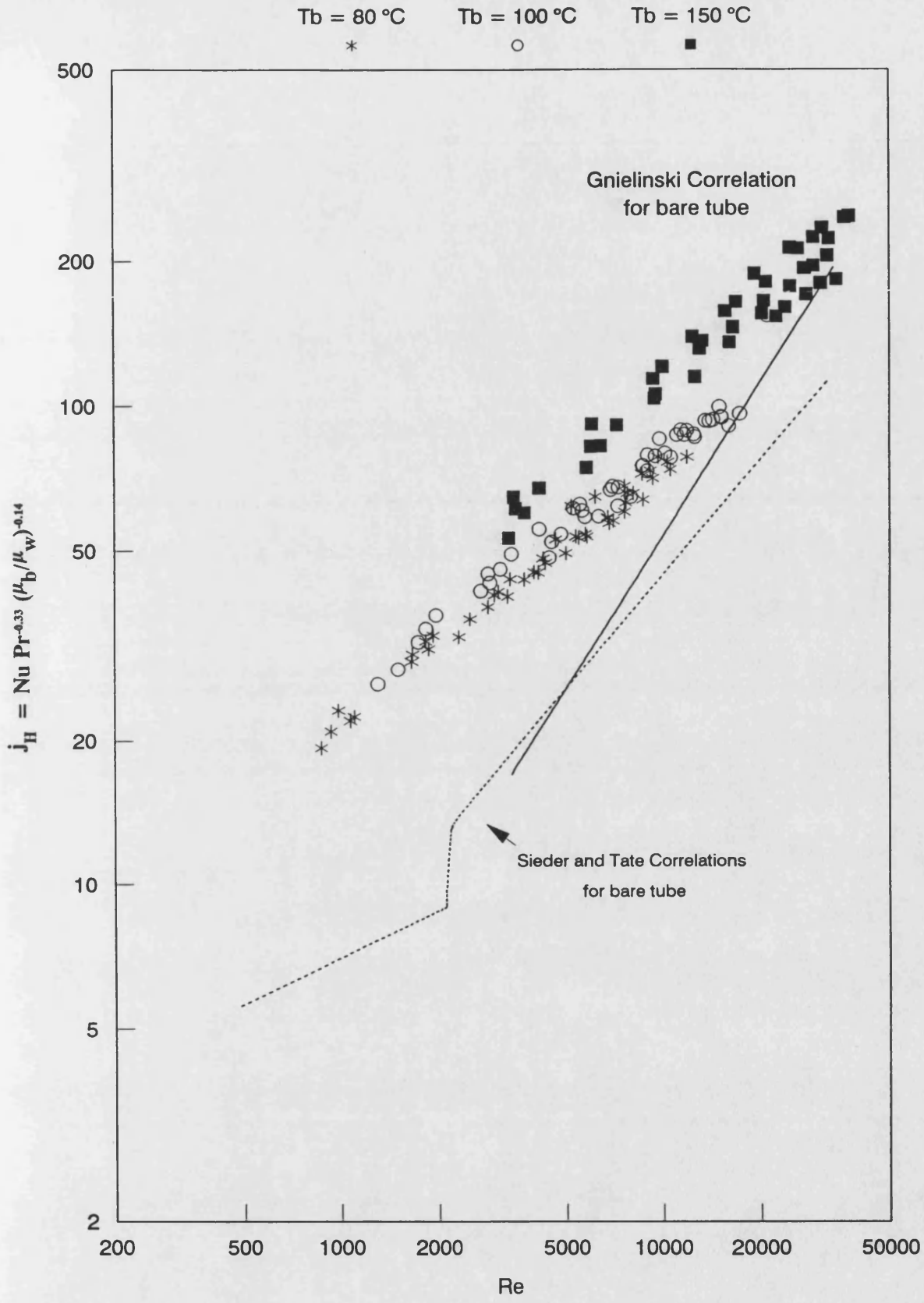

Fig (3.53) Heat transfer factor (j_H) vs Reynolds number (Re)

Santotherm 55 for tube fitted with LDI-A at 12 kW/m² < q < 60.2 kW/m²

(30 < Pr < 178)

3.69. For example , this product is about 0.19 to 0.21 for T_b < 100 °C , while it is 0.32 for T_b = 150 °C. Consequently, the values of j_H are about 30% higher at T_b = 150 °C than for the other bulk temperatures as seen in Fig 3.53 .

A comparison between LDI-A and LDI-B shows that the j_H-factor for a tube fitted with LDI-B is about 20% higher than that of same tube fitted with LDI-A, Figs 3.54 and 3.55. The reason behind this difference is possibly the same as that discussed in section 3.5.2.2.2-IV, (re-using the same insert) since the heat transfer and friction factor experiments were carried out at the same time.

Fig 3.53 clearly shows that a single good correlation for all the LDI-A data is not possible since the best fit would be within a ± 30% for Re > 2100. Thus a modified heat transfer factor (j_{HM}) is derived in section 3.5.2.4 .

II - Medium loop density inserts (MDI-A and MDI-B)

The effect of using five heat fluxes (12 < q < 60.2 kW/m^2) on j_H of the tube fitted with MDI-A is shown in Figs 3.56 , 3.57 and 3.58 at T_b equal to 80, 100 and 150 °C respectively. In all these Figures it can be seen that the effect of q on j_H is generally small for Re < 2100 . In general , for a given Re , j_H decreases with an increase in heat flux (q). The effect of bulk temperature on j_H is shown in Figs 3.59 and 3.60 for q = 24 and 48.2 kW/m^2

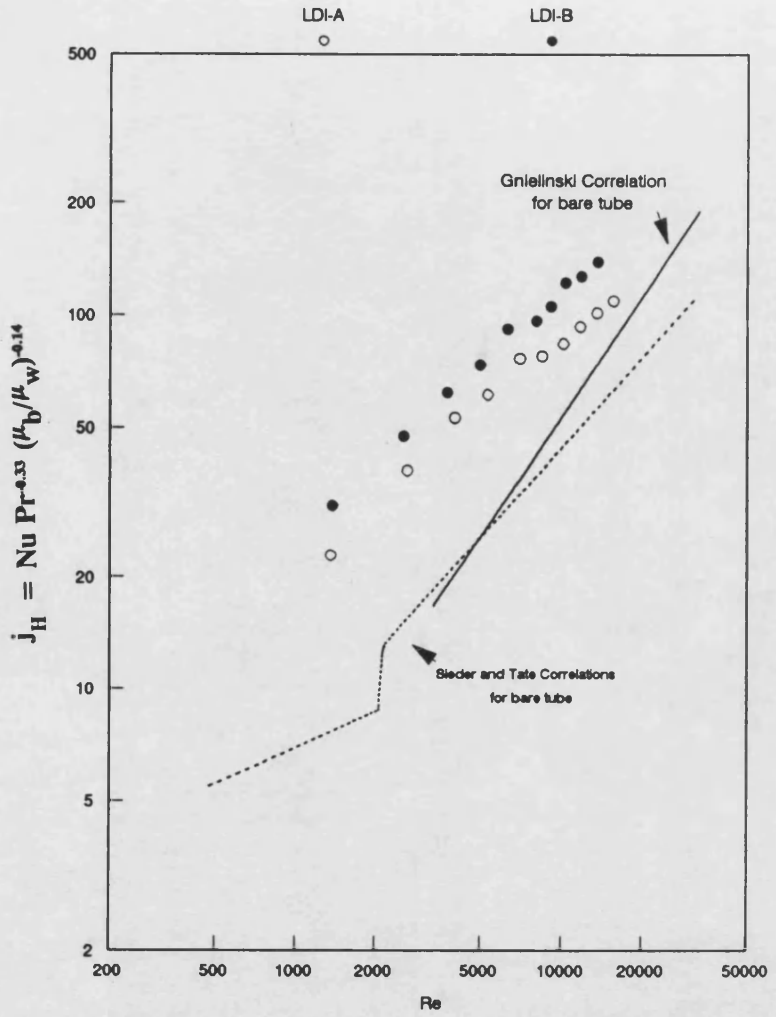

Fig (3.54) Heat transfer factor (j_H) vs Reynolds number (Re)

Comparsion between Inserts LDI-A and LDI-B fitted inside test section NO(2)
Santotherm 55 at q = 24 kW/m² ; Tb = 100 °C and 60 < Pr < 80

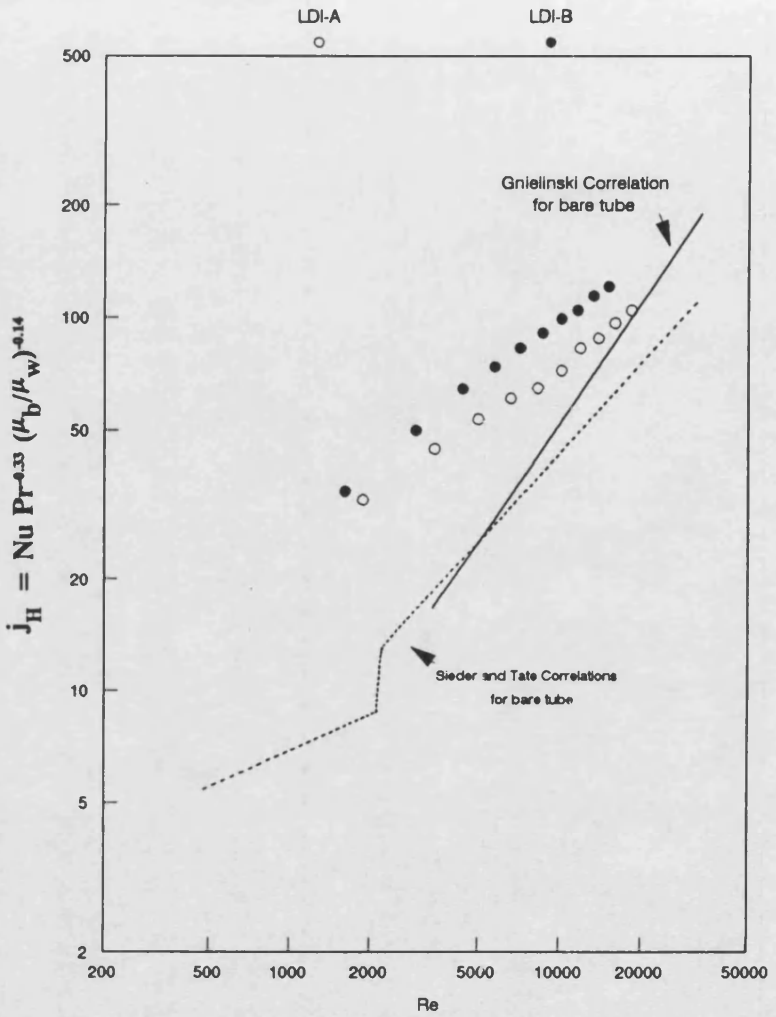

Fig (3.55) Heat transfer factor (j_H) vs Reynolds number (Re)

Comparsion between Inserts LDI-A and LDI-B fitted inside test section NO(2)
Santotherm 55 at q = 48.2 kW/m² ; Tb = 100 °C and 60 < Pr < 80

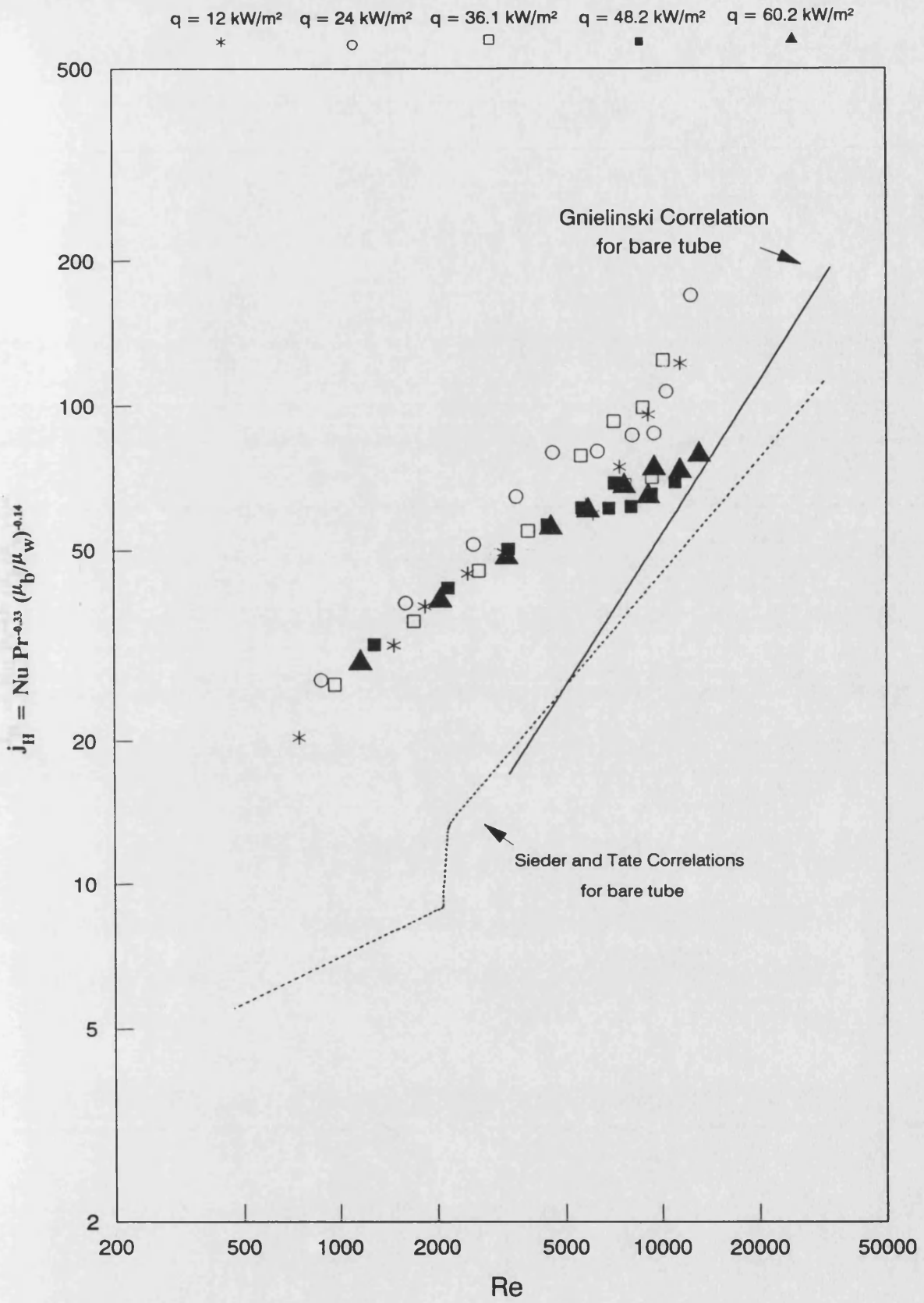

Fig (3.56) Heat transfer factor (j_H) vs Reynolds number (Re)

Santotherm 55 for tube fitted with MDI-A at Tb = 80 °C

(100 < Pr < 170)

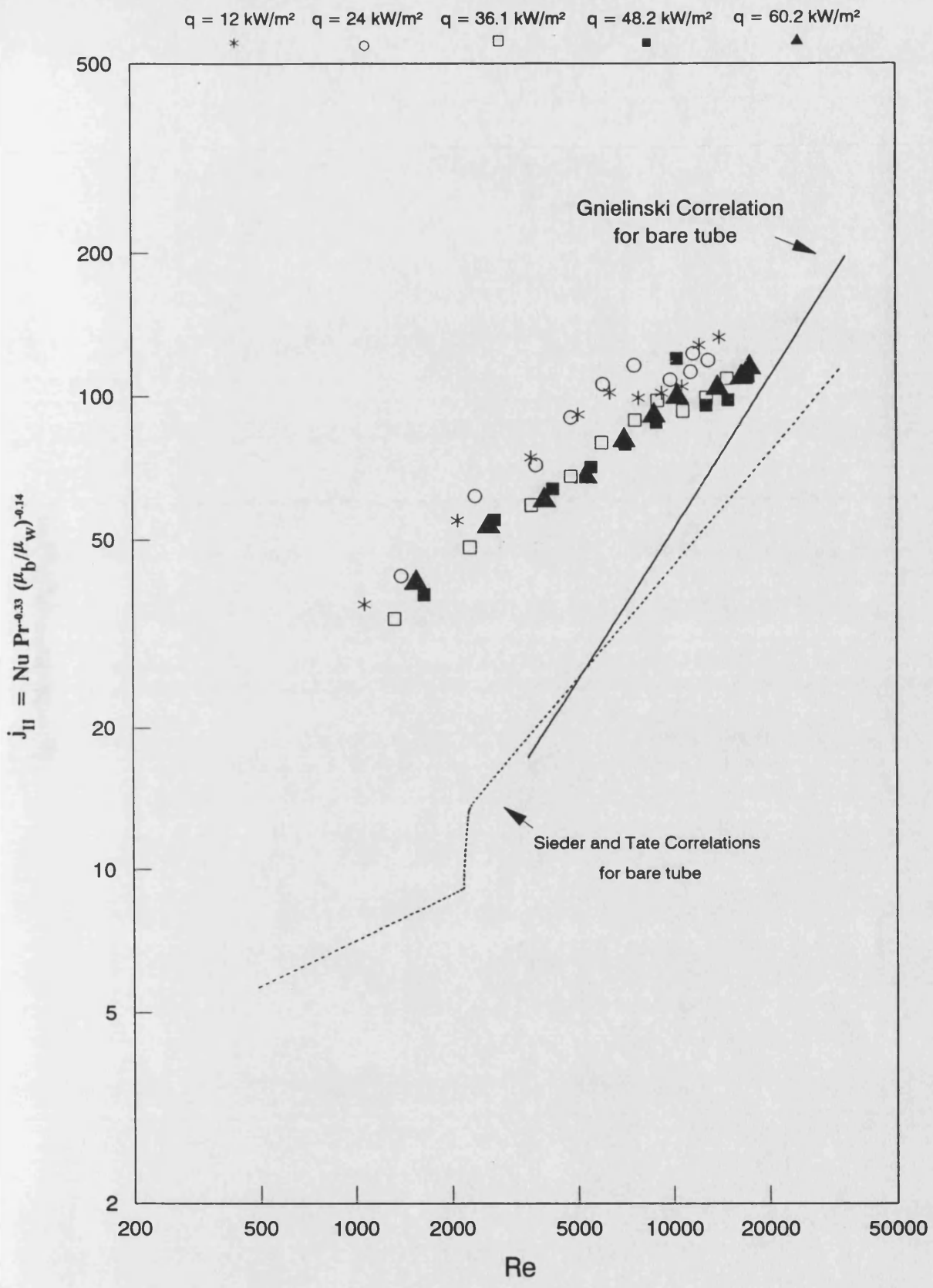

Fig (3.57) Heat transfer factor (j_H) vs Reynolds number (Re)

Santotherm 55 for tube fitted with MDI-A at Tb = 100 °C

(60 < Pr < 80)

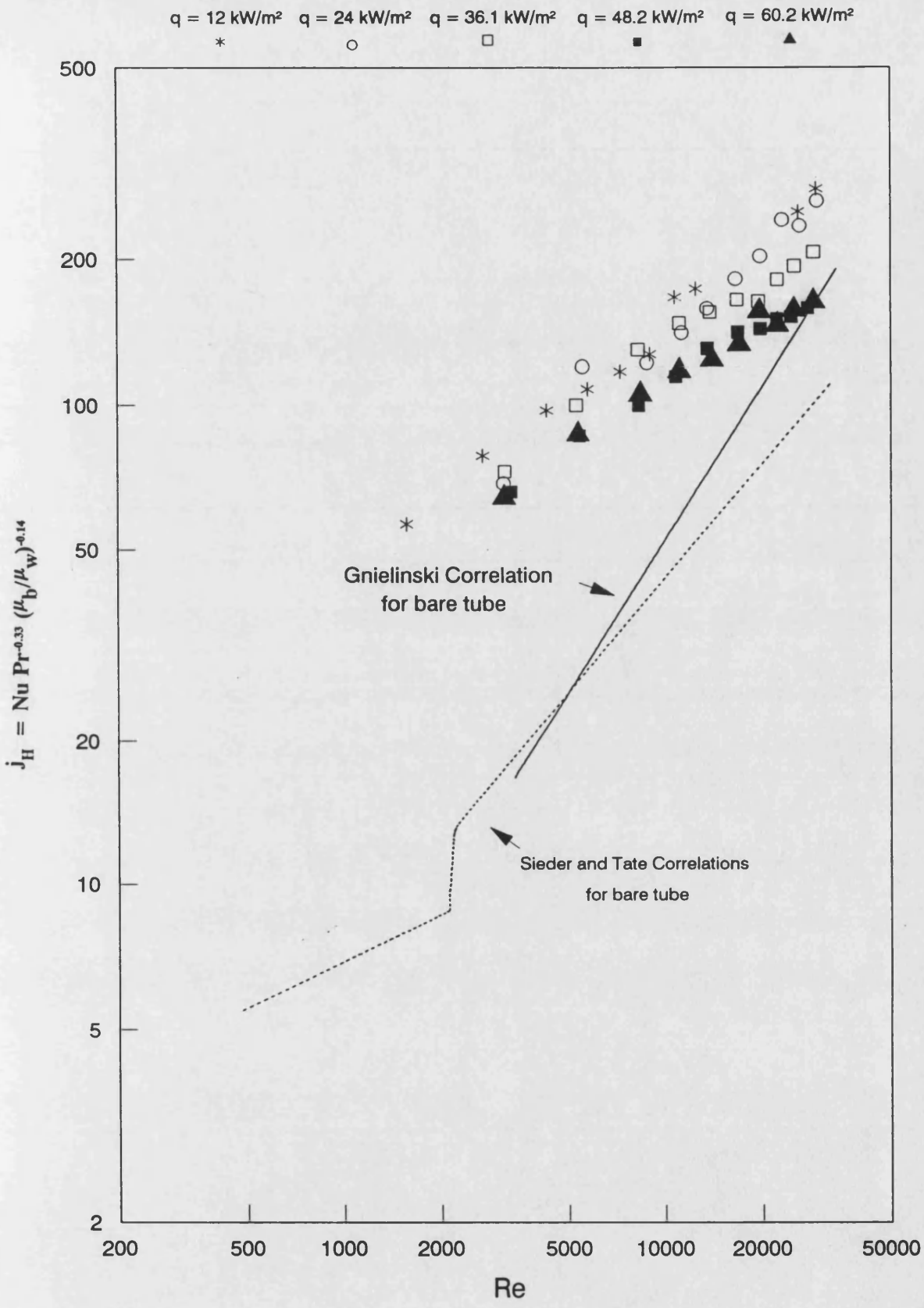

Fig (3.58) Heat transfer factor (j_H) vs Reynolds number (Re)

Santotherm 55 for tube fitted with MDI-A at Tb = 150 °C

(30 < Pr < 60)

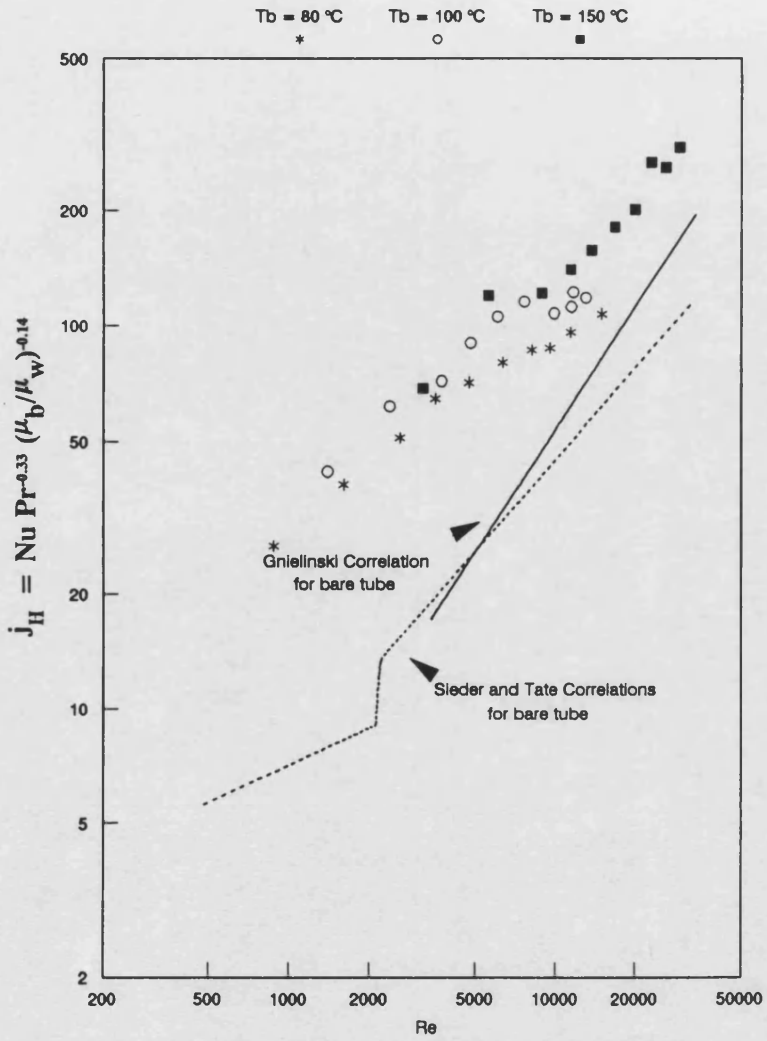

Fig (3.59) Heat transfer factor (j_H) vs Reynolds number (Re)

Santotherm 55 for tube fitted with MDI-A at q = 24 kW/m²

(30 < Pr < 178)

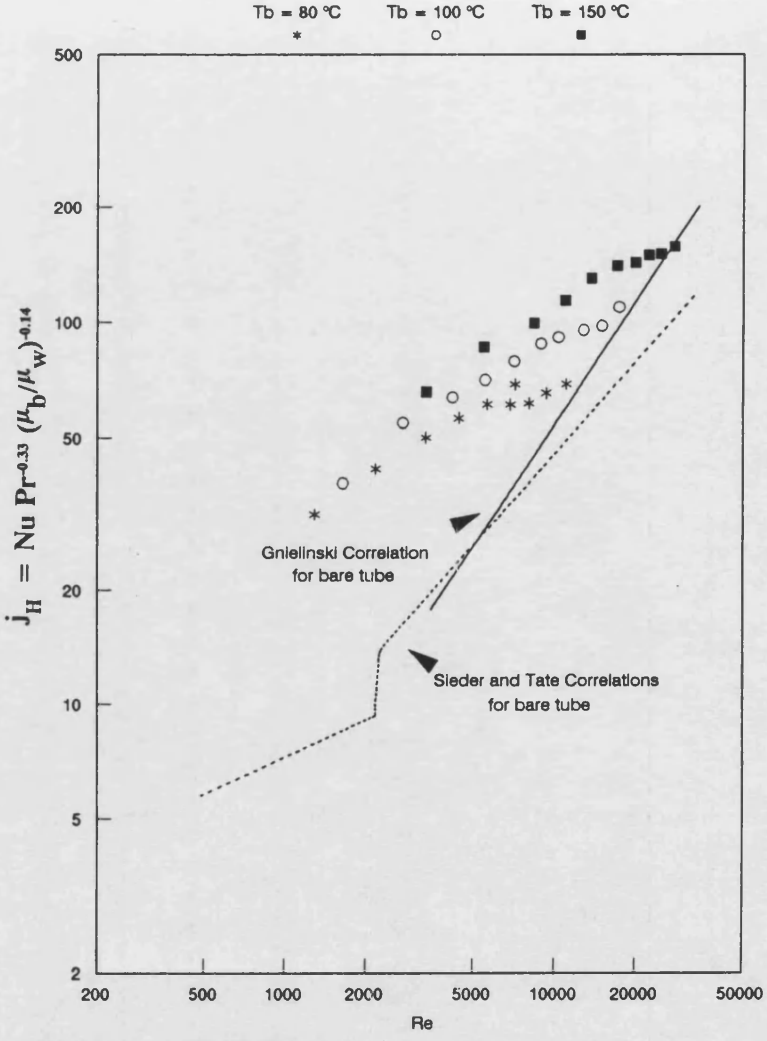

Fig (3.60) Heat transfer factor (j_H) vs Reynolds number (Re)

Santotherm 55 for tube fitted with MDI-A at q = 48.2 kW/m²

(30 < Pr < 178)

respectively. It can be seen that j_H is increased by increasing T_b at a constant heat flux (q).

Fig 3.61 shows the effect of T_b on j_H for all MDI-A data at $12 < q < 60.20$ kW/m^2. The scatter of data points is, once again, very large which makes a best fit correlation subject to ± 50% . For this reason j_{HM} was derived in section 3.5.2.4 .

Figs 3.62 to 3.67 show a comparison between j_H for both test sections (No (1) and No (2)) each fitted with an MDI-A insert and tested simultaneously. Although both inserts are similar (same manufacturer and same loop density), the insert fitted into test section No (2) gives a higher value of j_H (about 10 to 30%) than that fitted into test section No (1). There is no particular reason to expect that j_H for the insert fitted into test section (2) should be higher than that of test section (1), since both inserts had not been used previously and no difference in j_H for the bare tube case (both test sections) was noted (see Figs 3.40 to 3.42) . The only possible explanation for such a significant difference , is that the configuration of the insert inside test section No (1) was different from that in test section No (2) . The effect of insert configuration on j_H is investigated in section 3.5.2.3.2-V by rotating a HiTran insert inside a test section .

Fig. 3.68 shows all data points for both MDI-A inserts fitted into both test sections. The scatter

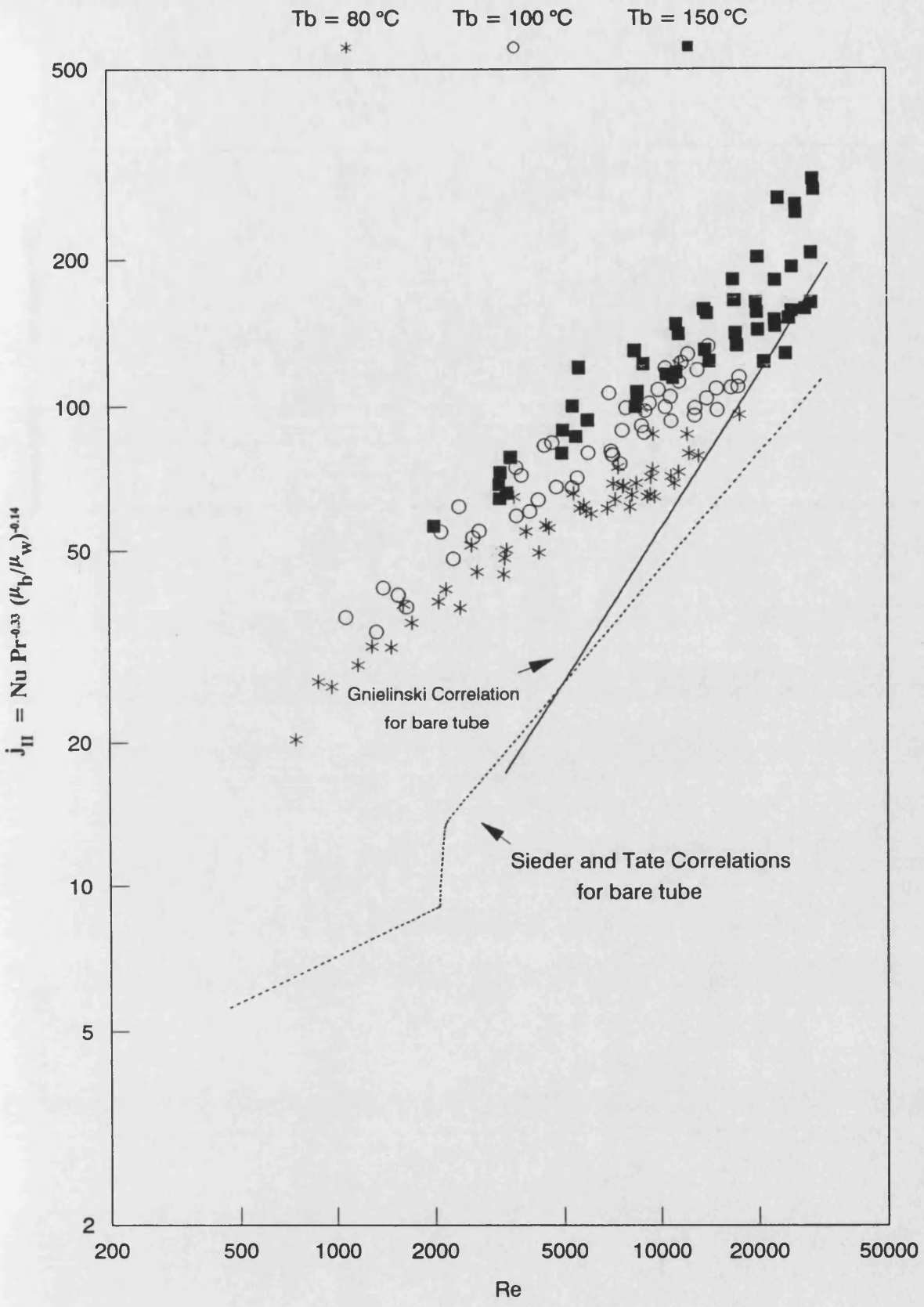

Fig (3.61) Heat transfer factor (j_H) vs Reynolds number (Re)

Santotherm 55 for tube fitted with MDI-A at 12 kW/m² < q < 60.2 kW/m²

(30 < Pr < 178)

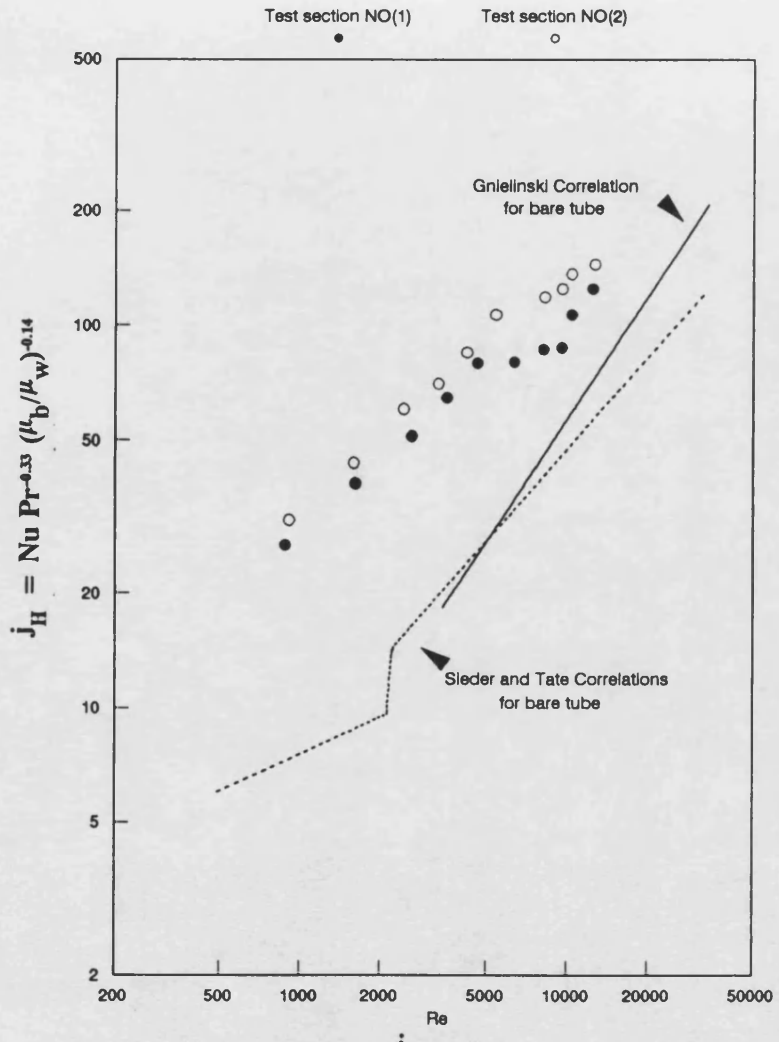

Fig (3.62) Heat transfer factor (j_{II}) vs Reynolds number (Re)

Comparsion between both test sections fitted with MDI-A at q = 24 kW/m²

(Tb = 80 °C and 100 < Pr < 187)

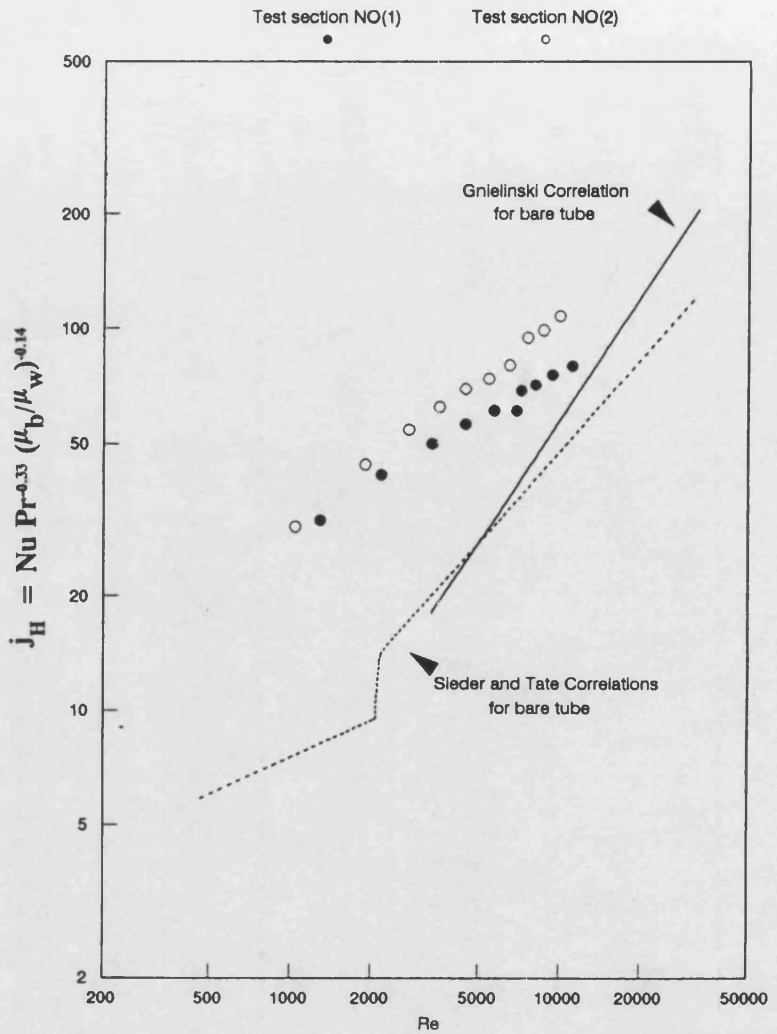

Fig (3.63) Heat transfer factor (j_H) vs Reynolds number (Re)

Comparsion between both test sections fitted with MDI-A at q = 48.2 kW/m²

(Tb = 80 °C and 100 < Pr < 187)

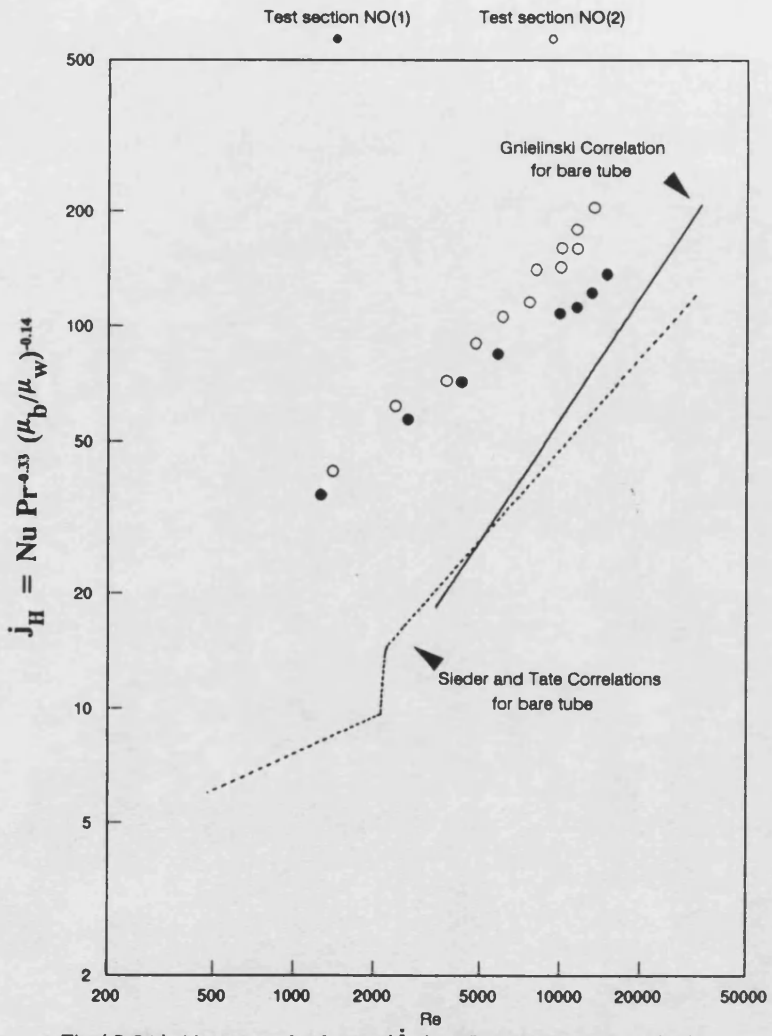

Fig (3.64) Heat transfer factor (j_H) vs Reynolds number (Re)

Comparsion between both test sections fitted with MDI-A at q = 24 kW/m²

(Tb = 100 °C and 60 < Pr < 80)

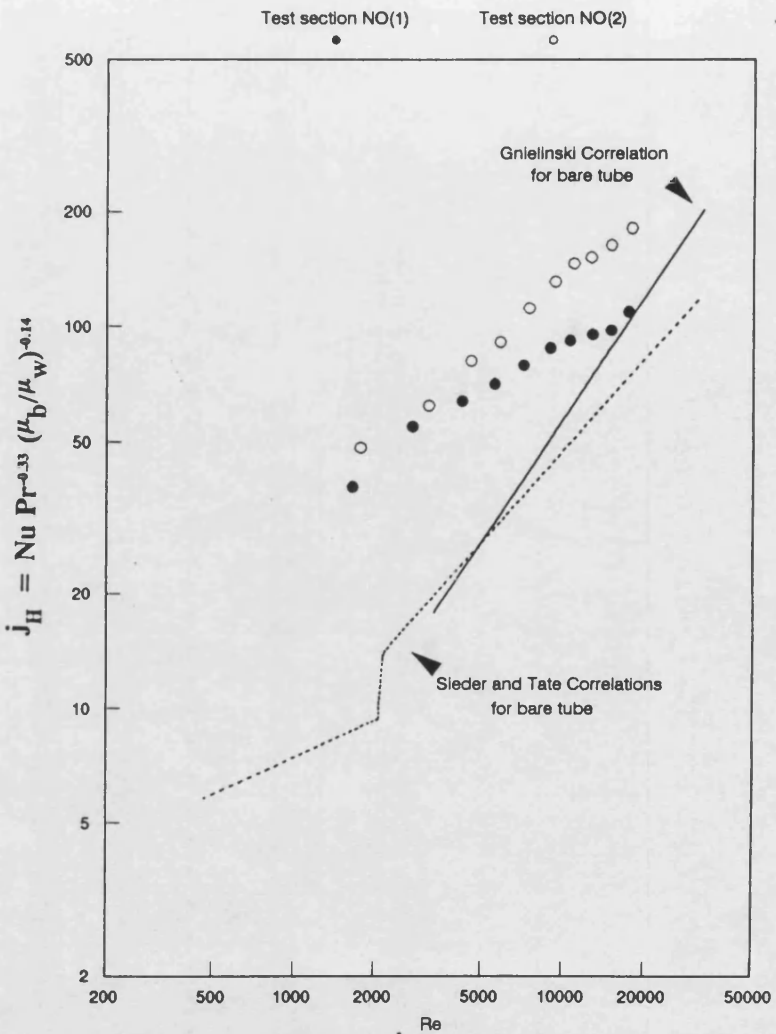

Fig (3.65) Heat transfer factor (j_H) vs Reynolds number (Re)

Comparsion between both test sections fitted with MDI-A at q = 48.2 kW/m²

(Tb = 100 °C and 60 < Pr < 80)

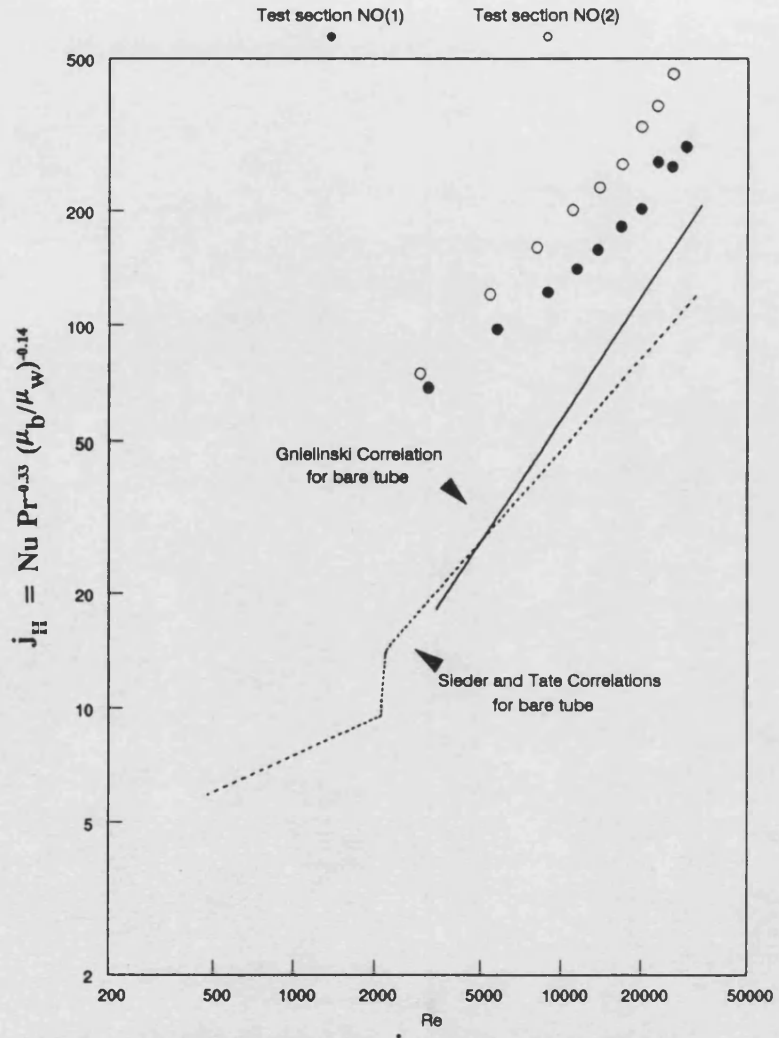

Fig (3.66) Heat transfer factor (j_H) vs Reynolds number (Re)

Comparsion between both test sections fitted with MDI-A at q = 24 kW/m²

(Tb = 150 °C and 30 < Pr < 60)

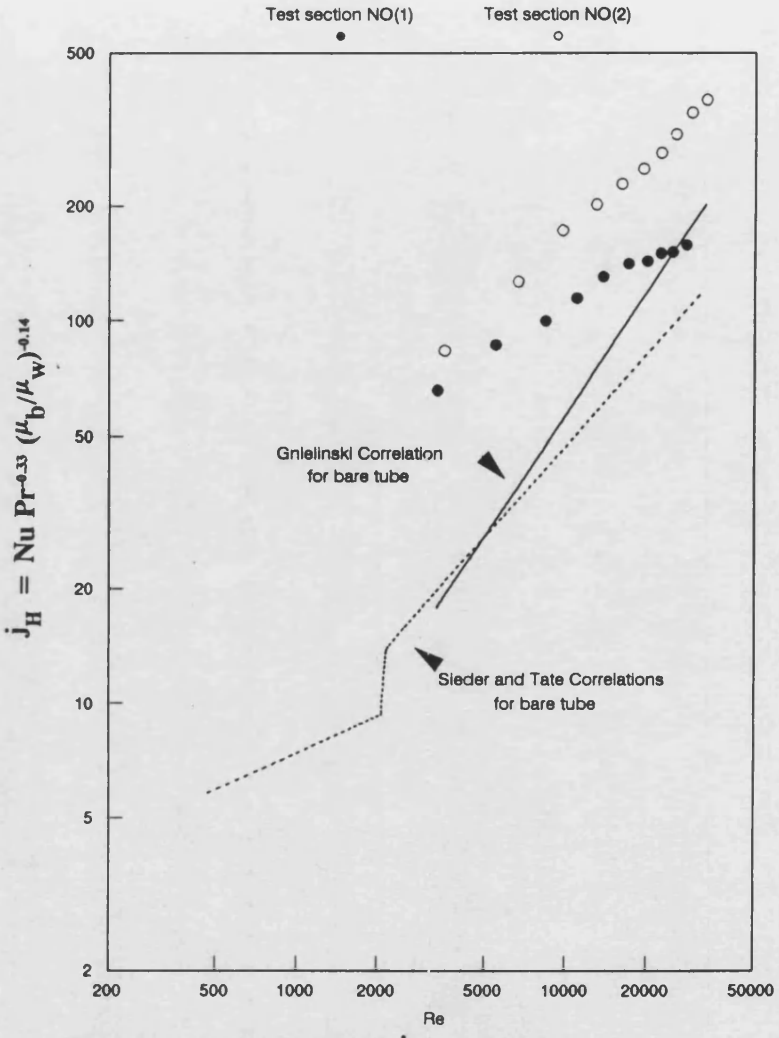

Fig (3.67) Heat transfer factor (j_H) vs Reynolds number (Re)

Comparsion between both test sections fitted with MDI-A at q = 48.2 kW/m²

(Tb = 150 °C and 30 < Pr < 60)

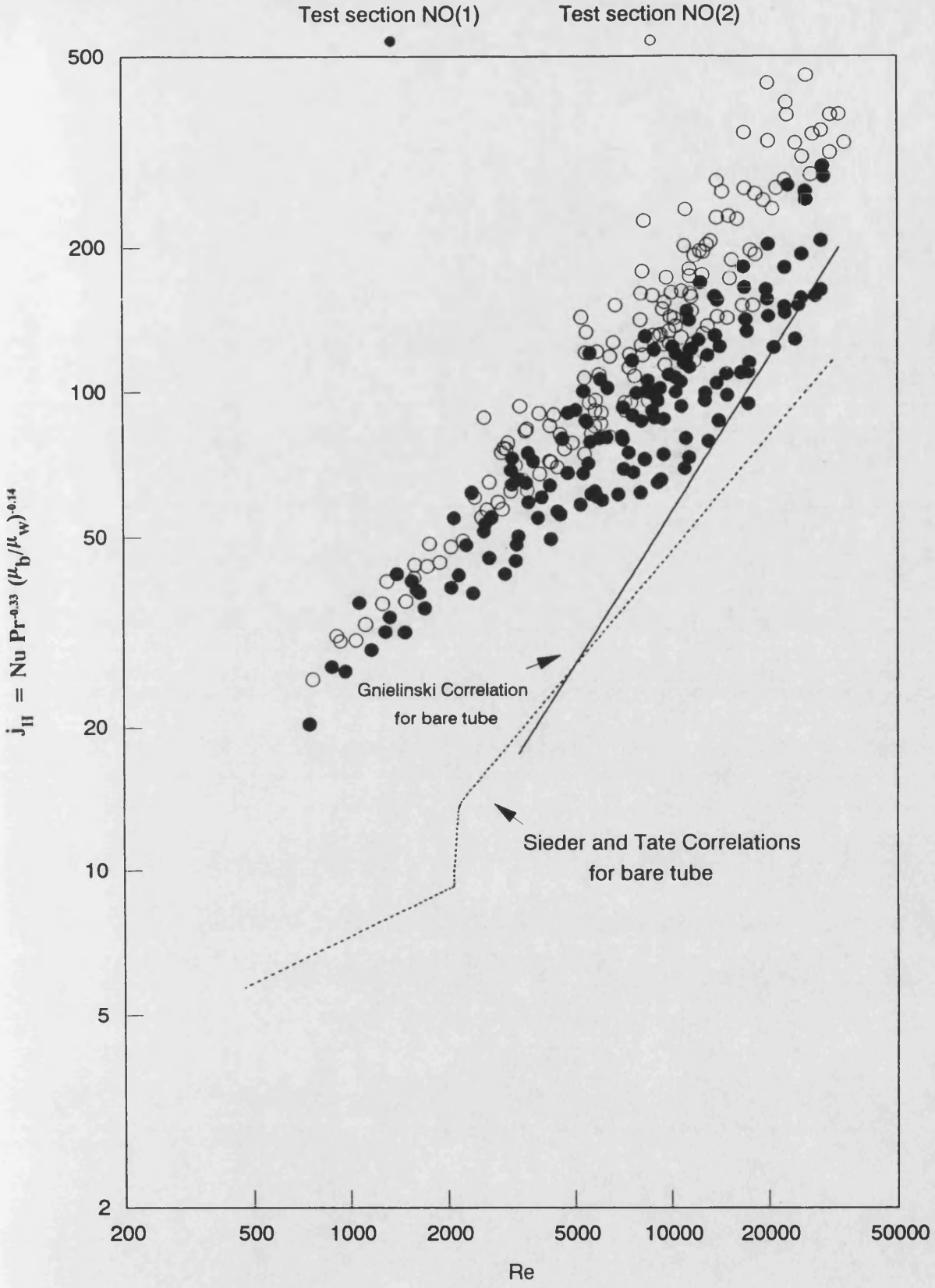

Fig (3.68) Heat transfer factor (j_H) vs Reynolds number (Re)

Comparsion between both test sections fitted with MDI-A

(12 kW/m² < q < 60.2 kW/m² ; 80 °C < Tb < 150 °C and 30 < Pr < 178)

of data shows that a best fit would be within ± 80% scatter .

A comparison between j_H of test section No (1) fitted with MDI-A and MDI-B is shown in Figs 3.69 and 3.70 . The comparison with the same inserts fitted into test section No (2) is shown in Figs 3.71 and 3.72 . It is clear that j_H for MDI-A is slightly higher than that for MDI-B.

III - High loop density inserts (HDI-A and HDI-B)

The effect of using three bulk temperatures (T_b = 80, 100 and 150 ^oC), on j_H for test section No(2) fitted with HDI-A at constant heat flux, is shown in Figs. 3.73 to 3.77 . The heat transfer factor is enhanced slightly by increasing the bulk temperature although the effect is less in this case than that of the previous cases with low and medium density inserts (LDI and MDI).

Fig. 3.78 shows all data points for HDI-A. The scatter of data is not large in this case, although a best fit would still be within a ± 20% variation.

A comparison between HDI-A and HDI-B fitted into test section No (1) is shown in Figs 3.79 and 3.80 at T_b = 100 ^oC for two heat fluxes (q = 24, and 48.16 kW/m^2). The performance of HDI-B is about 10% higher than that of HDI-A. On the other hand, a comparison between HDI-A and HDI-B fitted inside test section (2) shows very little difference in performance as illustrated in Figs 3.81 and 3.82 .

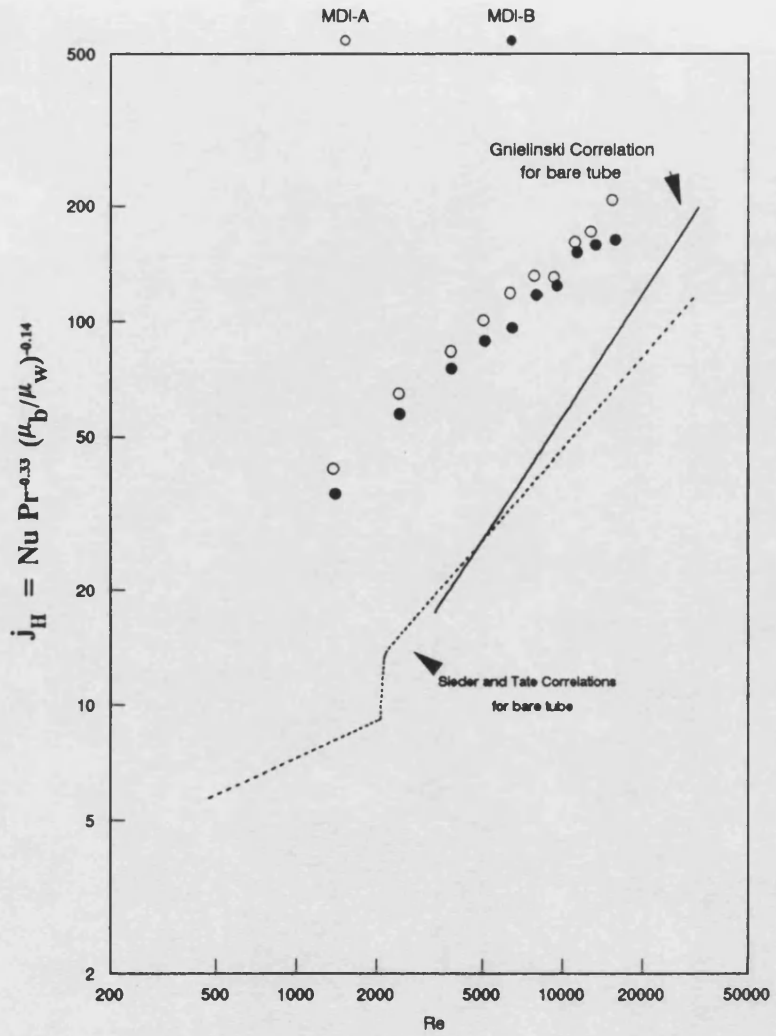

Fig (3.69) Heat transfer factor (j_H) vs Reynolds number (Re)

Comparsion between inserts MDI-A and MDI-B fitted into test section NO(1)
Santotherm 55 at q = 24 kW/m² ; Tb = 100 °C and 60 < Pr < 80

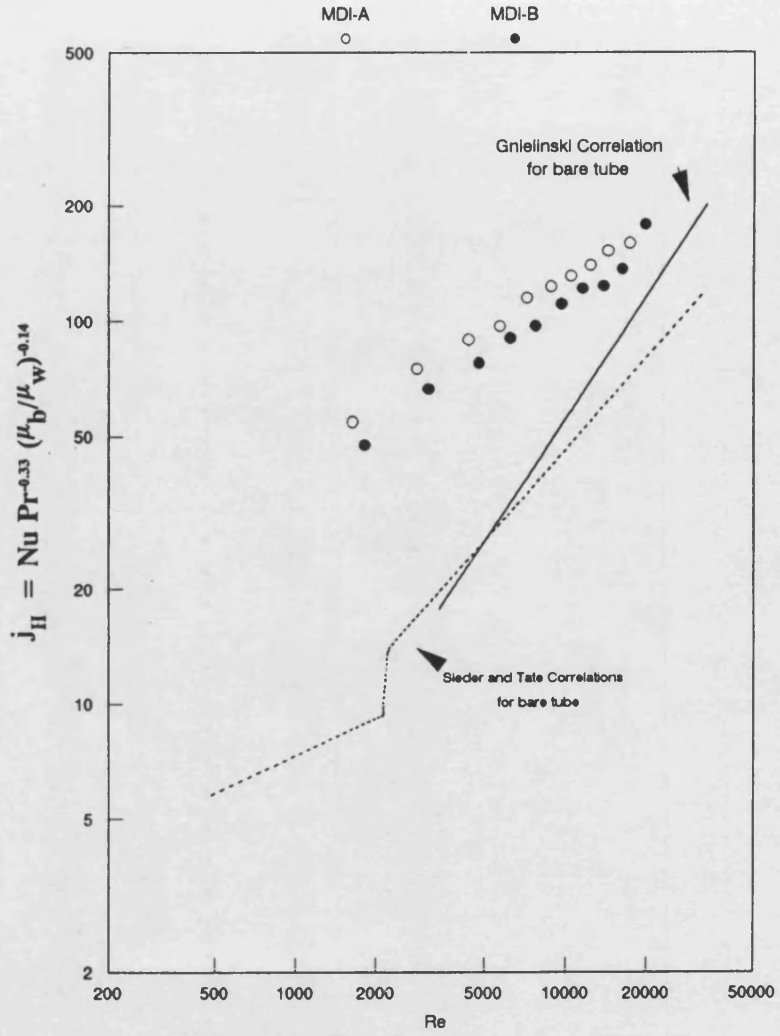

Fig (3.70) Heat transfer factor (j_H) vs Reynolds number (Re)

Comparsion between inserts MDI-A and MDI-B fitted into test section NO(1)
Santotherm 55 at q = 48.2 kW/m² ; Tb = 100 °C and 60 < Pr < 80

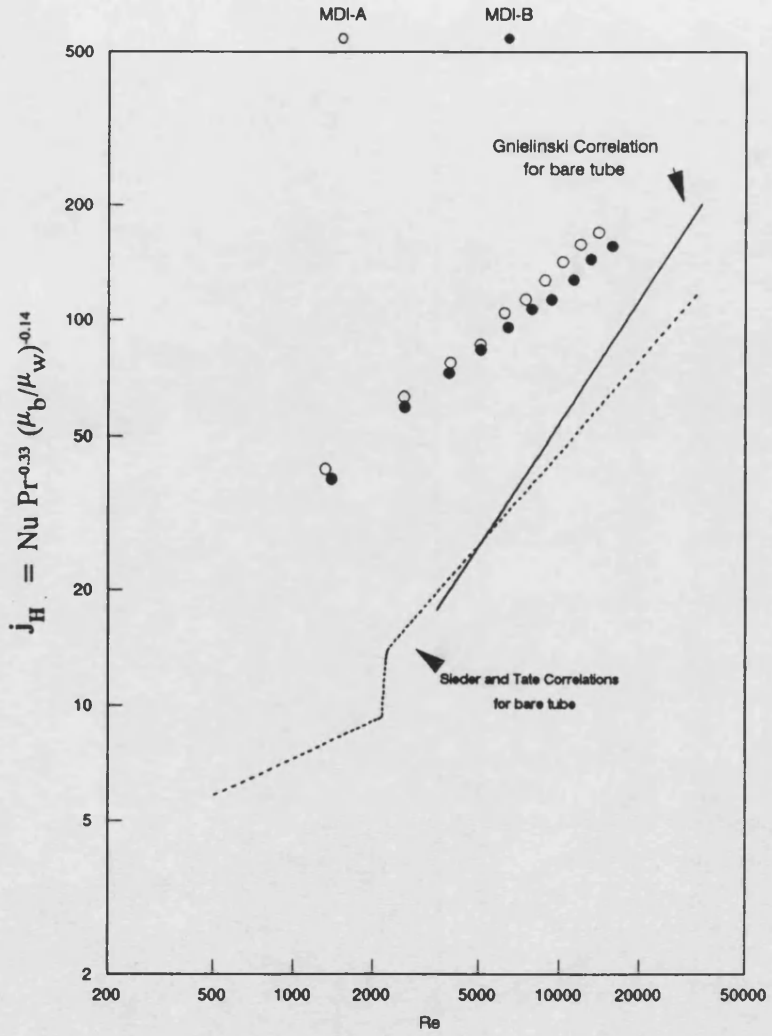

Fig (3.71) Heat transfer factor (j_H) vs Reynolds number (Re)

Comparsion between inserts MDI-A and MDI-B fitted into test section NO(2)
Santotherm 55 at q = 24 kW/m² ; Tb = 100 °C and 60 < Pr < 80

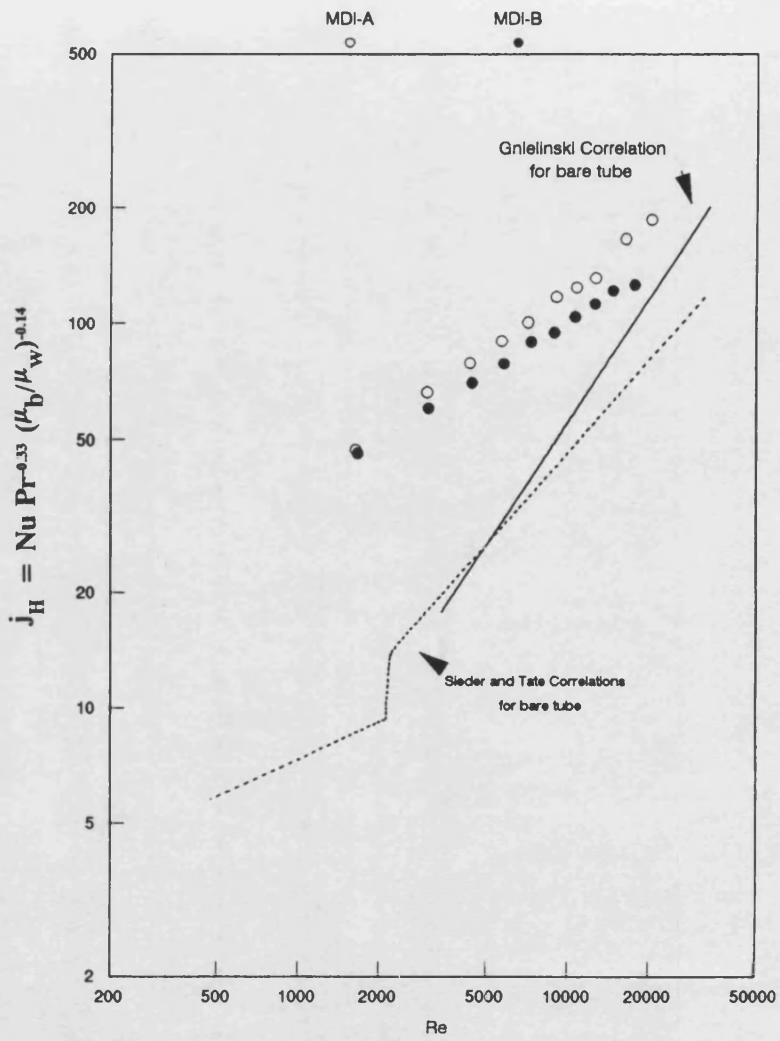

Fig (3.72) Heat transfer factor (j_H) vs Reynolds number (Re)

Comparsion between inserts MDI-A and MDI-B fitted into test section NO(2)
Santotherm 55 at q = 48.2 kW/m² ; Tb = 100 °C and 60 < Pr < 80

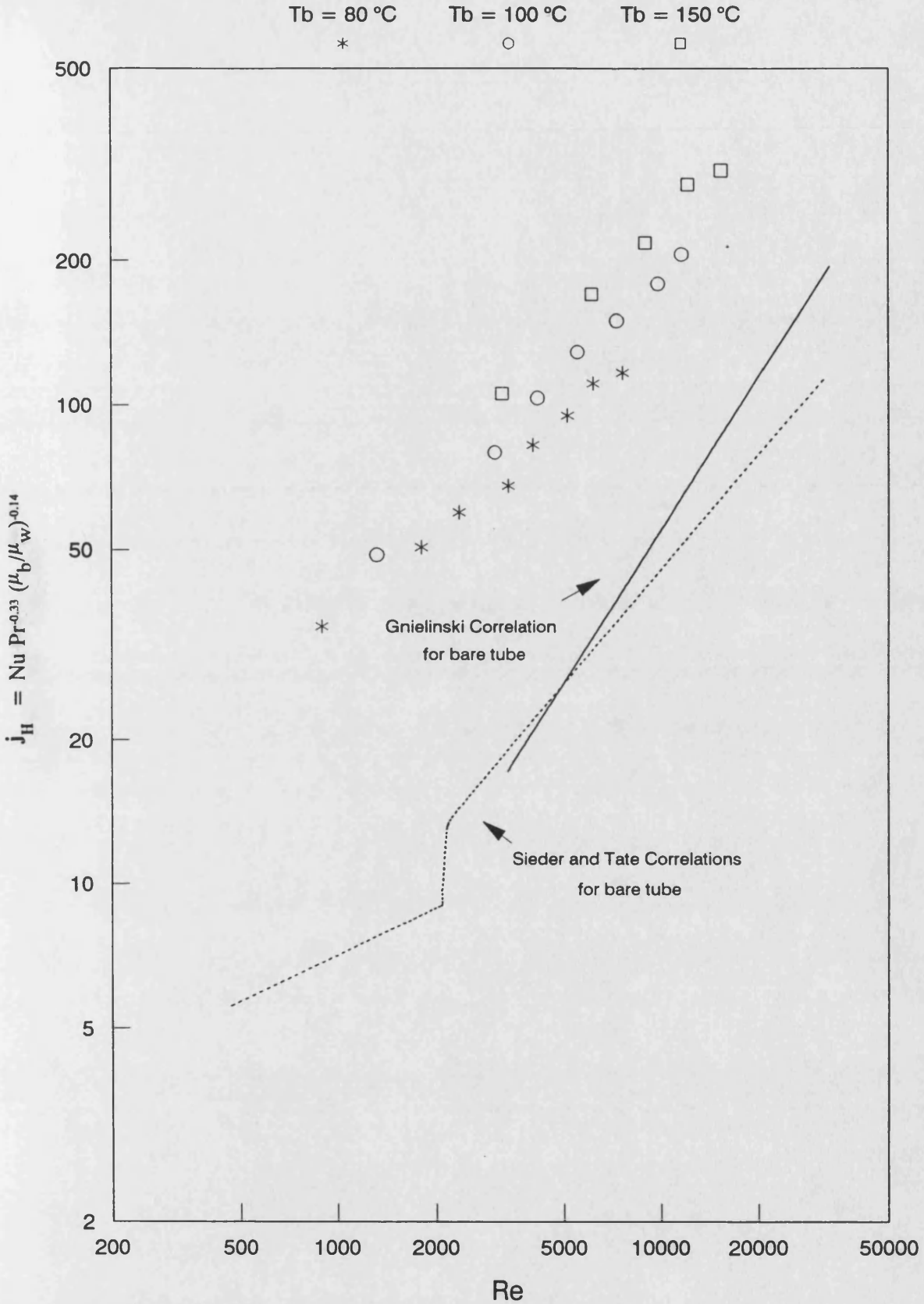

Fig (3.73) Heat transfer factor (j_H) vs Reynolds number (Re)

Santotherm 55 for tube fitted with HDI-A at q = 12 kW/m²

(80 °C < Tb < 150 °C and 30 < Pr < 178)

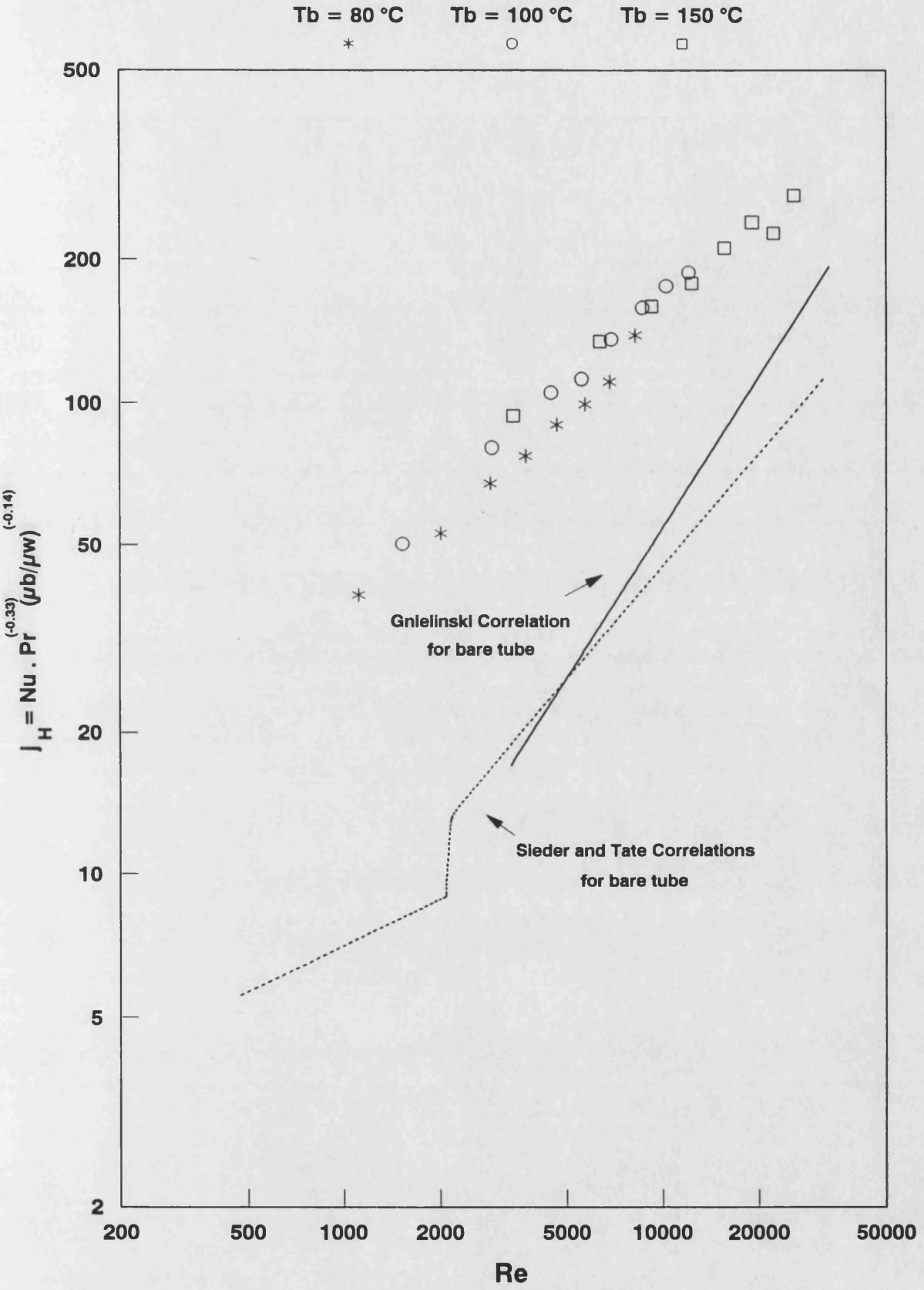

Fig (3.74) Heat transfer factor (j_H) vs Reynolds number (Re)

Santotherm 55 for tube fitted with HDI-A at q = 24 kW/m²

(80 °C < Tb < 150 °C and 30 < Pr < 178)

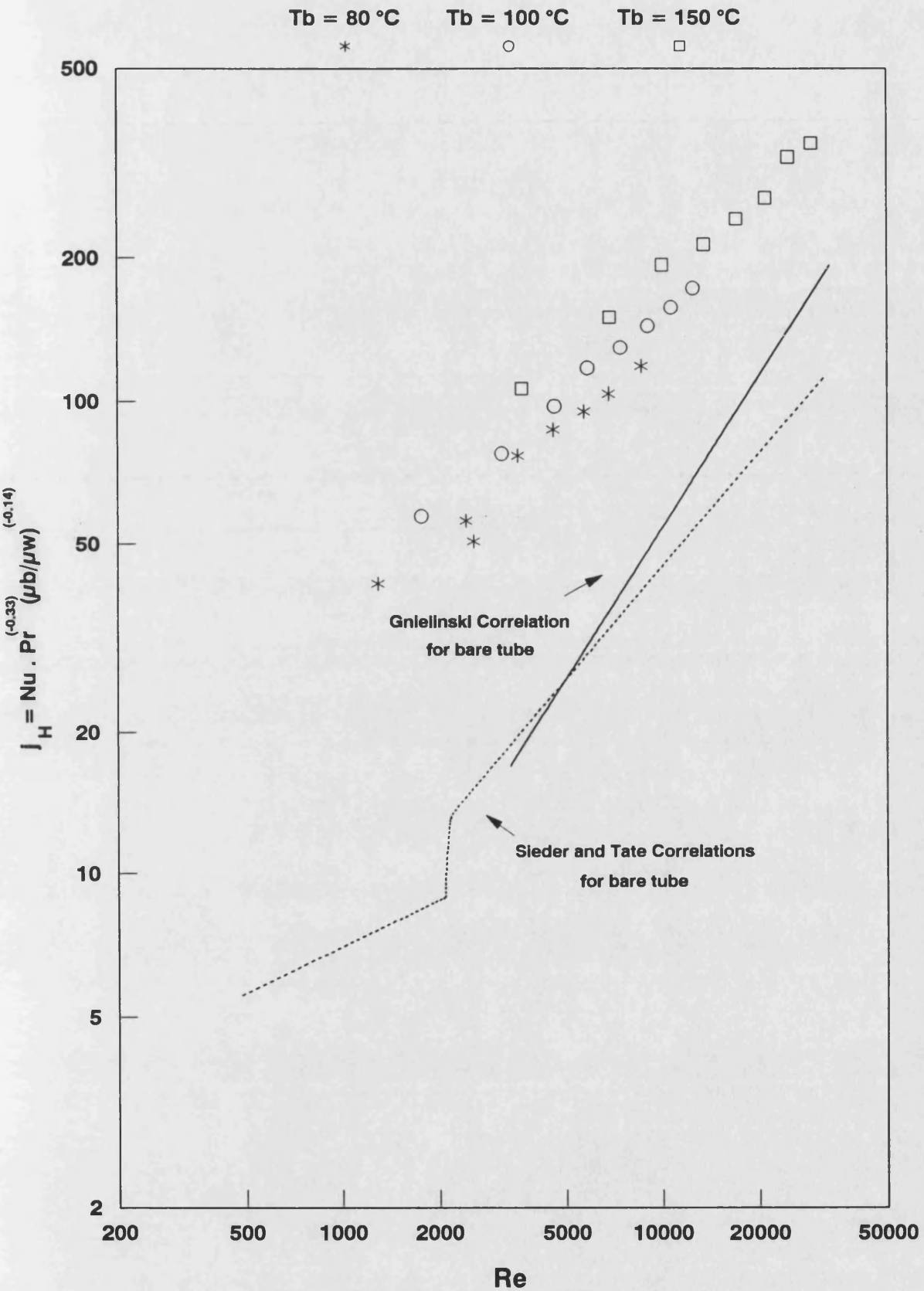

Fig (3.75) Heat transfer factor (j_H) vs Reynolds number (Re)

Santotherm 55 for tube fitted with HDI-A at q = 36.1 kW/m²

(80 °C < Tb < 150 °C and 30 < Pr < 178)

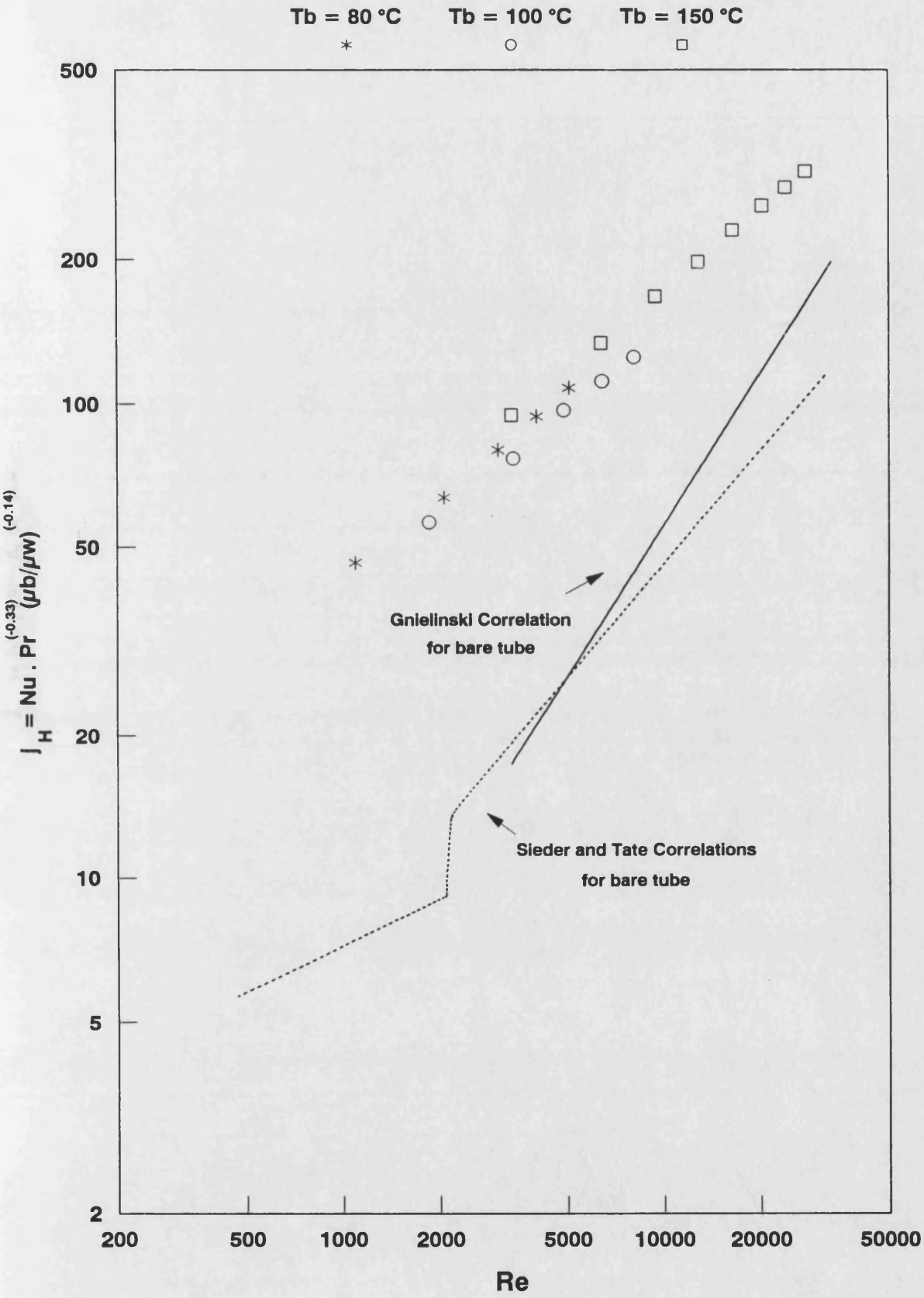

Fig (3.76) Heat transfer factor (j_H) vs Reynolds number (Re)

Santotherm 55 for tube fitted with HDI-A at q = 48.2 kW/m²
(80 °C < Tb < 150 °C and 30 < Pr < 178)

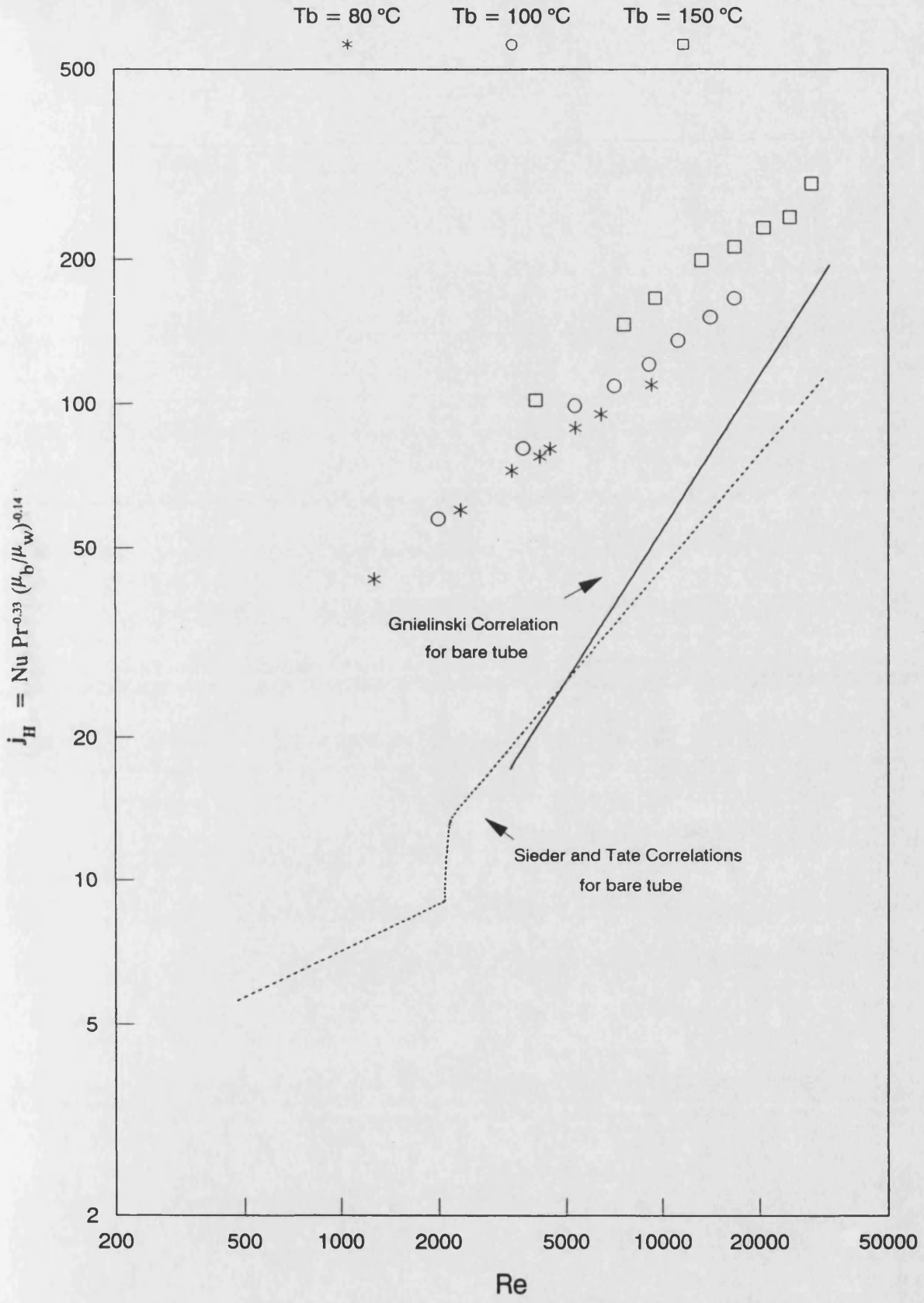

Fig (3.77) Heat transfer factor (j_H) vs Reynolds number (Re)

Santotherm 55 for tube fitted with HDI-A at q = 60.2 kW/m²

(80 °C < Tb < 150 °C and 30 < Pr < 178)

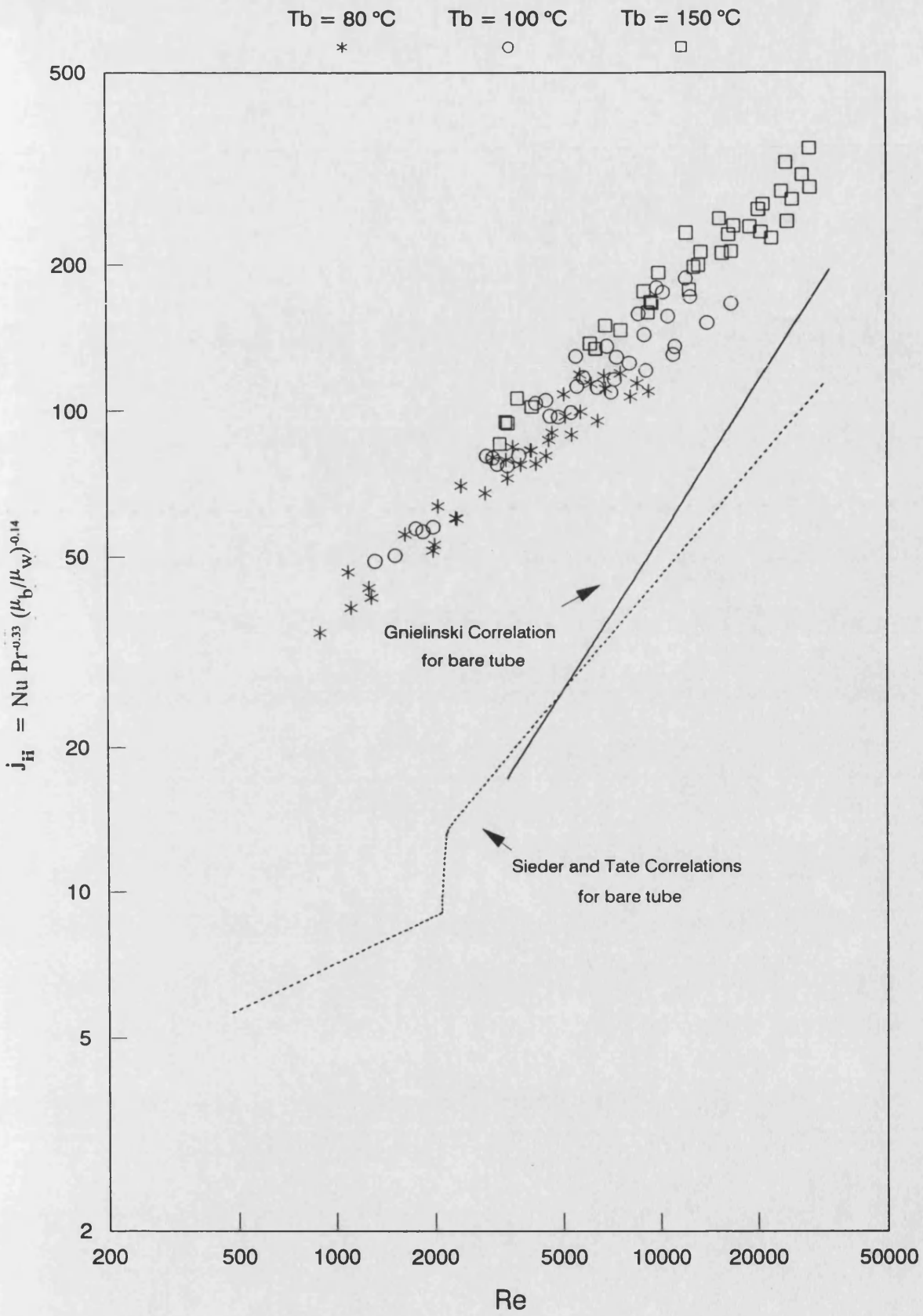

Fig (3.78) Heat transfer factor (j_H) vs Reynolds number (Re)

Santotherm 55 for tube fitted with HDI-A at 12 kW/m² < q < 60.2 kW/m²

(80 °C < Tb < 150 °C and 30 < Pr < 178)

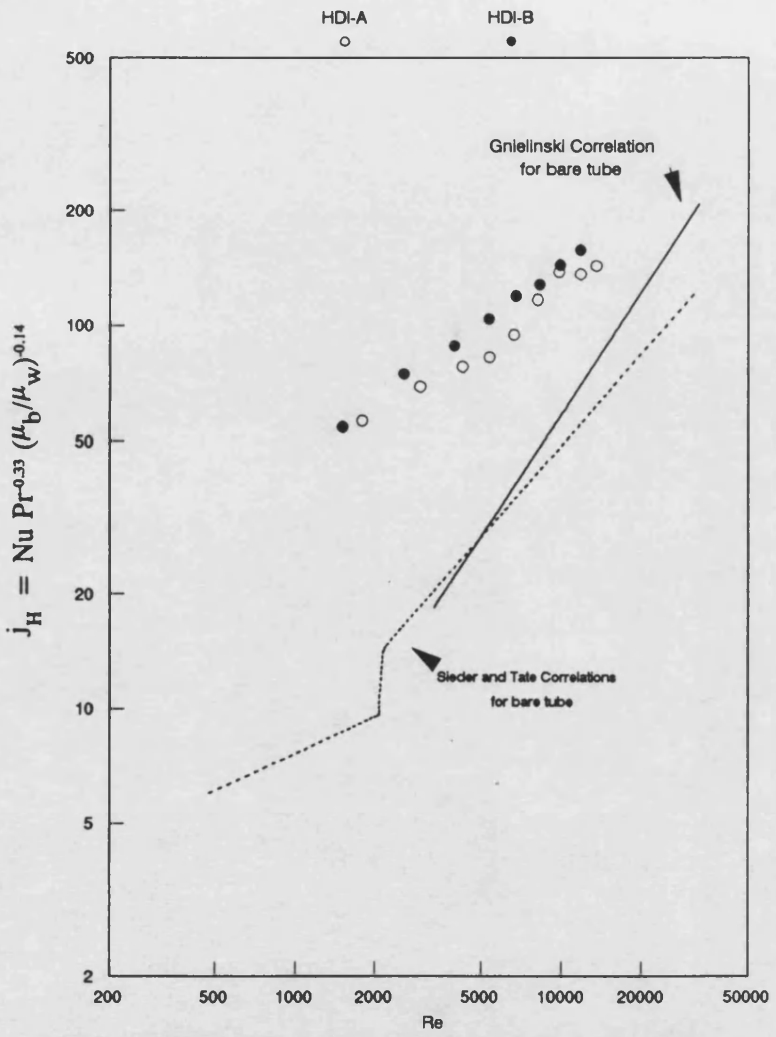

Fig (3.79) Heat transfer factor (j_H) vs Reynolds number (Re)

Comparsion between inserts HDI-A and HDI-B fitted into test section NO(1)
Santotherm 55 at q = 24 kW/m² ; Tb = 100 °C and 60 < Pr < 80

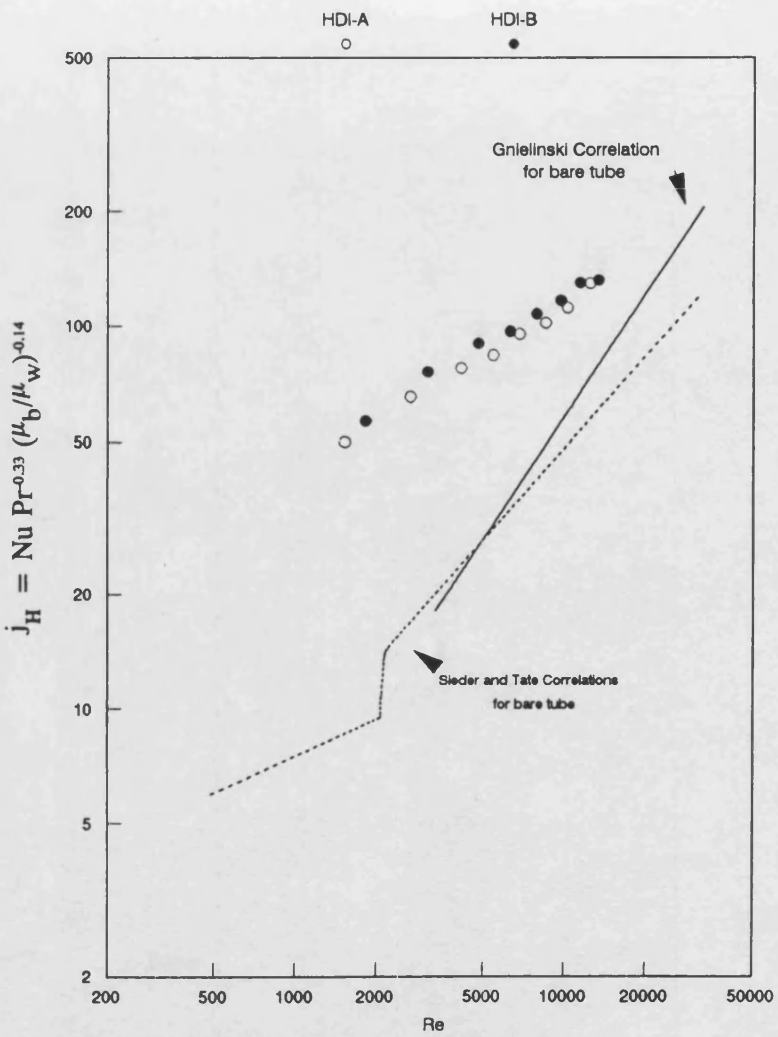

Fig (3.80) Heat transfer factor (j_H) vs Reynolds number (Re)

Comparsion between inserts HDI-A and HDI-B fitted into test section NO(1)
Santotherm 55 at q = 48.2 kW/m² ; Tb = 100 °C and 60 < Pr < 80

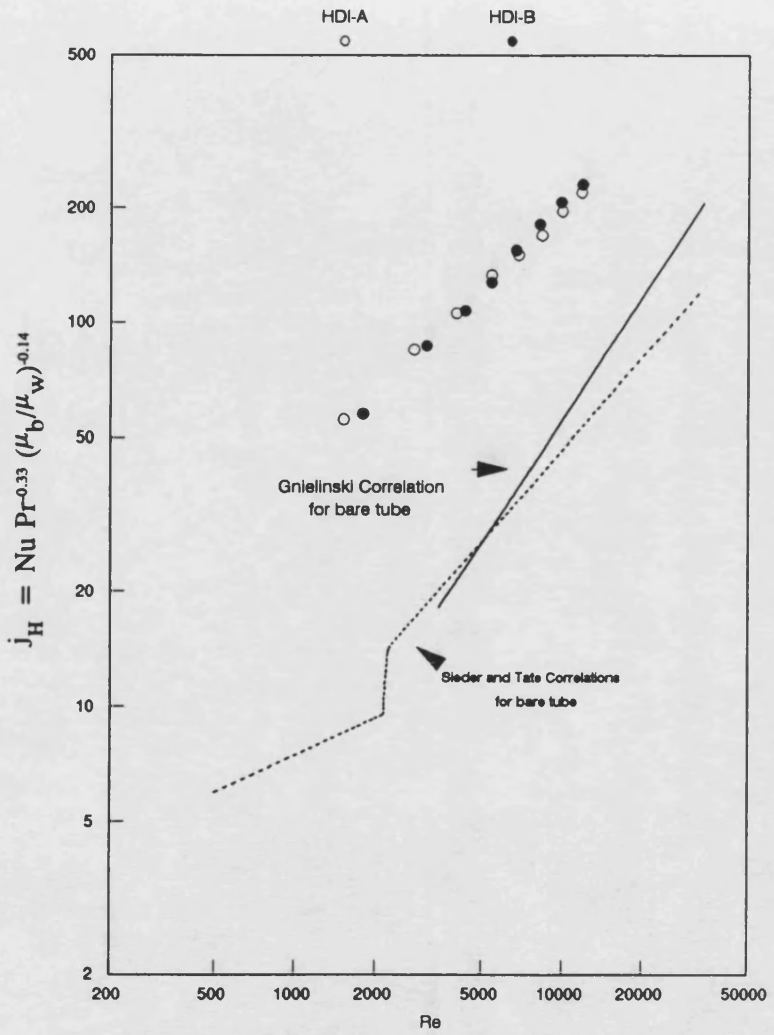

Fig (3.81) Heat transfer factor (j_H) vs Reynolds number (Re)

Comparsion between inserts HDI-A and HDI-B fitted into test section NO(2)
Santotherm 55 at q = 24 kW/m² ; Tb = 100 °C and 60 < Pr < 80

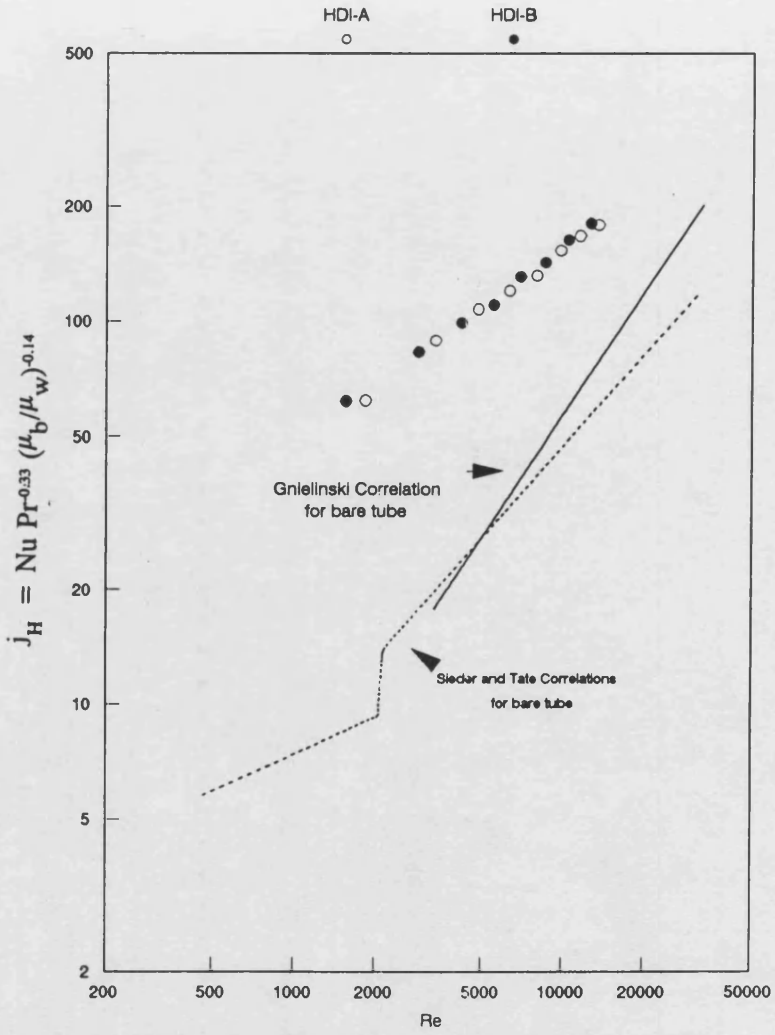

Fig (3.82) Heat transfer factor (j_H) vs Reynolds number (Re)

Comparsion between inserts HDI-A and HDI-B fitted into test section NO(2)
Santotherm 55 at q = 46.2 kW/m² ; Tb = 100 °C and 60 < Pr < 80

However, it is useful to mention that HDI-B was used for the first time in test section No (1), shown in Figs 3.79 and 3.80, then re-used in test section NO (2), Figs 3.81 and 3.82 , while the insert HDI-A had already been used several times before this comparison was made . The effect of re-using the same insert is discussed in the following section (3.5.2.3.2-IV).

IV- Effect of re-using the same HiTran insert

In order to demonstrate the effect of re-using the same HiTran insert , MDI-A was fitted into test section No (2) and tested at T_b = 100 °C with q = 24, and 48.16 kW/m^2 . MDI-A was then removed from the test section and re-fitted back in the same test section and then re-tested under similar conditions. The results of these two runs are shown in Figs 3.83 and 3.84 . The results of these two runs showed little difference. However, it should be noted that this insert (MDI-A) had already been used several times before these comparative experiments took place. A similar procedure was applied to MDI-B in test section No (1). The results of the two runs are shown in Figs 3.85 and 3.86 . In this case the j_H for insert MDI-B was higher by 15 to 20% in the first run. Moreover, MDI-B had only been used once prior to this experiment.

These experiments give clear evidence that the re-use of a HiTran insert can cause it to lose some

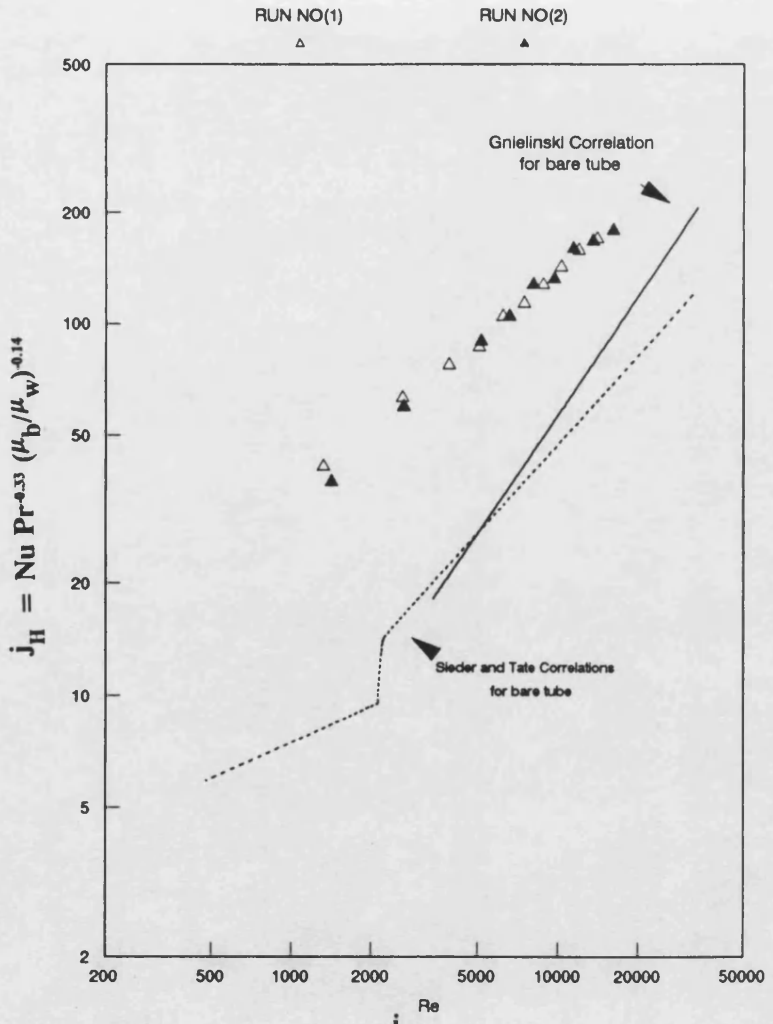

Fig (3.83) Heat transfer factor (j_H) vs Reynolds number (Re)
Effect of re-using MDI-A inside test section NO(2)
Santotherm 55 at q = 24 kW/m² ; Tb = 100 °C and 60 < Pr < 80

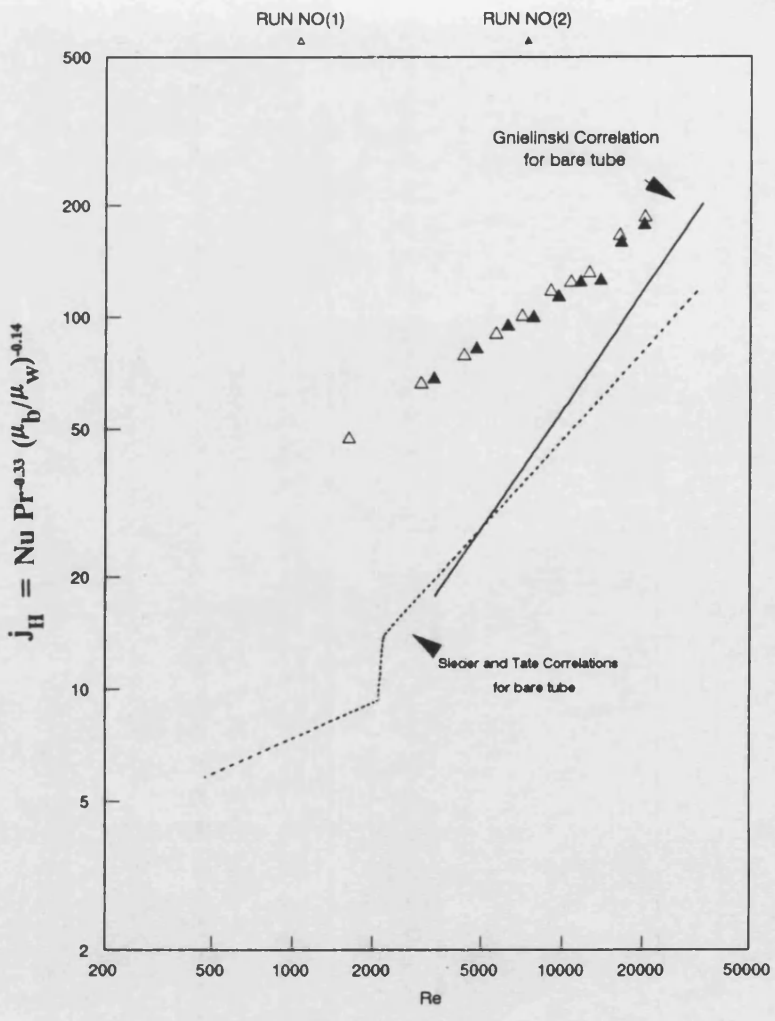

Fig (3.84) Heat transfer factor (j_H) vs Reynolds number (Re)
Effect of re-using MDI-A inside test section NO(2)
Santotherm 55 at q = 48.2 kW/m² ; Tb = 100 °C and 60 < Pr < 80

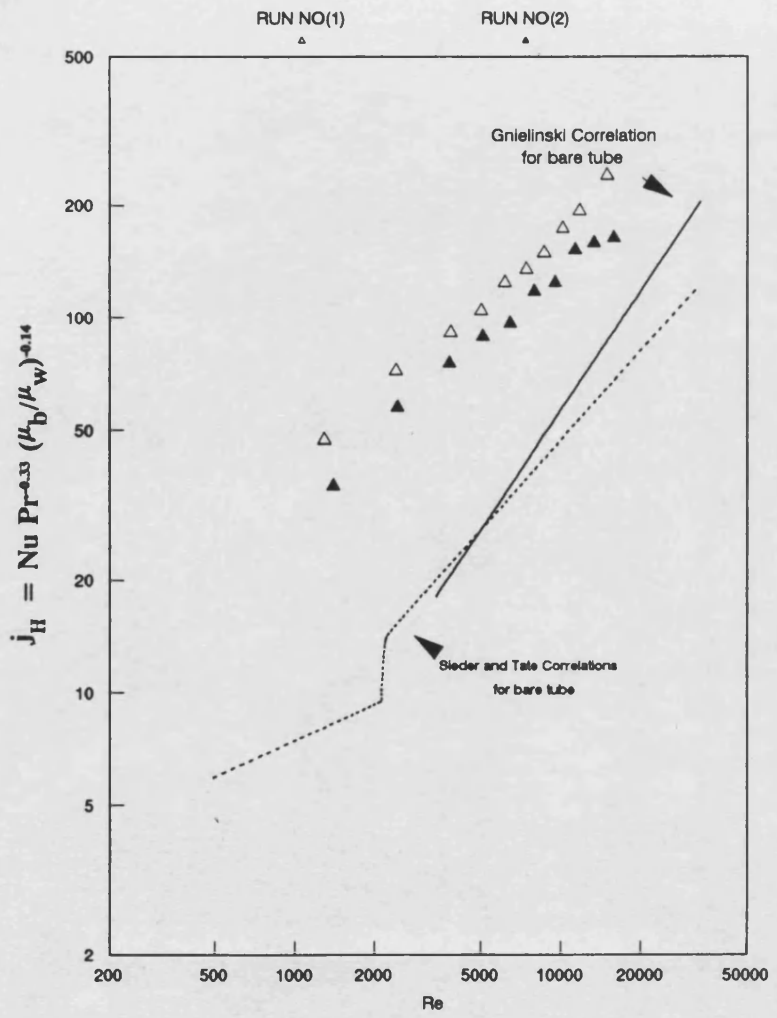

Fig (3.85) Heat transfer factor (j_H) vs Reynolds number (Re)
Effect of re-using MDI-B inside test section NO(1)
Santotherm 55 at q = 24 kW/m² ; Tb = 100 °C and 60 < Pr < 80

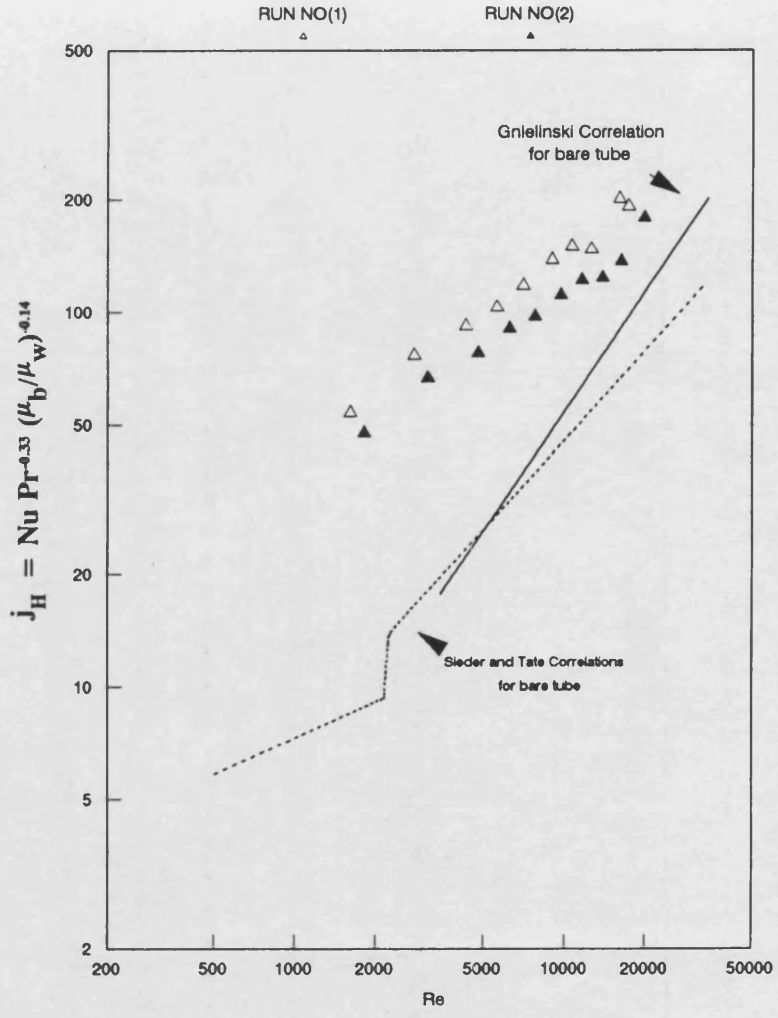

Fig (3.86) Heat transfer factor (j_H) vs Reynolds number (Re)
Effect of re-using MDI-B inside test section NO(1)
Santotherm 55 at q = 48.2 kW/m² ; Tb = 100 °C and 60 < Pr < 80

of it's heat transfer performance. However, a further decrease in performance is likely to disappear after several insertions. A reduction of 20% in j_H could perhaps be expected if a Hitran insert is re-used three times.

V- Effect of rotating a HiTran insert inside the test section

The effect of rotating a HiTran insert inside a test section was studied, but not to any great depth. Insert MDI-A was fitted into test section No(2) and then tested at T_b = 100 °C for q = 24, and 48.16 kW/m^2. The insert was then rotated 90° anti-clockwise and re-tested under identical operating conditions. The results are shown in Figs 3.87 and 3.88 . A large difference between the two runs is seen for both heat fluxes. This difference in performance increases as the Re is increased .

It was not the aim of this study to test the effect of rotation of HiTran inserts on j_H . However, an indepth investigation is needed in order to gain a better understanding of this phenomenon.

VI- Comparing the experimental data with Oliver - Aldington correlation

All the heat transfer experimental data in this study for tubes fitted with HiTran inserts (LDI , MDI and HDI) with Santotherm 55 fluid were compared with the Oliver and Aldington[23] correlation for a

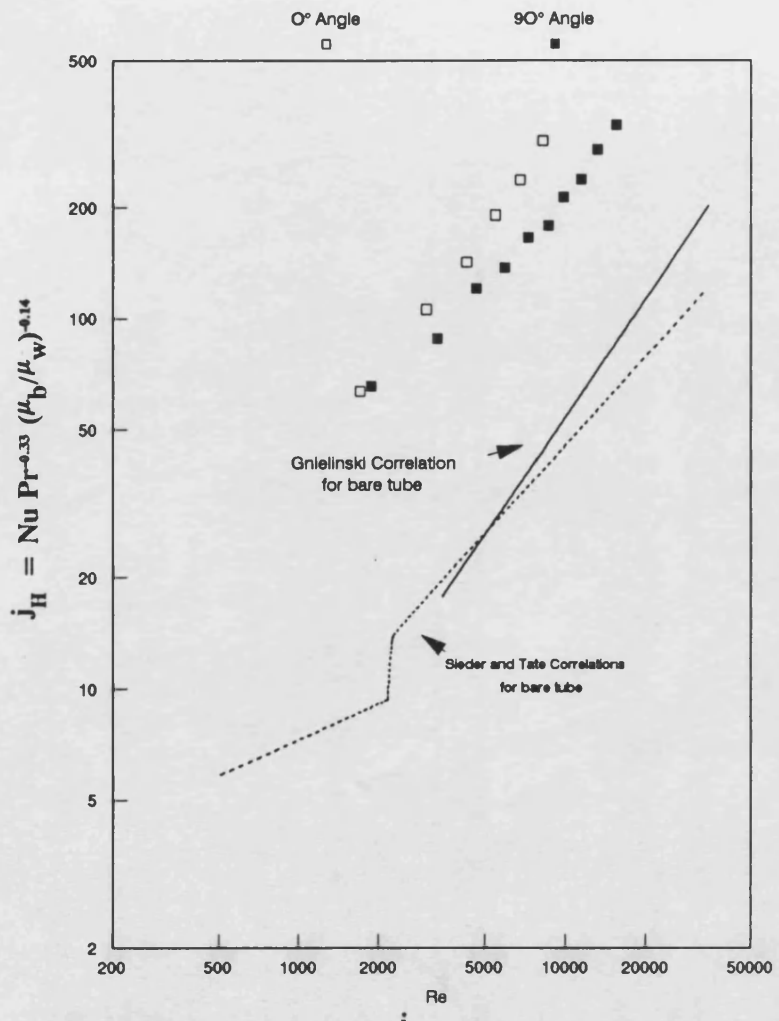

Fig (3.87) Heat transfer factor (j_H) vs Reynolds number (Re)
Effect of rotating of MDI-A inside test section NO(2)
Santotherm 55 at q = 24 kW/m² ; Tb = 100 °C and 60 < Pr < 80

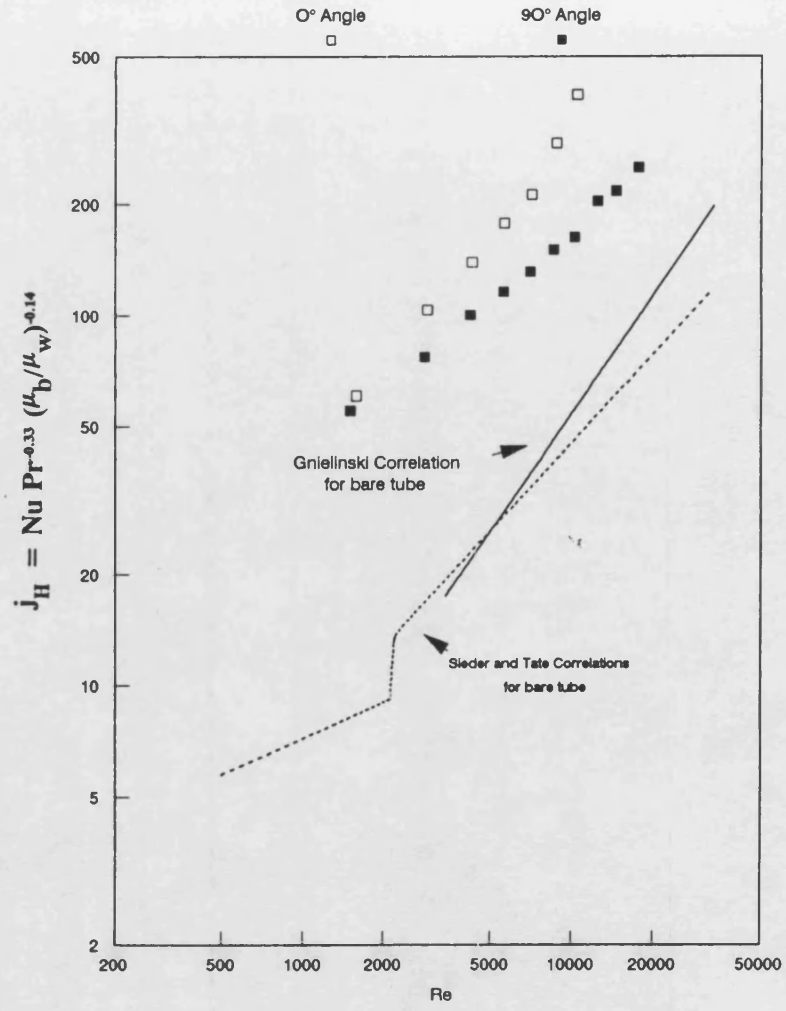

Fig (3.88) Heat transfer factor (j_H) vs Reynolds number (Re)
Effect of rotating of MDI-A inside test section NO(2)
Santotherm 55 at q = 48.2 kW/m² ; Tb = 100 °C and 60 < Pr < 80

tube fitted with an MDI insert with glycerol/water mixtures (equation 3.113) , in Fig 3.89 .

$$Nu = 0.232\, Re^{0.54} Pr^{0.46} \qquad (3.113)$$

There are no experimental data for Re < 500 . However , for Re equal to 600 and 1000 , equation 3.113 predicts values of Nu which are 10% and 15% respectively lower than those found experimentally in the present study . The accuracy of the Oliver and Aldington[23] correlation was not mentioned . It is important to re-state that equation 3.113 is only valid for 5 < Re < 1600 and 40 < Pr < 550 for glycerol/water mixtures in which the particular insert was tested . The Oliver and Aldington correlation may well be unsuitable for higher Re or fluids other than the glycerol/water mixtures. Furthermore, an empirical correlation in the specific form of equation 3.113 would probably fit all the experimental data in this study with a scatter of more than ±100% . Therefore a new form of correlation is derived in the following section (3.5.2.4) .

3.5.2.4 Modified heat transfer factor (j_{HM})

As the heat transfer factor (j_H), was found to be a relatively unsuccessful method for correlating the experimental results, a modified heat transfer factor (j_{HM}) was introduced as follows:

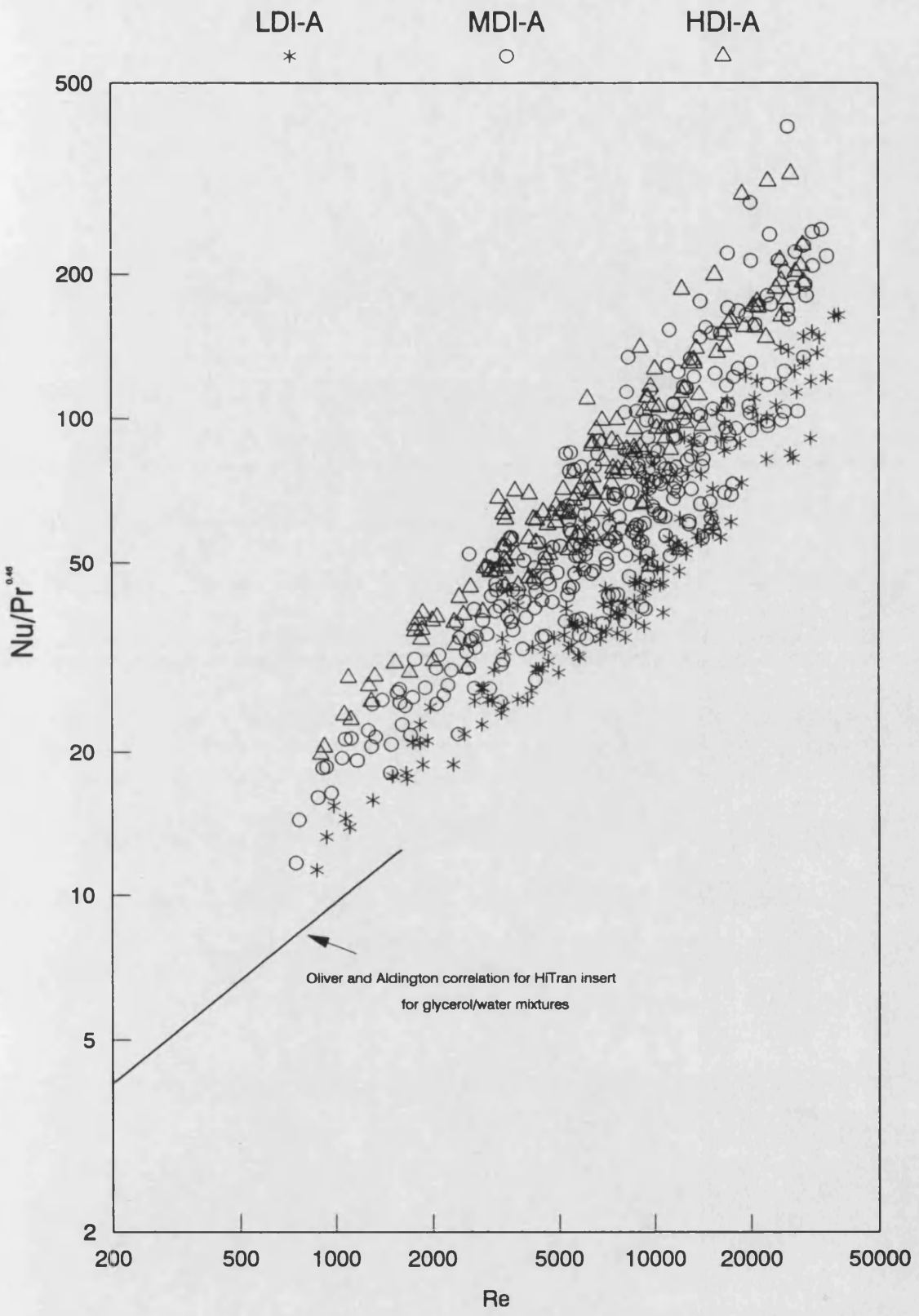

Fig (3.89) Comparing the experimental data with the Oliver and Aldington correlation
Santotherm 55 fluid for a tube fitted with different types of HiTran insert
80 °C < Tb < 150 °C and 30 < Pr < 150

$$j_{HM} = Nu\ [\ Pr\ f\ (\mu_b/\mu_w)\ ]^{0.14} \qquad (3.114)$$

By using the j_{HM}-factor, the bare tube as well as the **HiTran** insert results could be correlated as shown in Figs 3.90 to 3.93.

It is well recognised that the surface roughness can provide a remarkable increase in the film heat transfer coefficient[38]. Consequently, it is perhaps not surprising to find that j_{HM} , which contains the friction factor, can be used successfully to correlate the bare tube heat transfer experimental data for the ranges of $550 < Re < 34000$ and $30 < Pr < 187$ with an overall accuracy of ± 10% .

Fig 3.90 shows the j_{HM}-factor, which is calculated from equation 3.114 , for the bare tube test sections. The following correlation was found to fit the experimental data to within ± 10% :

$$j_{HM\,(bare)} = 0.7\ Re^{0.61} \qquad (3.115)$$

or,

$$Nu_{(bare)} = \frac{0.7\ Re^{0.61}}{[\ Pr\ f\ (\mu_b/\mu_w)\ ]^{0.14}} \qquad (3.116)$$

where, f is experimental friction factor of the bare tube. Clearly to be able to use this correlation for design purposes the friction factor must be known. For fully developed turbulent flow ($Re > 10^4$) equation 3.101 can be used with confidence .

Fig 3.90 also shows that the modified heat transfer factor (j_{HM}) is suitable for all ranges of

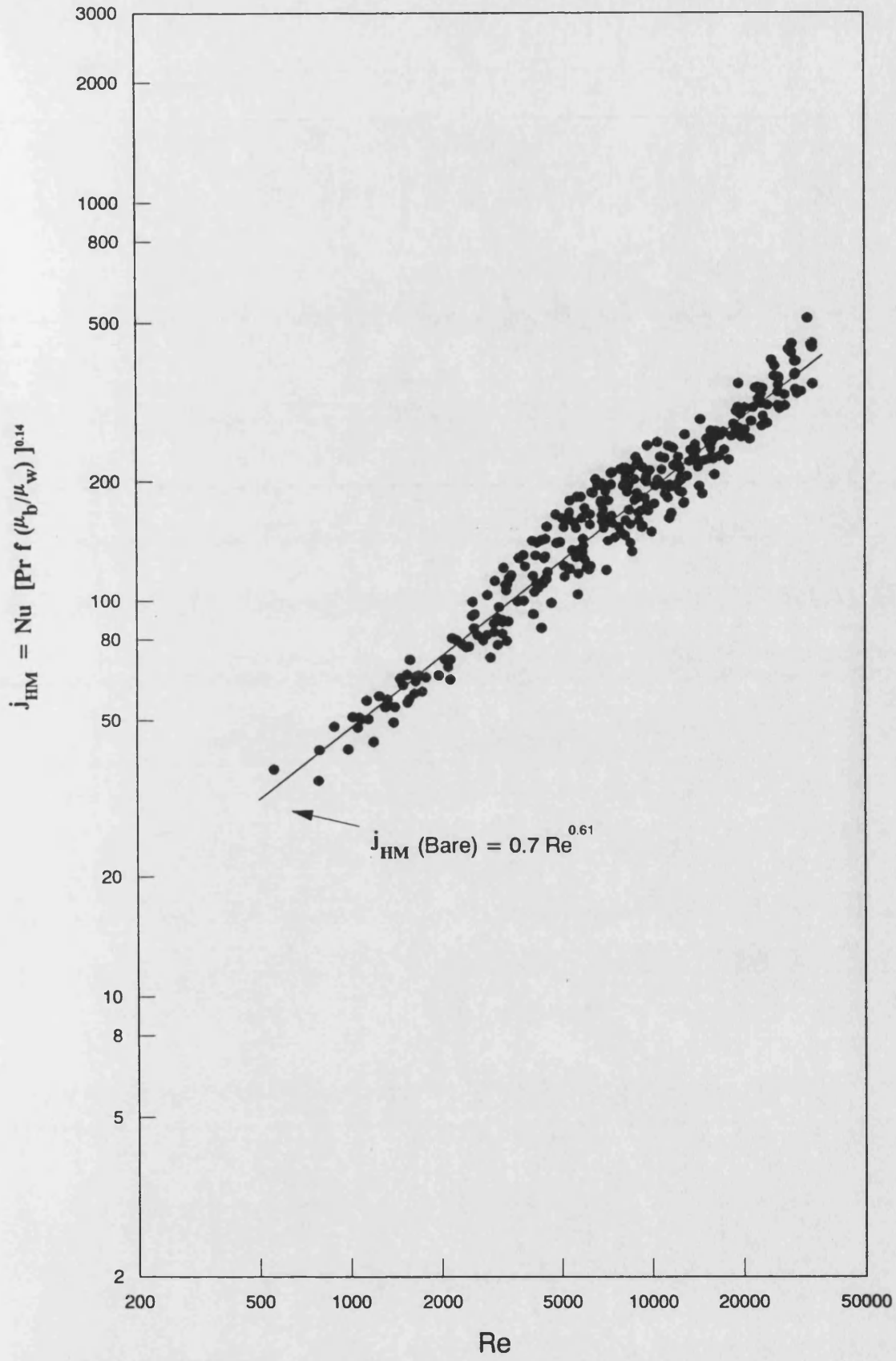

Fig (3.90) Modified Heat transfer factor (j_{HM}) vs Reynolds number (Re)

Santotherm 55 for bare tube ; 80 °C < Tb < 150 °C ; 30 < Pr < 187

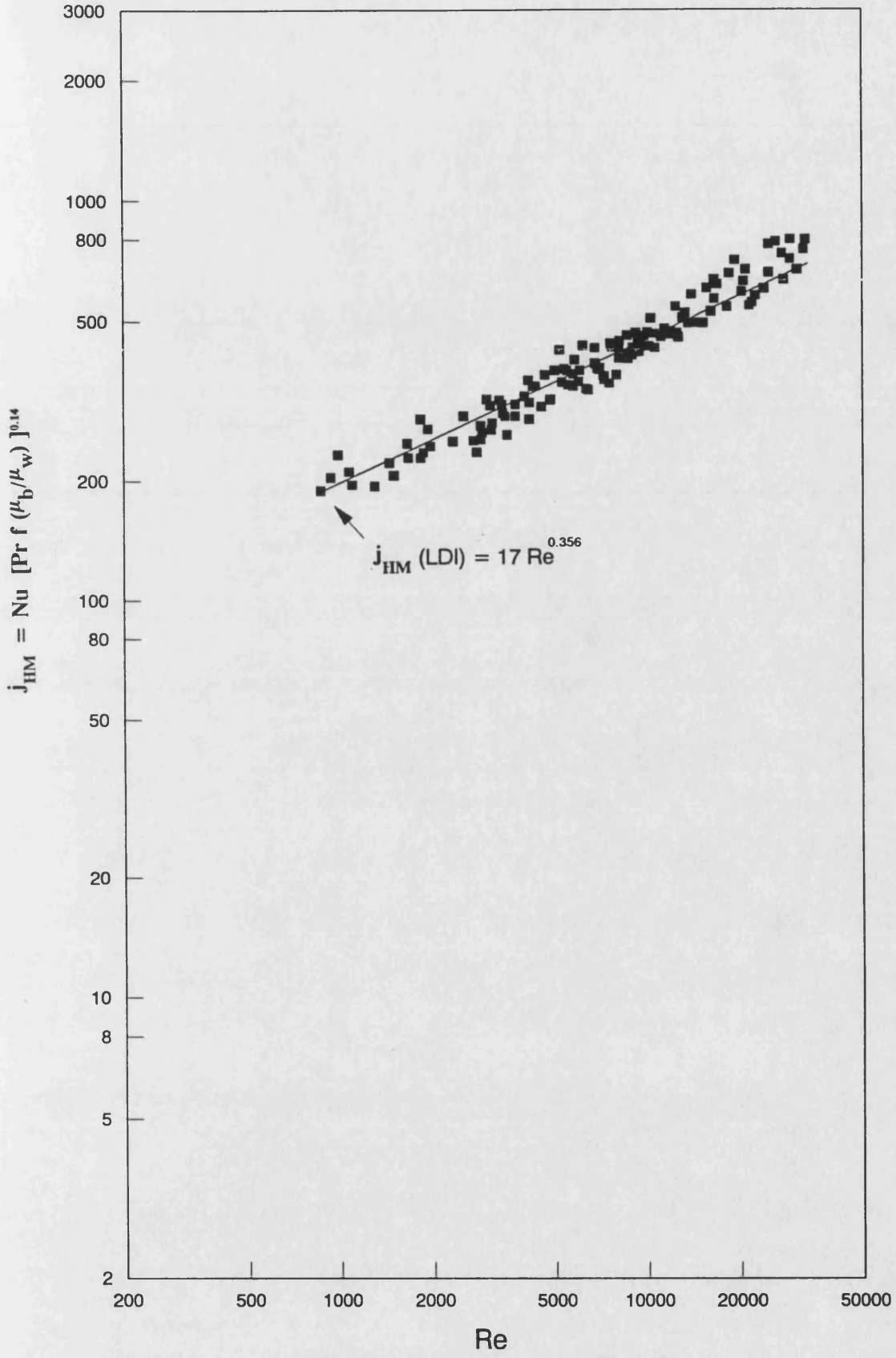

Fig (3.91) Modified Heat transfer factor (j_{HM}) vs Reynolds number (Re)

Santotherm 55 for tube fitted with LDI ; 80 °C < Tb < 150 °C ; 30 < Pr < 187

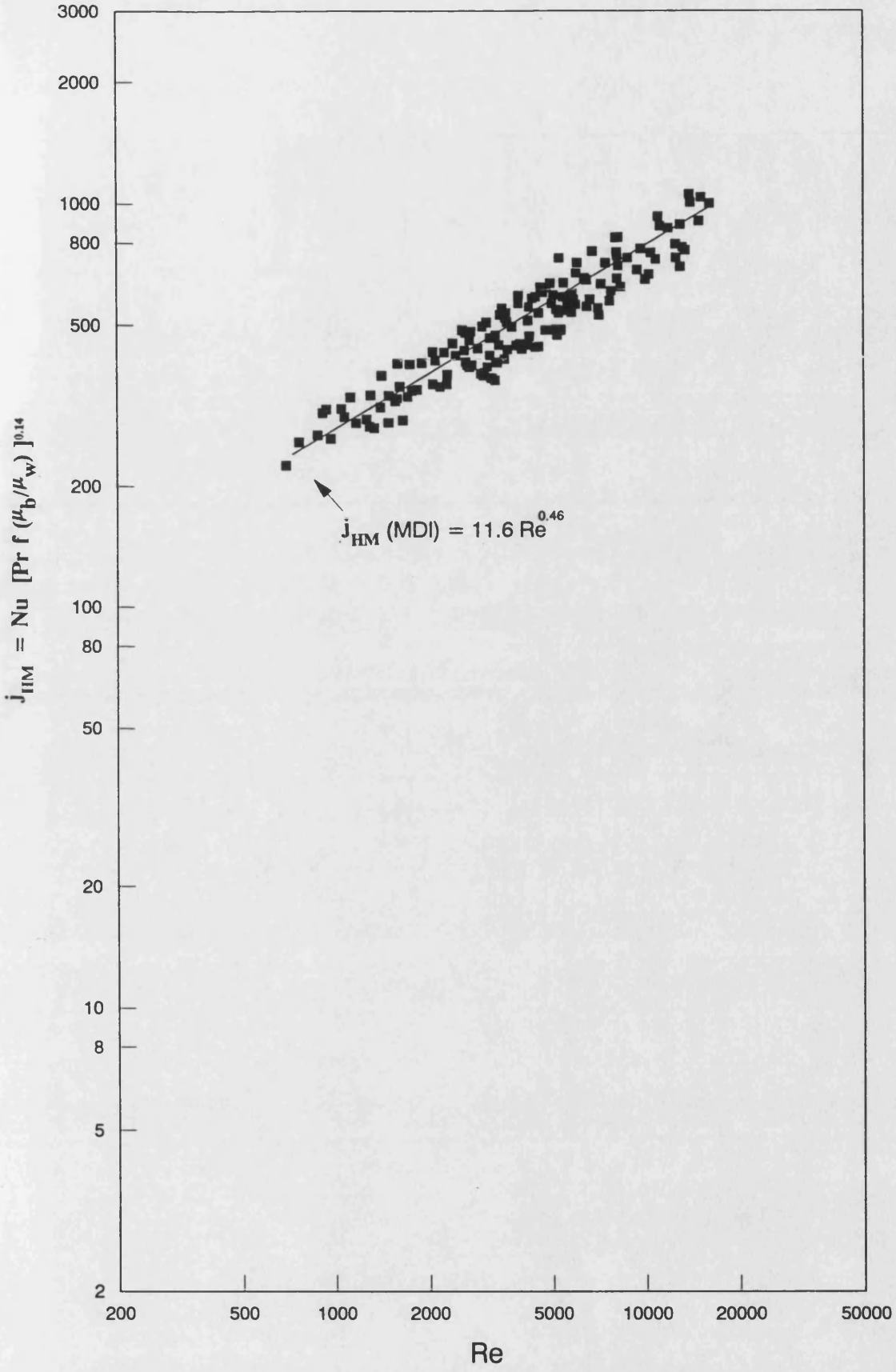

Fig (3.92) Modified Heat transfer factor (j_{HM}) vs Reynolds number (Re)

Santotherm 55 for tube fitted with MDI ; 80 °C < Tb < 150 °C ; 30 < Pr < 187

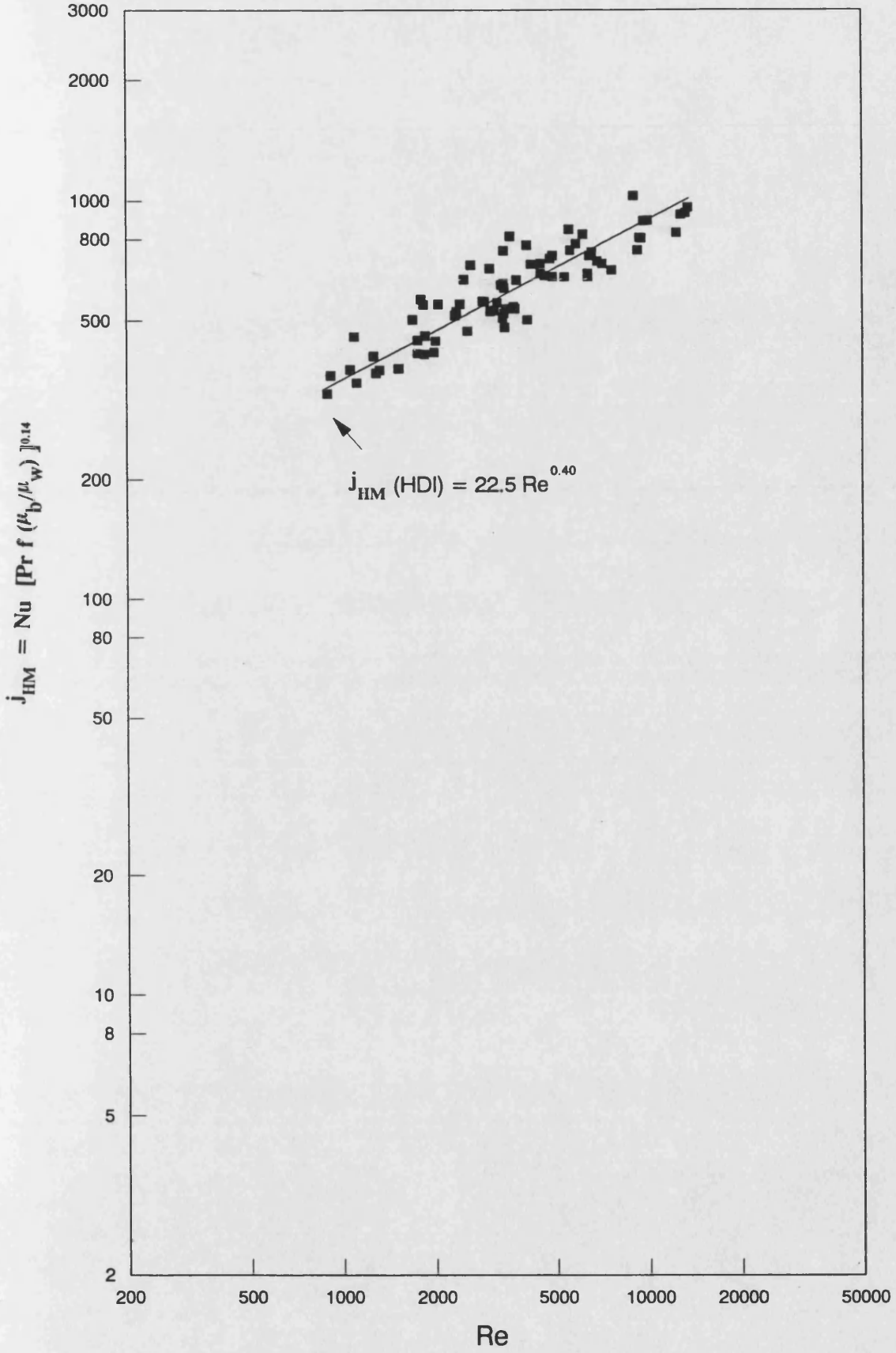

Fig (3.93) Modified Heat transfer factor (j_{HM}) vs Reynolds number (Re)

Santotherm 55 for tube fitted with HDI ; 80 °C < Tb < 150 °C ; 30 < Pr < 187

Reynolds number (Re) without distinguishing between laminar, transition and turbulent flow, as occurs in the Sieder and Tate j_H-factor. Moreover, this new correlation may be unaffected by the state of flow development, i.e it may be suitable for both developed and developing flows. However, different L/D ratios and also different fluids have to be studied in order to generate a comprehensive universal correlation for a bare tube.

Fig. 3.91 shows the results of j_{HM} for tubes fitted with LDI (for both LDI-A and LDI-B). The following correlation was found to correlate the experimental data to within ± 7.1% :

$$j_{HM\,(LDI)} = 17\,Re^{0.356} \qquad (3.117)$$

or,

$$Nu_{(LDI)} = \frac{17\,Re^{0.356}}{[\,Pr\,f\,(\mu_b/\mu_w)\,]^{0.14}} \qquad (3.118)$$

Fig 3.92 shows the results of MDI (both MDI-A and MDI-B) fitted in both test sections. The best correlation was found to be within ± 10% as follows,

$$j_{HM\,(MDI)} = 11.6\,Re^{0.46} \qquad (3.119)$$

or,

$$Nu_{(MDI)} = \frac{11.6\,Re^{0.46}}{[\,Pr\,.f\,(\mu_b/\mu_w)\,]^{0.14}} \qquad (3.120)$$

In Fig. 3.93 , j_{HM} results for HDI (both HDI-A and HDI-B) fitted in both test sections are shown. The following correlation fits all data within ± 6.2% :

$$j_{HM\ (HDI)} = 22.5\ Re^{0.4} \qquad (3.121)$$

or,

$$Nu_{(HDI)} = \frac{22.5\ Re^{0.4}}{[Pr\ .f\ .(\mu_b/\mu_w)]^{0.14}} \qquad (3.122)$$

The friction factor (f) shown in equations 3.115 to 3.122 is the experimental friction factor . Alternatively, equations 3.101 to 3.107 may be used to predict the friction factor of the bare tube (in fully developed turbulent flow) and for the tube fitted with **HiTran** inserts .

Comparisons between the experimental Nu and Nu predicted from equations 3.116 , 3.118 , 3.120 and 3.122 for the bare tube and for the tube fitted with different types of HiTran insert are shown in Fig 3.94 .

Use of the j_{HM}-factor makes it possible to compare the bare tube directly with a tube fitted with different types of HiTran insert, as shown in Fig. 3.95.

Although the current correlations are only valid under the present experimental conditions it is important to mention that the tubular test sections used are identical to those used in actual shell and tube heat exchangers . Therefore , the current correlations could be used to design a heat

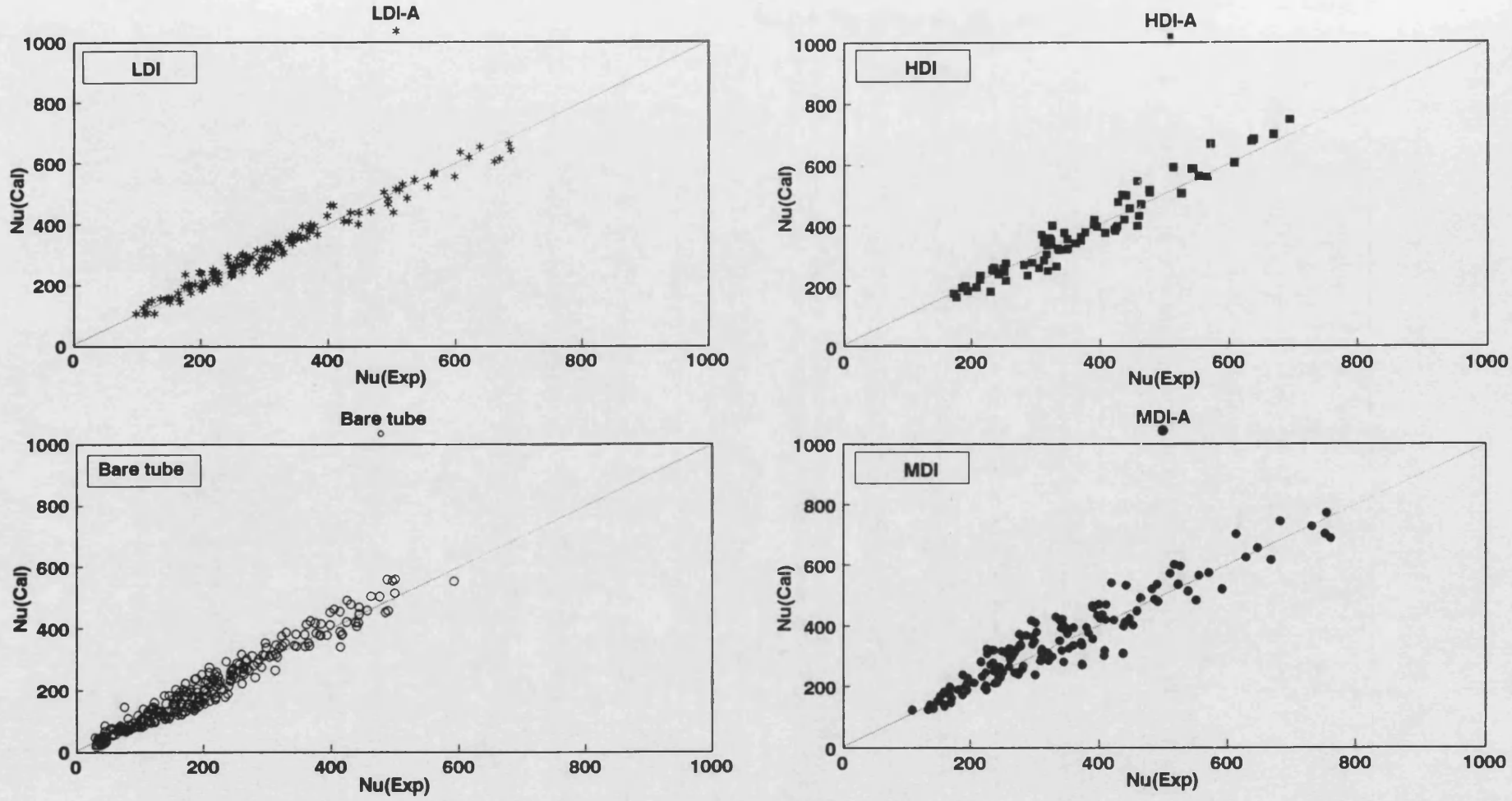

Fig (3.94) Comparsion between experimental and calculated Nusselt Number (Nu)

Santotherm 55 fluid for the bare tube and for tube fitted with different types of HITran insert

80 °C < Tb < 150 °C ; 30 < Pr < 187 and 550 < Re < 34000

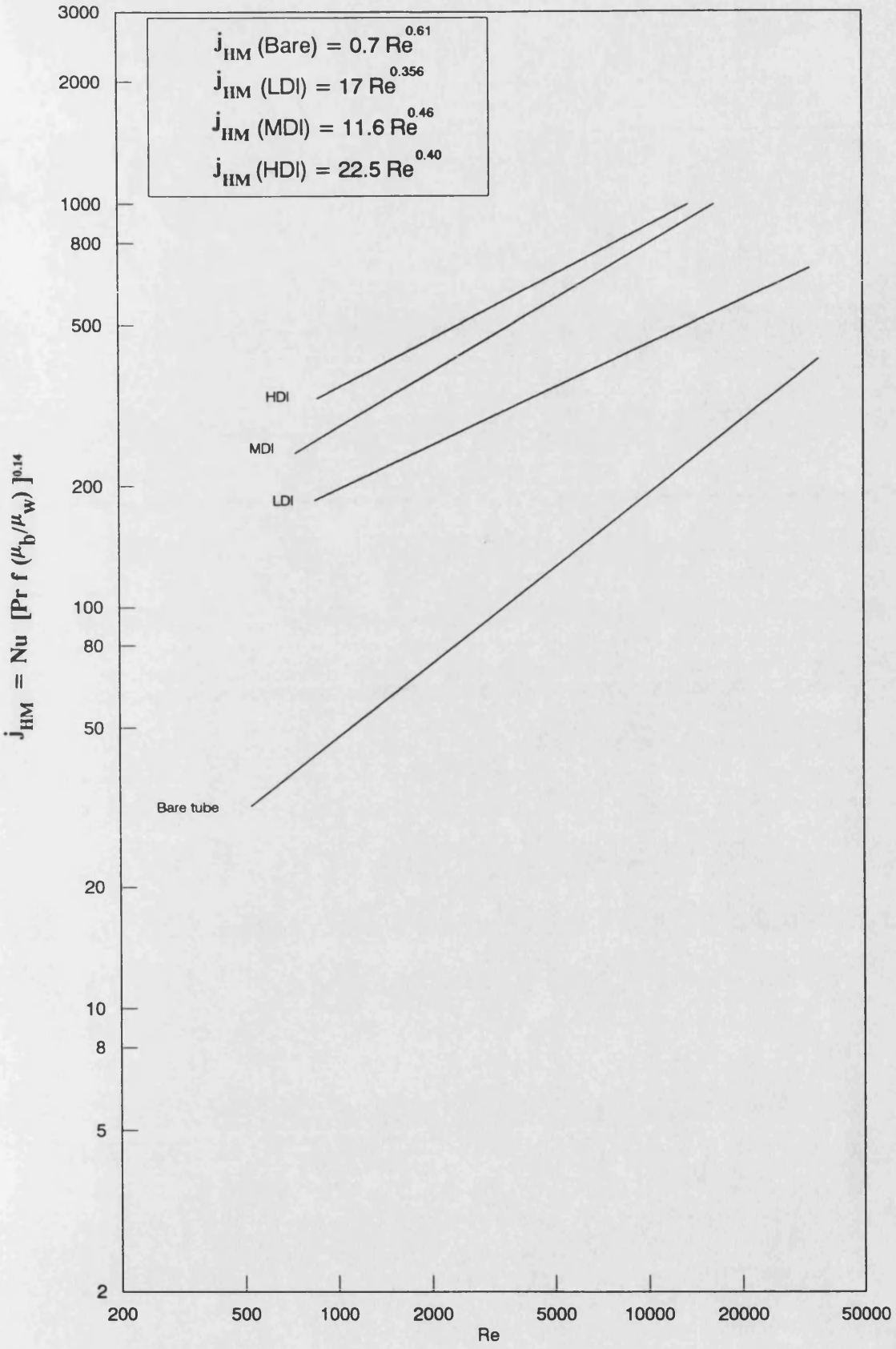

Fig (3.95) Modified Heat transfer factor (j_{HM}) vs Reynolds number (Re)

Comparison between bare tube and tube fitted with different types of HiTran insert

Santotherm 55 fluid ; 80 °C < Tb < 150 °C ; 30 < Pr < 187

exchanger in which the **HiTran** insert has been fitted inside the tubes .

3.5.2.5 Inner surface temperature (T_i) and temperature driving force (ΔT)

The inner surface temperature (T_i) and the temperature driving force ($\Delta T = T_i - T_b$), for the bare tube are compared with those for tubes fitted with different types of **HiTran** insert for 80 $^oC < T_b <$ 150 ^oC and q = 24 and 48.2 kW/m^2 in Figs. 3.96 to 3.101. The principal conclusions which may gained from these comparisons are summarised as follows :

1- It is expected from equation 1.13 ($T_i = T_b + \frac{q}{h_i}$) , that the use of a **HiTran** insert will provide a lower T_i and Δt for a given q , T_b and Re . This is seen to be specially true for Re < 10000 .

2- The effect of using a **HiTran** insert on T_i and Δt is similar to the effect of increasing the velocity in a bare tube . For example at T_b = 80 ^oC and q = 48.2 kW/m^2 , T_i of bare tube is equal to 110 ^oC at Re = 9000 . However , if a (LDI) **HiTran** insert is used under otherwise identical conditions then , T_i = 110 ^oC at Re = 1700 .

3- There is only a little difference between T_i of tubes fitted with LDI and HDI inserts . Thus if the aim is solely to get a low T_i

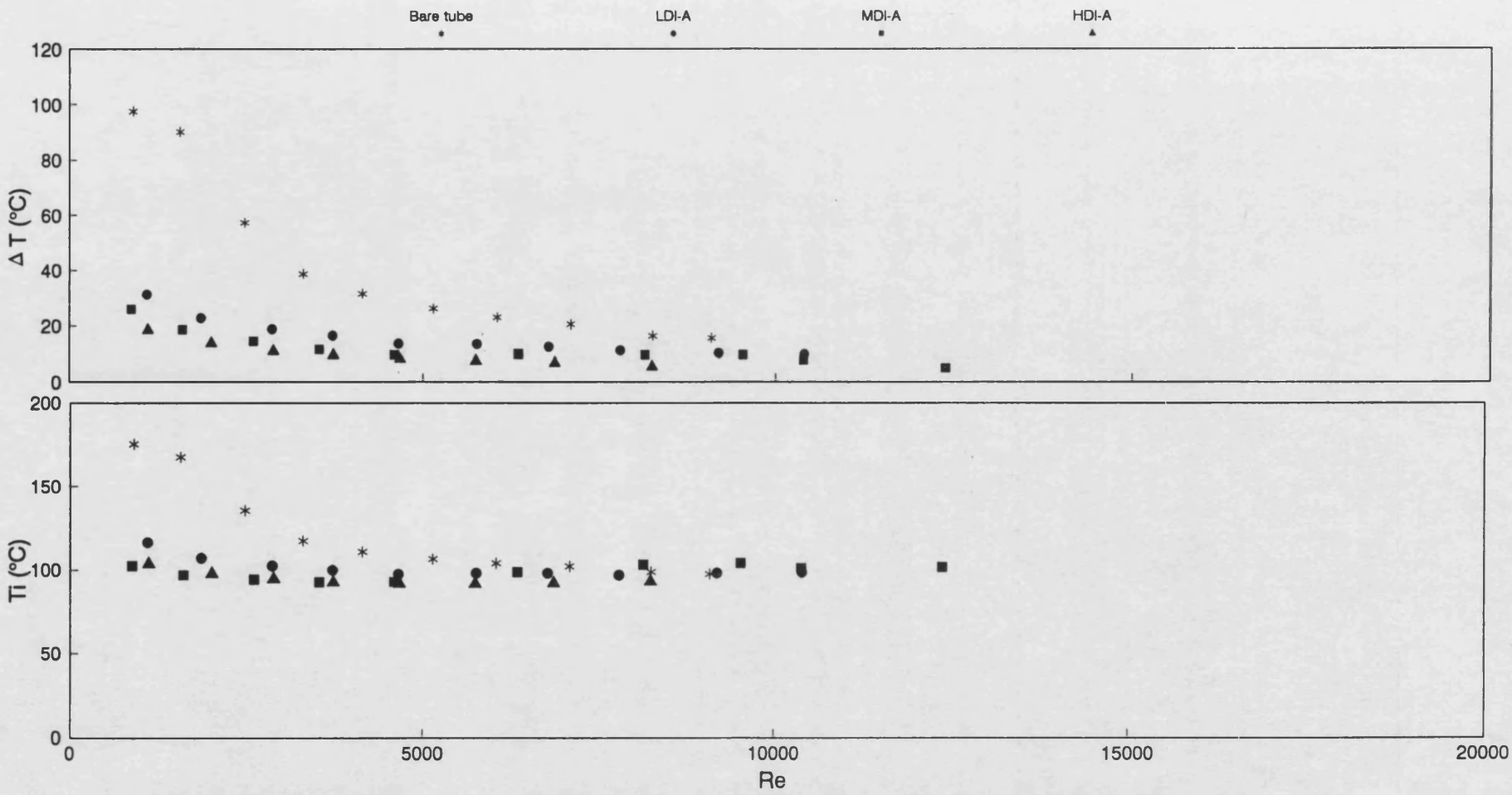

Fig (3.96) Inner surface temperature (Ti (°C)) and temperature driving force ΔT(°C) vs Reynolds number (Re)
Comparison between bare tube and a tube fitted with different HiTran inserts
Santotherm 55 fluid at Tb = 80 °C ; q = 24 kW/m² and 100 < Pr < 187

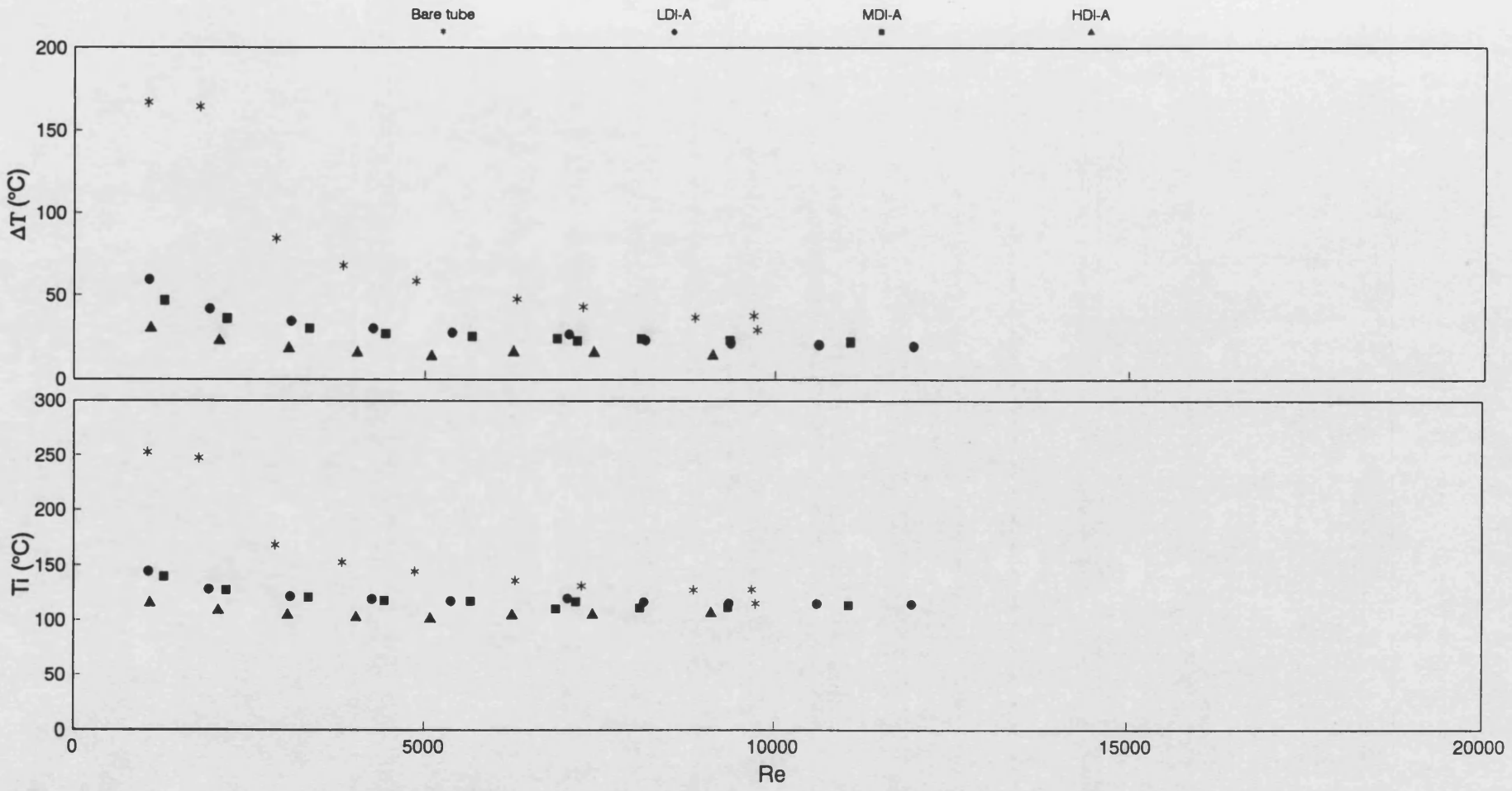

Fig (3.97) Inner surface temperature (Ti (°C)) and temperature driving force (ΔT(°C)) vs Reynolds number (Re)
Comparison between bare tube and a tube fitted with different types of HiTran insert
Santotherm 55 fluid at Tb = 80 °C ; q = 48.2 kW/m² and 100 < Pr < 187

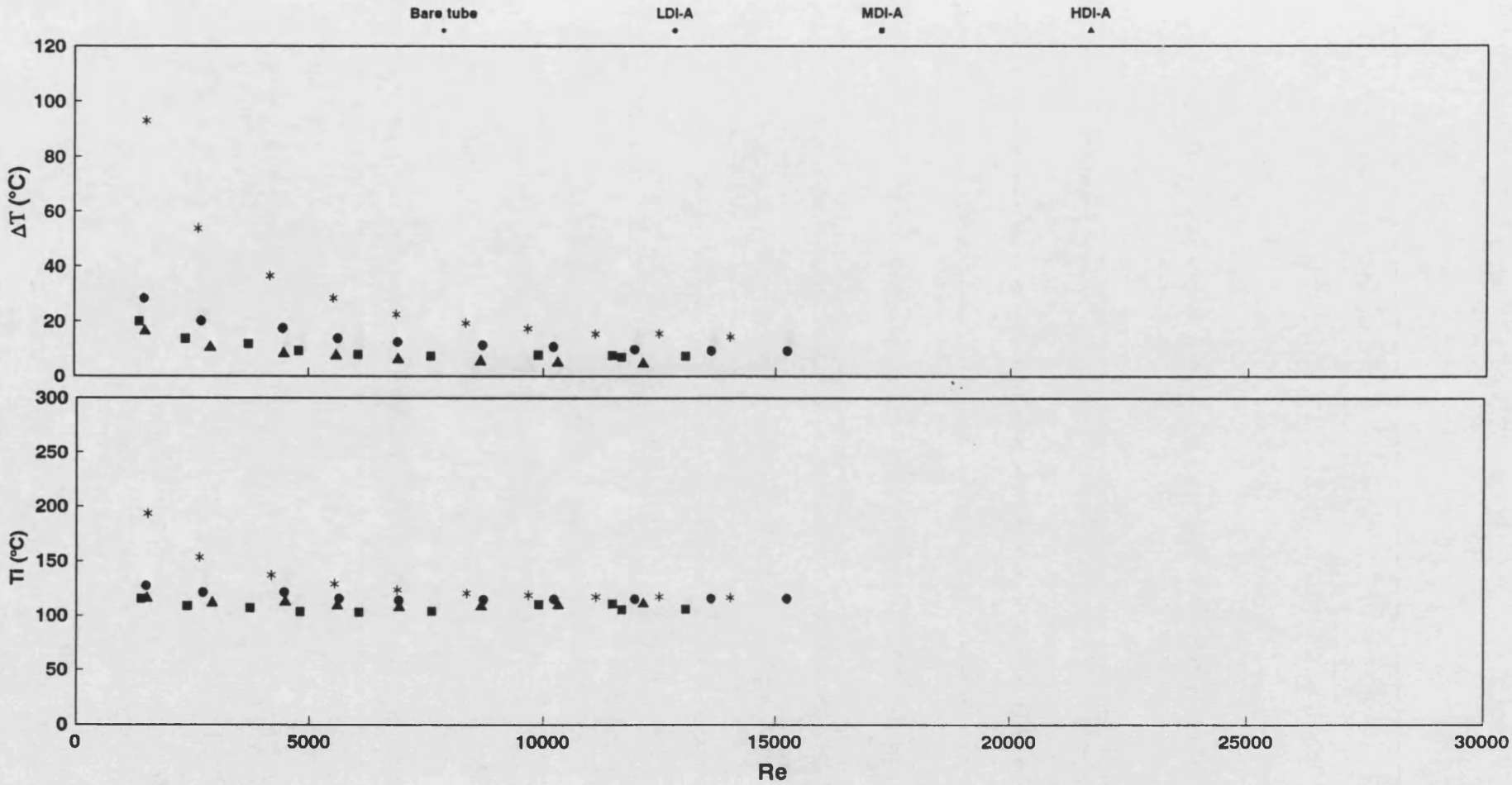

Fig (3.98) Inner surface temperature (Tl (°C)) and temperature driving force (ΔT(°C)) vs Reynolds number (Re)
Comparison between bare tube and a tube fitted with different types of HITran Insert
Santotherm 55 fluid at Tb = 100 °C ; q = 24 kW/m² and 60 < Pr < 80

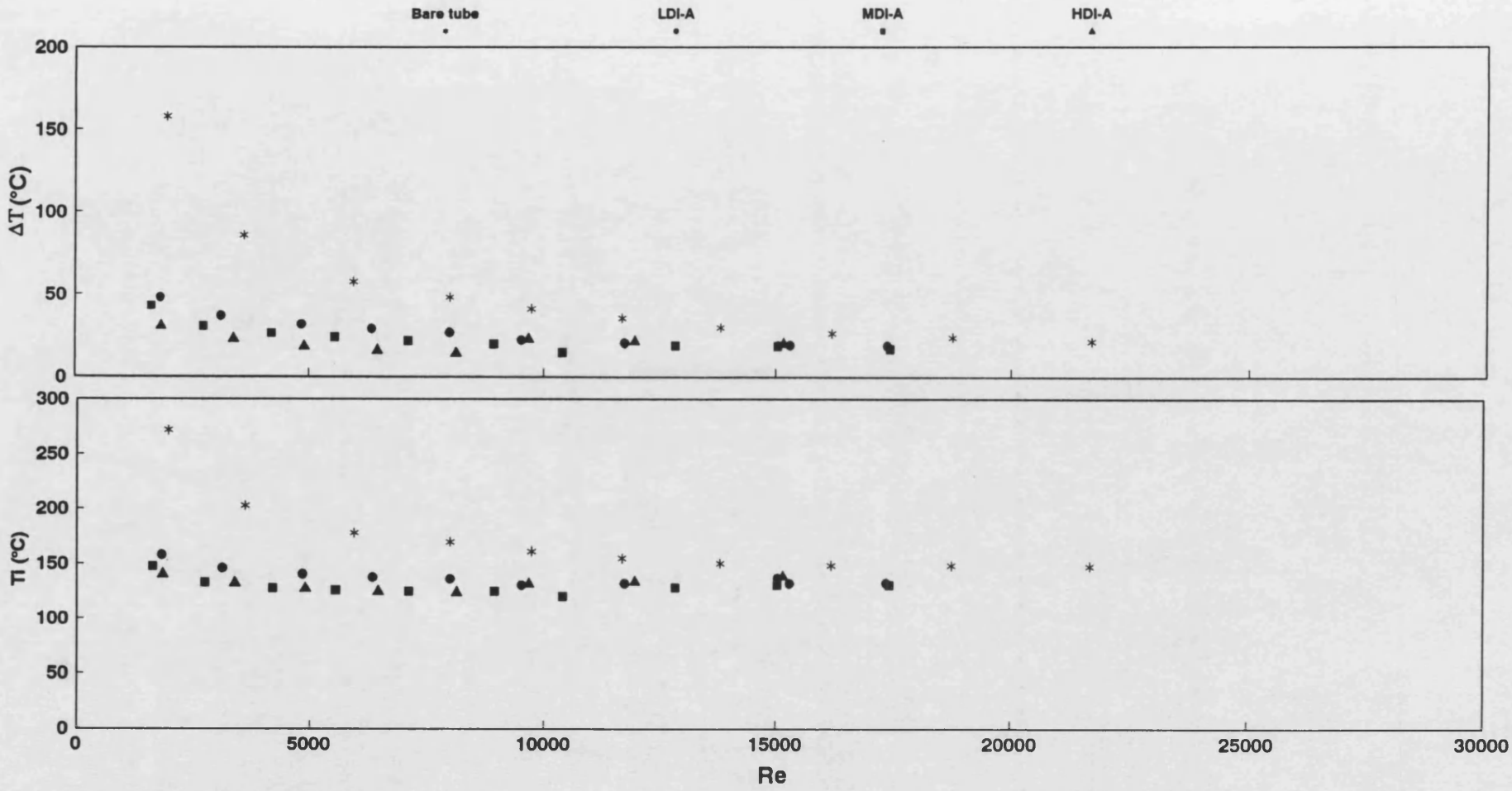

Fig (3.99) Inner surface temperature (Tl (°C)) and temperature driving force (ΔT(°C)) vs Reynolds number (Re)
Comparison between bare tube and a tube fitted with different types of HITran Insert
Santotherm 55 fluid at Tb = 100 °C ; q = 48.2 kW/m² and 60 < Pr < 80

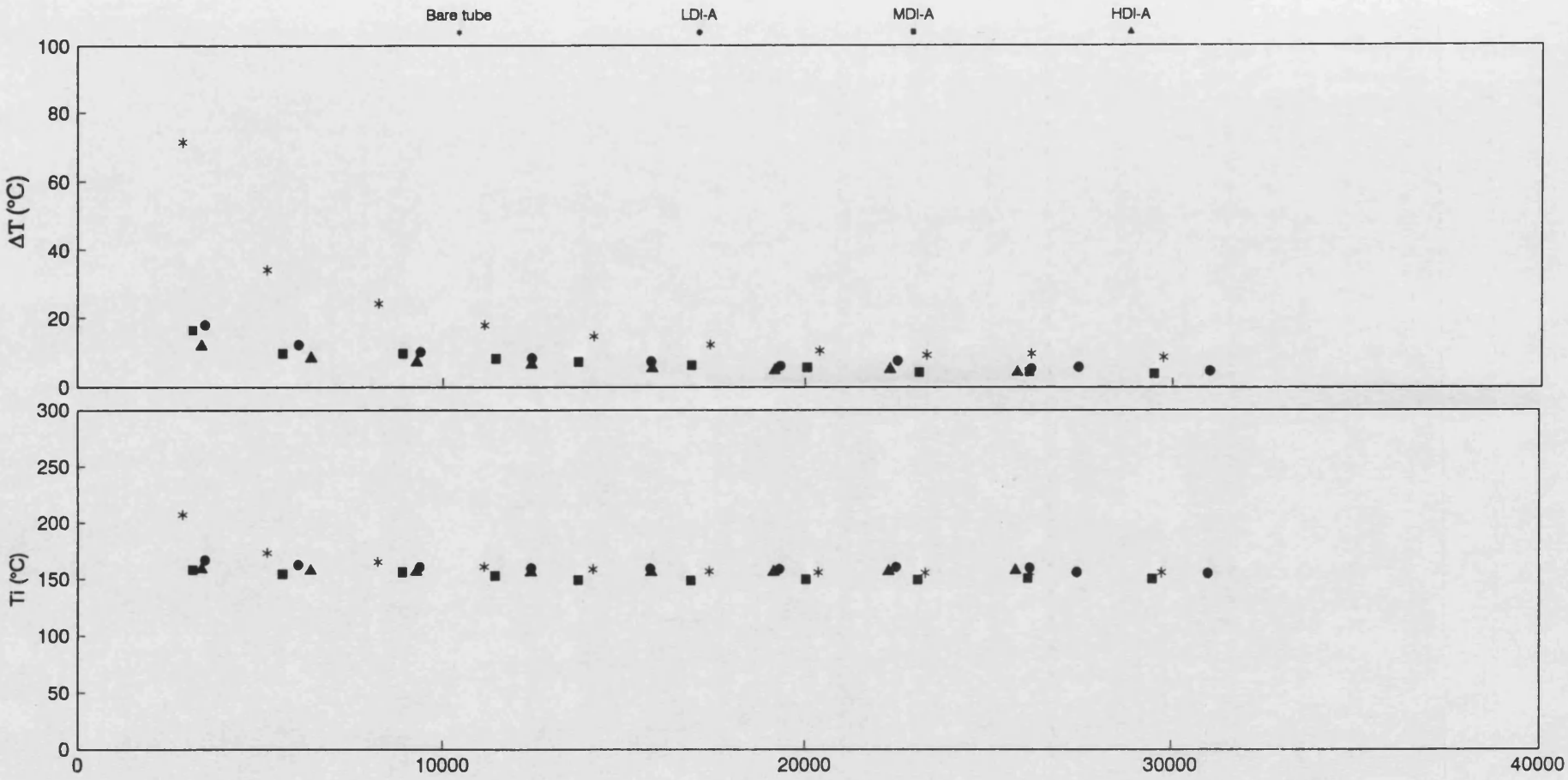

Fig (3.100) Inner surface temperature (Ti (°C)) and temperature driving force (ΔT(°C)) vs Reynolds number (Re)
Comparison between bare tube and a tube fitted with different types of HiTran insert
Santotherm 55 fluid at Tb = 150 °C ; q = 24 kW/m² and 30 < Pr < 60

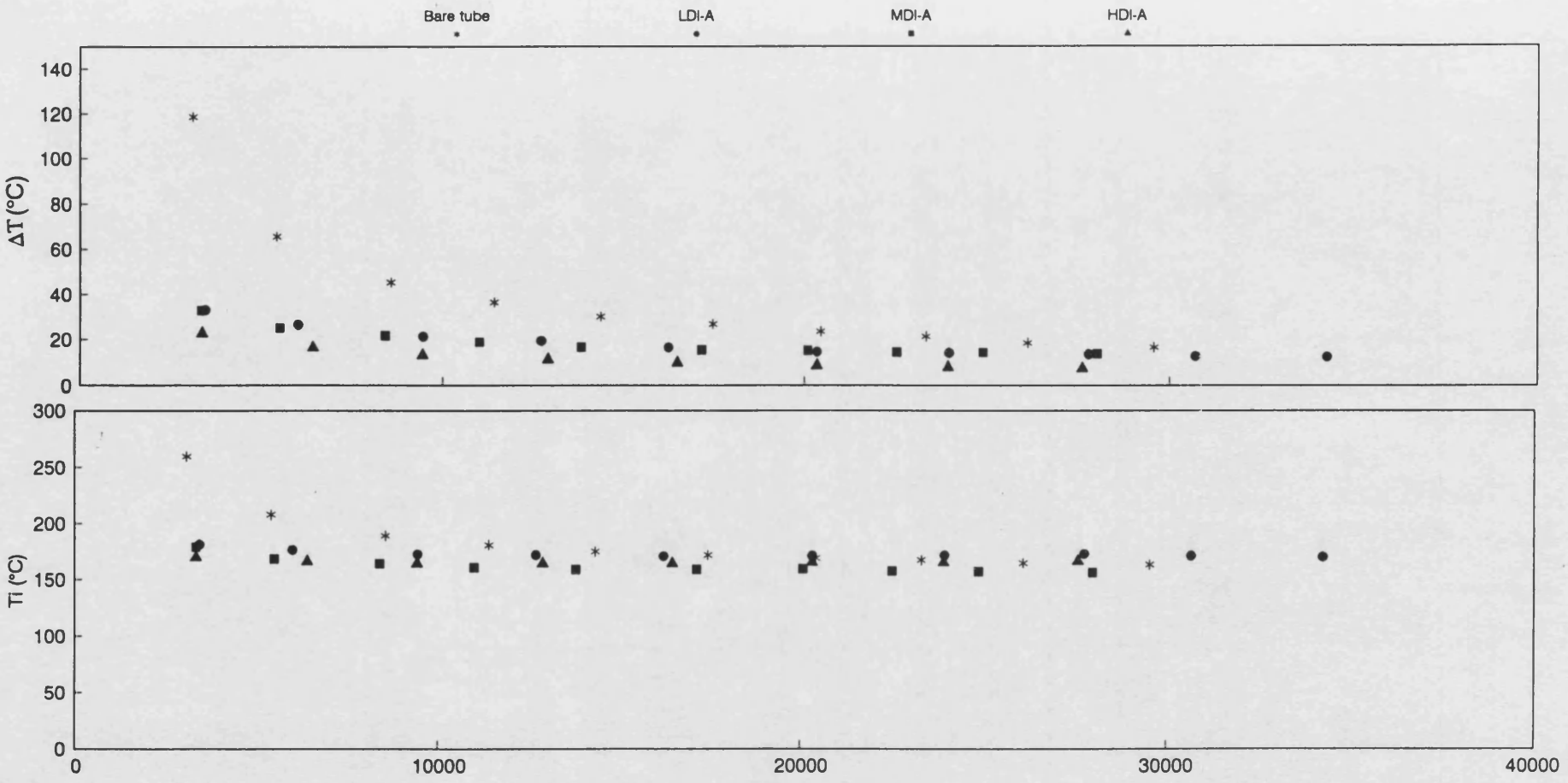

Fig (3.101) Inner surface temperature (Ti (°C)) and temperature driving force (ΔT(°C)) vs Reynolds number (Re)
Comparison between bare tube and a tube fitted with different types of HiTran insert
Santotherm 55 fluid at Tb = 150 °C ; q = 48.2 kW/m² and 30 < Pr < 60

then the use of higher loop density inserts may not be justified .

3.5.2.6 Enhancement factor (EF) of HiTran inserts

The enhancement factor (EF), calculated from equation 3.83 , is plotted vs Reynolds number (Re) in Figs 3.102 to 3.108 for the different types of **HiTran** insert used in the present study.

Fig. 3.102 shows the effect of heat flux ($12 < q < 60.20$ kW/m^2) on the enhancement factor (EF) of test section No (1) fitted with LDI-A at three different bulk temperatures (T_b = 80°C , 100°C and 150°C). EF decreases very rapidly by increasing Re in the laminar flow region (Re < 2100). However, for Re > 2100 the rate of decrease in EF with Re is very much reduced. EF was not affected by heat flux , although the greater values of EF were obtained at higher temperatures for a given Re . For example EF was about 0.51 at Re = 1000 for T_b 80°C , while about 0.8 at T_b 100°C . The lowest EF value was about 0.05 at the higher Re where it was not affected by increases in T_b .

A comparison between test section No (1) fitted with LDI-A and with LDI-B is shown in Fig 3.103 . At q = 24 kW/m^2 the EF values for both inserts are similar. However, at q = 48.2 kW/m^2 , the EF values for LDI-B are about 15% higher .

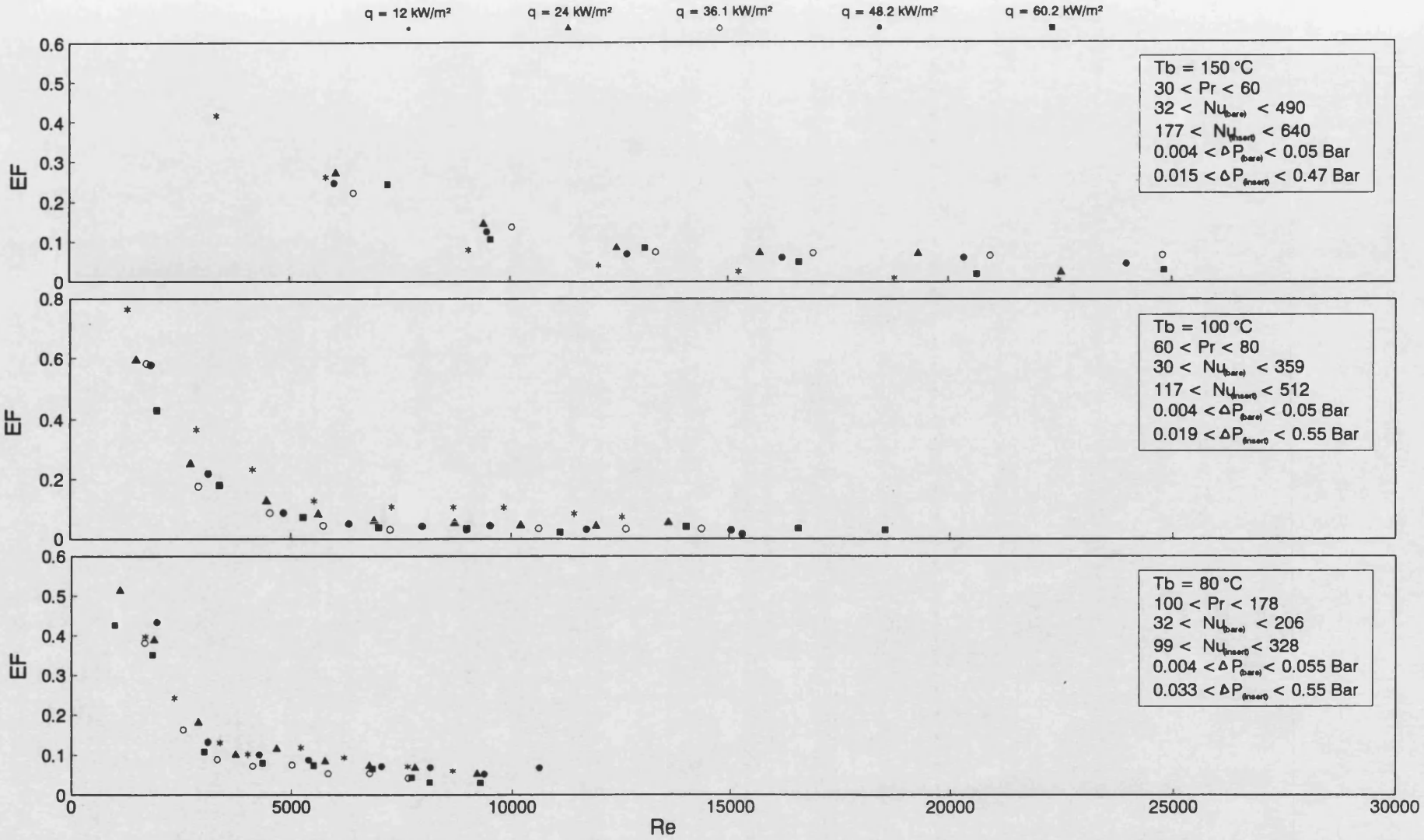

Fig (3.102) Enhancement factor (EF) vs Reynolds number (Re) for tube fitted with LDI-A ; effect of heat flux at constant bulk temperature

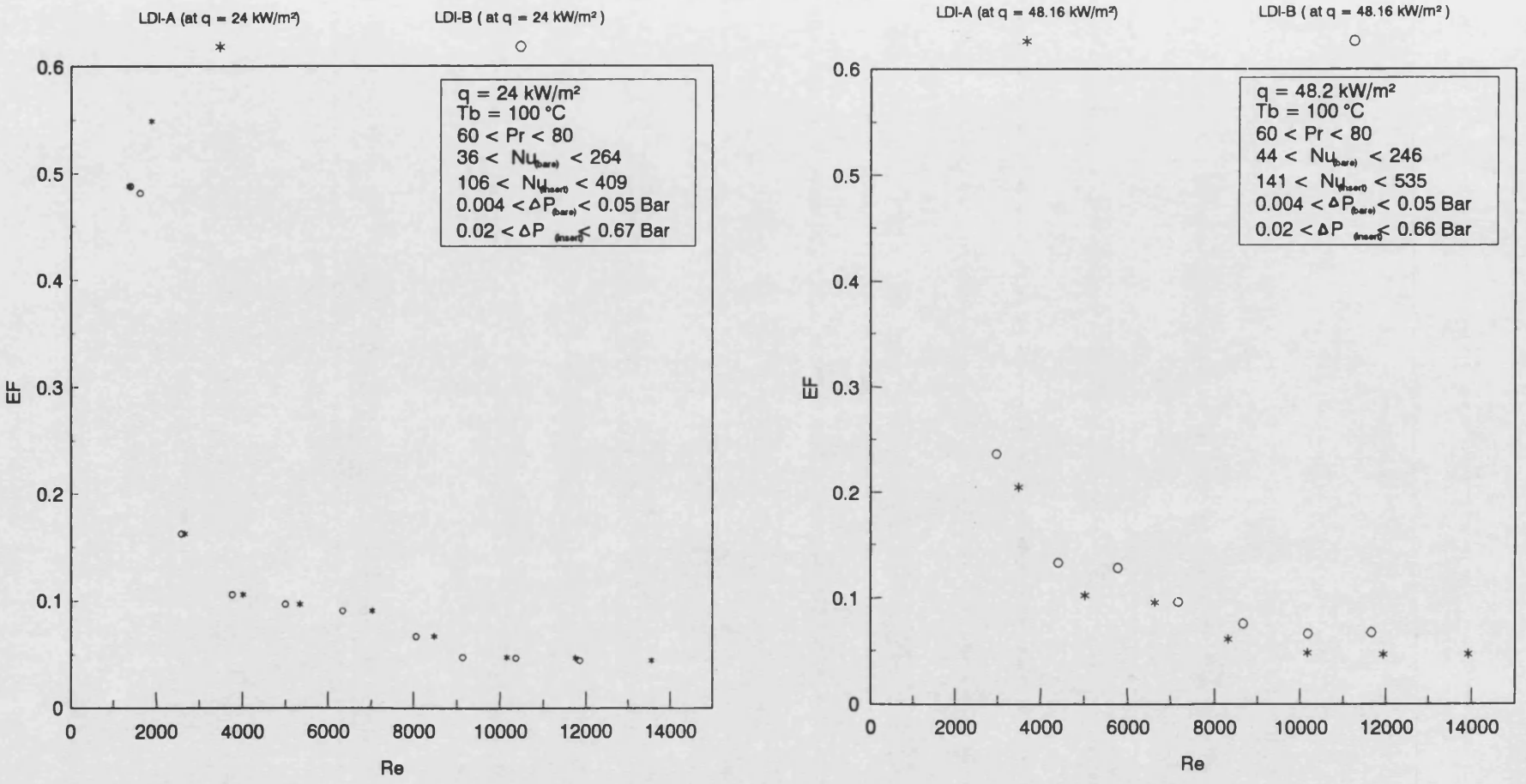

Fig (3.103) Enhancement factor (EF) vs Reynolds number (Re)

Comparison between LDI-A and LDI-B fitted inside test section No(1)

Santotherm 55 fluid at q = 24 and 48.16 kW/m² ; Tb = 100 °C and 60 < Pr < 80

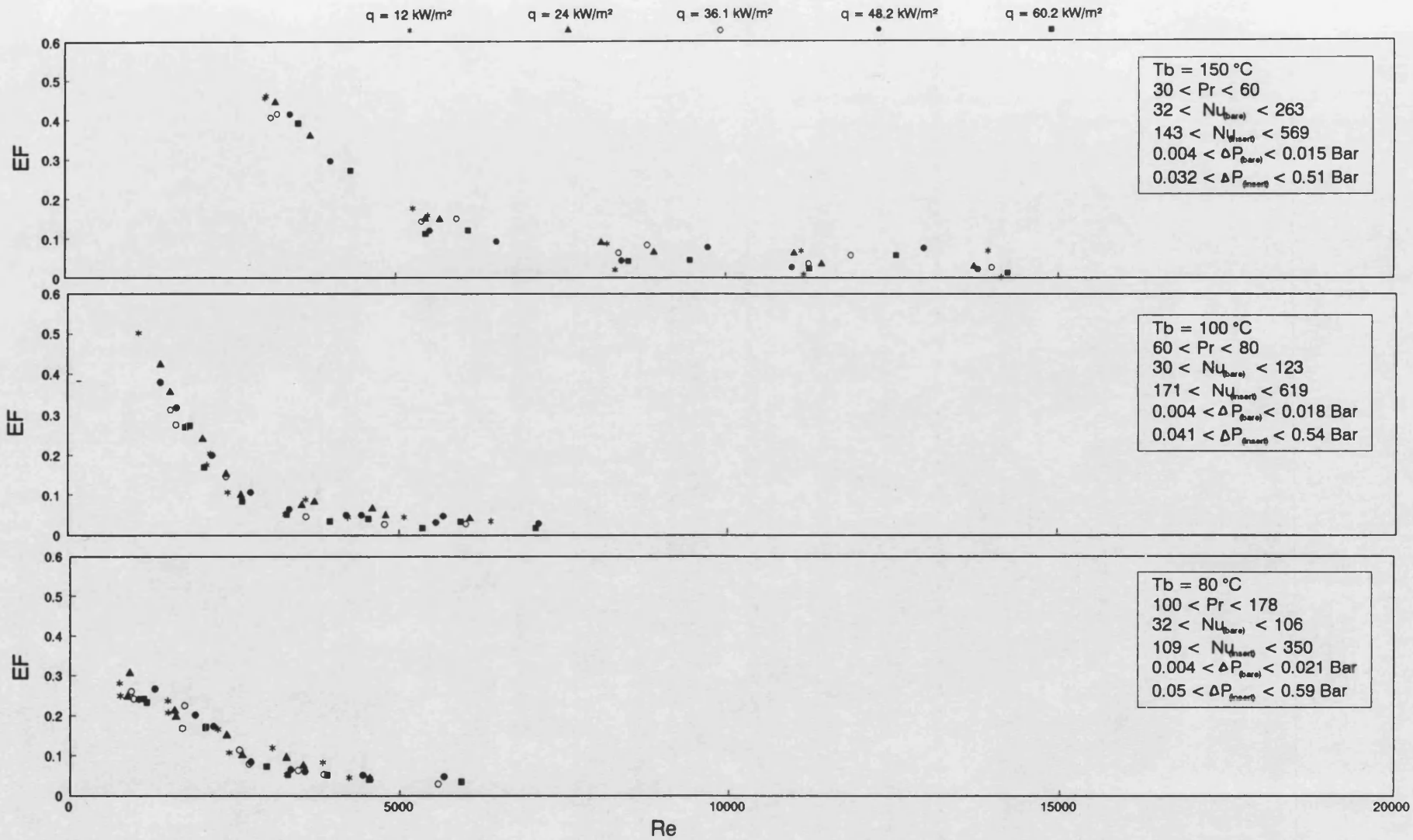

Fig (3.104) Enhancement factor (EF) vs Reynolds number (Re) for tube fitted with MDI-A ; effect of heat flux at constant bulk temperature

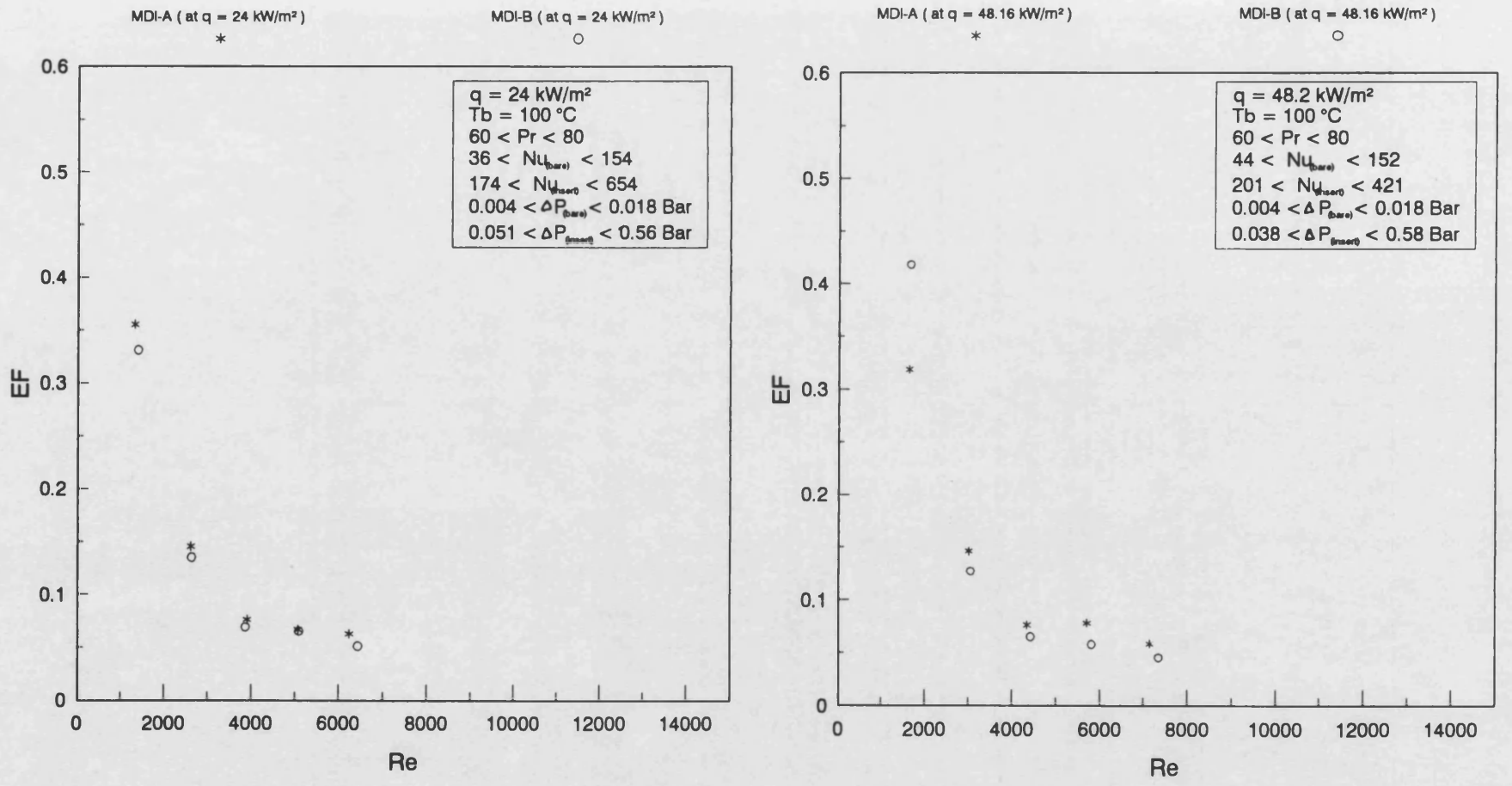

Fig (3.105) Enhancement factor (EF) vs Reynolds number (Re)

Comparison between MDI-A and MDI-B inserted inside test section No(1)

Santotherm 55 fluid at q = 24 and 48.16 kW/m² ; Tb = 100 °C and 60 < Pr < 80

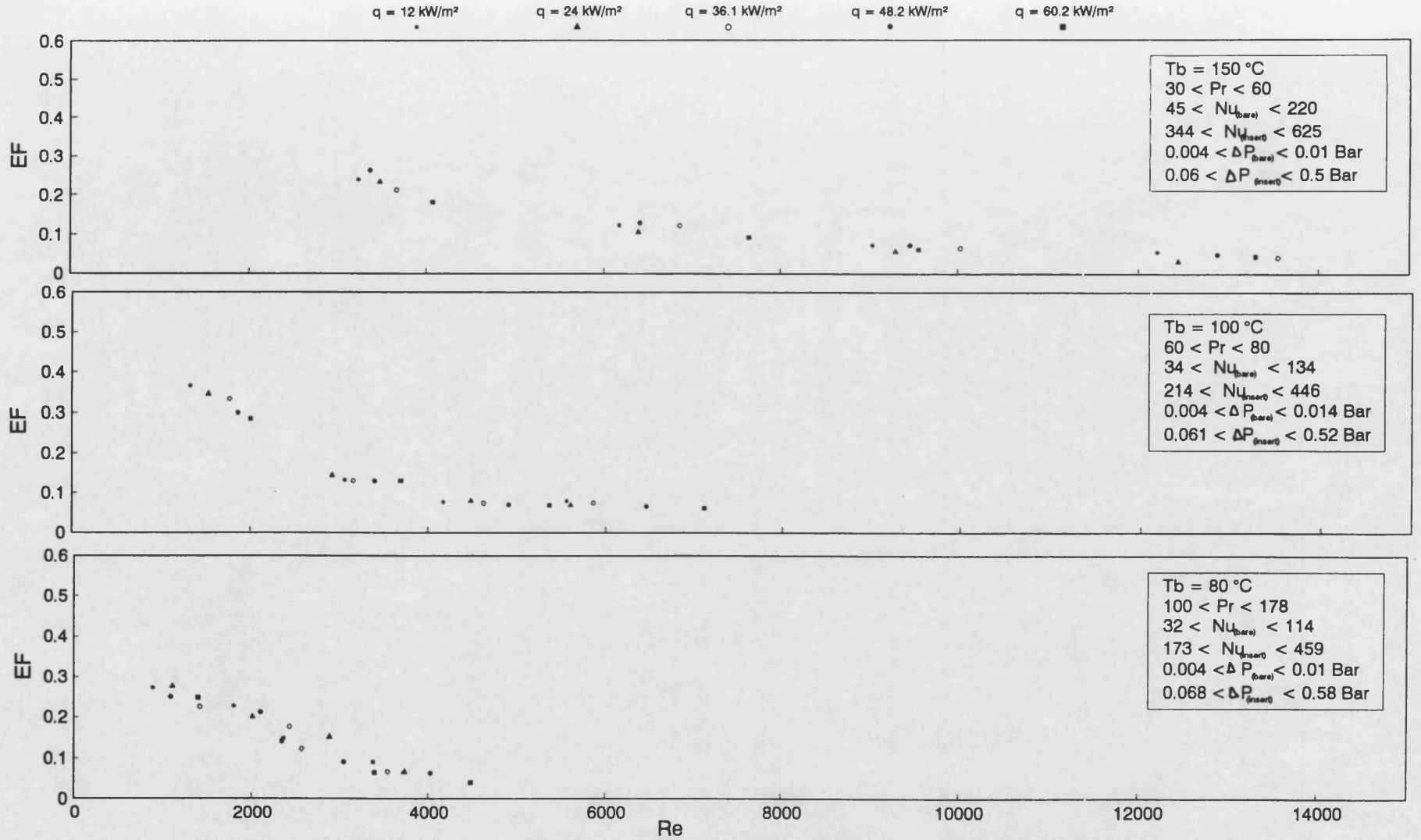

Fig (3.106) Enhancement factor (EF) vs Reynolds number (Re) for tube fitted with HDI-A ; effect of heat flux at constant bulk temperature

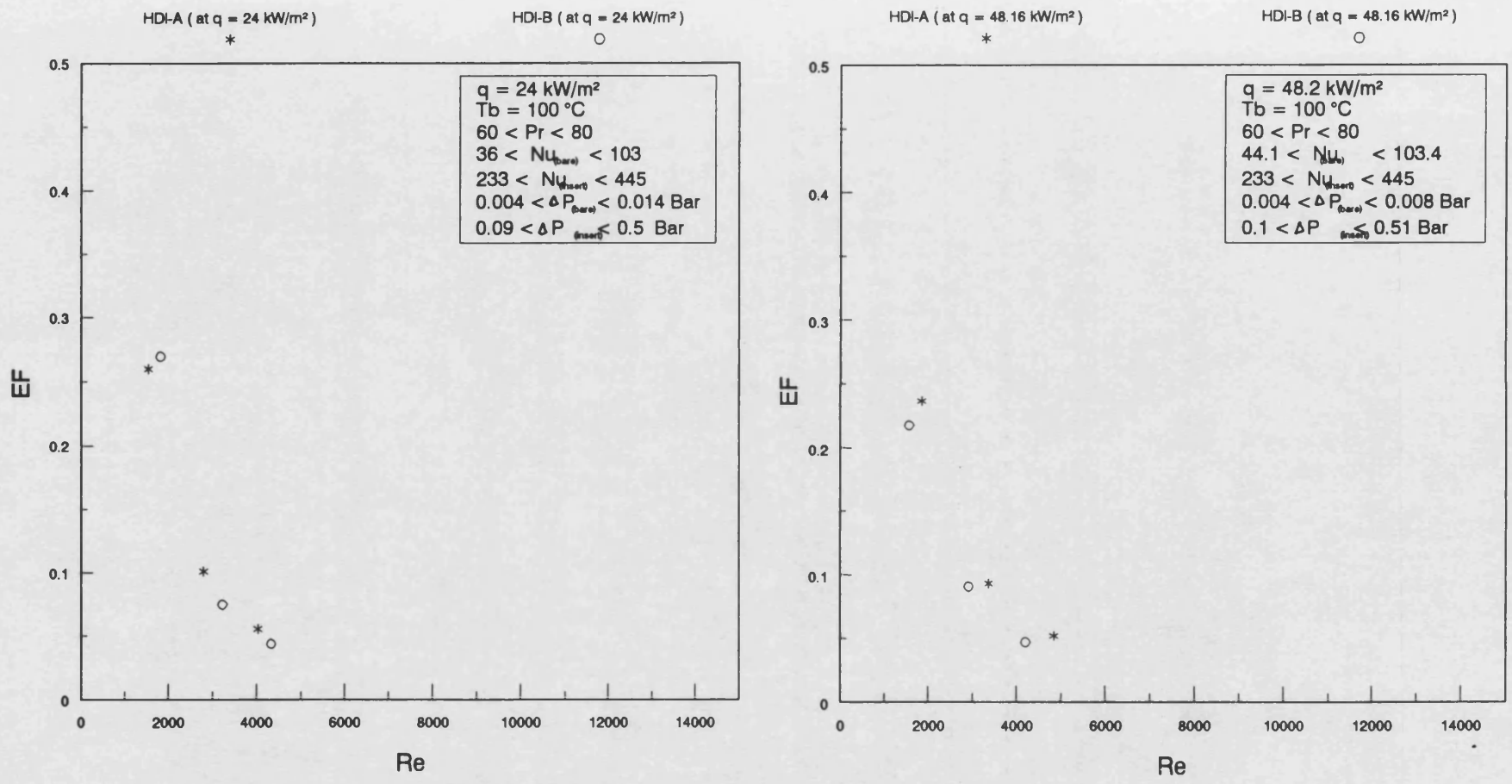

Fig (3.107) Enhancement factor (EF) vs Reynolds number (Re)

Comparison between HDI-A and HDI-B inserted inside test section No(1)

Santotherm 55 fluid at q = 24 and 48.16 kW/m² ; Tb = 100 °C and 60 < Pr < 80

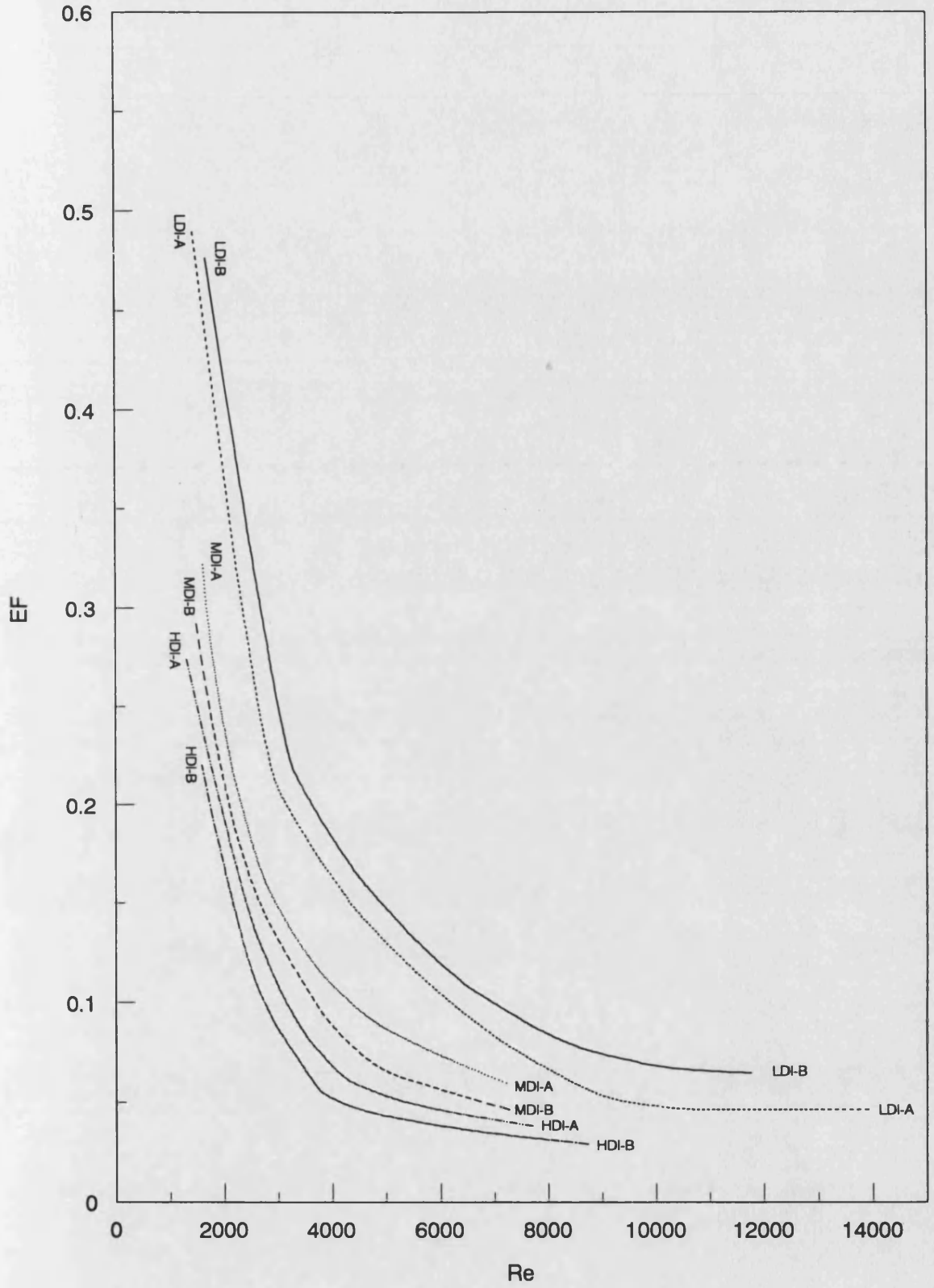

Fig (3.108) Enhancement factor (EF) vs Reynolds number (Re)

Comparison between all types of HiTran insert used in present study

Santotherm 55 fluid at Tb = 100 °C ; q = 48.2 kW/m² and 60 < Pr < 80

Fig 3.104 shows the effect of using different heat fluxes ($12 < q < 60.20$ kW/m^2), on the enhancement factor of both test sections fitted with MDI-A at T_b = 80 , 100 and 150°C . The highest value of EF (at the lower values of Re) was also affected by T_b . For Re = 1000 it is about 0.3 at 80°C and 0.5 at 100°C , these values being less than those obtained with the LDI insert. The lowest value of EF is about 0.03 which is also lower than that for the LDI case .

A comparison for test section No(1) fitted with MDI-A and then with MDI-B is shown in Fig 3.105. At q = 24 kW/m^2 , EF for the MDI-A case is only slightly higher than that for the MDI-B case. However, at q = 48 kW/m^2 , EF of MDI-A is about 10% higher than that of MDI-B for most of the Re range .

Fig 3.106 shows the effect of q and bulk temperature on EF of test section No(2) fitted with HDI-A. The highest value of EF was also affected by T_b . For Re = 1000 it was about 0.28 at T_b = 80°C and about 0.4 at T_b = 100°C , values which are less than the previous cases (with LDI-A and MDI-A). The lowest value of EF is very close to those in previous cases, i.e about 0.028 .

Fig 3.107 shows a comparison between test section No(1) fitted with HDI-A and the same test section fitted with HDI-B. At q = 24 kW/m^2 there is

little difference between both cases. However, at $q = 48.2\ kW/m^2$, HDI-A appears to give about a 20% higher value of EF than that of the HDI-B case.

An overall comparison between all six types of HiTran inserts, used in this study (LDI-A, LDI-B, MDI-A, MDI-B, HDI-A and HDI-B) is shown in Fig 3.108 for $T_b = 100°C$ and $q = 48.2\ kW/m^2$. For a given Re , the enhancement factor was increased by reducing the loop density of the HiTran insert. Among the HiTran inserts tested, LDI-B appears to give the highest EF. The enhancement factor for LDI-B is about 15%. 40%, 50%, 55% and 60% higher than EF of LDI-A, MDI-A, MDI-B, HDI-A and HDI-B respectively.

Fig 3.108 confirms that the use of HiTran inserts is useful in improving the performance of a heat exchanger if it is operating at relatively low Re , say $Re < 10000$. However, at higher flow rates ($Re > 10000$) less improvement can be achieved by the use of HiTran inserts.

3.6 Conclusions on the Santotherm 55 study

The principal conclusions on the Santotherm 55 study, are listed below:

1- The use of a **HiTran** insert enhanced the heat transfer factor (j_H) several times over that of a bare tube case. However, there was also a significant simultaneous increase in pressure drop (Δp). The average enhancement in j_H as well as the average increase in Δp for different **HiTran** inserts are summarised in Table 3.21 below.

Table 3.21 The enhancement in j_H and the increase in Δp provided by the use of HiTran inserts

Type of HiTran insert	Laminar flow 500<Re<2100		Transition flow 2100<Re<10000		Turbulent flow Re>10000	
	$\frac{j_H \text{ (insert)}}{j_H \text{ (bare)}}$	$\frac{\Delta p \text{ (insert)}}{\Delta p \text{ (bare)}}$	$\frac{j_H \text{ (insert)}}{j_H \text{ (bare)}}$	$\frac{\Delta p \text{ (insert)}}{\Delta p \text{ (bare)}}$	$\frac{j_H \text{ (insert)}}{j_H \text{ (bare)}}$	$\frac{\Delta p \text{ (insert)}}{\Delta p \text{ (bare)}}$
Low loop density insert LDI (2.7 loops per cm)	3.6	8.5	1.8	11.2	1.3	13
Medium loop density insert MDI (6.4 loops per cm)	4.8	19.5	2.0	30.0	1.6	36
High loop density insert HDI (10.5 loops per cm)	5.8	28	4.3	40	3.4	50

Moreover, the enhancement in j_H achieved by the same HiTran insert, was found to be affected by

the heat flux and bulk temperature as well as re-using and rotating the insert inside the tubular test section.

2- The experimental j_H of the bare tube was in close agreement with the Sieder and Tate[36] correlation for $100 < Pr < 187$. However it was about 20 to 30% higher at $30 < Pr < 60$. An overall agreement between the experimental results and the Gnielinski[37] correlation was achieved when the latter was modified with a viscosity correction factor. It is importsnt to note that the Santotherm 55 fluid was not fully developed for the whole ranges of Re and Pr studied (refer to Table 3.19). In the range of $1300 < Re < 2500$ where the fluid is expected to be still developing (both hydrodynamically and thermally) j_H of the bare tube was affected by both heat flux and bulk temperature.

3- The friction factor of the bare tube was affected by both heat flux and bulk temperature for the developing flow region (at $Re < 10000$). However, for fully developed flow ($Re > 10000$), the friction factor was not affected by q or T_b and it was possible to correlate with equation 3.101 which is in the form of the Churchill correlation[35] for a smooth bare tube . The friction factor of the tube fitted with a **HiTran** insert was unaffected either by heat

flux or by bulk temperature, but it was affected by the loop density . The friction factor was increased with an increase in the loop density. Moreover, f was also affected by re-using and rotating the same **HiTran** insert.

Table 3.22 summarises the Fanning friction factor equations generated in this study for the bare tube (equation 3.101) and for a tube fitted with different types of **HiTran** inserts (equations 3.102 to 3.107) .

Table 3.22 Fanning friction factor equations for bare tube and for a tube fitted with HiTran inserts

Conditions of the test sections	Equation	Recommended range	Accuracy and remarks
Bare tube	$f_{(bare)} = 0.117\ Re^{0.283}$	$Re > 10^4$ $30 < Pr < 187$	1- It is accurate to about ± 5% 2- About 7 to 10% higher comparing to equation 3.95.
Tube fitted with LDI HiTran insert (2.7 loops per cm)	$f_{(LDI)} = A_{11} + 60000/ Re^2$ Where : $Log_{10}(A_{11}) = 1.24 - 0.33\ Log_{10}(Re^3) + 0.01216\ (Log_{10}Re^3))^2$	$1000 < Re < 3.4x10^4$ $30 < Pr < 187$	accurate to about ± 8 %
Tube fitted with MDI HiTran insert (6.4 loops per cm)	$f_{(MDI)} = A_{12}$ Where : $Log_{10}(A_{12}) = 1.634 - 0.33\ Log_{10}(Re^3) + 0.01215\ (Log_{10}Re^3))^2$	$750 < Re < 15500$ $34 < Pr < 129$	accurate to about ± 7 %
Tube fitted with HDI HiTran insert (10.5 loops per cm)	$f_{(HDI)} = A_{13}$ Where : $Log_{10}(A_{13}) = 2.143 - 0.38\ Log_{10}(Re^3) + 0.01546\ (Log_{10}Re^3))^2$	$900 < Re < 13300$ $34 < Pr < 111$	accurate to about ± 2 %

5- It was not possible to correlate all the heat transfer results for the tube fitted with **HiTran** inserts by using the j_H-factor. Consequently, a modified heat transfer factor called j_{HM} was introduced (defined by equation 3.114). Using the j_{HM}-factor the heat transfer data for each type of **HiTran** insert as well as for the bare tube were correlated as shown in Table 3.23 (equations 3.115 to 3.122).

Table 3.23 Modified heat transfer factor (j_{HM}) equations for bare tube and for a tube fitted with HiTran inserts

Conditions of the test sections	Equation	Recommended range	Accuracy and remarks
Bare tube	$j_{HM\,(bare)} = 0.7\,Re^{0.61}$ Or, $Nu_{(bare)} = \frac{0.7\,Re^{0.61}}{[\,Pr\,f\,(\mu_b/\mu_w)\,]^{0.14}}$	$700 < Re < 3.4x10^4$ $30 < Pr < 187$	accurate to about ± 10 %
Tube fitted with LDI HiTran insert (2.7 loops per cm)	$j_{HM\,(LDI)} = 17\,Re^{0.356}$ Or, $Nu_{(LDI)} = \frac{17\,Re^{0.356}}{[\,Pr\,f\,(\mu_b/\mu_w)\,]^{0.14}}$	$800 < Re < 3.4x10^4$ $30 < Pr < 187$	accurate to about ± 7.1 %
Tube fitted with MDI HiTran insert (6.4 loops per cm)	$j_{HM\,(MDI)} = 11.6\,Re^{0.46}$ Or, $Nu_{(MDI)} = \frac{11.6\,Re^{0.46}}{[\,Pr\,f\,(\mu_b/\mu_w)\,]^{0.14}}$	$750 < Re < 15500$ $34 < Pr < 129$	accurate to about ± 10 %
Tube fitted with HDI HiTran insert (10.5 loops per cm)	$j_{HM\,(HDI)} = 22.5\,Re^{0.4}$ Or, $Nu_{(HDI)} = \frac{22.5\,Re^{0.4}}{[\,Pr\,f\,(\mu_b/\mu_w)\,]^{0.14}}$	$900 < Re < 13300$ $34 < Pr < 111$	accurate to about ± 6.2 %

The friction factor (f) used in the j_{HM}-factor was the experimental value. However, f calculated from the friction factor equations in Table 3.22 could be used with confidence.

6- The use of a HiTran insert caused an increase in both heat transfer and pressure drop, as mentioned above. In order to discover which **HiTran** insert would give the maximum improvement in the test section performance, the enhancement factor (EF) was used.
The enhancement factor is a combination of Nu and Δp in one formula, as follows:

$$EF = (R_{Nu} - 1) / (R_{\Delta p} - 1)$$

where:

$$R_{Nu} = \frac{\text{Nu for insert case}}{\text{Nu for bare tube case}}$$

$$R_{\Delta p} = \frac{\Delta p \text{ for insert case}}{\Delta p \text{ for bare tube case}}$$

The EF-factor was found to decrease with increasing loop density of the **HiTran** insert. Moreover , the enhancement factor decreased exponentially with Re. Among the six HiTran inserts tested in this study (LDI-A, LDI-B, MDI-A, MDI-B, HDI-A and HDI-B), LDI-B was found to give the highest EF-factor value, about 0.60 for laminar flow (at Re = 700) and about 0.08 for turbulent flow (for Re>12000). Consequently, if LDI-B was fitted into a heat

exchanger tube, then a marked improvement in it's performance would be expected. On the other hand, if a heat exchanger was designed to include a **HiTran** insert fitted inside the tube, then less heat transfer area would be required.

7- The inner surface temperature (T_i) of a tube fitted with a **HiTran** insert was found to be as much as 100°C lower than that for the bare tube at a similar flowrate. However, there is not much difference between T_i for the tube fitted with the LDI insert and the tube fitted with the HDI insert . Therefore, if the aim is solely to get a low T_i then the use of an HDI insert would not be justified .

The decrease of inner surface temperature (Ti) by using a **HiTran** insert, is useful for reducing the risk of in-tube fouling in those cases where fouling is known to be controlled by the inner surface temperature (this will be discussed in chapter 4 of this study).

Chapter 4
Crude oil Study

4.1 Introduction

The aim of this study was to investigate the effect of using a **HiTran** insert on the fouling of crude oil. Arabian light crude oil (A.L.crude) was chosen as a potentially fouling fluid. Test section No(2) was fitted with the low loop density insert (LDI-B) , which provided the greatest EF-factor in the Santotherm 55 study . Test section No(1) was left bare .

Seven fouling runs were carried out . Fouling did not occur in the first six runs , but it did occur in the seventh run . Many aspects which are believed to prevent fouling were individually investigated and thus the discussion of results has to be in the form of a case study .

The heat transfer coefficient and the friction factor of crude oil were determined for both test sections and compared with those for Santotherm 55 . The mathematical correlations of heat transfer and friction factor generated for Santotherm 55 were tested against the crude oil results . The effect of dissolved gases , such as nitrogen and helium , on the heat transfer coefficient (h_i) of crude oil and on the inner surface temperature (T_i) of the test sections was also investigated . The role of nitrogen gas for preventing fouling in the bare tube test section was demonstrated.

4.2 Specification of Arabian light crude oil

The broad specification of Arabian light crude oils was provided by the supplier (BP International Ltd.) and checked , whenever possible , against ASTM (American Society for Testing and Materials) and IP (Institute of Petroleum) standard methods.

4.2.1 Physical properties

The most important physical properties of Arabian light crude oil are listed in Table 4.1

Table 4.1 Physical properties of Arabian light crude oil

Gravity , °API	(Shalhi)	31.4
Specific gravity at 15/15 °C	(Shalhi)	0.8686
Density at 15 °C	(Shalhi)	868.2 (kg m^{-3})
Kinematic viscosity	(Shalhi)	
At 70 °F (21.1 °C)		18.77 (mm^2 s^{-1})
At 100 °F (37.8 °C)		10.95 (mm^2 s^{-1})
Watson Characterization factor (K)	(Shalhi)	11.4
Pour point	(BP)	-57 °C
Average molecular weight	(Shalhi)	192 (kg $kmol^{-1}$)
Boiling range		
ASTM distillation, vol % at 760 mm Hg	(Shalhi)	See Fig 4.1
TBP distillation , wt %	(BP)	See Fig 4.2
Water , % vol	(BP)	< 0.05 %
Sulphur content , % wt	(BP)	1.78 %
Carbon residue , % wt	(BP)	4.0 %
Asphaltenes , % wt	(BP)	1.0 %
Salt content (as Na C l)	(BP)	2.7 lb / 1000 bbl
Metallic elements :	(BP)	
Nickel		4 ppm
Vanadium		15 ppm

The variation of certain physical properties, such as density (ρ), specific heat (C_p), thermal conductivity

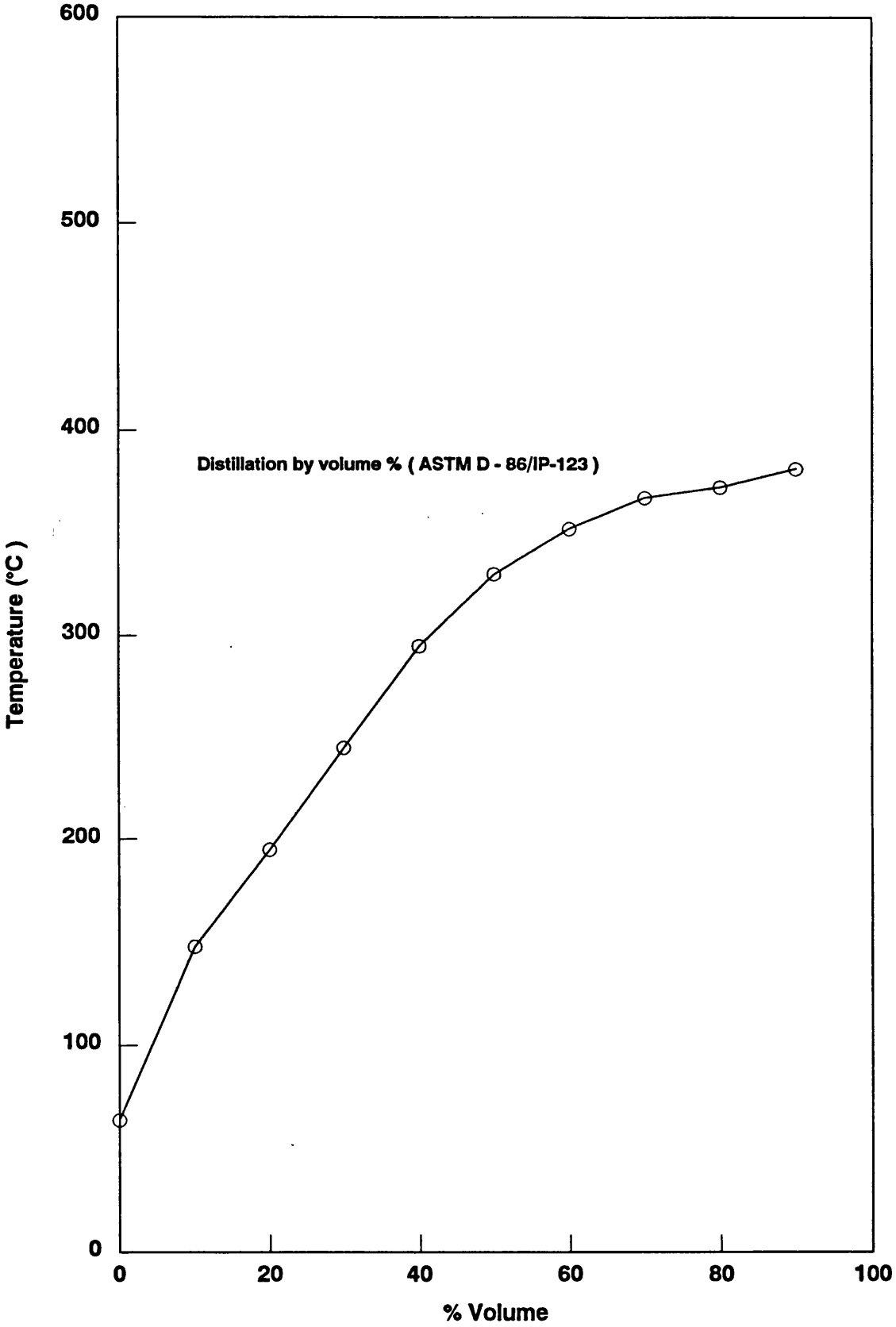

Fig(4.1) ASTM - Distillation of Arabian light crude oil (measured in the laboratory)

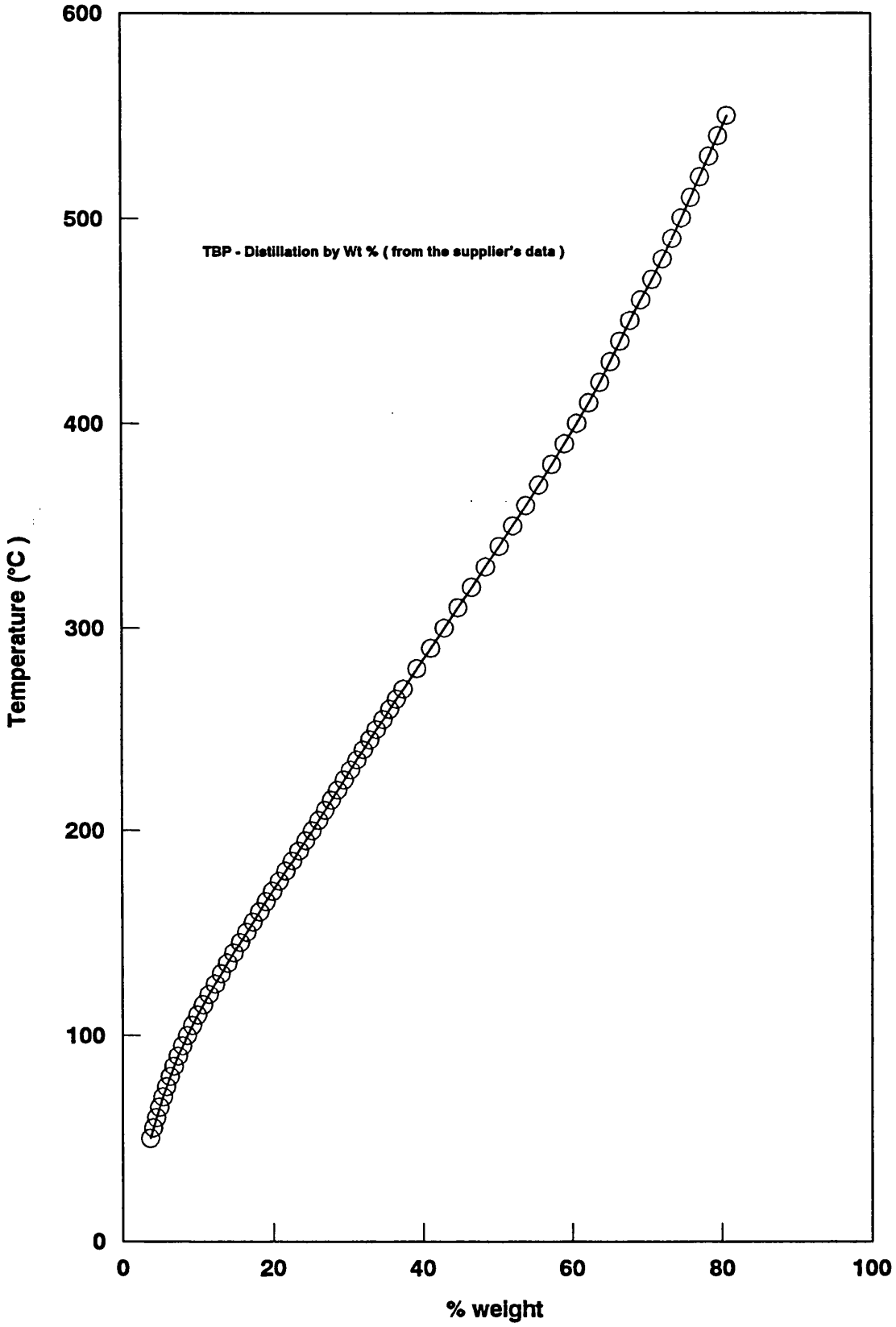

Fig(4.2) True boling point (TBP) Distillation of Arabian light crude oil (Supplied by BP)

blanket initially the tank , and a similar procedure was applied .

The results of the two experiments are shown in Fig 4.3 . An exponential relationship between pressure and temperature was obtained and correlated within ± 3% accuracy as follows :

$$\mathrm{Log}_{10}(P) = 1.94\,\mathrm{Log}_{10}(T) - 3.54$$

Or ,

$$P = 2.87 \times 10^{-4}\,(T)^{1.94} \qquad (4.5)$$

Where ,

P is the tank pressure (bar)

T is the temperature (^{o}C)

Equation 4.5 may be used to determine the pressure required to maintain the crude oil in the liquid phase or to suppress nucleate boiling in the test sections . For example , if the inner surface temperature (T_i) of the test section is 200 ^{o}C , then the pressure calculated from equation 4.5 would be 8.35 bar (see Fig 4.3). Consequently , the equipment pressure must be higher than 8.35 bar (absolute) in order to suppress any nucleate boiling .

4.3 Re - calibration of Flowmeters

Both flowmeters, No(1) and No(2), were re-calibrated using the Arabian light crude oil at three different bulk temperatures (25 , 33 and 45 ^{o}C). The calibration results are shown in Tables 4.2 and 4.3 below and correlated in equations 4.6 to 4.25 .

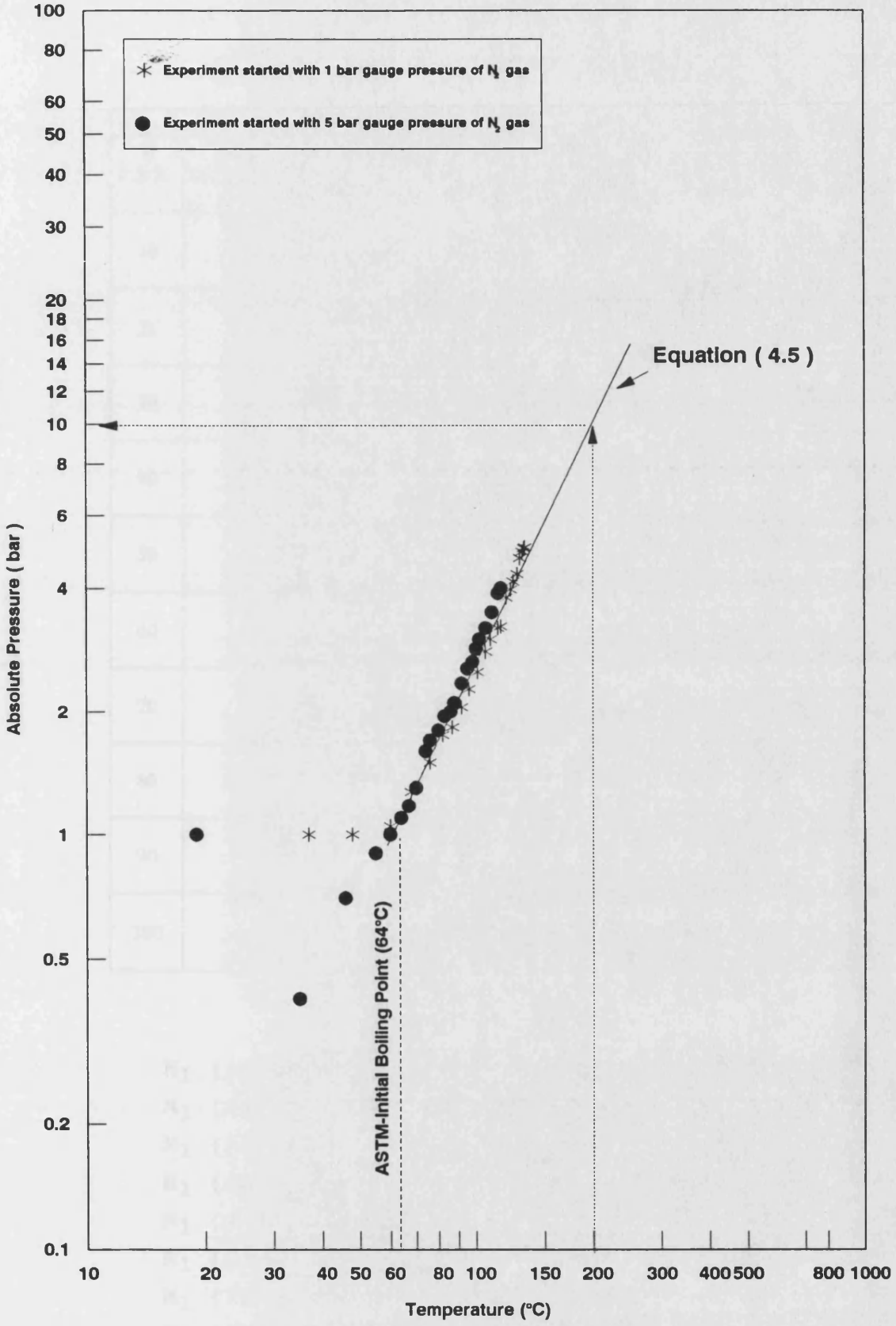

Fig(4.3) Tank pressure (Bar) Vs. temperature (°C)
for Arabian light crude oil

Table 4.2 Flowmeter calibrations

Flow meter No(1) for test section No(1)						
% F.S.R	Bulk Temperature (°C)	Mass Flow Rate ($kg\ hr^{-1}$)	Flowmeter Flow Rate ($m^3\ hr^{-1}$)	Velocity ($m\ s^{-1}$)	Kinematic Viscosity ($mm^2 s^{-1}$)	Re
10	25.3	267.9	0.3104	0.499	16.95	436.6
	36.6	266.2	0.3103	0.499	11.81	626.5
	45.4	264.2	0.3094	0.497	9.22	800.3
20	25.4	476.7	0.5523	0.888	16.89	779.5
	33.1	471.2	0.5482	0.881	13.13	995.3
	45.4	466.5	0.5463	0.878	9.22	1413.1
30	25.6	681.0	0.7892	1.269	16.77	1121.5
	33.3	674.5	0.7849	1.262	13.05	1433.7
	46.1	668.9	0.7836	1.260	9.05	2064.9
40	22.1	910.7	1.0535	1.693	18.97	1323.9
	34.9	904.0	1.0529	1.692	12.43	2020.1
	46.8	896.4	1.0506	1.689	8.88	2819.7
50	22.6	1132.9	1.3108	2.107	18.64	1677.1
	35.4	1123.9	1.3093	2.105	12.24	2550.3
	46.3	1117.8	1.3098	2.105	9.00	3469.5
60	21.2	1347.2	1.5576	2.504	19.60	1894.7
	33.5	1340.5	1.5600	2.507	12.97	2867.3
	46.4	1332.2	1.5610	2.509	8.98	4145.9
70	21.4	1555.8	1.7990	2.892	19.46	2204.2
	34.4	1548.5	1.8029	2.898	12.62	3406.8
	45.5	1542.4	1.8064	2.904	9.19	4684.8
80	22.4	1768.6	2.0462	3.290	18.77	2599.2
	34.5	1761.5	2.0511	3.297	12.58	3887.6
	45.4	1757.0	2.0577	3.308	9.22	5322.2
90	24.6	1979.7	2.2930	3.686	17.37	3147.9
	33.9	1968.3	2.2912	3.683	12.81	4263.6
	46.8	1957.7	2.2945	3.688	8.88	6158.4
100	25.3	2250.4	2.6075	4.191	16.95	3667.5
	35.2	2233.9	2.6021	4.183	12.32	5038.1
	47.2	2216.8	2.5987	4.177	8.79	7048.2

For Flowmeter No (1)

$$M_1\ (10\%) = 272.68 - 0.184\ T\ (^oC) \quad (4.6)$$

$$M_1\ (20\%) = 488.61 - 0.496\ T\ (^oC) \quad (4.7)$$

$$M_1\ (30\%) = 694.98 - 0.577\ T\ (^oC) \quad (4.8)$$

$$M_1\ (40\%) = 923.84 - 0.582\ T\ (^oC) \quad (4.9)$$

$$M_1\ (50\%) = 1147.08 - 0.639\ T\ (^oC) \quad (4.10)$$

$$M_1\ (60\%) = 1360.07 - 0.598\ T\ (^oC) \quad (4.11)$$

$$M_1\ (70\%) = 1567.67 - 0.557\ T\ (^oC) \quad (4.12)$$

$$M_1\ (80\%) = 1779.66 - 0.507\ T\ (^oC) \quad (4.13)$$

$$M_1\ (90\%) = 2002.88 - 0.978\ T\ (^oC) \quad (4.14)$$

$$M_1\ (100\%) = 2288.58 - 1.529\ T\ (^oC) \quad (4.15)$$

Table 4.3 Flowmeter calibrations

Flow meter No (2) for test section No(2)						
% F.S.R	Bulk Temperature (°C)	Mass Flow Rate ($kg\ hr^{-1}$)	Flowmetre Flow Rate ($m^3\ hr^{-1}$)	Velocity ($m\ s^{-1}$)	Kinematic Viscosity ($mm^2 s^{-1}$)	Re
10	25.7	262.1.	0.3037	0.488	16.72	433.1
	33.8	260.3	0.3146	0.506	12.85	583.5
	45.3	258.9	0.3032	0.487	9.24	782.1
20	25.7	464.2	0.5379	0.865	16.72	767.1
	33.9	462.5	0.5384	0.865	12.81	1001.8
	45.8	456.9	0.5353	0.860	9.12	1399.3
30	25.7	686.2	0.8038	1.292	16.72	1146.2
	35.8	679.5	0.7956	1.279	12.09	1568.6
	45.8	672.9	0.7874	1.266	9.12	2058.4
40	21.7	879.9	1.0175	1.636	19.25	1260.4
	35.8	875.0	1.0195	1.639	12.09	2009.9
	46.4	869.1	1.0184	1.637	8.98	2058.4
50	23.2	1124.4	1.3014	2.092	18.24	1700.9
	35.3	1117.7	1.3020	2.093	12.47	2528.4
	46.4	1111.9	1.3030	2.094	8.98	3460.7
60	21.6	1341.6	1.5514	2.922	19.32	1914.8
	34.8	1336.9	1.5570	2.503	12.47	2978.1
	45.5	1329.4	1.5570	2.503	9.19	4037.8
70	22.3	1571.4	1.8179	2.922	18.84	2301.0
	36.1	1557.0	1.8145	2.917	11.99	3609.5
	46.1	1549.2	1.8150	2.917	9.05	4037.8
80	23.6	1753.8	2.0303	3.263	17.99	2691.3
	34.9	1747.8	2.0356	3.272	12.43	3905.5
	46.7	1739.1	2.0382	3.276	8.91	5456.1
90	24.1	2009.4	2.3268	3.740	17.67	3139.1
	34.7	1994.0	2.3221	3.732	12.50	4428.1
	47.1	1982.0	2.3234	3.735	8.81	6284.9
100	26.1	2247.6	2.6054	4.188	16.49	3766.4
	35.6	2237.0	2.6062	4.189	12.17	5107.3
	47.2	2233.2	2.6180	4.208	8.79	7100.5

For Flowmeter No (2)

$$M_2\ (10\%) = 265.97 - 0.159\ T\ (^{o}C) \quad (4.16)$$

$$M_2\ (20\%) = 474.11 - 0.367\ T\ (^{o}C) \quad (4.17)$$

$$M_2\ (30\%) = 699.70 - 0.564\ T\ (^{o}C) \quad (4.18)$$

$$M_2\ (40\%) = 889.52 - 0.429\ T\ (^{o}C) \quad (4.19)$$

$$M_2\ (50\%) = 1136.77 - 0.536\ T\ (^{o}C) \quad (4.20)$$

$$M_2\ (60\%) = 1353.11 - 0.505\ T\ (^{o}C) \quad (4.21)$$

$$M_2\ (70\%) = 1591.99 - 0.941\ T\ (^{o}C) \quad (4.22)$$

$$M_2\ (80\%) = 1769.15 - 0.635\ T\ (^{o}C) \quad (4.23)$$

$$M_2\ (90\%) = 2036.94 - 1.184\ T\ (^{o}C) \quad (4.24)$$

$$M_2\ (100\%) = 2263.49 - 0.667\ T\ (^{o}C) \quad (4.25)$$

where:

M_1 and M_2 are mass flow rates in kg hr^{-1} for flowmeters No (1) and No (2) respectively, at given % F.S.R, and T is the bulk temperature in ^oC .

4.4 Check of thermal wall resistance

The thermal wall resistance for the bare tube test section (R_{w1}) was checked by applying Wilson's method with the crude oil. At similar bulk temperatures and heat fluxes as those used in the Santotherm 55 study, the overall heat transfer coefficient (U_t) was determined for a number of relatively high flow rates. The flow rate was kept high in order to prevent any formation of fouling in the Wilson experiment .

The data and results of Wilson's method for crude oil is shown in Table 4.4 . The graphs for both crude oil and Santotherm 55 are compared in Fig 4.4 . Both curves are identical and R_{w1} remained unchanged at 1.198×10^{-3} m^2 K W^{-1} . Wilson's method is only valid for a bare tube , therefore it was not applied to test section No(2) fitted with **HiTran** insert. It is assumed that R_{w2} for test section No(2) was also the same as that measured using Santotherm 55 at 6.75×10^{-4} m^2 K W^{-1} .

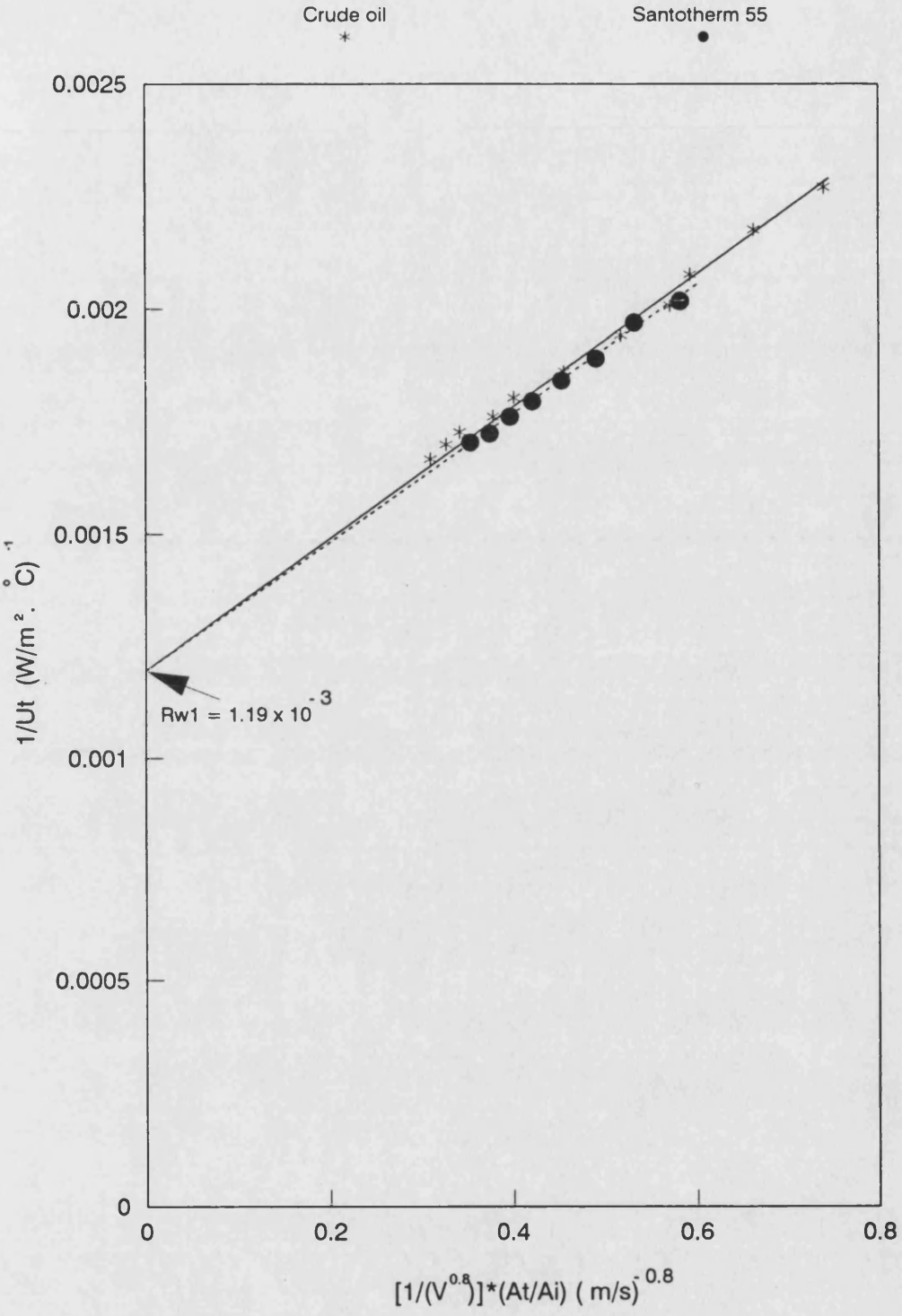

Fig (4.4) Wilson's plot for thermal resistance calculation

Comparsion between Santotherm 55 and Arabian Light Crude oil

4.5 Method of calculation for crude oil study

The methods of calculating the heat transfer coefficient , bulk and inner surface temperatures, friction factor and j_H-factor are identical to those used in the Santotherm 55 study. The efficiency of the test sections was calculated to be unchanged at 0.98 .

4.5.1 Fouling resistance

The fouling resistance is calculated as follows:

$$R_f = \frac{1}{U_t(t)} - \frac{1}{U_t(0)} \qquad (4.27)$$

Where ;

$U_t(t)$ is the overall heat transfer coefficient based on area A_t at time t ($W\ m^{-2}\ K^{-1}$)

$U_t(0)$ is the overall heat transfer coefficient based on area A_t at time zero ($W\ m^{-2}\ K^{-1}$)

U_t may be calculated from equations 3.25 and 3.29 as follows :

$$U_t = \frac{\eta\ Q_{(sup)}}{A_t\ (T_w - T_b)} \qquad (4.28)$$

where , η , $Q_{(sup)}$, A_t , T_w and T_b are defined in Chapter 3 (section 3.4)

Therefore , the fouling resistances for the test sections are calculated as follows :

$$R_{f1} = \left[\frac{(T_{w1} - T_{b1})}{\eta_1\ Q_{(sup)1}/A_{t1}}\right]_t - \left[\frac{(T_{w1} - T_{b1})}{\eta_1\ Q_{(sup)1}/A_{t1}}\right]_0 \qquad (4.29)$$

$$R_{f2} = \left[\frac{(T_{w2} - T_{b2})}{\eta_2\ Q_{(sup)2}/A_{t2}}\right]_t - \left[\frac{(T_{w2} - T_{b2})}{\eta_2\ Q_{(sup)2}/A_{t2}}\right]_0 \qquad (4.30)$$

Where :

$\eta 1 = \eta 2 = 0.98$

$A_{t1} = A_{t2} = 1.97 \times 10^{-2}$ (m^2)

T_{w1} , T_{w2} , T_{b1} and T_{b2} are calculated from equations 3.31 , 3.32 , 3.35 and 3.36 respectively . Therefore, at constant $Q_{(sup)}$ and T_b , R_{f1} and R_{f2} are calculated as follows:

$$R_{f1} = \frac{0.02\,(T_{w1(t)} - T_{w1(0)})}{Q_{(sup)1}} \qquad (4.31)$$

$$R_{f2} = \frac{0.02\,(T_{w2(t)} - T_{w2(0)})}{Q_{(sup)2}} \qquad (4.32)$$

where

$T_{w(0)}$ is the wall temperature at time = 0 (°C)

$T_{w(t)}$ is the wall temperature at time = t (°C)

The subscripts 1 and 2 denote test sections No(1) and No(2) respectively .

4.5.2 Solubility of gases in liquids

The solubility of a gas in a liquid may be estimated as follows[228] :

$$X_m = \left[\frac{R\,T}{P_{(g)}\,L(Ost)\,V°(l)} + 1\right]^{-1} \qquad (4.33)$$

Where ;

X_m is the mole fraction solubility at a gas partial pressure of 1 atm (kmol/kmol)

$P_{(g)}$ is the partial pressure of the gas (atm)

T is the local absolute temperature (K)

R is the universal gas constant

$R = 0.08205$ $\left(\frac{m^3\ atm}{kmol^{-1}\ K^{-1}}\right)$

$V^{o}(l)$ is the molar volume of liquid at 1 atm and the measured temperature (m^3 $kmol^{-1}$)

L(Ost) is the Ostwald coefficient which is defined as the ratio of the volume of gas absorbed to the volume of the absorbent liquid , all measured at the same temperature .

In order to use equation 4.33 , The Ostwald coefficient ($L_{(Ost)}$) has to be experimentally available for the particular gas soluble in the particular liquid. Unfortunately , Ostwald coefficients for nitrogen , oxygen and helium gases soluble in light crude oils (such as Arabian light crude oil) are not available in the literature e.g IUPAC, solubility data series[228]. Therefore , it is not possible to calculate accurately the mole fraction of nitrogen , oxygen or helium gases absorbed by Arabian light crude oil .

4.5.2.1 Effect of temperature and pressure on the solubility of gases

The solubility of a gas in a liquid is affected by both temperature and pressure . The solubilities of gases like nitrogen and oxygen in liquids decrease with increasing temperature. However the solubilities of inert gases such as helium or neon decrease with increasing temperature to a certain limit . When the temperature reaches 300 to 315 K , their solubilities start to increase with temperature .

Examples of the variation of solubility of nitrogen , oxygen and helium gases in water with temperature are shown in Fig 4.5 . The variations of solubility with pressure of oxygen gas in gas oil and nitrogen gas in polydimethyisiloxane oil are shown in Figs 4.6 and 4.7 respectively .

The effect of temperature and pressure on gas solubility depends on the type of gas but not on the absorbing liquid[228]. That is the solubilities of nitrogen and oxygen increase with increasing pressure and decreasing temperature . Consequently , it is a reasonable assumption that the solubilities of nitrogen and oxygen in Arabian light crude oil would follow similar behaviours to those shown in Figs 4.5 to 4.7 .

4.6 Results and discussion for crude oil study

4.6.1 Heat transfer and fouling results

The experimental conditions for the heat transfer studies with crude oil are summarised in Tables 4.5 to 4.19 , showing that around 4500 data points for both test sections were gathered .

The local heat transfer coefficient (hi) , with and without the use of the **HiTran** insert , has been obtained for liquid phase flow and for nucleate boiling conditions . The effects of pressure , heat flux and flow rate on h_i have been studied for the

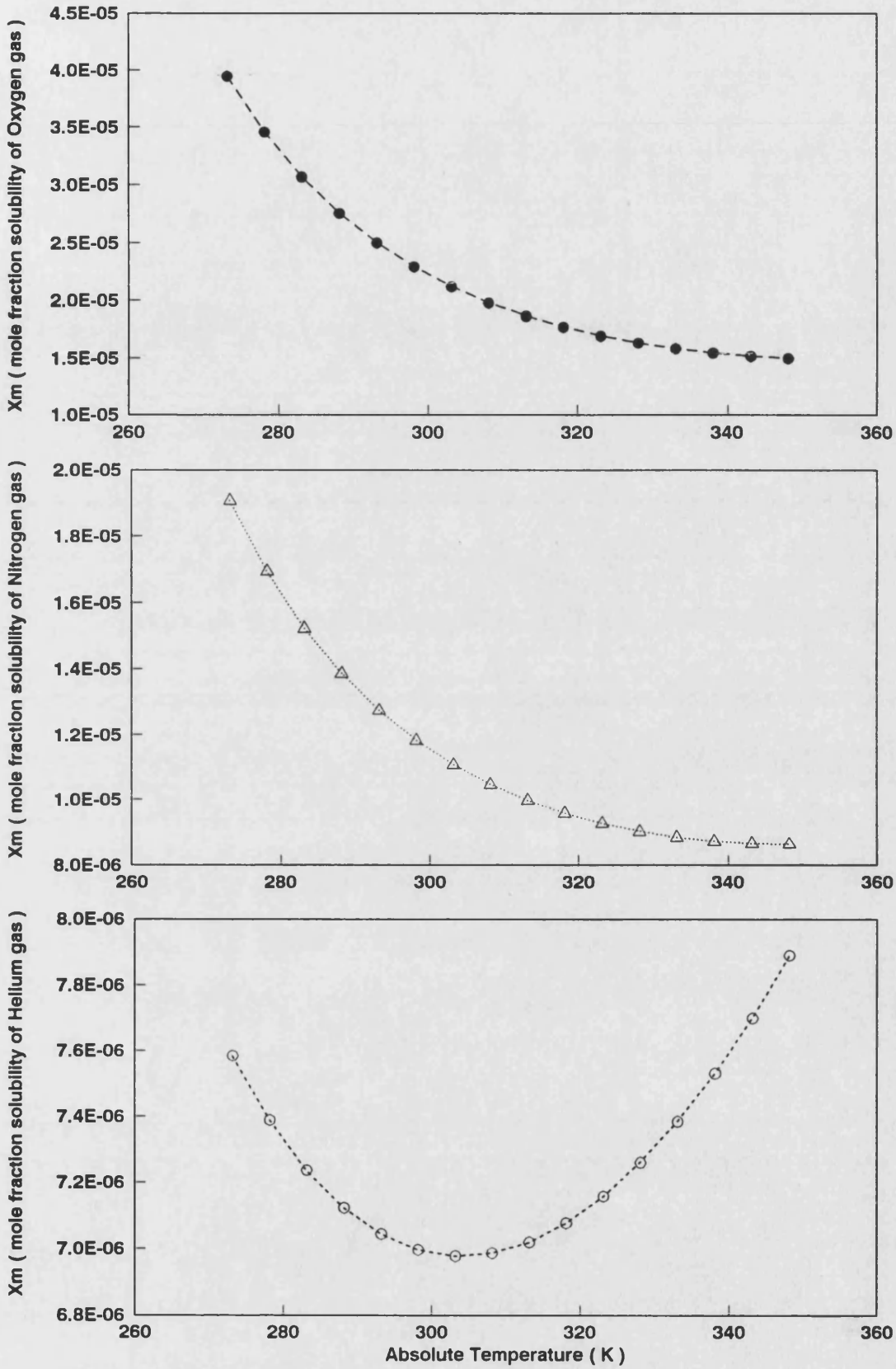

Fig (4.5) Variation of mole fraction solubility (Xm) with temperature (T)

solubility of Helium , Nitrogen and Oxygen gases in Water at 1 atm

[After IUPAC Solubility Data Series (228)]

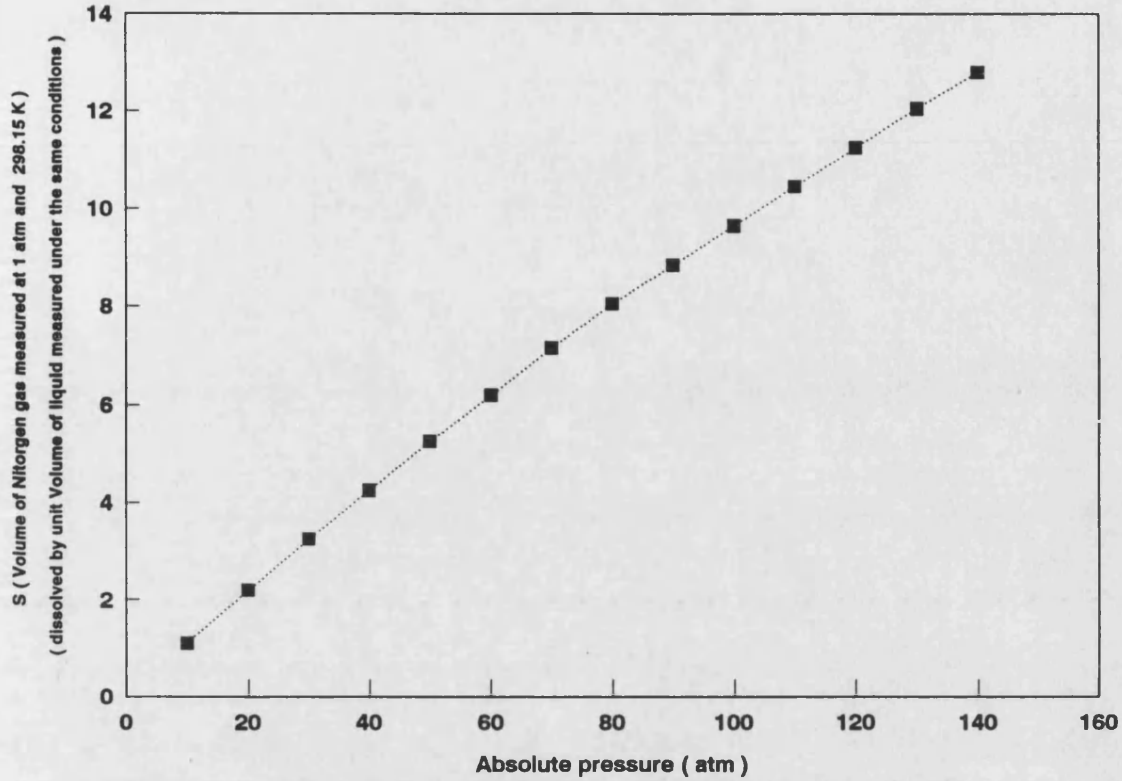

Fig (4.6) Variation of solubility (S) with pressure (P)

solubility of nitrogen gas in gas oil at 298 K

[After IUPAC Solubility Data Series (228)]

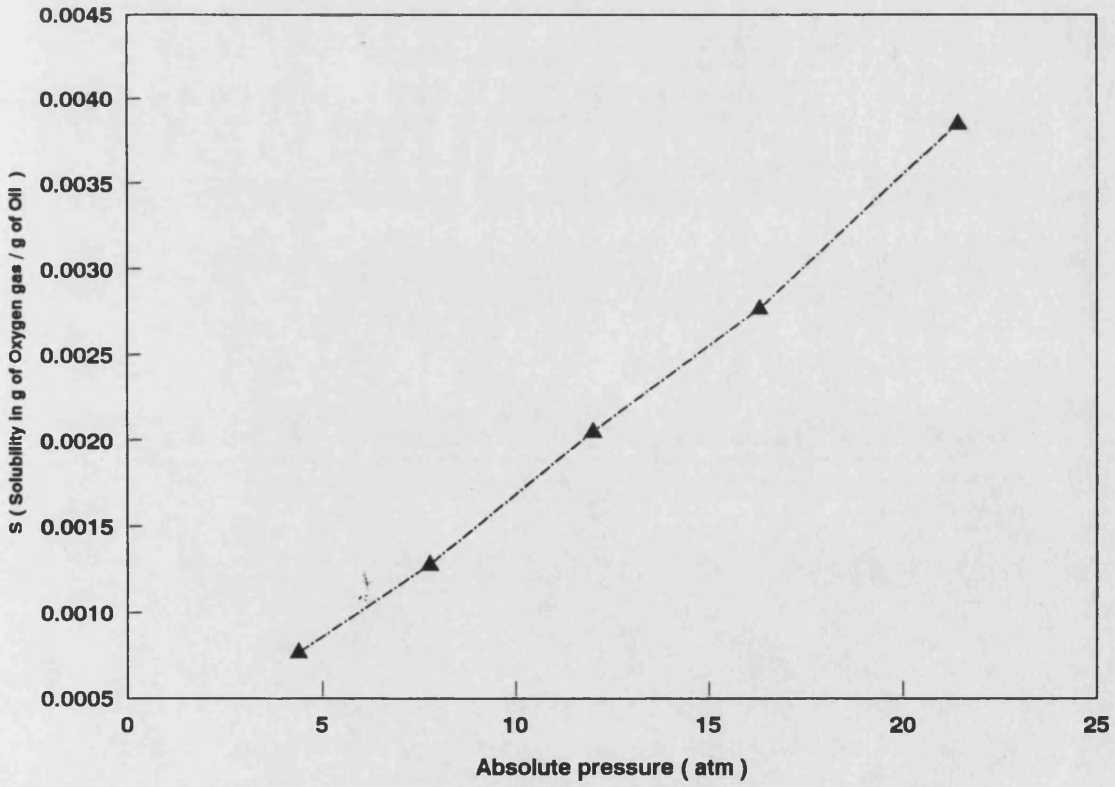

Fig (4.7) Variation of solubility (S) with pressure (P)

solubility of oxygen gas in polydimethylsiloxane oil at 303 K

[After IUPAC Solubility Data Series (228)]

Table No(4.5) Summary of Experimental Conditions of Crude heat transfer study

Test section No(2) is fitted with low loop density HiTran insert (LDI-B) and test section No(1) is a bare tube

Fluid (Arabian light crude oil)

Equipment under pressure of nitrogen (N_2) gas

| Total Pressure (bar gauge) | Bulk Temperature (°C) | Power supply (W) | Condition of test section | % F.S.R (full scale flow meter reading) | | |

Table No(4.6) Summary of Experimental Conditions of Crude heat transfer study

Test section No(2) is fitted with low loop density HITran insert (LDI-B) and test section No(1) is a bare tube

Fluid (Arabian light crude oil)

Equipment under pressure of nitrogen (N_2) gas

% F.S.R	Bulk Temperature (°c)	Power supply (W)	Condition of test section	Total pressure (bar gauge) 6	7	8	9	10	11	12	13	14	15
20 %	140	200	BARE	* * * * *				* * * * * * * * *			* * * * *		
			LDI - B	* * * * *				* * * * * * * * *			* * * * *		
		300	BARE										
			LDI - B										
		400	BARE	* * * * *				* * * * * * * * *			* * * * *		
			LDI - B	* * * * *				* * * * * * * * *			* * * * *		
		500	BARE										
			LDI - B										
		600	BARE	* * * * *				* * * * *		* * * * * * * * *			
			LDI - B	* * * * *				* * * * *		* * * * * * * * *			
		700	BARE										
			LDI - B										
		800	BARE	* * * * *				* * * * *		* * * * *		* * * * *	
			LDI - B	* * * * *				* * * * *		* * * * *		* * * * *	
		900	BARE										
			LDI - B										
		1000	BARE	* * * * *				* * * * *		* * * * *		* * * * *	
			LDI - B	* * * * *				* * * * *		* * * * *		* * * * *	
		1100	BARE										
			LDI - B										

T1 for test section No(1)
T5 for test section No(2)

T2 for test section No(1)
T6 for test section No(2)

T3 for test section No(1)
T7 for test section No(2)

T4 for test section No(1)
T8 for test section No(2)

ΔP1 for test section No(1)
ΔP2 for test section No(2)

Number of measurements :

x once
* twice
▲ three times
■ four times

Type of HITran inserts :

LDI - B (low loop density)

The supplier of HITran inserts :

B - set supplied by Norton Co.

Table No(4.7) Summary of Experimental Conditions of Crude heat transfer study

Test section No(2) is fitted with low loop density HITran insert (LDI-B) and test section No(1) is a bare tube

Fluid (Arabian light crude oil)

Equipment under pressure of nitrogen (N_2) gas

% F.S.R	Bulk Temperature (°c)	Power supply (W)	Condition of test section	Total pressure (bar gauge) 6	7	8	9	10	11	12	13	14	15
20 %	50	200	BARE	* * * * *		* * * * *		* * * * *		* * * * *		* * * * *	
			LDI - B	* * * * *		* * * * *		* * * * *		* * * * *		* * * * *	
		300	BARE										
			LDI - B										
		400	BARE	* * * * *		* * * * *		* * * * *		* * * * *		* * * * *	
			LDI - B	* * * * *		* * * * *		* * * * *		* * * * *		* * * * *	
		500	BARE										
			LDI - B										
		600	BARE	* * * * *		* * * * *		* * * * *		* * * * *		* * * * *	
			LDI - B	* * * * *		* * * * *		* * * * *		* * * * *		* * * * *	
		700	BARE										
			LDI - B										
		800	BARE	* * * * *		* * * * *		* * * * *		* * * * *			* * * * *
			LDI - B	* * * * *		* * * * *		* * * * *		* * * * *			* * * * *
		900	BARE										
			LDI - B										
		1000	BARE	* * * * *		* * * * *		* * * * *		* * * * *			* * * * *
			LDI - B	* * * * *		* * * * *		* * * * *		* * * * *			* * * * *
		1100	BARE										
			LDI - B										

T1 for test section No(1)
T5 for test section No(2)

T2 for test section No(1)
T6 for test section No(2)

T3 for test section No(1)
T7 for test section No(2)

T4 for test section No(1)
T8 for test section No(2)

ΔP1 for test section No(1)
ΔP2 for test section No(2)

Number of measurements :

x once
* twice
▲ three times
■ four times

Type of HITran inserts :

LDI - B (low loop density)

The supplier of HITran inserts :

B - set supplied by Norton Co.

Table No(4.8) Summary of Experimental Conditions of Crude heat transfer study

Test section No(2) is fitted with low loop density HiTran insert (LDI-B) and test section No(1) is a bare tube

Fluid (Arabian light crude oil with 10% by weight sludge)

Equipment under pressure of nitrogen (N_2) gas

% F.S.R	Bulk Temperature (°c)	Power supply (W)	Condition of test section	Total pressure (bar gauge) 5	6	7	8	9	10	12	13	14	15
10 %	140	200	BARE										
			LDI - B										
		300	BARE										
			LDI - B										
		400	BARE										
			LDI - B										
		500	BARE										
			LDI - B										
		600	BARE										
			LDI - B										
		800	BARE										
			LDI - B										
		900	BARE	x x x x x			x x x x x		x x x x x		x x x x x		x x x x x
			LDI - B	x x x x x			x x x x x		x x x x x		x x x x x		x x x x x
		1000	BARE										x x x x x
			LDI - B										x x x x x
		1100	BARE										x x x x x
			LDI - B										x x x x x
		1200	BARE									x x x x x	
			LDI - B									x x x x x	

T1 for test section No(1) / T5 for test section No(2)

T2 for test section No(1) / T6 for test section No(2)

T3 for test section No(1) / T7 for test section No(2)

T4 for test section No(1) / T8 for test section No(2)

ΔP1 for test section No(1) / ΔP2 for test section No(2)

Number of measurements :

x once

* twice

▲ three times

■ four times

Type of HiTran inserts :

LDI - B (low loop density)

The supplier of HiTran inserts :

B - set supplied by Norton Co.

Table No(4.9) Summary of Experimental Conditions of Crude heat transfer study

Test section No(2) is fitted with low loop density HiTran insert (LDI-B) and test section No(1) is a bare tube

Fluid (Arabian light crude oil with 10% by weight sludge)

Equipment under pressure of nitrogen (N_2) gas

% F.S.R	Bulk Temperature (°c)	Power supply (W)	Condition of test section	Total pressure (bar gauge) 5	6	7	8	9	10	11	12	13	14.5
20 %	140	200	BARE										
			LDI - B										
		300	BARE										
			LDI - B										
		400	BARE										
			LDI - B										
		500	BARE										
			LDI - B										
		600	BARE										
			LDI - B										
		800	BARE										
			LDI - B										
		900	BARE	x x x x x			x x x x x		x x x x x		x x x x x		* * * * *
			LDI - B	x x x x x			x x x x x		x x x x x		x x x x x		* * * * *
		1000	BARE										x x x x x
			LDI - B										x x x x x
		1100	BARE										x x x x x
			LDI - B										x x x x x
		1200	BARE										x x x x x
			LDI - B										x x x x x

T1 for test section No(1)
T5 for test section No(2)

T2 for test section No(1)
T6 for test section No(2)

T3 for test section No(1)
T7 for test section No(2)

T4 for test section No(1)
T8 for test section No(2)

Δ P1 for test section No(1)
Δ P2 for test section No(2)

Number of measurements :

x once
* twice
▲ three times
■ four times

Type of HiTran inserts :

LDI - B (low loop density)

The supplier of HiTran inserts :

B - set supplied by Norton Co.

Table No(4.12) Summary of Experimental Conditions of Crude heat transfer study

Test section No(2) is fitted with low loop density HiTran insert (LDI-B) and test section No(1) is a bare tube

Fluid (Arabian light crude oil with 10% by weight sludge)

Equipment under pressure of nitrogen (N_2) gas

% F.S.R	Bulk Temperature (°c)	Power supply (W)	Condition of test section	Total pressure (bar gauge) 5	5.5	7	8	9	9.5	10	11	11.5	12
40 %	65	200	BARE	x x x x x			x x x x x		x x x x x			x x x x x	
			LDI - B	x x x x x			x x x x x		x x x x x			x x x x x	
		300	BARE										
			LDI - B										
		400	BARE	x x x x x			x x x x x		x x x x x			x x x x x	
			LDI - B	x x x x x			x x x x x		x x x x x			x x x x x	
		500	BARE										
			LDI - B										
		600	BARE	x x x x x			x x x x x x x x x						x x x x x
			LDI - B	x x x x x			x x x x x x x x x						x x x x x
		700	BARE										
			LDI - B										
		800	BARE										
			LDI - B										
		900	BARE	x x x x x			x x x x x x x x x						x x x x x
			LDI - B	x x x x x			x x x x x x x x x						x x x x x
		1000	BARE										
			LDI - B										
		1100	BARE	x x x x x			x x x x x		x x x x x				x x x x x
			LDI - B	x x x x x			x x x x x		x x x x x				x x x x x

T1 for test section No(1)
T5 for test section No(2)

T2 for test section No(1)
T6 for test section No(2)

T3 for test section No(1)
T7 for test section No(2)

T4 for test section No(1)
T8 for test section No(2)

ΔP1 for test section No(1)
ΔP2 for test section No(2)

Number of measurements :

x once
* twice
▲ three times
■ four times

Type of HiTran Inserts :

LDI - B (low loop density)

The supplier of HiTran Inserts :

B - set supplied by Norton Co.

Table No(4.13) Summary of Experimental Conditions of Crude heat transfer study

Test section No(2) is fitted with low loop density HITran insert (LDI-B) and test section No(1) is a bare tube

Fluid (Arabian light crude oil with 10% by weight sludge)

Equipment under pressure of nitrogen (N_2) gas

% F.S.R	Bulk Temperature (°c)	Power supply (W)	Condition of test section	Total pressure (bar gauge) 4.5	5	7	8	9	9.5	10	11	11.5	12
60 %	65	200	BARE	x x x x x			x x x x x x x x x x				x x x x x		
			LDI - B	x x x x x			x x x x x x x x x x				x x x x x		
		300	BARE										
			LDI - B										
		400	BARE	x x x x x			x x x x x x x x x x				x x x x x		
			LDI - B	x x x x x			x x x x x x x x x x				x x x x x		
		500	BARE										
			LDI - B										
		600	BARE	x x x x x			x x x x x x x x x x				x x x x x		
			LDI - B	x x x x x			x x x x x x x x x x				x x x x x		
		700	BARE										
			LDI - B										
		800	BARE										
			LDI - B										
		900	BARE	x x x x x			x x x x x		x x x x x		x x x x x		
			LDI - B	x x x x x			x x x x x		x x x x x		x x x x x		
		1000	BARE										
			LDI - B										
		1100	BARE	x x x x x			x x x x x		x x x x x		x x x x x		
			LDI - B	x x x x x			x x x x x		x x x x x		x x x x x		

T1 for test section No(1)
T5 for test section No(2)

T2 for test section No(1)
T6 for test section No(2)

T3 for test section No(1)
T7 for test section No(2)

T4 for test section No(1)
T8 for test section No(2)

ΔP1 for test section No(1)
ΔP2 for test section No(2)

Number of measurements :

x once
* twice
▲ three times
■ four times

Type of HITran inserts :

LDI - B (low loop density)

The supplier of HITran inserts :

B - set supplied by Norton Co.

Table No(4.14) Summary of Experimental Conditions of Crude heat transfer study

Test section No(2) is fitted with low loop density HiTran insert (LDI-B) and test section No(1) is a Bare tube

Fluid (Arabian light crude oil with 10% by weight sludge)

Equipment under pressure of helium (He) gas

% F.S.R	Bulk Temperature (°c)	Power supply (W)	Condition of test section	Total pressure (bar gauge) 5	6	7	8	9	10	12	13	14	15
10 %	140	200	BARE										
			LDI - B										
		300	BARE										
			LDI - B										
		400	BARE										
			LDI - B										
		500	BARE										
			LDI - B										
		600	BARE										
			LDI - B										
		800	BARE										
			LDI - B										
		900	BARE										
			LDI - B										
		1000	BARE										
			LDI - B										
		1100	BARE						* * * * *				
			LDI - B						* * * * *				
		1200	BARE										
			LDI - B										

T1 for test section No(1)
T5 for test section No(2)

T2 for test section No(1)
T6 for test section No(2)

T3 for test section No(1)
T7 for test section No(2)

T4 for test section No(1)
T8 for test section No(2)

ΔP1 for test section No(1)
ΔP2 for test section No(2)

Number of measurements :

x once
* twice
▲ three times
■ four times

Type of HiTran Inserts :

LDI - B (low loop density)

The supplier of HiTran Inserts :

B - set supplied by Norton Co.

Table No(4.15) Summary of Experimental Conditions of Crude heat transfer study

Test section No(2) is fitted with low loop density HITran insert (LDI-B) and test section No(1) is a Bare tube

Fluid (Arabian light crude oil with 10% by weight sludge)

Equipment under pressure of heliume (He) gas

% F.S.R	Bulk Temperature (°c)	Power supply (W)	Condition of test section	Total pressure (bar gauge) 5	6	7	8	9	10	12	13	14	15
20 %	140	200	BARE										
			LDI - B										
		300	BARE										
			LDI - B										
		400	BARE										
			LDI - B										
		500	BARE										
			LDI - B										
		600	BARE										
			LDI - B										
		800	BARE										
			LDI - B										
		900	BARE				■ ■ ■ ■ ■		■ ■ ■ ■ ■				
			LDI - B				■ ■ ■ ■ ■		■ ■ ■ ■ ■				
		1000	BARE										
			LDI - B										
		1100	BARE						* * * * *				
			LDI - B						* * * * *				
		1200	BARE										
			LDI - B										

T1 for test section No(1)
T5 for test section No(2)

T2 for test section No(1)
T6 for test section No(2)

T3 for test section No(1)
T7 for test section No(2)

T4 for test section No(1)
T8 for test section No(2)

ΔP1 for test section No(1)
ΔP2 for test section No(2)

Number of measurements :

x once
* twice
▲ three times
■ four times

Type of HITran Inserts :

LDI - B (low loop density)

The supplier of HITran Inserts :

B - set supplied by Norton Co.

Table No(4.16) Summary of Experimental Conditions of Crude heat transfer study

Test section No(2) is fitted with low loop density HITran Insert (LDI-B) and test section No(1) is a bare tube

Fluid (Arabian light crude oil with 10% by weight sludge)

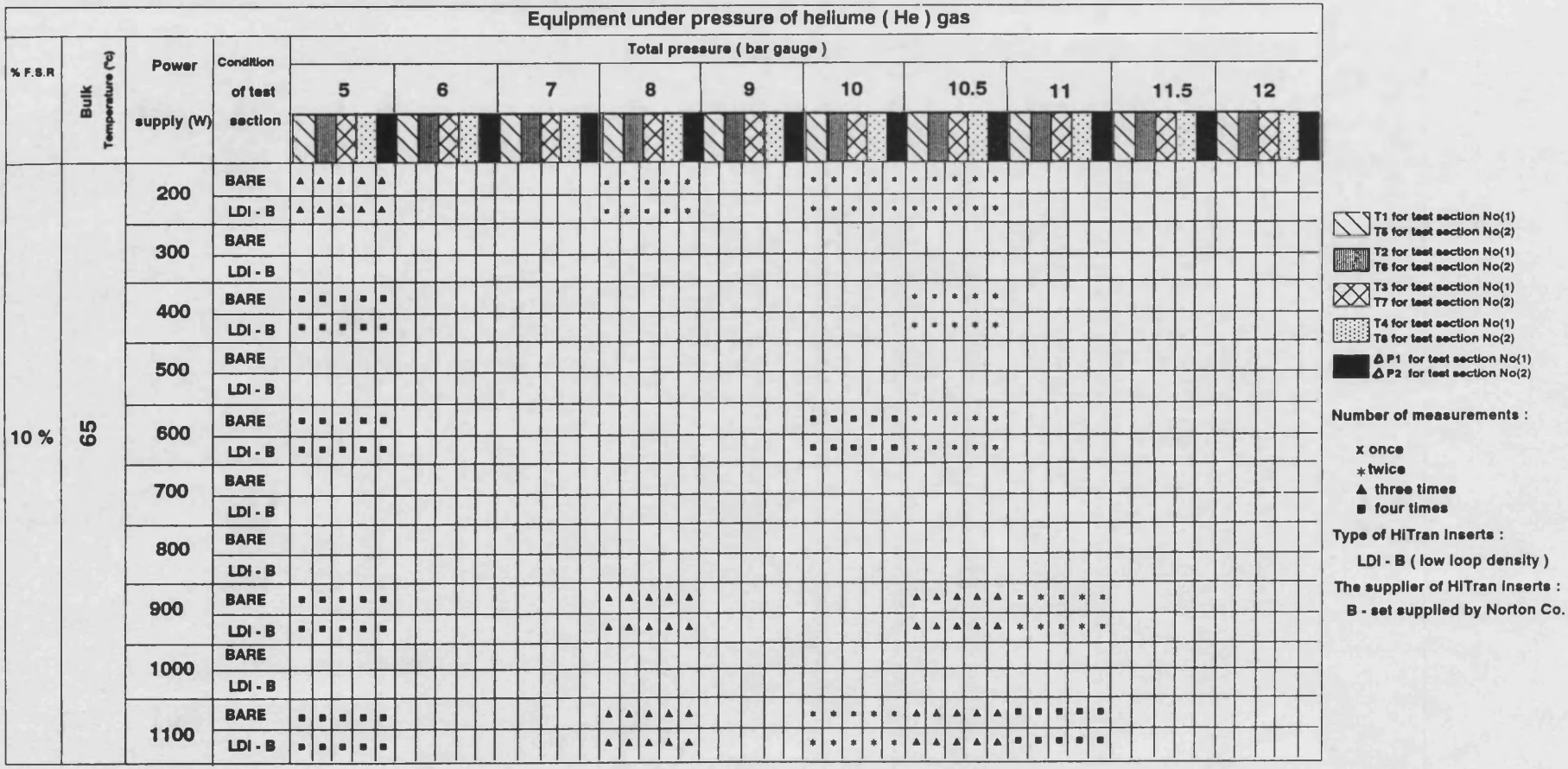

Table No(4.17) Summary of Experimental Conditions of Crude heat transfer study

Test section No(2) is fitted with low loop density HITran insert (LDI-B) and test section No(1) is a bare tube

Fluid (Arabian light crude oil with 10% by weight sludge)

Equipment under pressure of heliume (He) gas

% F.S.R	Bulk Temperature (°c)	Power supply (W)	Condition of test section	Total pressure (bar gauge) 5.5	6	7	8	9	10	10.5	11	11.5	12
20 %	65	200	BARE	x x x x x			* * * * *		* * * * *				
			LDI - B	x x x x x			* * * * *		* * * * *				
		300	BARE										
			LDI - B										
		400	BARE	▲ ▲ ▲ ▲ ▲			* * * * *		* * * * *				
			LDI - B	▲ ▲ ▲ ▲ ▲			* * * * *		* * * * *				
		500	BARE										
			LDI - B										
		600	BARE	* * * * *			* * * * *		* * * * *				
			LDI - B	* * * * *			* * * * *		* * * * *				
		700	BARE										
			LDI - B										
		800	BARE										
			LDI - B										
		900	BARE	* * * * *			▲ ▲ ▲ ▲ ▲		* * * * *				
			LDI - B	* * * * *			▲ ▲ ▲ ▲ ▲		* * * * *				
		1000	BARE										
			LDI - B										
		1100	BARE		* * * * *		* * * * *		* * * * *				
			LDI - B		* * * * *		* * * * *		* * * * *				

T1 for test section No(1)
T5 for test section No(2)

T2 for test section No(1)
T6 for test section No(2)

T3 for test section No(1)
T7 for test section No(2)

T4 for test section No(1)
T8 for test section No(2)

Δ P1 for test section No(1)
Δ P2 for test section No(2)

Number of measurements :

x once
* twice
▲ three times
■ four times

Type of HITran inserts :

LDI - B (low loop density)

The supplier of HITran inserts :

B - set supplied by Norton Co.

Table No(4.18) Summary of Experimental Conditions of Crude heat transfer study

Test section No(2) is fitted with low loop density HITran insert (LDI-B) and test section No(1) is a bare tube

Fluid (Arabian light crude oil with 10% by weight sludge)

Equipment under pressure of heliume (He) gas

% F.S.R	Bulk Temperature (°c)	Power supply (W)	Condition of test section	Total pressure (bar gauge) 5.5	6	7	8	9	10	10.5	11	11.5	12
40 %	65	200	BARE	x x x x x			x x x x x		* * * * *				
			LDI - B	x x x x x			x x x x x		* * * * *				
		300	BARE										
			LDI - B										
		400	BARE	x x x x x			x x x x x		* * * * *				
			LDI - B	x x x x x			x x x x x		* * * * *				
		500	BARE										
			LDI - B										
		600	BARE	x x x x x			x x x x x		* * * * *				
			LDI - B	x x x x x			x x x x x		* * * * *				
		700	BARE										
			LDI - B										
		800	BARE										
			LDI - B										
		900	BARE	* * * * *			x x x x x		* * * * *				
			LDI - B	* * * * *			x x x x x		* * * * *				
		1000	BARE										
			LDI - B										
		1100	BARE		* * * * *		x x x x x		* * * * *				
			LDI - B		* * * * *		x x x x x		* * * * *				

T1 for test section No(1)
T5 for test section No(2)

T2 for test section No(1)
T6 for test section No(2)

T3 for test section No(1)
T7 for test section No(2)

T4 for test section No(1)
T8 for test section No(2)

ΔP1 for test section No(1)
ΔP2 for test section No(2)

Number of measurements :

x once
* twice
▲ three times
■ four times

Type of HITran inserts :

LDI - B (low loop density)

The supplier of HITran inserts :

B - set supplied by Norton Co.

Table No(4.19) Summary of Experimental Conditions of Crude heat transfer study

Test section No(2) is fitted with low loop density HITran insert (LDI-B) and test section No(1) is a bare tube

Fluid (Arabian light crude oil with 10% by weight sludge)

Equipment under pressure of heliume (He) gas

% F.S.R	Bulk Temperature (°c)	Power supply (W)	Condition of test section	Total pressure (bar gauge) 5.5	6	7	8	9	10	10.5	11	11.5	12
60 %	65	200	BARE	x x x x x			x x x x x		* * * * *				
			LDI - B	x x x x x			x x x x x		* * * * *				
		300	BARE										
			LDI - B										
		400	BARE	x x x x x			x x x x x		x x x x x				
			LDI - B	x x x x x			x x x x x		x x x x x				
		500	BARE										
			LDI - B										
		600	BARE	x x x x x			x x x x x		x x x x x				
			LDI - B	x x x x x			x x x x x		x x x x x				
		700	BARE										
			LDI - B										
		800	BARE										
			LDI - B										
		900	BARE	x x x x x			x x x x x		x x x x x				
			LDI - B	x x x x x			x x x x x		x x x x x				
		1000	BARE										
			LDI - B										
		1100	BARE	x x x x x			x x x x x		x x x x x				
			LDI - B	x x x x x			x x x x x		x x x x x				

T1 for test section No(1)
T5 for test section No(2)

T2 for test section No(1)
T6 for test section No(2)

T3 for test section No(1)
T7 for test section No(2)

T4 for test section No(1)
T8 for test section No(2)

ΔP1 for test section No(1)
ΔP2 for test section No(2)

Number of measurements :

x once
* twice
▲ three times
■ four times

Type of HITran inserts :

LDI - B (low loop density)

The supplier of HITran inserts :

B - set supplied by Norton Co.

following ranges of Reynolds and Prandtl numbers : $1200 < Re < 38000$ and $27 < Pr < 110$.

The heat transfer factors (j_H) and the friction factors (f) for crude oil are compared with those for Santotherm 55 measured under similar experimental conditions. The empirical correlations generated in the Santotherm 55 study were tested with crude oil results .

Seven fouling runs have been carried out. In the first six runs the test equipment was maintained under elevated pressure using inert gases and no fouling occurred (the test sections were dismantled and physically inspected for fouling) . In the seventh run the equipment was filled up as completely as practicable with crude oil and pressurised to a desired value by means of a hand pump . In this last run fouling occurred in the bare tube only and not in the tube fitted with the **HiTran** insert . The experimental conditions of the fouling runs are summarised in Table 4.20 .

Examples heat transfer and fouling results are tabulated in Appendix C .

Table (4.20) Summary of Fouling Runs

Number Of Fouling Run	Bulk Temperature (°C)	Tank Pressure bar (gauge)	Fluid	Experimental Conditions	Duration Of experiment	Number of data points	Results and Comment
Run NO(1)	140	4.1 bar of crude vapour pressure 4.1 bar of 100 % N_2 Total pressure = 8.2 bar	Arabian Light Crude Oil	20 % F.S.R q = 42.14 kW/m² q = 54.18 kW/m²	20 hr for q = 42.14 kW/m² 49 hr for q = 54.18 kW/m² Total = 69 hrs	276 readings 1932 data points	Fouling did not occur , and the overall heat transfer coefficient increased with time . The following aspects were believed to be the cause of non-fouling :- (1) The absence of oxygen from the rig . (2) The concentration of asphaltene in the crude is too small . (3) The inner surface temperature is too low to cause fouling .
Run NO(2)	140	4.1 bar of crude vapour pressure 4.1 bar of 95 % N_2 and 5 % O_2 Total pressure = 8.2 bar	Arabian Light Crude Oil	20 % F.S.R q = 54.18 kW/m²	75 hrs	200 readings 1400 data points	Although , oxygen gas was used in this Run , fouling did not occur . The overall heat transfer coefficient was also increased with time . The tank pressure was decreas with time . The percentage of Asphaltene had to be increased in the next run .
Run NO(3)	140	4.1 bar of crude vapour pressure 4.1 bar of 95 % N_2 and 5 % O_2 Total pressure = 8.2 bar	Arabian Light Crude Oil with 10% by weight of Refinery sludge	20 % F.S.R q = 54.18 kW/m²	19 hrs	76 readings 532 data points	This run had to detemenated due to mechanical failure of the recirculation pump . No fouling occured . The next run had to be with similar experimental conditions as in this run .
Run NO(4)	140	4.1 bar of crude vapour pressure 4.1 bar of 95 % N_2 and 5 % O_2 Total pressure = 8.2 bar	Arabian Light Crude Oil with 10% by weight of Refinery sludge	20 % F.S.R q = 54.18 kW/m²	120 hrs	480 readings 3360 data points	The inner surface temperature (Ti) of bare tube decreased 10 °C in the first three hours then became steady . No fouling occured . In order to provide a higher (Ti) , the next run had to be under high pressure of nitrogen gas .
Run NO(5)	140	4.1 bar of crude vapour pressure 8.4 bar of 95 % N_2 and 5 % O_2 Total pressure = 12.5 bar	Arabian Light Crude Oil with 10% by weight of Refinery sludge	20 % F.S.R 10 % F.S.R q = 54.18 kW/m²	19 hr for 20 % F.S.R 29 hr for 10 % F.S.R Total = 48 hrs	192 readings 1344 data points	The inner surface temperature (Ti) of bare tube decreased 17 °C in the first three hours then became steady . No fouling occured . In order to provide a higher (Ti) , the next run had to be under pressure of less soluble gas . Helium gas was chosen to use in the next run .
Run NO(6)	74	10.2 bar of He gas (for 22 hrs) Then 12.0 bar of 84 % He and 16 % Air (to the end of the run)	Arabian Light Crude Oil with 10% by weight of Refinery sludge	10 % F.S.R q = 66.22 kW/m²	22 hr under He gas Pressure 53 hr under mixture of He and Air Total = 75 hrs	300 readings 2100 data points	The inner surface temperature (Ti) of bare tube was higher than the previous runs (240 °C) . Ti was reduced 4 °C under He pressure and 16 °C under the mixture of He and Air pressure . No fouling occured . Degassing of the gases (N_2 or He) on the inner surface of bare tube , was believed to be the couse of Ti reduction . The next run had to be under non-gas pressure (by filling up the test equipment with crude oil)
Run NO(7)	74	Varied between 4.5 bar and 13.1 bar unintentionally	Arabian Light Crude Oil with 10% by weight of Refinery sludge	10 % F.S.R q = 66.22 kW/m²	185 hrs	740 readings 5180 data points	The inner surface temperature (Ti) of bare tube was less the previous run (220 °C) . The fouling did start after 10 hrs. The pressure in the equipment was instable . The instability caused a fluctuation in Ti thus the fouling resistance of the bare tube was in the shape of saw-teeth .

4.6.2 Discussion of crude oil results

The results of the crude oil study are discussed in the form of a case study , under the following headings :

4.6.2.1 Comparison between Santotherm 55 and crude oil .
- 4.6.2.1.1 Friction factors .
- 4.6.2.1.2 j_H - factors .
- 4.6.2.1.3 Modified heat transfer factors (j_{HM}) .

4.6.2.2 Fouling run No 1 .

4.6.2.3 Heat transfer study on nucleate boiling of crude oil
- 4.6.2.3.1 Literature background .
- 4.6.2.3.2 Experimental investigation .

4.6.2.4 Fouling runs No 2 to No 5 .

4.6.2.5 Comparison between effect of nitrogen and helium gases on h_i and T_i .

4.6.2.6 Fouling runs No 6 and No 7 .

4.6.2.7 Conclusions on the crude oil results .

4.6.2.1 Comparison between Santotherm 55 and crude oil

4.6.2.1.1 Friction factors

Fig 4.8 shows a good agreement between the crude oil and Santotherm 55 data points for the bare tube test section No(1) . It also shows that , for fully developed turbulent flow ($Re > 10^4$) , the friction factor of the bare tube is well correlated by equation 3.101 .

Fig 4.9 shows the friction factor results for crude oil in test section No(2) fitted with LDI-B insert . The Santotherm 55 and crude oil results are in good agreement with equation 3.102 .

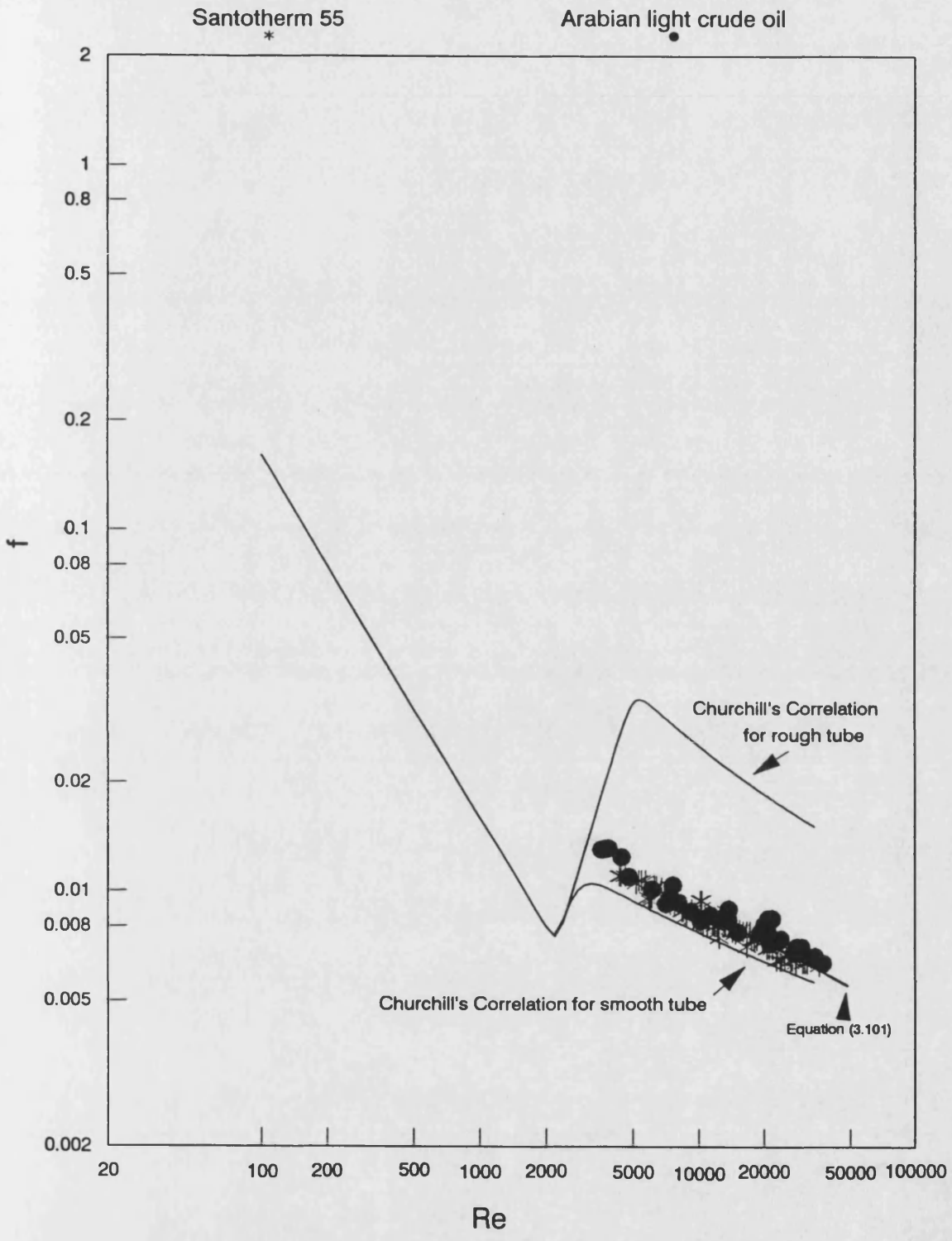

Fig (4.8) Friction factor (f) vs Reynolds number (Re)

Comparsion between Santotherm 55 and Arabian light crude oil

Bare tube test section No(1) ; $12 < q < 48.2$ kW/m² and $30 < Pr < 110$

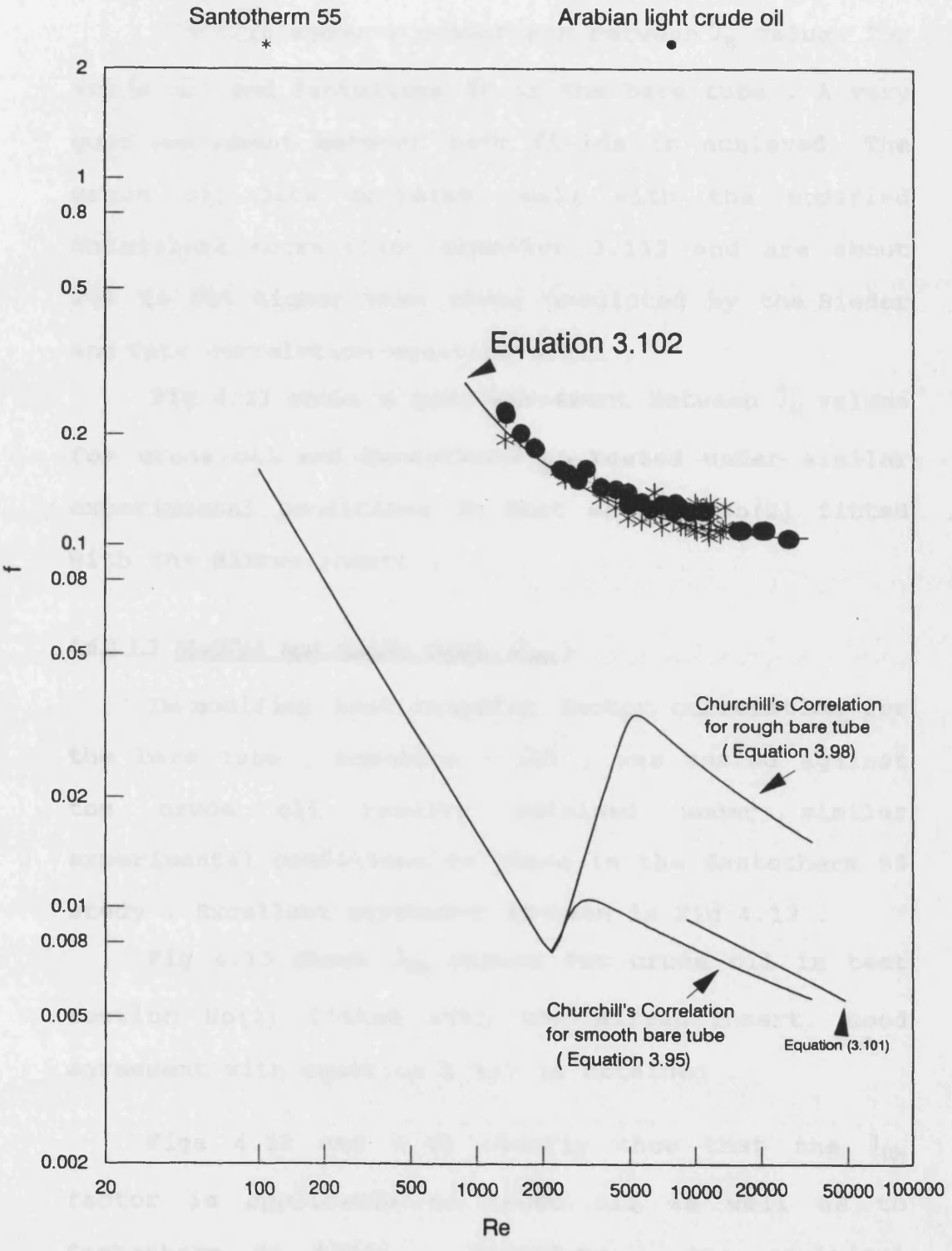

Fig (4.9) Friction factor (f) vs Reynolds number (Re)

Comparsion between Santotherm 55 and Arabian light crude oil

Test section No(2) fitted with LDI-B , $12 < q < 48.2$ kW/m^2 and $30 < Pr < 110$

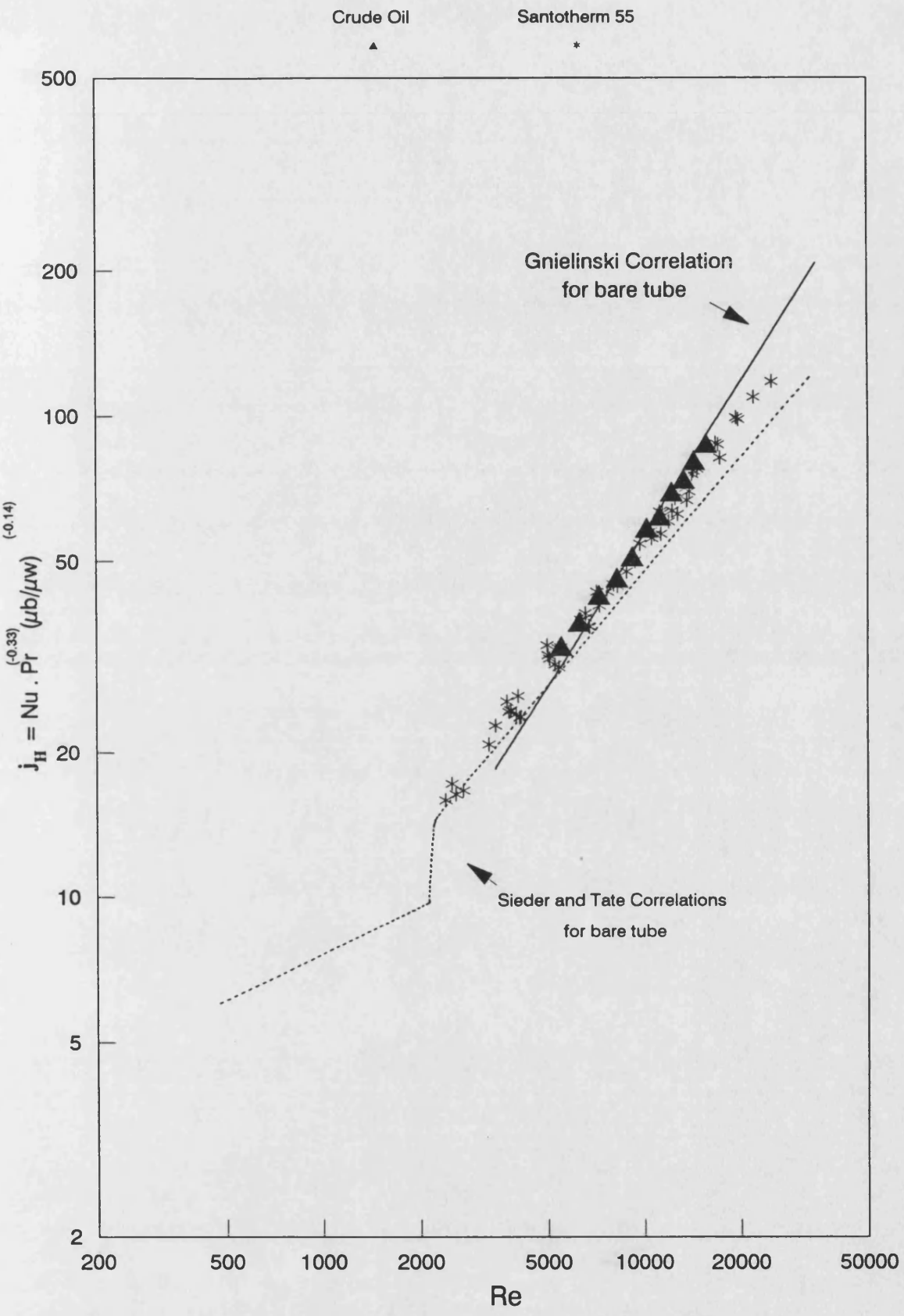

Fig (4.10) Heat transfer factor (j_H) vs Reynolds number (Re)

Comparison between Santotherm 55 fluid and Arabian light crude Oil

Bare tube test section No(1) at 60 < Pr < 85

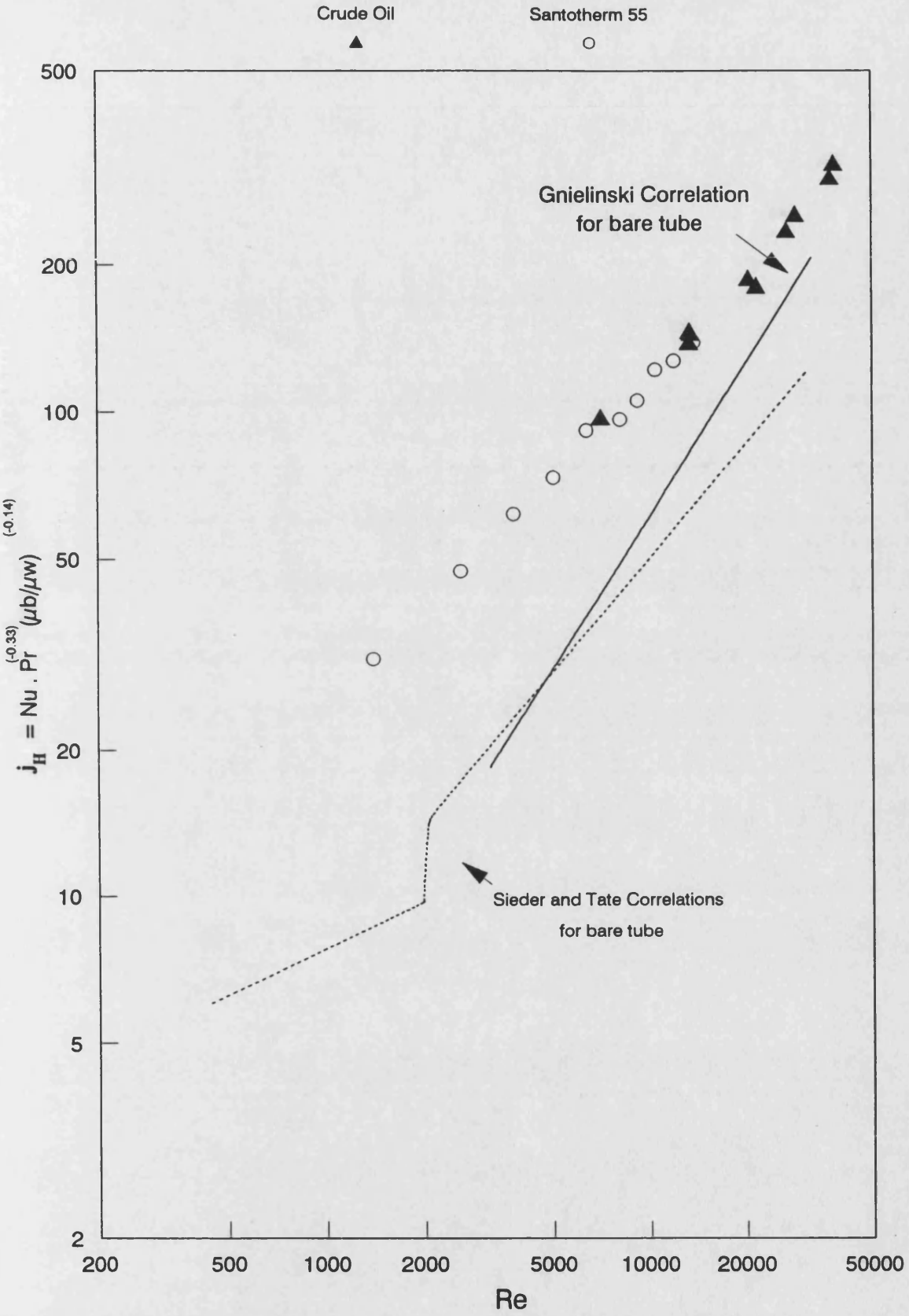

Fig (4.11) Heat transfer factor (j_H) vs Reynolds number (Re)

Comparison between Santotherm 55 fluid and Arabian light Crude Oil

Test section No(2) fitted with LDI-B at $12 < q < 48.2$ kW/m² ; $27 < Pr < 85$

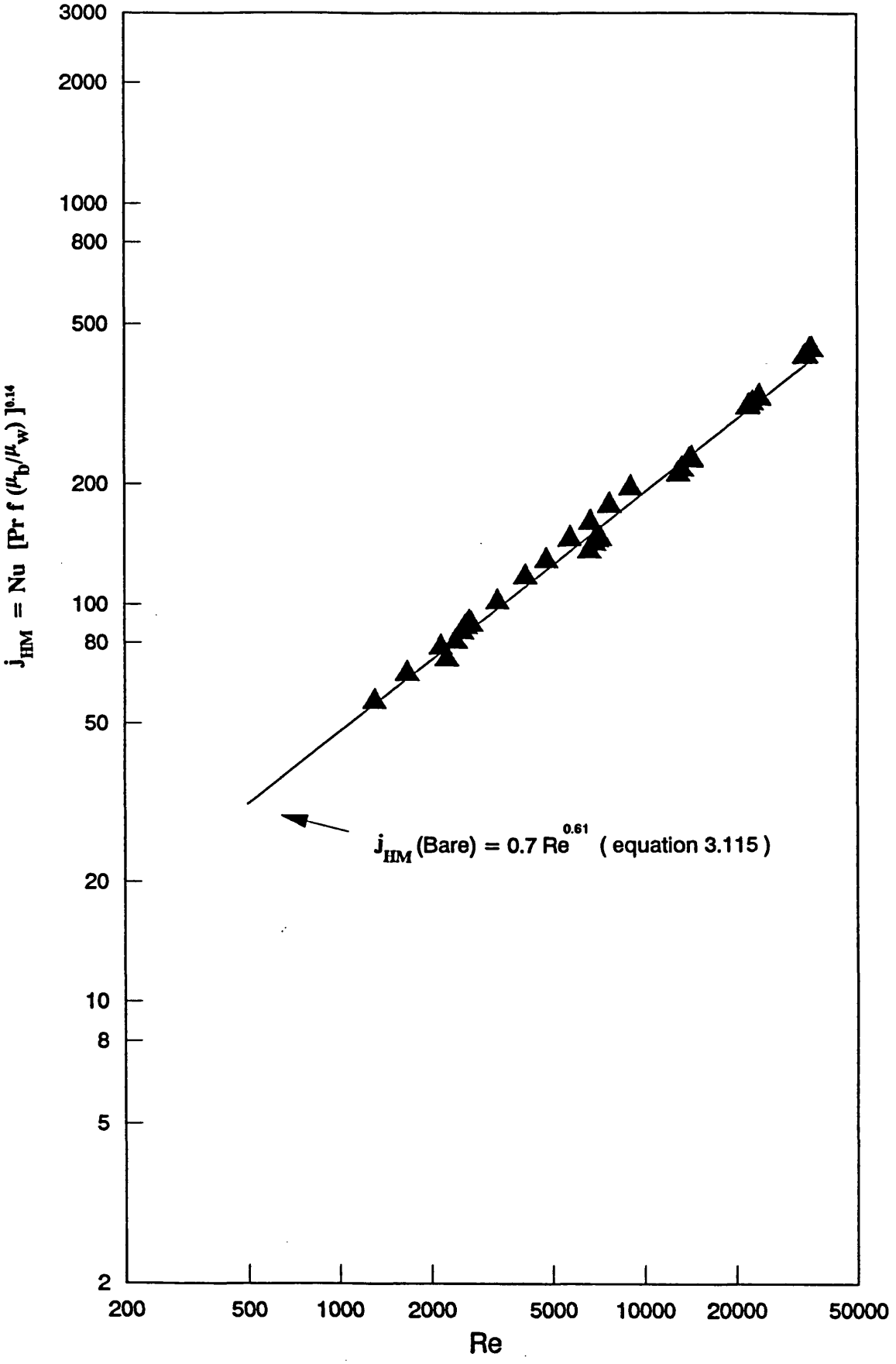

Fig (4.12) Modified Heat transfer factor (j_{HM}) vs Reynolds number (Re)

Test of equation 3.115 with crude oil results ; bare tube test section No(1)

Arabian light crude oil ; 60 °C < Tb < 150 °C ; 27 < Pr < 85

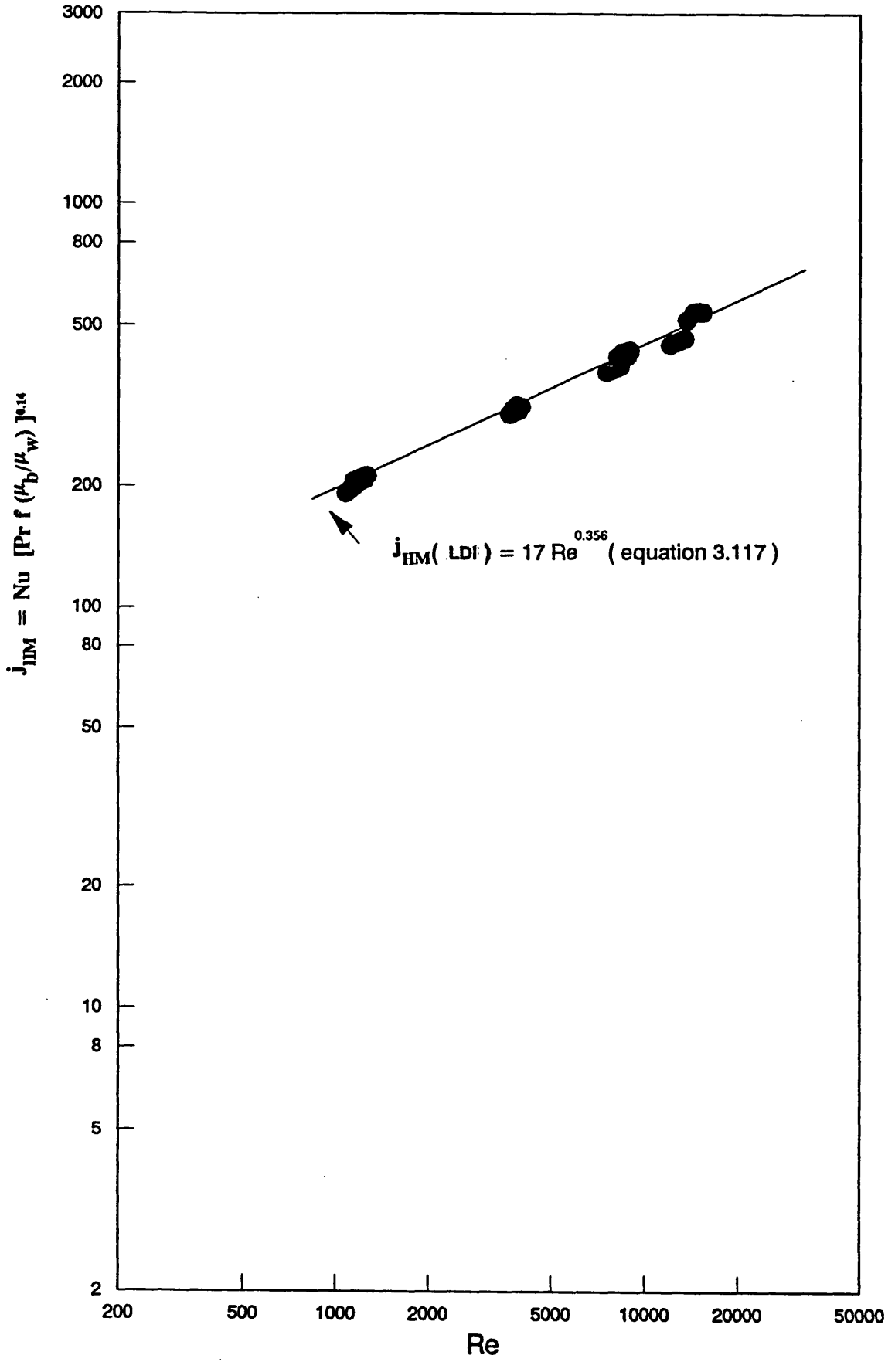

Fig (4.13) Modified Heat transfer factor (j_{HM}) vs Reynolds number (Re)

Test of equation 3.117 with crude oil results ; test section No(2) with LDI-B

Arabian light crude oil ; 60 °C < Tb < 150 °C ; 27 < Pr < 85

the crude oil but also possibly for any hydrocarbon fluid with specifications similar to those of Santotherm 55 . The ranges of Re and Pr have to be considered , however , for any further applications of equations 3.115 to 3.122 .

4.6.2.2 Fouling run No 1

The following experimental conditions were set-up for the first fouling run :

- Test section No 1 is the bare tube .
- Test section No(2) is fitted with the **HiTran** insert (LDI-B).
- Flow rate = 20 % F.S.R (for both test sections).
- Bulk fluid temperature (T_b) = 140 °C .

One bar (gauge) of nitrogen gas was used to blanket the crude oil in the tank . The crude oil was heated to 140 °C and the tank pressure increased to 5.1 bar (gauge) . In order to suppress nucleate boiling in the test sections , the tank pressure was then increased further to 8.2 bar (gauge) by supplying additional nitrogen.

In order to study the best conditions for fouling to occur , the effect of heat flux on heat transfer coefficient (h_i) and on surface temperature was examined .

In Fig 4.14 , h_i values for both test sections are plotted against heat flux in the range of $12 < q < 42.5$ kW/m^2 . It can be seen that h_i for the bare tube increases with heat flux whereas h_i for the test

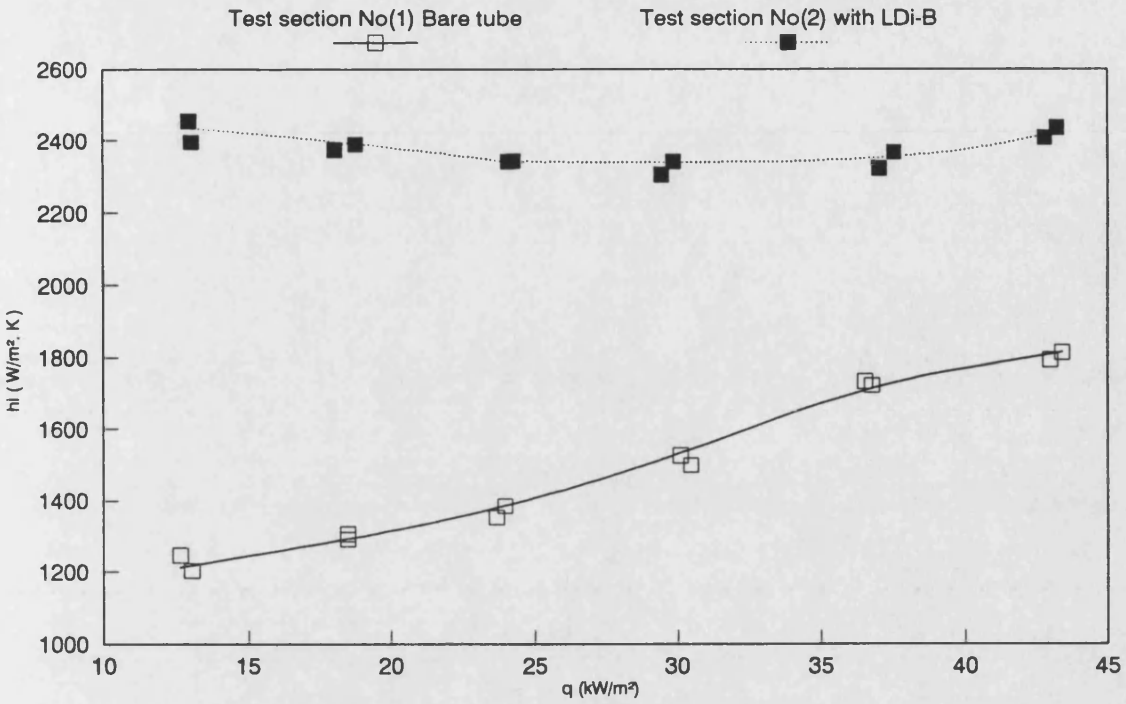

Fig (4.14) Heat transfer coefficient (hi) vs heat flux (q) for both test sections

Preparation for first fouling run for Arabian light crude oil

Tb = 140 °C ; 20% F.S.R ; P = 8.2 bar gauge of Nitrogen gas pressure

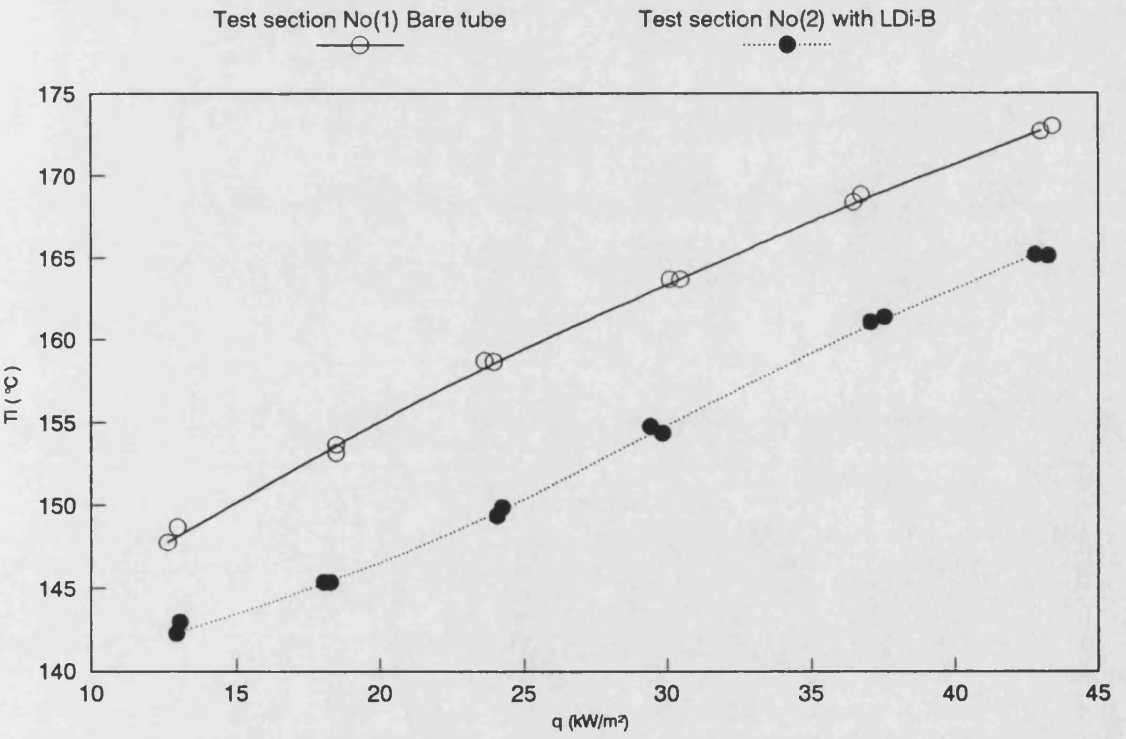

Fig (4.15) Inner surface temperature (Ti) vs heat flux (q) for both test sections

Preparation for first fouling run for Arabian light crude oil

Tb = 140 °C ; 20% F.S.R ; P = 8.2 bar gauge of Nitrogen gas pressure

section No(2) fitted with LDI-B was largely unaffected by q .

Fig 4.15 shows that the inner surface temperatures (T_i) of both test sections were increased by increasing q . For given q and flowrate , T_i of the bare tube was about 10 °C higher than that of the tube fitted with the insert .

Figs 4.16 and 4.17 show the effect of heat flux on the overall heat transfer coefficient (U_t) and on the wall temperature of both test sections (T_w). The value of U_t for test section No(2) , fitted with LDI-B , was almost twice that of the bare tube, test section No(1) .

The equipment was operated for one hour at q = 42.2 kW/m² . The bulk fluid and wall temperatures for both test sections as well as the tank pressure were monitored at 10 minute intervals. No changes in pressure or wall temperatures with time were observed. Consequently , steady state conditions were believed to have been established and the next set of readings were taken to be the clean conditions (time = 0) for the fouling run .

The initial T_i was 172°C for the bare tube and 164°C for test section No(2) , fitted with the **HiTran** insert .

The following readings were taken every 30 minutes for 69 hours (reference should be made to Fig 2.8 in Chapter 2 for the definitions of temperatures and pressure measuring points) :

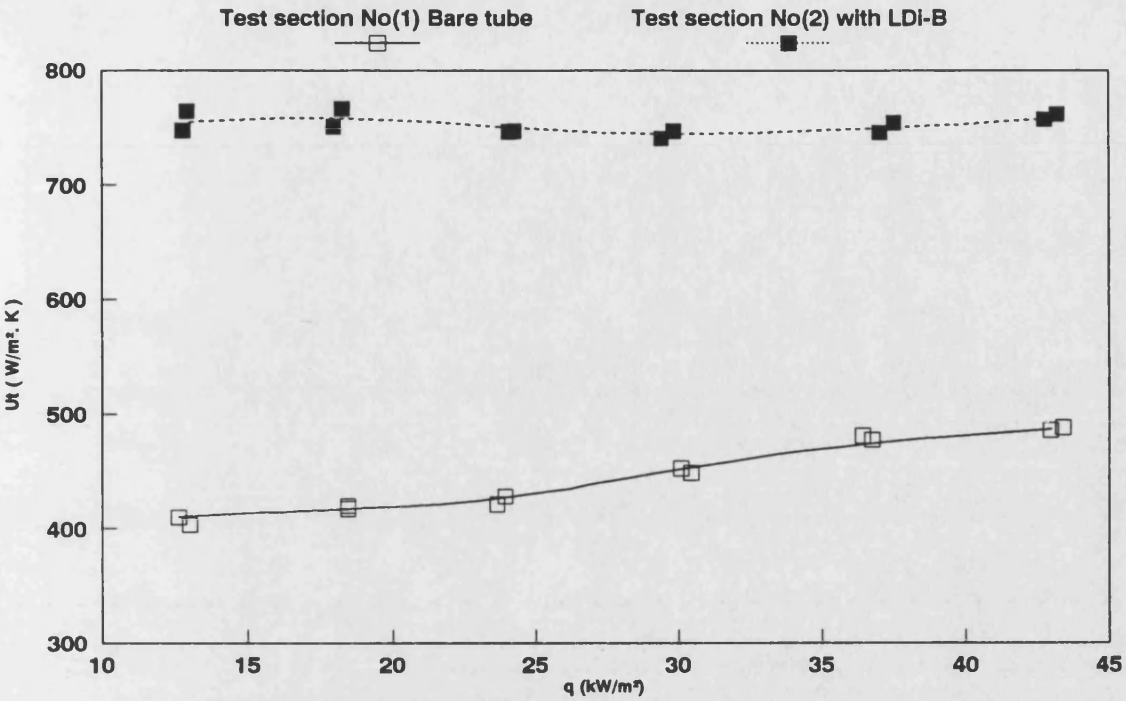

Fig (4.16) Overall heat transfer coefficient (Ut) vs heat flux (q) for both test sections

Preparation for first fouling run for Arabian light crude oil

Tb = 140 °C ; 20% F.S.R ; P = 8.2 bar gauge of Nitrogen gas pressure

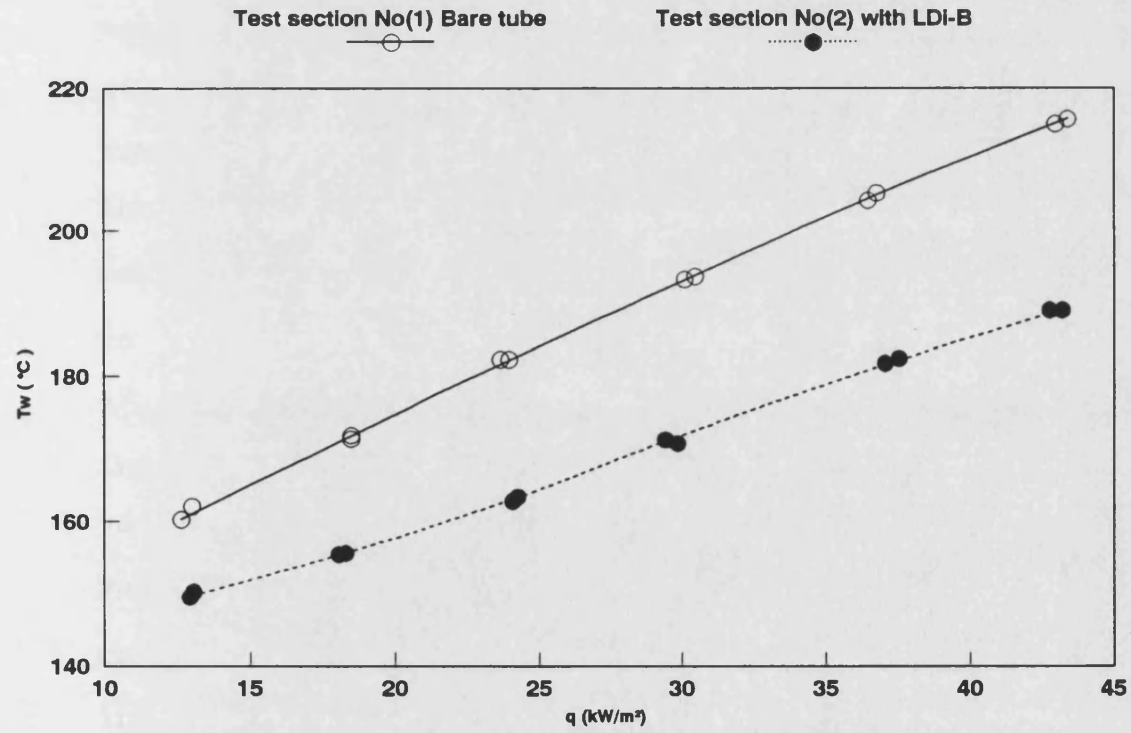

Fig (4.17) Wall temperature (Tw) vs heat flux (q) for both test sections

Preparation for first fouling run for Arabian light crude oil

Tb = 140 °C ; 20% F.S.R ; P = 8.2 bar gauge of Nitrogen gas pressure

Tank pressure (P_1)

T_1 , T_2 , T_3 , T_4 , ΔP_1 for test section No(1)

T_5 , T_6 , T_7 , T_8 , ΔP_2 for test section No(2)

The variation of tank pressure (P) , inner surface temperature (T_i) , overall heat transfer coefficient (U_t) and so called apparent fouling resistance ($R_{f(App)}$) , which is the difference between $\frac{1}{(U_t)_t}$ at any time and $\frac{1}{(U_t)_0}$ at the initial conditions (time = 0), are shown in Figs 4.18 and 4.19 for test sections No(1) and No(2) respectively. $R_{f(App)}$ was used in order to demonstrate whether fouling had occurred .

Fig 4.18 shows that the pressure decreased with time for the first 15 hrs . More N_2 gas was added to the equipment in order to reinstate the pressure to between 8.1 and 8.3 bar . After 20 hrs of operation at these experimental conditions no clear sign of fouling was apparent . The heat flux was therefore increased to 54.2 kW/m^2 in order to increase T_i of the bare tube to 182 °C and T_i of the LDI-B test section to 174°C. The experiment was operated for a further 49 hrs under the new conditions . U_t of the bare tube increased with time and therefore led to a negative values of $R_{f(App)}$ being calculated . These negative values of $R_{f(App)}$, however , are not believed to be caused by the mechanisms of many previous investigations[87,88,103]. That is , in this study a negative fouling resistance is not being caused by small amounts of deposit creating a rough surface in

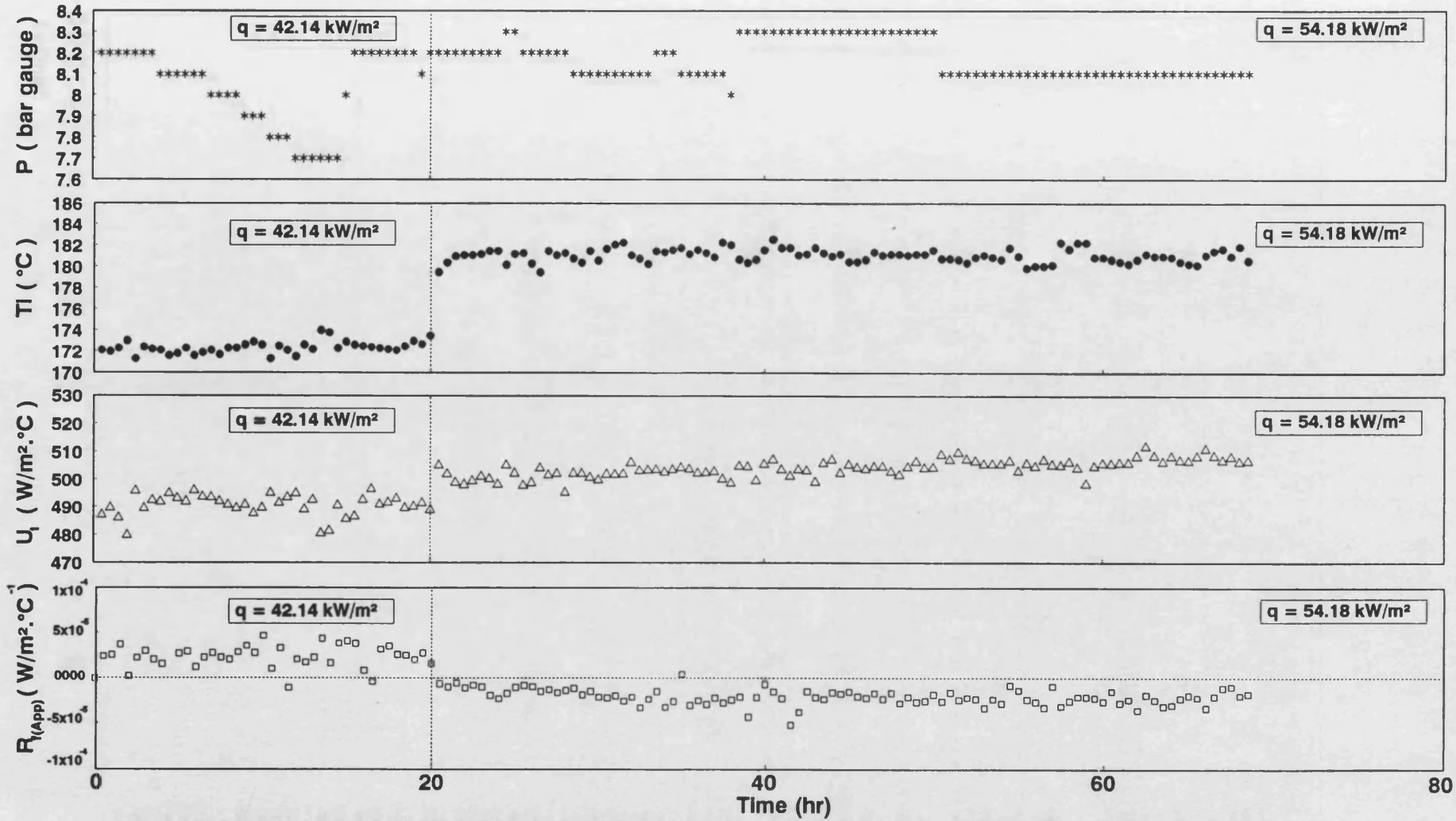

Fig (4.18) Fouling Run No(1) for bare tube test section No(1) [20% F.S.R ; Tb = 140 °C ; Re = 7000 ; Pr = 28]
Arabian light crude oil under pressure of nitrogen gas

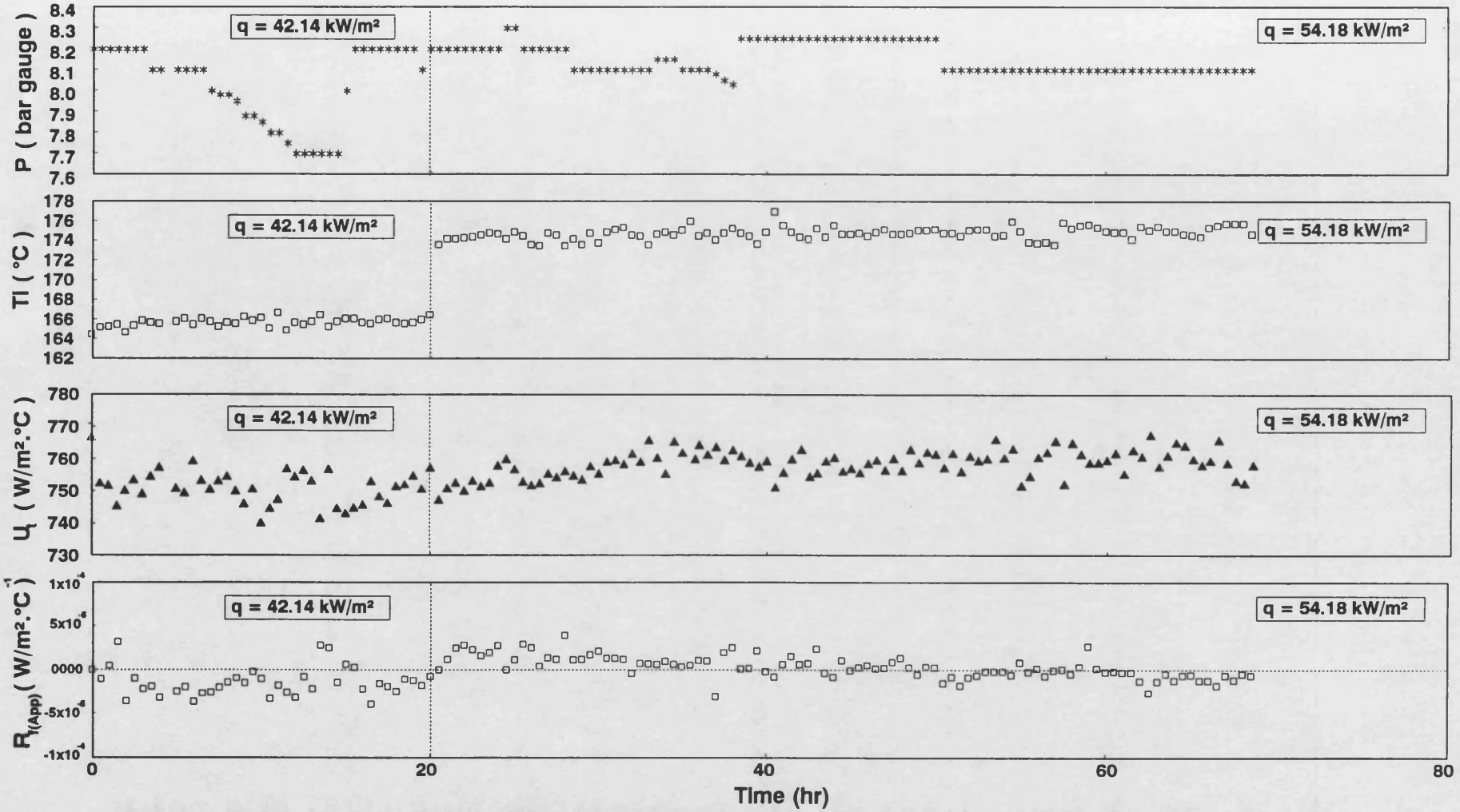

Fig (4.19) Fouling Run No(1) for test section No(2) fitted with LDI-B [20% F.S.R ; Tb = 140 °C ; Re = 7000 ; Pr = 28]
Arabian light crude oil under pressure of nitrogen gas

the early stages of fouling and thereby increasing the film heat transfer coefficient to an extent sufficient to counteract the additional thermal resistance due to the deposit itself[105] . In the current study fouling did not occur . Thus $R_{f(App)}$ was possibly due to an enhancement in h_i caused by nucleate boiling which contributes to an increase in U_t .To confirm this suggestion, Fig 4.19 shows that U_t of test section No(2) fitted with LDI-B , was not increased with time and $R_{f(App)}$ was zero . This is because the inner surface temperature was too low for nucleate boiling to occur when the insert was in place .

Fig 4.20 shows comparisons of T_i and U_t between both test sections . A comparison of $R_{f(App)}$ for both test sections is shown in Fig 4.21 .

The test sections were inspected and fouling did not occur in the first run . The following were considered to be the reasons why fouling did not occur :

1- The concentration of oxygen (O_2) gas dissolved in the crude oil was perhaps too low to cause oxidation reactions to occur .
2- The concentration of asphaltenes in the crude oil (1% by wt) was perhaps too low .
3- The inner surface temperature was perhaps below the break point temperature for fouling to be initiated .

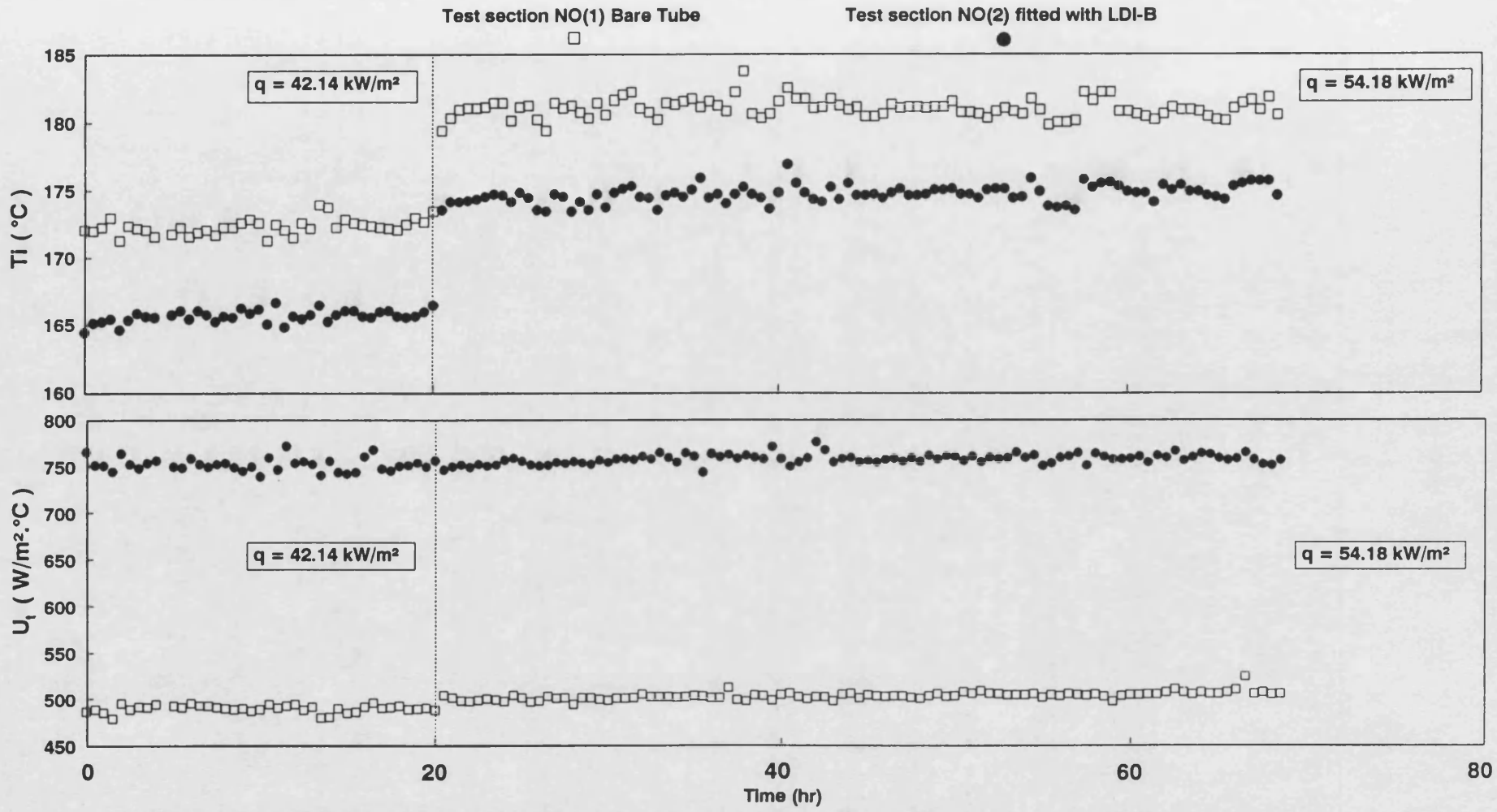

Fig (4.20) Comparison between overall heat transfer coefficient (Ut) and inner surface temperature (Ti) for both test sections

Fouling Run NO(1) ; Arabian light crude oil under pressure of nitrogen gas [20% F.S.R ; Tb = 140 °C ; Re = 7000 ; Pr = 28]

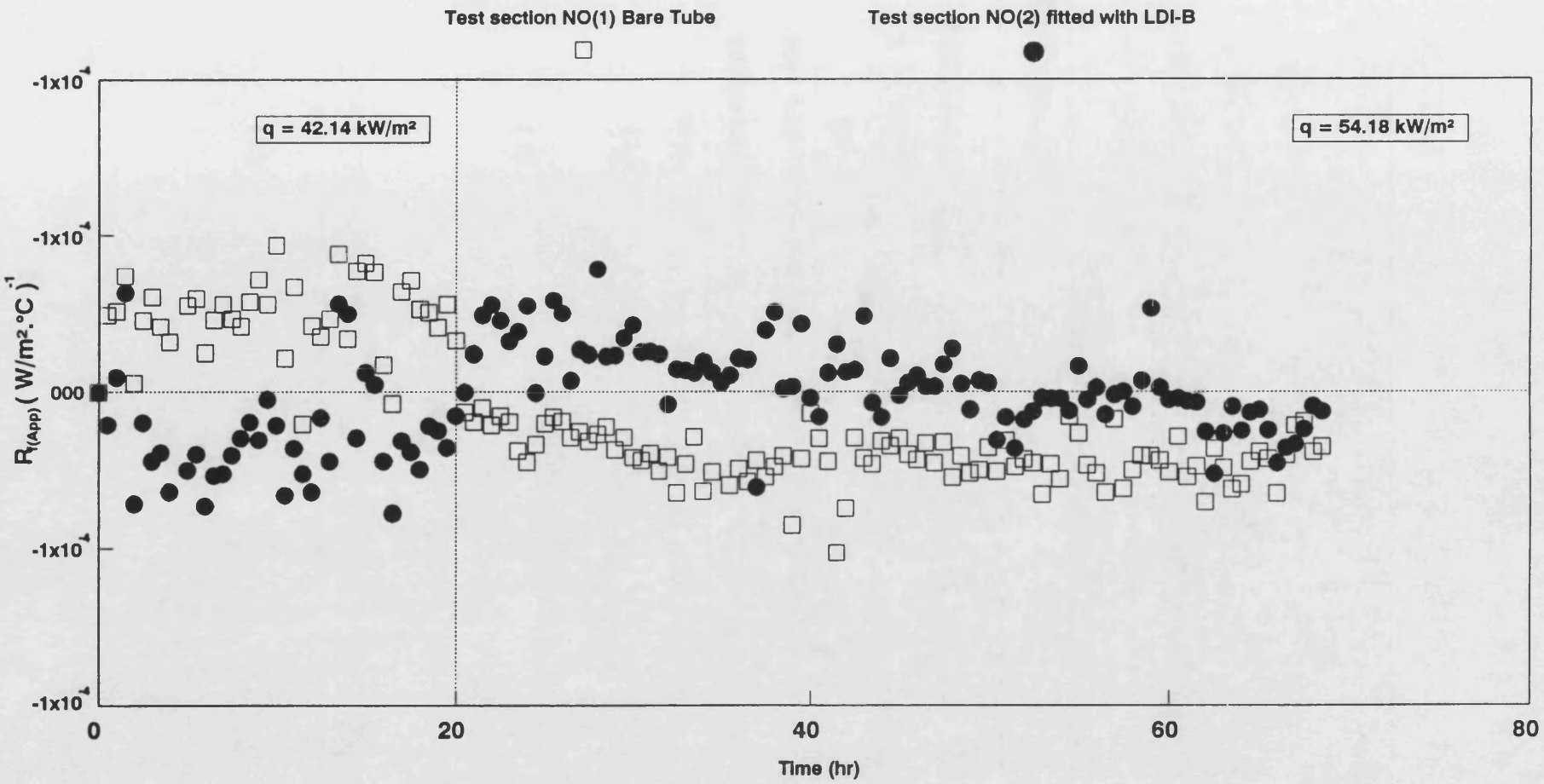

Fig (4.21) Comparison between apparent fouling resistance ($R_{f(App)}$) of both test sections

Fouling Run NO(1) ; Arabian light crude oil under pressure of nitrogen gas [20% F.S.R ; Tb = 140 °C ; Re = 7000 ; Pr = 28]

These three aspects are explored further in the following fouling runs .

In order to investigate the cause of the enhancement in the heat transfer coefficient for the bare tube with time when the heat flux was increased, the following heat transfer study on nucleate boiling of crude oil was carried out .

4.6.2.3 Heat transfer study on nucleate boiling of crude oil

4.6.2.3.1 Literature background

A - Boiling in general

Boiling can be divided into categories according to the mechanism occurring and according to the geometric situation[147].

The three mechanisms of boiling are :

(1) Nucleate boiling , where vapour bubbles are formed (usually at a solid surface) ;

(2) Convective boiling , where the heat is conducted through a thin film of liquid , the liquid then being evaporated at the vapour - liquid interface with no bubble formation , and

(3) Film boiling , where the heated surface is blanketed by a film of vapour , the heat being conducted through the vapour - liquid interface .

The two main geometric situations are ;

(1) Pool boiling , where the boiling occurs at a heated surface in a pool of liquid which , apart from any convection induced by the boiling , is stagnant .

(2) Flow boiling , where the liquid is pumped through a heated channel , typically a tube.

Nucleate boiling and film boiling occur in both pool boiling and flow boiling but convective boiling occurs only in flow boiling .

B - Pool boiling

An early investigation of pool boiling of water at its saturation temperature (100°C at 1 atm) was made by Nukiyama[152] in 1934 . His results and those of subsequent investigators were of the form shown in Fig 4.22 .

Nukiyama[152] found that as the temperature of a heated platinum wire increased above 100°C (212°F) , the rate of heat flux (calculated from the power input) increased smoothly until at 149°C (300°F) the temperature of the wire suddenly jumped to about 982°C (1000°F) . Further increases in the power input caused only regular increases in the wire temperature. A decrease in the power input from this point (point D in Fig 4.22) caused the wire temperature to decrease , as shown in Fig 4.22 , by the smooth curve between points D and C whereupon the temperature dropped suddenly to below 149°C (300°F) . Below this

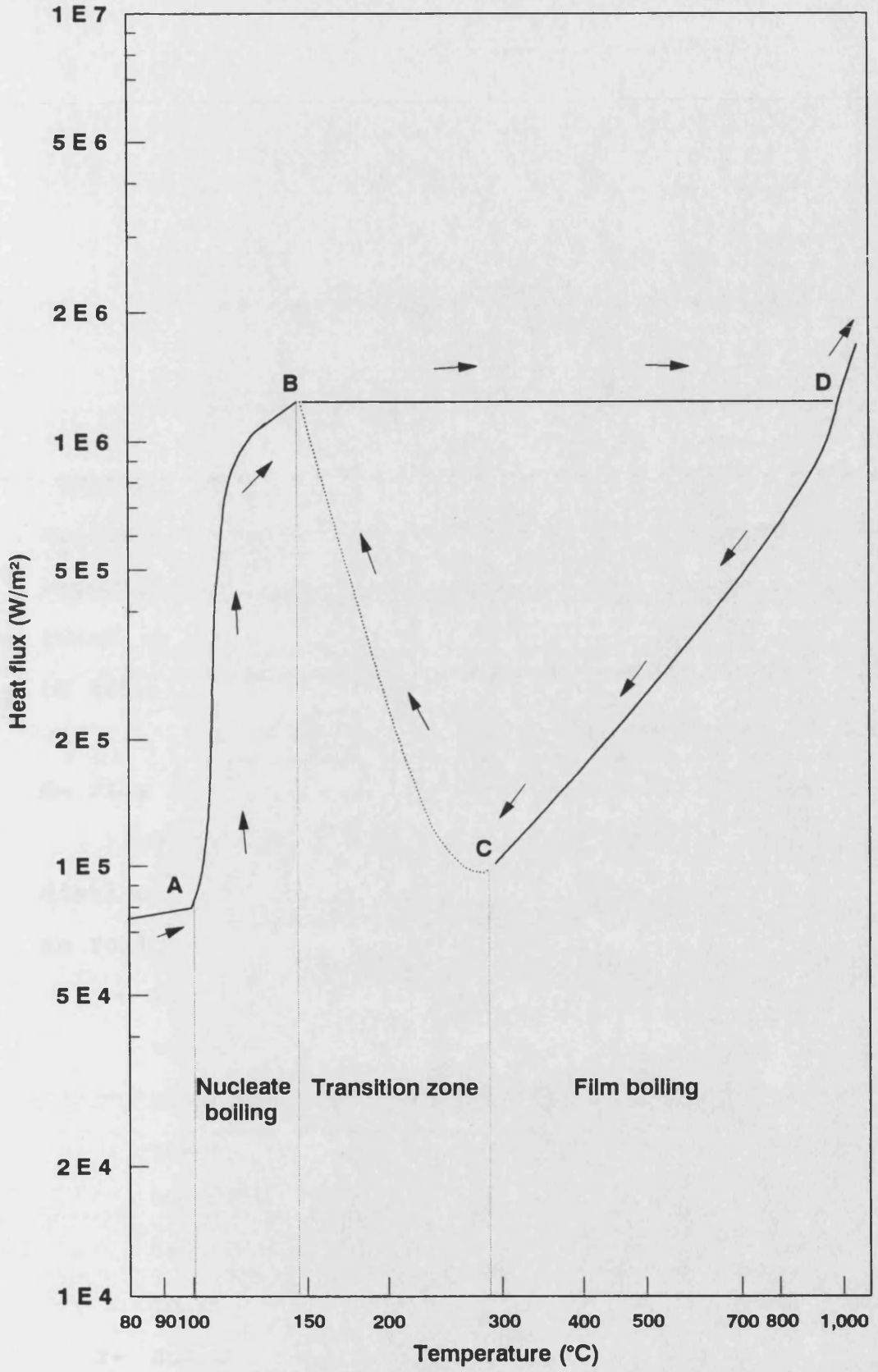

Fig(4.22) Boiling regimes for water at atmospheric pressure

point, it followed the curve B-A already established for increasing heat flux .

Nukiyama[152] concluded that at least three types of boiling existed :

1- Nucleate boiling between points A and B ,

2- Film boiling at points D upward , and

3- Transition zone between points B and C .

In the past many industrial boilers with the process fluid on the shell side , such as kettle reboilers , have been designed on the basis of pool boiling correlations. In contrast , it has been reported[148,150] that flow boiling curves cannot be based on pool boiling data but must rather be based on actual flow boiling data .

C- Flow boiling

For a fluid flowing in pipe , there are five distinct regions[147] , depending on the heat flux, as follows :

1- **Single -phase liquid forced convection** , in which the heat transfer coefficient is almost constant . Heat flux is less than that required for the onset of nucleate boiling (ONB) and T_b is much less than the saturation temperature (T_{sat}) corresponding to the system pressure.

2- **Subcooled nucleate boiling** , in which the heat transfer coefficient increases as the bulk fluid temperature approaches the

saturation temperature . Heat flux is at the onset of nucleate boiling (ONB) and T_b is less than T_{sat}. However, the presence of dissolved gases , such as air, nitrogen or oxygen, in the liquid can provide bubble nucleation on the hot surfaces[147] . The effect of dissolved gas on subcooled nucleate boiling has received very little research attention .

3- **Saturated nucleate boiling** , in which the heat transfer coefficient is almost constant. The heat flux is higher than that for ONB but less than the critical heat flux (CHF). T_b is equal to T_{sat} .

4- **Saturated convective boiling** , in which the heat transfer coefficient increases slowly with heat flux. The heat flux is equal or very close to the critical heat flux (CHF) , T_b is higher than T_{sat} .

5- **Post - critical heat flux** , in which the heat transfer coefficient is low . This regime gradually merges into a single phase vapour convection regime. The heat flux is higher than CHF and T_b is well above T_{sat} .

It is may be noted from the above , that the important heat fluxes are those for the onset of nucleate boiling (ONB) and the critical heat flux (CHF) .

(i) **Onset of nucleate boiling (ONB)**

Onset of nucleate boiling (ONB) is the minimum heat flux required for the nucleation boiling to start . The boiling of a mixture of liquids can exhibit significant differences from the boiling of a pure component. For a mixture , ONB occurs at a larger temperature difference (T_{sat} - T_b) than for a pure fluid[147].

A comprehensive review on flow boiling from (ONB) up to but not including the critical heat flux (CHF) has been made by Butterworth and Shock[150]. They noted that the workers in this field have concentrated on water and refrigerants to the exclusion of other fluids like hydrocarbons .

(ii) **Critical heat flux (CHF)**

Critical heat flux is defined as that condition under which a small increase in heat flux gives rise to an inordinate deterioration in heat transfer[151]. The critical heat flux (CHF) is described in various ways including dryout , burnout , and boiling crisis. However , the term critical heat flux has possibly the widest international recognition[151]. An intensive review on CHF in flow boiling is provided by Hewitt[151].

As mentioned above , nucleate boiling exists in two forms , namely subcooled nucleate boiling and saturated nucleate boiling . The main difference between these types is in what happens to the growing

bubbles at the heating surface . In a saturated liquid a bubble grows and then, aided by buoyancy , leaves the surface . As it leaves , fresh liquid flows towards the surface . Another bubble then begins to grow at the same point. In a subcooled liquid , the bubble grows and reaches out into the relatively cool liquid. Thus the vapour begins to condense , and in doing so causes the liquid temperature to rise slightly . The bubble collapses completely and , once again , new , cold liquid flows into the area near the wall and the process of bubble growth can then start again[147].

Generally, all liquids contain dissolved gases, especially air . However , the solubility of any gas in liquid, is a function of temperature and pressure, as mentioned in section 4.5.2 . In most cases the solubility of a gas in a liquid decreases with an increase in the temperature. Thus , when a cool liquid containing dissolved gases flows towards to a hot surface then , due to the difference in solubility between the bulk fluid and the wall temperatures, gas bubbles can grow and travel back into the relatively cool liquid to redissolve . When the bubbles collapse the latent heat is transfered to the liquid[147,153] . This type of bubble nucleation, which may be called " **bubble nucleation due to gas solubility difference (BNGSD)**" , is similar to subcooled nucleate boiling and it is difficult to distinguish between these two bubbling phenomena without visual experimental evidence .

The current study is concerned with the nucleate boiling (subcooled or otherwise) of crude oil in the presence of dissolved gases (air, nitrogen and helium) at two different bulk temperatures (50°C and 140°C). No previous work on this subject has been found in the literature . Thus, the present investigation appears to be the first in the field .

4.6.2.3.2 Experimental investigation

In order to investigate the effect of dissolved gases on the heat transfer coefficient (h_i) and the inner surface temperature (T_i) under nucleate boiling conditions , an experimental investigation was carried out in two stages ;

- In the first stage , the effect of nitrogen gas pressure on h_i and T_i of Arabian light crude oil was studied at two different bulk temperatures (50°C and 140°C) and at different flow rates. Flow rates, pressures and heat fluxes were in the ranges of $20\% < F.S.R < 80\%$; $6.2 < P < 14.2$ bar gauge and $12 < q < 60.2$ kW/m^2 respectively .
- In the second stage , after adding 10% wt of refinery sludge to the Arabian light crude oil, a comparative study of the effects of nitrogen and helium on h_i and T_i was carried out at experimental conditions similar to those in first stage. In order to keep the whole crude oil case study in chronological order

of investigation , the second stage will be discussed after fouling run No(5) , in section 4.6.2.5 .

Effect of N_2 gas pressure on the nucleate boiling of crude oil

a - At high bulk temperature (T_b = 140 °C)

When fouling run No(1) had been completed , the tank pressure was kept constant at 8.2 bar gauge and the first stage of investigation was carried out.

The results of the experiments are shown in Figs 4.23 and 4.24 for the bare tube test section No(1) and in Figs 4.25 and 4.26 for test section No(2) fitted with the **HiTran** insert (LDI-B) .

Fig 4.23 shows the effect of heat flux on h_i for the bare tube at constant flow rate (constant Re). For the lowest flow rate h_i is seen to increase with heat flux. However, for higher flow rates h_i appears not to be much affected by heat flux . This seemes to indicate that nucleate boiling existed only at the lowest flow rates.

Fig 4.24 shows that at constant flow rate T_i of the bare tube increases almost linearly with heat flux. Closer examination of Figs 4.23 and 4.24 reveals that the increase of h_i with heat flux for the lowest flow rate occurred at T_i > 154°C. Although T_i for higher Re exceeded the value of 154°C at q > 30 kW/m² , h_i was not affected by the heat flux. This indicates that nucleate boiling existed only at low flow rates and can be suppressed by an increase in the flow

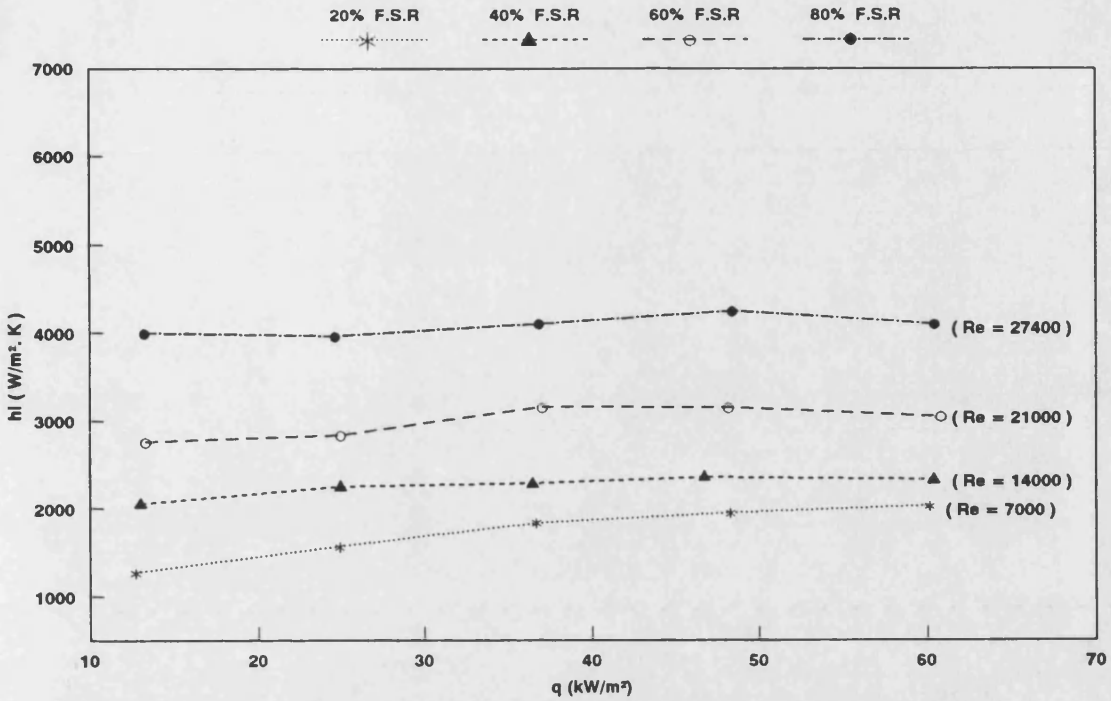

Fig (4.23) Heat transfer coefficient (hi) vs heat flux (q) for bare tube test section No(1)

Effect of heat flux on Arabian light crude oil

Tb = 140 °C ; 20% - 80% F.S.R and P = 8.2 bar gauge of nitrogen gas

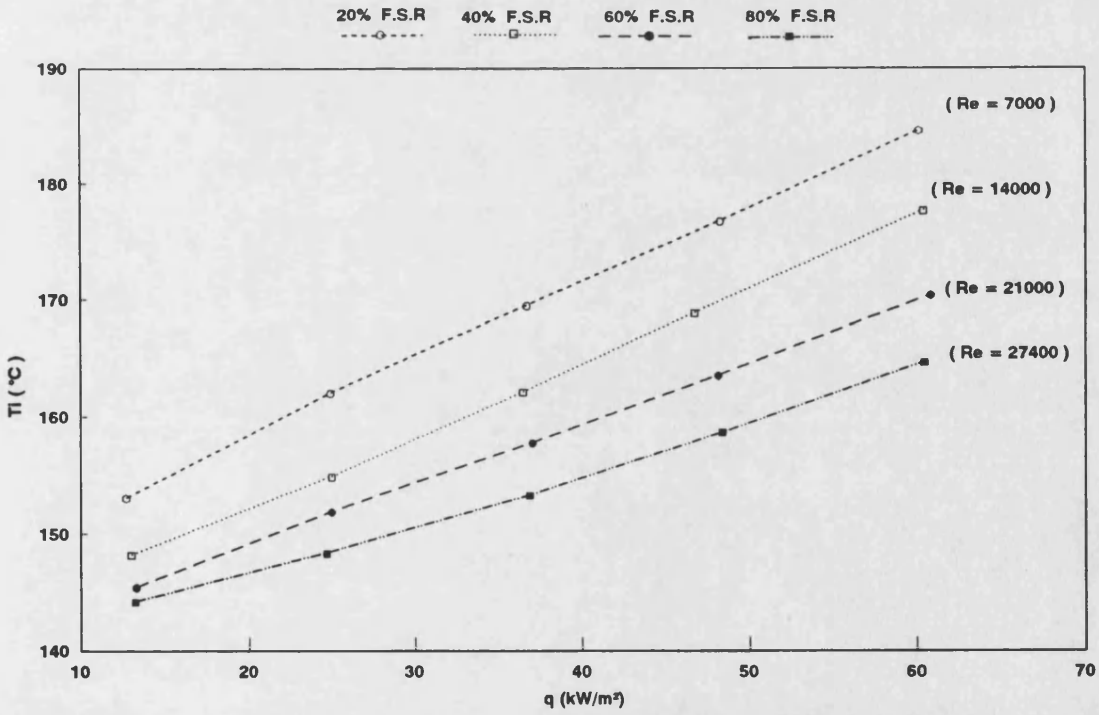

Fig (4.24) Inner surface temprature (Ti) vs heat flux (q) for bare tube test section No(1)

Effect of heat flux on Arabian light crude oil

Tb = 140 °C ; 20% - 80% F.S.R and P = 8.2 bar gauge of nitrogen gas

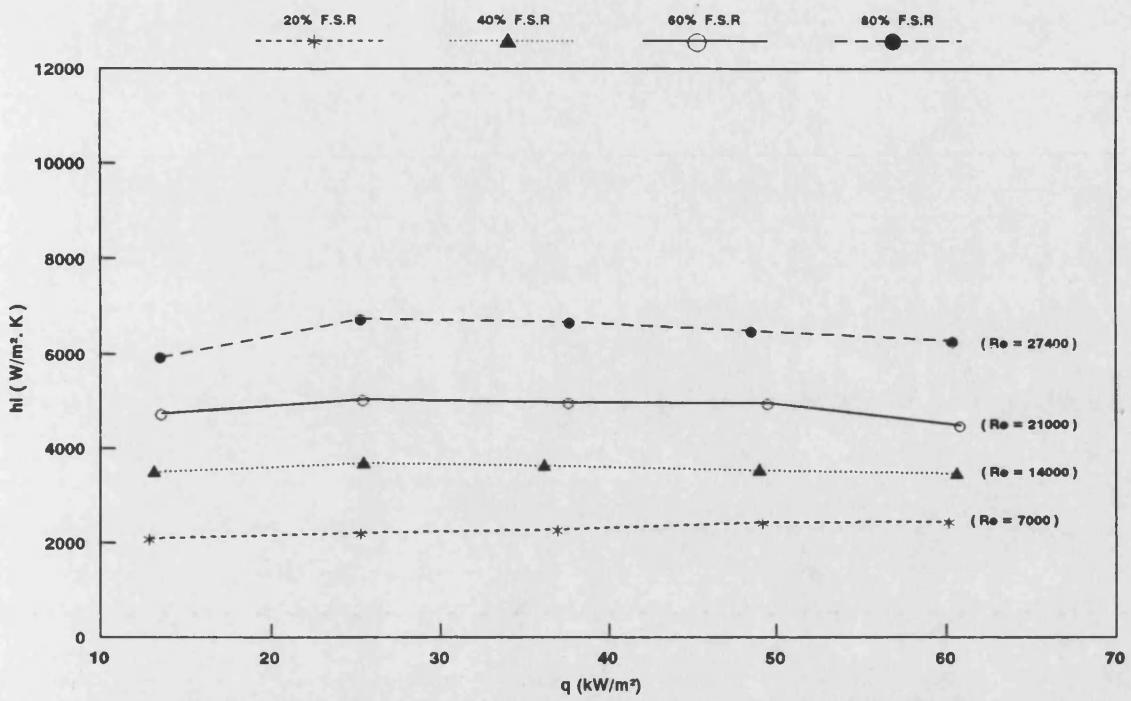

Fig (4.25) Heat transfer coefficient (hi) vs heat flux (q) for test section No(2) fitted with LDI-B

Effect of heat flux on Arabian light crude oil

Tb = 140 °C ; 20% - 80% F.S.R and P = 8.2 bar gauge of nitrogen gas

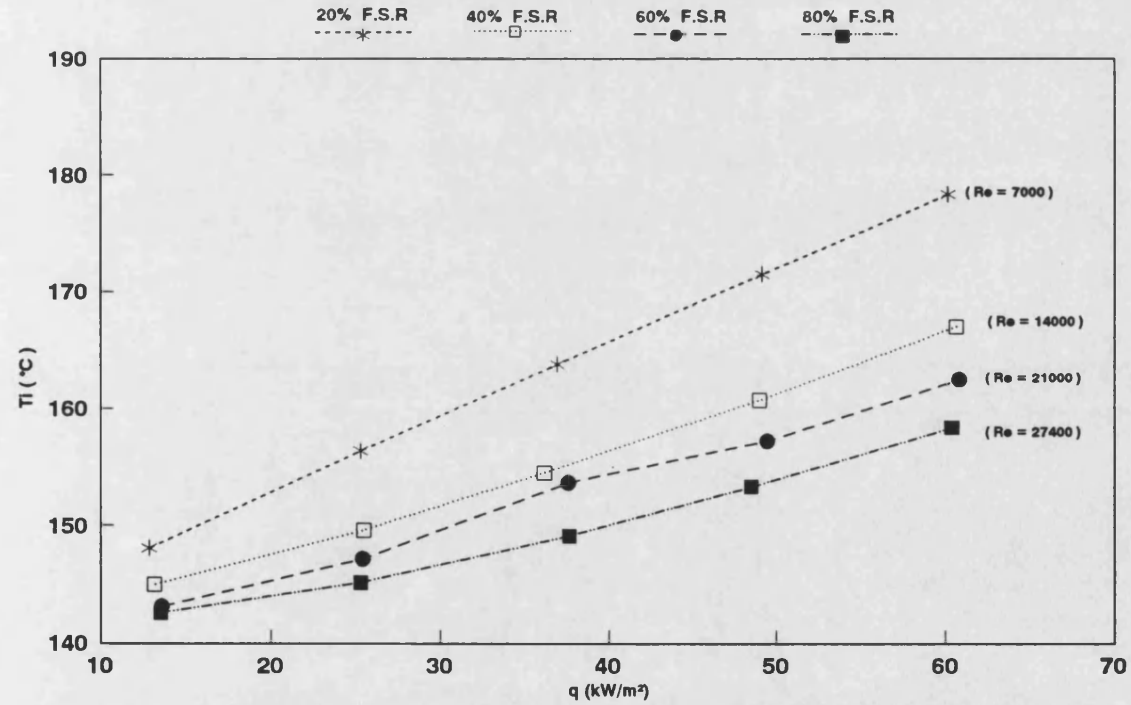

Fig (4.26) Inner surface temprature (Ti) vs heat flux (q) for test section No(2) fitted with LDI-B

Effect of heat flux on Arabian light crude oil

Tb = 140 °C ; 20% - 80% F.S.R and P = 8.2 bar gauge of nitrogen gas

rate. According to equation 4.5, T_{sat} = 210.2°C at the experimental pressure of 8.2 bar gauge . Thus the nucleate boiling occurring at low flow rate is possibly of the subcooled nucleate form .

Fig 4.25 shows that h_i of test section No(2), fitted with LDI-B , was largely unaffected by heat flux even at low flow rate . Fig 4.26 shows that T_i of test section No(2) also increased linearly with heat flux. Fig 4.26 shows also that T_i was greater than 154°C for q > 36 kW/m² . This seems to indicate that nucleate boiling did not exist even at low flow rate and high T_i .

Careful examinations of Figs 4.23 to 4.26 leads to the following conclusions :

1- Subcooled nucleate boiling occurred in the bare tube test section at the lowest flow rate (Re = 7000), but it could be suppressed by an increase in the flow rate (Re > 14000) .

2- Nucleate boiling did not occur in the tube fitted with the **HiTran** insert even at low flow rate (Re = 7000) and high heat flux, 30 < q < 60 kW/m² . Thus the **HiTran** insert may be used to suppress nucleate boiling at high heat fluxes .

3- The first fouling run was carried out under subcooled nucleate boiling conditions in the bare tube (flow rate 20% F.S.R ,

T_i = 172°C at q = 42.2 kW/m^2 and then 182°C at q = 54.2 kW/m^2) . This could help to explain why the overall heat transfer coefficient (U_t) was increased after 20 hours when the heat flux was increased , and why negative values for $R_{f(App)}$ were then calculated .

It was not immediately clear from Figs 4.23 to 4.26 whether the presence of nitrogen dissolved in the crude oil had any affect on the nucleate boiling. In order to investigate this aspect , the following experiment was carried out .

As nucleate boiling in the previous experiments was apparently present only at the lowest flow rates, the flow rates in both test sections were fixed at 20% F.S.R and the effects of nitrogen gas pressures in the range of 6.2 < P < 14.2 bar gauge and heat fluxes in the range of 12 < q < 60.2 kW/m^2 were studied. The results are shown in Figs 4.27 to 4.32 .

Fig 4.27 shows the variation of h_i for the bare tube with pressure (P) at constant heat flux (q) . The coefficient h_i was found to decrease with increase in pressure although the slope $(\frac{dh_i}{dp})$ depended upon the heat flux . The results indicate that nucleate boiling of the crude oil could be suppressed by increasing the gas pressure .

Fig 4.28 shows that h_i for the test section fitted with the **HiTran** insert decreased with pressure for

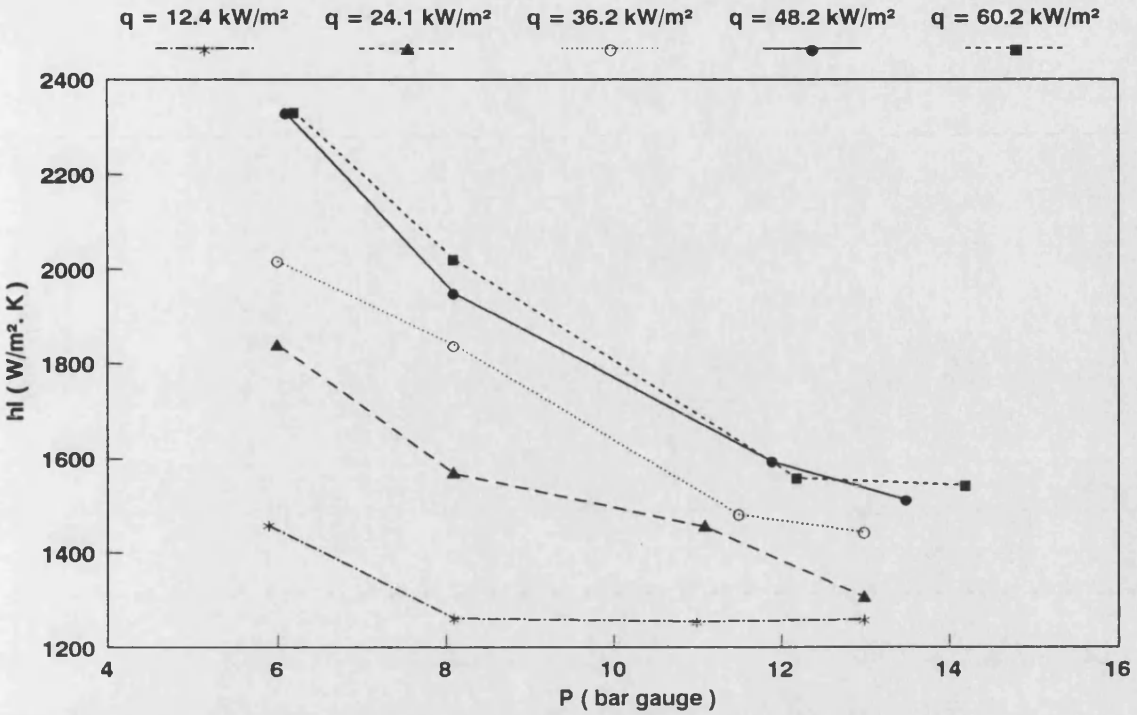

Fig (4.27) Heat transfer coefficient (hi) vs tank pressure (P) for bare tube test section No(1)
Effect of nitrogen gas pressure on Arabian light crude oil
Tb = 140 °C ; 20% F.S.R ; 12 < q < 60.2 kW/m² ; Re = 7000 and Pr = 28

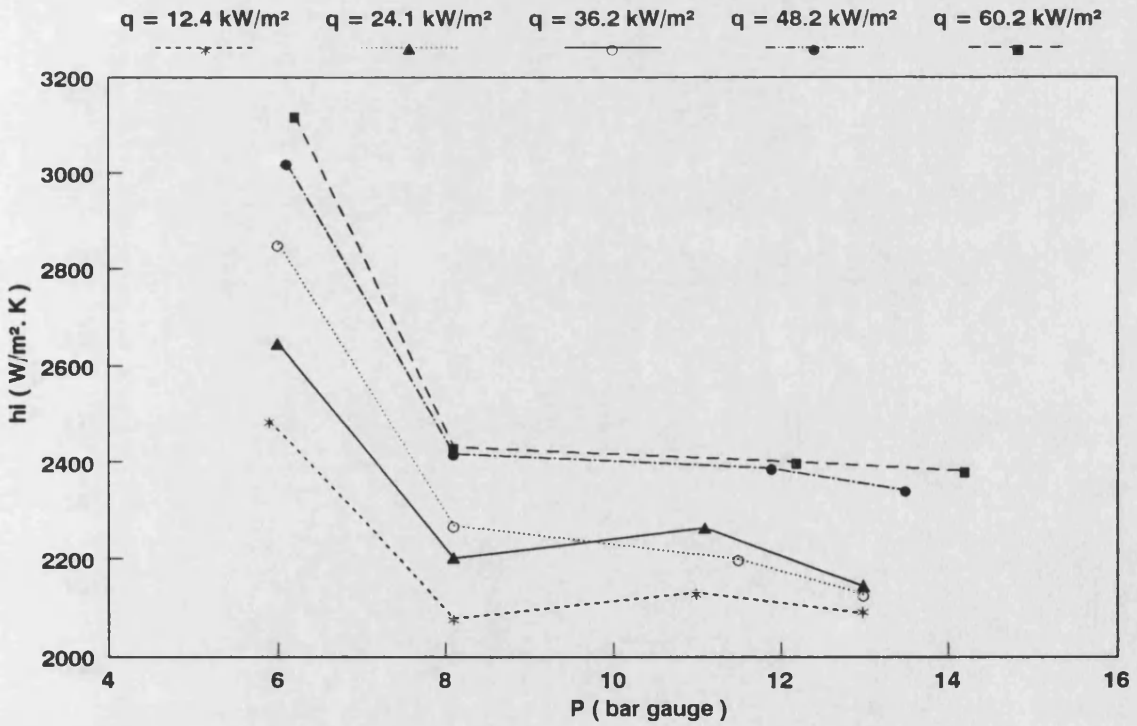

Fig (4.28) Heat transfer coefficient (hi) vs tank pressure (P) for test section No(2) fitted with LDI-B
Effect of nitrogen gas pressure on Arabian light crude oil
Tb = 140 °C ; 20% F.S.R ; 12 < q < 60.2 kW/m² ; Re = 7000 and Pr = 28

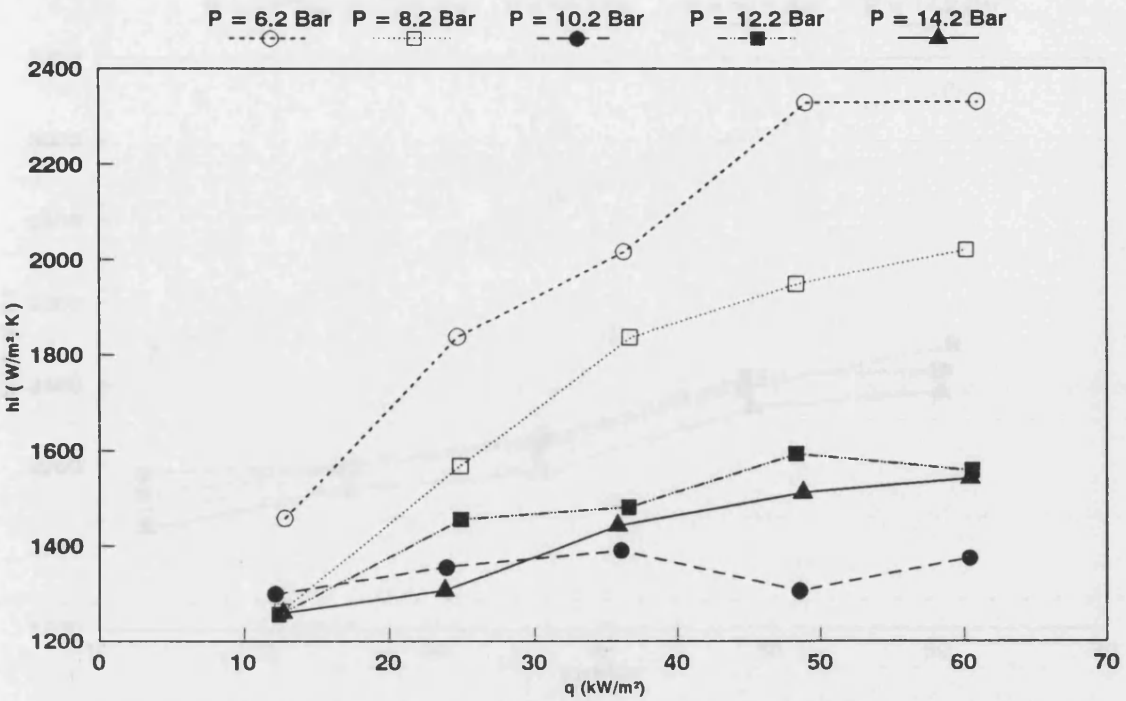

Fig (4.29) Heat transfer coefficient (hi) vs heat flux (q) for bare tube test section No(1)

Effect of heat flux on Arabian light crude oil

Tb = 140 °C ; 20% F.S.R and 6.2 < P < 14.2 bar gauge of nitrogen gas

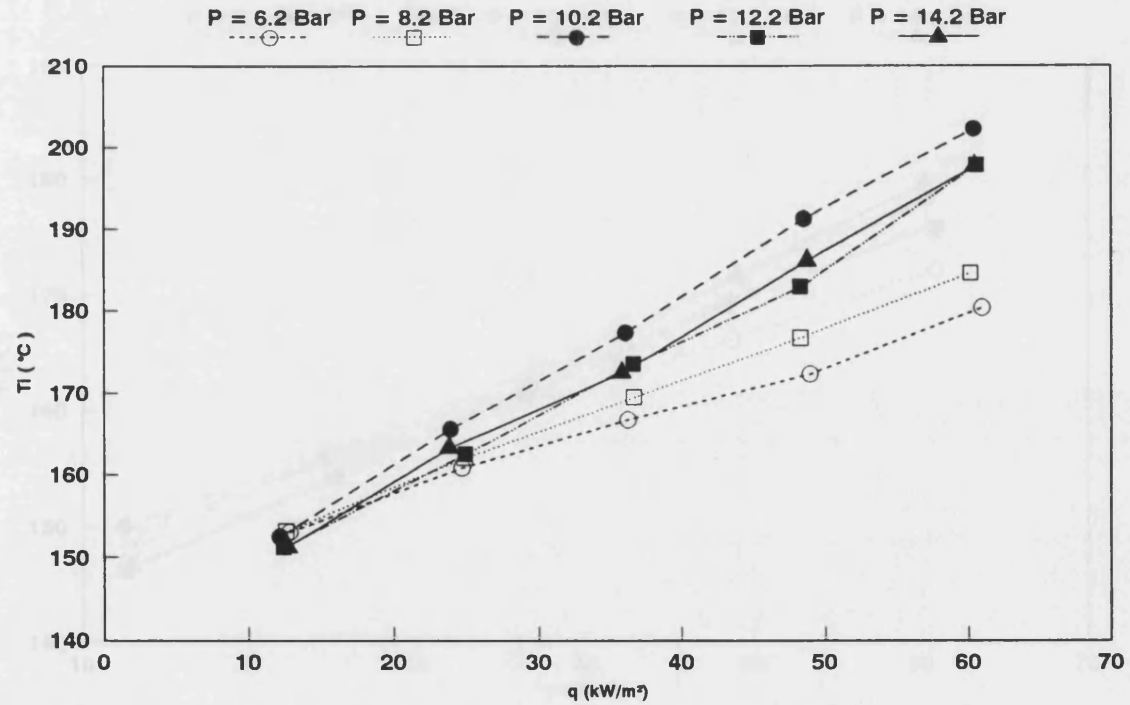

Fig (4.30) Inner surface temprature (Ti) vs heat flux (q) for bare tube test section No(1)

Effect of heat flux on Arabian light crude oil

Tb = 140 °C ; 20% F.S.R and 6.2 < P < 14.2 bar gauge of nitrogen gas

6.2 < P < 8.2 bar gauge . Pressure had no affect on h_i for P > 8.2 bar gauge. From equation 4.5 , T_{sat} is 182.6 °C at P = 6.2 bar gauge. Therefore, saturated nucleate boiling possibly existed at the lower pressures (P < 8.2).

Fig 4.29 shows h_i of the bare tube as a function of heat flux at constant pressure . For P = 6.2 bar gauge, the pressure at which nucleate boiling should occur, h_i increased rapidly with heat flux , as expected[147] . For P = 8.2 bar gauge , hi increased with q in a similar manner . For P = 10.2 bar gauge, the rate of increase of h_i with q , $\frac{dh_i}{dq}$, was the lowest among the whole range of pressures tested. This is possibly because nucleate boiling was completely suppressed by P = 10.2 bar gauge . However, for P = 12.2 bar gauge , h_i increased with q with $\frac{dh_i}{dq}$ being higher than for 10.2 bar . For P = 14.2 bar gauge, $\frac{dh_i}{dq}$ was for some reason between the two previous values .

Ideally, h_i should decrease with increasing pressure since the pressure can suppress the nucleate boiling process. However , the increase in h_i with q for P > 12.2 bar gauge is evidence that perhaps another type of nucleation may be occurring . The nucleation which enhanced h_i for P > 12.2 bar is possibly the bubble nucleation due to gas solubility difference (BNGSD) . As mentioned in section 4.5.2 the solubility

of nitrogen gas in any liquid can increase with pressure and decrease with temperature. Therefore it is a reasonable assumption that the solubility of nitrogen in crude oil would be increased by an increase in the system pressure . In contrast, an increase in pressure can suppress subcooled nucleate boiling on the inner surface of the bare tube test section . As T_i increases the temperature difference between T_b and T_i increases as well and thus the rate for BNGSD would also increase perhaps to an extent sufficient to control the nucleation process. Concluding this speculation , the enhancement in h_i may be controlled by the subcooled nucleate boiling for P < 10.2 bar gauge , and by BNGSD for P > 10.2 bar gauge .

Fig 4.30 shows the variation of T_i for the bare tube with heat flux at constant pressure. For P =10.2 bar gauge , T_i increased linearly with q. However, it seemed to increase non-linearly for pressures higher or lower than 10.2 bar . Moreover , at q = 12 kW/m^2, T_i was the same value (150°C) for all pressures tested . As the heat flux was increased , the effect of pressure on T_i became more noticeable . For example, at q = 60.2 kW/m^2 , T_i was as follows :

P (bar gauge)	6.2	8.2	10.2	12.2	14.2
T_i (°C)	180.4	184.6	202	197.8	197.7

It is clear from the above that the highest value of T_i occurred at P = 10.2 bar . This seems to

indicate that T_i was reduced whenever nucleate boiling or BNGSD was occurring and concurs with the work of Moore and Mesler[149] on the nucleate boiling of water at atmospheric pressure. They[149] came to the conclusion that the decrease in surface temperature indicates rapid removal of heat from the surface by bubbles .

Fig 4.31 shows that h_i for test section No(2) fitted with LDI-B , was relatively unaffected by heat flux for P > 8.2 bar gauge . For P = 6.2 bar , h_i increased with q . Fig 3.32 shows the T_i data for test section No(2).

b- <u>At low bulk temperature</u> (T_b = 50 °C)

In order to provide a clear distinction between nucleate boiling and BNGSD , the effect of nitrogen gas pressure on h_i and T_i was investigated at low bulk temperature (T_b = 50°C) but with similar heat fluxes , flow rates and preeures as those used at high T_b .

At T_b = 50°C the pressure in the reservoir is 0.56 bar absolute . Therefore , for P > 6 bar gauge (7 bar absolute) and q < 60.2 kW/m² , the chance of nucleate boiling occurring should be very small . The results of this study are shown in Figs 4.33 to 4.38.

Fig 4.33 shows that the rate of increase in h_i with q at constant p , $(\frac{dh_i}{dq})$ for the bare tube is

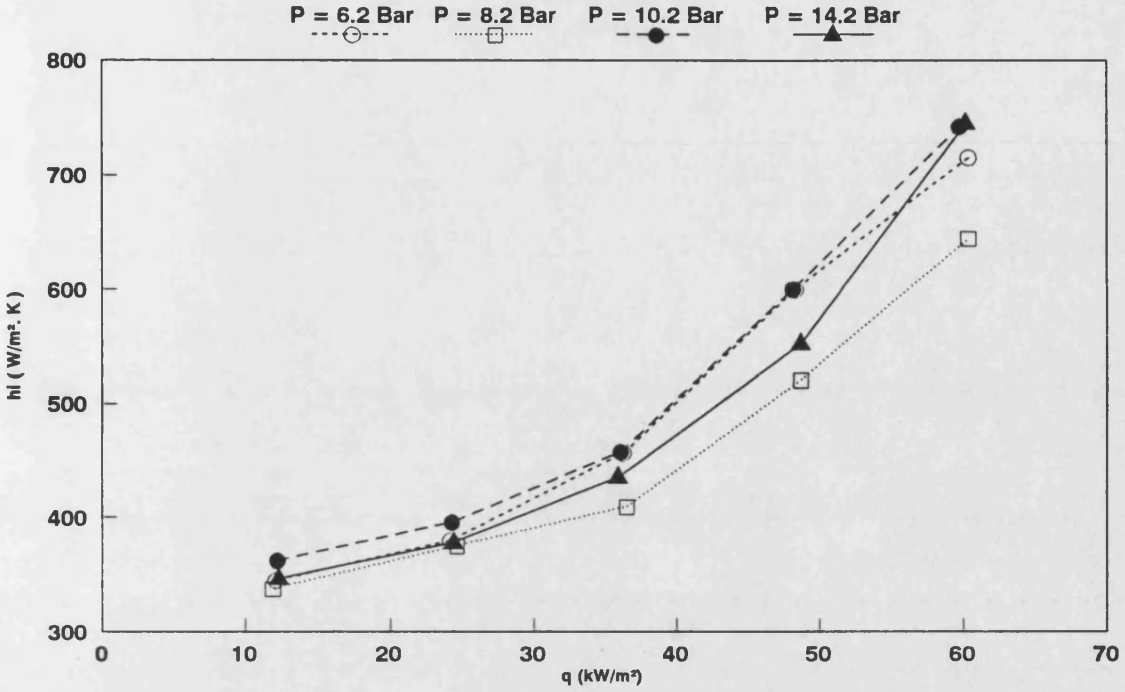

Fig (4.33) Heat transfer coefficient (hi) vs heat flux (q) for bare tube test section No(1)

Effect of heat flux on Arabian light crude oil

Tb = 50 °C ; 20% F.S.R and 6.2 < P < 14.2 bar gauge of nitrogen gas

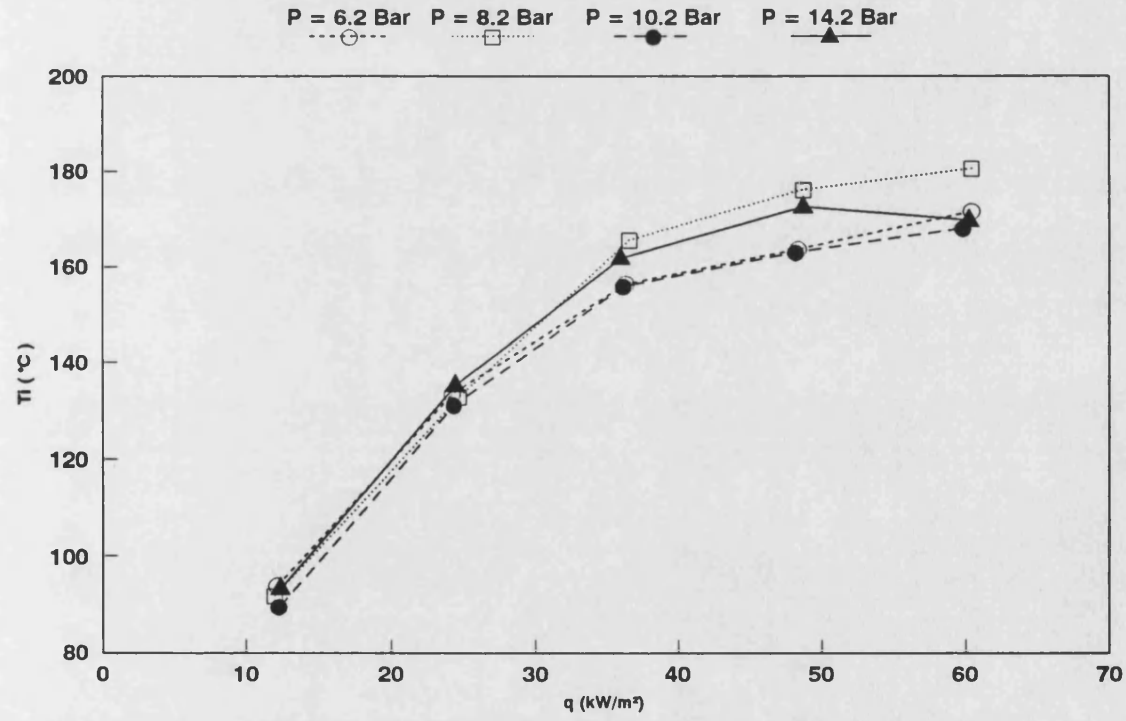

Fig (4.34) Inner surface temprature (Ti) vs heat flux (q) for bare tube test section No(1)

Effect of heat flux on Arabian light crude oil

Tb = 50 °C ; 20% F.S.R and 6.2 < P < 14.2 bar gauge of nitrogen gas

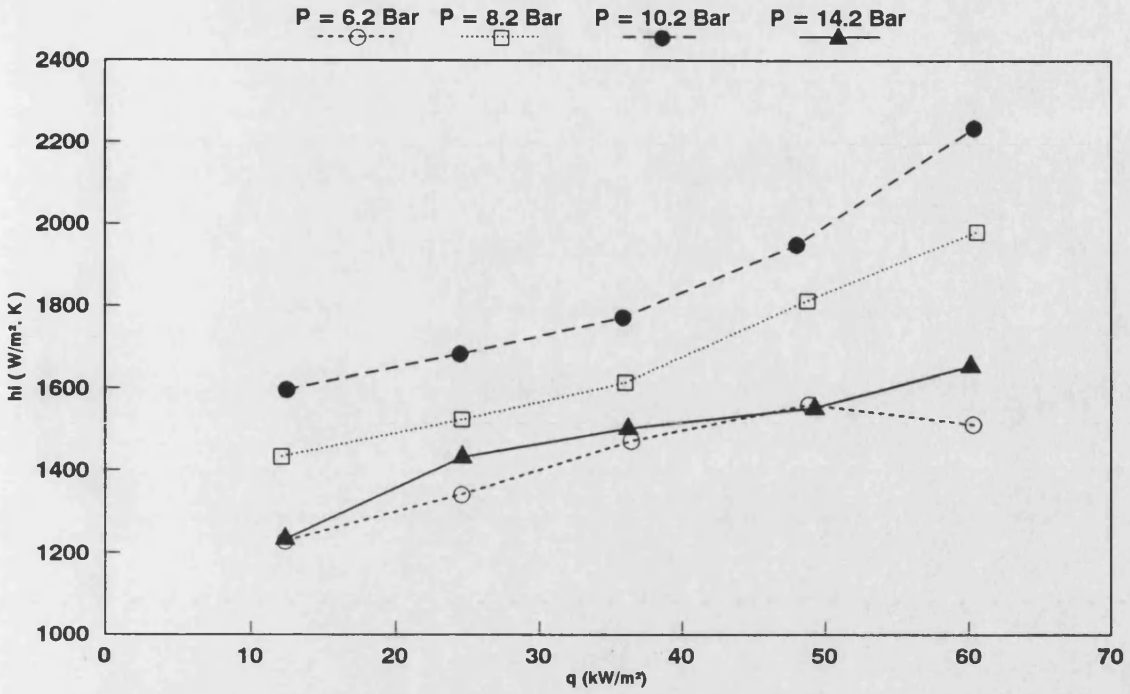

Fig (4.35) Heat transfer coefficient (hi) vs heat flux (q) for test section No (2) fitted with LDI-B

Effect of heat flux on Arabian light crude oil

Tb = 50 °C ; 20% F.S.R and 6.2 < P < 14.2 bar gauge of nitrogen gas

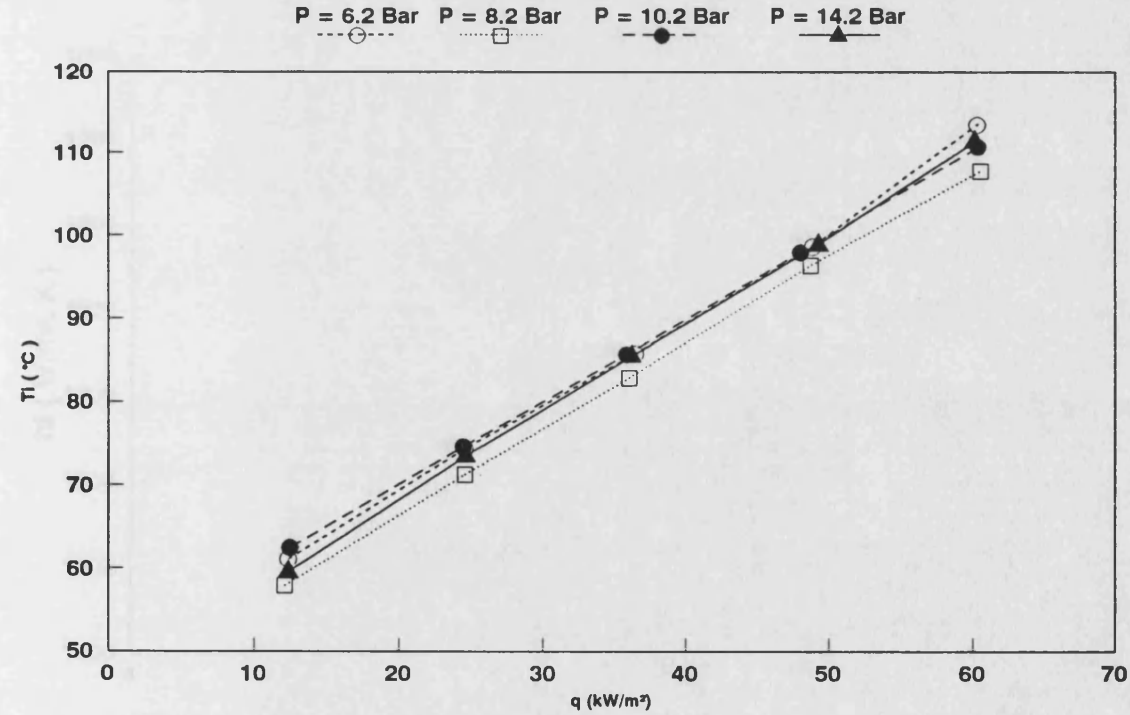

Fig (4.36) Inner surface temprature (Ti) vs heat flux (q) for test section No (2) fitted with LDI-B

Effect of heat flux on Arabian light crude oil

Tb = 50 °C ; 20% F.S.R and 6.2 < P < 14.2 bar gauge of nitrogen gas

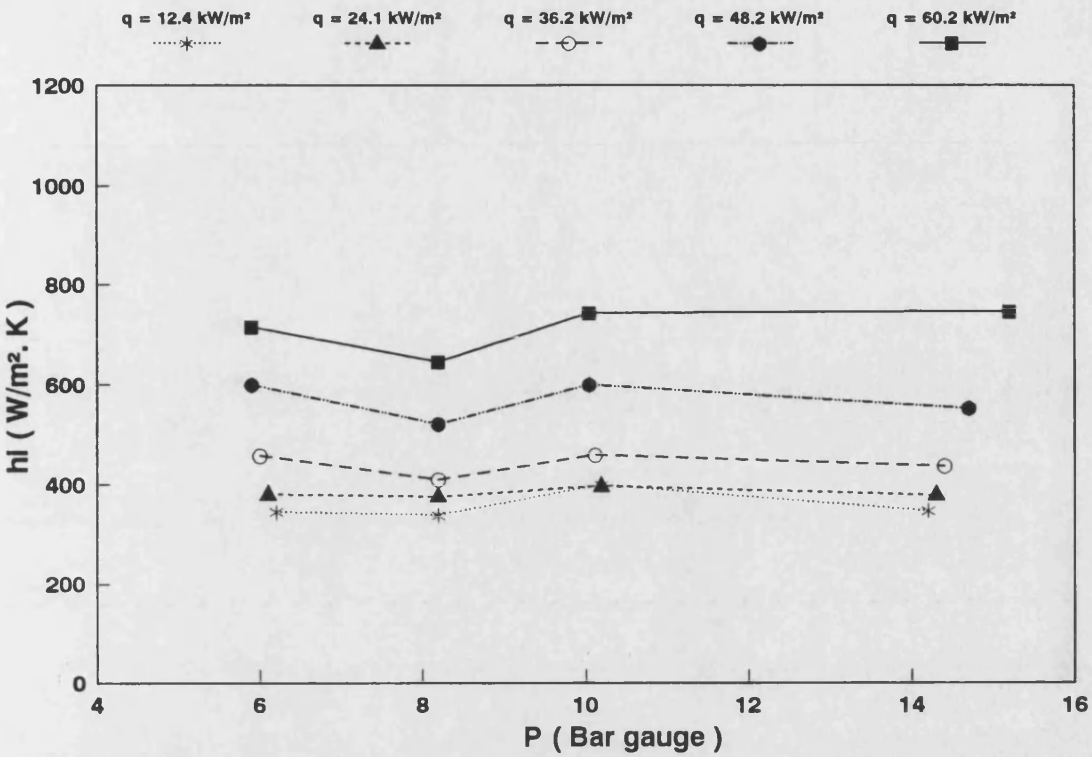

Fig (4.37) Heat transfer coefficient (hl) vs tank pressure (P) for bare tube test section No(1)
Effect of nitrogen gas pressure on Arabian light crude oil
Tb = 50 °C ; 20% F.S.R ; 12 < q < 60.2 kW/m² ; Re = 7000 and Pr = 100

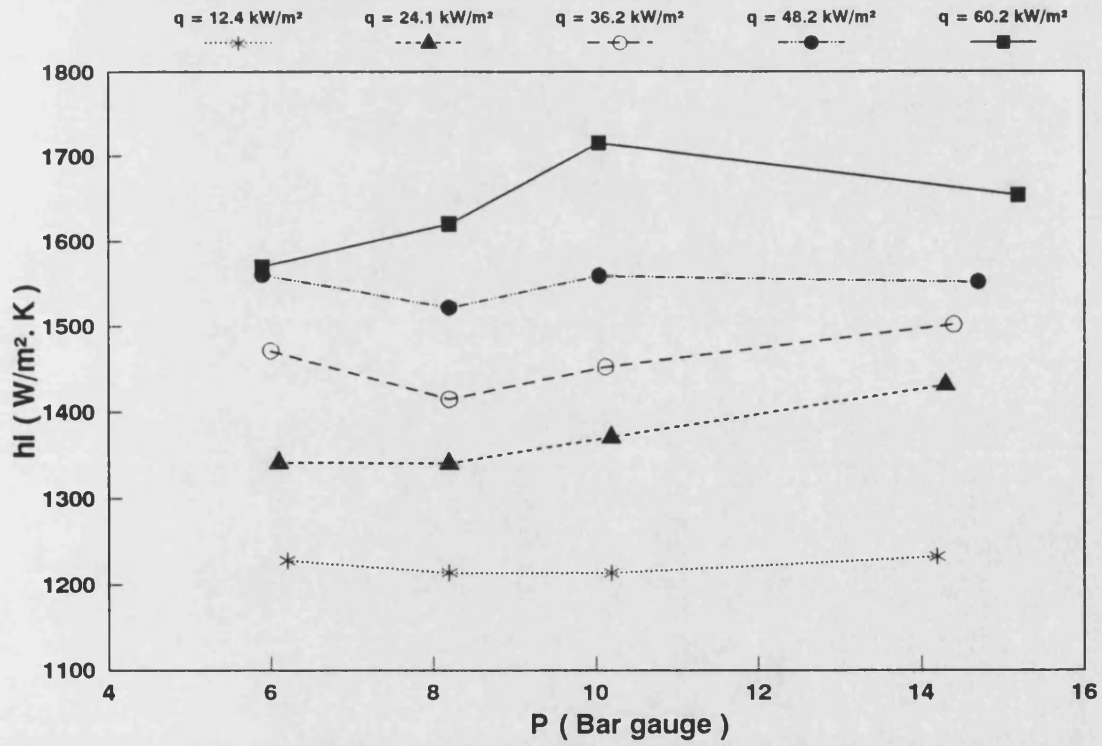

Fig (4.38) Heat transfer coefficient (hl) vs tank pressure (P) for test section No(2) fitted with LDI-B
Effect of nitrogen gas pressure on Arabian light crude oil
Tb = 50 °C ; 20% F.S.R ; 12 < q < 60.2 kW/m² ; Re = 7000 and Pr = 100

small for $q < 36$ kW/m^2 . However , for $q > 36$ kW/m^2 the gradient is noticeably higher. As nucleate boiling is unlikely to occur under these experimental conditions , it is a reasonable assumption that the enhancement in h_i was due to BNGSD . Fig 4.34 shows that T_i increased steeply with q for $q < 36$ kW/m^2 (the region where BNGSD was not expected) but for $q > 36$ kW/m^2 (the region where BNGSD was expected), T_i was not so dependent on heat flux.

Fig 4.35 shows a general increase in h_i with q for test section No(2) fitted with LDI-B . The gradients , $\frac{dh_i}{dq}$ were more or less constant over the range of heat fluxes tested ($12 < q < 60.2$ kW/m^2) but there was some variation with pressure . Fig 3.36 shows that T_i for test section No(2) increased linearly with q .

Fig 4.37 shows that h_i for the bare tube was affected slightly by pressure at constant q . Similar behaviour was noted for tube fitted with the **HiTran** insert , as may be seen in Fig 4.38 .

The principal conclusions which may be made from this experimental investigation on the nucleation of crude oil at high and low bulk temperatures , are listed below :

1- Two types of bubble nucleation probably exist in this study. The first is subcooled nucleate boiling which is controlled by

ΔT_{sat} (T_{sat} - T_b). Such bubble nucleation may be suppressed by increasing the pressure. The second type is bubble nucleation due to the solubility difference (BNGSD). Such bubble nucleation seems to be controlled by the temperature driving force ΔT_i (T_i - T_b) . This type of nucleation is likely to be enhanced by increasing the pressure, because pressure can increase the solubility of gas in the crude oil .

2- The heat transfer coefficient (h_i) of the bare tube can be enhanced by subcooled nucleate boiling and by BNGSD. However , the rate of enhancement by subcooled nucleate boiling is likely to be higher than by BNGSD.

3- The inner surface temperature T_i can be decreased by either subcooled nucleate boiling or BNGSD .

4- The **HiTran** insert may be used to suppress nucleate boiling . Thus , higher heat fluxes may be used . It is not clear, however , whether BNGSD can be suppressed by the **HiTran** insert.

5- Subcooled nucleate boiling as well as BNGSD can be suppressed by increasing the flow rate .

4.6.2.4 Fouling runs No 2 to No 5

a - Fouling run No(2)

It has been reported in many previous investigations[66,86,88,93,113,118,139,140] that the rate of chemical reaction fouling increases with increase in oxygen concentration in the feedstock . Thus , it was assumed that the absence of O_2 from the equipment was a major cause for the lack of fouling in the first run . In order to investigate this aspect , the experimental conditions for the second fouling run were kept similar to the first run , except that the pressurising gas was a mixture of 95% N_2 and 5% O_2 , instead of 100% N_2 in the first run .

The variation of pressure (P) , inner surface temperature (T_i) , overall heat transfer coefficient (U_t) and apparent fouling resistance ($R_{f(App)}$) with time are shown in Figs 4.39 and 4.40 for test sections No(1) and No(2) respectively .

Fig 4.39 shows that T_i of the bare tube was decreased by about 3.6°C (from 186.6 to 183 °C) in the first 13 hrs , then remained unchanged to the end of the run (50 hrs) . The pressure also started to decrease with time . However , it was then maintained in the range of 7.7 to 8.2 bar gauge by adding more N_2 gas pressure to the equipment . The overall heat transfer coefficient (U_t) increased from 430 to 492 W/m² °C in the first 13 hrs, then remained more or less constant to the end of the run. $R_{f(App)}$ reached

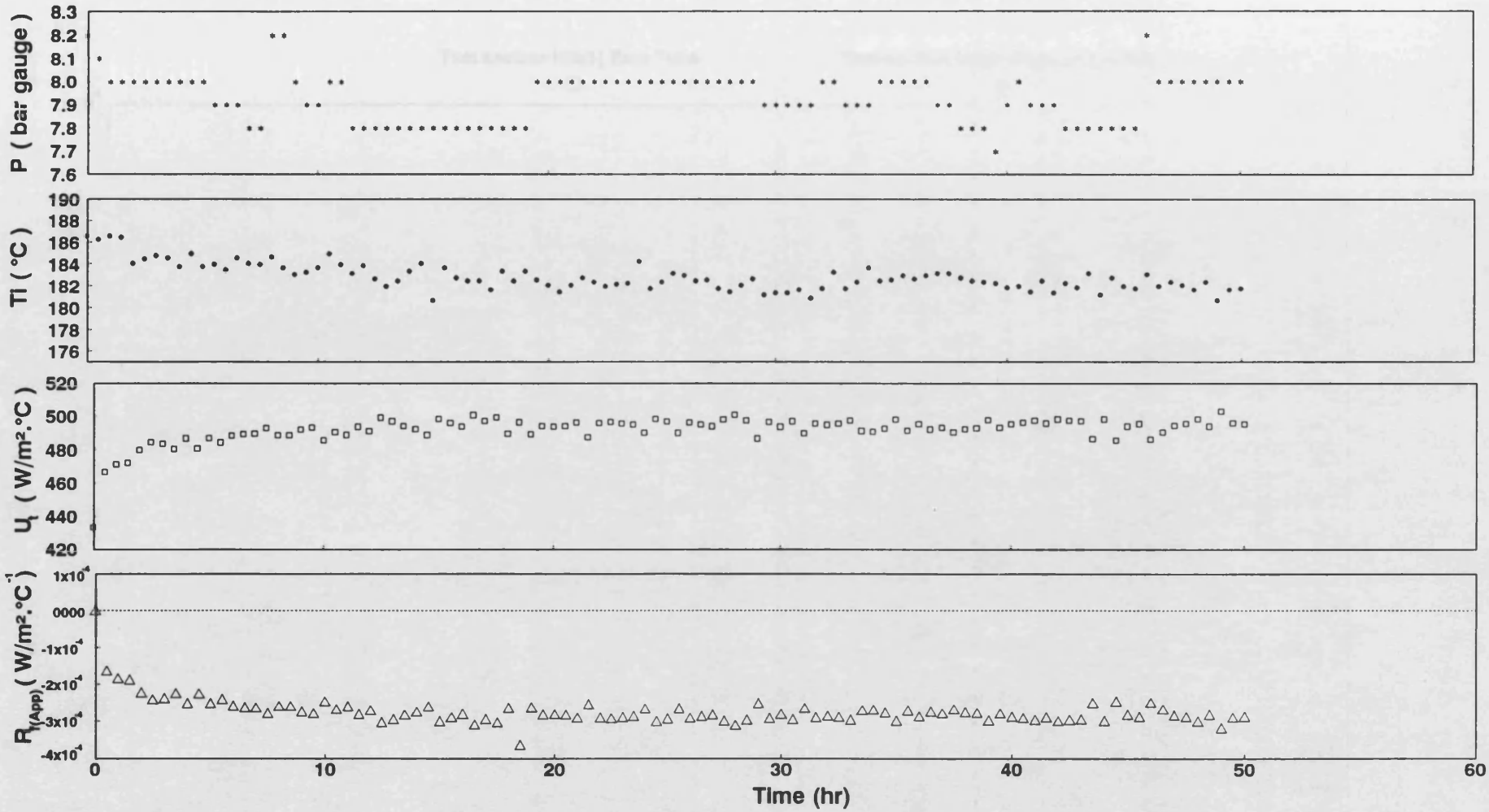

Fig (4.39) Fouling Run No(2) for bare tube test section No(1) [20% F.S.R ; Tb = 140 °C ; Re = 7000 ; Pr = 28 and q = 54.18 kW/m²]
Arabian light crude oil under pressure of 95% of nitrogen and 5% of oxygen gases

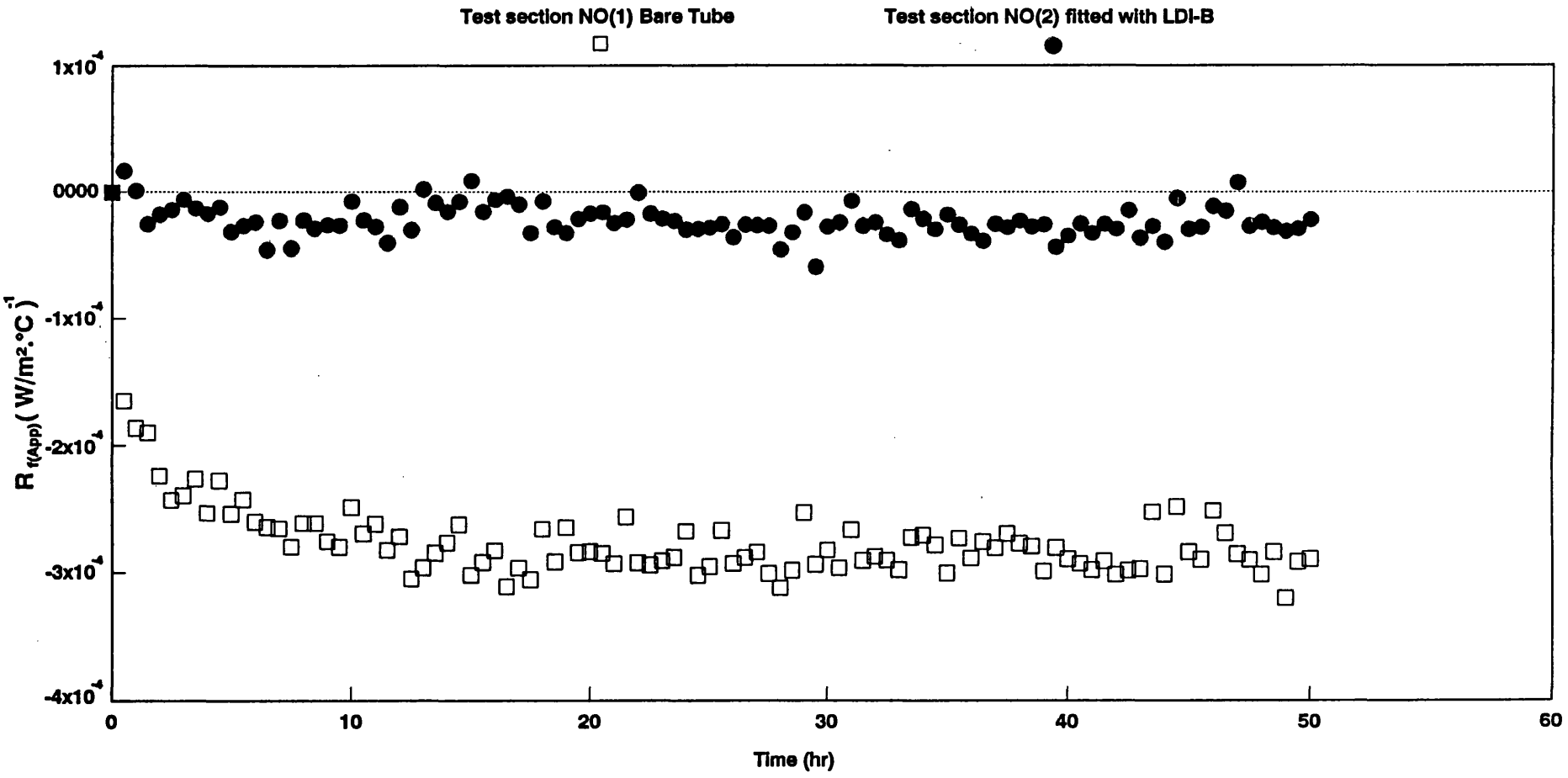

Fig (4.42) Comparison between apparent fouling resistance ($R_{f(App)}$) of both test sections for Fouling Run NO(2)

Arabian light crude oil under pressure of 95% nitrogen and 5% of oxygen gases [20% F.S.R ; Tb = 140 °C ; Re = 7000 ; Pr = 28 and q = 54.18 kW/m²]

it's lowest value [$-3x10^{-4}$ $(W/m^2\ °C)^{-1}$] after 13 hrs , then remained unchanged .

Fig 4.40 shows that T_i and U_t for test section No(2) fitted with LDI-B , remained unchanged with time . $R_{f(App)}$ was almost zero.

The test sections were physically inspected and fouling did not occur in this run as well . However, negative values of $R_{f(App)}$ in the bare tube is a clear evidence that h_i had been enhanced either by nucleate boiling and/or by BNGSD .

A comparison between U_t and T_i for both test sections is shown in Fig 4.41 . U_t (which includes R_w) of the tube fitted with the **HiTran** insert was almost twice that of the bare tube. T_i of the bare tube was about 10°C higher than that of test section No(1) . A comparison between $R_{f(App)}$ values for both test sections is shown in Fig 4.42 .

b - Fouling run No(3)

It has been noted[67] that asphaltene precipitation is one of the major mechanisms in crude oil heat exchanger fouling . Thus , it was believed that by increasing the asphaltene content of the crude oil fouling would be encouraged . Consequently , 10% by weight of refinery sludge (mixture of asphaltene and wax) , provided by ESSO Petroleum , was added to the Arabian light crude oil. No major changes in physical properties such as ρ , ν , C_p and k were found and thus

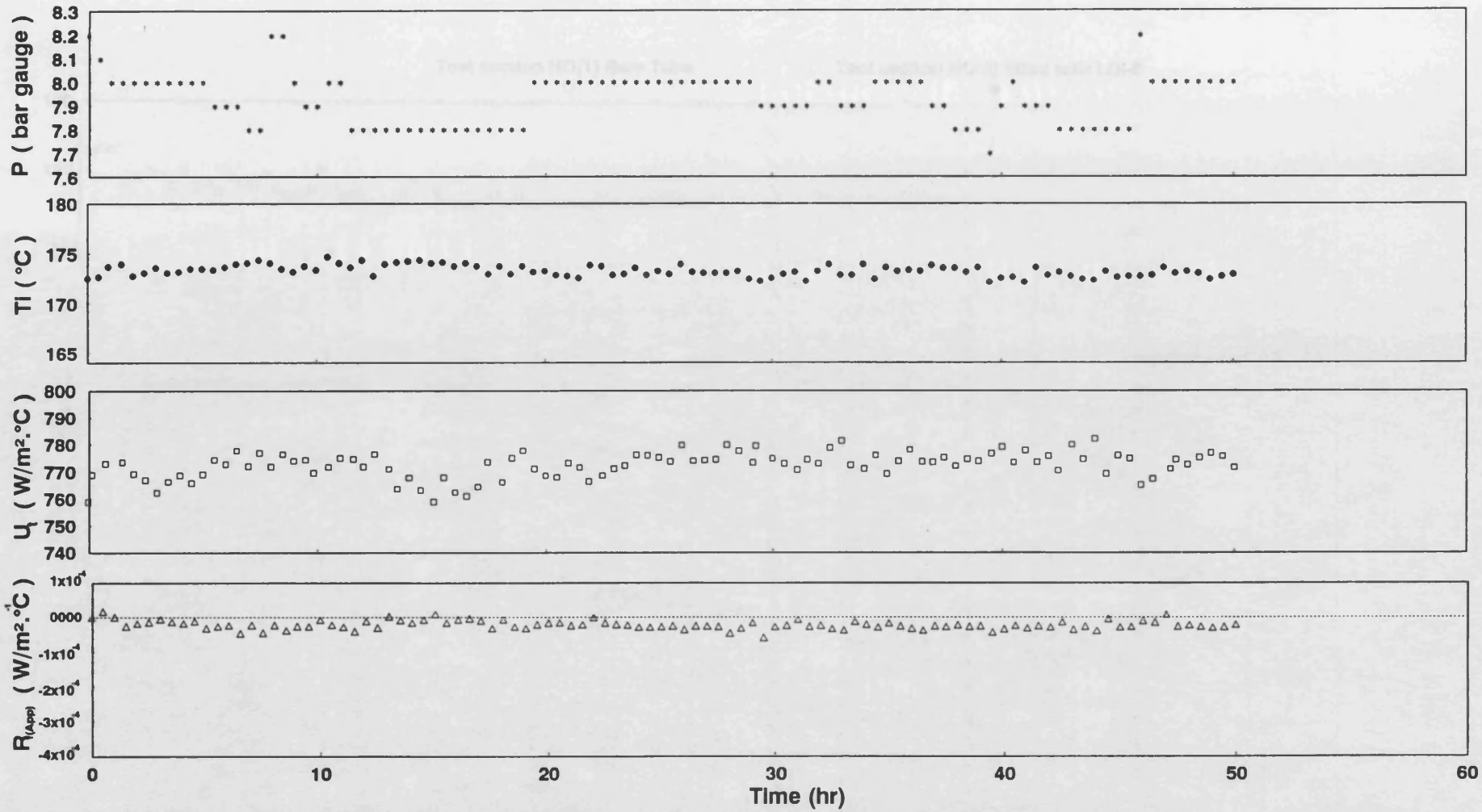

Fig (4.40) Fouling Run No(2) for test section No(2) fitted with LDI-B [20% F.S.R ; Tb = 140 °C ; Re = 7000 ; Pr = 28 and q = 54.18 kW/m²]
Arabian light crude oil under pressure of 95% of nitrogen and 5% of oxygen gases

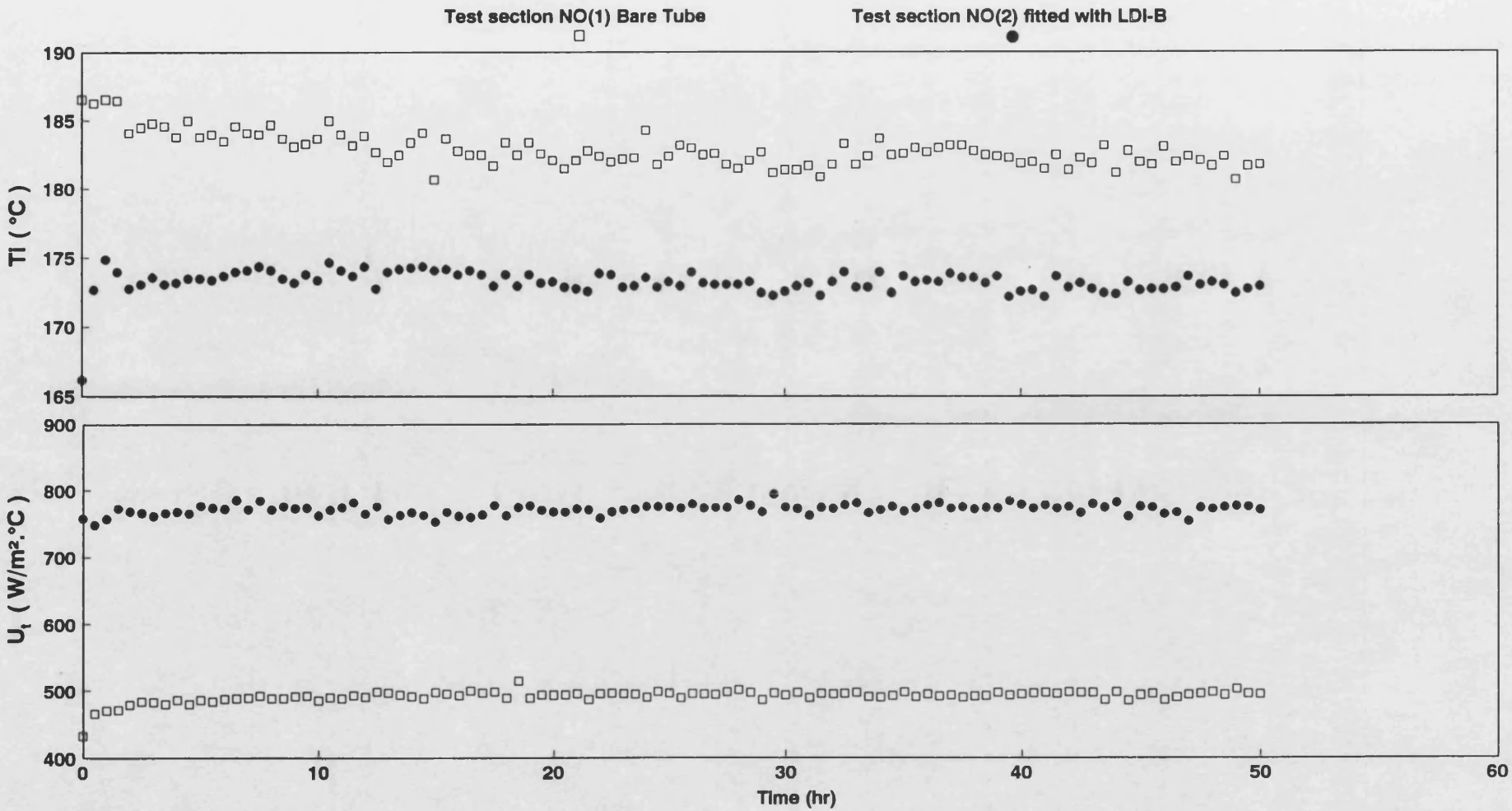

Fig (4.41) Comparison between the overall heat transfer coefficient (Ut) and the inner surface temperature (Ti) for both test sections

Fouling Run NO(2) ; Arabian light crude oil under pressure of 95% of nitrogen and 5% of Oxygen gases ; [20% F.S.R ; Tb = 140 °C ; Re = 7000 ; Pr = 28 ; q = 54.18 kW/m²]

equations 4.1 to 4.32 were applied to this new fluid mixture (Arabian light crude oil + 10% of refinery sludge) .

The experimental conditions for run 3 were similar to those for run 2 . Unfortunately , run 3 had to be terminated after 16 hrs due to mechanical failure of the hydrocarbon feed pump . Nonetheless the variations of P , T_i , U_t and $R_{f(App)}$ with time are shown in Figs 4.43 and 4.44 for test sections No(1) and No(2) respectively .

Fig 4.43 shows that T_i for the bare tube decreased by about 3°C in the first 3 hrs and then remained constant . U_t was increased by 13 W/m² °C in the same period . On average P decreased with time although it was maintained in the range of 7.9 to 8.2 bar gauge. $R_{f(App)}$ decreased to $-5x10^{-5}$ $(W/m^2\ °C)^{-1}$ after 3 hrs and then remained unchanged .

Fig 4.44 shows that T_i and U_t for test section No(2) , fitted with LDI-B , were unchanged with time and that $R_{f(App)}$ remained equal to zero .

Fig 4.45 shows a comparison between U_t and T_i for both test sections . A comparison between $R_{f(App)}$ for both test sections is shown in Fig 4.46 .

c - Fouling run No(4)

This run was under similar experimental conditions as the previous run , but with a longer running time (120 hrs).

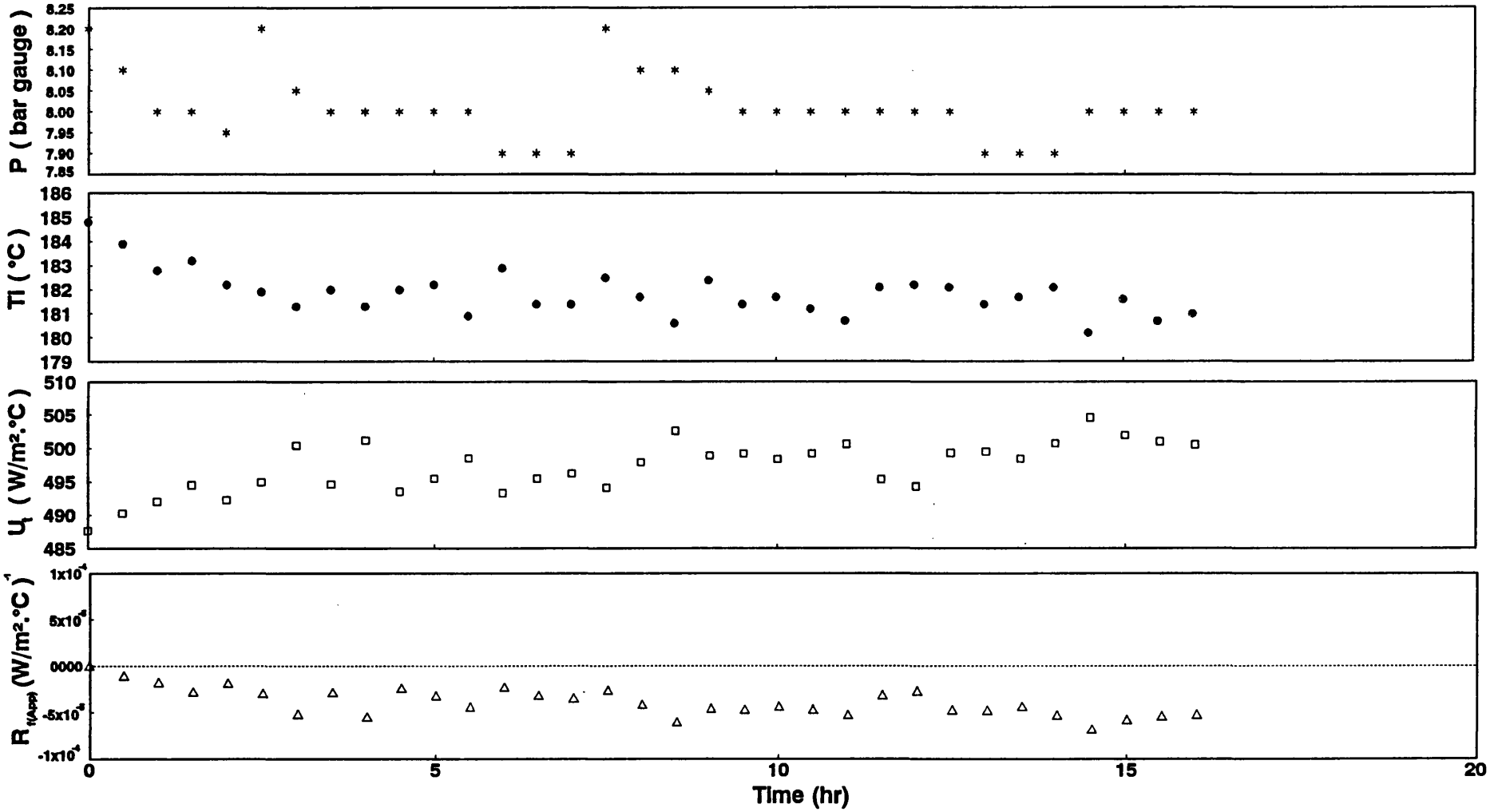

Fig (4.43) Fouling Run No(3) for bare tube test section No(1) [20% F.S.R ; Tb = 140 °C ; Re = 7000 ; Pr = 28 and q = 54.18 kW/m²]

Arabian light crude oil with 10% by weight of refinery sludge under pressure of 95% of nitrogen and 5% of oxygen gases

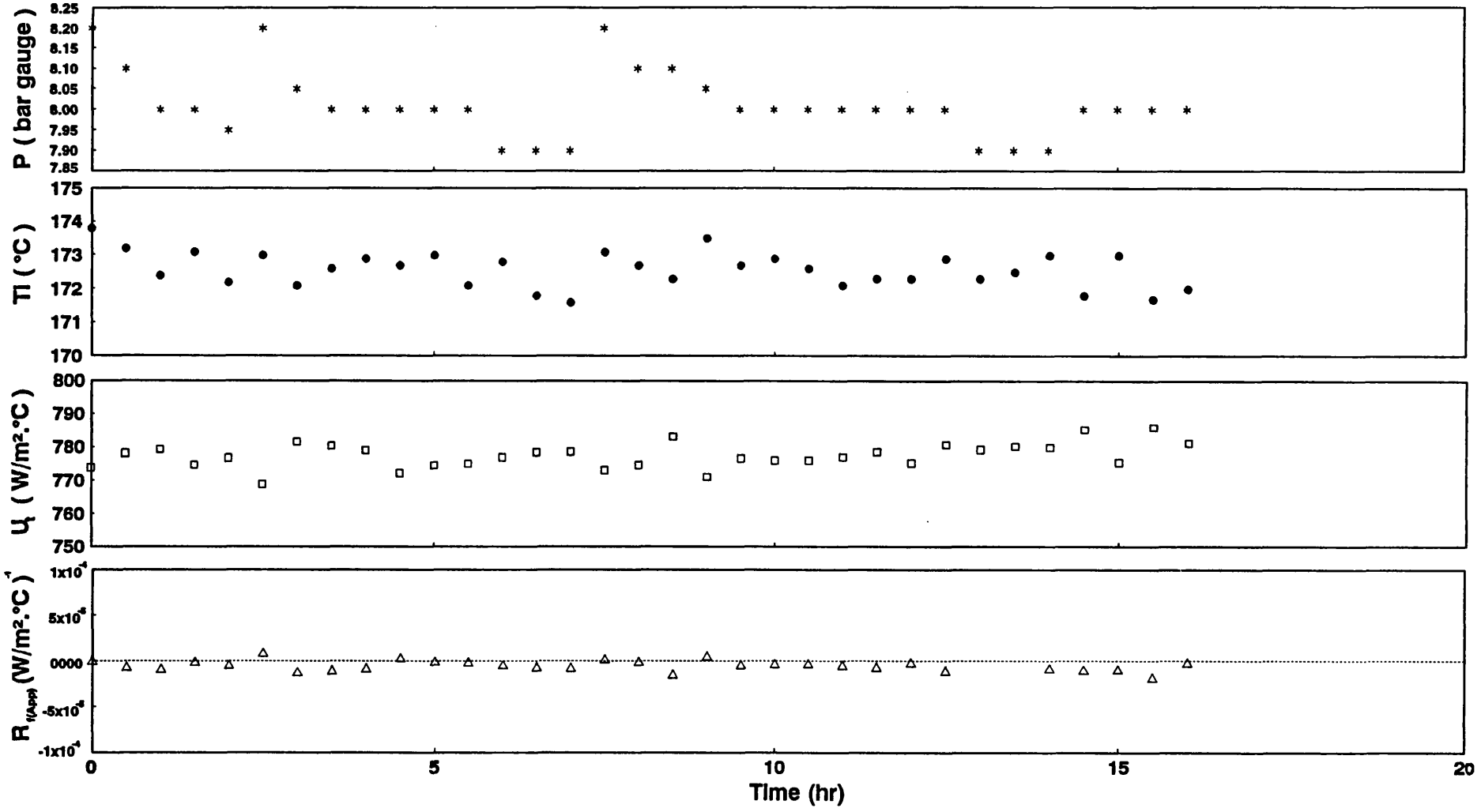

Fig (4.44) Fouling Run No(3) for test section No(2) fitted with LDI-B [20% F.S.R ; Tb = 140 °C ; Re = 7000 ; Pr = 28 ; q = 54.18 kW/m²]

Arabian light crude oil with 10% by weight of refinery sludge under pressure of 95% of nitrogen and 5% of oxygen gases

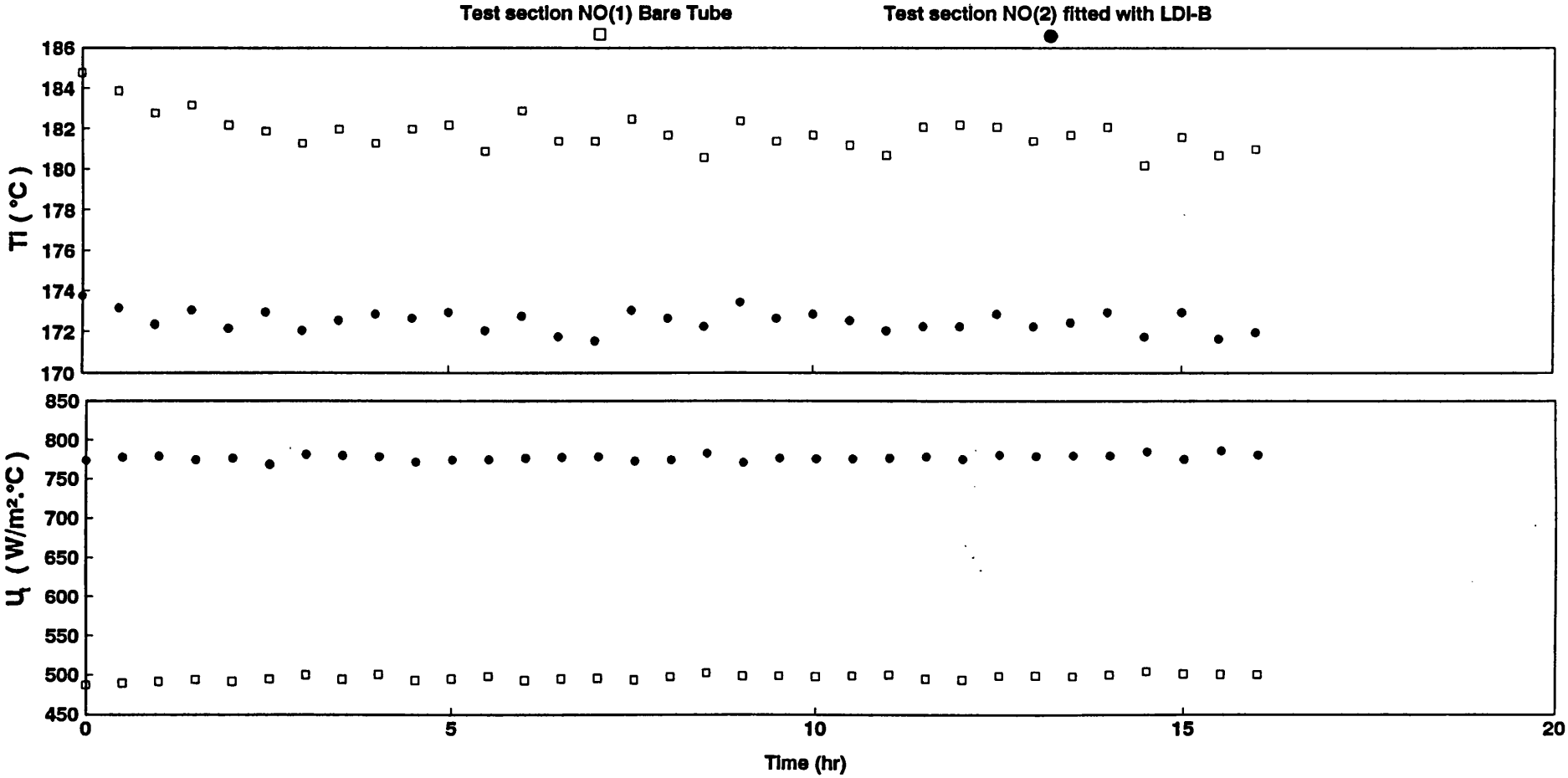

Fig (4.45) Comparison between the overall Heat Transfer coefficient (Ut) and inner surface temperature (Ti) for both test sections

Arabian light crude oil with 10% by weight of refinery sludge under pressure of 95% nitrogen and 5% of oxygen gases

Fouling Run NO(3) [20% F.S.R ; Tb = 140 °C ; Re = 7000 ; Pr = 28 and q = 54.18 kW/m²]

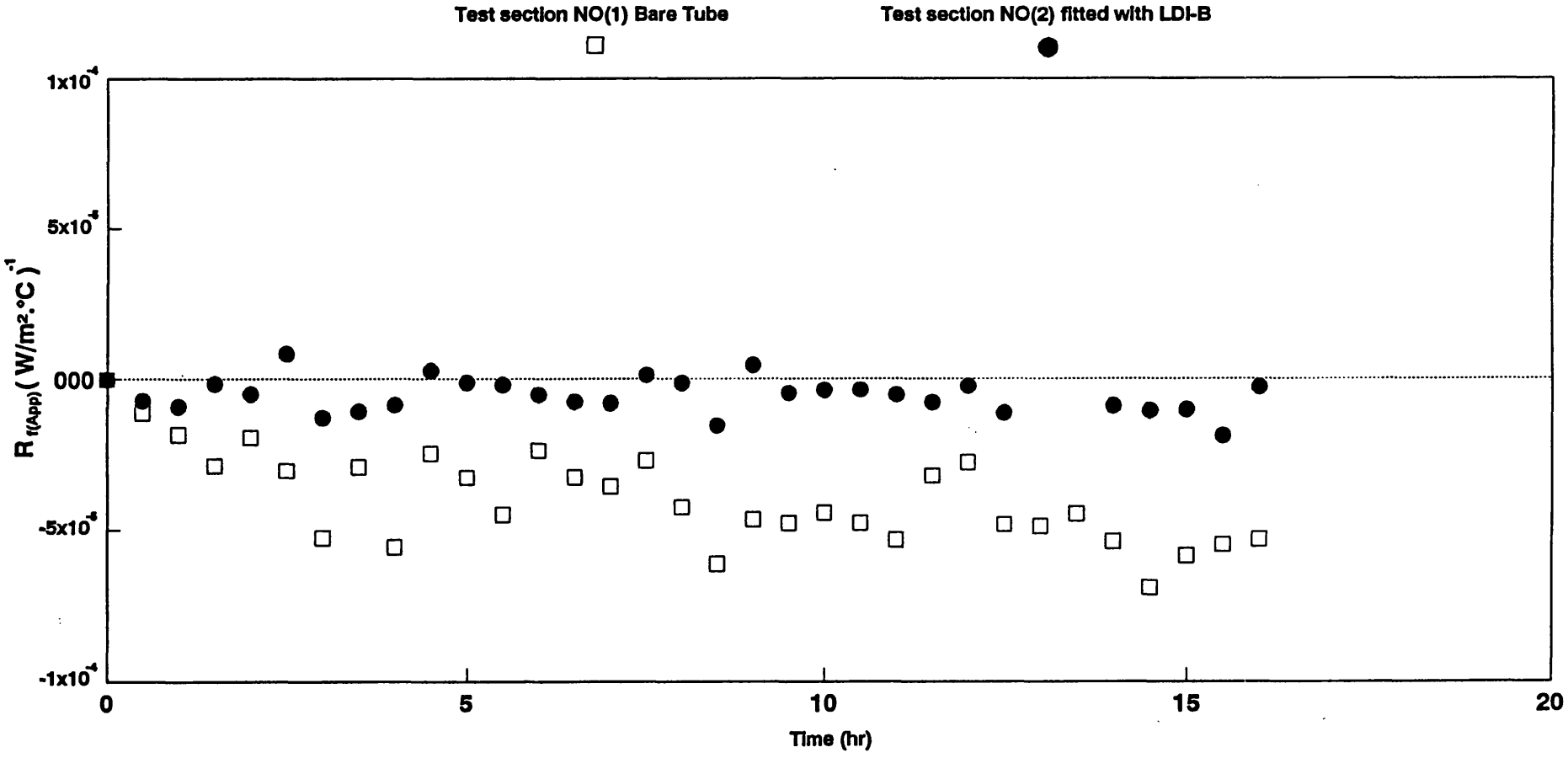

Fig (4.46) Comparison between apparent fouling resistance ($R_{f(App)}$) of both test sections for Fouling Run NO(3)

Arabian light crude oil with 10% by weight of refinery sludge under pressure of 95% nitrogen and 5% of oxygen gases
[20% F.S.R ; Tb = 140 °C ; Re = 7000 ; Pr = 28 and q = 54.18 kW/m²]

The variations of P , T_i , U_t and $R_{f(App)}$ with time are shown in Figs 4.47 and 4.48 for test sections No(1) and No(2) respectively .

Although this run is a repetition of run No(3), the variation of T_i , U_t and $R_{f(App)}$ with time for both test sections were different. Fig 4.47 shows that T_i of bare tube was decreased by about 12 °C in the first 3 hrs (instead of by 3°C in the previous run) and then remained constant to the end of the run . U_t was increased by about 52 W/m^2 °C in 3 hrs instead of by 13 W/m^2 °C in the previous run and then became steady until the end of the run. $R_{f(App)}$ decreased from zero to $-2.5x10^{-4}$ $(W/m^2\ °C)^{-1}$ in the first 3 hrs and then remained constant. P was maintained constant at about 8.2 bar gauge by regularly adding more N_2 gas pressure to the equipment. This possibly increased the solubility of N_2 in the crude and thus BNGSD had possibly increased as well .

The increase of U_t during the first 3 hrs of operation may be explained by the mechanism of bubble nucleation in the bare tube test section . Bubble nucleation (either subcooled nucleate boiling or BNGSD) is likely to need some time before reaching steady state conditions. During the unsteady conditions h_i was enhanced with time and thus U_t increased , while T_i would be expected to decrease as seen in Fig 4.47. This , however, is discussed in more detail in fouling run No(5) .

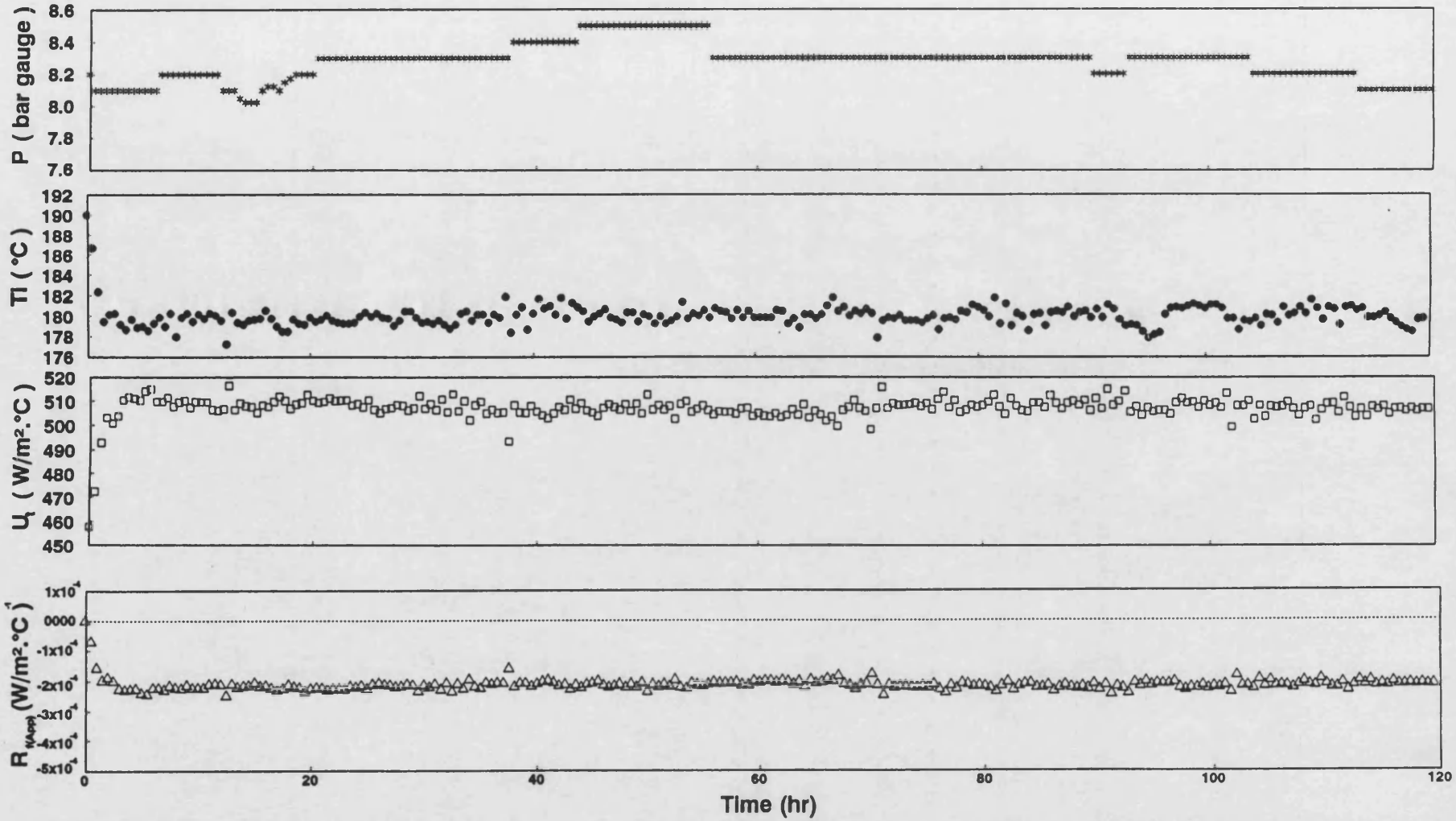

Fig (4.47) Fouling Run No(4) for bare tube test section No(1) [20% F.S.R ; Tb = 140 °C ; Re = 7000 ; Pr = 28 and q = 54.18 kW/m²]

Arabian light crude oil with 10% by weight of refinery sludge under pressure of 95% of nitrogen and 5% of oxygen gases

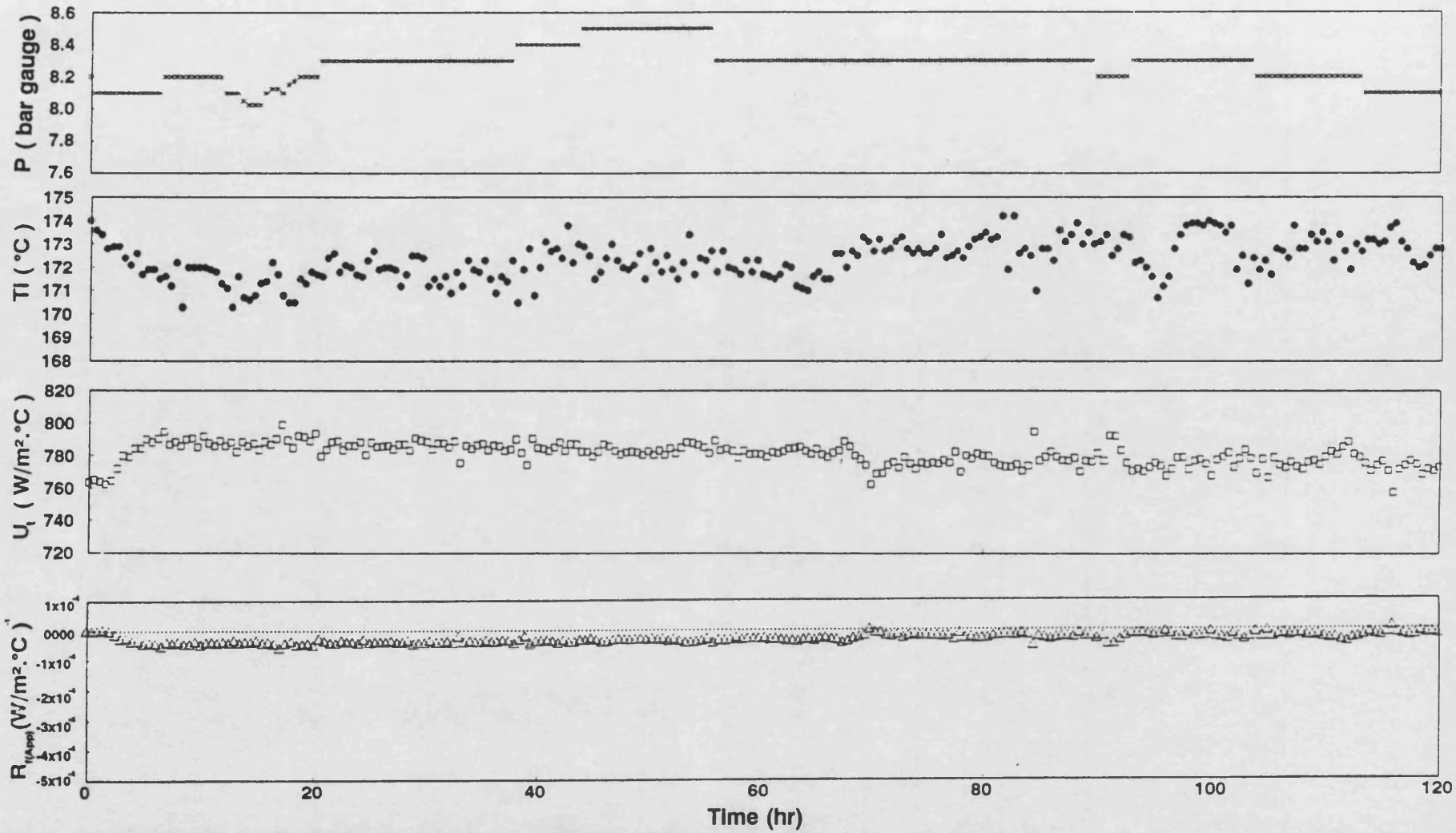

Fig (4.48) Fouling Run No(4) for test section No(2) fitted with LDI-B [20% F.S.R ; Tb = 140 °C ; Re = 7000 ; Pr = 28 and q = 54.18 kW/m²]

Arabian Light Crude Oil with 10% by weight of Refinery Sludge under pressure of 95% N_2 and 5% O_2 gases

Fig 4.48 shows that Ti of test section No(2) , fitted with LDI-B , was slightly decreased (3°C) in the first 3 hours of the operation . U_t was increased by about 30 W/m^2 °C in the same period of time. $R_{f(App)}$ became a small negative value . This is the first occasion in this equipment that a egative value of $R_{f(App)}$ was calculated for the tube fitted with a **HiTran** insert and indicated that BNGSD possibly occurred in test section No(2) .

A comparison between T_i and U_t for both test sections is shown in Fig 4.49. The initial difference between T_i of both test sections was 16°C but reduced to 7°C after 3 hrs . U_t of test section No(2) was about 1.6 times that of the bare tube.

Fig 4.50 shows a comparison between $R_{f(App)}$ for both test sections . $R_{f(App)}$ of test section No(2) is closer to zero than that of the bare tube test section No(1) .

Visual inspection showed that fouling did not occur in this run . Thus the next run had to be under different experimental conditions .

d - Fouling run No(5)

It has been reported[66,115,117] that for any particular fluid there is a break-point surface temperature above which fouling occurs and below which none occurs. It was suspected that all previous runs were carried out at surface temperatures below

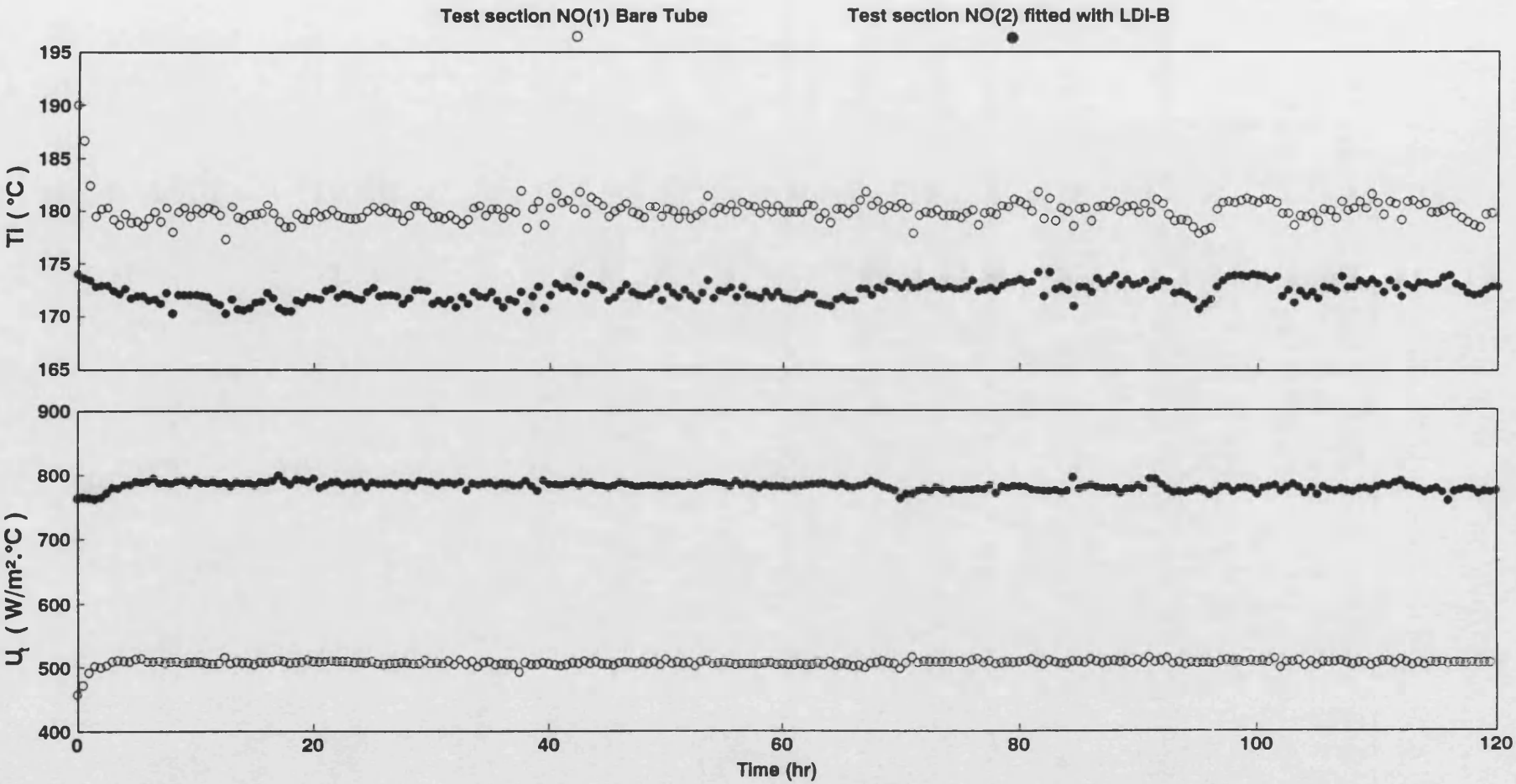

Fig (4.49) Comparison between the overall heat transfer coefficient (Ut) and inner surface temperature (Ti) for both test sections

Arabian light crude oil with 10% by weight of refinery sludge under pressure of 95% of nitrogen and 5% of oxygen gases

Fouling Run NO(4) [20% F.S.R ; Tb = 140 °C ; Re = 7000 ; Pr = 28 and q = 54.18 kW/m²]

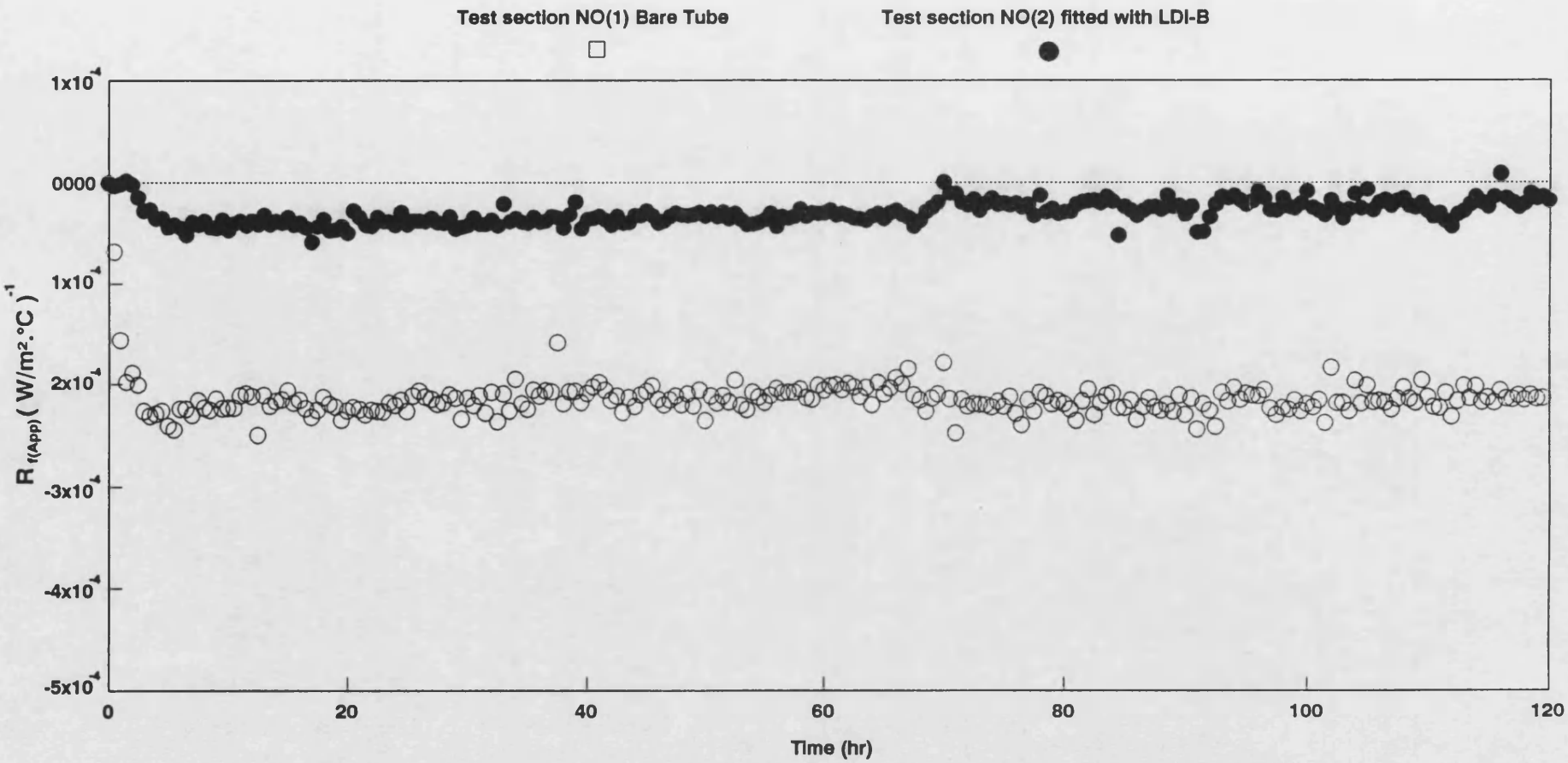

Fig (4.50) Comparison between apparent fouling resistance ($R_{f(App)}$) of bothtest sections for fouling Run NO(4)

Arabian light crude oil with 10% by weight of refinery sludge under pressure of 95% of nitrogen and 5% of oxygen gases

[20% F.S.R ; Tb = 140 °C ; Re = 7000 ; Pr = 28 and q = 54.18 kW/m²]

the break-point temperature of the crude oil . Thus , run 5 was designed to have a higher inner surface temperature. Clearly, the effect of nucleate boiling and/or BNGSD on reducing T_i for the bare tube was considered to be a potential problem in raising T_i .

In order to determine the highest possible T_i under N_2 gas pressure, the variation of T_i and h_i with time were investigated over a short period of time (250 mins).

Fig 4.51 shows the variation of h_i , T_i and P with time at fixed flow rate and heat flux for both test sections . The heat flux was increased after 150 minutes. Initially at q = 54.2 kW/m^2 and P = 12.2 bar gauge , T_i for the bare tube was 198°C and that for LDI-B tube was 175°C, whilst h_i for the bare tube was 1320 W/(m^2 K) and for test section No(2) was 2380 W/(m^2 K). After 30 min P was manually increased to 12.6 bar gauge . However , T_i of the bare tube was decreased to 196.5°C and h_i increased to 1360 W/(m^2 K). No change was noted in T_i or h_i for test section No(2) . The pressure was left to fall with time and its value as well as the surface temperatures were monitored every 30 minutes. After 120 mins T_i of the bare tube had been decreased to 187°C and h_i increased to 1700 W/(m^2 K) . The pressure had decreased to 11.95 bar gauge. Again no changes in T_i or h_i for test section No(2) were observed. After 150 minutes , P and q were manually increased to 12.0 bar

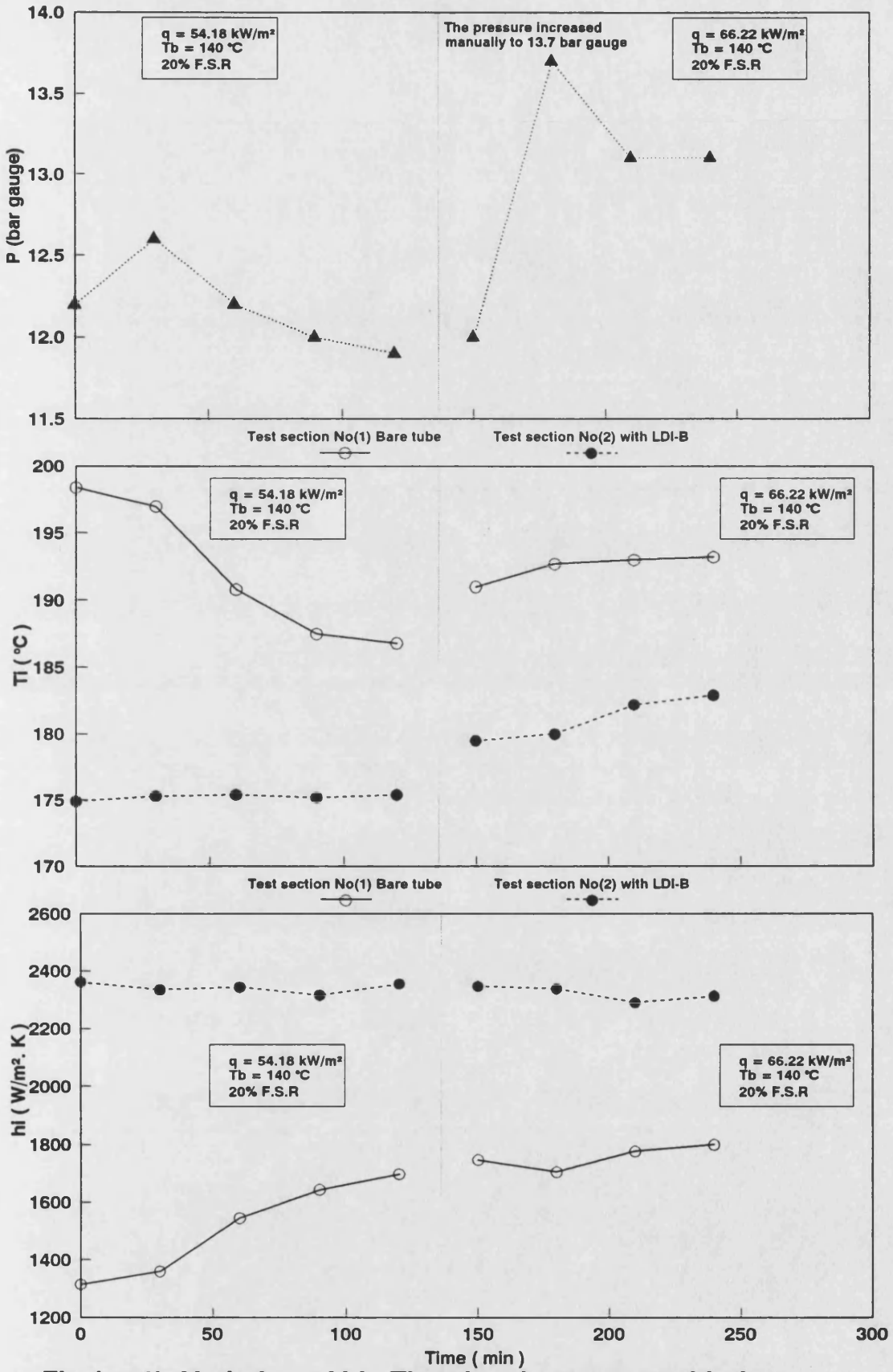

Fig (4.51) Variation of hi , Ti and tank pressure with time

Preparation for fouling Run No(5) for Arabian light crude oil + 10% wt sludge

20% F.S.R ; under pressure of nitrogen gas ; Re = 7000 ; Pr = 27

gauge and 66.22 kW/m² respectively. At the new conditions , T_i of the bare tube became 191°C and for the tube fitted with LDI-B 178°C. The coefficient h_i of the bare tube increased to 1750 W/(m^2 K) while h_i of the tube with LDI-B remained essentially unchanged. By increasing the pressure (manually) to 13.7 bar gauge , T_i for the bare tube was increased just 1°C to 192°C , while h_i remained virtually unchanged. T_i and h_i of the tube fitted with LDI-B were also unchanged . The pressure was then left to fall again. After a total time of 210 minutes , P was steady at 13.0 bar gauge and no further changes in T_i or h_i were observed .

Conclusions gained from Fig 4.51 are summarized below ;

1- For each heat flux, for the bare tube, steady state conditions may need at least 120 minutes to establish .

2- During the unsteady state conditions P decreases T_i decreases and h_i increases for any initial pressure .

3- As the initial pressure is increased more N_2 gas could be dissolved in the crude oil and thus the tank pressure can slowly decrease. Thus the possibility of BNGSD occurring in the bare tube could also be increased by increasing T_i.

4- Since T_i and h_i of the tube fitted with the **HiTran** insert were not changed with time, BNGSD was believed not to occur in test section No(2) .

Following this initial study, it was decided that fouling run 5 would be carried out at $T_b = 140°C$, $q = 54.2\ kW/m^2$ and P = 12.5 bar gauge . The flow rate was 20% F.S.R (Re = 7000) for the first 19 hrs and was then decreased to 10% F.S.R in order to increase T_i for the bare tube . The variations of P , T_i , U_t and $R_{f(App)}$ with time are shown in Figs 4.52 and 4.53 for test sections No(1) and No(2) respectively.

Fig 4.52 shows that T_i of the bare tube decreased from 197°C to 180°C in the first 3 hrs then became steady . After 19 hrs the flow rate was decreased intentionally to 10% F.S.R in order to increase T_i to 195°C . The pressure decreased to 12.0 bar in first 2 hrs . However , it was maintained constant at 12.5 bar , by adding more N_2. U_t increased from 420 to 500 $W/(m^2\ °C)$ in the first 2 hrs to become constant until the flow rate was changed to 10% F.S.R . At this flow rate (10% F.S.R) , U_t remained constant at 440 $W/(m^2\ °C)$. $R_{f(App)}$ became negative at 20% F.S.R but returned to zero at 10% F.S.R .

Fig 4.53 shows that T_i of test section No(2) was slightly decreased from 174°C to 172°C in the first 5

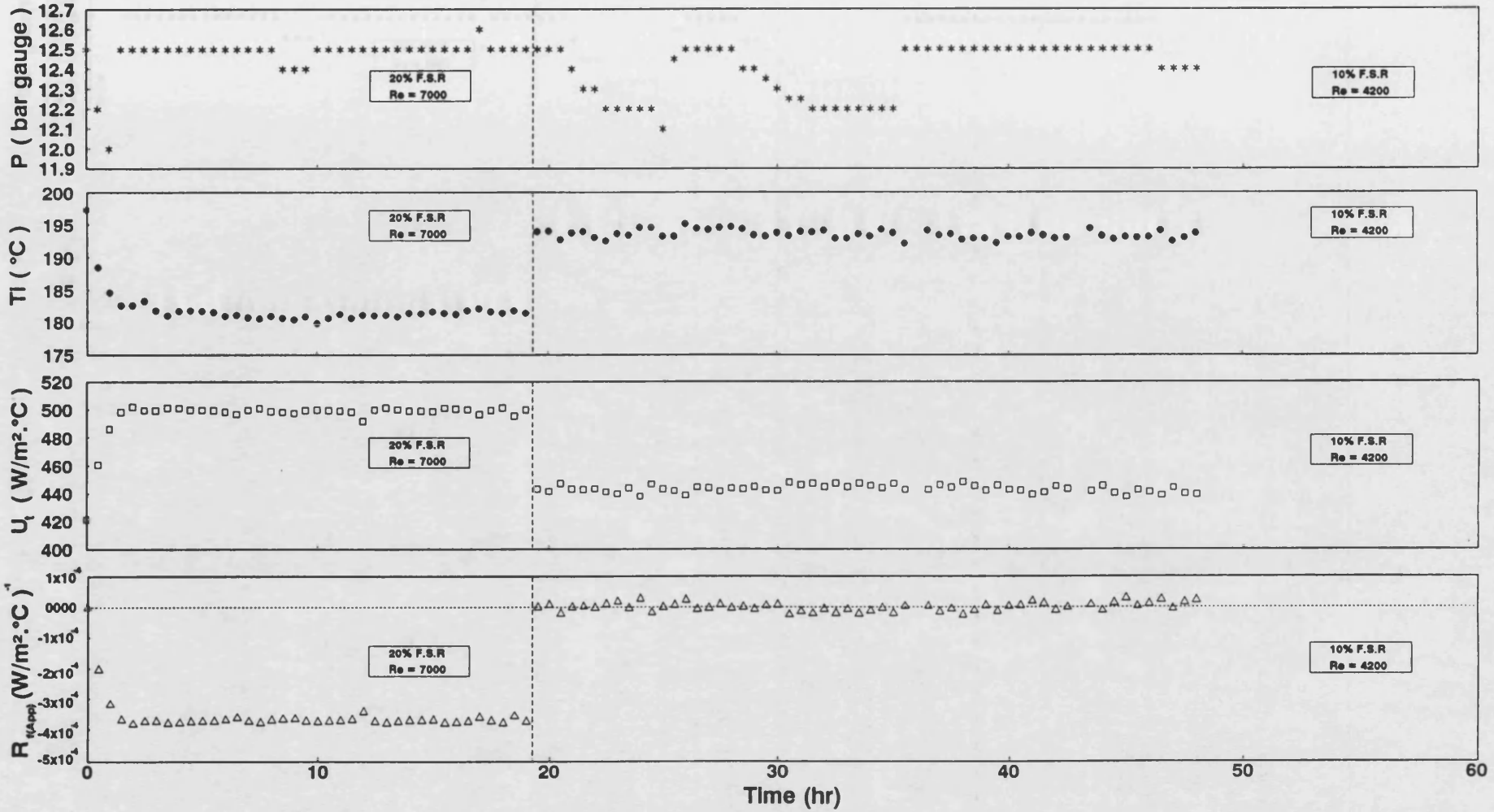

Fig (4.52) Fouling Run No(5) for bare tube test section No(1) [20% & 10% F.S.R ; Tb = 140 °C ; Re = 7000 & 4200 ; Pr = 28 ; q = 54.18 kW/m²]
Arabian light crude oil with 10% by weight of refinery sludge under pressure of 95% of nitrogen and 5% of oxygen gases

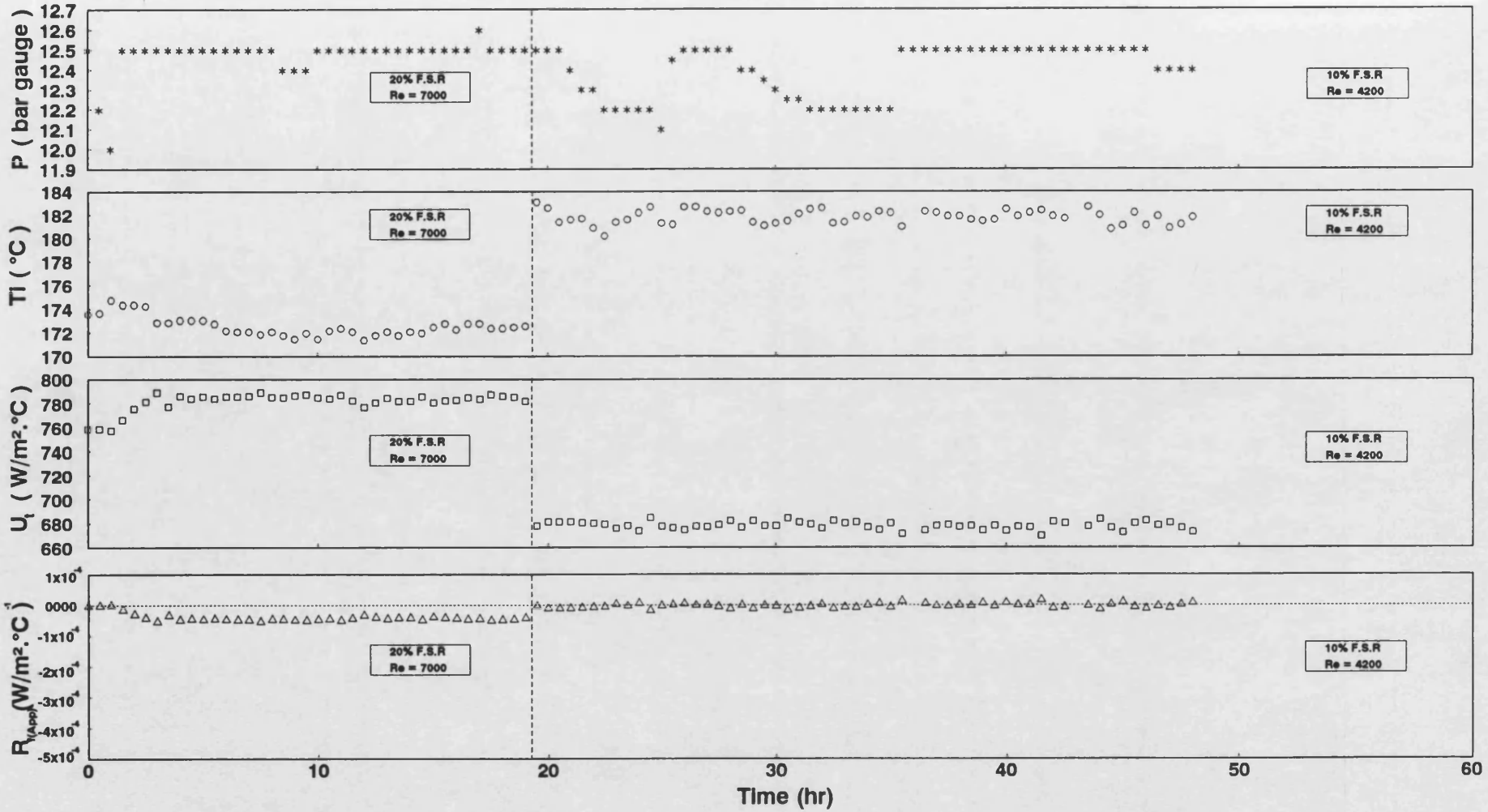

Fig (4.53) Fouling Run No(5) for test section No(2) fitted with LDI-B [20% & 10% F.S.R ; Tb = 140 °C ; Re = 7000 & 4200 ; Pr = 28 ; q = 54.18 kW/m²]
Arabian light crude oil with 10% by weight of refinery sludge under pressure of 95% of nitrogen and 5% of oxygen gases

hours and then became steady. When the flow rate was decreased to 10% F.S.R , T_i increased to 182°C and then remained unchanged. U_t was increased from 760 to 790 W/(m^2 °C) in the first 5 hours and then remained constant until the flow rate was reduced. At 10% F.S.R, U_t was constant at 660 W/(m^2 °C) . $R_{f(App)}$ was slightly negative at 20% F.S.R and zero at 10% F.S.R .

A comparison between U_t and T_i for both test sections are shown in Fig 4.54 . The initial difference between T_i of both test sections was 24°C. However, after 3 hrs that difference became only 8°C. When the flow rate was reduced to 10% F.S.R the difference in T_i became 13°C and remained unchanged. At 20% F.S.R , U_t of test section No(2) was initially 1.9 times that of the bare tube, reduced to 1.6 times after 3 hrs . For 10% F.S.R , U_t of test section No(2) was about 1.55 times that of the bare tube.

A comparison between $R_{f(App)}$ of both test sections is shown in Fig 4.55. For 20% F.S.R , $R_{f(App)}$ for both test sections was negative . However, for 10% F.S.R , both values were zero .

The test sections were visually inspected and no fouling occurred in run No(5) . The next run was carried out under pressure of helium gas which shows a reverse solubility behaviour with temperature, as seen in Fig 4.5 , Section 4.5.2.1 .

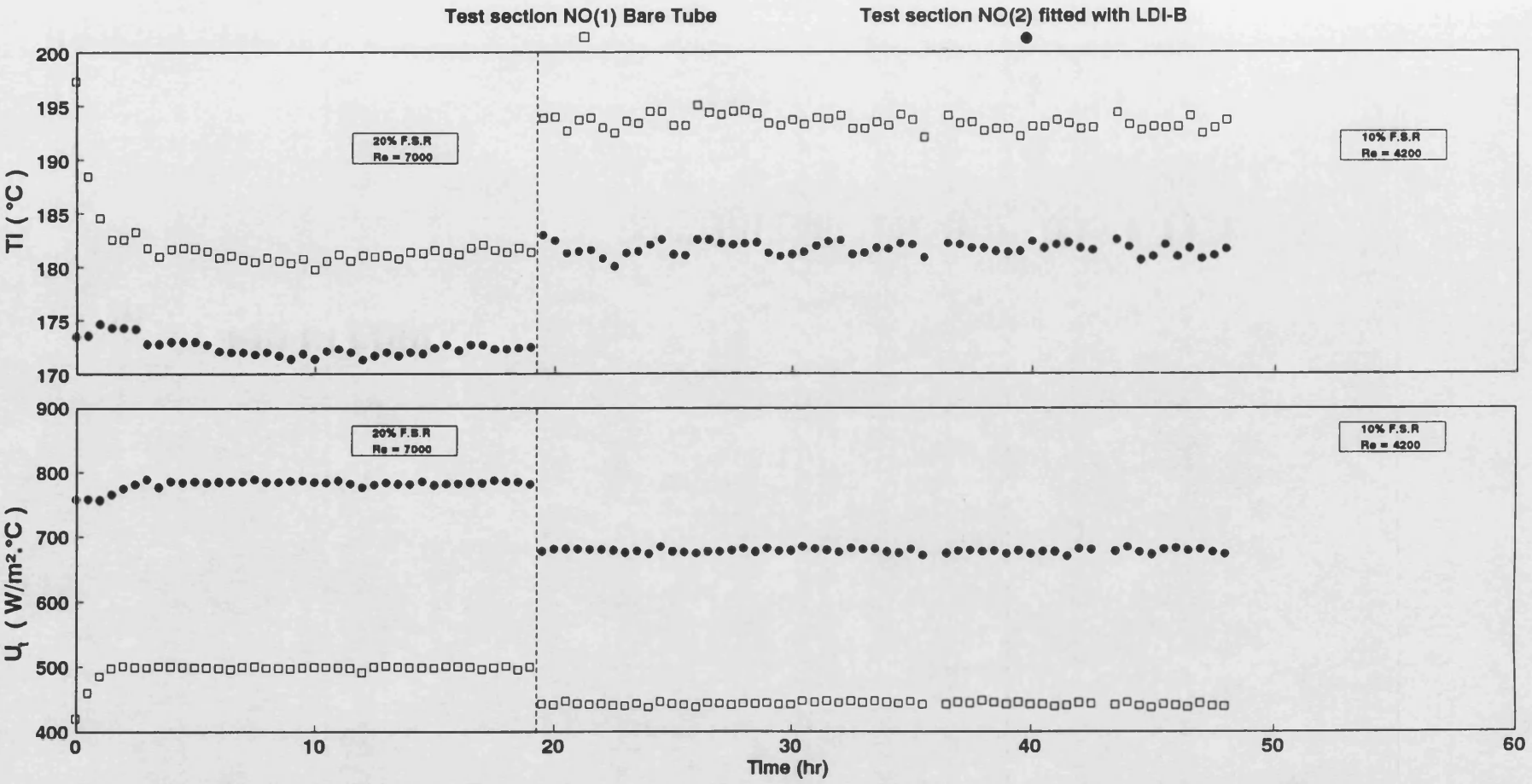

Fig (4.54) Comparison between the overall heat transfer coefficient (Ut) and inner surface temperature (TI) for both test sections

Arabian light crude oil with 10% by weight of refinery sludge under pressure of 95% of nitrogen and 5% of oxygen gases

Fouling Run NO(5) [20% & 10% F.S.R ; Tb = 140 °C ; Re = 7000 & 4200 ; Pr = 28 ; q = 54.18 kW/m²]

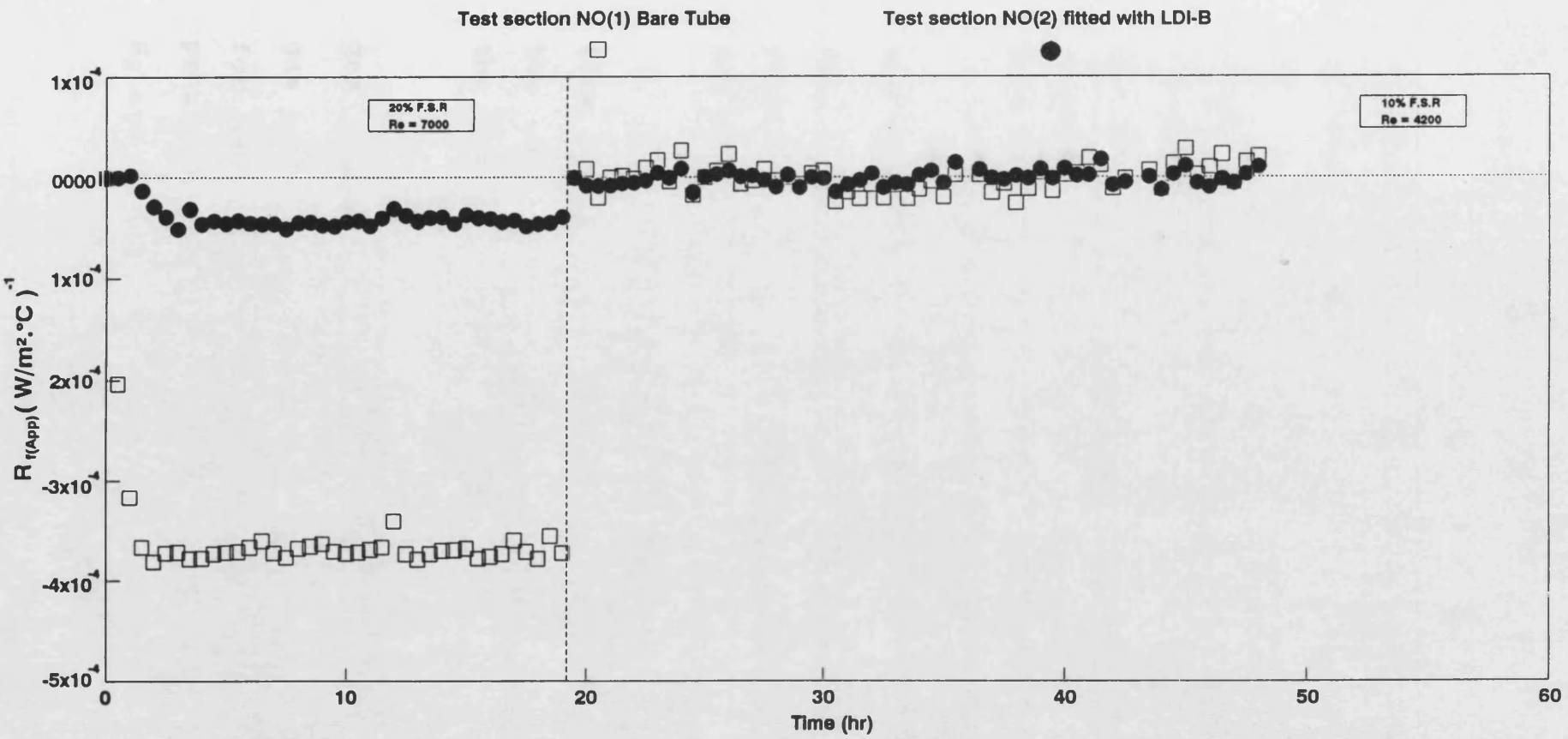

Fig (4.55) Comparison between apparent fouling resistance ($R_{f(App)}$) of both test sections for Fouling Run NO(5)

Arabian light crude oil with 10% by weight of refinery sludge under pressure of 95% of nitrogen and 5% of oxygen gases

[20% & 10% F.S.R ; Tb = 140 °C ; Re = 7000 & 4200 ; Pr = 28 ; q = 54.18 kW/m²]

4.6.2.5 Comparison between effect of nitrogen and helium gases on h_i and T_i

It has been noted in Fig 4.5 , Section 4.5.2.1 , that the solubility of helium gas in water at 1 atm is increased (rather than decreased) with temperature for T > 305 K (32°C). Consequently , if the solubility of helium gas in crude oil is similar in behaviour to that in Fig 4.5 , then bubble nucleation due to gas solubility difference (BNGSD) might be expected to disappear if the equipment is pressurised with helium rather than with nitrogen .

In order to provide a clear comparison between the effect of N_2 and He gases on h_i with the crude oil, a set of experiments was carried out at different experimental conditions . The results of these experiments are shown in Figs 4.56 to 4.71.

The effect of q on h_i at constant pressure and flow rate is shown in Figs 4.56 , 4.58 and 4.60 for the bare tube and in Figs 4.57 , 4.59 and 4.61 for the test section No(2) fitted with LDI-B .

At low pressure (P = 5 bar gauge) , h_i with He gas pressure was slightly higher than that with N_2 gas pressure (Fig 4.56 for the bare tube and Fig 4.57 for the tube fitted with LDI-B). However , for higher pressures (P = 8 and 10 bar gauge) , h_i with both N_2 and He were almost virtually the same .

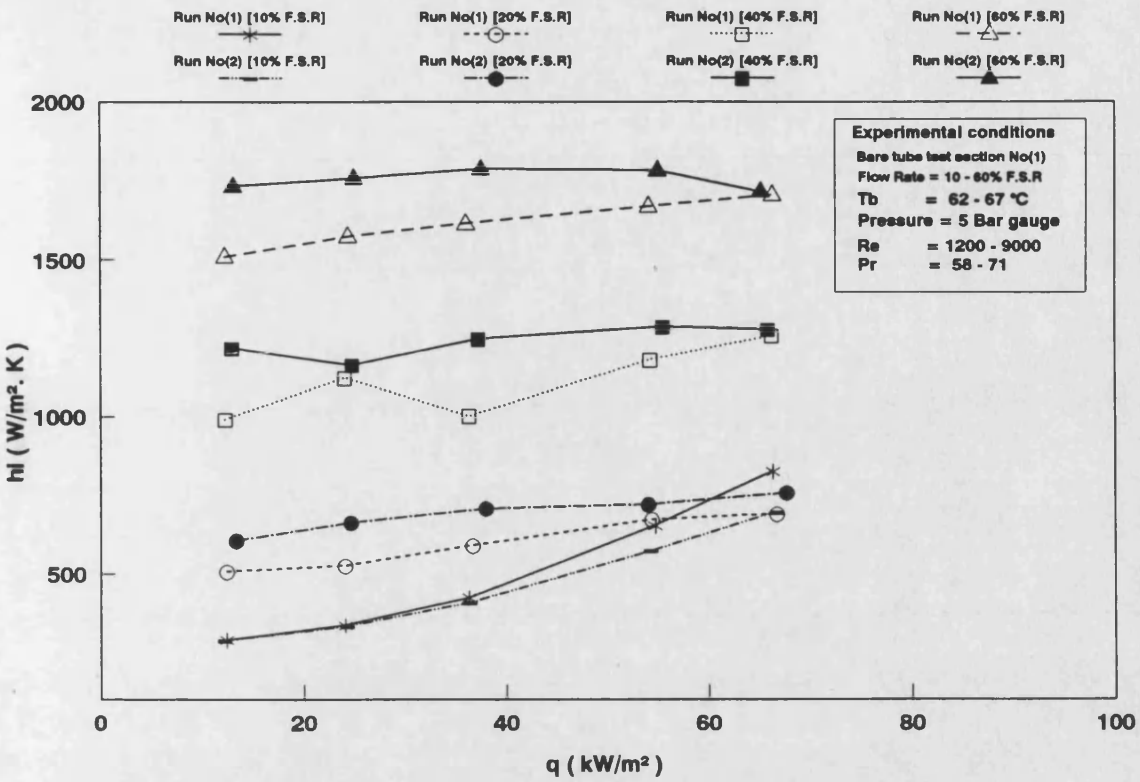

Fig (4.56) Heat transfer coefficient (hi) vs Heat Flux (q)

pressurising of the Arabian light crude oil (with 10% wt sludge)

Run No(1) under Nitrogen (N2) gas and Run No(2) under Helium (He) gas pressure

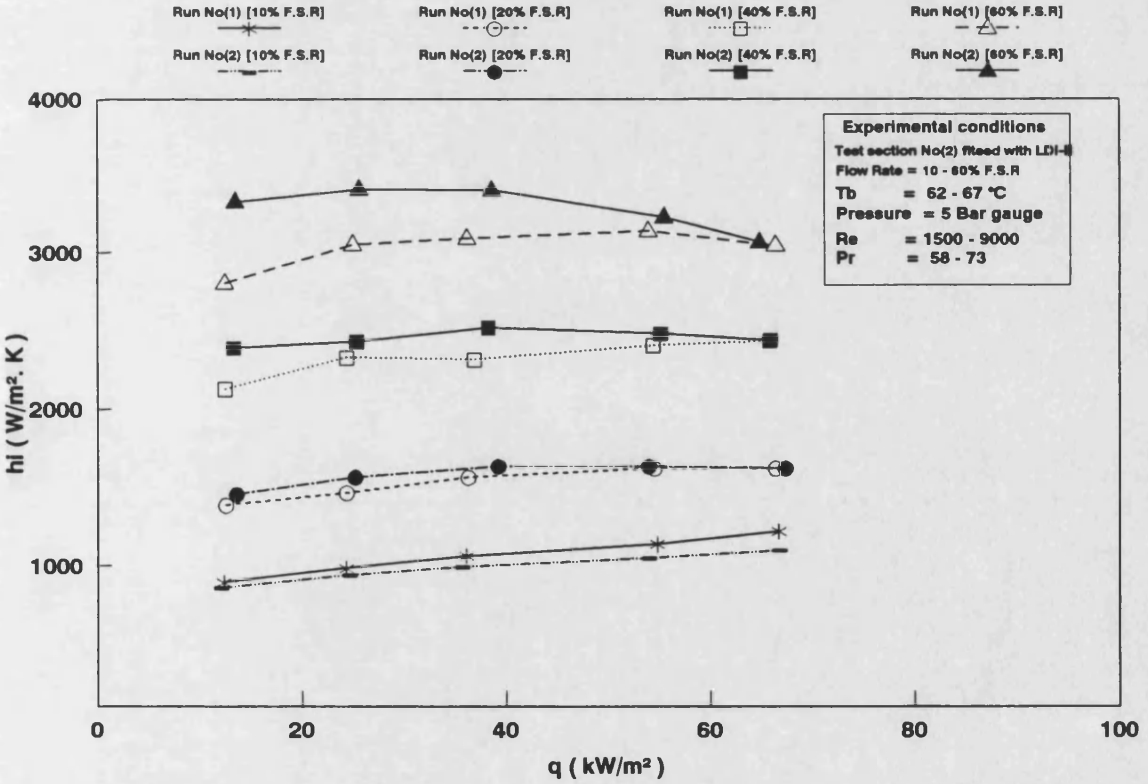

Fig (4.57) Heat transfer coefficient (hi) vs Heat Flux (q)

pressurising of the Arabian light crude oil (with 10% wt sludge)

Run No(1) under Nitrogen (N2) gas and Run No(2) under Helium (He) gas pressure

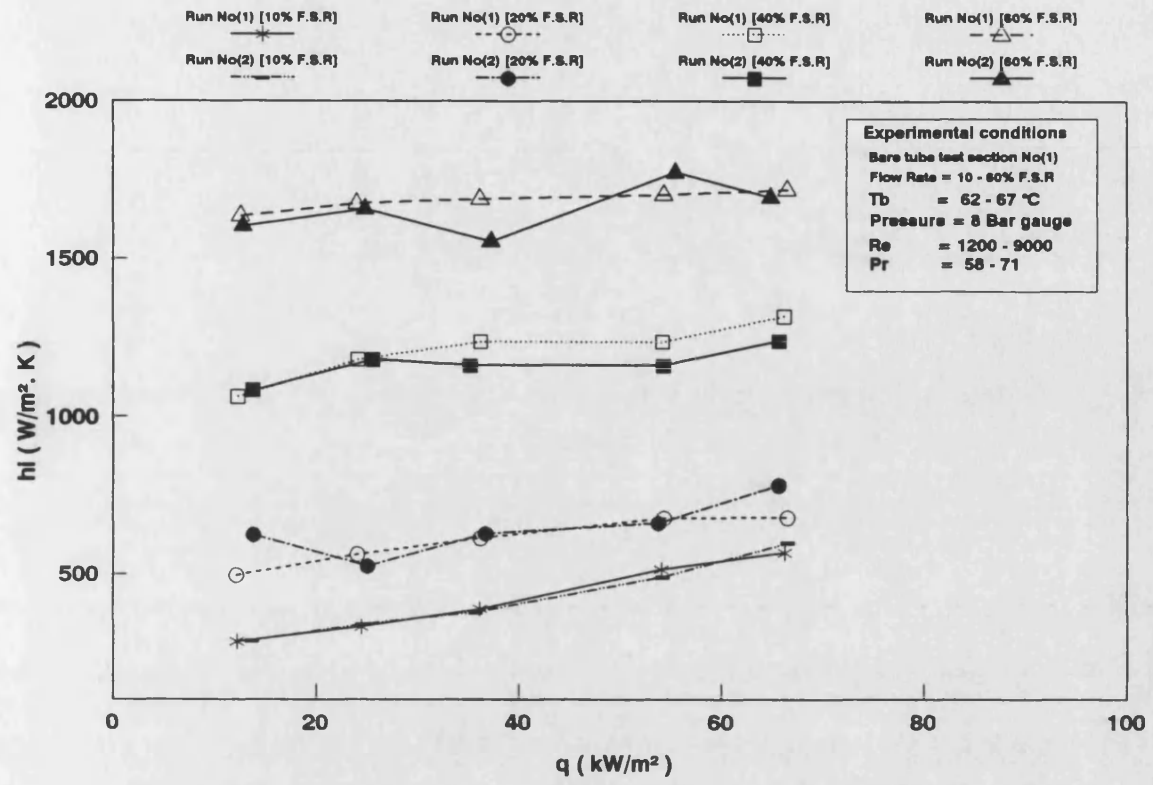

Fig (4.58) Heat transfer coefficient (hi) vs Heat Flux (q)

pressurising of the Arabian light crude oil (with 10% wt sludge)

Run No(1) under Nitrogen (N2) gas and Run No(2) under Helium (He) gas pressure

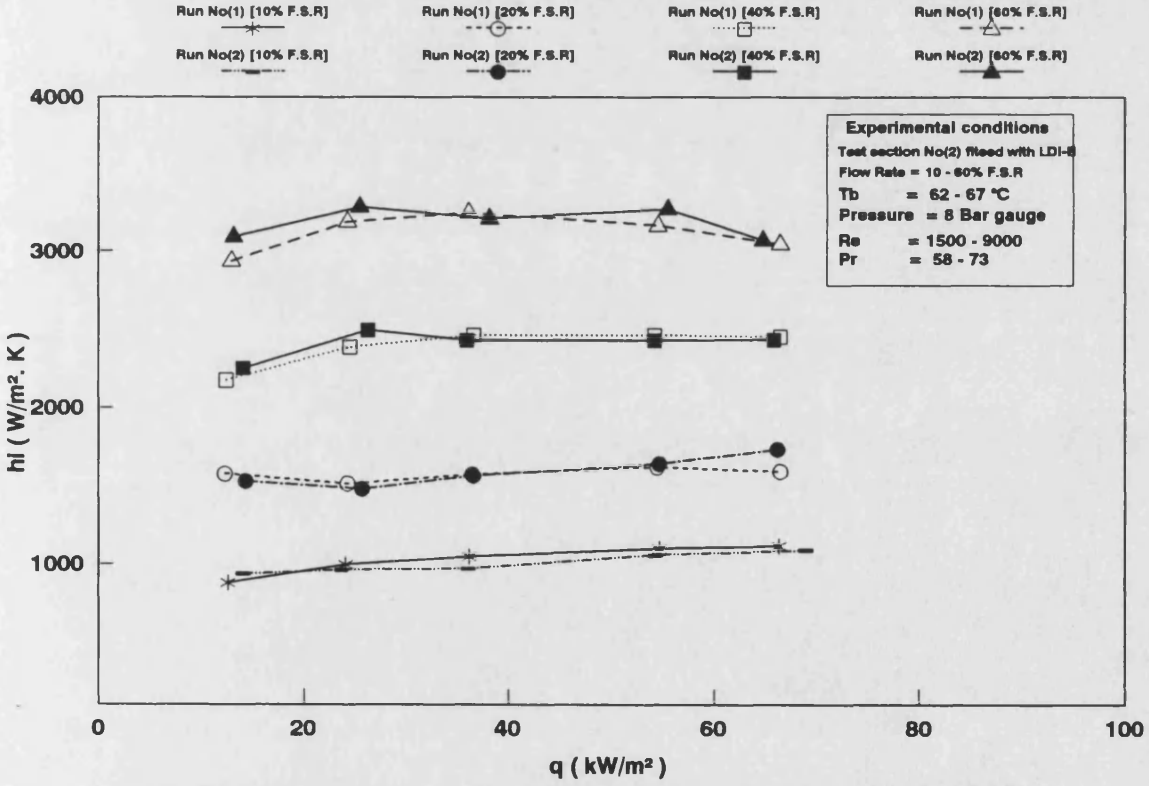

Fig (4.59) Heat transfer coefficient (hi) vs Heat Flux (q)

pressurising of the Arabian light crude oil (with 10% wt sludge)

Run No(1) under Nitrogen (N2) gas and Run No(2) under Helium (He) gas pressure

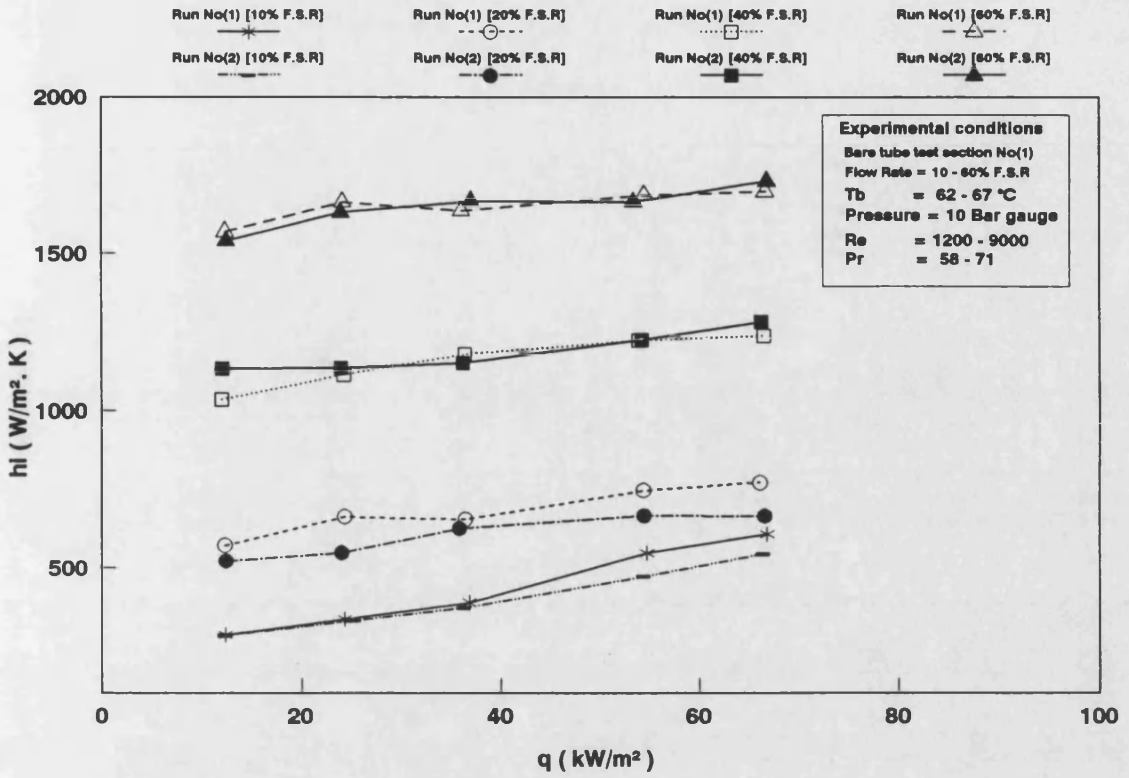

Fig (4.60) Heat transfer coefficient (hi) vs Heat Flux (q)

pressurising of the Arabian light crude oil (with 10% wt sludge)

Run No(1) under Nitrogen (N2) gas and Run No(2) under Helium (He) gas pressure

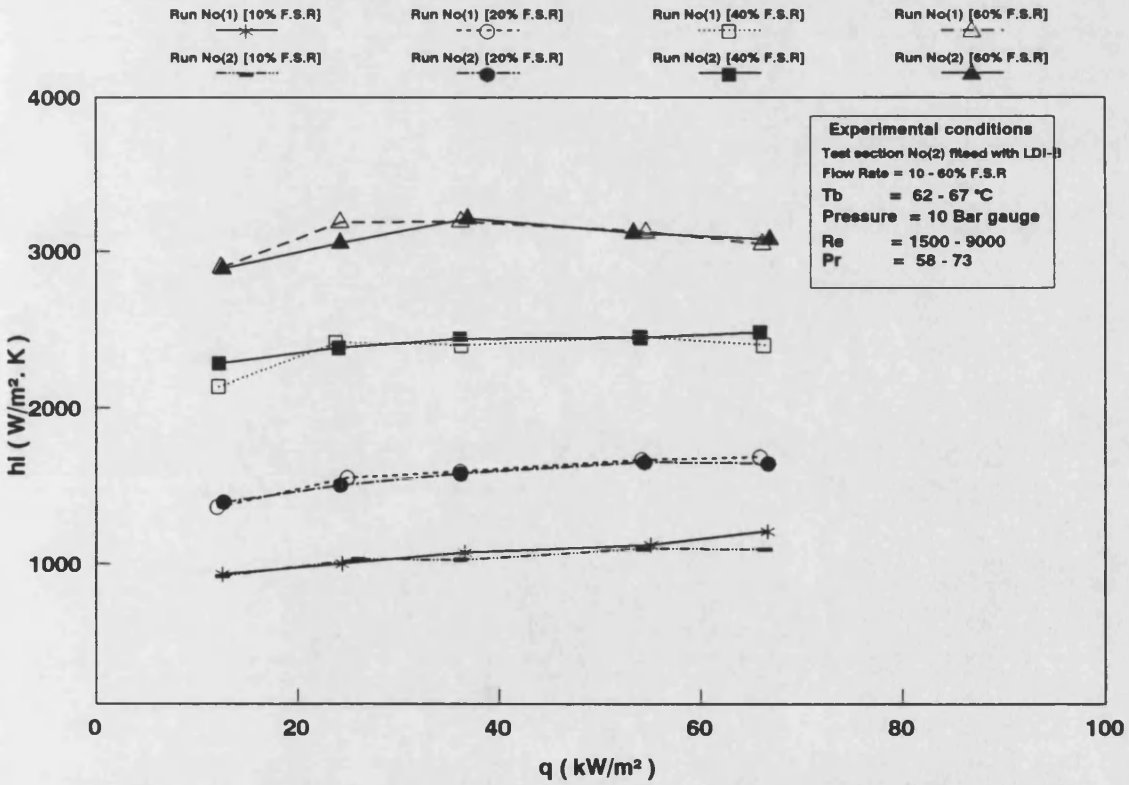

Fig (4.61) Heat transfer coefficient (hi) vs Heat Flux (q)

pressurising of the Arabian light crude oil (with 10% wt sludge)

Run No(1) under Nitrogen (N2) gas and Run No(2) under Helium (He) gas pressure

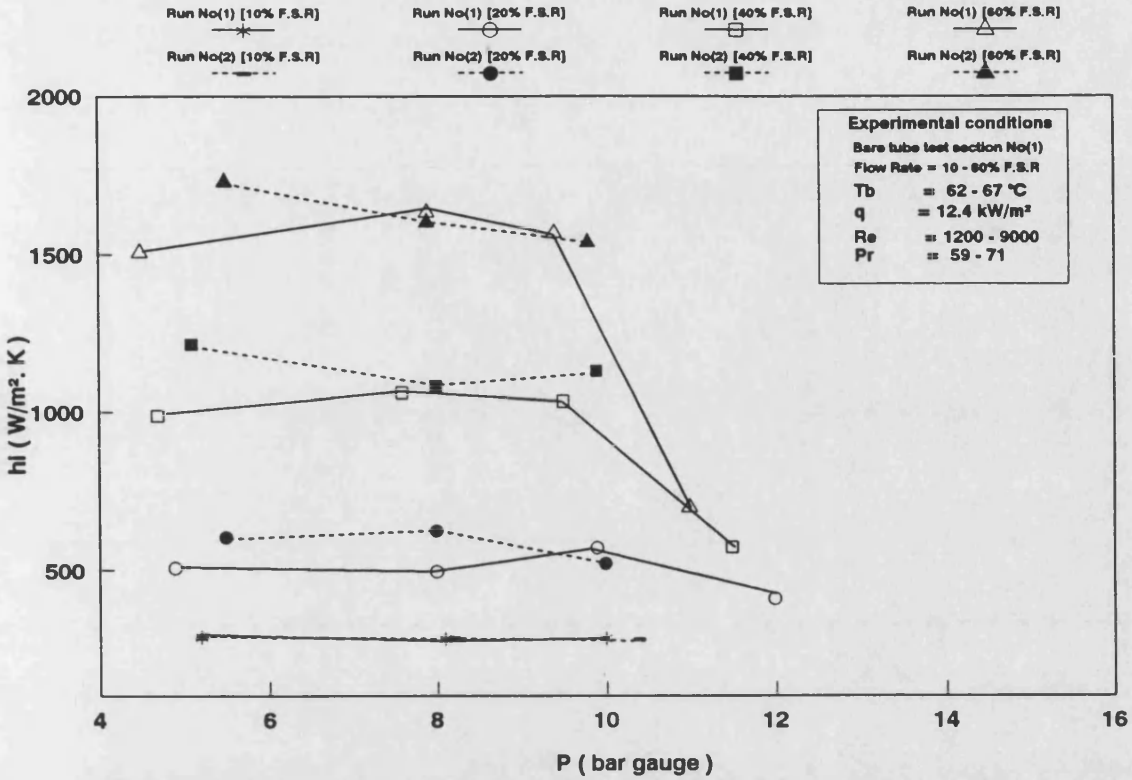

Fig (4.62) Heat transfer coefficient (hi) vs total pressure (P)

pressurising of the Arabian light crude oil (with 10% wt sludge)

Run No(1) under Nitrogen (N2) gas and Run No(2) under Helium (He) gas pressure

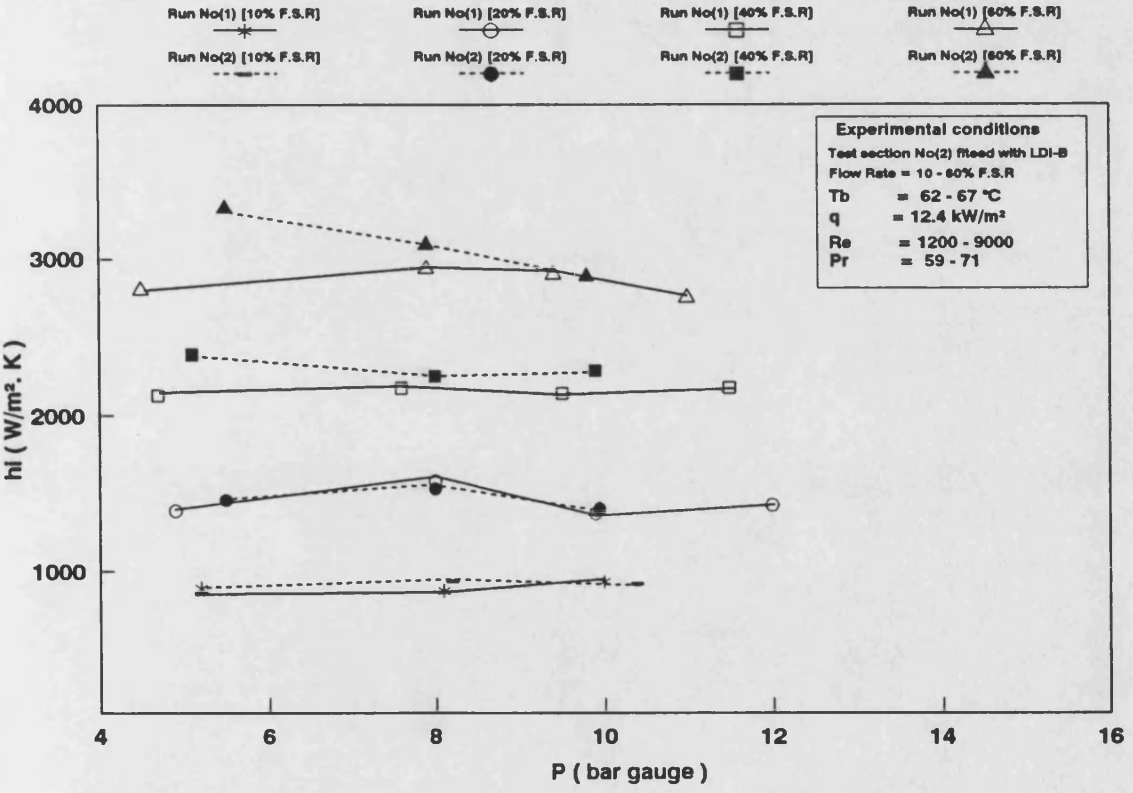

Fig (4.63) Heat transfer coefficient (hi) vs total pressure (P)

pressurising of the Arabian light crude oil (with 10% wt sludge)

Run No(1) under Nitrogen (N2) gas and Run No(2) under Helium (He) gas pressure

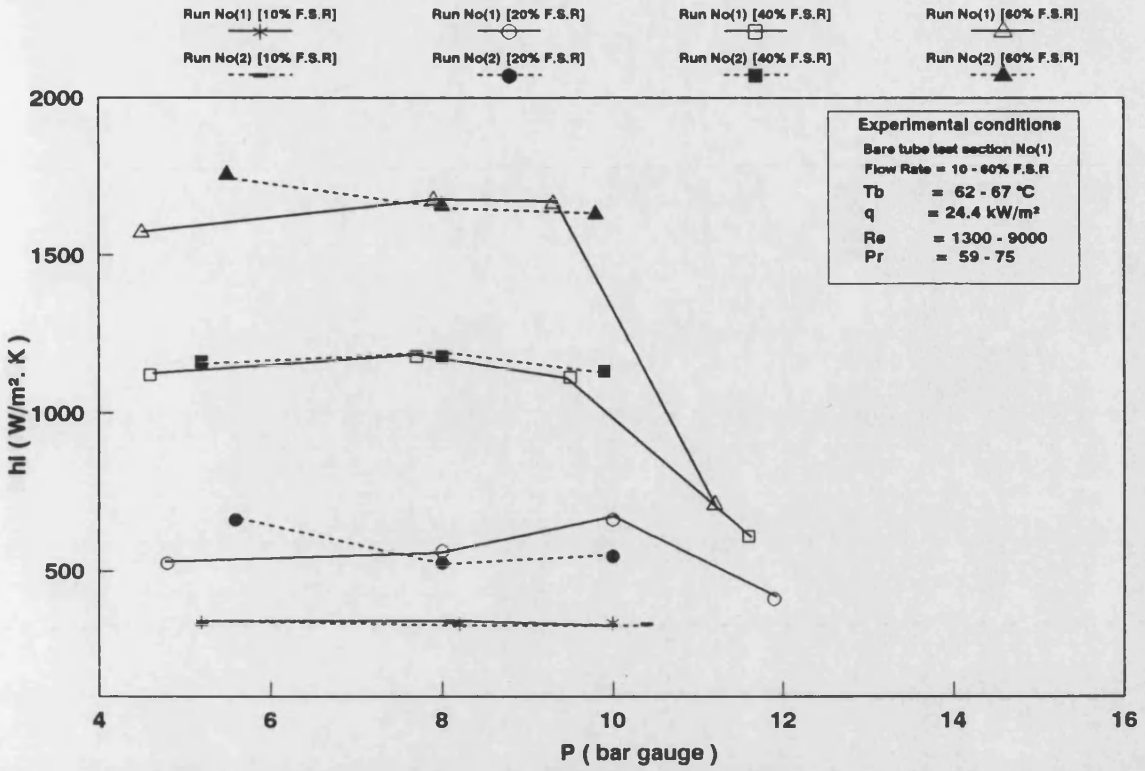

Fig (4.64) Heat transfer coefficient (hi) vs total pressure (P)

pressurising of the Arabian light crude oil (with 10% wt sludge)

Run No(1) under Nitrogen (N2) gas and Run No(2) under Helium (He) gas pressure

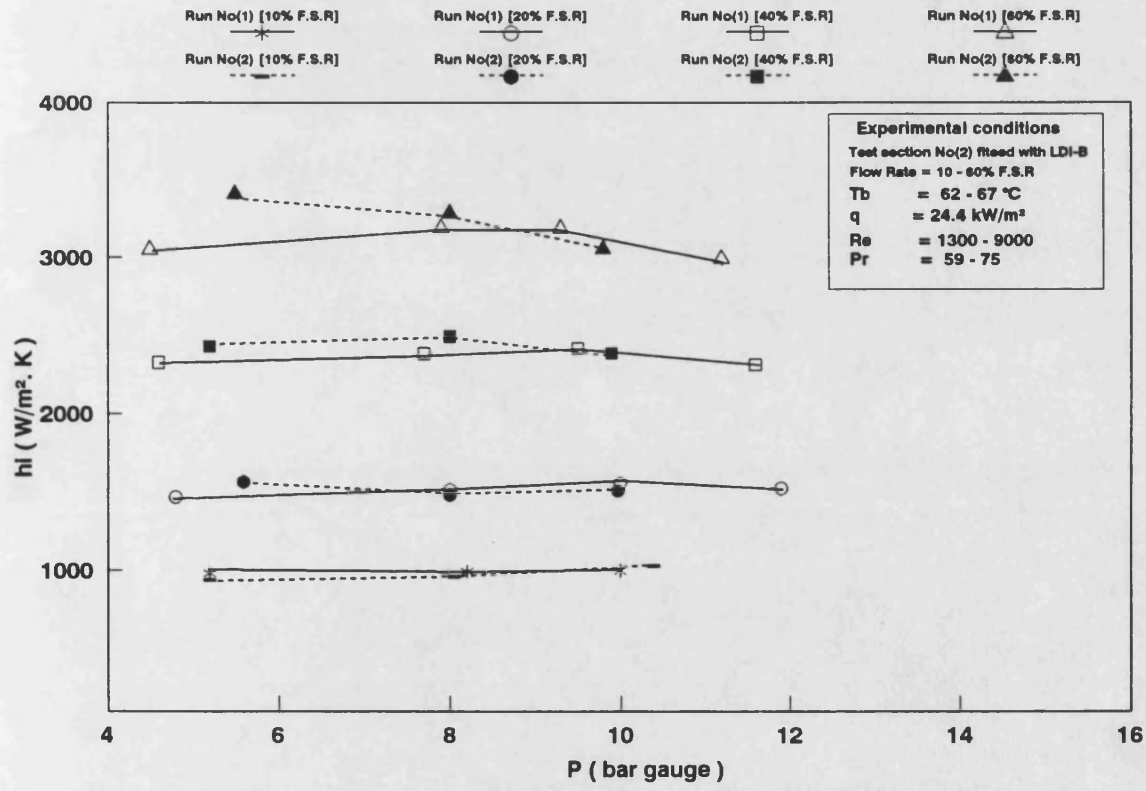

Fig (4.65) Heat transfer coefficient (hi) vs total pressure (P)

pressurising of the Arabian light crude oil (with 10% wt sludge)

Run No(1) under Nitrogen (N2) gas and Run No(2) under Helium (He) gas pressure

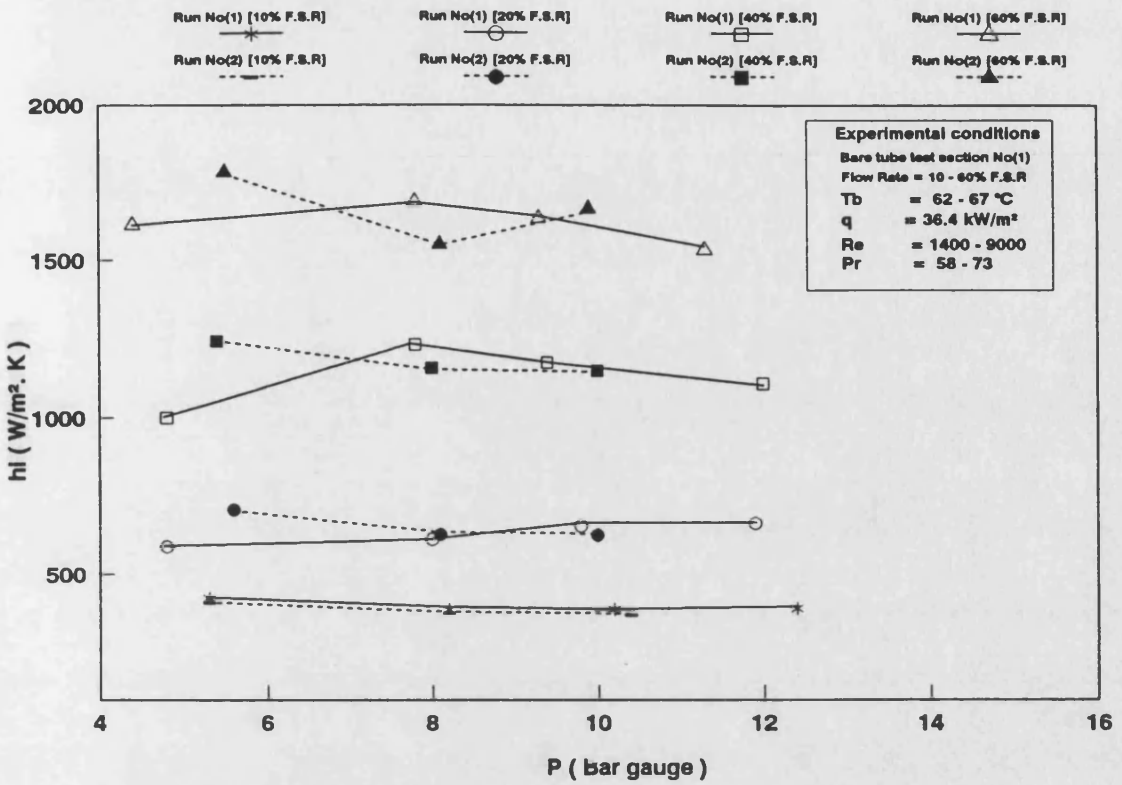

Fig (4.66) Heat transfer coefficient (hi) vs total pressure (P)

pressurising of the Arabian light crude oil (with 10% wt sludge)

Run No(1) under Nitrogen (N2) gas and Run No(2) under Helium (He) gas pressure

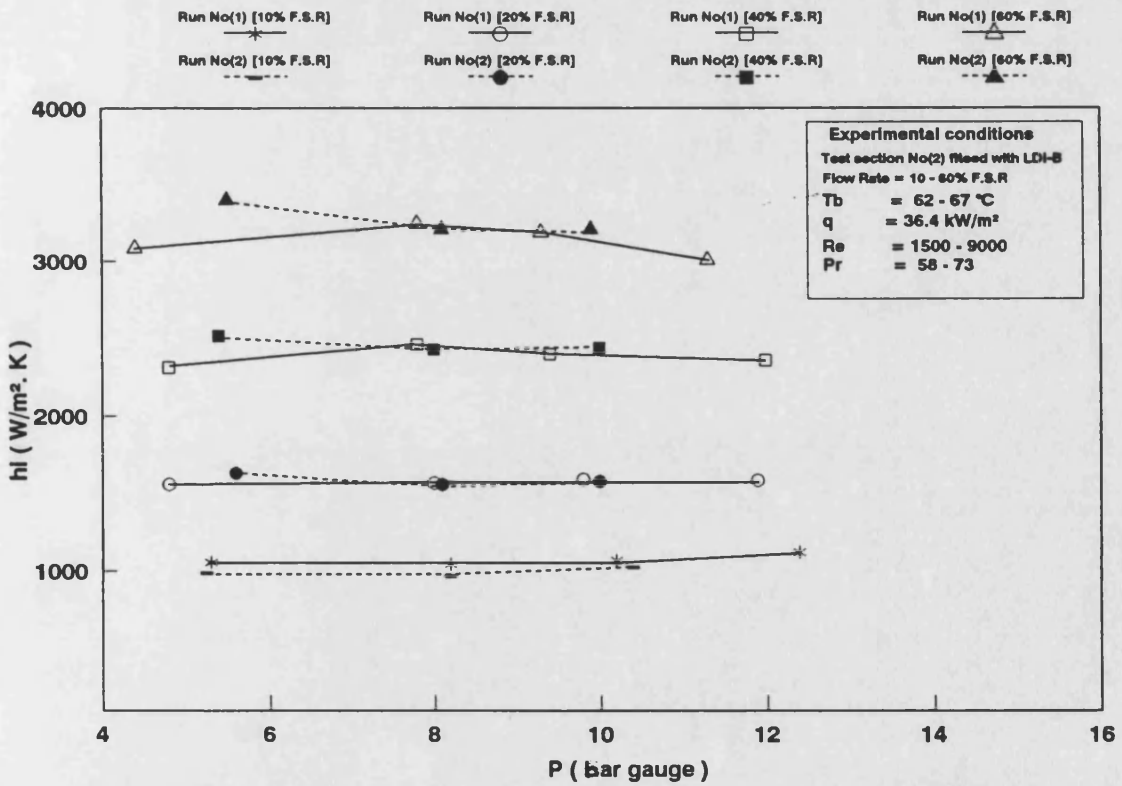

Fig (4.67) Heat transfer coefficient (hi) vs total pressure (P)

pressurising of the Arabian light crude oil (with 10% wt sludge)

Run No(1) under Nitrogen (N2) gas and Run No(2) under Helium (He) gas pressure

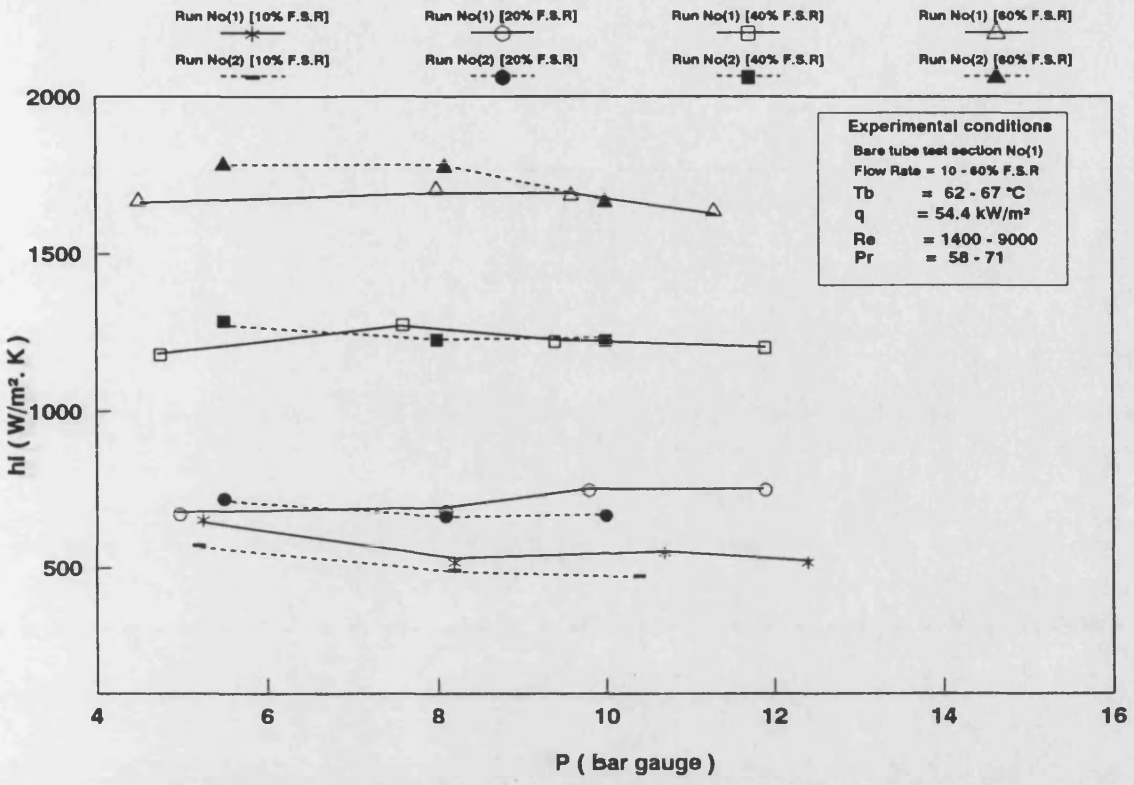

Fig (4.68) Heat transfer coefficient (hi) vs total pressure (P)

pressurising of the Arabian light crude oil (with 10% wt sludge)

Run No(1) under Nitrogen (N2) gas and Run No(2) under Helium (He) gas pressure

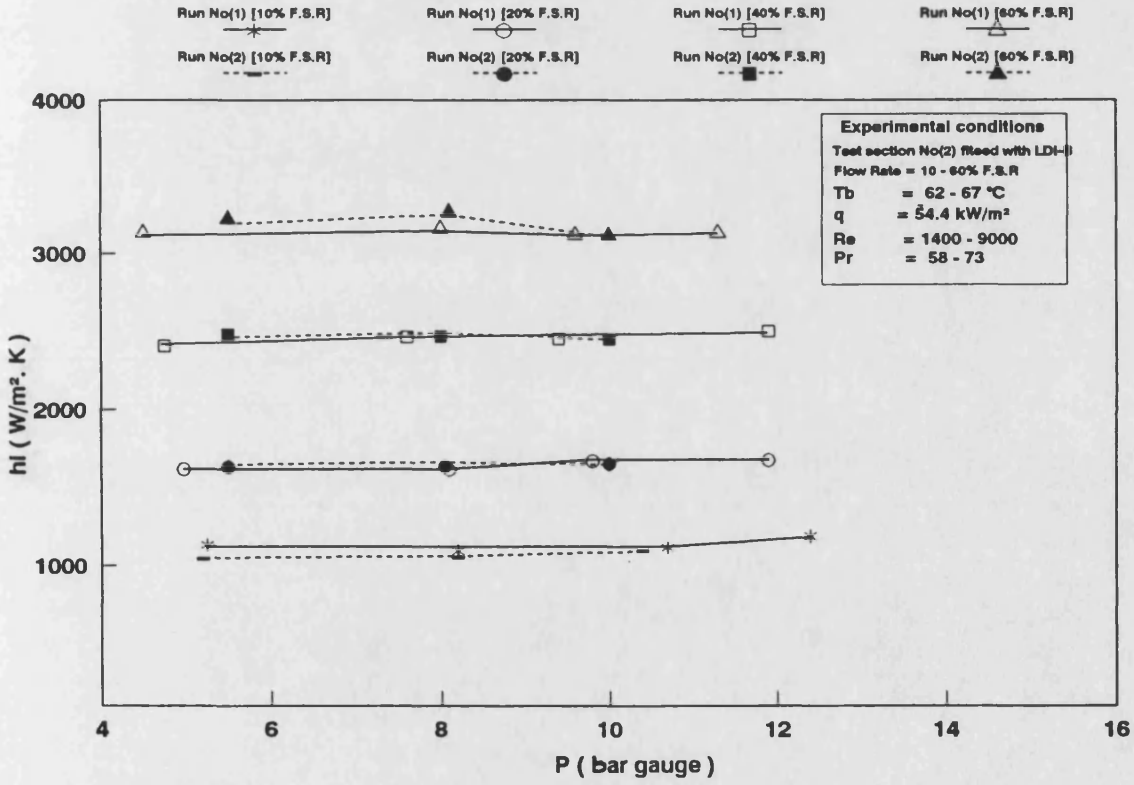

Fig (4.69) Heat transfer coefficient (hi) vs total pressure (P)

pressurising of the Arabian light crude oil (with 10% wt sludge)

Run No(1) under Nitrogen (N2) gas and Run No(2) under Helium (He) gas pressure

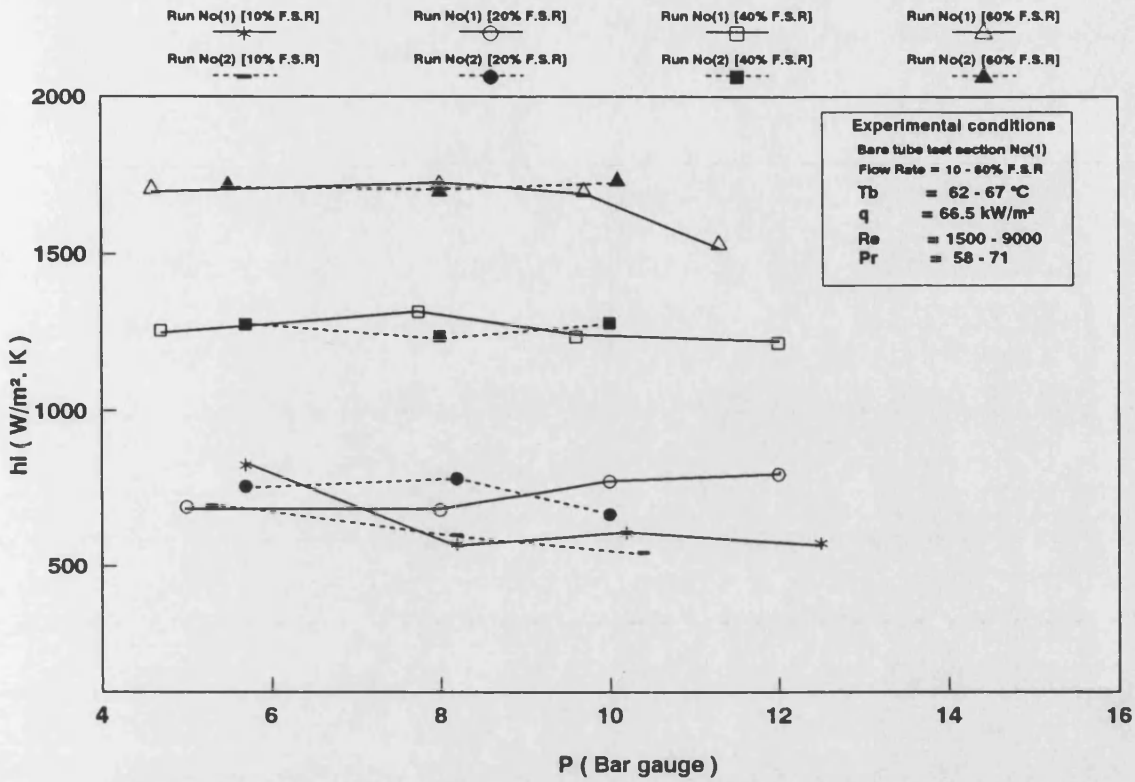

Fig (4.70) Heat transfer coefficient (hi) vs total pressure (P)

pressurising of the Arabian light crude oil (with 10% wt sludge)
Run No(1) under Nitrogen (N2) gas and Run No(2) under Helium (He) gas pressure

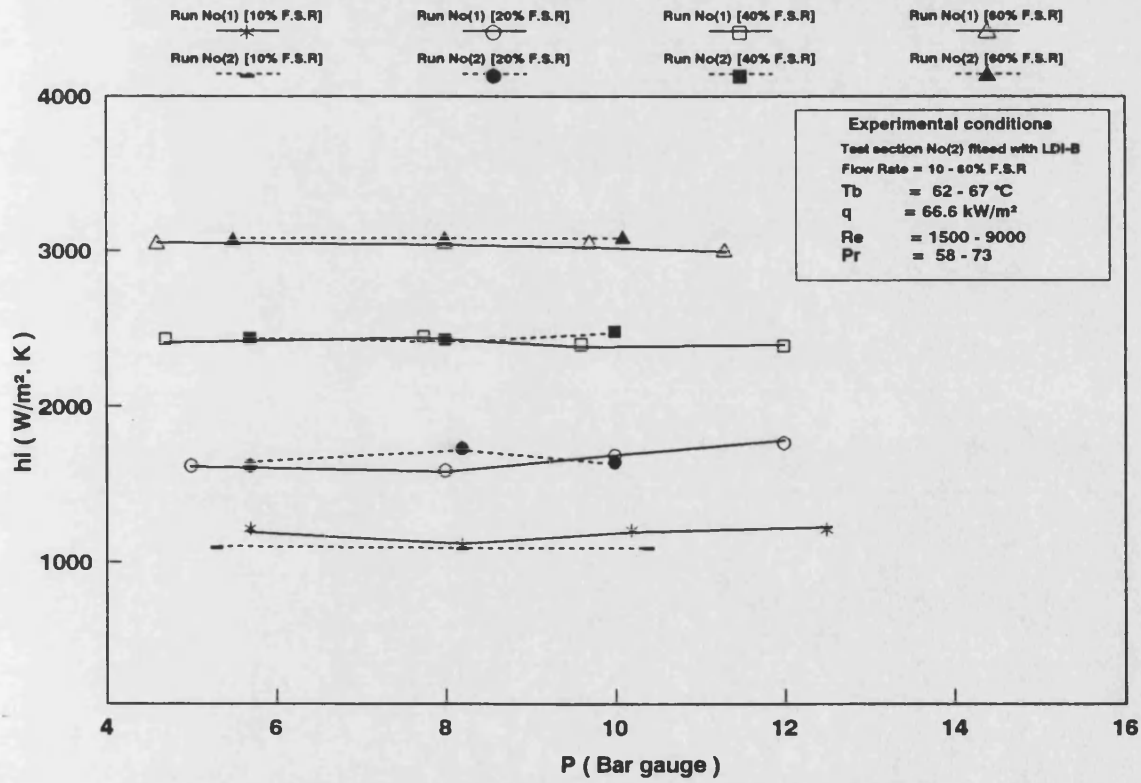

Fig (4.71) Heat transfer coefficient (hi) vs total pressure (P)

pressurising of the Arabian light crude oil (with 10% wt sludge)
Run No(1) under Nitrogen (N2) gas and Run No(2) under Helium (He) gas pressure

The effect of pressure on h_i at constant flow rate and heat flux is shown in Figs 4.62 , 4.64 , 4.66 , 4.68 and 4.70 for the bare tube test section No(1) and in Figs 4.63 , 4.65 , 4.67, 4.69 and 4.71 for test section No(2) fitted with the **HiTran** insert.

At low heat flux , $q < 24.4$ kW/m^2 , h_i of crude oil with He pressure was slightly higher than that with N_2 gas pressure. However , for $q > 36.4$ kW/m^2 the opposite was noted . This is a possible indication that, under conditions where subcooled nucleate boiling or BNGSD are not expected , h_i of crude oil with He pressure is higher . However, under conditions for which nucleation might be expected (subcooled or BNGSD) , h_i of crude oil with N_2 is enhanced, while with He gas pressure no such enhancement is likely .

As a result of this comparative study between the effects of N_2 and He gas pressures, it was considered worthwhile to carry out a fouling run with He gas pressure .

4.6.2.6 Fouling runs No 6 and No 7

a - Fouling run No(6)

In order to determine the highest possible T_i under helium gas pressure , the variations of T_i and h_i with time were investigated over a short period of time (180 mins) .

Fig 4.72 shows the variation of h_i and T_i with time at fixed flow rate , heat flux and pressure . The tank pressure did not decrease as it did for the nitrogen case (refer to Fig 4.51) . At a pressure of 8.1 bar gauge T_i for the bare tube decreased from 187 to 183 °C in 55 minutes and h_i increased by about 300 W/(m^2 K) in the same period. This is possibly because of nucleate boiling occurring . Only small changes in T_i or h_i were noted for test section No(2) fitted with the LDI-B insert . After 60 minutes the pressure was manually increased to 10.5 bar gauge . At p = 10.5 bar Ti and hi for both test sections remained essentially constant. After 125 minutes the heat flux was manually increased to 66.2 kW/m^2 . T_i for the bare tube increased to 190 °C and for the tube with LDI-B insert to 183 °C . When the flow rate was decreased to 10% F.S.R , Ti for the bare tube increased to 200 °C and that for test section No(2) to 194 °C . At 10% F.S.R , h_i was 1600 W/(m^2 K) for the bare tube and 1800 W/(m^2 K) for the tube with LDI-B .

Fig 4.73 shows the effects of the bulk temperature (T_b) on the inner surface temperature (T_i) and on the heat transfer cofficient (h_i). At 10% F.S.R and T_b = 74 °C the inner surface temperature (T_i) for the bare tube is 238 °C while it is 200 °C at T_b = 140 °C .

The experimental conditions for the sixth fouling run were as follows:

Bulk temperature (T_b) = 74 °C

Flow rate = 10% F.S.R

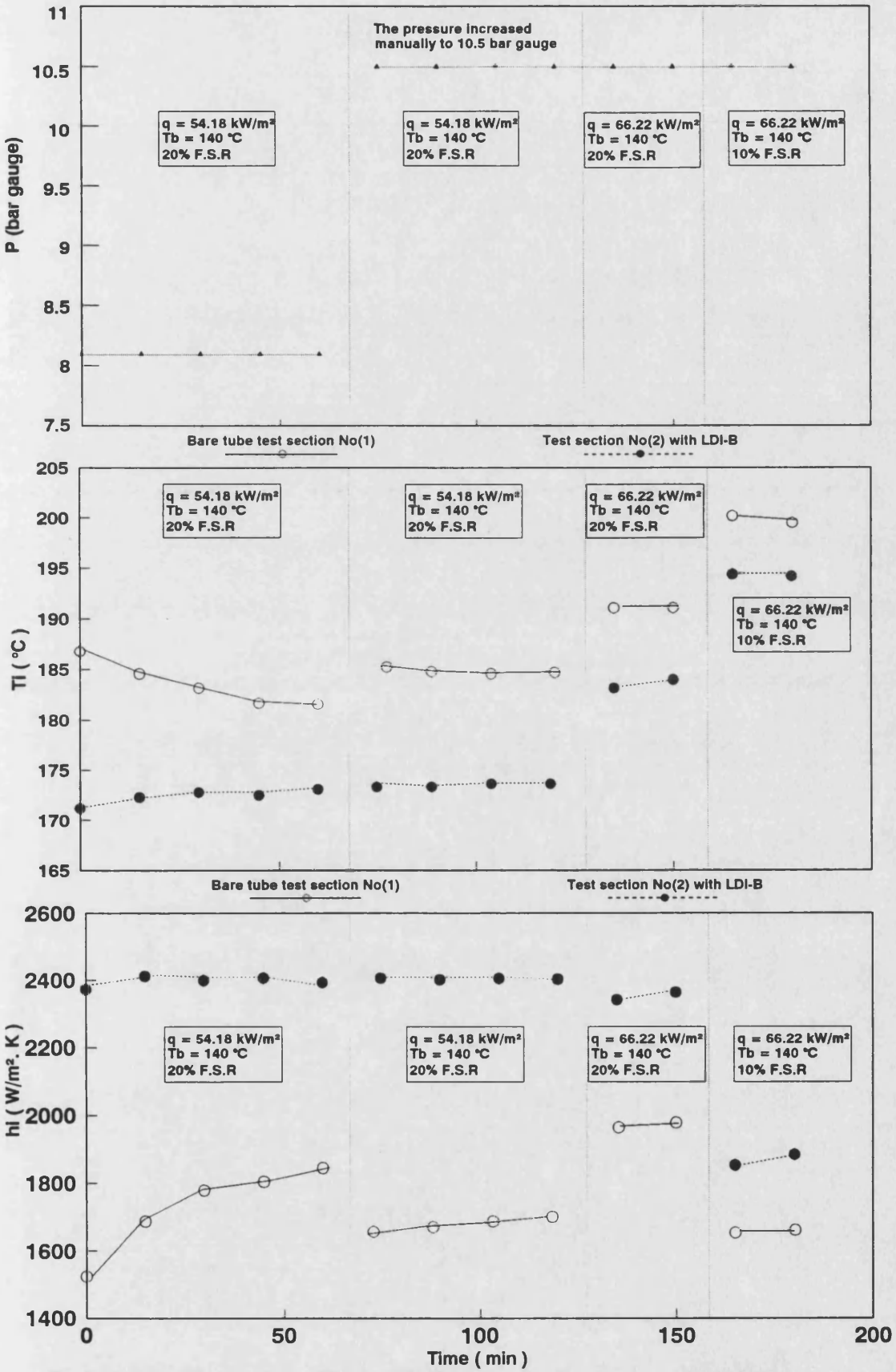

Fig (4.72) Variation of hi , Ti and tank pressure with time

Preparation for fouling Run No(6) for Arabian light crude oil + 10% wt sludge

10% & 20% F.S.R ; under pressure of Helium gas ; Re = 4200 - 7000 ; Pr = 27

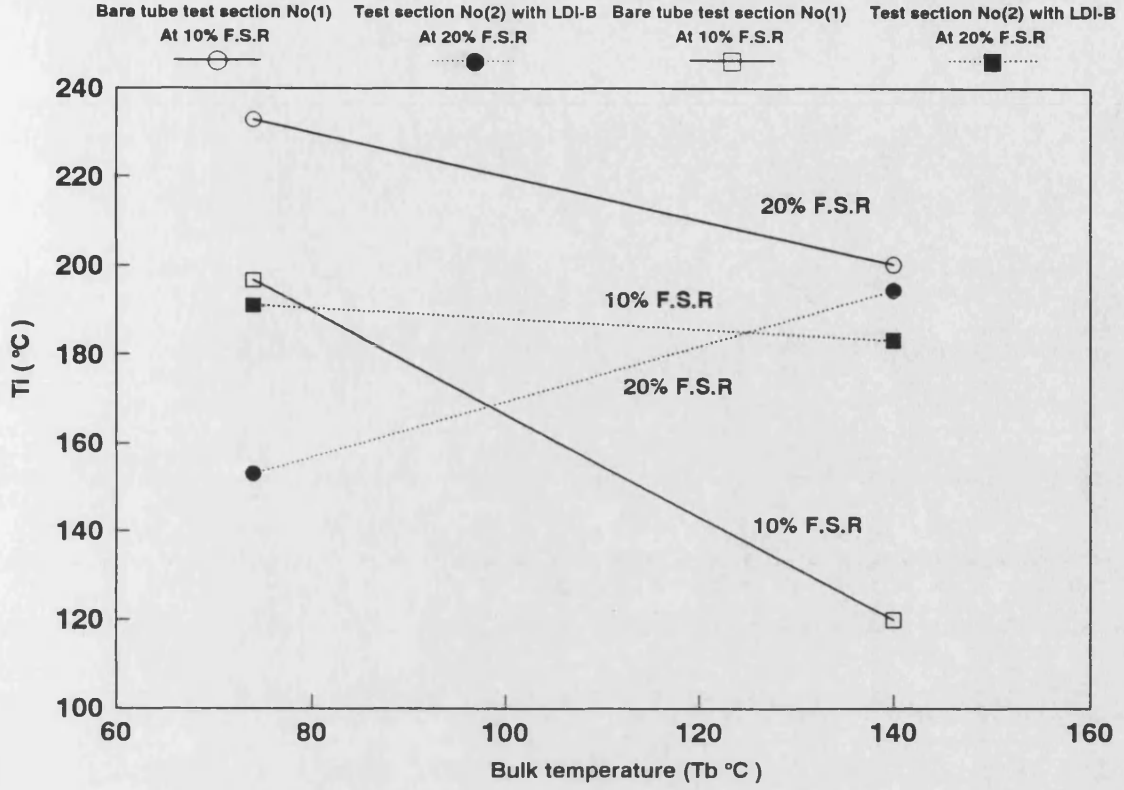

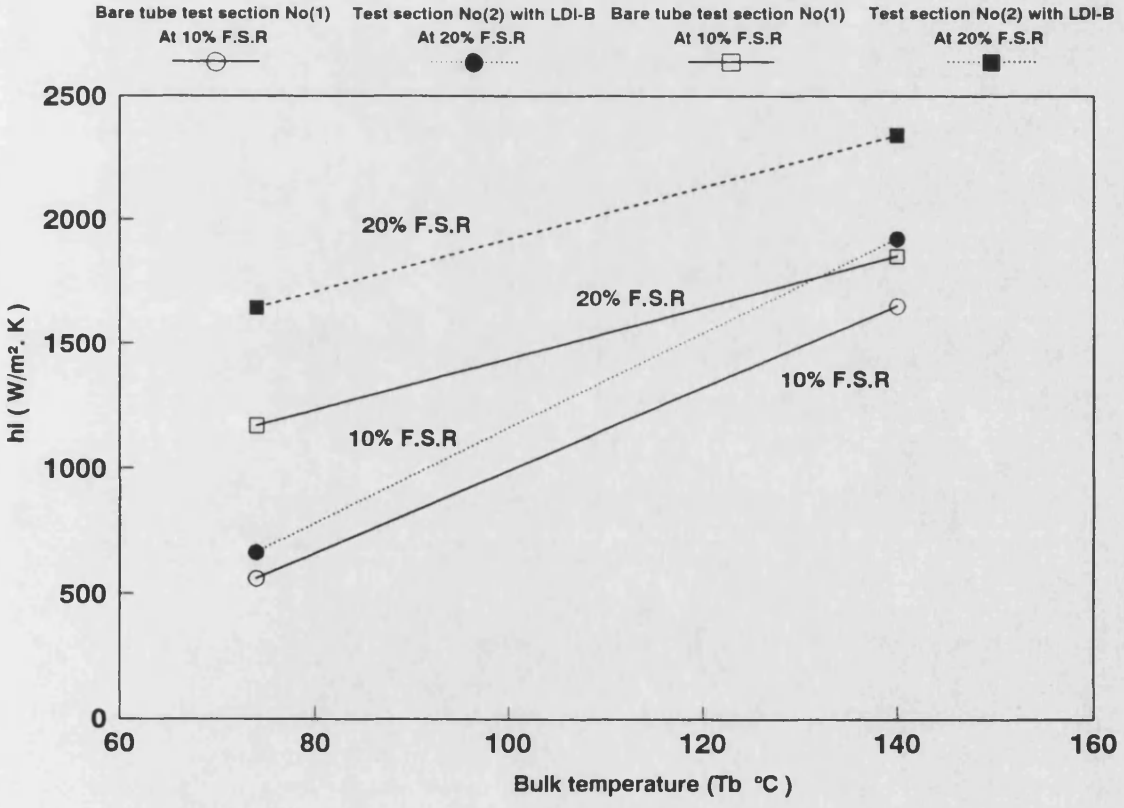

Fig (4.73) Variation of hi and Ti with bulk temperature (Tb)

Preparation for fouling Run No(6) for Arabian light crude oil + 10% wt sludge

10% & 20% F.S.R ; under pressure of Helium gas ; Re = 4200 - 7000 ; Pr = 27

Heat flux = 66.2 kW/m^2

Pressure = 10.4 bar gauge of helium gas

Initial T_i of bare tube test section No(1) = 238 °C

Initial T_i of test section No(2) fitted with LDI-B = 154°C

The fluid is the same as that used in Runs No 3 to No 5

The variation of pressure , T_i , U_t and $R_{f(App)}$ with time are shown in Figs 4.74 and 4.75 for test sections No(1) and No(2) respectively .

Fig 4.74 shows that T_i of the bare tube was decreased by about 4 °C in the first 2 hrs , then became constant. U_t was increased by about 10 W/m^2 °C in the same period and then became constant . $R_{f(App)}$ became negative . P , however, was constant at 10.4 bar . The reason behind the reduction of T_i and the enhancement in U_t , while the pressure remained unchanged may have been because the crude oil had already contained N_2 gas absorbed in the previous runs.

After 22 hrs of operation with no apparant fouling , 1.6 bar of air was added to the equipment in order to provide O_2 gas in the crude oil . The tank pressure became 12.0 bar gauge, T_i of the bare tube became 243°C and U_t 235 $W/(m^2$ °C) . 6 hrs after the air had had been added, T_i decreased to 231°C and U_t increased to 255 $W/(m^2$ °C). Interestingly these T_i and U_t values were identical to those which existed before the air had been added to the equipment . P also decreased to 11.2 bar gauge and $R_{f(App)}$ took a negative value . At 42 hours the tank pressure was

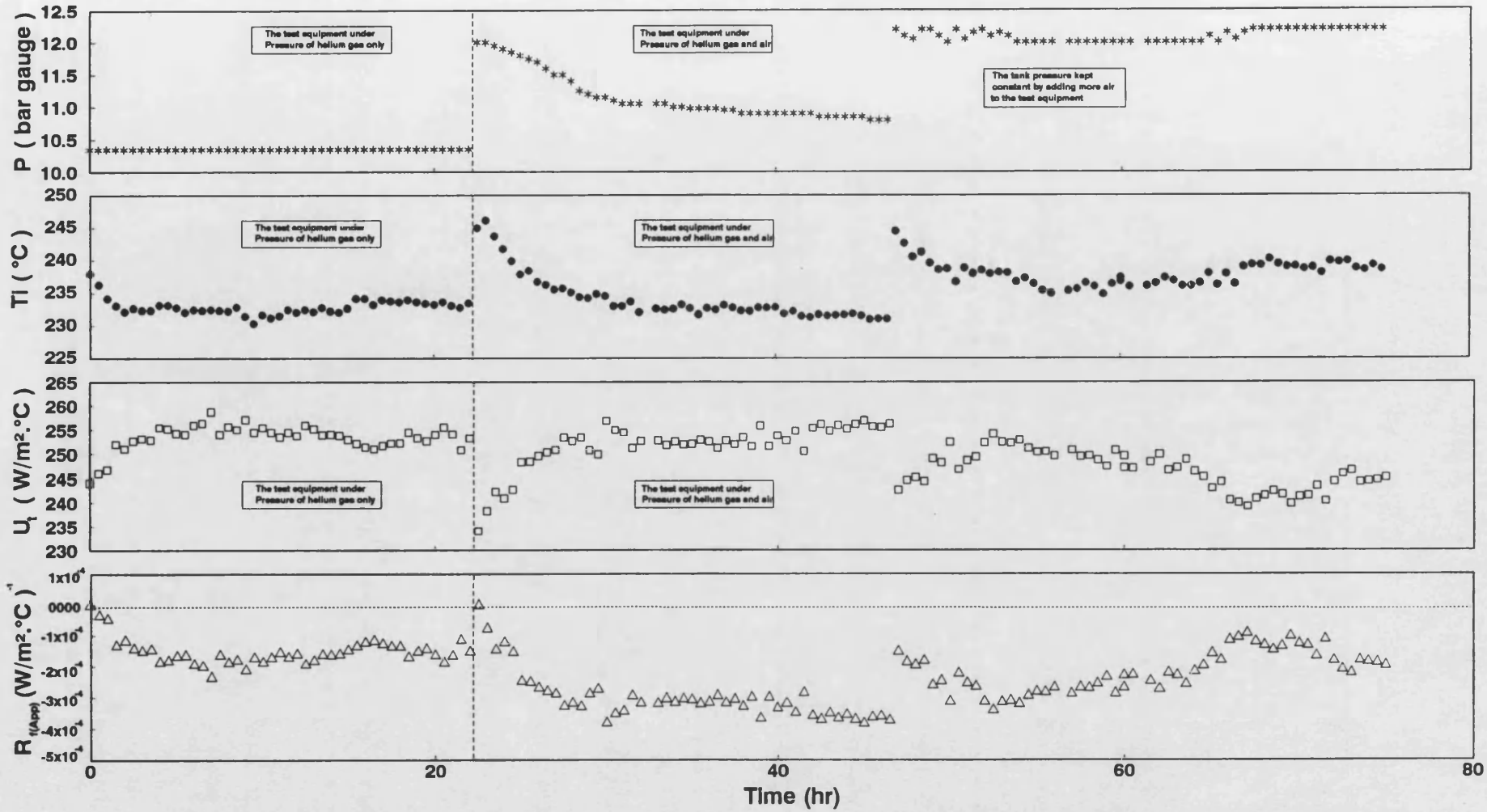

Fig (4.74) Fouling Run No(6) for bare tube test section No(1) [10% F.S.R ; Tb = 74 °C ; Re = 1600 ; Pr = 60 and q = 66.22 kW/m²]

Arabian light crude oil with 10% by weight of refinery sludge under pressure of Helium (He) gas for 22 hrs and then mixture of 84% He and 16% air

increased to and kept constant at about 12 bar gauge by adding more air to the equipment .

Fig 4.75 shows that T_i , U_t and $R_{f(App)}$ of test section No(2) , fitted with LDI-B , were almost unaffected either by time or by the changes in the operating conditions . $R_{f(App)}$ was more or less zero for the whole run which lasted 79 hrs.

A comparison between U_t and T_i of both test sections is shown in Fig 4.76 . T_i of the bare tube test section was about 85 °C higher than that for the LDI-B case .

A comparison between $R_{f(App)}$ for both test sections is shown in Fig 4.77 . $R_{f(App)}$ for the LDI-B case was virtually zero , but that for the bare tube was quite variable with time .

The test sections were dismantled and checked. No fouling occurred in this run and a tentative conclusion was reached that fouling would not occur as long as the equipment was under gas pressure .

The results for runs 1 to 6 seem to show that the presence of dissolved gases (especially N_2) , can provide inhibition of fouling. The role of dissolved N_2 gas as a fouling inhibitor is complex but perhaps may be summarised as follows :

1- N_2 may be degassing on the hot surface due to the solubility difference at

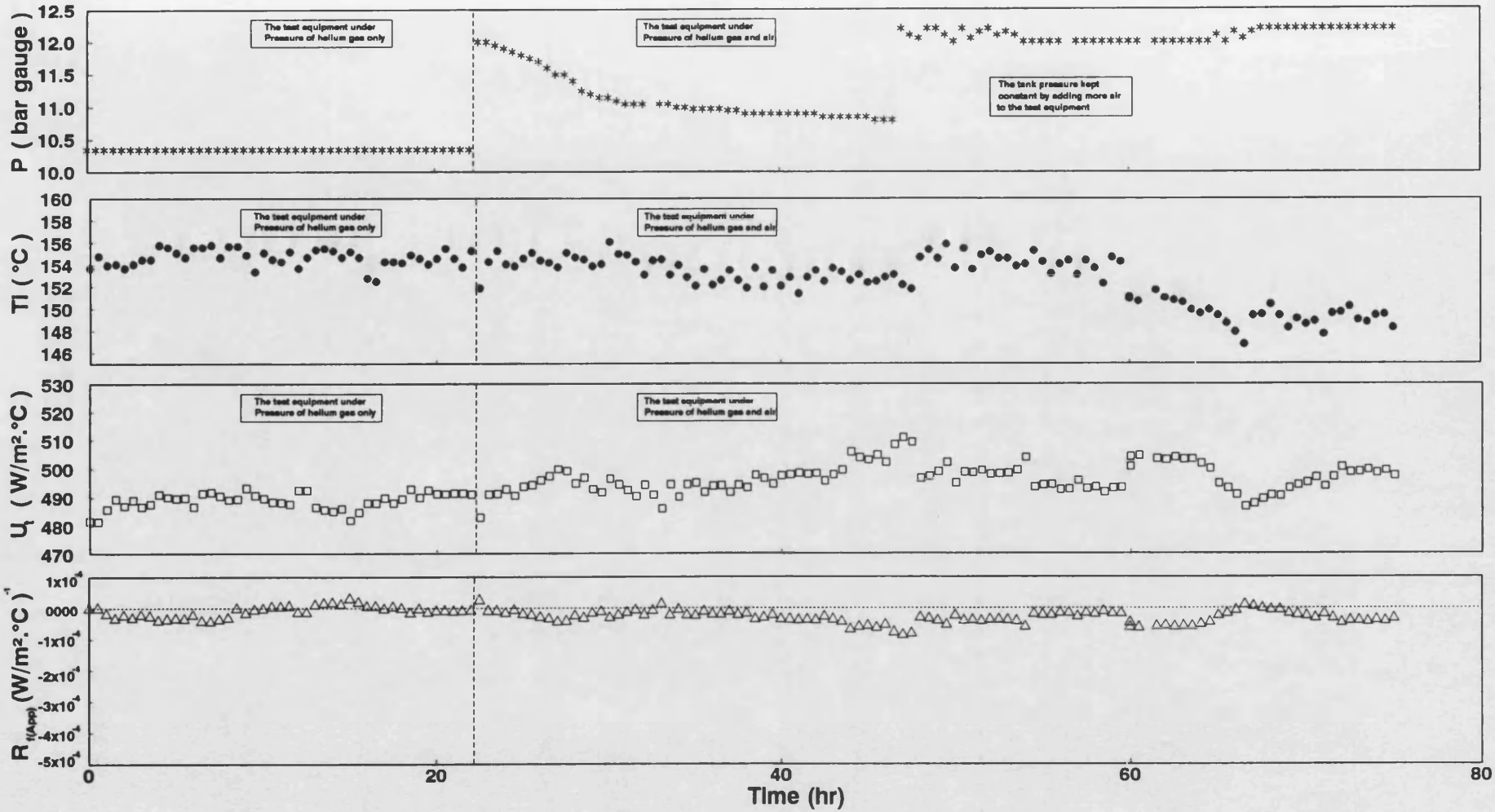

Fig (4.75) Fouling Run No(6) for test section No(2) fitted with LDI-B [10% F.S.R ; Tb = 74 °C ; Re = 1600 ; Pr = 60 and q = 66.22 kW/m²]

Arabian light crude oil with 10% by weight of refinery sludge under pressure of Helium (He) gas for 22 hrs and then mixture of 84% He and 16% air

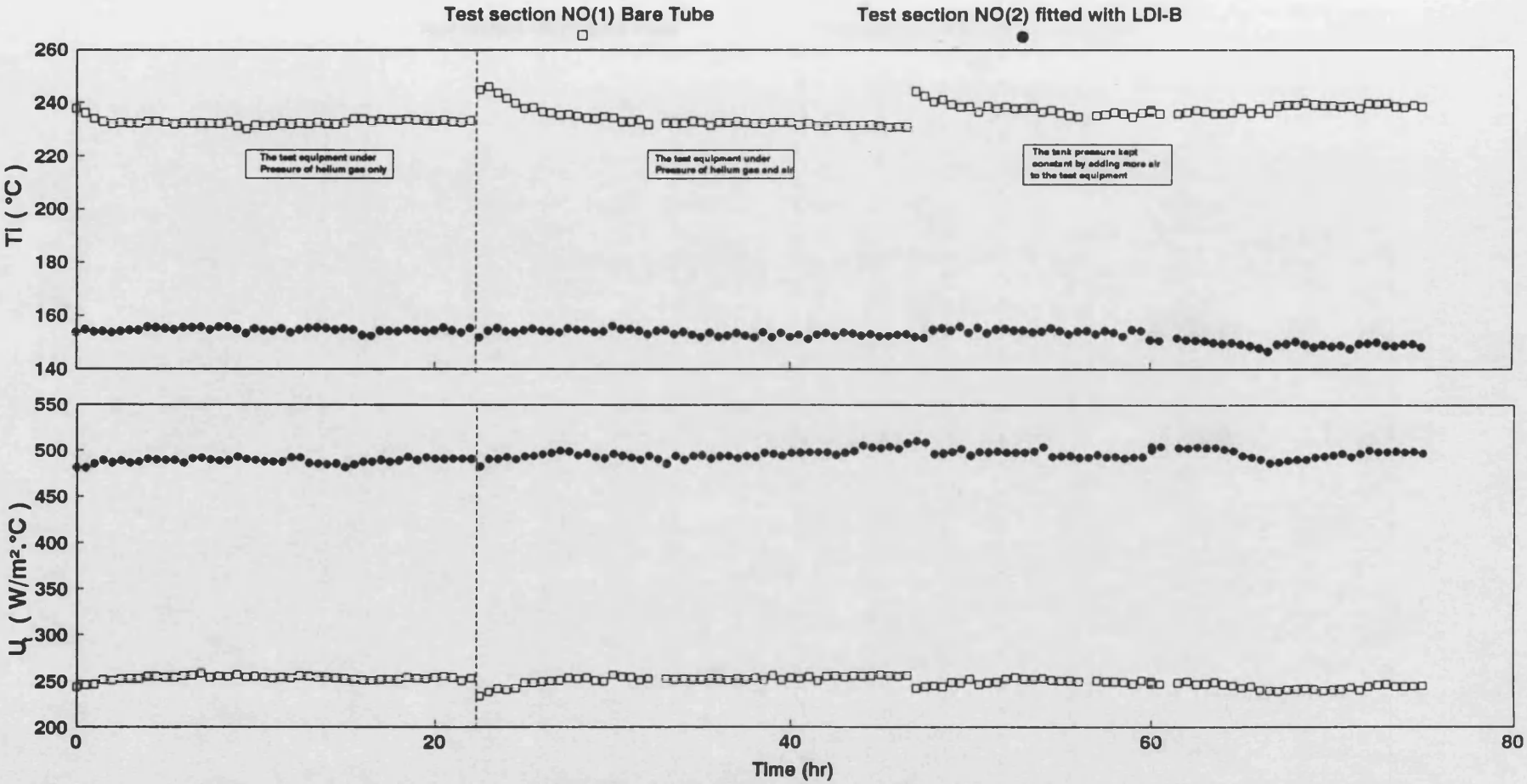

Fig (4.76) Comparison between the overall heat transfer coefficient (Ut) and inner surface temperature (Ti) for both test sections

Arabian light crude oil with 10% by weight of refinery sludge under pressure of helium (He) gas for 22 hrs and then under mixture of 84% He and 16% air

Fouling Run NO(6) [10% F.S.R ; Tb = 74 °C ; Re = 1600 ; Pr = 60 and q = 66.122 kW/m²]

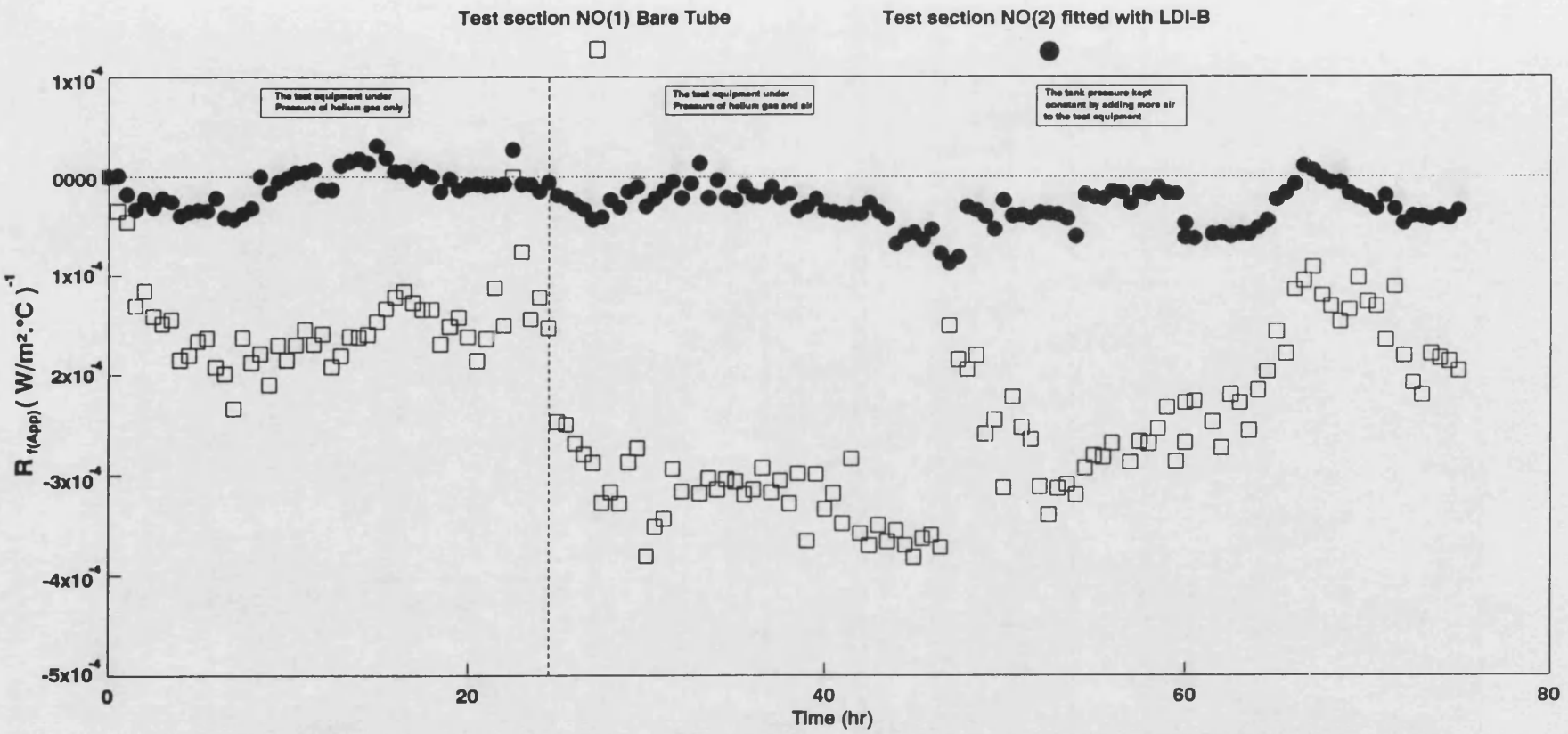

Fig (4.77) Comparison between apparent fouling resistance ($R_{f(App)}$) of both test sections for Fouling Run NO(6)

Arabian light crude oil with 10% by weight of refinery sludge under pressure of helium (He) gas for 22 hrs and then under mixture of 84% He and 16% air

[10% F.S.R ; Tb = 74 °C ; Re = 1600 ; Pr = 60 and q = 66.122 kW/m²]

temperatures T_b and T_i . This provides a reduction in T_i and an enhancement in h_i .

2- N_2 gas bubbles on the hot surface could possibly prevent O_2 gas from contacting the surface. Consequently, the chance of chemical reaction fouling via outoxidation might be lowered .

Fouling under nucleate boiling conditions has received little attention . Palen and Westwater[135] studied the heat transfer and fouling rates of calcium sulphate solutions during pool boiling and came to the conclusion that deposition creates additional nucleate boiling sites which in turn cause an increase in the heat transfer coefficient. They also noted that the fouling rate was a minimum under nucleate conditions. Muller-Steinhagen et al[136], in a recent study on fouling of alumina particles suspended in heptane during boiling and non-boiling conditions , found that the fouling rate was less under nucleate boiling conditions. Khater[47] reported that the fouling rate of vaporising kerosene in a certain range of conditions was decreased by an increase in the temperature. One possibility is that the heat transfer coefficient had been enhanced by nucleate boiling and thus the overall heat transfer coefficient had been increased, rather than decreased, with time.

b - Fouling run No(7)

In order to confirm that the presence of compression gases in the equipment was the main cause of fouling inhibition in the previous six runs an attempt was made in the seventh to eliminate gas from the apparatus .

The equipment was filled as completaly as possible with crude oil and pressurised to 1 bar gauge by using a liquid hand pump. The crude oil was heated up to 74°C , and then pressurised to 13 bar gauge (using the same hand pump) . The set point of the pressure relief valve was 13.2 bar .

The experimental conditions for fouling run No(7) were as follows :

Bulk temperature = 74 °C
Flow rate = 10% F.S.R
Heat flux = 66.2 kW/m²
Initial T_i of bare tube test section No(1) = 213 °C
Initial T_i of test section No(2) fitted with LDI-B = 152°C
The fluid is the same as that used in Runs No 3 to No 6

The variations of P , wall temperature T_w , U_t and $R_{f(App)}$ with time are shown in Fig 4.78 for the bare tube and in Fig 4.79 for test section No(2) fitted with LDI-B . Fouling did occur in this run and thus the variation of T_w (rather than T_i) with time[47,49] has to be plotted as shown in Figs 4.78 and 4.79 .

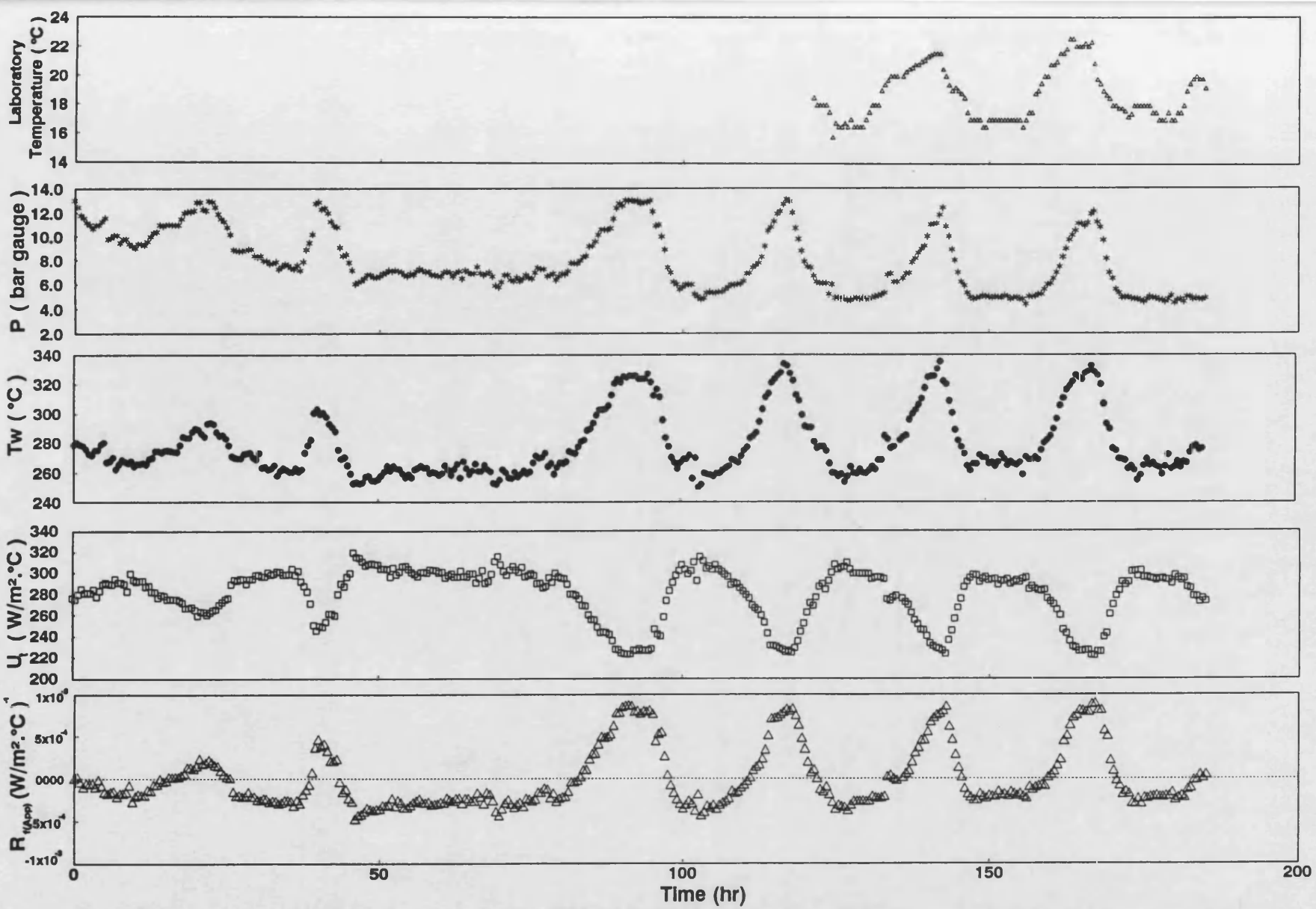

Fig (4.78) Fouling Run No(7) for bare tube test section No(1) [10% F.S.R ; Tb = 74 °C ; Re = 1600 ; Pr = 60 ; q = 66.22 kW/m²]

Arabian light crude oil with 10% by weight of refinery sludge under liquid pressure (the equipment full up with liquid)

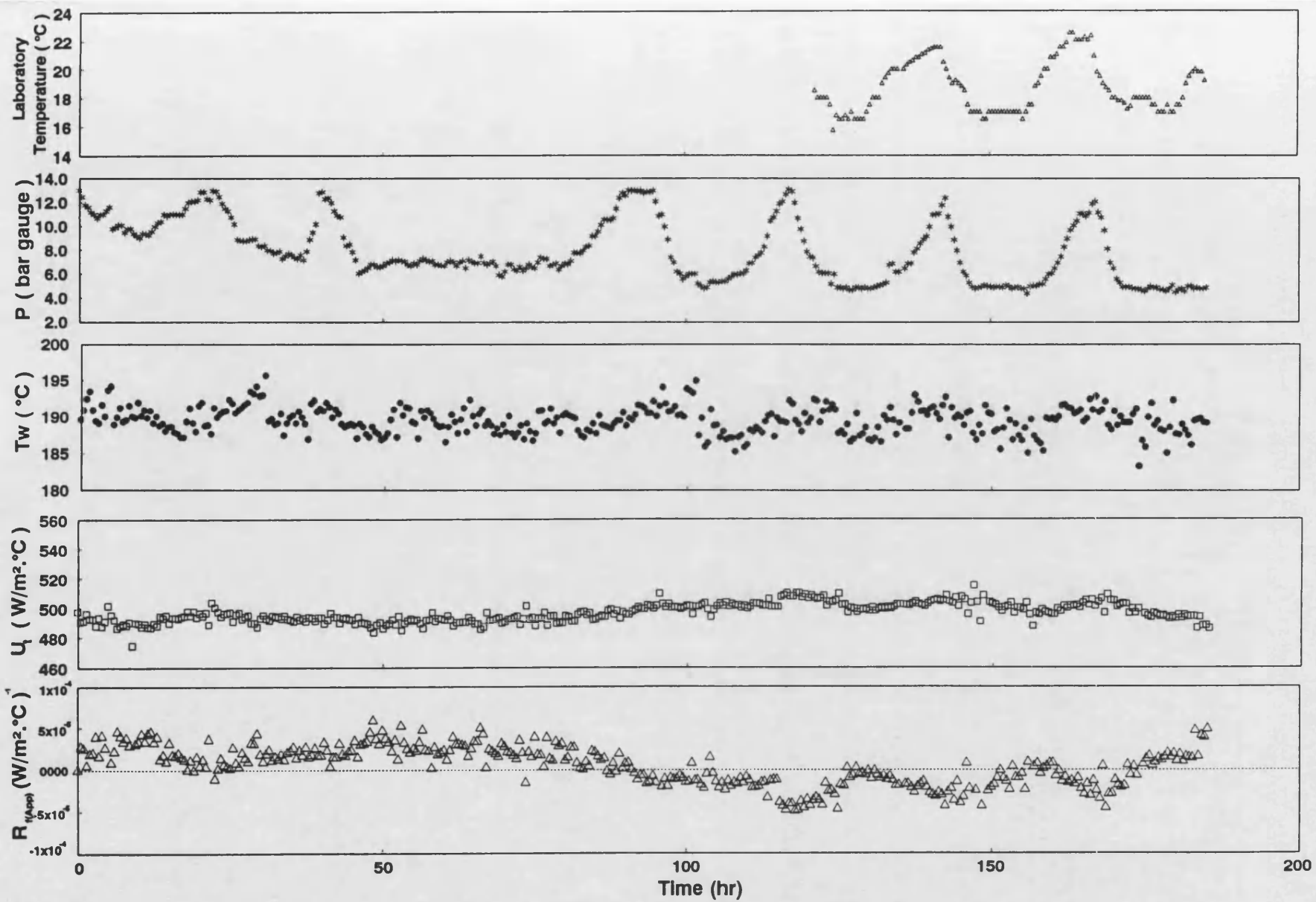

Fig (4.79) Fouling Run No(7) for test section No(2) fetted with LDI-B [10% F.S.R ; Tb = 74 °C ; Re = 1600 ; Pr = 60 and q = 66.22 kW/m²]

Arabian light crude oil with 10% by weight of refinery sludge under liquid pressure (the equipment full up with liquid)

Fig 4.78 shows that the pressure was not stable. P fluctuated between 5 and 13.2 bar and the fluctuation correlated strongly with the variation in laboratory temperatures (between 16°C at night to 21°C during the day time). This variation of pressure caused T_w and U_t to fluctuate as well , as seen in Fig 4.78. Positive values of fouling resistance did occur in this run , but the variation of $R_{f(App)}$ with time was in the shape of saw-teeth .

Fig 4.79 shows that T_w of the tube fitted with the **HiTran** insert was only slightly affected by the variation in the pressure , while U_t was largely unaffected . $R_{f(App)}$ was more or less zero .

A comparison between U_t and T_w for both test sections is shown in Fig 4.80 . A comparison between $R_{f(App)}$ of both test sections is also shown in Fig 4.81 .

Fig 4.82 shows the variation of T_w and U_t with time for bare tube test section No(1) at particular pressures in the run. The variation of $R_{f(App)}$ with time at particular pressures is shown in Fig 4.83 . It seems from these Figures that had it been possible to keep the pressure constant, then fouling would have increased steadily with time .

The conclusions which can be gained from this fouling run are summarised below :

1- The major cause for inhibition of fouling in the previous six runs was the presence

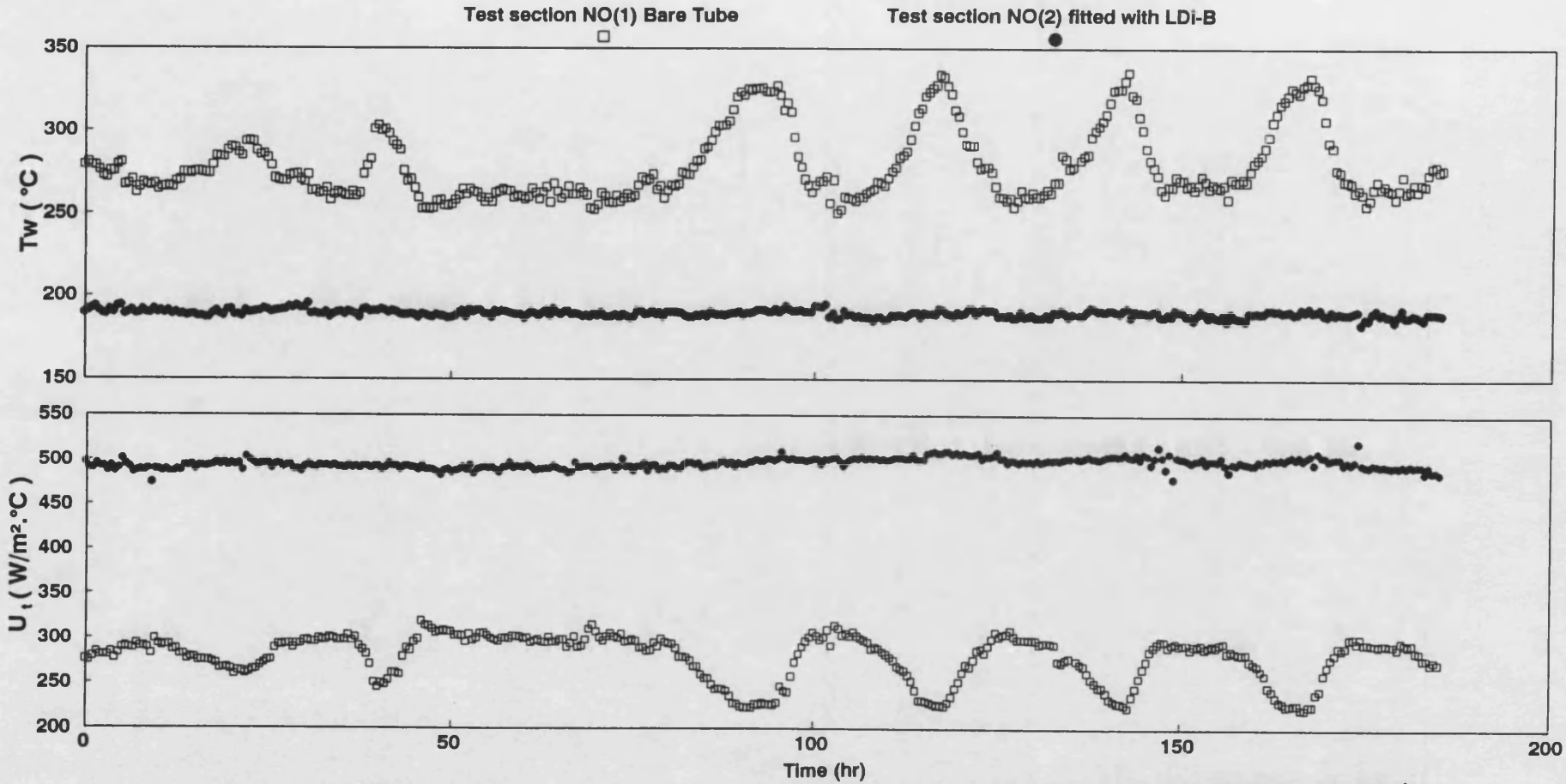

Fig (4.80) Comparison between the overall heat transfer coefficient (Ut) and wall temperature (Tw) for both test sections

Arabian light crude oil with 10% by weight of refinery sludge under liquid pressure (the equipment full up with liquid)

Fouling Run NO(7) [10% F.S.R ; Tb = 74 °C ; Re = 1600 ; Pr = 60 and q = 66.22 kW/m²]

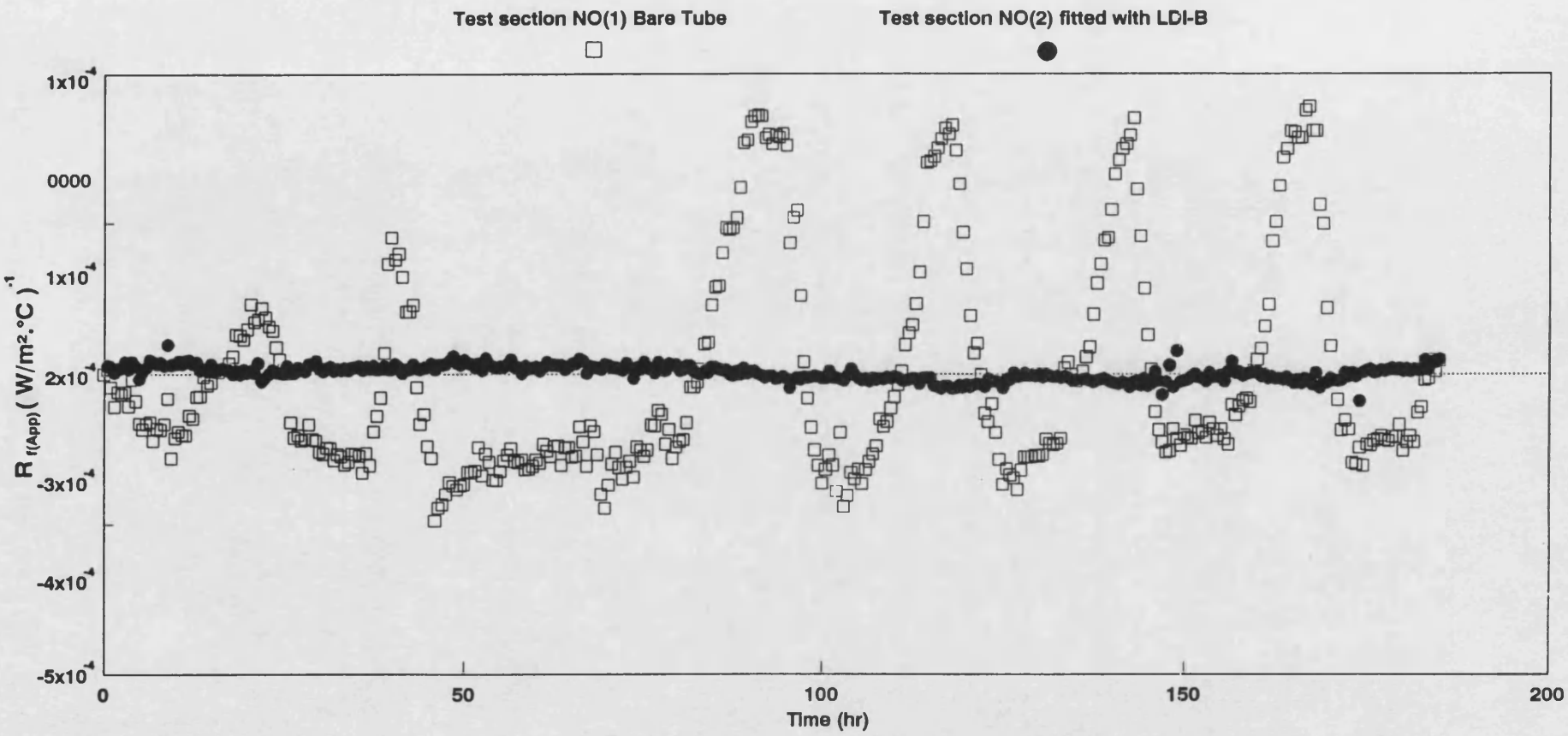

Fig (4.81) Comparison between apparent fouling resistance ($R_{f(App)}$) of both test sections for Fouling Run NO(7)

Arabian light crude oil with 10% by weight of refinery sludge under liquid pressure (the equipment full up with liquid)

[10% F.S.R ; Tb = 74 °C ; Re = 1600 ; Pr = 60 ; q = 66.122 kW/m²]

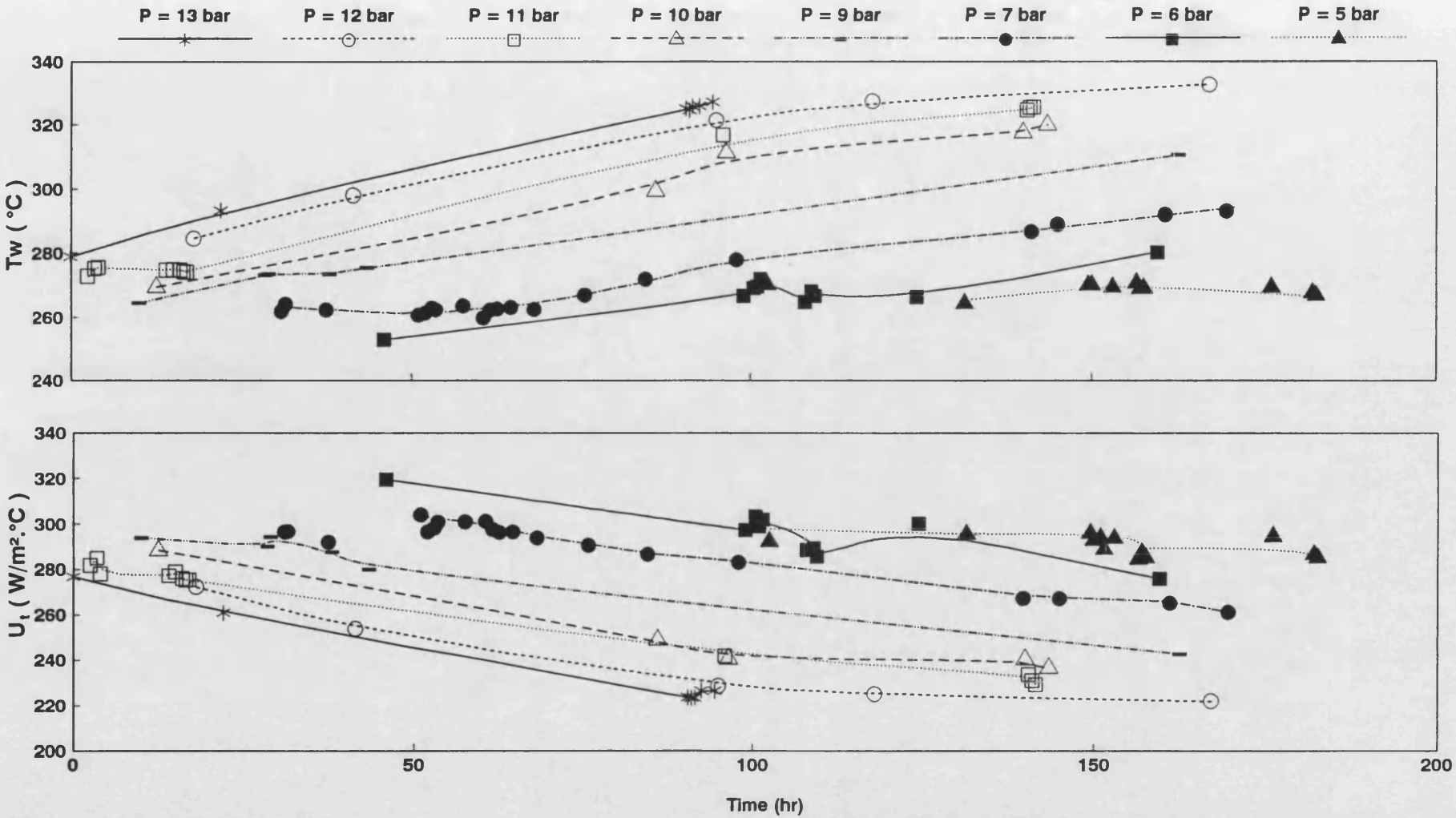

Fig (4.82) Variation of the overall heat transfer coefficient (Ut) and wall temperature (Tw) with time (t) at constant pressure

Arabian light crude oil with 10% by weight of refinery sludge under liquid pressure (the equipment full up with liquid)

Fouling Run NO(7) [10% F.S.R ; Tb = 74 °C ; Re = 1600 ; Pr = 60 and q = 66.22 kW/m²]

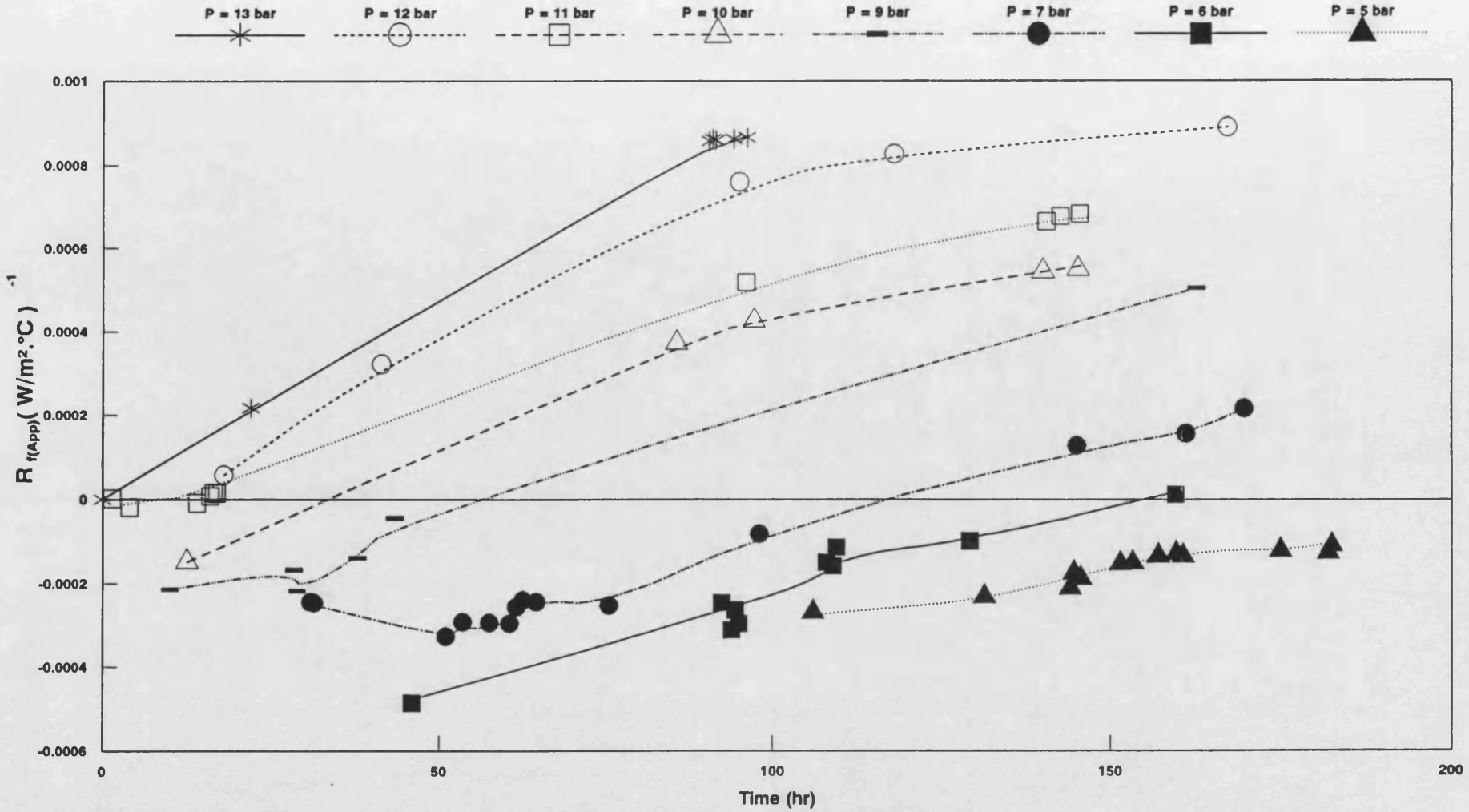

Fig (4.83) Variation of apparent fouling resistance ($R_{f(App)}$) with time at constant pressure

Arabian light crude oil with 10% by weight of refinery sludge under liquid pressure (the equipment full up with liquid)

Fouling Run NO(7) [10% F.S.R ; Tb = 74 °C ; Re = 1600 ; Pr = 60 and q = 66.22 kW/m²]

of dissolved gases (especially nitrogen gas) in the crude oil .

2- A fluctuation of pressure could cause T_w , T_i and U_t to fluctuate accordingly .

3- At low pressure , nucleate boiling could occur in the bare tube and h_i could be enhanced to an extent sufficient to increase the value of U_t, thus creating negative values for $R_{f(App)}$ from equation 4.27.

4- At high pressure , nucleate boiling could not occur . Consequently, there would not be any enhancement in h_i and therefore , U_t values would decrease if fouling occurred and positive $R_{f(App)}$ values would be calculated.

5- At any given pressure in the pressure fluctuations (Figs 4.82 and 4.83), the fouling resistance for the bare tube increased with time. Therefore, in the negative $R_{f(App)}$ regions it appears that existing fouling deposits were not removed from the surface .

6- The test sections were dismantled and checked . Fouling did occur in the bare tube but not in the test section No(2) in which the **HiTran** insert was fitted .

4.6.2.7 Conclusions on the crude oil study results

The principal conclusions of the crude oil study are as follows :

1- The empirical correlations for friction factor and heat transfer, which were generated in the Santotherm 55 study , are applicable to crude oil under similar ranges of Re and Pr .

2- Under nucleate boiling conditions, h_i at lower flow rates (Re < 7000) can increase with heat flux and decrease with pressure. However for higher flow rates (Re > 14000), P and q have no effect on h_i .

3- The solubility of N_2 gas in crude oil is likely to decrease with temperature and increase with pressure . Thus due to the difference in gas solubility at the bulk fluid and surface temperatures, bubble nucleation can occur on the hot surfaces . This bubble nucleation may be called bubble nucleation due to gas solubility difference (BNGSD). The difference between nucleate boiling and BNGSD is that the latter may be enhanced by increasing the pressure , whilst nucleate boiling would be suppressed by increasing the pressure . Nucleate boiling is controlled by ΔT_{sat} , $(T_{sat} - T_{b)}$, whilst BNGSD is likely to be

controlled by the temperature driving force ΔT_i , $(T_i - T_b)$.

4- Both nucleate boiling and BNGSD enhance the heat transfer coefficient and hence reduce the inner surface temperature .

5- Nitrogen gas may be used as a fouling inhibitor. N_2 gas can degass, due to the BNGSD mechanism , on the hot surfaces to prevent O_2 gas from contacting the surface. Thus the chemical reaction fouling mechanism might be restricted. N_2 bubbles can also reduce the inner surface temperature and hence reduce the rate of a chemical reaction fouling mechanism.

6- Negative fouling resistances, which have been reported in many previous fouling studies , can clearly be due to an enhancement in h_i during the early period of an experiment and be caused by nucleate boiling and/or BNGSD . Fouling deposits in the early stages could create additional nucleate boiling sites which would increase nucleate boiling and/or BNGSD. If the order of magnitude of the enhancement in h_i is sufficient to counteract the thermal resistance of the deposit itself, then an increase, rather than a decrease, in the overall heat transfer coefficient (U_t) would occur and a negative fouling

resistance (R_f) would be calculated from equation 4.27. Moreover, if the enhancement in h_i is just equivalent to the deposit thermal resistance , then no change in U_t would be found and R_f would be zero . This could explain the induction period observed in some fouling studies. On the other hand, if the enhancement in h_i is insufficient to counteract the deposit thermal resistance , then a decrease in U_t would occur and a positive fouling resistance R_f would be calculated .

7- The **HiTran** insert can decrease the inner surface temperature T_i , increase the heat transfer coefficient and create mixing in the bulk of fluid . Thus, fouling has less chance to occur . The present study shows that when the bare tube was fouled (Run 7), the tube fitted with the **HiTran** insert did not .

8- The **HiTran** insert was believed to suppress nucleate boiling and thus a higher heat flux could be applied to a tube fitted with a **HiTran** insert .

Chapter 5

Conclusions and Recommendations for Further Work

5.1 Conclusions

The principal conclusions of the present study are as follows :

1- Over the range of experimental conditions studied , the use of a **HiTran** insert enhances the heat transfer factor (j_H) over that of a bare tube. The enhancement ranges between 3.6 and 5.8 times for 500 < Re < 2100 , between 1.8 and 4.3 times for 2100 < Re < 10000 and between 1.3 and 3.4 times for 10000< Re < 34000. However, there is also a significant concomitant increase in pressure drop (Δp) in the range of 8.5 to 50 times for 500 < Re < 34000 over that of a bare tube case.

2- The heat transfer results for a bare tube and for a tube fitted with different types of **HiTran** insert were correlated by a modified heat transfer factor (j_{HM}) which defined as follows:

$$j_{HM} = Nu\,[\,Pr\,f\,(\mu_b/\mu_w)\,]^{0.14}$$

The empirical correlations which were generated for Santotherm 55 fluid and tested with data obtained using Arabian light crude oil are believed to be valid for hydrocarbons in general subject to the ranges of Reynolds number (Re) and Prandtl number (Pr) shown in Table 5.1 below .

Table 5.1 Heat transfer and friction factor correlations for a bare tube and for a tube fitted with different types of HiTran insert

Conditions of the test sections	Correlation	Recommended range	Accuracy and remarks
Bare tube	$Nu_{(bare)} = \frac{0.7\ Re^{0.61}}{[\ Pr\ f\ (\mu_b/\mu_w)\ ]^{0.14}}$ $f_{(bare)} = 0.117\ Re^{0.283}$	for friction factor $Re > 10^4$ $30 < Pr < 187$ and for Nu $700 < Re < 3.4 \times 10^4$ $30 < Pr < 187$	1- The friction factor correlation accurate to about ± 5% 2- Nu correlation accurate to about ± 10%
Tube fitted with LDI HiTran insert (2.7 loops per cm)	$Nu_{(LDI)} = \frac{17\ Re^{0.356}}{[\ Pr\ f\ (\mu_b/\mu_w)\ ]^{0.14}}$ $f_{(LDI)} = A_{11} + 60000/\ Re^2$ Where : $Log_{10}(A_{11}) = 1.24 - 0.33\ Log_{10}(Re^3) + 0.01216\ (Log_{10}Re^3)^2$	$1000 < Re < 3.4 \times 10^4$ $30 < Pr < 187$	1- The friction factor correlation accurate to about ±8% 2- Nu correlation accurate to about ±7.1%
Tube fitted with MDI HiTran insert (6.4 loops per cm)	$Nu_{(MDI)} = \frac{11.6\ Re^{0.46}}{[\ Pr\ f\ (\mu_b/\mu_w)\ ]^{0.14}}$ $f_{(MDI)} = A_{12}$ Where : $Log_{10}(A_{12}) = 1.634 - 0.33\ Log_{10}(Re^3) + 0.01215\ (Log_{10}Re^3)^2$	$750 < Re < 15500$ $34 < Pr < 129$	1- The friction factor correlation accurate to about ±7% 2- Nu correlation accurate to about ±10%
Tube fitted with HDI HiTran insert (10.5 loops per cm)	$Nu_{(HDI)} = \frac{22.5\ Re^{0.4}}{[\ Pr\ f\ (\mu_b/\mu_w)\ ]^{0.14}}$ $f_{(HDI)} = A_{13}$ Where : $Log_{10}(A_{13}) = 2.143 - 0.38\ Log_{10}(Re^3) + 0.01546\ (Log_{10}Re)^2$	$900 < Re < 13300$ $34 < Pr < 111$	1- The friction factor correlation accurate to about ±2% 2- Nu correlation accurate to about ±6.2%

3- The overall performance of the test section fitted with **HiTran** inserts was determined by using the enhancement factor (EF). The enhancement factor, which is a combination of Nu and Δp in one formula , was found to decrease with increasing loop density of the **HiTran** insert and with increasing Re .

4- The use of a **HiTran** insert provides a substantial reduction in the inner surface temperature which is useful for controlling in - tube fouling .

5- Nucleate boiling in a bare tube test section can enhance the heat transfer coefficient and so reduce the inner surface temperature .

6- Dissolved nitrogen can degass on hot surfaces due to the mechanism of solubility difference at the bulk and surface temperatures . The effect of bubble nucleation due to gas solubility difference on heat transfer coefficient and inner surface temperature is similar to that provided by nucleate boiling .

7- Fouling may be inhibited by both nucleate boiling and bubble nucleation due to gas solubility difference .

8- The **HiTran** insert is useful for suppressing nucleate boiling and thus a higher heat flux could be applied to a tube fitted with a **HiTran** insert .

5.2 Recommendations for Further Work

It is recommended that further research on heat transfer and fouling of hydrocarbons, with or without inserts , should be carried out as follows :

1- A device to stabilise the pressure should be installed on the hydrocarbon feed tank, in order to avoid the pressure fluctuations experienced in fouling run 7 in this study.

2- With a pressure stabiliser installed, the effects of nucleate boiling and bubble nucleation due to gas solubility difference (BNGSD) on both heat transfer and fouling should be examined further. Both these nucleation phenomena are likely to occur in crude oil preheat exchangers. Consideration should be given to whether a visual section can be installed in the apparatus. The dark colour of crude oil and the need to work at elevated pressures and temperatures present substantial technical and safety difficulties in this respect .

3-With a pressure stabiliser installed, the effects of flowrate, heat flux, surface temperature and bulk temperature on fouling from a range of crude oils should be studied for both the bare tube and for a tube fitted with different types of insert. The effect of insert re-use and rotation should also be explored.

4- Consideration should also be given to the length - to - diameter ratio of each test section . The effects of different test section diameters, perhaps using different materials of constriction, could be studied .

References

1- Holman , J.P.

Experimental Methods for Engineers, 5th Edition , McGraw - Hill , New York , 1989, pp 6-12 .

2- Chatfield , C.

Problem Solving ; A Statistician's Guide, 1st Edition , Chapman and Hal , Lndon , 1988, pp 200 - 205 .

3- McAdams , W.H.

Heat Transmission , 3rd Edition , McGraw - Hill , New York , 1954, pp 165-182 .

4- Perry , R.H. and Chilton , C

Chemical Engineers' Handbook , 5th Edition , McGraw - Hill , Tokyo , 1973 .

5- Churchill , S.W. and Chu , H.H.S.

Int.J.Heat & Mass Transfer , vol.18 , 1975, p 1049 .

6- Welty , J.R. ; Wicks , C.E. and Wilson , R.E.

Fundamentals of Momentum , Heat, and Mass Transfer , 3rd Edition , Jphn Wiley & Sons , New York , 1984, pp 754 - 780 .

7- Incropera, F.P. and DeWitt, D.P.

Introduction to Heat Transfer , 2nd Edition, John Wiley & Sons , New York , 1990 .

8- Bennett, C.O. and Myers,J.E.

Momentum, Heat, and Mass Transfer ,3th Edition , McGraw - Hill, Singapore, 1983 .

9- Fischer, P. ; Suitor, J.W. , and Ritter,R.B.

Chem. Eng. Prog. , vol. 71 , July 1975, PP 66 - 72 .

10 Knudsen, J.G.

In Fouling of Heat Transfer Equipment, Eds, Somerscales, E.F.C. and Knudsen, J.G. ; Hemisphere, Washington, 1981, pp 57 - 81 .

11- Wilson, E.E.

Trans. ASME, vol. 37 , 1915 , PP 47 - 89 .

12- **Dittus, P.W. and Boelter, L.M.K.**
University of California Pub.Eng. , vol.2, No 13, Oct. 17 , 1930 , PP 443 - 461 ; reprinted in Int. comm. Heat Mass Transfer, vol.12, 1985, PP 3 - 22 .

13- **Shah , R.K. and London, A.L.**
Laminar flow forced convection in Ducts , Supplement 1 to Advanced in Heat Transfer , Academic Press Inc., New York , 1978, P 30.

14- **Kakaç , S. et al**
Handbook of Single - Phase convection Heat Transfer , 1st Edition, John Wiley & Sons , New York , 1987 .

15- **Moody, L.F.**
Tran.of ASME, Nov.1944, PP 671 - 684 .

16- **Noel de Nevers**
Fluid Mechanics For Chemical Engineers, 2nd Edition, McGraw - Hill , New York , 1991 .

17- **Coulson, J.M. and Richardson, J.F.**
Chemical Engineering , vol. 1 , 3th Edition, Pergamon press , Oxford , 1977 .

18- **Agrawal, A.K. and Sangupta, S.**
Int.J.Heat and Fluid Flow, vol. 11 , No 1, Mar. 1990 , PP 54 - 89 .

19- **Gough, M.J. ; Rogers, J.V. and Russell, C.M.B.**
12th HTFS Res Symp University of Warwick , Paper RS 417 .

20- **Crittenden, B.D. and Kolaczkowski, S.T.**
Hydrocarbon Processing, Aug.1987, PP 45 - 46.

21- **Gough, M.J. and Rogers, J.V.**
Heat Transfer - Pittsburgh 1987 , AIChE Symposium series, vol. 83, No 257, PP 17-21.

22- **Aldington, R.W.J.**
Ph.D. Thesis, Birmingham University, U.K.,1987.

23- **Oliver, D.R. and Aldington, R.W.J.**
Chem.Eng.Res.Des. , vol. 66, Nov.1988, pp 555 - 565 .

24- Rorers, J.V. ; Bowen, J.E. and Gough, M.J.
Heat Transfer - Philadelphia, 1989, AIChE Symposium serier, vol. 85, No 269, PP 160-156

25- Gough, M. and Rogers, J.
Processing , July 1991, PP 15-16 .

26- Chen, R.Y.
J.Fluid Eng. , vol. 95 , 1973, PP 153 - 158 .

27- Hornbeck, R.W.
Appl.Sci.Res., section A 13, 1964, PP 224-232

28- Liu, J.
Ms Thesis , University of Wisconsin Milwaukee, USA, 1974 .

29- Keys, W.M. and Crawford, M.W.
Convective Heat and Mass Transfer, 2nd Edition, McGraw - Hill , New York , 1980 .

30- Shah, R.K.
Proc.Natl.Heat Mass Transfer conf., 3rd , Indion Inst. Techonol., Bomobay, vol. I, 1975. Pap. No HMT-!!-75 .

31- Al-Arabi, M.
Heat Transfer Eng. , vol. 3 , 1983, PP 76-83 .

32- Latzko, H.Z.
Angew. Math.U.Mech., 1, 1921, PP 268 - 290; English translation, Natl. Advisory Comm. Aeronaut.,Tech. Mem., 1944, P 1068.

33- Notter,R.H. and Sleicher, C.A.
Chem.Eng.Sci. , vol. 27 , 1972, PP 2073-2093 .

34- Kays, W.M. and London, A.L.
Compact heat exchangers , 3rd Edition, McGraw - Hill , New York , 1984 .

35- Churchill, S.W.
Ind.Eng.Chem., Fundam., vol. 16, No 1, 1977, PP 109 - 116 .

36- Sieder, E.B. and Tate, G.E.
Ind.Eng.Chem., vol. 28, 1936, PP 1429-1435 .

37- Gnielinski, V.
Int.Chem.Eng. , vol. 16, 1976, PP 359 -368 .

38- **Walker, R.A. and Bott, T.R.**
The chemical Engineer, Mar.1973, PP 151-156 .

39- **Garrett-Price, B.A.** ***et al***
Fouling of Heat Exchanger, Noyes Publications, New Jersey, 1985.

40- **Bott, T.R.**
Fouling Notebook, Inst.of Chem. Eng., Rugby, 1990 .

41- **Walker, R.A.**
Ph.D. Thesis, Birmingham University, U.K.,1973.

42- **Gudmundsson, J.S.**
Ph.D. Thesis, Birmingham University, U.K.,1977.

43- **Kolaczkowski, S.T.**
Ph.D. Thesis, Bath University, U.K.,1977.

44- **Hall, J.**
Ph.D. Thesis, Liverpool University, U.K.,1978.

45- **Loo, C.E.**
Ph.D. Thesis, Oxford University, U.K.,1979.

46- **Harty, D.W.S.**
Ph.D. Thesis, Birmingham University, U.K.,1980.

47- **Khater, E.M.H.**
Ph.D. Thesis, Bath University, U.K.,1982.

48- **Hussain, C.I.**
Ph.D. Thesis, Birmingham University, U.K.,1982.

49- **Hout, S.A.**
Ph.D. Thesis, Bath University, U.K.,1983.

50- **Nesuratnam, R.N.**
Ph.D. Thesis, Birmingham University, U.K.,1984.

51- **Alderman, N.J.**
Ph.D. Thesis, Bath University, U.K.,1986.

52- **Zhang, G.**
M.Ph. Thesis, Birmingham University, U.K.,1988.

53- **Lowe, M.J.**
Ph.D. Thesis, Birmingham University, U.K.,1988.

54- **Somerscales, E.F.C. and Knudsen, J.K. ; Eds.**
Fouling of Heat Transfer Equipment, Hemisphere, Washington, 1981 .

55- **Chenoweth, J.M. and Impagliazzo, M. ; Eds.**
Fouling in Heat Exchange Equipment, HTD-vol.17, ASME, New York, 1981 .

56- Suitor, J.W. and Pritchard, A.M. ; Eds.
Fouling in Heat Exchange Equipment, HTD-vol.35, ASME, New York, 1984 .

57- Bryery, R.W. ; Ed.
Fouling of Heat Exchange Surfaces, Proce. of the Engineering Foundation Conference held Oct.31 Nov. 5 , 1982 at the Hershey Pocono Resort, White Haven,Pennsylvania, U.S.A.

58- Melo, L.F.; Bott, T.R. and Bernardo, C.A.; Eds.
Fouling Science and technology ; Kluwer Academic Publishers, Dordrecht, The Netherlands, 1988 .

59- Somerscales, E.F.C.
Fouling of Heat Transfer Surfaces: An Historiacl review, in History of Heat Transfer, essays in honor of 50^{th} anniversary of the ASME heat transfer division; Layto, E.T.and Lienhard,J.H, Eds.,ASME, 1988 .

60- Epstein, N.
Proc. 6^{th} Int. Heat Transfer conf. Toronto, Canada, vol. 6, Hemisphere Pub. Corp, Washington, 1978, PP 235-254 .

61- Epstein, N.
In Fouling of Heat Transfer Equipment, Somerscales, E.F.C. and Knudsen, J.G.; Eds, Hemisphere, Washington, 1981, pp 31 - 53 .

62- Epstein, N.
Heat Transfer Engineering, vol. 4, No 1, 1983, PP 43 - 56 .

63- Bohnet, M.
Chem. Eng. Technol. , 10, 1987, PP 113 - 125 .

64- Crittenden, B.D.
In Fouling Science and Technology; Melo, L.F, *et al* ,Eds. , Kluwer Academic Publishers, Dordrecht, The Netherlands, 1988, PP 293-313 .

65- Crittenden, B.D.
In Fouling Science and Technology; Melo, L.F, *et al* ,Eds. , Kluwer Academic Publishers, Dordrecht, The Netherlands, 1988, PP 315-332 .

66- Braun, R.
Materials Performance, Nov. 1977, PP 35 - 41 .
67- Dickakian, G. and Seay, S.
Oil & Gas Journal, Mar. 7, 1988, PP 47 - 50 .
68- Fields, D.E. ; Freeman , R.F. and Wright, B.E.
Energy Progress, vol. 8, No 4, Dec 1988,
PP 220 - 225 .
69- Nelson, W.L.
Refinery and Natural Gasoline Manufacturer,
vol.13, No 7 , PP 271-276 ; No 8 , PP 292-298,
1934 .
70- Nelson, W.L.
Petroleum Refinery Engineering, 4^{th} Edition,
McGraw - Hill , New York , 1958 .
71- Tubular Exchanger Manufacturers Association
Standards of the Tubular Exchangers
Manufacturers Association, 1^{st} Edition
New York, 1941 .
72- Bott, T.R. and Walker, R.A.
The Chemical Engineer, Nov. 1971, PP 391-395 .
73- Lambourn, G.A. and Durrieu, M.
In Heat Exchangers Theory and Practice;
Taborek, J ; Hewitt, G.F and Afgan, N. ; Eds,
Hemisphere, Washington, 1983, pp 841-852 .
74- Tubular Exchanger Manufacturers Association
Standards of the Tubular Exchangers
Manufacturers Association, 7^{th} Edition
New York, 1988 .
75- Chenoweth, J.
Heat Transfer Eng. , vol. 11, No 1,1990,
PP 73-107 .
76- Taborek, J.
Heat Transfer - Philadelphia, 1989, AIChE
Symposium serier, vol. 85, No 269, PP 79-83.
77- Van Nostrand, W.L.; Leach, S.H. and Haluska,J.L.
In Fouling of Heat Transfer Equipment,
Somerscales, E.F.C. and Knudsen, J.G.; Eds,
Hemisphere, Washington, 1981, PP 619 - 643.

78- **Crittenden,B.D. and Kolaczkowski, S.T.**
Technical Report on Fouling, Selectamaster Ltd, Bath , Dec. 1991 .

79- **Froment, G.F.**
In Fouling of Heat Transfer Equipment, Somerscales, E.F.C. and Knudsen, J.G.; Eds, Hemisphere, Washington, 1981, PP 411 - 435.

80- **Crittenden,B.D.; Kolaczkowski,S.T. and Hout, S.A.**
Chem.Eng.Res.Des., vol.65, Mar.1987, PP 171-179

81- **Crittenden,B.D.; Hout, S.A. and Alderman, N.J.**
Chem.Eng.Res.Des., vol.65, Mar.1987, PP 165-170

82- **Watkinson, A.P.**
Critical Review of Organic fluid fouling: final report, ANL/CNSV - TM - 208, 1988.

83- **Crittenden, B.D. and Downey, I.L.**
In Fouling Science and Technology; Melo, L.F, *et al* ,Eds. , Kluwer Academic Publishers, Dordrecht, The Netherlands, 1988, PP 727-729 .

84- **Epstein, N.**
In Fouling Science and Technology; Melo, L.F, *et al* ,Eds. , Kluwer Academic Publishers, Dordrecht, The Netherlands, 1988, PP 15 -29 .

85- **Kern, D.Q. and Seaton, R.E.**
Brit.Chem.Eng., vol. 4, No 5, 1959, PP 258-262.

86- **Eaton, P. and Lux, R.**
ASME HTD-vol. 35 , 1984 , PP 33 - 42 .

87- **Crittenden, B.D. and Khater, E.M.H.**
ASME HTD-vol. 35 , 1984 , PP 54 - 64 .

88- **Crittenden, B.D. and Khater, E.M.H.**
J. of Heat Tran., vol. 109, Aug.1987,PP 583-587

89- **Crittenden,B.D.; Downey, I.L.and Kolaczkowski,S.T.**
Intl.Conf.Fouling in Process Plant, Inst. Corr. Sc.Tech. and Inst. Chem. Eng.,Oxford, U.K , 1988, PP 32 - 51 .

90- **Atkins, G.T.**
Petro/Chem.Eng., vol.34, Apr. 1962 , PP 20-25.

91- **Dahlin, K.E.; Daniel,S.R. and Worstell, J.H.**
Fuel ,vol. 60, 1981, PP 477 - 480.

92- Gillies, W.V.
In Fouling - Science or Art ? , Inst.Corr. Sc. Tech. and Inst Chem. Engs, Univ. of Surrey, Guidford, U.K, 1979 , PP 188 - 196 .

93- Butler, R.C. ; Mc Curdy, W.N. and Linden, N.J.
Trans. ASME,vol. 71, 1949, PP 843- 847 .

94- Chantry, W.A. and Church, D.M.
Chem.Eng.Prog., vol. 54, No 10, 1958, PP 64-67.

95- Katz, D.L. *et al*
Petr.Refiner, Vol.33, No 4 , 1954, PP 123-125 .

96- Dugan, C.L.; Van Nostrand,Jr.W.L, and Haluska,J.L.
Chem.Eng.Prog., vol. 74, No 5, 1978 , PP 53-57.

97- Crittenden,B.D.; Kolaczkowski,S.T. and Downey, I.L
Trans. I.Chem E , 1992 , 1n Press .

98- Hausler, R.H.
Oil & Gas J. ,vol. 71, 4 July 1973, PP 56 - 63.

99- Kolaczkowski,S.T.; Crittenden,B.D. and Varley,R.
Intl.Conf.Fouling in Process Plant, Inst. Corr. Sc.Tech. and Inst. Chem. Eng.,Oxford, U.K , 1988, PP 52 - 67 .

100- Crittenden,B.D. and Kolaczkowski,S.T.
In Fouling - Science or Art ? , Inst.Corr. Sc. Tech. and Inst Chem. Engs, Univ. of Surrey, Guidford, U.K, 1979. PP 169 - 187 .

101- Crittenden,B.D. and Kolaczkowski,S.T.
In Energy for Industry; O'Callaghan, P.W., Ed., Pergamon, Oxford, 1979, PP 257 - 266 .

102- Taborek, J. *et al* .
Chem.Eng.Prog. , vol. 68, No 2 , PP 59-67; No 7, PP 69-78, 1972 .

103- Bott, T.R. and Gudmundsson. J.S.
Proc. 6th Int. Heat Transfer conf. Toronto, Canada, vol. 4, Hemisphere Pub. Corp, Washington, 1978, PP 373-378 .

104- Ritter, R.B.
ASME HTD-vol. 17 , 1984 , PP 67 - 72 .

105- Crittenden,B.D.; and Alderman, N.J.
Chem.Eng.Scin.,vol. 43, No 4, 1988, PP 829-838

106- **Lobo, S.L.**
In Fouling Science and Technology; Melo, L.F, *et al* ,Eds. , Kluwer Academic Publishers, Dordrecht, The Netherlands, 1988, PP 333 -349 .

107- **Watkinson, A.P. and Epstein, N.**
Chem.Eng.Prog.Symp.ser.,vol 65,No 92,1969, PP 84 - 90 .

108- **Smith, G.T.**
Ind.Engng.Chem.Proc.Des.Dev.,vol 8,1969, PP 299 - 308 .

109- **Vranos, A. ; Marteney, P.J. and Knight, B.A.**
In Fouling of Heat Transfer Equipment, Somerscales, E.F.C. and Knudsen, J.G.; Eds, Hemisphere, Washington, 1981, PP 489 - 499.

110- **Weiland, J.H. ; McCay, R.C. and Barnes, J.E.**
Trans. ASME, vol. 71, 1949 , PP 849 - 853 ,

111- **Shah, Y.T. ; Stuart, E.B. and Sheth, K.D.**
Ind.Engng.Chem.Proc.Des.Dev.,vol 15,1976, PP 518 - 524 .

112- **Sundaram, K.F. and Froment, G.F.**
Chem. Eng.Sci., vol. 34, 1979, PP 635 - 644 .

113- **Taylor, W.F.**
The study of hudrocarbon fuel vapor deposits, Air Force Repoat, AFAPL-TR-69-77 , Sep. 1969 .

114- **Takatsuka, T. ; *et al* .**
J.Chem.Eng.Japan,vol 22,No 2, 1989, PP 149-154.

115- **Zengel, A.E.**
A Comparison of the Capabilities of a Fuel Coker and the Minex Heat Exchanger for Determining hydrocarbon Fuel Thermal Stability, Air Force Report, AFAPL-TR-64-154, Mar. 1965 .

116- **Watt, J.J. ; Evans, A. and Hibbard, R.R.**
NASA Report, TN D-4958, Dec. 1968 .

117- **Hausler, R.H. and Thalmayer, C.E.**
API Refining 40th Mid - Year Meeting, Chicago, U.S.A, 1975 .

118- **Taylor, W.F.**
Ind.Engng.Chem.Proc.Des.Dev.,vol 13,1974, PP 133 - 138 .

119- Eaton, P.E. and Weeter, G.Y.
16th Nat. Heat. Tran. Conf. 76. ,CSME/CSChe-22, St. Louis, U.S.A , 1976 .

120- Fetissoff, P.E. ; Watkinson,A.P. and Epstein, N.
Proc. 7th Int. Heat Trans. Conf. , Munchen, Germany, vol 6, 1982, PP 391 - 396 .

121- Latos, E.J. and Franke, F.H.
Corrosion 82 , NACE, Mar 1982, Paper No 103 .

122- Scarborough, C.E. , *et al* .
Chem. Eng. Prog., vol 75, No 7, 1979,PP 41-46 .

123- Chen, J and Maddock, M.J.
Hydr. Proc. , vol 52, No 5, 1973, PP 147-150 .

124- Fernandez - Baujin, J.M. and Solomon, S.M.
In Industrial and Laboratory Pyrolyses, Albright, L.F. , and Crynes, B.L. ; Eds., ACE Symp. ser. No 32, Washington, 1976, PP 345 - 372 .

125- Thackery, P .
In Fouling - Science or Art ? , Inst.Corr. Sc. Tech. and Inst Chem. Engs, Univ. of Surrey, Guidford, U.K, 1979. PP 1 - 9 .

126- Thompson, R.B. , *et al* .
Ind.Eng.Chem., vol 43 , Apr 1951, PP 935-939 .

127- Haluska, J.L.
Hydr. Proc. ,vol 55, No 7, 1976 , PP 153 - 156.

128- Jones, L. ; *et al* .
Fuel , vol 63, Aug. 1984, PP 1152 - 1156 .

129- Pedley, J.F.; Hiley, R.W. and Hancock, R.A.
Fuel , vol 68, Jan. 1989, PP 27 - 31 .

130- Sanford, E.C. and Kirchen, R.P.
Oil & Gas J. , Dec. 19, 1988, PP 35 - 41 .

131- Yen, L.C., Wrench, R.E. and Ong, A.S.
Oil & Gas J. , Jan. 11, 1988, PP 67 - 70 .

132- Albright, L.F.
Oil & Gas J. , Aug 1 , PP 35-40, Aug 29, PP 45 - 48 , 1988 .

133- Martin, J.F.
Hydr. Proc. , Nov. 1988 , PP 63 - 67 .

134- Knudsen, J.G.
Chem. Eng. Prog. , Feb. 1984, PP 63-69 .

135- Palen, J.W. and Westwater, J.W.
Chem. Eng. Prog. Symp. Ser. ,vol 62, No 64, 1966 , PP 77 - 86 .

136- Muller-Steinhagen, H. , *et al* .
Proc. 8th Int. Heat Trans. Conf.,San Francisco, U.S.A, vol 5, 1986, PP 2555 - 2560 .

137- Speight, J.G.
Chemistry and Technology of Petrolum , Marcel Dekker Inc., New York, 1980, Chp. 7.

138- Dickakian, G.B.
Eur. Pat. app., P. No 0 241 233 A2, Oct 87, and P. No 0 261 960 A2 , Mar 1988 .

139- Canapary, R.C.
Oil & Gas J., Oct 9, 1961, PP 114 - 118 .

140- Taylor, W.F. and Frankenfeld, J.W.
Ind.Engng.Chem.Prod.Res.Dev.,vol 17, No 1, 1978, PP 86 - 90 .

141- Merry, H. and Polley, G.T.
In Fouling of Heat Transfer Equipment, Somerscales, E.F.C. and Knudsen, J.G.; Eds, Hemisphere, Washington, 1981, PP 83 - 94 .

142- Chenoweth, J.W.
In Fouling Science and Technology; Melo, L.F, *et al* ,Eds. , Kluwer Academic Publishers, Dordrecht, The Netherlands, 1988, PP 49 -65 .

143- Somerscales, E.F.C.
In Fouling of Heat Transfer Equipment, Somerscales, E.F.C. and Knudsen, J.G.; Eds, Hemisphere, Washington, 1981, PP 1 - 27 .

144- Melo, L.F. and Pinheiro, J. de D. R. S.
ASME HTD - vol35, 1984 , PP 43 - 49 .

145- Frazier, A.W. , Huddle, J.G. and Power, W.R.
Oil & Gas J. , Mar 3 , 1965 , PP 117 - 122.

146- Harty, D.W.S. and Bott, T.R.
In Fouling of Heat Transfer Equipment, Somerscales, E.F.C. and Knudsen, J.G.; Eds, Hemisphere, Washington, 1981, PP 335 - 344 .

147- Whalley, P.B.
Boiling, Condensation and Gas-Liquid Flow, Clarendon Press, Oxford, 1987 .

148- Bergles, A.E. and Rohsenow, W.M.
Tran. ASME J. Heat Transfer, Aug 1964, PP 365-372

149- Moore, F.D. and Mesler, R.B.
AIChE Journal, vol 7 , Dec 1961, PP 620-624 .

150- Butterworth, D. and Shock, R.A.W.
Proc. 7th Int. Heat Trans. Conf. , Munchen, Germany, vol 1, 1982, PP 11 - 30 .

151- Hewitt, G.F.
Proc. 6th Int. Heat Transfer conf. Toronto, Canada, vol. 6, Hemisphere Pub. Corp,, Washington, 1978, PP 143 - 171 .

152- Nukiyama, S.
J. Japan Soc.Mevh. Eng. , 37, 367, 1934; English Trans. : Int.J.Heat Mass Trans.,vol 9, 1966, PP 1419 - 1433 .

153- Blander, M. and Katz, J.
AIChE Journal, Vol 21, No 5, Sep 1975, PP 833-848 .

154- Arpaci, V.S. and Larsen, P.S.
Convective Heat Transfer, Prentic - Hall, Englewood Cliffs, 1984 .

155- Burmeister, L.C.
Convective Heat Transfer, Wiley-Interscience, New York, 1983 .

156- Nunner, W.
VDI-Forschungsheft 445, Ser.B , vol 22 , 1956 , PP 5 - 39 : English Transl. , Atomic Energy Research Establishment, Harwell,U.K.

157- Nikuradse, j.
Forsch.Arb.Ing.Wes., No 361, 1933, English Transl., NACA TM 1292 .

158- Savage, D.W. and Myers, J.E.
AIChE Journal, vol 9, No 5, Sep 1963, PP 694-703 .

159- Webb,R.L. and Eckert, E.R.C.
Int.J.Heat Mass Transfer, vol 15, 1972, PP 1647 - 1658 .

160- Poiseuille, J.
C.R.Acad.Sci. 11 ,PP 961-967,PP 1041-1048, 1840 ; 12, PP 112-115, 1841 , (in German).

161- Blasius, H.
Forschg.Arb.Ing. - Wes., No 131, Berlin, 1913, (in German) .

162- van Kàrmàn, T.
Nachr.Ges.Wiss.Gottingen, Math.Phys.Klasse, No 5, 1930, PP 58-76 , English Trans. NACA TM 611, 1931 .

163- Drew, T.B. ; Koo, E.C. and McAdams, W.H.
Trans. AIChE, vol 28, 1932, PP 56-72 .

164- Colebrook, C.F.
J.Inst.Civ.Eng., vol 11, 1939, PP 133-156 .

165- Techo, R ; Tickner, R.R. and James, R.E.
J.Appl.Wech., vol 32, 1965, PP 443-446 .

166- Nikuradse, j.
Forsch.Arb.Ing.Wes., No 356, 1932, English Transl., NACA TT F-10,359, 1966.

167- van Kàrmàn, T.
J.Aerosp.Sci., vol 7 , 1934, PP 1-20 .

168- Prandtl, L.
Fuhrrer durch die Stomungslehr, vieweg, Braunschweig, 1944, P 359 ; English Transl., Blackie, London, 1952 .

169- Swamee, P.K. , and Jain, A.K.
J. Hydroulic Div. ASCE, vol 102, 1976, PP 57 - 664 .

170- Round, G.H.
Can.J.Chem.Eng., vol 58, 1980, PP 122 -123.

171- Haaland, S.H.
J.Fluids Eng., vol 105, 1983, PP 89 - 90 .

172- Bhatt, M.S. and Shah, R.K.
In Handbook of Single - Phase Convective Heat Transfer, Kakaç *et al* ,Eds, John Wiley & Sons, New York, 1987, Chp. 4 .

173- Churchill, S.W.
Chem.Eng., 1977, PP 91-92 .

174- Nusselt, W.
Z.VDI, vol.53 , 1909, PP 1750-1755 and 1809 1812 .

175- Nusselt, W.
Z.VDI, vol.54 , 1910, PP 1154 - 1158 .

176- Lévêque, M.A.
Annls. Mines Carbur., Paris, vol 13, No 201, 1928 .

177- Coulson,J.M. ;Richardson, J.F. and Sinnott,R.K.
Chemical Engineering, vol 6, 1st , Pergamon Press , Oxford, 1983 .

178- Reynolds, O.
Proc. Manchester Lit.Philos. Soc., vol 14 , 1874, PP 7-12 .

179- Prandtl, L.
Z. Physik, vol 11 , 1910 , PP 1072 - 1078 .

180- Taylor, G.I.
British Advisory Committee for Aeronautics, voi 2 , R & M No 272, 1916, PP 423 - 429 .

181- Colburn, A.P.
Tran. AIChE, vol19, 1933, PP 174-210 ; reprinted in Int.J. Heat Mass Transfer , vol 7, 1964, PP 1359-1384 .

182- van Kàrmàn, T.
Trans. ASME, vol 61, 1939 , PP 705 - 710 .

183- Drexel, R.E. and McAdams, W.H.
NACA ARR No 4F28; also Wartime Report W -108 , 1945 .

184- Martinelli, R.C.
Trans. ASME, vol 69, 1947, PP 947-959 .

185- Friend, W.L. and Metzner, A.B.
AIChE Journal, vol 4 , 1958, PP 393-402.

186- Petukhov, B.S.; Kirillov, V.V. and Popov, V.N.
Teploenergetika, vol 4, No 4,1958,PP 63-68, (in Russion) ; see also Petukhov, B.S., In Advances in Heat Transfer, Hartnett, J.P and Irvine, T.F., Eds, vol 6, Acdemic Press, New York, 1970, PP 503 - 565 .

187- Dipprey, D.F. and Sabersky, R.H.
Int.J.Heat Mass Transfer,vol 6, 1963,
PP 329-353 .

188- Gowen, R.A. and Smith, J.W.
Int.J.Heat Mass Transfer,vol 11, 1968,
PP 1657 - 1673 .

189- Butterworth, D.
Introduction to Heat Transfer, Engineering
Design Guide No 18, Oxford U.P.

190- Engineering Sciences Data Unit (ESDU)
Forced Convection Heat Transfer in Circular
Tube. Pare I : Corrections for fully
developed turbulent flow - their scope and
limitations . Item No 67016, 1967 .

191- Sandall, O.C. ; Hanna, O.T. and Mazet, P.R.
Can.J.Chem.Eng., vol 58 , 1980, PP 443-447.

192- Kawase, Y. and De, A.
Int.J.Heat Mass Transfer, vol 27, 1984,
PP 140-142 .

193- Kern, D.Q.
Process Heat Transfer, McGraw - Hill,
New York, Intr. Edition , 1965 .

194- Bergles, A.E.
Proc. 6th Int. Heat Transfer conf. Toronto,
Canada, vol. 6, Hemisphere Pub. Corp,
Washington, 1978, PP 89-108 .

195- Bergles, A.E.
Heat Exchanger Design Handbook, vol 2,
Hemisphere Pub. Corp, Washington, 1983,
Section 2.5.11 .

196- Bergles, A.E.
Trans.ASME,J.Heat Trans.,vol 110, Nov 1988,
PP 1082 - 1096 .

197- Webb,R.L.
Heat Tran.Eng, vol 1, No 3, 1980, PP 33-49 .

198- Webb,R.L.
Heat Tran.Eng, vol 2, Nos 3-4, 1981, PP 46-69 .

199- Webb,R.L.
Heat Tran.Eng, vol 4, Nos 3-4, 1983, PP 71-82 .

200- Webb,R.L.
In Handbook of Single - Phase Convective Heat Transfer, Kakaç *et al* ,Eds, John Wiley & Sons, New York, 1987, Chp. 17 .

201- Joule, J.P.
Philosophical Transactions of the Royal Socity of London,vol 151, 1861, PP 133-160.

202- Bergles, A.E. and Joshi, S.D.
In Heat Exchanger Sourcebook, Palen, J.W., Ed.; Hemisphere Pub. Corp, Washington, 1986, PP 619-644 .

203- Smith, J.W. and Gowen, R.A.
AIChE Jounal, vol 11 , 1965, PP 941-943 .

204- White, A.
Nature, vol 227, 1970, PP 487-490 .

205- Thomas, D.G.
Ind. & E.C. Process desing and development, Vol 6, No 3, July 1967, PP 385-390 .

206- Gluck, D.F.
Ms Thesis , University of Delaware, USA, 1959.

207- Blumenkrantz, A.R. and Taborek, J.
Heat Transfer Research Inc. Report 2439-300-8, 1971 .

208- Rozqlowski, G.R. and Gater, R.A.
ASME , Paper No 75-HT-40 , 1975 .

209- Watkinson,A.P.; Milett, D.L., and Tarassoff,P.
AIChE Symp. Series, vol 69, No 131, PP 94-103 .

210- Scott, M.J. and Webb, R.L.
Trans. ASME, Journal of Heat Trans., vol 103, Aug 1981, PP 422-428 .

211- Trupp, A.C and Soliman, H.M.
In Heat Exchangers Theory and Practice; Taborek, J ; Hewitt, G.F and Afgan, N. ; Eds, Hemisphere, Washington, 1983, pp 899-916 .

212- DeLorenzo, B. and Anderson, E.D.
ASME, PaPer No 44-A-64, 1944 .

213- Koch, R.
Verein Deutscher Ingenieure-Forschungsheft, Series B, vol 24 , No 469, 1958, PP 1-44 .

214- Grace, C.D.
Chemical and Process Engineering,July 1971, PP 57-59 .

215- Van Der Meer, TH.H. and Hoogendoorn, C.J.
Chem.Eng.Sci.,vol 33, 1978, PP 1277-1282; see also, In Heat Exchangers Theory and Practice; Taborek, J ; Hewitt, G.F and Afgan, N. ; Eds,Hemisphere, Washington, 1983, pp 953 - 964 .

216- Kumar, P. and Judd,R.L.
The Canadian Journal of Chem. Eng., vol 48, Aug 1970, PP 378-383 .

217- Uttarwar, S.B. and Raja Rao, M.
Trans. ASME, Jour. of Heat Trans., vol 107, Nov 1985. PP 930-935 .

218- Gough, M.J. and Rogers, J.V.
U.K Patent No 2097910, European Patent No 0061154 and USA Patent No 4481154, 1982.

219- Siegel, R. and Perlmutter, M.
J.Appl.Mech. , vol 25, 1958, PP 295-297 .

220- Abdel-Salam, M.S. ; Hilal,M.M. and Khalil,E.E.
In Heat Exchagers Theory and Practice; Taborek, J ; Hewitt, G.F and Afgan, N. ; Eds, Hemisphere, Washington, 1983, pp 933-944 .

221- Klepper, O.H.
AIChE Symp. Ser., vol 69, No 131, PP 87-93.

222- Date, A.W.
Int.J.Heat Mass Transfer, vol 17, 1974, PP 845-859 .

223- Hong,S.W. and Bergles, A.E.
J.Heat Transfer, vol 98, 1976 , PP 251-256.

225- Watkinson , A.P.
Heat Transfer Eng. , vol 11 , No 3, 1990, PP 632-640 .

226- Kim, N.H. and Webb, R.L.
Int. J. Heat Mass Trnsfer, vol 34, No 11, 1991, PP 2727-2738 .

227- Someah, K.
Chem.Eng.Prog. , July 1992 , PP 39-45 .

228- IUPAC
Solubility Data Series, Pergamon Press, Oxford, vol 1 Helium and Neon , 1979 ; vol 7 Oxygen , 1981 ; vol 10 Nitrogen and Air , 1982 .

229- Nijsing, R
Eur 543. e , European Atomic Energy Community, EURATOM,1964.

230- Perera, W.G. and Rafique, K.
The Chem.Eng. , Feb. 1976.

231- Watkins, R.W ; Robertson, C.R. and Acrivos, A.
Int. J. Heat Mass Trnsfer, vol 19, 1976, PP 693 - 695 .

232- Van Rooyen, R.S and Keöger, D.A.
Proc. 6th Int. Heat Transfer conf. Toronto, Canada, vol. 2, Hemisphere Pub. Corp, Washington, 1978, PP 577-581 .

233- Hagge, J.K. and Junkhan, G.H.
J. Heat Trnsfer, vol 97, 1975, PP 516-520.

234- McElhiney, J.E. and Preckshot, G.W.
Int. J. Heat Mass Trnsfer, vol 20, 1977, PP 847 - 854 .

235- Mori, J. and Nakayama, W.
Int. J. Heat Mass Trnsfer, vol 20, 1977, PP 847 - 854 .

236- Mori, J. ; Fukada,T. and Nakayama, W.
Int. J. Heat Mass Trnsfer, vol 14, 1971, PP 1807 - 1824 .

237- Hiyazaki, H.
Int. J. Heat Mass Trnsfer, vol 14, 1971, PP 1295 - 1309 .

238- Bergles, A.E.
Progress in Heat and Mass Transfer, vol 1, Pergamon press, New York, 1969, PP 331 - 424 .

239- Moissis, R. and Maroti, L.A.
Dynatech Corporation report No 322, July,1962.

240- Newton, D.C. and Allen, P.H.G.
Letters in Heat and Mass Transfer, vol 4,
No 1 , PP 9 - 16 .
241- Mizushina, T. ; Ueda, H. and Matsumoto, T.
J. Chem. Eng. of Japan, vol 9, 1976,
PP 97-102.
242- Kinney, R.B.
Int. J. Heat Mass Trnsfer, vol 11, 1968,
PP 1393 - 1401 .

Appendix A
Examples of data recorded sheets

Date 20-3-90	Test cell no. 1	Condition tested WITHOUT INSERT	
Comments RUN Nº 1		Fluid SANTOTHERM 55	Data recorded by

Time (h)	Power (w)	Flow (%)	Flow (kg h^{-1})	ΔP (b)	T tank (°C)	T(1) inlet (°C)	T(2) outlet (°C)	T(3) wall (°C)	T(4) wall (°C)
	800	10		0·007	84·0	78·3	86·8	299·3	304·1
		20		0·005	84·0	80·2	83·2	294·2	298·3
		30		0·0080	85·0	82·3	84·1	216·5	218·5
		40		0·012	85·0	83·3	84·6	198·1	205·2
		50		0·0190	86·0	84·7	85·7	188·5	198·5
		60		0·028	89·0	87·5	88·4	180·8	189·7
		70		0·034	89·0	87·6	88·2	176·6	184·3
		80		0·041	93·0	90·4	90·9	172·7	180·9
		90		0·042	90·0	89·5	90·0	173·1	181·0
		100		0·065	87·0	85·3	87·9	161·0	164·7

Date	Test cell no. 2	Condition tested WITHOUT INSERT	
Comments RUN Nº1		Fluid SANTOTHEME 55	Data recorded by

Time (h)	Power (w)	Flow (%)	Flow (kg h^{-1})	ΔP (b)	T tank (°C)	T(5) inlet (°C)	T(6) outlet (°C)	T(7) wall (°C)	T(8) wall (°C)
	800*	10		0·005	78·0	74·6	80·0	277·3	280·8
	〃	20		0·007	79·0	75·3	78·1	270·2	274·1
	〃	30		0·008	79·0	77·5	79·6	196·6	202·4
	〃	40		0·013	80·0	78·2	79·8	179·2	185·2
	〃	50		0·019	80·0	78·7	80·0	166·0	172·4
	〃	60		0·026	81·0	78·9	80·1	156·6	163·2
	〃	70		0·035	81·0	78·9	79·8	149·5	156·3
	〃	80		0·044	80·0	78·7	79·6	145·9	152·8
	〃	90		0·058	80·0	78·2	79·0	142·1	149·1
	〃	94		0·060	78·0	77·6	78·4	139·9	147·2
	804	100		0·070	83·0	77·6	79·8**	137·3	143·8

* Add 40 W

* Now Thermocouple No (6) Defect (1.80)

Date 11-6-90	Test cell no. 1	Condition tested WITH INSERT (LDI-A)
Comments RUN (1)	Fluid	Data recorded by

Time (h)	Power (w)	Flow (%)	Flow (kg h^{-1})	ΔP (b)	T tank (°C)	T(1) inlet (°C)	T(2) outlet (°C)	T(3) wall (°C)	T(4) wall (°C)
4:35	429	10		0.0225	100	92.2	96.8	145.9	147.2
4:55	424	20		0.0475	100	93.3	97.0	137.4	138.8
5:05	418	30		0.0950	100	94.0	97.3	134.2	135.7
5:20	426	40		0.1450	100	94.7	98.1	133.1	134.6
5:38	418	50		0.2220	100	96.2	99.1	131.4	132.8
11:07	420	60		0.32	102	98.8	101.7	133.5	135.1
11:25	421	70		0.41	102	97.8	100.6	131.5	133.1
11:38	420	80		0.52	101	97.4	100.2	130.1	131.6
11:50	421	90		0.63	101	98.2	101.2	131.2	132.8
12:10	423	100		OVER SCALE	103	99.7	102.5	132.1	133.7

Appendix B
Examples of heat transfer and friction factor results for Santotherm 55 study

Bare tube test section No(1)

Run NO = (1)
Avr. T(in) = 85 °C
q(based on Ao) = 48160 W/m²
At(surface) = 0.01970 m²
Ai(surface) = 0.01268 m²
Efficiency = 0.98 -
Rw(1) = 0.00119 (W/m².K)

Q(supp) W	% F.S.R	ΔP bar	Tb °C	Tw °C	Ai kg/hr	Ti °C	v m/sec	hi (Exp.) W/m².°C	Re	Pr	Nu (Exp.)	jH (Exp.)	f (Exp.)
821.5	10	0.004	85.9	301.7	256.76	253.1	0.487	379.80	1060.6	94.11	42.993	7.027	0.039672
821.5	20	0.006	82.9	296.3	442.21	247.6	0.838	385.55	1788.1	95.93	43.617	7.098	0.020076
821.5	30	0.008	84.0	217.5	684.84	168.9	1.299	747.93	2874.9	92.75	84.705	15.394	0.011148
821.5	40	0.012	84.5	201.7	896.52	153.0	1.702	927.13	3833.9	91.22	105.058	19.756	0.009752
821.5	50	0.020	85.7	193.5	1105.26	144.9	2.101	1072.55	4873.0	88.75	121.646	23.526	0.010683
821.5	60	0.028	88.4	185.3	1337.75	136.6	2.548	1316.30	6298.9	83.67	149.588	30.248	0.010187
821.5	70	0.034	88.2	180.5	1541.39	131.8	2.936	1456.23	7249.3	83.76	165.485	33.775	0.009318
821.5	80	0.041	90.9	176.8	1764.04	128.2	3.367	1705.54	8854.2	79.03	194.211	41.088	0.00856
821.5	90	0.055	90.0	177.1	1973.22	128.4	3.764	1653.93	9690.0	80.58	188.204	39.421	0.009184
798.7	100	0.065	85.6	162.9	2198.82	115.6	4.180	2062.39	9741.6	88.37	233.945	48.255	0.008771

Run NO = (2)
Avr. T(in) = 118 °C
q(based on Ao) = 48160 W/m²
At(surface) = 0.01970 m²
Ai(surface) = 0.01268 m²
Efficiency = 0.98 -
Rw(1) = 0.00119 (W/m².K)

Q(supp) W	% F.S.R	ΔP bar	Tb °C	Tw °C	Ai kg/hr	Ti °C	v m/sec	hi (Exp.) W/m².°C	Re	Pr	Nu (Exp.)	jH (Exp.)	f (Exp.)
821.5	10	0.004	114.1	320.6	255.42	272.0	0.496	402.26	1976.1	53.95	46.511	9.803	0.0392
821.5	20	0.006	116.8	251.5	434.43	202.8	0.846	738.22	3620.8	50.57	85.613	19.934	0.0202
821.5	30	0.009	120.0	226.4	670.25	177.8	1.309	1099.21	5950.1	47.89	127.814	31.600	0.0127
821.5	40	0.011	121.1	218.2	879.66	169.5	1.720	1313.01	7994.7	46.93	152.826	38.634	0.0090
821.5	50	0.018	119.9	209.8	1093.55	161.2	2.136	1538.32	9742.0	47.74	178.898	45.447	0.0096
821.5	60	0.021	119.1	203.3	1327.92	154.7	2.593	1785.87	11685.6	48.25	207.580	53.040	0.0076
821.5	70	0.029	120.2	198.8	1537.54	150.2	3.005	2120.45	13805.1	47.42	246.680	64.072	0.0078
821.5	80	0.038	121.8	197.0	1751.26	148.3	3.427	2398.59	16192.6	46.24	279.389	73.715	0.0079
821.5	90	0.045	124.0	196.7	1954.87	148.1	3.832	2643.14	18763.5	44.77	308.378	82.688	0.0074
821.5	100	0.055	125.8	196.1	2191.80	147.5	4.303	2938.00	21697.5	43.60	343.253	93.340	0.0072

Run NO = (3)
Avr. T(in) = 143 °C
q(based on Ao) = 48160 W/m²
At(surface) = 0.01970 m²
Ai(surface) = 0.01268 m²
Efficiency = 0.98 -
Rw(1) = 0.00119 (W/m².K)

Q(supp) W	% F.S.R	ΔP bar	Tb °C	Tw °C	Ai kg/hr	Ti °C	v m/sec	hi (Exp.) W/m².°C	Re	Pr	Nu (Exp.)	jH (Exp.)	f (Exp.)
821.5	10	0.004	141.1	308.7	254.16	260.0	0.505	534.11	3106.8	36.46	63.053	16.248	0.0387
821.5	20	0.006	142.1	256.7	428.56	208.0	0.852	964.29	5411.2	35.48	113.989	31.369	0.0204
821.5	30	0.008	143.7	238.1	660.54	189.4	1.316	1390.62	8573.1	34.67	164.623	46.902	0.0114
821.5	40	0.010	144.4	229.9	868.88	181.2	1.732	1724.69	11407.2	34.34	204.293	59.143	0.0082
821.5	50	0.015	144.7	223.8	1085.01	175.1	2.164	2089.07	14326.3	34.17	247.529	72.466	0.0079
821.5	60	0.021	144.8	220.7	1319.67	172.0	2.632	2335.81	17462.0	34.11	276.797	81.484	0.0075
821.5	70	0.027	145.3	217.9	1534.51	169.3	3.062	2652.89	20449.4	33.91	314.490	93.242	0.0071
821.5	80	0.032	145.7	216.2	1741.38	167.5	3.475	2914.63	23338.1	33.75	345.623	102.991	0.0066
821.5	90	0.040	145.9	213.5	1943.05	164.8	3.879	3364.13	26133.0	33.65	399.000	119.579	0.0066
821.5	100	0.050	146.2	211.9	2188.23	163.2	4.370	3743.13	29576.1	33.51	444.070	133.699	0.0065

Avr.T(in) = 77 °C
q(based on Ao) = 36120 W/m²
At(surface) = 0.0197 m²
Ai(surface) = 0.01268 m²
Efficiency = 0.98
Rw(2) = 0.00068 (W/m².K)⁻¹

Q(supp) W	% F.S.R	ΔP bar	Tb °C	Tw °C	M2 kg/hr	Ti °C	v m/sec	hi (Exp.) W/m².°C	Re	Pr	Nu (Exp.)	jH (Exp.)	f (Exp.)
634.9	10	0.004	73.9	232.9	262.23	211.6	0.493	356.54	817.0	121.50	40.053	6.034	0.0384
634.9	20	0.006	72.8	226.4	480.85	205.0	0.904	371.35	1500.2	121.34	41.717	6.337	0.0171
634.9	30	0.008	72.9	183.2	693.91	161.8	1.306	551.80	2192.4	119.96	62.010	10.064	0.0110
634.9	40	0.010	78.3	157.2	900.39	135.8	1.701	853.02	3297.4	104.91	96.235	17.469	0.0081
634.9	50	0.020	74.3	147.1	1109.93	125.8	2.091	953.45	3655.6	115.51	107.261	18.984	0.0107
634.9	60	0.028	74.8	141.1	1338.12	119.8	2.522	1091.79	4480.1	113.80	122.877	22.205	0.0103
634.9	70	0.038	76.0	135.2	1552.33	113.8	2.928	1298.66	5376.3	110.35	146.290	27.215	0.0104
634.9	80	0.048	77.8	132.1	1771.24	110.8	3.346	1490.35	6444.1	105.54	168.107	32.200	0.0100
634.9	90	0.060	79.0	129.1	1989.21	107.8	3.761	1702.95	7458.3	102.70	192.246	37.600	0.0099
599.2	100	0.070	80.4	126.7	2214.21	106.6	4.191	1766.54	8607.5	99.40	199.627	39.789	0.0094

Run NO (2)
Avr.T(in) = 103 °C
q(based on Ao) = 36120 W/m²
At(surface) = 0.0197 m²
Ai(surface) = 0.01268 m²
Efficiency = 0.98
Rw(2) = 0.00068 (W/m².K)⁻¹

Q(supp) W	% F.S.R	ΔP bar	Tb °C	Tw °C	M2 kg/hr	Ti °C	v m/sec	hi (Exp.) W/m².°C	Re	Pr	Nu (Exp.)	jH (Exp.)	f (Exp.)
634.9	10	0.004	102.9	261.7	257.55	240.3	0.496	357.16	1634.3	64.19	40.991	8.161	0.0388
634.9	20	0.006	102.8	200.2	470.79	178.8	0.907	645.35	3015.1	63.67	74.092	15.921	0.0174
634.9	30	0.008	103.0	179.0	679.50	157.7	1.309	897.52	4396.4	63.10	103.081	22.992	0.0112
634.9	40	0.014	103.4	168.7	891.68	147.4	1.719	1115.44	5822.3	62.59	128.152	29.224	0.0113
634.9	50	0.018	103.7	161.0	1102.64	139.6	2.126	1366.06	7258.5	62.14	156.991	36.456	0.0095
634.9	60	0.024	104.2	156.6	1329.77	135.3	2.565	1579.81	8851.3	61.54	181.628	42.746	0.0087
634.9	70	0.030	104.5	153.9	1544.24	132.6	2.980	1749.38	10351.4	61.16	201.175	47.753	0.0081
634.9	80	0.042	104.9	151.3	1756.28	130.0	3.390	1960.63	11891.0	60.63	225.551	54.062	0.0087
634.9	90	0.050	105.5	149.5	1976.82	128.1	3.818	2173.31	13545.0	59.99	250.128	60.498	0.0082
634.9	100	0.056	106.1	148.3	2204.49	126.9	4.260	2361.51	15285.4	59.37	271.909	66.273	0.0074

Run NO (3)
Avr.T(in) = 150 °C
q(based on Ao) = 36120 W/m²
At(surface) = 0.0197 m²
Ai(surface) = 0.01268 m²
Efficiency = 0.98
Rw(2) = 0.00068 (W/m².K)⁻¹

Q(supp) W	% F.S.R	ΔP bar	Tb °C	Tw °C	M2 kg/hr	Ti °C	v m/sec	hi (Exp.) W/m².°C	Re	Pr	Nu (Exp.)	jH (Exp.)	f (Exp.)
634.9	10	0.004	143.7	247.9	251.09	226.5	0.500	592.57	3219.2	35.03	70.104	19.019	0.0395
634.9	20	0.006	146.4	216.0	456.19	194.6	0.911	1016.85	6122.6	33.71	120.590	34.594	0.0179
634.9	30	0.008	148.7	203.8	657.60	182.5	1.315	1454.29	9152.6	32.71	172.806	51.147	0.0115
634.9	40	0.010	150.2	198.3	875.39	177.0	1.753	1831.17	12455.2	32.11	217.852	65.577	0.0081
634.9	50	0.016	151.8	195.0	1090.70	173.7	2.188	2244.36	15892.4	31.49	267.364	81.663	0.0083
634.9	60	0.022	152.5	192.2	1316.01	170.8	2.642	2680.95	19370.2	31.22	319.557	98.431	0.0078
634.9	70	0.028	153.3	190.0	1530.34	168.6	3.074	3208.76	22782.7	30.93	382.716	118.835	0.0074
634.9	80	0.034	154.7	189.3	1728.79	168.0	3.477	3708.57	26237.5	30.44	442.818	138.716	0.0070
634.9	90	0.042	155.3	188.6	1953.61	167.2	3.931	4099.32	29865.2	30.26	489.681	154.029	0.0068
634.9	100	0.050	156.0	188.3	2185.67	166.9	4.400	4472.87	33721.3	30.04	534.587	168.862	0.0064

Test section No(1) fitted with low density insert (LDI-H)

Run NO = (1)
Avr. T(in) = 84 °C
q(based on Ao) = 24000 W/m²
At(surface) = 0.01970 m²
Ai(surface) = 0.01268 m²
Efficiency = 0.98
Rw(1) = 0.00119 (W/m².K)⁻¹

Q(supp) W	% F.S.R	ΔP bar	Tb °C	Tw °C	Mi kg/hr	Ti °C	v m/sec	hi (Exp.) W/m².°C	Re	Pr	Nu (Exp.)	jH (Exp.)	f (Exp.)
398.3	10	0.0190	85.1	140.3	256.69	116.7	0.4875	976.533	1105.80	90.62	110.68	22.4936	0.188305
397.3	20	0.0475	84.1	130.6	441.79	107.1	0.8385	1334.14	1870.73	92.03	151.13	31.2269	0.159008
399.3	30	0.0900	83.6	126.3	684.84	102.6	1.2995	1623.04	2874.91	92.75	183.82	38.2920	0.125412
400.3	40	0.1550	83.1	123.6	897.05	99.9	1.7016	1843.48	3728.53	93.58	208.72	43.6192	0.125924
398.3	50	0.2300	83.6	121.2	1105.90	97.6	2.0987	2208.59	4659.76	92.44	250.16	52.9413	0.122891
401.3	60	0.3200	84.4	122.0	1338.95	98.2	2.5427	2247.38	5761.10	90.72	254.71	54.2924	0.116561
399.3	70	0.4100	85.3	121.7	1541.74	98.1	2.9297	2409.83	6772.71	89.04	273.29	58.8114	0.112564
401.3	80	0.5200	85.5	120.8	1766.29	97.0	3.3570	2687.85	7796.93	88.65	304.86	65.9474	0.108754
400.3	90	0.6500	87.7	122.0	1974.44	98.3	3.7593	2922.52	9198.54	84.47	332.02	73.2573	0.108597
399.3	100	-	88.4	122.2	2198.33	98.6	4.1879	3027.13	10412.18	83.23	344.07	76.3962	

Run NO = (2)
Avr. T(in) = 102 °C
q(based on Ao) = 24000 W/m²
At(surface) = 0.01970 m²
Ai(surface) = 0.01268 m²
Efficiency = 0.98
Rw(1) = 0.00119 (W/m².K)⁻¹

Q(supp) W	% F.S.R	ΔP bar	Tb °C	Tw °C	Mi kg/hr	Ti °C	v m/sec	hi (Exp.) W/m².°C	Re	Pr	Nu (Exp.)	jH (Exp.)	f (Exp.)
400.0	10	0.018	99.0	151.1	256.05	127.4	0.4916	1087.62	1508.41	68.54	124.50	28.2695	0.177329
401.0	20	0.042	101.2	145.3	437.87	121.5	0.8425	1528.59	2730.12	65.19	175.33	41.3320	0.141185
400.0	30	0.085	103.8	145.2	676.67	121.5	1.3048	1747.83	4458.91	62.09	200.87	48.4927	0.119385
400.0	40	0.143	101.8	139.6	888.44	115.9	1.7106	2199.95	5637.55	64.19	252.49	60.7715	0.116686
400.0	50	0.215	101.3	137.8	1099.84	114.1	2.1169	2426.43	6914.52	64.71	278.39	67.0326	0.114518
401.0	60	0.301	103.2	138.6	1332.94	114.8	2.5695	2678.67	8721.33	62.48	307.77	75.2478	0.108982
403.0	70	0.390	104.0	138.9	1539.48	115.0	2.9695	2821.28	10226.56	61.65	324.33	79.7781	0.105794
402.0	80	0.480	105.2	139.0	1758.13	115.2	3.3945	3107.22	11963.07	60.36	357.52	88.8141	0.099739
400.0	90	0.640	106.1	139.3	1964.51	115.6	3.7959	3235.18	13621.42	59.37	372.50	93.1772	0.106431
402.0	100	-	106.2	139.4	2195.22	115.6	4.2420	3292.15	15251.21	59.27	379.09	94.9088	

Run NO = (3)
Avr. T(in) = 150 °C
q(based on Ao) = 24000 W/m²
At(surface) = 0.01970 m²
Ai(surface) = 0.01268 m²
Efficiency = 0.98
Rw(1) = 0.00119 (W/m².K)⁻¹

Q(supp) W	% F.S.R	ΔP bar	Tb °C	Tw °C	Mi kg/hr	Ti °C	v m/sec	hi (Exp.) W/m².°C	Re	Pr	Nu (Exp.)	jH (Exp.)	f (Exp.)
400.0	10	0.015	148.7	190.5	253.76	166.8	0.5074	1709.33	3507.48	32.90	203.03	61.3411	0.144468
400.0	20	0.042	150.2	186.2	426.68	162.5	0.8545	2507.1	6050.19	32.20	298.21	91.6633	0.142856
408.0	30	0.080	150.5	184.8	657.79	160.6	1.3178	3095.34	9391.14	32.02	368.32	113.8790	0.114447
410.0	40	0.135	151.0	183.7	865.88	159.4	1.7355	3763.88	12446.72	31.84	448.04	139.2058	0.111408
410.0	50	0.200	151.6	183.4	1082.68	159.1	2.1712	4227.53	15711.68	31.59	503.50	157.1226	0.105506
403.0	60	0.280	152.3	182.4	1317.31	158.5	2.6434	5025.07	19311.12	31.33	598.83	187.8267	0.099714
410.0	70	0.370	152.4	184.4	1533.65	160.1	3.0780	4103.45	22528.10	31.28	489.06	153.1037	0.0972
402.0	80	0.480	154.2	183.6	1737.86	159.8	3.4932	5614.16	26166.43	30.64	670.05	212.0147	0.098052
401.0	90	0.590	149.8	179.5	1941.11	155.8	3.8866	5230.71	27448.56	32.28	622.08	193.1696	0.096982
402.0	100	-	150.0	178.8	2187.63	155.0	4.3809	6320.28	31019.57	32.20	751.78	234.0298	

Avr. T(in) = 85 °C
q(based on Ao) = 24000 W/m2
At(surface) = 0.0197 m2
Ai(surface) = 0.01268 m2
Efficiency = 0.98
Rw(1) = 0.00119 (W/m2.K)-1

Q(supp) W	% F.S.R	ΔP bar	Tb °C	Tw °C	Ai kg/hr	Ti °C	v m/sec	hi (Exp.) W/m2.°C	Re	Pr	Nu (Exp.)	jH (Exp.)	f (Exp.)
424.2	10	0.0480	76.3	127.7	257.10	102.6	0.4848	1248.53	880.87	111.44	140.60	26.8042	0.477544
424.2	20	0.1210	78.1	122.2	443.15	97.1	0.8372	1731.68	1612.28	105.54	195.33	38.8259	0.404460
424.2	30	0.2390	79.8	119.6	686.40	94.5	1.2985	2230.48	2613.94	101.27	251.91	51.4738	0.332538
424.2	40	0.3750	81.0	118.1	898.02	92.9	1.7006	2751.72	3540.34	98.15	311.08	64.8337	0.304505
424.2	50	0.5750	83.1	118.2	1106.07	93.0	2.0982	3310.53	4603.02	93.48	374.83	79.9620	0.307255
424.2	60	-	88.5	123.9	1337.65	98.7	2.5484	3189.26	6343.11	83.14	362.52	80.4918	
424.2	70	-	93.2	128.3	1540.78	103.1	2.9465	3314.44	8147.01	75.44	378.05	86.9179	
424.2	80	-	94.3	129.3	1762.65	104.1	3.3736	3318.35	9540.56	73.89	378.78	87.7317	
424.2	90	-	93.1	126.3	1971.52	101.1	3.7699	4063.22	10401.30	75.59	463.42	107.0307	
424.2	100	-	96.2	126.6	2196.97	101.4	4.2114	6221.65	12410.84	71.14	711.20	169.0303	

Run NO (2)
Avr. T(in) = 96 °C
q(based on Ao) = 24000 W/m2
At(surface) = 0.0197 m2
Ai(surface) = 0.01268 m2
Efficiency = 0.98
Rw(1) = 0.00119 (W/m2.K)-1

Q(supp) W	% F.S.R	ΔP bar	Tb °C	Tw °C	Ai kg/hr	Ti °C	v m/sec	hi (Exp.) W/m2.°C	Re	Pr	Nu (Exp.)	jH (Exp.)	f (Exp.)
424.2	10	0.0380	95.4	140.7	256.21	115.6	0.4906	1628.08	1402.17	73.17	185.91	42.0186	0.374922
424.2	20	0.1180	94.9	133.9	439.31	108.7	0.8410	2363.36	2393.66	73.46	269.83	61.9202	0.396054
424.2	30	0.2100	95.0	132.2	680.20	107.0	1.3025	2726.17	3730.75	73.02	311.32	71.9628	0.293945
424.2	40	0.3610	94.1	128.8	891.98	103.7	1.7069	3427.60	4801.29	74.25	391.18	90.4971	0.294040
424.2	50	0.5410	95.0	128.4	1101.98	103.3	2.1104	3977.78	6064.08	72.81	454.30	106.2209	0.288482
424.2	60	-	96.7	129.5	1335.02	104.4	2.5602	4290.00	7623.72	70.46	490.57	116.1984	
400.3	70	-	102.4	134.1	1539.67	110.4	2.9660	3847.60	9901.09	63.44	441.80	108.4030	
398.3	80	-	103.1	134.4	1758.98	110.8	3.3906	3973.76	11485.57	62.59	456.54	112.6348	
424.2	90	-	98.5	130.9	1968.61	105.8	3.7806	4479.47	11683.70	68.09	512.91	123.0593	
424.2	100	-	98.6	131.3	2196.55	106.1	4.2187	4331.56	13064.23	67.96	496.01	119.0026	

Run NO (3)
Avr. T(in) = 143 °C
q(based on Ao) = 24000 W/m2
At(surface) = 0.0197 m2
Ai(surface) = 0.01268 m2
Efficiency = 0.98
Rw(1) = 0.00119 (W/m2.K)-1

Q(supp) W	% F.S.R	ΔP bar	Tb °C	Tw °C	Ai kg/hr	Ti °C	v m/sec	hi (Exp.) W/m2.°C	Re	Pr	Nu (Exp.)	jH (Exp.)	f (Exp.)
424.2	10	0.0340	141.4	183.1	254.09	158.0	0.5051	1982.38	3175.52	35.78	234.22	68.8762	0.328546
424.2	20	0.0850	144.5	179.4	427.95	154.3	0.8531	3363.71	5618.34	34.34	398.44	120.3260	0.288735
424.2	30	0.1940	146.4	181.2	659.39	156.1	1.3167	3383.97	8912.26	33.51	401.46	122.3126	0.277100
424.2	40	0.3350	144.5	178.0	868.74	152.9	1.7322	3924.62	11454.33	34.21	464.99	141.0138	0.276066
424.2	50	0.5200	141.6	174.1	1086.04	149.0	2.1603	4458.15	13732.80	35.43	527.04	158.2052	0.274859
424.2	60	-	142.1	173.6	1320.50	148.5	2.6278	5107.35	16831.81	35.20	604.04	182.0815	
424.2	70	-	143.8	174.7	1534.67	149.6	3.0584	5633.79	20047.48	34.48	667.16	202.7415	
424.2	80	-	144.9	174.4	1741.67	149.3	3.4740	7417.87	23111.51	34.03	879.16	269.0391	
424.2	90	-	145.8	175.5	1943.08	150.3	3.8787	7174.45	26114.95	33.67	850.89	261.2581	
424.2	100	-	146.0	175.2	2188.26	150.0	4.3690	8078.79	29514.07	33.57	958.33	294.8293	

q(based on Ao) = 48160 W/m²
At(surface) = 0.0197 m²
Ai(surface) = 0.01268 m²
Efficiency = 0.98
Rw(2) = 0.00068 (W/m².K)⁻¹

Q(supp) W	% F.S.R	ΔP bar	Tb °C	Tw °C	M2 kg/hr	Ti °C	v m/sec	hi (Exp.) W/m².°C	Re	Pr	Nu (Exp.)	jH (Exp.)	f (Exp.)
833.3	10	0.0500	83.5	157.3	260.72	129.3	0.4940	1407.562	1047.61	96.48	159.21	30.509	0.481381
833.3	20	0.1150	82.2	142.6	477.78	114.6	0.9051	1989.718	1902.84	97.25	225.00	44.415	0.329789
833.3	30	0.2400	81.8	136.5	689.76	108.5	1.3066	2415.277	2743.59	97.37	273.11	54.714	0.330241
833.3	40	0.3700	81.5	133.0	899.31	105.0	1.7034	2744.139	3568.06	97.59	310.28	62.657	0.299521
833.3	50	0.5600	81.8	131.0	1109.42	103.0	2.1020	3032.862	4440.89	96.81	343.01	69.912	0.297798
833.3	60	-	82.1	130.2	1336.07	102.2	2.5322	3202.2	5402.42	95.93	362.27	74.325	
833.3	70	-	83.3	130.1	1550.42	102.1	2.9413	3425.528	6468.28	93.27	387.88	80.695	
833.3	80	-	84.3	128.5	1767.73	100.5	3.3563	3975.049	7559.49	91.22	450.43	95.143	
833.3	90	-	85.1	128.8	1986.36	100.8	3.7740	4120.824	8683.55	89.43	467.25	99.577	
833.3	100	-	86.5	129.1	2211.91	101.1	4.2072	4417.506	10002.38	86.76	501.40	108.331	

Run NO (2)
Avr. T(in) = 106 °C
q(based on Ao) = 48160 W/m²
At(surface) = 0.0197 m²
Ai(surface) = 0.01268 m²
Efficiency = 0.98
Rw(2) = 0.00068 (W/m².K)⁻¹

Q(supp) W	% F.S.R	ΔP bar	Tb °C	Tw °C	M2 kg/hr	Ti °C	v m/sec	hi (Exp.) W/m².°C	Re	Pr	Nu (Exp.)	jH (Exp.)	f (Exp.)
833.3	10	0.0360	107.3	171.2	256.92	143.2	0.50	1795.87	1765.67	59.84	206.71	48.556	0.350142
833.3	20	0.1000	105.6	161.8	469.95	133.8	0.91	2285.33	3166.01	60.89	262.86	62.375	0.290932
833.3	30	0.2000	104.9	154.7	678.70	126.7	1.31	2957.22	4540.37	61.27	340.05	81.670	0.279058
833.3	40	0.3450	103.6	151.0	891.64	123.0	1.72	3322.76	5833.94	62.48	381.77	91.564	0.279157
833.3	50	0.5300	105.2	149.3	1104.01	121.3	2.13	4000.55	7467.35	60.68	460.21	112.399	0.279358
833.3	60	-	107.0	149.0	1329.02	121.0	2.57	4604.29	9324.53	58.76	530.38	131.669	
833.3	70	-	110.0	148.9	1542.88	120.9	2.99	5927.37	11493.95	55.76	684.35	174.325	
833.3	80	-	108.3	150.4	1754.46	122.4	3.40	4570.54	12674.59	57.28	527.07	132.050	
833.3	90	-	111.1	152.5	1974.25	124.5	3.83	4827.40	15046.08	54.66	557.84	142.316	
833.3	100	-	113.9	151.8	2201.57	123.8	4.28	6518.06	17692.77	52.20	754.80	197.230	

Run NO (3)
Avr. T(in) = 151 °C
q(based on Ao) = 48160 W/m²
At(surface) = 0.0197 m²
Ai(surface) = 0.01268 m²
Efficiency = 0.98
Rw(2) = 0.00068 (W/m².K)⁻¹

Q(supp) W	% F.S.R	ΔP bar	Tb °C	Tw °C	M2 kg/hr	Ti °C	v m/sec	hi (Exp.) W/m².°C	Re	Pr	Nu (Exp.)	jH (Exp.)	f (Exp.)
802	10	0.0330	151.7	205.2	249.90	178.2	0.5006	2342.03	3562.89	32.06	278.66	83.801	0.327121
800	20	0.0960	152.9	197.7	454.05	170.8	0.9111	3460.40	6656.15	31.33	412.37	126.819	0.287766
800	30	0.2000	153.6	193.7	655.35	166.8	1.3161	4666.60	9723.83	31.02	556.49	173.043	0.287563
800	40	0.3300	153.4	191.7	874.28	164.8	1.7559	5433.17	12989.57	30.98	647.95	202.235	0.266580
802	50	0.5100	152.9	189.9	1092.95	163.0	2.1941	6143.15	16130.14	31.16	732.35	228.641	0.263732
803	60	-	152.7	188.9	1315.99	161.9	2.6417	6721.46	19395.77	31.19	801.23	250.430	
800	70	-	152.6	187.9	1530.81	161.0	3.0728	7384.65	22546.82	31.21	880.25	275.483	
800	80	-	152.8	187.2	1729.89	160.3	3.4731	8231.49	25564.70	31.12	981.38	307.882	
800	90	-	153.7	187.3	1954.35	160.4	3.9269	9297.70	29250.65	30.80	1109.30	349.784	
800	100	-	154.7	187.8	2186.15	160.9	4.3965	9991.08	33178.68	30.44	1192.98	377.959	

Test section No(2) fitted with high density insert (HDI-A)

Run NO (1)
Avr. T(in) = 86 °C
q(based on Ao) = 60200 W/m²
At(surface) = 0.0197 m²
Ai(surface) = 0.01268 m²
Efficiency = 0.98
Rw(2) = 0.00068 (W/m².K)⁻¹

Q(supp) W	% F.S.R	ΔP bar	Tb °C	Tw °C	M2 kg/hr	Ti °C	v m/sec	hi (Exp.) W/m².°C	Re	Pr	Nu (Exp.)	jH (Exp.)	f (Exp.)
1003.0	10	0.0670	91.8	167.9	259.42	134.2	0.4948	1832.45	1271.02	80.75	208.50	43.1065	0.647294
1001.0	20	0.1700	91.4	156.3	474.75	122.6	0.9058	2480.08	2352.98	79.92	282.29	60.1295	0.490231
1005.0	30	0.3400	91.1	151.2	685.35	117.4	1.3077	2953.93	3404.60	79.76	336.26	72.5618	0.470437
1002.0	40	0.5600	91.3	148.8	895.96	115.1	1.7101	3255.46	4486.77	79.19	370.67	80.7218	0.453248
1004.0	50	-	79.4	135.6	1109.99	101.9	2.0990	3458.48	4172.64	102.46	390.46	77.6702	
1010.0	60	-	82.1	136.3	1336.11	102.3	2.5320	3852.44	5382.20	96.26	435.78	89.2325	
1002.0	70	-	83.5	136.3	1550.40	102.6	2.9414	4050.33	6476.26	93.17	458.65	95.3414	
1000.0	80	-	93.3	145.0	1762.79	111.4	3.3708	4278.50	9300.09	75.59	487.97	109.6947	

Run NO (2)
Avr. T(in) = 114 °C
q(based on Ao) = 60200 W/m²
At(surface) = 0.0197 m²
Ai(surface) = 0.01268 m²
Efficiency = 0.98
Rw(2) = 0.00068 (W/m².K)⁻¹

Q(supp) W	% F.S.R	ΔP bar	Tb °C	Tw °C	M2 kg/hr	Ti °C	v m/sec	hi (Exp.) W/m².°C	Re	Pr	Nu (Exp.)	jH (Exp.)	f (Exp.)
1006.0	10	0.0600	114.0	185.9	255.86	152.1	0.4969	2041.91	2001.75	53.43	236.20	57.6828	0.585250
1006.0	20	0.1500	113.7	175.4	467.16	141.6	0.9077	2791.68	3695.85	52.91	323.08	80.8278	0.438671
997.0	30	0.3200	113.5	169.8	674.39	136.3	1.3107	3384.83	5365.03	52.66	391.81	99.2726	0.448948
1006.0	40	0.5200	113.9	168.7	887.95	134.9	1.7265	3699.50	7129.42	52.24	428.39	109.2754	0.420642
1009.0	50	-	115.6	168.9	1101.51	135.0	2.1449	4033.99	9147.53	50.73	467.76	121.0217	
1004.0	60	-	116.7	167.8	1326.13	134.0	2.5848	4471.55	11253.22	49.79	518.96	135.7559	
1020.0	70	-	121.2	171.7	1539.59	137.4	3.0120	4849.86	14150.17	46.48	564.77	151.7414	
1007.0	80	-	123.7	172.5	1745.74	138.6	3.4226	5216.92	16770.22	44.74	608.69	166.2147	

Run NO (3)
Avr. T(in) = 157 °C
q(based on Ao) = 60200 W/m²
At(surface) = 0.0197 m²
Ai(surface) = 0.01268 m²
Efficiency = 0.98
Rw(2) = 0.00068 (W/m².K)⁻¹

Q(supp) W	% F.S.R	ΔP bar	Tb °C	Tw °C	M2 kg/hr	Ti °C	v m/sec	hi (Exp.) W/m².°C	Re	Pr	Nu (Exp.)	jH (Exp.)	f (Exp.)
1004.0	10	0.0550	162.2	224.5	248.26	190.7	0.5017	2721.12	4056.22	28.66	326.33	101.9275	0.547638
1002.0	20	0.1400	164.6	218.6	450.21	184.9	0.9122	3812.13	7652.13	27.75	458.27	146.5745	0.422750
1006.0	30	0.3000	152.3	203.2	656.02	169.4	1.3159	4546.04	9552.28	31.50	541.54	166.4500	0.430967
1003.0	40	0.5000	155.4	203.6	873.63	169.9	1.7573	5347.51	13302.74	30.36	638.64	199.7249	0.403877
1005.0	50	-	156.1	203.6	1092.21	169.8	2.1985	5671.93	16817.84	30.08	677.82	212.9636	
1003.0	60	-	157.7	204.0	1314.58	170.3	2.6498	6163.59	20681.70	29.56	737.50	233.5905	
1005.0	70	-	160.4	206.3	1528.62	172.5	3.0884	6393.82	24912.17	28.72	766.66	245.4531	
1005.0	80	-	163.3	207.6	1724.13	173.8	3.4921	7406.55	29159.41	27.86	890.10	288.7146	

Table (B-7) Heat transfer and friction factor results for Santotherm 55 study

Comparison between LDI-A and LDI-B fitted inside test section No(2)

Run NO (1) With LDI-A
Avr. T(in) = 100 °C
q(based on Ao) = 48160 W/m²
At(surface) = 0.0197 m²
Ai(surface) = 0.01268 m²
Efficiency = 0.98
Rw(2) = 0.00068 (W/m².K)⁻¹

Q(supp) W	% F.S.R	ΔP bar	Tb °C	Tw °C	M2 kg/hr	Ti °C	v m/sec	hi (Exp.) W/m².°C	Re	Pr	Nu (Exp.)	jH (Exp.)	f (Exp.)
818	10	0.0200	110.5	189.7	256.40	162.2	0.497	1222.29	1879.3	56.56	141.032	41.550	0.1948
816	20	0.0500	110.2	176.5	468.33	149.1	0.907	1623.34	3469.0	56.04	187.382	54.061	0.1459
820	30	0.0975	110.0	170.5	676.23	142.9	1.310	1925.77	5004.2	56.09	222.284	63.390	0.1365
823	40	0.1520	110.1	167.1	889.38	139.5	1.723	2169.08	6613.0	55.85	250.413	70.990	0.1230
824	50	0.2320	110.7	166.1	1102.73	138.4	2.138	2295.36	8309.2	55.21	265.129	75.163	0.1220
826	60	0.3200	111.4	164.4	1327.74	136.7	2.576	2527.76	10157.1	54.48	292.145	82.723	0.1160
821	70	0.4300	111.9	161.6	1542.31	134.0	2.994	2871.04	11932.2	53.95	331.966	93.661	0.1155
820	80	0.5400	113.3	161.9	1751.70	134.3	3.404	3020.05	13909.8	52.74	349.556	99.076	0.1123
827	90	0.6600	114.7	162.0	1972.57	134.2	3.838	3277.71	16071.7	51.58	379.772	108.046	0.1081
828	100	-	116.3	162.5	2200.66	134.6	4.287	3495.87	18474.3	50.26	405.544	116.003	

Run NO (2) With LDI-B
Avr. T(in) = 100 °C
q(based on Ao) = 48160 W/m²
At(surface) = 0.0197 m²
Ai(surface) = 0.01268 m²
Efficiency = 0.98
Rw(2) = 0.00068 (W/m².K)⁻¹

Q(supp) W	% F.S.R	ΔP bar	Tb °C	Tw °C	M2 kg/hr	Ti °C	v m/sec	hi (Exp.) W/m².°C	Re	Pr	Nu (Exp.)	jH (Exp.)	f (Exp.)
818	10	0.0250	102.6	176.6	257.67	149.1	0.496	1358.18	1609.9	65.07	155.794	43.777	0.2427
820	20	0.0550	102.0	162.7	471.14	135.1	0.907	1913.85	2952.8	64.89	219.558	60.089	0.1597
820	30	0.1080	103.1	157.0	679.54	129.5	1.309	2404.10	4387.8	63.21	276.092	75.027	0.1505
820	40	0.1720	102.9	153.6	891.87	126.1	1.718	2741.64	5758.8	63.21	314.856	84.934	0.1392
822	50	0.2600	103.0	151.4	1104.51	123.8	2.128	3052.20	7153.6	63.04	350.560	94.136	0.1372
822	60	0.3700	103.2	149.9	1330.08	122.2	2.564	3334.31	8658.6	62.76	383.031	102.577	0.1346
820	70	0.4950	103.5	148.7	1544.66	121.1	2.978	3608.51	10168.2	62.14	414.698	110.963	0.1334
823	80	0.6300	103.9	148.4	1756.86	120.7	3.389	3792.02	11647.1	61.76	435.899	116.657	0.1312
823	90	-	104.9	148.1	1977.12	120.5	3.816	4097.24	13372.9	60.68	471.331	126.461	
820	100	-	105.8	148.1	2204.62	120.6	4.259	4303.80	15181.0	59.73	495.420	133.325	

Appendix C
Examples of heat transfer , friction factor and fouling results for crude oil study

Table (C-1) Heat transfer and friction factor results for crude oil study

Effect of nitrogen gas pressure on hi and Ti
Bare tube test section No (1)
Flow rate = 20% F.S.R
Tb = 50 °C

P (bar)	Q(Sup) W	q (kW/m2)	hi (W/m2.°C)	Re	Ti (°C)	jH (Exp.)	Pr	f (Exp.)
6.2	202	12.2	345.5	1593.3	93.9	8.22	105.6	0.0366
8.2	199	12.0	338.1	1484.7	91.8	7.86	112.8	0.0364
10.2	204	12.3	398.9	1637.1	89.4	9.58	103.0	0.0366
11.8	206	12.4	618.7	2194.0	88.8	16.43	78.5	0.0374
14.2	206	12.4	347.0	1567.8	93.3	8.21	107.2	0.0365
6.1	403	24.2	379.9	1685.5	133.4	9.22	100.3	0.0367
8.2	411	24.7	375.7	1561.9	132.8	8.88	107.6	0.0365
10.2	405	24.4	396.2	1718.2	131.0	9.67	98.5	0.0368
12.0	407	24.5	677.3	2289.7	110.6	18.20	75.5	0.0375
14.3	407	24.5	378.4	1740.8	135.2	9.28	97.3	0.0368
6.0	604	36.4	457.2	1792.9	156.4	11.33	94.7	0.0369
8.2	608	36.6	409.7	1655.2	165.5	9.88	102.0	0.0367
10.1	601	36.2	458.2	1809.7	155.8	11.39	93.8	0.0369
12.1	598	36.0	713.5	2334.7	132.4	19.36	74.2	0.0376
14.4	598	36.1	435.9	1843.5	161.8	10.90	92.3	0.0369
5.9	804	48.4	600.2	2006.3	163.7	15.45	85.3	0.0372
8.2	810	48.8	520.6	1858.4	176.2	13.06	91.6	0.0370
10.1	801	48.2	600.3	2019.6	162.9	15.49	84.8	0.0372
12.1	810	48.8	726.8	2320.4	151.8	19.67	74.6	0.0376
14.7	810	48.7	552.3	1990.8	172.5	14.18	85.9	0.0371
5.9	1004	60.4	715.8	2148.1	171.6	18.87	80.1	0.0374
8.2	1004	60.4	644.7	2021.8	180.6	16.64	84.7	0.0372
10.1	994	59.8	742.8	2224.2	167.9	19.82	77.6	0.0375
12.2	1001	60.3	589.5	2039.6	192.2	15.26	84.0	0.0372
15.2	1001	60.3	745.6	2277.9	169.6	20.05	75.8	0.0375

Table (C-2) Heat transfer and friction factor results for crude oil study

Effect of nitrogen gas pressure on hi and Ti
Bare tube test section No (1)
Flow rate = 20% F.S.R
Tb = 140 °C

P (bar)	Q(Sup) (W)	q (kW/m2)	hi (W/m2.°C)	Re	Ti (°C)	jH (Exp.)	Pr	f (Exp.)
5.9	214	12.8	1459.2	6911.9	153.1	58.06	28.01	0.0393
8.1	210	12.6	1262.4	6806.2	153.2	49.94	28.39	0.0321
10.2	203	12.2	1298.7	6847.1	152.5	51.49	28.24	0.0392
11.0	207	12.4	1255.2	6680.4	151.3	49.32	28.85	0.0390
13.0	212	12.7	1259.2	6663.4	151.3	49.43	28.92	0.0390
6.0	411	24.7	1838.1	7024.6	160.9	73.57	27.62	0.0394
8.1	414	24.9	1569.1	6898.2	162.1	62.38	28.06	0.0321
10.2	398	23.9	1552.8	7082.8	165.6	62.34	27.42	0.0395
11.1	415	24.9	1456.2	6796.0	162.5	57.58	28.43	0.0392
13.0	409	23.8	1306.4	6711.0	163.3	51.41	28.74	0.0391
6.0	603	36.3	2017.5	7021.2	166.7	80.74	27.63	0.0394
8.1	610	36.7	1837.6	7021.2	169.5	73.54	27.63	0.0322
10.2	600	36.1	1390.9	7045.2	177.4	55.73	27.55	0.0394
11.5	609	36.6	1482.1	6894.8	173.6	58.91	28.07	0.0393
13.0	596	35.8	1443.8	6782.4	172.5	57.04	28.47	0.0392
6.1	814	49.0	2329.8	7117.1	172.3	93.70	27.31	0.0395
8.1	803	48.3	1949.2	7079.4	176.7	78.24	27.44	0.0323
10.2	807	48.5	1301.9	6983.6	191.2	52.00	27.76	0.0394
11.9	803	48.3	1594.3	7021.2	182.9	63.80	27.63	0.0394
13.5	811	48.8	1512.6	7058.9	186.1	60.65	27.51	0.0394
6.2	1013	60.9	2331.4	7202.9	180.3	94.19	27.03	0.0396
8.1	1000	60.2	2021.3	7165.1	184.6	81.50	27.15	0.0324
10.5	1004	60.4	1374.3	7120.5	202.2	55.28	27.30	0.0395
12.2	1007	60.6	1559.2	7292.2	197.8	63.28	26.74	0.0397
14.2	1005	60.5	1543.8	7226.9	197.6	62.44	26.95	0.0396

Table (C-3) Heat transfer and friction factor results for crud oil study

Effect of nitogen gas pressure on hi and Ti
Test section No(2) fitted with LDI-B insert
Flow rate = 20% F.S.R
Tb = 50 °C

P (bar)	Q(Sup) W	q (kW/m2)	hi (W/m2.°C)	Re	Ti (°C)	jH (Exp.)	Pr	f (Exp.)
6.2	206	12.4	1228.2	1553.4	61.1	29.17	106.3	0.1895
8.2	202	12.1	1214.1	1432.9	57.9	28.06	114.6	0.1888
10.2	208	12.5	1213.6	1596.6	62.5	29.09	103.7	0.1897
11.8	209	12.5	1420.2	2170.2	74.0	37.75	78.3	0.1925
14.2	206	12.4	1232.9	1495.4	59.5	28.91	110.1	0.1892
6.1	409	24.6	1341.5	1644.6	74.4	32.48	100.9	0.1899
8.2	409	24.6	1340.6	1524.3	71.2	31.64	108.2	0.1893
10.2	407	24.5	1370.9	1683.1	74.6	33.45	98.8	0.1901
12.0	398	23.9	1545.0	2251.8	84.5	41.59	75.7	0.1928
14.3	410	24.6	1431.7	1672.9	73.5	34.86	99.3	0.1901
6.0	606	36.4	1471.4	1761.3	85.8	36.46	94.7	0.1905
8.2	599	36.0	1414.9	1614.6	82.9	34.04	102.6	0.1898
10.1	596	35.8	1452.7	1771.8	85.7	36.06	94.2	0.1906
12.1	604	36.3	1618.9	2265.9	94.1	43.67	75.2	0.1929
14.4	602	36.2	1501.8	1788.5	85.4	37.40	93.4	0.1907
5.9	812	48.8	1560.4	1938.6	98.6	39.93	86.8	0.1914
8.2	810	48.7	1522.2	1811.7	96.4	38.07	92.3	0.1908
10.1	798	48.0	1559.1	1949.5	98.0	39.97	86.3	0.1914
12.1	812	48.9	1624.9	2205.0	102.8	43.43	77.1	0.1926
14.7	819	49.3	1551.9	1929.8	98.9	39.65	87.1	0.1913
5.9	1002	60.3	1512.3	2099.2	113.5	39.75	80.7	0.1921
8.2	1006	60.5	1620.4	1980.4	107.8	41.76	85.1	0.1916
10.1	1003	60.4	1715.8	2235.4	110.7	46.07	76.2	0.1928
12.2	1006	60.6	1558.0	1978.1	109.2	40.14	85.2	0.1916
15.2	999	60.1	1653.8	2214.3	111.4	44.26	76.9	0.1927

Table (C-4) Heat transfer and friction factor results for crud oil study

Effect of nitogen gas pressure on hi and Ti
Test section No(2) fitted with LDI-B insert
Flow rate = 20% F.S.R
Tb = 140 °C

P (bar)	Q(Sup) W	q (kW/m2)	hi (W/m2.°C)	Re	Ti (°C)	jH (Exp.)	Pr	f (Exp.)
5.9	219	13.2	2486.2	7013.8	149.3	99.12	27.9	0.1930
8.1	214	12.9	2078.9	6864.7	148.1	82.25	28.3	0.1926
10.2	210	12.6	2137.8	6850.5	151.0	54.19	28.4	0.1925
11.0	210	12.6	2131.8	6744.5	146.1	83.81	28.8	0.1922
13.0	216	13.0	2258.9	6762.1	146.6	88.89	28.7	0.1922
6.0	422	25.4	2645.2	7117.2	156.2	106.01	27.5	0.1934
8.1	421	25.3	2202.2	6949.8	156.3	87.51	28.1	0.1928
10.2	406	24.4	2011.7	7028.0	156.2	80.26	27.8	0.1931
11.1	418	25.2	2263.0	6864.7	154.6	89.53	28.3	0.1926
13.0	416	25.0	2144.4	6772.7	154.0	84.43	28.7	0.1923
6.0	618	37.2	2851.8	7124.3	160.8	114.33	27.5	0.1934
8.1	614	36.9	2269.0	7028.0	163.8	90.52	27.8	0.1931
10.2	607	36.5	2120.6	7127.9	166.5	85.03	27.5	0.1934
11.5	601	36.2	2429.3	6964.0	161.4	96.60	28.1	0.1929
13.0	608	36.6	2127.0	6836.4	162.2	84.02	28.4	0.1925
6.1	809	48.7	3020.8	7188.6	166.1	121.50	27.3	0.1936
8.1	818	49.2	2417.2	7170.7	171.5	97.13	27.4	0.1935
10.2	806	48.5	2738.6	7188.6	169.5	110.15	27.3	0.1936
11.9	805	48.4	2388.2	7035.2	169.1	95.32	27.8	0.1931
13.5	813	48.9	2342.3	7142.2	171.7	93.99	27.5	0.1934
6.2	1012	60.9	3118.7	7296.1	172.2	126.11	26.9	0.1939
8.1	1000	60.2	2431.8	7260.2	178.4	98.16	27.1	0.1938
10.5	1004	60.4	2472.2	7267.4	178.5	99.82	27.1	0.1938
12.2	1013	60.9	1987.4	7353.5	187.3	80.58	26.8	0.1941
14.2	1002	60.3	2381.8	7303.3	179.7	96.34	26.9	0.1940

Table (C-5) Fouling results
Fouling Run No(7) for bare tube test section No(1)

Fluid	=	Arabian light crude oil with 10% wt sludge	
Pressure	=	4.5 to 13.1	bar gauge (liquid pressure)
Bulk Temp.	=	74	°C
Q(supp)	=	1100	W
At	=	0.0197	m²
Ai	=	0.01268	m²
Efficiency	=	0.98	
Rw(1)	=	0.00119	(m² K / W)

Time Of Running	Date and Time	Tank Pressure (bar)	Q(supp) W	% F.S.R	Tw °C	Ti °C	v m/sec	UE (W/m² K)	Rf (m² K / W)	Re	Pr	Nu (Exp.)	jH (Exp.)	f (Exp.)
	17/1/91													
0	19.00	13.05	1110	10	279.0	213.2	0.495	276.66	0.000E+00	1651.7	61.22	73.633	18.68	0.0775
0.5	19.30	12.50	1115	10	280.6	214.5	0.495	275.44	1.60E-05	1647.1	61.37	73.141	18.54	0.1065
1.0	20.00	11.80	1128	10	279.1	212.3	0.495	280.03	-4.36E-05	1637.9	61.68	74.955	18.97	0.1065
1.5	20.30	11.60	1145	10	278.5	210.7	0.495	285.16	-1.08E-04	1636.4	61.73	77.030	19.49	0.1065
2.0	21.00	11.20	1116	10	276.1	210.0	0.495	281.29	-5.95E-05	1633.4	61.83	75.450	19.08	0.1065
2.5	21.30	11.00	1101	10	273.0	207.8	0.495	281.92	-6.74E-05	1631.9	61.88	75.702	19.14	0.1065
3.0	22.00	10.70	1094	10	271.8	207.1	0.495	281.32	-5.99E-05	1625.8	62.09	75.448	19.05	0.1065
3.5	22.30	11.00	1127	10	275.3	208.5	0.495	285.05	-1.06E-04	1628.8	61.99	76.971	19.45	0.1065
4.0	23.00	11.00	1100	10	275.6	210.4	0.495	278.07	-1.83E-05	1633.4	61.83	74.159	18.75	0.1065
4.5	23.30	11.30	1142	10	279.3	211.7	0.495	283.68	-8.94E-05	1639.5	61.63	76.430	19.35	0.1065
5.0	00.00	11.60	1173	10	280.6	211.2	0.495	289.77	-1.64E-04	1644.0	61.47	78.944	20.00	0.1065
	18/1/91													
5.5	0.30	9.80	1107	10	267.4	201.9	0.495	291.34	-1.82E-04	1624.3	62.14	79.562	20.09	0.1065
6.0	1.00	9.90	1106	10	266.2	202.7	0.495	289.99	-1.66E-04	1625.8	62.09	79.000	19.95	0.1065
6.5	1.30	10.10	1115	10	270.5	204.4	0.495	289.32	-1.58E-04	1630.3	61.94	78.731	19.90	0.0871
7.0	2.00	10.10	1091	10	262.8	198.2	0.495	294.68	-2.21E-04	1628.8	61.99	80.972	20.46	0.0871
7.5	2.30	9.50	1096	10	266.0	201.1	0.495	291.23	-1.81E-04	1630.3	61.94	79.525	20.10	0.0871
8.0	3.00	9.80	1114	10	268.7	202.7	0.495	291.51	-1.84E-04	1625.8	62.09	79.635	20.11	0.0871
8.5	3.30	9.80	1102	10	267.6	202.3	0.495	289.92	-1.65E-04	1624.3	62.14	78.966	19.94	0.0871
9.0	4.00	9.40	1072	10	266.8	203.3	0.495	283.07	-8.19E-05	1621.2	62.25	76.149	19.21	0.0871
9.5	4.30	9.20	1143	10	268.0	200.3	0.495	299.81	-2.79E-04	1619.7	62.30	83.147	20.97	0.0871
10.0	5.00	9.05	1100	10	264.7	199.5	0.495	294.00	-2.13E-04	1622.8	62.19	80.674	20.36	0.0871
10.5	5.30	9.40	1103	10	266.2	200.9	0.495	292.11	-1.91E-04	1621.2	62.25	79.876	20.15	0.0871
11.0	6.00	9.40	1106	10	266.1	200.6	0.495	293.00	-2.02E-04	1619.7	62.30	80.247	20.24	0.0871
11.5	6.30	9.30	1109	10	266.8	201.1	0.495	293.12	-2.03E-04	1624.3	62.14	80.305	20.27	0.0871
12.0	7.00	9.60	1084	10	266.0	201.8	0.495	287.56	-1.37E-04	1619.7	62.30	77.982	19.67	0.0871
12.5	7.30	10.00	1109	10	269.5	203.8	0.495	288.44	-1.48E-04	1615.2	62.46	78.337	19.74	0.0871
13.0	8.00	10.30	1090	10	270.3	205.8	0.495	282.61	-7.62E-05	1621.2	62.25	75.964	19.17	0.0774
13.5	8.30	10.40	1114	10	274.6	208.6	0.495	282.48	-7.45E-05	1622.8	62.19	75.914	19.16	0.0774
14.0	9.00	11.00	1095	10	274.8	209.9	0.495	277.31	-8.47E-06	1625.8	62.09	73.843	18.65	0.0774
14.5	9.30	10.90	1098	10	274.0	209.0	0.495	279.62	-3.82E-05	1633.4	61.83	74.779	18.91	0.0775
15.0	10.00	11.00	1101	10	276.1	209.9	0.495	278.94	-2.95E-05	1634.9	61.78	74.509	18.85	0.0775
15.5	10.30	11.05	1088	10	275.2	210.0	0.495	275.66	1.20E-05	1637.9	61.68	73.220	18.53	0.0775
16.0	11.00	11.00	1090	10	274.9	210.3	0.495	276.06	7.86E-06	1630.3	61.94	73.356	18.54	0.0774
16.5	11.30	11.00	1084	10	274.4	210.2	0.495	275.42	1.63E-05	1633.4	61.83	73.108	18.49	0.0775
17.0	12.00	11.00	1082	10	274.3	210.2	0.495	275.49	1.53E-05	1637.9	61.68	73.146	18.51	0.0775
17.5	12.30	11.50	1102	10	276.9	213.6	0.495	274.03	3.47E-05	1637.9	61.68	72.568	18.37	0.0775
18.0	13.00	12.00	1125	10	284.7	218.1	0.495	272.28	5.81E-05	1645.5	61.42	71.898	18.22	0.0775
18.5	13.30	12.10	1099	10	283.9	218.8	0.495	267.04	1.30E-04	1647.1	61.37	69.873	17.71	0.0775
19.0	14.00	12.10	1100	10	283.9	218.8	0.495	267.28	1.27E-04	1647.1	61.37	69.966	17.74	0.0775
19.5	14.30	12.20	1125	10	288.0	221.4	0.495	268.12	1.15E-04	1650.1	61.27	70.293	17.83	0.0775
20.0	15.00	12.90	1127	10	290.2	223.5	0.495	265.78	1.48E-04	1648.6	61.32	69.393	17.60	0.0775
20.5	15.30	12.90	1098	10	289.4	224.4	0.495	260.07	2.31E-04	1653.2	61.17	67.240	17.07	0.0775
21.0	16.00	12.30	1100	10	286.6	221.5	0.495	264.05	1.73E-04	1651.7	61.22	68.738	17.44	0.0775
21.5	16.30	12.20	1089	10	284.7	220.2	0.495	263.47	1.81E-04	1645.5	61.42	68.509	17.36	0.0775
22.0	17.00	13.00	1123	10	293.5	227.0	0.495	260.94	2.18E-04	1651.7	61.22	67.566	17.14	0.0775
22.5	17.30	12.95	1135	10	294.1	226.9	0.495	263.07	1.87E-04	1656.2	61.07	68.375	17.36	0.0775
23.0	18.00	12.50	1136	10	293.2	226.0	0.495	265.11	1.57E-04	1670.0	60.62	69.173	17.61	0.0775
23.5	18.30	11.90	1113	10	287.8	221.9	0.495	266.12	1.43E-04	1662.4	60.87	69.548	17.68	0.0775
24.0	19.00	11.50	1117	10	285.2	219.0	0.495	270.05	8.85E-05	1654.7	61.12	71.045	18.04	0.0775
24.5	19.30	11.30	1131	10	285.8	218.8	0.495	273.02	4.81E-05	1659.3	60.97	72.212	18.35	0.0775
25.0	20.00	10.80	1130	10	283.4	216.5	0.495	275.46	1.57E-05	1651.7	61.22	73.160	18.56	0.0775
25.5	20.30	10.20	1110	10	279.7	213.0	0.495	276.50	2.08E-06	1644.0	61.47	73.556	18.64	0.0775
26.0	21.00	8.90	1120	10	271.3	204.9	0.495	289.48	-1.60E-04	1636.4	61.73	78.810	19.94	0.0871
26.5	21.30	8.85	1131	10	270.3	203.3	0.495	293.85	-2.11E-04	1636.4	61.73	80.539	20.40	0.0871
27.0	22.00	8.80	1126	10	269.8	203.1	0.495	293.15	-2.03E-04	1631.9	61.88	80.333	20.31	0.0871
27.5	22.30	8.80	1133	10	269.9	202.8	0.495	294.64	-2.21E-04	1633.4	61.83	80.965	20.48	0.0871
28.0	23.00	8.90	1147	10	272.8	204.9	0.495	294.19	-2.15E-04	1634.9	61.78	80.779	20.43	0.0871
28.5	23.30	8.95	1134	10	273.3	206.1	0.495	290.07	-1.67E-04	1634.9	61.78	79.051	20.00	0.0871
29.0	00.00	8.95	1152	10	273.7	205.5	0.495	294.32	-2.17E-04	1636.4	61.73	80.836	20.45	0.0871
	19/1/91													
29.5	0.30	8.40	1136	10	270.6	203.4	0.495	294.69	-2.21E-04	1633.4	61.83	80.989	20.48	0.0871
30.0	1.00	8.30	1140	10	269.2	201.7	0.495	297.99	-2.59E-04	1633.4	61.83	82.390	20.84	0.0871
30.5	1.30	8.40	1168	10	273.5	204.3	0.495	298.58	-2.65E-04	1634.9	61.78	82.647	20.91	0.0871
31.0	2.00	8.00	1106	10	263.8	198.3	0.495	296.67	-2.44E-04	1622.8	62.19	81.807	20.65	0.0871
31.5	2.30	7.95	1110	10	264.3	198.6	0.495	296.85	-2.46E-04	1621.2	62.25	81.878	20.66	0.0871
32.0	3.00	7.75	1112	10	262.4	196.6	0.495	300.45	-2.86E-04	1621.2	62.25	83.426	21.05	0.0871
32.5	3.30	7.80	1109	10	263.0	197.3	0.495	298.68	-2.67E-04	1622.8	62.19	82.668	20.87	0.0871
33.0	4.00	7.90	1125	10	265.3	198.7	0.495	299.37	-2.74E-04	1624.3	62.14	82.964	20.95	0.0871
33.5	4.30	7.30	1094	10	258.4	193.6	0.495	301.69	-3.00E-04	1615.2	62.46	83.949	21.16	0.0871
34.0	5.00	7.50	1109	10	261.7	196.0	0.495	300.86	-2.91E-04	1621.2	62.25	83.605	21.10	0.0871
34.5	5.30	7.70	1111	10	263.3	197.5	0.495	298.58	-2.65E-04	1619.7	62.30	82.616	20.84	0.0871
35.0	6.00	7.60	1103	10	262.2	196.9	0.495	298.61	-2.66E-04	1622.8	62.19	82.636	20.86	0.0871
35.5	6.30	7.40	1098	10	260.9	195.9	0.495	299.08	-2.71E-04	1619.7	62.30	82.834	20.90	0.0871
36.0	7.00	7.30	1117	10	260.8	194.6	0.495	304.21	-3.27E-04	1616.7	62.40	85.055	21.44	0.0871
36.5	7.30	7.60	1110	10	263.3	197.6	0.495	298.31	-2.62E-04	1619.7	62.30	82.501	20.81	0.0871
37.0	8.00	7.20	1109	10	260.8	195.1	0.495	301.95	-3.03E-04	1616.7	62.40	84.068	21.19	0.0871
37.5	8.30	7.90	1081	10	262.5	198.5	0.495	292.07	-1.91E-04	1624.3	62.14	79.867	20.16	0.0871
38.0	9.00	8.90	1126	10	273.7	207.0	0.495	287.73	-1.39E-04	1637.9	61.68	78.088	19.76	0.0871
38.5	9.30	9.50	1133	10	278.7	211.6	0.495	282.80	-7.86E-05	1647.1	61.37	76.089	19.29	0.0872
39.0	10.00	10.20	1107	10	282.6	217.0	0.495	271.48	6.90E-05	1656.2	61.07	71.604	18.18	0.0872
39.5	10.30	12.80	1116	10	301.0	234.9	0.495	251.22	3.66E-04	1667.0	60.72	64.008	16.28	0.0872
40.0	11.00	12.90	1103	10	303.4	238.1	0.495	245.82	4.53E-04	1670.0	60.62	62.060	15.80	0.0872
40.5	11.30	12.30	1105	10	300.1	234.6	0.495	250.34	3.80E-04	1676.2	60.42	63.492	16.23	0.0872
41.0	12.00	12.40	1105	10	301.0	235.5	0.495	249.10	4.00E-04	1671.6	60.57	63.239	16.10	0.0872
41.5	12.30	12.00	1115	10	298.3	232.2	0.495	253.97	3.23E-04	1665.4	60.77	65.000	16.53	0.0872
42.0	13.00	11.30	1122	10	293.3	226.9	0.495	261.76	2.06E-04	1663.9	60.82	67.892	17.26	0.0872
42.5	13.30	10.95	1109	10	291.0	225.3	0.495	261.66	2.07E-04	1670.0	60.62	67.868	17.28	0.0872
43.0	14.00	10.80	1094	10	288.2	223.4	0.495	260.19	2.29E-04	1642.5	61.53	67.267	17.04	0.0872
43.5	14.30	9.10	1110	10	275.6	209.8	0.495	280.00	-4.31E-05	1628.8	61.99	74.924	18.93	0.0871
44.0	15.00	8.40	1114	10	269.5	203.5	0.495	289.94	-1.66E-04	1625.8	62.09	78.980	19.95	0.0871
44.5	15.30	8.50	1110	10	270.6	204.8	0.495	287.23	-1.33E-04	1624.3	62.14	77.855	19.66	0.0871
45.0	16.00	7.85	1115	10	265.3	199.3	0.495	296.31	-2.40E-04	1618.2	62.35	81.643	20.59	0.0871
45.5	16.30	7.20	1095	10	259.7	194.9	0.495	299.60	-2.79E-04	1615.2	62.46	83.134	20.95	0.0871
46.0	17.00	6.05	1128	10	253.1	186.3	0.495	319.68	-4.86E-04	1601.6	62.93	91.998	23.13	0.0871
46.5	17.30	6.20	1116	10	253.7	187.6	0.495	315.36	-4.44E-04	1603.1	62.88	90.012	22.64	0.0871
47.0	18.00	6.30	1108	10	253.0	187.4	0.495	314.26	-4.32E-04	1603.1	62.88	89.510	22.51	0.0871
47.5	18.30	6.50	1100	10	253.6	188.4	0.495	311.03	-3.99E-04	1604.6	62.82	88.055	22.15	0.0871
48.0	19.00	6.80	1110	10	257.6	191.8	0.495	307.03	-3.58E-04	1606.1	62.77	86.275	21.71	0.0871
48.5	19.30	6.80	1118	10	258.2	192.0	0.495	308.22	-3.70E-04	1606.1	62.77	86.800	21.84	0.0871
49.0	20.00	6.60	1104	10	255.1	189.7	0.495	309.44	-3.83E-04	1604.6	62.82	87.341	21.97	0.0871
49.5	20.30	6.60	1097	10	254.8	189.8	0.495	308.24	-3.70E-04	1606.1	62.77	86.809	21.84	0.0871
50.0	21.00	6.70	1102	10	255.8	190.6	0.495	307.82	-3.66E-04	1606.1	62.77	86.623	21.80	0.0871
50.5	21.30	6.90	1103	10	258.3	193.0	0.495	303.92	-3.24E-04	1606.1	62.77	84.902	21.36	0.0871
51.0	22.00	7.00	1120	10	260.9	194.6	0.495	304.12	-3.26E-04	1604.6	62.82	84.986	21.38	0.0871
51.5	22.30	7.20	1140	10	264.8	197.3	0.495	303.56	-3.20E-04	1612.2	62.56	84.760	21.35	0.0871
52.0	23.00	7.10	1096	10	261.6	196.7	0.495	296.58	-2.43E-04	1607.6	62.72	81.740	20.57	0.0871
52.5	23.30	7.20	1145	10	264.8	197.0	0.495	305.06	-3.36E-04	1615.2	62.46	85.422	21.53	0.0871
53.0	00.00	7.10	1109	10	263.1	197.4	0.495	298.47	-2.64E-04	1618.2	62.35	82.565	20.82	0.0871

Table (C-5) (Continuation 1)

Time Of Running	Date and Time	Tank Pressure (bar)	Q(supp) W	% F.S.R	Te °C	Ti °C	u m/sec	Ot (W/m2 K)	Rf (m2 K / W)	Re	Pr	Nu (Exp.)	jH (Exp.)	F (Exp.)
	20/1/91													
53.5	0.30	7.05	1116	10	262.6	196.5	0.495	300.96	-2.92E-04	1615.2	62.46	83.633	21.08	0.0871
54.0	1.00	6.80	1117	10	259.6	193.4	0.495	306.30	-3.50E-04	1612.2	62.56	85.961	21.65	0.0871
54.5	1.30	6.70	1104	10	257.1	191.7	0.495	306.51	-3.52E-04	1607.6	62.72	86.045	21.66	0.0871
55.0	2.00	6.90	1107	10	259.3	193.8	0.495	303.70	-3.22E-04	1610.7	62.61	84.816	21.36	0.0871
55.5	2.30	6.80	1085	10	257.1	192.9	0.495	300.58	-2.88E-04	1603.1	62.88	83.443	20.98	0.0871
56.0	3.00	7.10	1108	10	262.5	196.9	0.495	298.88	-2.69E-04	1615.2	62.46	82.738	20.85	0.0871
56.5	3.30	7.30	1106	10	263.5	198.0	0.495	296.87	-2.46E-04	1616.7	62.40	81.881	20.64	0.0871
57.0	4.00	7.20	1130	10	265.0	198.1	0.495	300.72	-2.89E-04	1613.7	62.51	83.527	21.05	0.0871
57.5	4.30	7.05	1124	10	263.8	197.2	0.495	301.14	-2.94E-04	1613.7	62.51	83.708	21.09	0.0871
58.0	5.00	7.10	1120	10	263.7	197.3	0.495	300.25	-2.84E-04	1615.2	62.46	83.325	21.00	0.0871
58.5	5.30	6.80	1109	10	259.9	194.2	0.495	303.26	-3.17E-04	1612.2	62.56	84.629	21.32	0.0871
59.0	6.00	6.80	1115	10	260.8	194.8	0.495	303.01	-3.14E-04	1607.6	62.72	84.508	21.27	0.0871
59.5	6.30	6.70	1108	10	260.2	194.6	0.495	302.18	-3.05E-04	1607.6	62.72	84.147	21.18	0.1064
60.0	7.00	6.70	1092	10	258.7	194.0	0.495	300.22	-2.84E-04	1606.1	62.77	83.295	20.96	0.0871
60.5	7.30	7.00	1104	10	260.0	194.6	0.495	301.25	-2.95E-04	1604.6	62.82	83.738	21.06	0.0871
61.0	8.00	7.10	1112	10	265.2	199.3	0.495	295.69	-2.33E-04	1613.7	62.51	81.373	20.50	0.0871
61.5	8.30	7.00	1104	10	262.5	197.1	0.495	297.72	-2.56E-04	1612.2	62.56	82.234	20.72	0.0871
62.0	9.00	6.70	1090	10	258.8	194.2	0.495	299.34	-2.74E-04	1603.1	62.88	82.909	20.85	0.0871
62.5	9.30	7.00	1103	10	262.9	197.6	0.495	296.28	-2.39E-04	1606.1	62.77	81.609	20.53	0.0871
63.0	10.00	7.10	1120	10	266.1	199.8	0.495	296.18	-2.38E-04	1612.2	62.56	81.575	20.55	0.0871
63.5	10.30	6.50	1087	10	256.9	192.5	0.495	301.83	-3.01E-04	1604.6	62.82	83.988	21.13	0.0871
64.0	11.00	7.20	1132	10	268.0	200.9	0.495	296.71	-2.44E-04	1615.2	62.46	81.808	20.62	0.0871
64.5	11.30	7.05	1105	10	263.3	197.9	0.495	296.64	-2.44E-04	1613.7	62.51	81.777	20.61	0.0871
65.0	12.00	6.90	1093	10	259.4	194.6	0.495	299.37	-2.74E-04	1609.1	62.66	82.937	20.88	0.0871
65.5	12.30	6.95	1110	10	261.8	196.0	0.495	299.17	-2.72E-04	1597.1	63.09	82.823	20.81	0.0870
66.0	13.00	7.50	1101	10	266.4	201.2	0.495	290.77	-1.75E-04	1612.2	62.56	79.296	19.98	0.0871
66.5	13.30	6.95	1090	10	261.5	197.0	0.495	295.04	-2.25E-04	1607.6	62.72	81.084	20.41	0.0871
67.0	14.00	6.80	1116	10	261.6	195.5	0.495	302.31	-3.07E-04	1612.2	62.56	84.212	21.21	0.0871
67.5	14.30	6.90	1095	10	265.3	200.5	0.495	290.35	-1.70E-04	1610.7	62.61	79.120	19.93	0.0871
68.0	15.00	7.05	1085	10	262.7	198.4	0.495	292.06	-1.91E-04	1613.7	62.51	79.839	20.12	0.0871
68.5	15.30	6.70	1100	10	261.2	196.0	0.495	298.82	-2.68E-04	1618.2	62.35	82.719	20.86	0.0871
69.0	16.00	5.90	1098	10	253.3	188.3	0.495	310.98	-3.99E-04	1603.1	62.88	88.027	22.14	0.0871
69.5	16.30	5.80	1111	10	252.6	186.8	0.495	315.54	-4.45E-04	1595.6	63.14	90.077	22.62	0.0870
70.0	17.00	6.20	1102	10	255.5	190.3	0.495	307.99	-3.68E-04	1600.1	62.98	86.685	21.79	0.0870
70.5	17.30	6.60	1120	10	262.5	196.2	0.495	301.54	-2.98E-04	1609.1	62.66	83.873	21.12	0.0871
71.0	18.00	6.80	1095	10	260.6	195.7	0.495	298.08	-2.60E-04	1609.1	62.66	82.381	20.74	0.0871
71.5	18.30	6.40	1092	10	257.1	192.4	0.495	302.62	-3.10E-04	1604.6	62.82	84.333	21.21	0.0871
72.0	19.00	6.30	1102	10	256.6	191.4	0.495	306.14	-3.48E-04	1603.1	62.88	85.872	21.60	0.0871
72.5	19.30	6.60	1114	10	260.8	194.9	0.495	302.61	-3.10E-04	1607.6	62.72	84.394	21.23	0.0871
73.0	20.00	6.30	1090	10	257.5	192.9	0.495	300.76	-2.90E-04	1595.6	63.14	83.509	20.97	0.0870
73.5	20.30	6.50	1117	10	259.5	193.4	0.495	305.49	-3.41E-04	1603.1	62.88	85.586	21.52	0.0871
74.0	21.00	6.80	1099	10	261.9	196.8	0.495	296.53	-2.42E-04	1603.1	62.88	81.707	20.55	0.0871
74.5	21.30	6.60	1089	10	259.7	195.2	0.495	297.46	-2.53E-04	1603.1	62.88	82.104	20.65	0.0871
75.0	22.00	6.50	1102	10	261.0	195.7	0.495	299.31	-2.74E-04	1607.6	62.72	82.907	20.87	0.0871
75.5	22.30	7.00	1131	10	267.1	200.1	0.495	297.44	-2.53E-04	1610.7	62.61	82.112	20.68	0.0871
76.0	23.00	7.40	1128	10	271.7	204.9	0.495	290.18	-1.68E-04	1619.7	62.30	79.065	19.94	0.0871
76.5	23.30	7.30	1120	10	270.0	203.7	0.495	290.48	-1.72E-04	1619.7	62.30	79.192	19.98	0.0871
77.0	00.00	7.30	1108	10	270.7	205.1	0.495	286.25	-1.21E-04	1616.7	62.40	77.437	19.52	0.0774
	21/1/91													
77.5	0.30	6.70	1127	10	273.6	206.8	0.495	287.22	-1.33E-04	1630.3	61.94	77.861	19.68	0.0774
78.0	1.00	6.80	1109	10	264.6	198.9	0.495	295.70	-2.33E-04	1612.2	62.56	81.374	20.50	0.0774
78.5	1.30	6.90	1104	10	266.6	201.2	0.495	291.40	-1.83E-04	1615.2	62.46	79.568	20.05	0.0774
79.0	2.00	6.40	1095	10	259.5	194.6	0.495	299.88	-2.80E-04	1609.1	62.66	83.157	20.94	0.0871
79.5	2.30	6.70	1110	10	263.9	198.2	0.495	296.58	-2.43E-04	1607.6	62.72	81.739	20.57	0.0871
80.0	3.00	6.90	1121	10	267.1	200.7	0.495	294.97	-2.24E-04	1613.7	62.51	81.066	20.43	0.0871
80.5	3.30	6.85	1115	10	266.6	200.5	0.495	294.44	-2.18E-04	1616.7	62.40	80.850	20.38	0.0871
81.0	4.00	7.10	1106	10	267.8	202.3	0.495	289.56	-1.61E-04	1610.7	62.61	78.793	19.84	0.0871
81.5	4.30	7.60	1106	10	274.7	209.2	0.495	280.08	-4.41E-05	1621.2	62.25	74.941	18.91	0.0871
82.0	5.00	7.60	1101	10	273.8	208.6	0.495	280.06	-4.39E-05	1624.3	62.14	74.938	18.92	0.0871
82.5	5.30	7.75	1094	10	273.3	208.5	0.495	278.79	-2.76E-05	1619.7	62.30	74.423	18.77	0.0871
83.0	6.00	8.00	1104	10	277.7	212.3	0.495	275.45	1.59E-05	1625.8	62.09	73.108	18.46	0.0871
83.5	6.30	8.30	1100	10	281.5	216.4	0.495	269.33	9.83E-05	1627.3	62.04	70.722	17.86	0.0871
84.0	7.00	8.40	1103	10	282.3	217.1	0.495	268.93	1.04E-04	1625.8	62.09	70.562	17.82	0.0871
84.5	7.30	9.20	1102	10	289.0	223.8	0.495	260.22	2.28E-04	1627.3	62.04	67.254	16.99	0.0871
85.0	8.00	9.25	1090	10	290.1	225.5	0.495	256.26	2.88E-04	1633.4	61.83	65.791	16.64	0.0871
85.5	8.30	9.60	1110	10	294.1	228.4	0.495	255.94	2.93E-04	1630.3	61.94	65.669	16.60	0.0871
86.0	9.00	10.15	1104	10	299.5	234.1	0.495	248.96	4.02E-04	1642.5	61.53	63.144	15.99	0.0872
86.5	9.30	10.60	1098	10	303.1	238.1	0.495	243.91	4.85E-04	1648.6	61.32	61.346	15.56	0.0872
87.0	10.00	10.60	1100	10	303.2	238.1	0.495	244.31	4.79E-04	1653.2	61.17	61.496	15.61	0.0872
87.5	10.30	10.55	1100	10	303.6	238.4	0.495	243.92	4.85E-04	1651.7	61.22	61.354	15.57	0.0872
88.0	11.00	10.70	1103	10	305.9	240.6	0.495	242.02	5.17E-04	1648.6	61.32	60.680	15.39	0.0872
88.5	11.30	11.50	1107	10	312.8	247.2	0.495	236.14	6.20E-04	1656.2	61.07	58.642	14.89	0.0872
89.0	12.00	12.40	1106	10	320.8	255.3	0.495	228.07	7.70E-04	1660.8	60.92	55.895	14.21	0.0872
89.5	12.30	12.80	1117	10	323.6	257.5	0.495	227.62	7.79E-04	1657.8	61.02	55.742	14.16	0.0872
90.0	13.00	12.60	1091	10	321.6	257.0	0.495	224.49	8.40E-04	1667.0	60.72	54.706	13.92	0.0872
90.5	13.30	13.05	1103	10	325.3	260.1	0.495	223.60	8.58E-04	1670.0	60.62	54.417	13.85	0.0872
91.0	14.00	13.00	1099	10	324.8	259.7	0.495	223.35	8.63E-04	1671.6	60.57	54.335	13.84	0.0872
91.5	14.30	13.05	1105	10	326.0	260.5	0.495	223.48	8.60E-04	1673.1	60.52	54.381	13.85	0.0872
92.0	15.00	12.95	1122	10	325.7	259.3	0.495	227.26	7.86E-04	1677.7	60.37	55.646	14.18	0.0872
92.5	15.30	13.00	1120	10	326.1	259.7	0.495	226.63	7.98E-04	1682.3	60.22	55.443	14.14	0.0873
93.0	16.00	12.80	1118	10	324.0	257.8	0.495	228.29	7.66E-04	1685.4	60.12	56.005	14.30	0.0873
93.5	16.30	12.90	1110	10	323.8	258.0	0.495	226.81	7.94E-04	1683.9	60.17	55.505	14.16	0.0873
94.0	17.00	12.90	1112	10	324.0	258.1	0.495	227.12	7.88E-04	1685.4	60.12	55.609	14.19	0.0873
94.5	17.30	13.00	1123	10	327.4	260.9	0.495	226.47	8.01E-04	1693.1	59.88	55.403	14.16	0.0873
95.0	18.00	12.10	1107	10	321.6	256.1	0.495	228.58	7.60E-04	1694.7	59.83	56.115	14.35	0.0873
95.5	18.30	10.90	1151	10	312.4	244.3	0.495	246.96	4.35E-04	1686.9	60.08	62.492	15.96	0.0873
96.0	19.00	11.00	1149	10	316.9	248.9	0.495	241.93	5.19E-04	1688.5	60.03	60.706	15.50	0.0873
96.5	19.30	10.00	1116	10	311.5	245.4	0.495	240.53	5.43E-04	1688.5	60.03	60.214	15.38	0.0873
97.0	20.00	6.90	1124	10	296.1	229.5	0.495	258.23	2.58E-04	1662.4	60.87	66.569	16.92	0.0872
97.5	20.30	7.40	1126	10	284.0	217.3	0.495	273.73	3.86E-05	1656.2	61.07	72.486	18.41	0.0870
98.0	21.00	7.00	1131	10	278.0	211.0	0.495	283.02	-8.13E-05	1651.7	61.22	76.186	19.33	0.08720
98.5	21.30	6.20	1121	10	270.6	204.2	0.495	290.93	-1.77E-04	1644.0	61.47	79.426	20.12	0.0872
99.0	22.00	6.00	1125	10	267.0	200.4	0.495	297.46	-2.53E-04	1639.5	61.63	82.176	20.80	0.0871
99.5	22.30	5.60	1120	10	263.0	196.6	0.495	302.09	-3.04E-04	1631.9	61.88	84.161	21.28	0.0871
100.0	23.00	5.80	1164	10	267.1	198.1	0.495	307.55	-3.63E-04	1634.9	61.78	86.563	21.90	0.0871
100.5	23.30	6.00	1162	10	269.4	200.6	0.495	303.33	-3.18E-04	1636.4	61.73	84.710	21.43	0.0871
101.0	00.00	6.00	1147	10	269.7	201.8	0.495	299.02	-2.70E-04	1639.5	61.63	82.849	20.97	0.0871
	22/1/91													
101.5	0.30	6.00	1173	10	272.1	202.7	0.495	301.97	-3.03E-04	1636.4	61.73	84.115	21.28	0.0871
102.0	1.00	5.20	1111	10	256.4	190.6	0.495	310.13	-3.90E-04	1622.8	62.19	87.690	22.13	0.0871
102.5	1.30	5.00	1130	10	270.3	203.4	0.495	292.33	-1.94E-04	1615.2	62.46	79.957	20.15	0.0871
103.0	2.00	4.80	1096	10	250.5	185.6	0.495	315.14	-4.41E-04	1601.6	62.93	89.908	22.60	0.0871
103.5	2.30	4.90	1096	10	252.4	187.5	0.495	311.54	-4.05E-04	1598.6	63.04	88.269	22.18	0.0870
104.0	3.00	5.30	1115	10	260.1	194.0	0.495	304.19	-3.27E-04	1606.1	62.77	85.022	21.39	0.0871
104.5	3.30	5.40	1120	10	259.4	193.1	0.495	306.20	-3.49E-04	1601.6	62.93	85.896	21.60	0.0871
105.0	4.00	5.30	1106	10	259.0	193.5	0.495	303.27	-3.17E-04	1603.1	62.88	84.613	21.28	0.0871
105.5	4.30	5.30	1117	10	257.9	191.8	0.495	307.75	-3.65E-04	1598.6	63.04	86.574	21.75	0.0870
106.0	5.00	5.40	1114	10	260.1	194.2	0.495	303.37	-3.18E-04	1600.1	62.98	84.652	21.28	0.0870
106.5	5.30	5.40	1105	10	260.0	194.6	0.495	300.92	-2.91E-04	1597.1	63.09	83.580	21.00	0.0870
107.0	6.00	5.60	1109	10	262.2	196.5	0.495	298.68	-2.66E-04	1601.6	62.93	82.623	20.77	0.0871
107.5	6.30	5.80	1109	10	263.6	197.9	0.495	296.29	-2.40E-04	1600.1	62.98	81.599	20.51	0.0870
108.0	7.00	6.00	1087	10	265.0	200.7	0.495	288.59	-1.50E-04	1606.1	62.77	78.383	19.72	0.0871
108.5	7.30	5.95	1118	10	269.2	203.0	0.495	290.68	-1.74E-04	1610.7	62.61	79.257	19.96	0.0871
109.0	8.00	6.05	1109	10	268.4	202.7	0.495	289.32	-1.58E-04	1607.6	62.72	78.687	19.80	0.0871
109.5	8.30	6.05	1087	10	267.0	202.6	0.495	285.64	-1.14E-04	1607.6	62.72	77.170	19.42	0.0871
110.0	9.00	6.30	1100	10	271.5	206.3	0.495	282.64	-7.65E-05	1613.7	62.51	75.959	19.14	0.0871
110.5	9.30	6.90	1109	10	275.4	209.7	0.495	279.39	-3.54E-05	1616.7	62.40	74.656	18.82	0.0871
111.0	10.00	6.95	1106	10	277.6	212.1	0.495	276.09	7.47E-06	1625.8	62.09	73.360	18.53	0.0871
111.5	10.30	7.40	1110	10	283.8	218.0	0.495	269.52	9.58E-05	1637.9	61.68	70.811	17.92	0.0871
112.0	11.00	7.60	1107	10	285.3	219.7	0.495	266.74	1.34E-04	1637.9	61.68	69.740	17.65	0.0871

Table (C-5) (Continuation 2)

Time Of Runing	Date and Time	Tank Pressure (bar)	Q(supp) W	% F.S.R	Tw °C	Ti °C	v m/sec	Ut (W/m² K)	Rf (m² K / W)	Re	Pr	Nu (Emp.)	jH (Emp.)	f (Emp.)
112.5	11.30	7.80	1110	10	287.5	221.7	0.495	264.86	1.61E-04	1641.0	61.58	69.030	17.48	0.0872
113.0	12.00	8.30	1128	10	294.9	228.1	0.495	260.01	2.31E-04	1645.5	61.42	67.205	17.03	0.0872
113.5	12.30	9.20	1139	10	303.4	235.9	0.495	253.07	3.37E-04	1654.7	61.12	64.656	16.41	0.1066
114.0	13.00	10.50	1130	10	311.4	244.5	0.495	242.74	5.05E-04	1665.4	60.77	60.959	15.51	0.0872
114.5	13.30	10.80	1090	10	313.9	249.4	0.495	231.62	7.03E-04	1668.5	60.67	57.108	14.53	0.0872
115.0	14.00	11.30	1122	10	321.3	254.9	0.495	231.29	7.09E-04	1673.1	60.52	57.004	14.52	0.0872
115.5	14.30	11.90	1129	10	323.8	256.9	0.495	230.49	7.24E-04	1676.2	60.42	56.736	14.46	0.0872
116.0	15.00	12.10	1132	10	326.3	259.3	0.495	228.98	7.53E-04	1683.9	60.17	56.235	14.35	0.0873
116.5	15.30	12.70	1128	10	328.1	261.3	0.495	227.42	7.83E-04	1702.4	59.59	55.733	14.27	0.0873
117.0	16.00	13.10	1150	10	334.3	266.2	0.495	225.58	8.18E-04	1690.0	59.98	55.102	14.08	0.0873
117.5	16.30	12.95	1148	10	333.0	265.0	0.495	226.62	7.98E-04	1699.3	59.69	55.462	14.19	0.0873
118.0	17.00	12.00	1116	10	327.6	261.5	0.495	225.09	8.28E-04	1703.9	59.54	54.956	14.07	0.0873
118.5	17.30	10.70	1115	10	322.8	256.7	0.495	229.35	7.46E-04	1703.9	59.54	56.387	14.44	0.0873
119.0	18.00	9.80	1099	10	312.8	247.7	0.495	235.52	6.31E-04	1696.2	59.78	58.483	14.96	0.0873
119.5	18.30	8.80	1125	10	309.1	242.5	0.495	244.85	4.70E-04	1688.5	60.03	61.741	15.77	0.0873
120.0	19.00	7.90	1114	10	299.7	233.8	0.495	252.35	3.48E-04	1677.7	60.37	64.427	16.42	0.0872
120.5	19.30	7.50	1119	10	291.8	225.6	0.495	262.68	1.92E-04	1670.0	60.62	68.251	17.37	0.0872
121.0	20.00	7.40	1153	10	291.0	222.7	0.495	271.51	6.86E-05	1665.4	60.77	71.632	18.22	0.0872
121.5	20.30	6.70	1143	10	291.1	223.4	0.495	269.17	1.01E-04	1667.0	60.72	70.728	17.99	0.0872
122.0	21.00	6.20	1124	10	281.3	214.7	0.495	276.88	-2.93E-06	1654.7	61.12	73.727	18.72	0.0872
122.5	21.30	6.10	1142	10	277.0	209.4	0.495	287.06	-1.31E-04	1647.1	61.37	77.828	19.73	0.0872
123.0	22.00	6.10	1156	10	278.0	209.5	0.495	289.32	-1.58E-04	1648.6	61.32	78.765	19.97	0.0872
123.5	22.30	6.10	1137	10	278.0	210.7	0.495	284.51	-9.97E-05	1650.1	61.27	76.788	19.48	0.0872
124.0	23.00	5.20	1153	10	275.0	206.7	0.495	292.33	-1.94E-04	1637.9	61.68	80.003	20.25	0.0871
124.5	23.30	6.00	1135	10	266.6	199.4	0.495	300.26	-2.84E-04	1627.3	62.04	83.359	21.06	0.0871
125.0	00.00	4.90	1128	10	260.3	193.5	0.495	307.95	-3.67E-04	1615.2	62.46	86.700	21.85	0.0871
	23/1/91													
125.5	0.30	4.90	1110	10	260.0	194.3	0.495	303.07	-3.15E-04	1609.1	62.66	84.541	21.28	0.0871
126.0	1.00	4.80	1103	10	258.0	192.7	0.495	304.95	-3.35E-04	1613.7	62.51	85.373	21.51	0.0871
126.5	1.30	4.90	1116	10	259.5	193.4	0.495	305.85	-3.45E-04	1612.2	62.56	85.764	21.60	0.0871
127.0	2.00	4.70	1098	10	254.3	189.3	0.495	309.53	-3.84E-04	1606.1	62.77	87.383	21.99	0.0871
127.5	2.30	4.70	1100	10	258.0	192.8	0.495	303.41	-3.19E-04	1601.6	62.93	84.669	21.29	0.0871
128.0	3.00	4.90	1122	10	264.3	197.8	0.495	299.47	-2.75E-04	1607.6	62.72	82.976	20.88	0.0871
128.5	3.30	4.90	1098	10	260.2	195.2	0.495	299.51	-2.76E-04	1606.1	62.77	82.991	20.88	0.0871
129.0	4.00	4.80	1097	10	259.8	194.8	0.495	299.42	-2.75E-04	1598.6	63.04	82.937	20.84	0.0870
129.5	4.30	4.90	1113	10	262.7	196.8	0.495	298.95	-2.70E-04	1598.6	63.04	82.734	20.79	0.0870
130.0	5.00	4.80	1100	10	260.4	195.3	0.495	299.19	-2.72E-04	1600.1	62.98	82.841	20.82	0.0870
130.5	5.30	4.80	1096	10	260.1	195.2	0.495	298.80	-2.68E-04	1600.1	62.98	82.673	20.78	0.0870
131.0	6.00	4.90	1090	10	262.0	197.4	0.495	294.25	-2.16E-04	1601.6	62.93	80.736	20.30	0.0774
131.5	6.30	5.00	1111	10	264.5	198.8	0.495	295.52	-2.31E-04	1606.1	62.98	81.274	20.43	0.0774
132.0	7.00	5.10	1100	10	262.6	197.5	0.495	295.98	-2.36E-04	1607.6	62.72	81.481	20.51	0.0774
132.5	7.30	5.20	1134	10	268.8	201.7	0.495	295.48	-2.30E-04	1609.1	62.66	81.273	20.46	0.0774
133.0	8.00	5.30	1129	10	269.0	202.1	0.495	294.10	-2.14E-04	1612.2	62.56	80.695	20.33	0.0871
133.5	8.30	6.80	1140	10	285.3	217.8	0.495	275.26	1.84E-05	1644.0	61.47	73.066	18.51	0.0872
134.0	9.00	6.90	1123	10	283.1	216.6	0.495	273.79	3.78E-05	1642.5	61.53	72.485	18.36	0.0872
134.5	9.30	6.20	1103	10	277.0	211.7	0.495	276.80	-1.88E-06	1634.9	61.78	73.659	18.63	0.0871
135.0	10.00	6.20	1114	10	278.0	212.1	0.495	278.55	-2.45E-05	1641.0	61.58	74.365	18.83	0.0872
135.5	11.00	6.50	1128	10	282.4	215.6	0.495	275.96	9.15E-06	1642.5	61.53	73.339	18.58	0.0872
136.0	11.30	6.90	1125	10	284.6	218.0	0.495	272.43	5.61E-05	1647.1	61.37	71.958	18.24	0.0872
136.5	12.00	6.95	1120	10	285.7	219.4	0.495	270.03	8.87E-05	1653.2	61.17	71.037	18.03	0.0872
137.0	12.30	7.85	1140	10	296.4	228.9	0.495	262.42	1.96E-04	1673.1	60.52	68.156	17.36	0.0872
137.5	13.00	8.15	1129	10	300.4	233.5	0.495	255.44	3.00E-04	1677.7	60.37	65.560	16.71	0.0872
138.0	13.30	8.60	1124	10	303.0	236.4	0.495	251.35	3.64E-04	1679.2	60.32	64.065	16.34	0.0872
138.5	14.00	8.95	1120	10	306.3	239.9	0.495	246.42	4.44E-04	1674.6	60.47	62.280	15.87	0.0872
139.0	14.30	9.20	1136	10	310.4	243.2	0.495	245.93	4.52E-04	1685.4	60.12	62.122	15.86	0.0873
139.5	15.00	10.00	1145	10	317.6	249.8	0.495	240.36	5.46E-04	1686.9	60.08	60.154	15.36	0.0873
140.0	15.30	11.00	1145	10	324.9	257.1	0.495	233.61	6.66E-04	1699.3	59.69	57.830	14.80	0.0873
140.5	16.00	11.05	1136	10	325.6	258.4	0.495	231.05	7.14E-04	1697.7	59.73	56.955	14.57	0.0873
141.5	16.30	11.10	1126	10	325.7	259.0	0.495	229.10	7.50E-04	1702.4	59.59	56.300	14.41	0.0873
141.5	17.00	11.80	1144	10	330.6	262.9	0.495	228.28	7.66E-04	1705.5	59.49	56.028	14.35	0.0873
142.0	17.30	12.40	1160	10	335.7	267.0	0.495	226.77	7.95E-04	1707.0	59.44	55.524	14.23	0.0873
142.5	18.00	10.85	1085	10	322.2	257.9	0.495	223.87	8.52E-04	1702.4	59.59	54.547	13.97	0.0873
143.0	18.30	10.00	1138	10	320.1	252.7	0.495	236.43	6.15E-04	1691.6	59.93	58.792	15.02	0.0873
143.5	19.00	8.90	1127	10	308.8	242.0	0.495	245.56	4.58E-04	1682.3	60.22	61.984	15.81	0.0873
144.0	19.30	8.00	1138	10	300.9	233.5	0.495	256.54	2.84E-04	1674.6	60.47	65.961	16.81	0.0872
144.5	20.00	7.00	1123	10	289.4	222.9	0.495	267.11	1.29E-04	1671.6	60.57	69.940	17.81	0.0872
145.0	20.30	6.20	1122	10	282.1	215.6	0.495	275.51	1.51E-05	1654.7	61.12	73.183	18.58	0.0872
145.5	21.00	5.90	1144	10	277.8	210.1	0.495	286.50	-1.24E-04	1645.5	61.42	77.594	19.67	0.0872
146.0	21.30	5.30	1138	10	273.1	205.7	0.495	291.52	-1.84E-04	1636.4	61.73	79.661	20.16	0.0871
146.5	22.00	4.95	1106	10	265.0	199.5	0.495	295.04	-2.25E-04	1625.8	62.09	81.122	20.49	0.0871
147.0	22.30	4.80	1100	10	261.8	196.7	0.495	297.98	-2.59E-04	1615.2	62.46	82.350	20.76	0.0871
147.5	23.00	4.90	1125	10	266.5	199.9	0.495	297.64	-2.55E-04	1619.7	62.30	82.216	20.74	0.0871
148.0	23.30	4.95	1099	10	266.3	201.2	0.495	291.27	-1.81E-04	1622.8	62.19	79.528	20.07	0.0871
148.5	00.00	5.10	1144	10	272.3	204.6	0.495	294.11	-2.14E-04	1628.8	61.99	80.732	20.40	0.0871
	24/1/91													
149.0	0.30	5.00	1141	10	270.3	202.8	0.495	296.03	-2.37E-04	1624.3	62.14	81.538	20.59	0.0871
149.5	1.00	5.00	1130	10	270.4	203.5	0.495	292.93	-2.01E-04	1619.7	62.30	80.218	20.24	0.0871
150.0	1.30	4.90	1113	10	266.6	200.7	0.495	293.82	-2.11E-04	1615.2	62.46	80.583	20.31	0.0871
150.5	2.00	5.00	1120	10	267.3	201.0	0.495	294.07	-2.14E-04	1609.1	62.66	80.675	20.31	0.0871
151.0	2.30	4.95	1086	10	264.8	200.5	0.495	288.67	-1.53E-04	1606.1	62.77	78.499	19.75	0.0871
151.5	3.00	4.90	1115	10	267.6	201.5	0.495	292.43	-1.95E-04	1607.6	62.72	79.982	20.13	0.0871
152.0	3.30	5.10	1141	10	272.8	205.2	0.495	291.96	-1.89E-04	1618.2	62.35	79.806	20.13	0.0871
152.5	4.00	5.00	1130	10	269.7	202.8	0.495	293.81	-2.11E-04	1616.7	62.40	80.582	20.32	0.0871
153.0	4.30	4.80	1090	10	265.3	200.7	0.495	289.51	-1.61E-04	1609.1	62.66	78.770	19.83	0.0871
153.5	5.00	4.90	1110	10	267.8	202.1	0.495	291.27	-1.81E-04	1613.7	62.51	79.511	20.03	0.0871
154.0	5.30	4.95	1110	10	266.4	200.6	0.495	293.22	-2.04E-04	1609.1	62.66	80.320	20.22	0.0871
154.5	6.00	4.80	1098	10	265.6	200.6	0.495	291.27	-1.81E-04	1607.6	62.72	79.500	20.01	0.0871
155.0	6.30	4.80	1120	10	267.4	201.1	0.495	294.13	-2.15E-04	1610.7	62.61	80.703	20.32	0.0871
155.5	7.00	4.40	1082	10	259.2	195.1	0.495	295.72	-2.33E-04	1598.1	63.41	81.331	20.48	0.0870
156.0	7.30	5.00	1105	10	271.0	205.6	0.495	284.59	-1.01E-04	1604.6	62.82	76.736	19.30	0.0871
156.5	8.00	5.05	1103	10	269.2	203.9	0.495	287.30	-1.34E-04	1612.2	62.56	77.859	19.61	0.0871
157.0	8.30	5.05	1096	10	269.3	204.4	0.495	285.06	-1.07E-04	1609.1	62.66	76.936	19.37	0.0871
157.5	9.00	5.20	1096	10	270.9	206.0	0.495	283.51	-8.74E-05	1621.2	62.25	76.327	19.26	0.0871
158.0	9.30	5.20	1084	10	269.3	205.1	0.495	282.85	-7.91E-05	1622.8	62.19	76.062	19.20	0.0871
158.5	10.00	5.60	1123	10	275.7	209.2	0.495	283.83	-9.14E-05	1628.8	61.99	76.474	19.32	0.0871
159.0	10.30	6.00	1115	10	280.6	214.6	0.495	275.76	1.18E-05	1644.0	61.47	73.261	18.56	0.0872
159.5	11.00	6.10	1116	10	282.8	216.7	0.495	272.98	4.87E-05	1644.0	61.47	72.170	18.29	0.0872
160.0	11.30	6.50	1120	10	285.3	219.0	0.495	270.37	8.41E-05	1644.0	61.47	71.150	18.03	0.0872
160.5	12.00	7.00	1119	10	290.0	223.7	0.495	265.08	1.58E-04	1659.3	60.97	69.145	17.57	0.0872
161.0	12.30	7.50	1132	10	296.8	229.8	0.495	260.16	2.29E-04	1670.0	60.62	67.302	17.13	0.0872
161.5	13.00	8.30	1118	10	305.7	239.5	0.495	246.59	4.41E-04	1670.0	60.62	62.336	15.87	0.0872
162.0	13.30	9.00	1123	10	310.7	244.2	0.495	242.67	5.06E-04	1679.2	60.32	60.955	15.54	0.0872
162.5	14.00	9.75	1118	10	316.4	250.2	0.495	235.77	6.27E-04	1682.3	60.22	58.552	14.94	0.0873
163.0	14.30	10.10	1105	10	318.9	253.5	0.495	230.61	7.22E-04	1685.4	60.12	56.789	14.50	0.0873
163.5	15.00	10.50	1110	10	321.9	256.2	0.495	229.13	7.50E-04	1694.7	59.83	56.301	14.39	0.0873
164.0	15.30	11.10	1114	10	326.3	260.3	0.495	226.06	8.09E-04	1699.3	59.69	55.273	14.14	0.0873
164.5	16.00	11.10	1109	10	324.7	259.0	0.495	226.23	8.06E-04	1694.7	59.83	55.324	14.15	0.0873
165.0	16.30	10.90	1107	10	323.2	257.7	0.495	227.21	7.87E-04	1693.1	59.88	55.650	14.22	0.0873
165.5	17.00	11.15	1126	10	327.6	260.9	0.495	227.12	7.88E-04	1696.2	59.78	55.626	14.23	0.0873
166.0	17.30	11.90	1109	10	328.9	263.2	0.495	222.58	8.78E-04	1700.8	59.64	54.118	13.85	0.0873
166.5	18.00	12.10	1122	10	332.9	266.5	0.495	221.94	8.91E-04	1710.1	59.35	53.920	13.82	0.0873
167.0	18.30	11.20	1124	10	328.6	262.0	0.495	226.00	8.10E-04	1703.9	59.54	55.260	14.15	0.1067
167.5	19.00	10.80	1113	10	326.1	260.2	0.495	226.00	8.10E-04	1700.8	59.64	55.257	14.14	0.0873
168.0	19.30	9.70	1150	10	320.0	251.9	0.495	239.39	5.63E-04	1693.1	59.88	59.824	15.29	0.0873
168.5	20.00	8.15	1107	10	306.9	241.4	0.495	243.14	4.98E-04	1679.2	60.32	61.123	15.59	0.0872
169.0	20.30	7.00	1119	10	293.5	227.3	0.495	260.98	2.17E-04	1671.6	60.57	67.612	17.22	0.0872
169.5	21.00	6.50	1138	10	290.2	222.8	0.495	269.78	9.22E-05	1671.6	60.57	70.969	18.07	0.0872
170.0	21.30	5.60	1103	10	276.7	211.4	0.495	278.32	-2.16E-05	1650.1	61.27	74.290	18.84	0.0872
170.5	22.00	5.30	1116	10	275.4	209.3	0.495	283.25	-8.41E-05	1647.1	61.37	76.271	19.34	0.0872
171.0	22.30	4.95	1121	10	269.8	203.4	0.495	291.52	-1.84E-04	1624.3	62.14	79.636	20.11	0.0871
171.5	23.00	4.95	1110	10	269.6	203.8	0.495	288.80	-1.52E-04	1619.7	62.30	78.492	19.80	0.0871
172.0	23.30	4.95	1115	10	268.7	202.6	0.495	291.33	-1.82E-04	1618.2	62.35	79.545	20.06	0.0871
172.5	00.00	4.85	1123	10	263.2	196.7	0.495	301.04	-2.93E-04	1606.1	62.77	83.652	21.05	0.0871

Table (C-5) (Continuation 3)

Time Of Runing	Date and Time	Tank Pressure (bar)	Q(supp) W	% F.S.R	Tw °C	Ti °C	v m/sec	Ut (W/m² K)	Rf (m² K / W)	Re	Pr	Nu (Exp.)	jH (Exp.)	f (Exp.)
	25/1/91													
173.0	0.30	4.80	1136	10	264.9	197.7	0.495	301.59	-2.99E-04	1601.6	62.93	83.877	21.09	0.0871
173.5	1.00	4.80	1100	10	262.2	197.0	0.495	296.66	-2.44E-04	1604.6	62.82	81.766	20.57	0.0871
174.0	1.30	4.70	1082	10	255.5	191.4	0.495	301.97	-3.03E-04	1597.1	63.09	84.035	21.11	0.0870
174.5	2.00	4.60	1077	10	258.7	194.9	0.495	295.62	-2.32E-04	1598.6	63.04	81.313	20.43	0.0870
175.0	2.30	4.80	1115	10	265.3	199.2	0.495	295.86	-2.35E-04	1604.6	62.82	81.424	20.48	0.0871
175.5	3.00	5.00	1136	10	269.7	202.5	0.495	294.59	-2.20E-04	1607.6	62.72	80.895	20.36	0.0871
176.0	3.30	4.90	1110	10	265.6	199.8	0.495	294.06	-2.14E-04	1604.6	62.82	80.663	20.29	0.0871
176.5	4.00	4.90	1116	10	267.1	201.0	0.495	293.17	-2.04E-04	1603.1	62.88	80.285	20.19	0.0871
177.0	4.30	4.75	1108	10	264.9	199.3	0.495	294.35	-2.17E-04	1601.6	62.93	80.780	20.31	0.0871
177.5	5.00	4.70	1105	10	263.9	198.5	0.495	294.73	-2.22E-04	1595.6	63.14	80.930	20.32	0.0870
178.0	5.30	4.60	1075	10	259.5	195.8	0.495	293.46	-2.07E-04	1592.6	63.25	80.385	20.18	0.0870
178.5	6.00	4.80	1106	10	264.8	199.3	0.495	293.52	-2.08E-04	1594.1	63.19	80.416	20.19	0.0870
179.0	6.30	5.10	1136	10	272.7	205.4	0.495	290.00	-1.66E-04	1606.1	62.77	78.966	19.87	0.0871
179.5	7.00	4.50	1110	10	263.0	197.3	0.495	297.50	-2.53E-04	1595.6	63.14	82.107	20.62	0.0870
180.0	7.30	4.70	1109	10	264.4	198.7	0.495	294.99	-2.25E-04	1594.1	63.19	81.036	20.34	0.0870
180.5	8.00	4.80	1120	10	268.2	201.9	0.495	293.20	-2.04E-04	1616.7	62.40	80.324	20.25	0.0871
181.0	8.30	4.60	1107	10	263.9	198.4	0.495	294.93	-2.24E-04	1588.1	63.41	80.999	20.31	0.0870
181.5	9.00	5.00	1097	10	268.0	203.0	0.495	286.68	-1.26E-04	1601.6	62.93	77.586	19.51	0.0871
182.0	9.30	5.05	1086	10	267.2	202.9	0.495	285.21	-1.08E-04	1606.1	62.77	76.993	19.37	0.0871
182.5	10.00	4.80	1097	10	274.1	209.1	0.495	278.10	-1.87E-05	1610.7	62.61	74.130	18.67	0.0871
183.0	10.30	4.90	1113	10	277.8	211.9	0.495	277.65	-1.29E-05	1624.3	62.14	73.976	18.68	0.0871
183.5	11.00	4.80	1100	10	278.8	213.7	0.495	272.97	4.89E-05	1624.3	62.14	72.129	18.21	0.0871
184.0	11.30	4.80	1096	10	275.8	211.0	0.495	275.86	1.05E-05	1621.2	62.25	73.261	18.49	0.0871
184.5	12.00	4.90	1090	10	276.8	212.3	0.495	273.23	4.54E-05	1625.8	62.09	72.233	18.24	0.0871

Table (C-6) Fouling results
Fouling Run No(7) for test section No(2) fitted with LDI-B

Fluid = Arabian light crude oil with 10% wt sludge
Pressure = 4.5 to 13.1 bar gauge (liquid pressure)
Bulk Temp. = 74 °C
Q(sup) = 1100 W
At = 0.0197 m²
Ai = 0.01268 m²
Efficiency = 0.98
Rw(2) = 0.00068 (m² K / W)

Time Of Runing	Date and Time	Tank Pressure (bar)	Q(sup) W	% F.S.R	Tw °C	Ti °C	V m/sec	Ut (W/m² K)	Rf (m² K / W)	Re	Pr	Nu (Exp.)	jH (Exp.)	f (Exp.)
	17/1/91													
0.0	19.00	13.05	1114	10	189.7	152.2	0.486	497.89	0.000E+00	1608.8	61.63	133.8	33.8	0.3016
0.5	19.30	12.50	1112	10	191.0	153.6	0.486	491.16	2.75E-05	1605.8	61.73	131.1	33.1	0.3016
1.0	20.00	11.80	1129	10	192.5	154.5	0.486	491.63	2.56E-05	1601.3	61.88	131.2	33.2	0.3019
1.5	20.30	11.60	1152	10	193.5	154.8	0.486	496.60	5.23E-06	1596.8	62.04	133.2	33.6	0.3016
2.0	21.00	11.20	1121	10	191.0	153.4	0.486	493.16	1.93E-05	1593.9	62.14	131.8	33.2	0.3015
2.5	21.30	11.00	1106	10	189.5	152.3	0.486	492.94	2.02E-05	1592.4	62.19	131.7	33.2	0.3015
3.0	22.00	10.70	1094	10	189.2	152.5	0.486	488.19	3.99E-05	1587.9	62.35	129.8	32.7	0.3015
3.5	22.30	11.00	1129	10	191.7	153.7	0.486	493.79	1.67E-05	1592.4	62.19	132.1	33.3	0.3015
4.0	23.00	11.00	1100	10	190.1	153.1	0.486	487.97	4.08E-05	1592.4	62.19	129.8	32.7	0.3015
4.5	23.30	11.30	1141	10	193.7	155.4	0.486	491.38	2.66E-05	1598.3	61.99	131.1	33.1	0.3015
5.0	00.00	11.60	1169	10	194.2	154.9	0.486	501.87	-1.59E-05	1599.8	61.94	135.4	34.2	0.3015
	18/1/91													
5.5	0.30	9.80	1109	10	189.0	151.8	0.486	495.78	8.57E-06	1587.9	62.35	132.9	33.5	0.3015
6.0	1.00	9.90	1110	10	190.0	152.7	0.486	492.41	2.24E-05	1589.4	62.30	131.5	33.2	0.3015
6.5	1.30	10.10	1111	10	191.3	153.9	0.486	486.83	4.57E-05	1587.9	62.35	129.3	32.6	0.3015
7.0	2.00	10.10	1096	10	189.4	152.6	0.486	488.16	4.00E-05	1586.4	62.40	129.8	32.7	0.3012
7.5	2.30	9.50	1102	10	189.6	152.6	0.486	489.62	3.39E-05	1586.4	62.40	130.4	32.8	0.3015
8.0	3.00	9.80	1120	10	191.6	154.0	0.486	488.68	3.79E-05	1580.4	62.61	130.0	32.7	0.3014
8.5	3.30	9.80	1110	10	190.1	152.8	0.486	490.66	2.95E-05	1580.4	62.61	130.8	32.9	0.3015
9.0	4.00	9.40	1073	10	189.9	153.9	0.486	474.89	9.73E-05	1578.9	62.66	124.6	31.3	0.3015
9.5	4.30	9.20	1128	10	192.0	154.1	0.486	490.29	3.11E-05	1578.9	62.66	130.6	32.9	0.3014
10.0	5.00	9.05	1109	10	190.2	152.9	0.486	489.73	3.35E-05	1578.9	62.66	130.4	32.8	0.3015
10.5	5.30	9.40	1112	10	191.0	153.6	0.486	487.59	4.24E-05	1578.9	62.66	129.6	32.6	0.3014
11.0	6.00	9.40	1106	10	189.9	152.7	0.486	489.71	3.36E-05	1578.9	62.66	130.4	32.8	0.3014
11.5	6.30	9.30	1111	10	190.9	153.6	0.486	487.42	4.31E-05	1580.4	62.61	129.5	32.6	0.3014
12.0	7.00	9.60	1095	10	189.2	152.4	0.486	486.96	4.51E-05	1571.5	62.93	129.3	32.5	0.3014
12.5	7.30	10.00	1112	10	190.1	152.7	0.486	489.75	3.34E-05	1567.1	63.09	130.4	32.7	0.3014
13.0	8.00	10.30	1095	10	188.8	152.0	0.486	488.42	3.90E-05	1573.0	62.88	129.6	32.6	0.3014
13.5	8.30	10.40	1112	10	189.1	151.7	0.486	494.78	1.27E-05	1576.0	62.77	132.4	33.3	0.3014
14.0	9.00	11.00	1099	10	188.1	151.2	0.486	493.58	1.76E-05	1577.5	62.72	131.9	33.2	0.3014
14.5	9.30	10.90	1105	10	188.6	151.5	0.486	495.43	9.99E-06	1587.9	62.35	132.7	33.4	0.3015
15.0	10.00	11.00	1093	10	188.7	152.0	0.486	490.05	3.22E-05	1590.9	62.25	130.6	32.9	0.3015
15.5	10.30	11.05	1093	10	187.9	151.2	0.486	493.61	1.74E-05	1590.9	62.25	132.0	33.3	0.3015
16.0	11.00	11.00	1091	10	187.7	151.0	0.486	493.82	1.65E-05	1590.9	62.25	132.1	33.3	0.3015
16.5	11.30	11.00	1085	10	187.2	150.8	0.486	493.13	1.94E-05	1590.9	62.25	131.8	33.3	0.3015
17.0	12.00	11.00	1088	10	187.2	150.6	0.486	494.27	1.47E-05	1587.9	62.35	132.3	33.3	0.3015
17.5	12.30	11.50	1109	10	189.4	152.2	0.486	494.94	1.20E-05	1595.3	62.09	132.6	33.4	0.3015
18.0	13.00	12.00	1133	10	191.2	153.2	0.486	497.95	-2.37E-07	1595.3	62.09	133.8	33.7	0.3015
18.5	13.30	12.10	1105	10	189.2	152.0	0.486	495.20	1.09E-05	1602.8	61.83	132.7	33.5	0.3012
19.0	14.00	12.10	1100	10	188.0	151.1	0.486	498.12	-9.36E-07	1602.8	61.83	133.9	33.8	0.3016
19.5	14.30	12.20	1125	10	191.6	153.8	0.486	494.10	1.54E-05	1607.3	61.68	132.3	33.5	0.3016
20.0	15.00	12.90	1136	10	192.0	153.8	0.486	496.86	4.19E-06	1601.3	61.88	133.3	33.7	0.3016
20.5	15.30	12.90	1100	10	188.8	151.9	0.486	494.92	1.21E-05	1604.3	61.78	132.6	33.5	0.3016
21.0	16.00	12.30	1107	10	188.9	151.7	0.486	497.12	3.14E-06	1599.8	61.94	133.4	33.7	0.3015
21.5	16.30	12.20	1080	10	187.7	151.4	0.486	489.07	3.62E-05	1593.9	62.14	130.2	32.8	0.3015
22.0	17.00	13.00	1145	10	191.3	152.9	0.486	504.17	-2.50E-05	1605.8	61.73	136.3	34.5	0.3016
22.5	17.30	12.95	1113	10	190.0	152.6	0.486	500.64	-1.10E-05	1626.9	61.02	135.0	34.2	0.3017
23.0	18.00	12.50	1117	10	190.5	153.0	0.486	497.62	1.11E-06	1622.4	61.17	133.7	33.9	0.3017
23.5	18.30	11.90	1114	10	190.8	153.4	0.486	494.51	1.37E-05	1619.3	61.27	132.5	33.6	0.3017
24.0	19.00	11.50	1120	10	190.9	153.2	0.486	496.46	5.81E-06	1614.8	61.42	133.2	33.7	0.3017
24.5	19.30	11.30	1136	10	192.4	154.2	0.486	496.91	3.99E-06	1614.8	61.42	133.4	33.8	0.3017
25.0	20.00	10.80	1134	10	191.9	153.8	0.486	497.51	1.54E-06	1610.3	61.58	133.6	33.8	0.3016
25.5	20.30	10.20	1110	10	190.6	153.3	0.486	491.37	2.67E-05	1602.8	61.83	131.1	33.1	0.3016
26.0	21.00	8.90	1127	10	191.0	153.1	0.486	495.92	7.99E-06	1590.9	62.25	132.9	33.5	0.3015
26.5	21.30	8.85	1132	10	191.3	153.3	0.486	497.02	3.52E-06	1593.9	62.14	133.4	33.6	0.3015
27.0	22.00	8.80	1126	10	191.7	153.8	0.486	492.86	2.05E-05	1593.9	62.14	131.7	33.2	0.3015
27.5	22.30	8.80	1134	10	192.0	153.9	0.486	494.41	1.42E-05	1590.9	62.25	132.3	33.4	0.3015
28.0	23.00	8.90	1150	10	193.5	154.8	0.486	495.47	9.81E-06	1592.4	62.19	132.8	33.5	0.3015
28.5	23.30	8.95	1135	10	193.2	155.1	0.486	490.07	3.21E-05	1592.4	62.19	130.6	32.9	0.3015
29.0	00.00	8.95	1144	10	194.2	155.8	0.486	490.13	3.18E-05	1595.3	62.09	130.6	33.0	0.3015
	19/1/91													
29.5	0.30	8.40	1127	10	192.9	155.1	0.486	487.46	4.30E-05	1589.4	62.30	129.6	32.7	0.3015
30.0	1.00	8.30	1142	10	193.0	154.6	0.486	493.31	1.67E-05	1586.4	62.40	131.9	33.3	0.3015
30.5	1.30	8.40	1172	10	195.7	156.3	0.486	495.46	9.85E-06	1590.9	62.25	132.7	33.5	0.3015
31.0	2.00	8.00	1108	10	189.5	152.2	0.486	493.23	1.90E-05	1584.9	62.46	131.8	33.2	0.3014
31.5	2.30	7.98	1110	10	189.8	152.5	0.486	491.97	2.42E-05	1580.4	62.61	131.3	33.1	0.3015
32.0	3.00	7.75	1109	10	189.0	151.7	0.486	495.06	1.15E-05	1580.4	62.61	132.6	33.4	0.3014
32.5	3.30	7.80	1108	10	189.2	152.0	0.486	494.00	1.58E-05	1584.9	62.46	132.1	33.3	0.3014
33.0	4.00	7.90	1122	10	190.5	152.8	0.486	494.65	1.32E-05	1580.4	62.51	132.4	33.3	0.3015
33.5	4.30	7.30	1092	10	187.5	150.8	0.486	493.27	1.88E-05	1576.0	62.77	131.8	33.2	0.3014
34.0	5.00	7.50	1110	10	189.2	151.9	0.486	494.89	1.22E-05	1584.9	62.46	132.5	33.4	0.3015
34.5	5.30	7.70	1113	10	190.0	152.6	0.486	492.81	2.07E-05	1581.9	62.56	131.7	33.1	0.3014
35.0	6.00	7.60	1114	10	190.3	152.8	0.486	492.33	2.27E-05	1583.4	62.51	131.5	33.1	0.3015
35.5	6.30	7.40	1103	10	189.2	152.2	0.486	491.28	2.70E-05	1580.4	62.61	131.0	33.0	0.3015
36.0	7.00	7.30	1126	10	190.8	153.0	0.486	494.39	1.42E-05	1578.9	62.66	132.3	33.3	0.3015
36.5	7.30	7.60	1113	10	190.0	152.6	0.486	492.15	2.34E-05	1578.9	62.66	131.4	33.1	0.3014
37.0	8.00	7.20	1108	10	189.1	151.9	0.486	493.56	1.76E-05	1578.9	62.66	131.9	33.2	0.3015
37.5	8.30	7.90	1081	10	187.0	150.7	0.486	491.26	2.71E-05	1583.4	62.51	131.0	33.0	0.3015
38.0	9.00	8.90	1132	10	191.9	153.6	0.486	494.14	1.62E-05	1589.4	62.30	132.2	33.4	0.3015
38.5	9.30	9.50	1132	10	192.3	154.3	0.486	493.54	1.77E-05	1599.8	61.94	132.0	33.4	0.3016
39.0	10.00	10.20	1111	10	190.8	153.4	0.486	491.49	2.62E-05	1602.8	61.83	131.2	33.2	0.3016
39.5	10.30	12.80	1115	10	191.2	153.7	0.486	493.70	1.71E-05	1617.8	61.32	132.1	33.5	0.3017
40.0	11.00	12.90	1111	10	190.9	153.5	0.486	493.68	1.71E-05	1620.8	61.22	132.1	33.5	0.3017
40.5	11.30	12.30	1114	10	192.0	154.6	0.486	489.93	3.26E-05	1619.3	61.27	130.6	33.1	0.3017
41.0	12.00	12.40	1114	10	191.4	154.0	0.486	492.16	2.34E-05	1617.8	61.32	131.5	33.4	0.3017
41.5	12.30	12.00	1111	10	190.0	152.6	0.486	490.95	3.83E-05	1619.3	61.27	130.4	33.1	0.3017
42.0	13.00	11.30	1117	10	191.0	153.5	0.486	494.09	1.55E-05	1610.3	61.58	132.3	33.5	0.3017
42.5	13.30	10.95	1108	10	190.5	153.2	0.486	494.12	1.54E-05	1620.8	61.22	132.3	33.6	0.3017
43.0	14.00	10.80	1092	10	189.1	152.4	0.486	490.11	3.19E-05	1601.3	61.88	130.6	33.0	0.3016
43.5	14.30	9.10	1098	10	188.7	151.8	0.486	493.25	1.89E-05	1592.4	62.19	131.9	33.3	0.3015
44.0	15.00	8.40	1103	10	188.9	151.8	0.486	493.71	1.70E-05	1586.4	62.40	132.0	33.3	0.3015
44.5	15.30	8.50	1103	10	189.1	152.1	0.486	492.60	2.16E-05	1586.4	62.40	131.6	33.2	0.3015
45.0	16.00	7.85	1103	10	188.9	151.9	0.486	492.21	2.32E-05	1578.9	62.66	131.4	33.1	0.3015
45.5	16.30	7.20	1081	10	187.1	150.8	0.486	489.47	3.46E-05	1574.5	62.82	130.3	32.8	0.3014
46.0	17.00	6.05	1111	10	189.1	151.7	0.486	494.12	1.53E-05	1570.0	62.98	132.1	33.2	0.3014
46.5	17.30	6.20	1102	10	188.7	151.7	0.486	490.39	3.07E-05	1562.6	63.25	130.6	32.8	0.3013
47.0	18.00	6.30	1092	10	187.7	151.0	0.486	490.16	3.17E-05	1561.1	63.30	130.5	32.8	0.3013
47.5	18.30	6.50	1085	10	187.3	150.8	0.486	489.62	3.40E-05	1565.6	63.14	130.3	32.7	0.3014
48.0	19.00	6.80	1092	10	188.7	152.0	0.486	487.03	4.48E-05	1568.5	63.04	129.3	32.5	0.3014
48.5	19.30	6.80	1078	10	188.0	151.8	0.486	483.66	5.91E-05	1570.0	62.98	128.0	32.2	0.3014
49.0	20.00	6.60	1087	10	187.7	151.1	0.486	488.85	3.72E-05	1568.5	63.04	130.0	32.7	0.3014
49.5	20.30	6.60	1083	10	186.9	150.5	0.486	490.37	3.08E-05	1568.5	63.04	130.6	32.8	0.3014
50.0	21.00	6.70	1078	10	187.2	151.0	0.486	486.51	4.70E-05	1564.1	63.19	129.1	32.4	0.3013
50.5	21.30	6.90	1087	10	187.8	151.2	0.486	488.80	3.74E-05	1570.0	62.98	130.0	32.7	0.3014
51.0	22.00	7.00	1108	10	189.7	152.4	0.486	489.73	3.35E-05	1567.1	63.09	130.4	32.8	0.3014
51.5	22.30	7.20	1125	10	191.0	153.3	0.486	492.38	2.25E-05	1574.5	62.82	131.5	33.1	0.3014
52.0	23.00	7.10	1083	10	187.3	150.9	0.486	489.26	3.54E-05	1571.5	62.93	130.2	32.7	0.3014
52.5	23.30	7.20	1140	10	192.0	153.7	0.486	494.81	1.25E-05	1574.5	62.82	132.4	33.3	0.3014
53.0	00.00	7.10	1102	10	190.3	153.3	0.486	485.13	5.28E-05	1573.0	62.88	128.6	32.3	0.3014

Table (C-6) (Contiuation 1)

Time Of Runing	Date and Time	Tank Pressure (bar)	Q(sup) W	% F.S.R	Tw °C	Ti °C	v m/sec	Ut (W/m2 K)	Rf (m2 K / W)	Re	Pr	Nu (Exp.)	jH (Exp.)	f (Exp.)
	20/1/91													
53.5	0.30	7.05	1122	10	191.4	153.7	0.486	489.99	3.24E-05	1577.5	62.72	130.5	32.8	0.3014
54.0	1.00	6.80	1125	10	191.3	153.5	0.486	491.73	2.52E-05	1577.5	62.72	131.2	33.0	0.3014
54.5	1.30	6.70	1112	10	189.4	152.0	0.486	492.86	2.05E-05	1568.5	63.04	131.6	33.1	0.3014
55.0	2.00	6.90	1106	10	189.2	152.1	0.486	491.68	2.54E-05	1573.0	62.88	131.2	33.0	0.3014
55.5	2.30	6.80	1088	10	187.1	150.5	0.486	492.36	2.26E-05	1570.0	62.98	131.4	33.1	0.3014
56.0	3.00	7.10	1117	10	190.9	153.3	0.486	489.74	3.34E-05	1574.5	62.82	130.4	32.8	0.3014
56.5	3.30	7.30	1100	10	190.0	153.1	0.486	486.36	4.76E-05	1577.5	62.72	129.1	32.5	0.3014
57.0	4.00	7.20	1123	10	191.0	153.2	0.486	491.98	2.41E-05	1576.0	62.77	131.3	33.1	0.3014
57.5	4.30	7.05	1119	10	190.6	153.0	0.486	492.35	2.26E-05	1577.5	62.72	131.5	33.1	0.3014
58.0	5.00	7.10	1123	10	189.8	152.0	0.486	497.29	2.43E-06	1577.5	62.72	133.4	33.6	0.3014
58.5	5.30	6.80	1103	10	189.0	152.0	0.486	491.23	2.73E-05	1573.0	62.88	131.0	32.9	0.3014
59.0	6.00	6.80	1104	10	188.7	151.6	0.486	493.32	1.86E-05	1576.0	62.77	131.8	33.2	0.3014
59.5	6.30	6.70	1104	10	188.8	151.7	0.486	492.77	2.09E-05	1573.0	62.88	131.6	33.1	0.3014
60.0	7.00	6.70	1083	10	186.6	150.2	0.486	492.11	2.36E-05	1570.0	62.98	131.3	33.0	0.3014
60.5	7.30	7.00	1108	10	188.7	151.4	0.486	495.00	1.17E-05	1573.0	62.88	132.5	33.3	0.3014
61.0	8.00	7.1	1118	10	190.4	152.9	0.486	492.13	2.35E-05	1574.5	62.82	131.4	33.1	0.3014
61.5	8.30	7.00	1100	10	189.4	152.4	0.486	488.36	3.92E-05	1573.0	62.88	129.9	32.7	0.3014
62.0	9.00	6.70	1090	10	187.8	151.1	0.486	490.49	3.03E-05	1570.0	62.98	130.7	32.9	0.3014
62.5	9.30	7.00	1108	10	189.7	152.5	0.486	490.33	3.10E-05	1571.5	62.93	130.6	32.9	0.3014
63.0	10.00	7.10	1122	10	191.3	153.6	0.486	490.63	2.97E-05	1577.5	62.72	130.8	32.9	0.3014
63.5	10.30	6.50	1095	10	186.0	151.2	0.486	490.79	2.91E-05	1565.6	63.14	130.8	32.9	0.3013
64.0	11.00	7.20	1141	10	192.4	154.1	0.486	493.90	1.63E-05	1576.0	62.77	132.1	33.2	0.3014
64.5	11.30	7.05	1116	10	190.2	152.7	0.486	491.68	2.54E-05	1571.5	62.93	131.2	33.0	0.3014
65.0	12.00	6.90	1096	10	188.9	152.0	0.486	489.59	3.41E-05	1577.5	62.72	130.4	32.8	0.3014
65.5	12.30	6.95	1114	10	190.5	153.1	0.486	489.50	3.44E-05	1571.5	62.93	130.3	32.8	0.3014
66.0	13.00	7.50	1109	10	191.1	153.8	0.486	485.80	5.00E-05	1577.5	62.72	128.9	32.4	0.3014
66.5	13.30	6.95	1093	10	188.9	152.1	0.486	487.43	4.31E-05	1573.0	62.88	129.5	32.5	0.3014
67.0	14.00	6.80	1121	10	189.5	151.8	0.486	497.24	2.64E-06	1573.0	62.88	133.4	33.6	0.3014
67.5	14.30	6.90	1101	10	188.9	151.9	0.486	491.71	2.53E-05	1580.4	62.61	131.2	33.1	0.3015
68.0	15.00	7.05	1092	10	187.7	151.0	0.486	492.38	2.25E-05	1576.0	62.77	131.5	33.1	0.3014
68.5	15.30	6.70	1100	10	188.5	151.6	0.486	493.03	1.98E-05	1580.4	62.61	131.7	33.2	0.3015
69.0	16.00	5.90	1098	10	187.6	150.7	0.486	493.91	1.62E-05	1565.6	63.14	132.0	33.2	0.3014
69.5	16.30	5.80	1106	10	189.0	151.8	0.486	490.20	3.15E-05	1556.7	63.46	130.5	32.7	0.3013
70.0	17.00	6.20	1096	10	188.0	151.1	0.486	490.96	2.83E-05	1561.1	63.30	130.8	32.8	0.3013
70.5	17.30	6.80	1118	10	190.2	152.7	0.486	492.61	2.15E-05	1573.0	62.88	131.5	33.1	0.3014
71.0	18.00	6.80	1094	10	187.8	151.0	0.486	492.78	2.08E-05	1574.5	62.82	131.6	33.1	0.3014
71.5	18.30	6.40	1092	10	187.3	150.6	0.486	493.67	1.72E-05	1571.5	62.93	132.0	33.2	0.3014
72.0	19.00	6.30	1102	10	187.9	150.8	0.486	494.60	1.34E-05	1565.6	63.14	132.3	33.2	0.3014
72.5	19.30	6.60	1098	10	188.9	152.0	0.486	489.22	3.56E-05	1570.0	62.98	130.2	32.7	0.3014
73.0	20.00	6.30	1090	10	187.0	150.3	0.486	492.82	2.07E-05	1564.1	63.19	131.6	33.1	0.3013
73.5	20.30	6.50	1130	10	189.2	151.2	0.486	501.68	-1.52E-05	1567.1	63.09	135.2	33.9	0.3014
74.0	21.00	6.80	1098	10	188.1	151.2	0.486	492.53	2.19E-05	1570.0	62.98	131.5	33.1	0.3013
74.5	21.30	6.60	1090	10	186.8	150.2	0.486	493.94	1.61E-05	1567.1	63.09	132.1	33.2	0.3014
75.0	22.00	6.50	1086	10	187.8	151.3	0.486	488.30	3.95E-05	1568.5	63.04	129.8	32.6	0.3014
75.5	22.30	7.00	1125	10	190.9	153.1	0.486	493.29	1.87E-05	1576.0	62.77	131.8	33.1	0.3014
76.0	23.00	7.40	1125	10	191.0	153.2	0.486	493.46	1.80E-05	1580.4	62.61	131.9	33.2	0.3014
76.5	23.30	7.30	1116	10	189.2	151.7	0.486	497.01	3.55E-06	1578.9	62.66	133.3	33.5	0.3014
77.0	00.00	7.30	1100	10	189.5	152.6	0.486	488.53	3.85E-05	1577.5	62.72	129.9	32.7	0.3014
	21/1/91													
77.5	0.30	6.70	1125	10	191.2	153.4	0.486	494.55	1.36E-05	1592.4	62.19	132.4	33.4	0.3015
78.0	1.00	6.80	1112	10	189.2	151.8	0.486	495.06	1.15E-05	1577.5	62.72	132.5	33.4	0.3014
78.5	1.30	6.90	1106	10	190.0	152.8	0.486	489.66	3.38E-05	1580.4	62.61	130.4	32.8	0.3015
79.0	2.00	6.40	1092	10	187.9	151.2	0.486	490.82	2.89E-05	1573.0	62.88	130.8	32.9	0.3014
79.5	2.30	6.70	1112	10	190.3	152.9	0.486	490.19	3.16E-05	1576.0	62.77	130.6	32.9	0.3014
80.0	3.00	6.90	1122	10	190.6	152.9	0.486	495.07	1.14E-05	1595.3	62.09	132.6	33.5	0.3016
80.5	3.30	6.85	1120	10	190.3	152.7	0.486	494.22	1.49E-05	1577.5	62.72	132.2	33.3	0.3014
81.0	4.00	7.10	1112	10	190.1	152.8	0.486	491.22	2.73E-05	1577.5	62.72	131.0	33.0	0.3014
81.5	4.30	7.80	1108	10	189.9	152.7	0.486	491.25	2.71E-05	1584.9	62.46	131.0	33.0	0.3015
82.0	5.00	7.80	1101	10	188.2	151.2	0.486	495.94	7.92E-06	1586.4	62.40	132.9	33.5	0.3015
82.5	5.30	7.75	1098	10	187.5	150.6	0.486	497.34	2.23E-06	1584.9	62.46	133.5	33.7	0.3015
83.0	6.00	8.00	1096	10	187.3	150.4	0.486	497.74	6.14E-07	1586.4	62.40	133.7	33.7	0.3015
83.5	6.30	8.30	1099	10	188.3	151.3	0.486	495.48	9.76E-06	1592.4	62.19	132.8	33.5	0.3015
84.0	7.00	8.40	1102	10	188.1	151.0	0.486	496.84	4.27E-06	1586.4	62.40	133.3	33.6	0.3015
84.5	7.30	9.20	1100	10	189.2	152.2	0.486	492.31	2.28E-05	1593.9	62.14	131.5	33.2	0.3016
85.0	8.00	9.25	1087	10	187.8	151.3	0.486	492.63	2.14E-05	1598.3	61.99	131.6	33.3	0.3016
85.5	8.30	9.60	1115	10	190.3	152.9	0.486	493.92	1.62E-05	1593.9	62.14	132.1	33.4	0.3016
86.0	9.00	10.15	1103	10	189.0	152.0	0.486	494.87	1.23E-05	1599.8	61.94	132.5	33.5	0.3016
86.5	9.30	10.60	1098	10	188.8	151.9	0.486	494.41	1.41E-05	1605.8	61.73	132.4	33.5	0.3016
87.0	10.00	10.60	1105	10	188.7	151.5	0.486	498.29	-1.62E-06	1607.3	61.68	134.0	33.9	0.3017
87.5	10.30	10.55	1105	10	188.5	151.3	0.486	499.25	-5.47E-06	1608.8	61.63	134.3	34.0	0.3017
88.0	11.00	10.70	1104	10	189.2	152.1	0.486	495.94	7.91E-06	1607.3	61.68	133.0	33.7	0.3017
88.5	11.30	11.50	1113	10	189.6	152.2	0.486	498.41	-2.08E-06	1610.3	61.58	134.0	33.9	0.3017
89.0	12.00	12.40	1100	10	189.6	152.7	0.486	493.08	1.96E-05	1614.8	61.42	131.9	33.4	0.3017
89.5	12.30	12.80	1119	10	190.7	153.1	0.486	497.51	1.54E-06	1619.3	61.27	133.7	33.9	0.3017
90.0	13.00	12.60	1098	10	188.9	152.0	0.486	495.98	7.73E-06	1617.8	61.32	133.1	33.8	0.3017
90.5	13.30	13.05	1106	10	189.9	152.8	0.486	495.72	8.80E-06	1622.4	61.17	133.0	33.8	0.3017
91.0	14.00	13.00	1107	10	189.7	152.5	0.486	497.79	4.13E-07	1626.9	61.02	133.8	34.0	0.3018
91.5	14.30	13.05	1116	10	190.4	152.9	0.486	498.91	-4.08E-06	1629.9	60.92	134.3	34.1	0.3018
92.0	15.00	12.95	1130	10	191.7	153.7	0.486	500.78	-1.16E-05	1635.9	60.72	135.1	34.4	0.3018
92.5	15.30	13.00	1125	10	191.5	153.8	0.486	499.51	-6.50E-06	1640.5	60.57	134.6	34.3	0.3019
93.0	16.00	12.80	1122	10	191.3	153.6	0.486	499.52	-6.53E-06	1640.5	60.57	134.6	34.3	0.3019
93.5	16.30	12.90	1120	10	190.6	153.0	0.486	501.99	-1.64E-05	1643.5	60.47	135.6	34.6	0.3019
94.0	17.00	12.90	1118	10	190.5	153.0	0.486	501.38	-1.40E-05	1645.0	60.42	135.3	34.5	0.3019
94.5	17.30	13.00	1129	10	192.2	154.3	0.486	499.73	-7.37E-06	1649.6	60.27	134.7	34.4	0.3019
95.0	18.00	12.10	1113	10	190.2	152.8	0.486	501.62	-1.49E-05	1651.1	60.22	135.5	34.6	0.3019
95.5	18.30	10.80	1148	10	191.5	153.8	0.486	500.70	-1.65E-05	1640.5	60.57	138.8	35.3	0.3019
96.0	19.00	11.00	1156	10	194.1	155.2	0.486	502.85	-1.98E-05	1643.5	60.47	139.9	34.6	0.3019
96.5	19.30	10.00	1129	10	191.9	154.0	0.486	500.62	-1.09E-05	1646.5	60.37	135.0	34.4	0.3019
97.0	20.00	8.90	1129	10	190.8	152.9	0.486	502.80	-1.96E-05	1626.9	61.02	135.9	34.5	0.3018
97.5	20.30	7.40	1127	10	190.9	153.0	0.486	500.35	-9.85E-06	1617.8	61.32	134.8	34.2	0.3017
98.0	21.00	7.00	1136	10	191.5	153.3	0.486	500.77	-1.15E-05	1611.8	61.53	135.0	34.2	0.3017
98.5	21.30	6.20	1125	10	190.3	152.5	0.486	500.52	-1.06E-05	1607.3	61.68	134.9	34.1	0.3017
99.0	22.00	6.00	1125	10	190.4	152.6	0.486	499.46	-6.30E-06	1602.8	61.83	134.4	34.0	0.3016
99.5	22.30	5.60	1126	10	190.1	152.2	0.486	500.35	-9.86E-06	1596.8	62.04	134.7	34.1	0.3016
100.0	23.00	5.80	1166	10	193.9	154.7	0.486	501.61	-1.49E-05	1598.3	61.99	135.3	34.2	0.3016
100.5	23.30	6.00	1162	10	193.6	154.5	0.486	501.41	-1.41E-05	1598.3	61.99	135.2	34.2	0.3016
101.0	00.00	6.00	1146	10	193.3	154.8	0.486	495.84	8.29E-06	1599.8	61.94	132.9	33.6	0.3016
	22/1/91													
101.5	0.30	6.00	1175	10	195.0	155.5	0.486	501.15	-1.31E-05	1601.3	61.88	135.1	34.2	0.3016
102.0	1.00	5.20	1105	10	187.5	150.3	0.486	500.97	-1.23E-05	1587.9	62.35	135.0	34.1	0.3015
102.5	1.30	5.00	1134	10	189.9	151.8	0.486	502.33	-1.78E-05	1581.9	62.56	135.5	34.1	0.3015
103.0	2.00	4.80	1101	10	186.0	149.0	0.486	503.33	-2.17E-05	1571.5	62.93	135.9	34.2	0.3014
103.5	2.30	4.90	1098	10	186.5	149.6	0.486	499.16	-5.09E-06	1567.1	63.09	134.2	33.7	0.3014
104.0	3.00	5.30	1130	10	191.1	153.1	0.486	494.08	1.55E-05	1570.0	62.98	132.1	33.2	0.3014
104.5	3.30	5.40	1120	10	188.9	151.3	0.486	498.90	-4.06E-06	1573.0	62.88	134.1	33.7	0.3014
105.0	4.00	5.30	1126	10	189.0	151.2	0.486	501.42	-1.41E-05	1571.5	62.93	135.1	34.0	0.3014
105.5	4.30	5.30	1115	10	187.3	149.8	0.486	503.21	-2.12E-05	1567.1	63.09	135.8	34.1	0.3013
106.0	5.00	5.40	1120	10	188.0	150.4	0.486	501.77	-1.55E-05	1565.6	63.14	135.2	34.0	0.3013
106.5	5.30	5.40	1114	10	187.0	149.6	0.486	503.90	-2.39E-05	1567.1	63.09	136.1	34.2	0.3014
107.0	6.00	5.60	1109	10	187.2	150.0	0.486	501.13	-1.30E-05	1568.5	63.04	135.0	33.9	0.3013
107.5	6.30	5.80	1112	10	187.2	149.8	0.486	502.77	-1.95E-05	1570.0	62.98	135.6	34.1	0.3014
108.0	7.00	6.00	1090	10	185.3	148.7	0.486	501.66	-1.51E-05	1571.5	62.93	135.2	34.0	0.3014
108.5	7.30	5.95	1110	10	187.3	150.0	0.486	502.14	-1.70E-05	1577.5	62.72	135.4	34.1	0.3014
109.0	8.00	6.05	1111	10	187.5	150.2	0.486	500.39	-1.00E-05	1567.1	63.09	134.7	33.8	0.3014
109.5	8.30	6.05	1095	10	185.9	149.1	0.486	501.68	-1.51E-05	1578.9	62.66	135.2	34.1	0.3015
110.0	9.00	6.30	1095	10	186.3	149.5	0.486	499.90	-8.08E-06	1577.5	62.72	134.5	33.9	0.3014
110.5	9.30	6.90	1115	10	188.3	150.8	0.486	500.93	-1.22E-05	1581.9	62.56	134.9	34.0	0.3015
111.0	10.00	6.95	1116	10	188.0	150.6	0.486	503.20	-2.12E-05	1587.9	62.35	135.9	34.3	0.3015
111.5	10.30	7.40	1120	10	188.7	151.0	0.486	503.13	-2.09E-05	1592.4	62.19	135.9	34.3	0.3015
112.0	11.00	7.60	1114	10	188.3	150.8	0.486	502.76	-1.94E-05	1596.8	62.04	135.7	34.3	0.3016

Table (C-6) (Continuation 3)

Time Of Runing	Date and Time	Tank Pressure (bar)	Q(sup) W	% F.S.R	Tw °C	Ti °C	v m/sec	Ut (W/m² K)	Rf (m² K / W)	Re	Pr	Nu (Exp.)	jH (Exp.)	f (Exp.)
	25/1/91													
173.0	0.30	4.80	1144	10	191.2	152.8	0.486	499.54	-6.63E-06	1570.0	62.98	134.3	33.8	0.3014
173.5	1.00	4.80	1110	10	183.4	146.1	0.486	520.81	-8.84E-05	1573.0	62.88	143.2	36.0	0.3014
174.0	1.30	4.70	1096	10	186.9	150.1	0.486	496.16	7.03E-06	1565.6	63.14	132.9	33.4	0.3014
174.5	2.00	4.60	1085	10	186.0	149.5	0.486	494.66	1.31E-05	1562.6	63.25	132.3	33.2	0.3013
175.0	2.30	4.80	1120	10	190.0	152.4	0.486	493.71	1.70E-05	1570.0	62.98	132.0	33.2	0.3014
175.5	3.00	5.00	1144	10	192.0	153.6	0.486	496.54	5.46E-06	1574.5	62.82	133.1	33.5	0.3014
176.0	3.30	4.90	1114	10	189.0	151.6	0.486	495.68	8.96E-06	1570.0	62.98	132.8	33.4	0.3014
176.5	4.00	4.90	1117	10	189.6	152.1	0.486	494.41	1.41E-05	1571.5	62.93	132.3	33.3	0.3014
177.0	4.30	4.75	1107	10	188.4	151.2	0.486	495.00	1.17E-05	1567.1	63.09	132.5	33.3	0.3014
177.5	5.00	4.70	1104	10	188.2	151.1	0.486	494.16	1.52E-05	1565.6	63.14	132.1	33.2	0.3014
178.0	5.30	4.60	1074	10	185.2	149.1	0.486	492.92	2.02E-05	1559.7	63.36	131.6	33.0	0.3013
178.5	6.00	4.80	1110	10	188.7	151.4	0.486	494.12	1.53E-05	1561.1	63.30	132.1	33.2	0.3013
179.0	6.30	5.10	1140	10	192.4	154.1	0.486	493.03	1.98E-05	1573.0	62.88	131.7	33.1	0.3014
179.5	7.00	4.50	1103	10	187.8	150.8	0.486	495.22	1.09E-05	1564.1	63.19	132.6	33.3	0.3013
180.0	7.30	4.70	1100	10	187.7	150.8	0.486	493.37	1.84E-05	1556.7	63.46	131.8	33.1	0.3013
180.5	8.00	4.80	1110	10	189.1	151.8	0.486	495.33	1.04E-05	1584.9	62.46	132.7	33.5	0.3015
181.0	8.30	4.60	1109	10	188.3	151.0	0.486	493.96	1.60E-05	1547.8	63.79	132.0	33.1	0.3012
181.5	9.00	5.00	1100	10	187.6	150.7	0.486	494.31	1.45E-05	1561.1	63.30	132.2	33.2	0.3013
182.0	9.30	5.05	1087	10	186.3	149.8	0.486	494.38	1.43E-05	1564.1	63.19	132.2	33.2	0.3013
182.5	10.00	4.80	1097	10	189.6	152.7	0.486	486.59	4.66E-05	1576.0	62.77	129.2	32.5	0.3009
183.0	10.30	4.90	1113	10	189.8	152.4	0.486	493.91	1.62E-05	1584.9	62.46	132.1	33.3	0.3009
183.5	11.00	4.80	1100	10	189.9	152.9	0.486	487.97	4.08E-05	1586.4	62.40	129.7	32.7	0.3009
184.0	11.30	4.80	1096	10	189.4	152.5	0.486	488.33	3.93E-05	1584.9	62.46	129.9	32.7	0.3009
184.5	12.00	4.90	1090	10	189.3	152.6	0.486	486.14	4.86E-05	1586.4	62.40	129.0	32.5	0.3009